



ISSN 1454-8518

**ANNALS
OF THE UNIVERSITY OF
PETROȘANI**

ELECTRICAL ENGINEERING

VOL. 26 (LIII)

**UNIVERSITAS PUBLISHING HOUSE
PETROȘANI, ROMANIA 2024**

EDITOR OF PUBLICATION

Prof. Sorin Mihai RADU Ph.D, Email: sorin_mihai_radu@yahoo.com

ADVISORY BOARD

Prof. Alexandru BITOLEANU, Ph.D. - University of Craiova, *Romania*; Full Professor Emeritus Stanislaw CIERPISZ – Silesian University of Technology, *Poland*; Prof. Tiberiu COLOȘI, Ph.D., - Member of the Academy of Technical Science of *Romania*, President of Cluj Branch; Prof. Dr. Predrag DAŠIĆ - High Technological Technical School, Krusevac, *Serbia and Montenegro*; Dr. Eng. Nicolae DAN - Dessault Systems Simulia Corp., Providence, *USA*; Assoc. Prof. Daniel DUBOIS, Ph.D. - University of Liège, *Belgium*; Eng. Emilian GHICIOI, Ph.D. - INCD INSEMEX Petrosani, *Romania*; Prof. Emerit Mircea EREMIA, Ph.D. – Member of the Academy of Technical Science of *Romania*; Prof. Dr. Vladimir KEBO – VSB, Technical University of Ostrava, *Czech Republic*; Assoc. Prof. Eng. Vladimir CABLIK, Ph.D., VSB - Technical University of Ostrava. *Czech Republic*; Assoc. Prof. Dr. Ernő KOVÁCS - University of Moskolc, *Hungary*; Prof. Gheorghe MANOLEA, Ph.D. - University of Craiova, *Romania*; Prof. Radu MUNTEANU, Ph.D. – Member of the Academy of Technical Science of *Romania*, *Vice President*; Prof. Dan NEGRUT, Ph.D. – University of Wisconsin, Madison, *USA*; Acad. Prof. Dr. Genadiy PIVNYAK – National Mining University Dnepropetrovsk, *Ukraine*; Prof. Flavius Dan ȘURIANU, Ph.D. – “Politehnica” University of Timișoara, *Romania*; Prof. Willibald SZABO, Ph.D. – “Transilvania” University of Brașov, *Romania*; Prof. Alexandru VASILIEVICI, Ph.D. – “Politehnica” University of Timișoara, *Romania*, Prof. Susana ARAD, Ph.D. – University of Petroșani, *Romania*; Assoc. Prof. Liliana Brana SAMOILĂ, Ph.D. – University of Petroșani, *Romania*.

EDITORIAL BOARD

Editor-in-chief:

Assoc. Prof. Marius Daniel MARCU, Ph.D., University of Petroșani

Deputy Editor:

Assoc. Prof. Dragoș PĂSCULESCU, Ph.D., University of Petroșani

Associate Editors:

Assoc. Prof. Nicolae PĂTRĂȘCOIU, Ph.D., University of Petroșani

Assoc. Prof. Ilie UȚU, Ph.D., University of Petroșani

Assoc. Prof. Florin Gabriel POPESCU, Ph.D., University of Petroșani

Assoc. Prof. Olimpiu STOICUȚA, Ph.D., University of Petroșani

Editor Secretary:

Lecturer Ioan Răzvan SLUSARIUC, Ph.D., University of Petroșani

Editorial office address: University of Petroșani, 20 University Street, 332006 Petroșani, Romania, Phone: (40) 254/54.29.94; 54.25.80; 54.25.81; 54.33.82; Fax: (40) 254/54.34.91; 54.62.38,

Contact person: Marius Daniel MARCU, e-mail: mariusmarcu@upet.ro

This publication is spread in 28 countries.

CONTENTS

1. Roland Iosif Moraru , <i>Occupational risk assessment for maintenance electricians within an automotive production company</i>	7
2. Georgeta Buică, Anca Elena Antonov, Constantin Beiu, Dragos Pasculescu, Mircea Risteiu , <i>Managing the risks of injury and occupational disease in the maintenance activity of wind farms</i>	25
3. Dragoş Fotău, Marcel Rad, Diana Sălăşan, Valentin Sîrbu , <i>Aspects regarding the usage of the high voltage impulse generator in order to verify the insulation systems of electric motors used in potentially explosive atmosphere</i>	35
4. Maria Daniela Stochitoiu, Ilie Utu , <i>The modern technology implementation for safe energy transition</i>	43
5. Florin Mureşan-Grecu, Roland Iosif Moraru , <i>Health and safety risk assessment for three representative workstations from a local company that manufactures electrical lighting equipment</i>	51
6. Sebastian Daniel Rosca, Marius Marcu, Monica Leba, Daniel Ioan Dinea, Dumitru Cristian Iacobescu Dinea , <i>The impact of meditation in a video game based on BCI</i>	69
7. Constantin Beiu, Georgeta Buică, Antonov Anca Elena, Dragos Pasculescu, Remus Dobra, Mircea Risteiu , <i>Arc flash detection on photovoltaic systems</i>	79
8. Valery Boroday, Olga Nesterova, Vladyslav Naida , <i>Application of altera programmed logic integrated circuit in efficient asynchronous drive system</i>	89
9. Alina Stepanek, Fabian Arun Panaite , <i>A literature review on integrating ai and blockchain technologies in animatronics for children's entertainment and education</i>	97
10. Leon Pană, Florin Gabriel Popescu, Sebastian Daniel Rosca <i>ATEX thermistor motor protection relays in on board electrical installations</i>	107
11. Stanislav Shykhov, Vladyslav Knysh, Oleksii Plahunov , <i>Development of a mobile platform with a manipulator robot</i>	115
12. Emanuel Muntean, Monica Leba , <i>Mimicking humanoid robot gait using human motion data from IMU</i>	123

13. Lucian Moldovan, Mihai Magyari, Clementina Moldovan, Sorin Râșnoveanu, <i>Particularities regarding the determination of maximum surface temperature of junction boxes with type of protection increased safety “e” designed for use in gaseous explosive atmospheres</i>	133
14. Cosmin Rus, Monica Leba, <i>Autonomous indoor navigation system concept: hardware and software integration for electric vehicles</i>	141
15. Simona Riurean, Tatiana Antipova, <i>Prebunking, an effective defense mechanism to strengthen consumers’ cyber awareness</i>	155
16. Alexandra Soica, Nicoleta Negru, Razvan Bogdan Itu, Susana Apostu, <i>Public opinion about the impact of renewable energy sources on the environment of Jiu Valley</i>	169
17. Florin Mureșan-Grecu, Florin Gabriel Popescu, Marius Daniel Marcu, Dragos Pasculescu, Mircea Risteiu, Teodora Lazar, <i>Modernization of electrical installations for lighting and power in the electroenergetics laboratory of the University of Petroșani</i>	177
18. Nicolae Patrascoiu, <i>Hardware and software used for the study of angular motion by remote control</i>	197
19. Zoltan Vass, Marius Șuvar, Bogdan Șimon-Marinică, Laurențiu Muntean, <i>Developing a programmable electronic circuit for the controlled ignition of explosive mixtures</i>	207
20. Maria-Isabela Ghicaianu (Cașotă), Dan Codruț Petrilean, <i>Energy consumption and resource allocation made more efficient through artificial intelligence: AI-driven design optimization for HVAC (heating, ventilation, and air conditioning) system</i>	237
21. Alina Panciu, Mihai Victor Zerbis, Lucian Lobonț, <i>Is the European infrastructure ready for long haul electric transportation? An analysis of a freight transport from Romania to Germany using an electric semi-trailer truck</i>	247
22. Dan Gabor, Mihaela Părăian, Anca Tăzlăuanu, <i>Reliability of blasting machines used to initiate electrical detonators</i>	263
23. Mihai Magyari, Dragoș Fotău, Sorin Zsido, <i>Aspects regarding the use of variable speed drives in the case of explosion protected electric motors used in explosive environments</i>	273
24. Mirela Ancuța Radu, Cătălin Mihai Popa, Ana Petrina Păun, <i>Aspects of earthing of installations in environments with potentially explosive atmospheres</i>	285

25. Remus Sibişanu, Tudor Manole, Cosmin Rus , <i>Developing an autonomous drone for early detection of forest fires</i>	295
26. Alexandru Costinaş, Marius Leonard Olar, Sebastian Daniel Roşca , <i>Challenges in integrating artificial intelligence for enhanced robotic autonomy and interaction</i>	307
27. Alexandra Soica, Nicoleta Negru, Sorin Mihai Radu, Angela Egri , <i>Research on reducing PM10 particles in the Jiu Valley area as a result of using photovoltaic panels in electricity production</i>	315
28. Victor Triohin, Tudor Manole , <i>Modelling and implementation of the dashboard interface for electric vehicles using advanced simulation technologies and navigation APIs</i>	329
29. Ilie Utu, Maria Daniela Stochitoiu , <i>Energy transition as the necessity for achieve a climate-neutral Europe</i>	341
30. Sebastian Daniel Rosca, Monica Leba, Dragos Pasculescu, Leon Pană, Florin Gabriel Popescu , <i>Analyzing the impact of motor imagery in a BCI video game</i>	347
31. Maria Daniela Stochitoiu, Ilie Utu , <i>Increasing the transmission capacity of 220kV line using a static synchronounous series compensator</i>	355
32. Andrei Cristian Rada , <i>Charging through electric field - the limiting electric charge of particles in electrostatic filters</i>	361
33. Nadia Elena Stoicuta , <i>Evolution of electricity production from thermoelectric power plants in Romania: an econometric approach</i>	373
34. Sebastian Daniel Rosca, Simona Riurean, Gabriela Popescu, Teodora Lazar, Florin Gabriel Popescu , <i>Development of a BCI video game for mental state recognition</i>	383
35. Olimpiu Stoicuta, Vali – Chivuta Sirb, Nadia Elena Stoicuta , <i>Direct rotor flux-oriented control of induction motors using hysteresis current controllers and VSI inverter</i>	391

OCCUPATIONAL RISK ASSESSMENT FOR MAINTENANCE ELECTRICIANS WITHIN AN AUTOMOTIVE PRODUCTION COMPANY

ROLAND IOSIF MORARU¹

Abstract: This work represents an attempt to highlight, in a concise form, through accessible arguments, combined with scientific rigor, the potentiality of methods for evaluating occupational risk factors for the "Maintenance and Repair Electrician" job. At the same time, we tried to capture, in a broad, relational, systematic, concise, but also attractive framework, the essential aspects of the assessment of the risk factors found at the level of workplaces within the investigated company. The aim was to offer an interesting perspective, in the aspect of a particular vision of the organizational reality or a new paradigm regarding the impact of the assessment of risk factors on competitive success, which would bring a genuine increase in knowledge, facilitate the understanding of the respective issue or the new reference for explaining organizational performance and to have relevance for the professionalization of activities in the field.

Key words: risk at work, injury and occupational illness, maintenance electrician, automotive industry.

1. INTRODUCTION

Any organization operating in an environment that influence the risks but creates at the same time, a context that fixes the limits within which risks must be managed [1], [2], [3]. Moreover, each organization has partners relying on their approach for achieving the goals [4], [5] As emphasized by Moraru et al. (2011, 2014), an effective risk management for occupational health and safety (OHS) must take into account the priorities established by the partners too with respect to risk management processes [6], [7]. Therefore, the environment in which the organization subsists is not neutral. In theory and practice devoted to risk we are speaking even about the extended organization (at the level of the interacting environment) [8]. Risk management must be subordinated to the objectives that form an integrated, coherent and converging system, towards the overall objectives, so that activity levels to support each other [9], [10], [27], [29], [31].

This approach allows the organization to define and implement a risk management strategy that starts from the top and is integrated into routine activities and operations of the organization. In all working systems and all the jobs the employer has

¹ Professor., Ph.D. Eng., University of Petroșani, roland_moraru@yahoo.com

a general duty to protect the life, integrity and health of workers against occupational hazards that may occur in the workplace and create working conditions designed to ensure their physical, psychological and social comfort. [11], [12]. Adoption by the employer, within its responsibilities, of prevention and protection measures aimed at preventing occupational risks, information and training of workers and ensuring the organizational framework and means required for health and safety at work imposes to perform the occupational risk assessment [13]. Therefore, it can be stated that the primary goal of occupational risk assessment is always prevention of occupational risks, even if this objective is not always achievable in practice [14]. Where it is not possible to eliminate hazards, risks should be reduced so that the residual risks are kept under control [15]. In later stages and under a rigorous control program, residual risks will be reassessed, analyzing the possibility to further eliminate or reduce them, following developments in scientific and technical knowledge [16], [28], [30], [34].

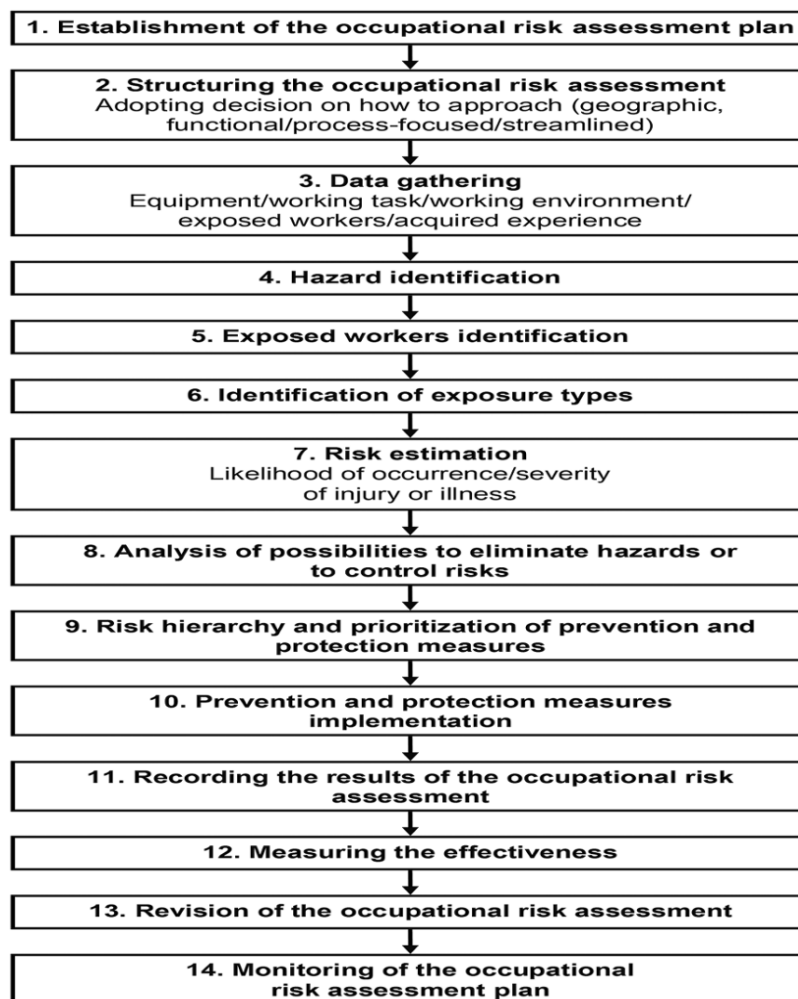


Fig.1. The overall chart of the occupational risks assessment and management process (adapted after [26])

Starting from the legislative, normative and methodological requirements, it can be stated that the occupational risk assessment is the systematic study of all aspects of the work process that are likely to generate unwanted events, of the means of eliminating hazards and applicable prevention and protection measures to control the associated risks [17], [18], [19], [20].

The assessment should cover the occupational risks that are reasonably foreseeable. Risks resulting from day-to-day activities are normally considered insignificant and require no special attention unless professional activity implies their aggravation [21]. The methodology and criteria for assessing occupational risks must be defined according to the scope, nature and time scheduling to ensure they are proactive rather than reactive and are used in a systematic manner [22]. Organizations can use different risk assessment methods as part of their global strategy to deal with various hazards or activities. The complexity of the risk assessment method does not depend on the size of the organization but on the hazards associated with the organization's activities. Figure 1 presents the general chart of the occupational risk assessment process that includes some elements of occupational risk management [23], [32].

To be effective and sustainable, the risk assessment process should be simple, practical, and easy to understand. Its success highly depends upon management commitment, involvement and adequate resources allotment [24]. The process should be performed by people with proper skills supported by technology that is correctly sized for the working task. Risk assessment must be part of a larger framework that uses the information gathered to make decisions about risk responses and monitoring, and returns information back into the overall strategic planning process [25], [33].

2. WORK PROCESSES IN THE INVESTIGATED COMPANY

Commercial company S.C. XYZ ROMANIA LLC. is located in the N-E part of the ABC municipality, and owns the site of 6.75 ha of the headquarters, the built surface is $A_c = 14,490 \text{ m}^2$ and the developed surface is $A_d = 16,320 \text{ m}^2$. The company provides its employees with appropriate spaces for carrying out their activity, environmental motivations for quality services. Activity profile: CAEN code 2932 - *manufacture of other parts and accessories for motor vehicles and motor vehicle engines*. Number of employees: 551. They carry out their activities in the main headquarters, as follows:

a) ***Company management and support departments:***

- Secretariat;
- Technical office: HSE (Safety and health at work, Emergency situations and Environment);
- Human resources office;
- Financial office - accountant;
- Archive;
- Engineering;
- IT;
- Logistics office;

- Personal training rooms;
- Dining room;
- Changing rooms-lockers;
- Medical office.

b) Production/manufacturing departments:

1. Warehouse raw materials production space
2. BPP sector (sandblasting, adhesive application)
3. Press sector
4. Clamping/unclamping sector
5. Ovens sector
6. GSP sector
7. Accessories sector
8. Packaging sector
9. Finished product warehouse sector
10. Quality laboratory
11. Maintenance

The specific activities of each section are carried out based on the work procedures and integrated management plans for quality, environment, safety and health at work, established for each of them within the implemented SMI (integrated management system).

c) Technical space annexes:

- Compressor technical space;
- Thermal power plant technical space;
- Electricity transformer building;

d) Warehouses:

- Storage of chemical materials;
- Storage of raw materials;
- Residuary wastes.

Description of activities:

The production hall, the property of the company, is authorized and approved by the local administration bodies, sanitary, the authority for environmental protection, fire safety and safety and health at work, in an area of 11,564 square meters. The following sections are organized in this space:

1. Raw material warehouse section for production space

The raw material warehouse for production space is equipped with 3 forklifts and 3 electric forklifts that also serve the production sector, shelves for storing raw materials and materials. Also here is the installation to send the mix to the press bunkers. In this warehouse, the raw material (mix, metal plates, chemicals, etc.) is received, a preliminary quality check is made and they are placed on the shelves (fig.2).



Fig.2. Raw material warehouse section for production space

2. Section BPP sandblasting adhesive application

The BPP sandblasting and adhesive application section receives the plates from the raw material warehouse, it is equipped with a plate sandblasting plant, an adhesive application plant, a plate heating oven, a cooling oven, a conveyor belt, a plate recovery tank, shelves for keeping sandblasted plates and for which the adhesive was applied. The metal plates are sandblasted, then a layer of adhesive is applied, they go through the oven and then the cooler, then they are transported to the press section (fig.3).



Fig.3. Section BPP sandblasting adhesive application

3. Presses section

At the press section there are 2 types of pressing procedures:

- Hot pressing: FHP presses, 3 pieces
- Cold pressing: FSP presses, 6 pieces, KZP 4 pieces, SSP 2 pieces.

The plates coming from the adhesive application section are placed in the press warehouse, the mix is brought through pipes from the warehouse to the hopper, and the pressing operation is done automatically (fig.4).



Fig.4. Section „presses”

4. Clamping/unclamping section

The clamping/unclamping section contains 10 workstations. When clamping, they are fixed in frames to prevent expansion in the ovens, then they are placed in the

oven at a temperature lower than 300°C and left for a few hours for the baking process. Then they are put into the cooler where they are removed from the frames (fig. 5).



Fig.5. Clamping/unclamping section

5. Furnace section

Furnace section contains a number of 6 ovens where the plates are inserted into the oven at a temperature lower than 300°C and are left for a few hours for the baking process (fig. 6).



Fig.6. Furnace section

6. GSP section

The GSP section has 5 production lines. At GSP, the first process is the grinding process, where the edges of the plates are made (they are ground), then on the metal side, the back of the plate, a paint is applied in an electrostatic field (in painting booths), then the plates are inserted into the painting oven (paint oven) then follows the cooler and the rotary table from where they are taken manually by the operator. At GSP, the plates are transported between processes on a conveyor belt (fig.7).



Fig.7. GSP section

7. Accessories section

The accessory section has 10 work lines. For accessories, various accessories are applied on the back of the plates, the sensor (only on certain types) 10 work tables, 10 devices for inscription, 10 stations with operators who mount accessories and inscribe the barcode and company logo on the plate (fig.8).

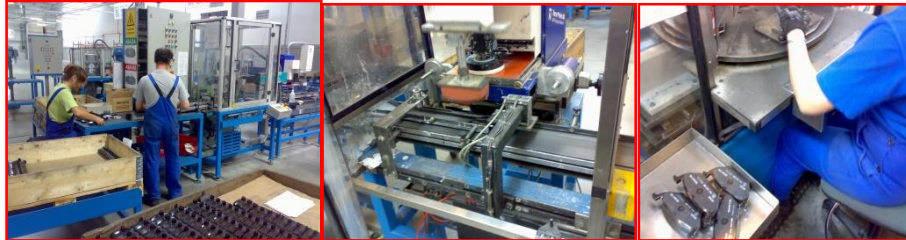


Fig.8. Accessories section

8. The packing department

The packing section has 3 work lines, consisting of work tables, box support stacks. When packing, the pairs of plates are put into boxes, along with the instructions, the boxes are closed and sealed, checked and ready for delivery. At each section and completion of operation or process there are stations for checking product operations by quality checkers (fig.9).



Fig.9. The packing department

9. Finished Product Warehouse Section

The product warehouse is equipped with 2 forklifts and 2 electric forklifts that also serve the production sector, shelves for storing finished products. At the finished product warehouse, the products are placed in transport boxes and the rolls are loaded for transport (fig. 9)



Fig. 9. Finished Product Warehouse Section

10. Quality Laboratory Section

At the quality laboratory, specific tests are performed (friction, detachment, etc.) being equipped with devices and equipment for performing tests and checks (fig. 10).



Fig.10. Quality Laboratory Section

11. Maintenance Section

The maintenance department is equipped with welding machines (electric and autogenous), drilling machine, cutter with abrasive stone (fixed and mobile), grinder, welding table, lathe, planer, milling machine, grinding machine, tool kit, air compressor, workbenches, vices, sandblasting machine etc. The maintenance section provides repairs and interventions to production machinery in the event of defects, malfunctions in the process and technological flow (fig.11).



Fig.11. Maintenance Section

The jobs that were analyzed and for which the risk assessment for safety and health at work was carried out are presented in table 1.

Table 1. The list of jobs for which the risk assessment was carried out

Nr. crt.	Job/workstation	Number of workers
1.	Operator of industrial robot presses FSP - CAEN code 817001	27
2.	Maintenance and repair electrician - CAEN code 724507	7
3	Mechanical locksmith - CAEN code 721424	4
Total		38

3. ASSESSMENT OF INJURY AND OCCUPATIONAL DISEASE RISKS FOR THE MAINTENANCE AND REPAIR ELECTRICIAN

The purpose of the work process is to check, maintain and repair the electrical installations within the unit. Figures 12, 13 and 14 show some of the

identified forms of manifestation of specific risks. Applying the tools and the procedure specific to the INCDPM Bucharest method [26], the concrete forms of manifestation of the risks were identified, the severity classes and the probability classes related to each of the identified risks were assigned, and then - using the scale of framing the risk levels, the partial risk levels were set.

The results obtained are centralized in Table 2. The meaning of the notations in table 2 is as follows:

- *WSE - Work system element; IR - identified risk; RF – risk factor; MC - Maximum consequence; S - Severity; Likelihood; RL - Risk level; WE - Working equipment; OE - Occupational environment; WT - Working task; HF - Human factor;*
- *N-negligible; LTI 3-45 – Lost Time Injury from 3 to 35 days; LTI 45-180 – Lost Time Injury from 45 to 180 days; INV I – first degree invalidity; INV II – second degree invalidity; INV III – third degree invalidity; D – death.*



Fig.12. Machine parts in motion - hand grip when placing the plates in the magazine.



Fig.13. Projection of dust mix in the eye, particles carried by the air currents to the abrasive belt, dropping-jumping pads



Fig.14. Falling from a height due to imbalance, slipping, tripping – when checking the level of mix in the mix in the hopper, when manually loading and emptying the hopper

Table 2. Risk Assessment Card for „Maintenance Electrician”

UNIT: S.C. XYZ LLC.		WORKPLACE EVALUATION SHEET	Number of people exposed: 7			
DEPARTMENT: Maintenance			Duration of exposure: 8 h/shift			
Workstation: Electrician de întreținere și reparații 724507			<i>Evaluation team:</i> Administrator, Head of maintenance, Head of internal OSH service, Occupational medicine doctor			
WSE	IR	Risk Factors	MC	S	L	RL
WE	Mech. RF	1. Machine parts in motion - grip, drive by transmissions with couplings, with belts.	INV III	4	2	3
		2. Movements of means of transport - hit by means of transport - access to the	INV III	4	1	2

OCCUPATIONAL RISK ASSESSMENT FOR MAINTENANCE ELECTRICIANS WITHIN
AN AUTOMOTIVE PRODUCTION COMPANY

		workplace by means of vehicles				
		3. Dangerous surfaces or contours – direct contact of the epidermis with cutting, prickly, slippery surfaces	LTI 3-45	2	5	3
	Thermal RF	4. Lowered temperature – cold metal surfaces touched directly	LTI 3-45	2	6	3
		5. Flames from the accidental priming of the electric arc in the switching devices.	D	7	1	3
	Electric RF	6. Electrocutation by direct contact	D	7	2	4
		7. Electrocutation by indirect contact or by the appearance of step voltage	D	7	2	4
	Chemical RF	8. Flammable substances, adhesive, adhesive solution, paints, thinners	LTI 45-180	3	3	3
	OE	Physical RF	9. High relative air humidity	LTI 3-45	2	6
10. High noise level especially in the test bench area			INV III	4	2	3
11. Low lighting level – lack of lighting lamps			INV III	4	2	3
Chemical RF		12. High level of exhaust gases, etc.	D	7	1	3
WT	Physical overload	13. Forced working positions.	LTI 3-45	2	6	3
		14. Dynamic effort – long intervention route, repeated movements between machines.	LTI 3-45	2	5	3
	Mental overload	15. Difficult decisions in a short time made in an environment of noise and exhaust gases.	LTI 3-45	2	5	3
HF	Wrong actions	16. Execution of works that exceed the competence or authorization of the worker	D	7	2	4
		17. Actions due to erroneous identification of equipment elements	D	7	2	4
		18. Out of sync when working in a team	LTI 45-180	3	2	2

		19. Falling on the same level by unbalancing, slipping, tripping – slippery, uneven surfaces	LTI 45-180	3	3	3
		20. Falling from a height on the nacelle, by stepping in the void, unbalancing or slipping	D	7	1	3
	Omissions	21. Failure to use personal protective equipment: electrical insulating boots, electrical insulating gloves, protective helmet and visor	D	7	2	4

The overall risk level of the job is:

$$N_{rg} = \frac{\sum_{i=1}^{21} r_i \cdot R_i}{\sum_{i=1}^{21} r_i} = \frac{5 \cdot (4 \times 4) + 14 \cdot (3 \times 3) + 2 \cdot (2 \times 2)}{5 \times 4 + 14 \times 3 + 2 \times 2} = \frac{214}{66} = 3,24 \quad (1)$$

The partial levels of risk by risk factors are represented graphically in fig. 15, the prevention and protection measures intended to minimize the risks located in the unacceptable field being centralized in table 3.

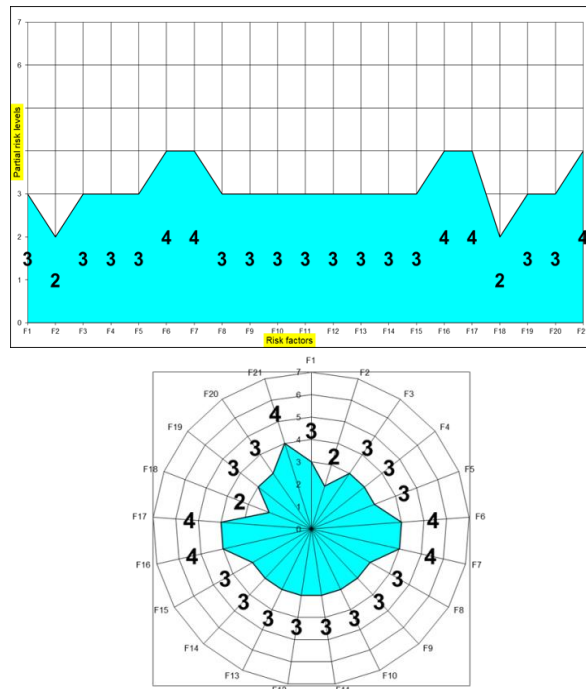


Fig.15. Partial risk levels by risk factors at work: maintenance and repair electrician

OCCUPATIONAL RISK ASSESSMENT FOR MAINTENANCE ELECTRICIANS WITHIN
AN AUTOMOTIVE PRODUCTION COMPANY

Table 3 . Sheet of proposed measures: "Maintenance and repair electrician" workplace

Risk factor	Risk level	Proposed measures
F06 - Electrocution by direct contact	4	<p>Technical measures:</p> <ul style="list-style-type: none"> • identification of the installations to be worked on; • visual check of the integrity of the electrical conductor insulation; • the use, as appropriate, of a head protection helmet, a face protection visor, electro-insulating gloves, electro-insulating shoes or carpet and tools with an electro-insulating handle; • execution of technical security measures by trained and authorized personnel. <p>Organizational measures:</p> <ul style="list-style-type: none"> • training and authorization according to the legal provisions in force, as well as periodic testing of the technical and work safety knowledge acquired by the executor; • execution according to the authorized procedures of all interventions, regardless of their nature; • periodical control with the aim of complying with electrical safety measures.
F07 - Electrocution by indirect contact or the appearance of step voltage	4	<p>Technical measures:</p> <ul style="list-style-type: none"> • visual check of the integrity of the grounding of the equipment casings, poles and metal and concrete supports in the work area • discharging the capacitive load of the installation to be worked on; • the use, as appropriate, of electro-insulating gloves, shoes or electro-insulating carpet and tools with an electro-insulating handle.
F16 - Execution of works that exceed the competence or authorization of the worker	4	<p>Organizational measures:</p> <ul style="list-style-type: none"> • the duties of the maintenance electrician will include only activities for which he is authorized and trained; • for interventions that exceed the competence or authorization of the maintenance electrician, natural or legal persons with the necessary competence will be contacted.
F17 - Actions due to erroneous identification of equipment elements	4	<p>Technical measures:</p> <ul style="list-style-type: none"> • all interventions performed on the electrical installations will comply with the provisions contained in the technical books of the equipment. <p>Organizational measures:</p> <ul style="list-style-type: none"> • the maintenance electrician will be periodically trained on how to operate the technical equipment used by the unit in the production process.

F21 - Failure to use individual protective equipment and other protective means provided	4	<p>Technical measures:</p> <ul style="list-style-type: none"> equipping workers with individual protective equipment corresponding to the activity to be carried out. <p>Organizational measures:</p> <ul style="list-style-type: none"> wearing protective equipment will be mandatory.
--	---	--

4. INTERPRETATION OF RISK ASSESSMENT RESULTS

The global risk level calculated for the job "*Maintenance and repair electrician*" is equal to 3.24, a value that places it in the category of jobs with a low to medium risk level, not exceeding the maximum acceptable limit (3.5).

The analysis of the data from the "Assessment Sheet" highlights the fact that out of the total of 21 risk factors identified, only 5 exceed, as a partial level of risk, the value of 3, 5 falling into the category of medium risk factors.

The risk factors that are in the unacceptable range are:

- F06 - Electrocution by direct contact – partial risk level 4;
- F07 - Electrocution by indirect contact or the appearance of step voltage - partial risk level 4;
- F16 - Execution of works that exceed the competence or authorization of the worker - partial risk level 4;
- F17 - Actions through erroneous identification of equipment elements - partial risk level 4;
- F21 - Non-use of individual protective equipment and other protective means provided - partial risk level 4.

In order to reduce or eliminate the 5 risk factors (which are in the unacceptable field), the generic measures presented in the "Proposed measures sheet" are necessary. The distribution of risk factors by generating sources is presented as follows (fig. 16):

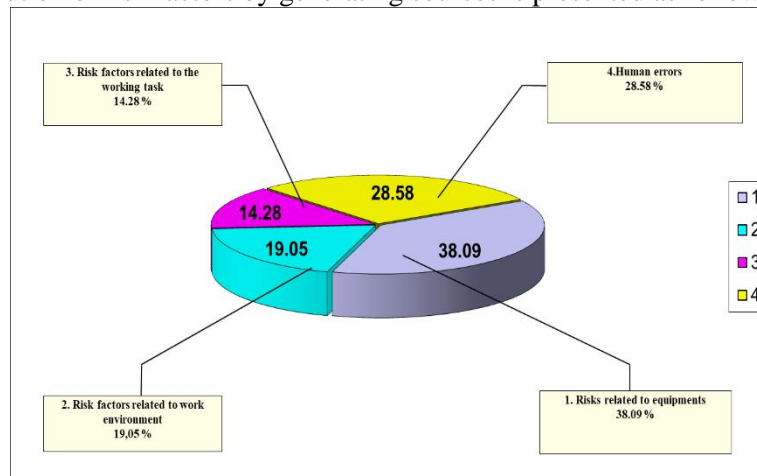


Fig.16. The share of risk factors identified by the generating source

- 38.09%, factors specific to the work equipments;

- 19.05%, factors specific to the work environment;
- 14.28%, factors specific to the workload;
- 28.58%, human factors.

From the analysis of the Risk Assessment Card, it is found that 38.10% of the identified risk factors can have irreversible consequences on the performer (death or disability), so that the workplace cannot be classified among those with a particular risk of injury.

5. CONCLUSIONS

The work concerned the assessment of risks for the job "Maintenance and repair electrician" within an industrial company in the automotive field, in accordance with the provisions of art. 7, para. 4, lit. b, art. 12, para. 1, lit. and art. 13 of Law no. 319/2006 and art. 15, para. 1, points 1 and 2 of H.G. no. 1425/2006.

The risk assessment was carried out on the basis of the data provided to the investigated company through the job descriptions, the lists of technical equipment, their technical books, the regulations for granting individual protective equipment, information about technological processes and the development of the work process for each job, received from the management and technical staff of the company, as well as the own observations made during the documentation visits and follow-up of the activity for each workplace.

The list of jobs evaluated in the overall research is shown in table 4.

Table 4. The centralizer of the results of risk assessments at the investigated company

Crt. No.	No. card	Workstation	Overall risk level
1	F01	Operator of industrial robot presses FSP 817001	3,11
2	F02	Maintenance and repair electrician 724507	3,24
3	F03	Locksmiths 721424	3,23

The overall risk level per company is:

$$N_{gs} = \frac{\sum_{i=1}^3 r_i \cdot N_{gi}}{\sum_{i=1}^3 r_i} = 3,19 \quad (2)$$

According to the ranking, it is found that all jobs have a global risk level below the allowed limit (3.5), they fall into the category of those with a low to medium risk level. The value of the aggregate global risk level per company $N_{gs} = 3.19$, determines its inclusion in the category of those with a low to medium risk level.

The ranking of workstations, depending on the overall level of risk, is shown in table 5.

Table 5. Risk ranking

Crt. No.	No. card	Workstation	Overall risk level
1	F01	Maintenance and repair electrician 724507	3,24
2	F02	Locksmiths 721424	3,23
3	F03	Operator of industrial robot presses FSP 817001	3,11

The realization of the work consisted in going through the following stages: analysis of the activities carried out within the company; establishing the workplaces for which the risk assessment for safety and health at work was carried out; identification of risk factors for each job; establishing the maximum foreseeable consequence of the action of the risk factors on the human body, for each individual risk factor; classification into gravity classes; classification into probability classes (frequency); determination of the partial risk level for each identified risk factor; calculation of the global risk level for each job; interpretation of the results of the risk assessment for safety and health at work for each workplace, through the lens of current legislation; preparation of measures sheets for each workplace, for risk factors that exceed the acceptable level.

In the current activity of the investigated company, the employer has always shown the conviction that the success, performance and competitiveness of the modern organization depend, to a large extent, on the integration of the assessment of risk factors into the business strategy, beyond the legal provisions that require this or the threat of stopping the activity or fines applied by labor inspectors. Beyond these considerations, the discrepancies also reflect the shock produced by an interdisciplinary, relatively new field of concern and action on a society, not always sufficiently prepared in terms of information, but also of the lack of multiple choices, therefore of knowledge and receptivity to new and change.

Through this paper, we tried not only to present an aspectual assessment, from the point of view of the occupational safety and health field, of a workplace, but also to satisfy the need for information on the activity profile as a whole and to cover a void strongly felt in the specialized literature. Because of claims, often apathetic, lacking in depth, of false conditioning focused only on one method, of obvious mistrust, of the perpetuation of de facto resistance or lack of specialized literature, translated into Romanian, it should not be limited the action and not diminished the tendency of the assessment of professional risk factors to integrate more and more deeply in the organizational management, in general, or even in the management of human resources in particular, beyond the activities of the Internal Service of Prevention and Protection, as one of the modern directions of their development.

The paper invites to analysis, provokes reflection and hopefully interest, while being susceptible to improvement and development, and some of the issues and aspects require continuous improvement and examination. The work is, however, a point of departure and analysis of research that is based on reducing the risk and reducing the occurrence of work accidents.

REFERENCES

- [1]. Aven T., Zio E., *Some considerations on the treatment of uncertainties in risk assessment for practical decision making*, Reliability Engineering & System Safety, Volume 96, Issue 1, Pages 64-74, 2011.
- [2]. Azadeh-Fard N., Schuh A., Rashedi E., Camelio J.A., *Risk assessment of occupational injuries using accident severity grade*. Saf Sci 76:160–167, 2015.
- [3]. Bedford T., Cooke R., *Probabilistic risk analysis: foundations and methods*. Cambridge: Cambridge University Press, 2001.
- [4]. Cioca L.-I., Ivascu, L., *Risk Indicators and Road Accident Analysis for the Period 2012–2016*. Sustainability, 9, 1530., 2017.
- [5]. HSE, *Risk assessment: A brief guide to controlling risks in the workplace*, Leaflet INDG163 (rev4), Health and Safety Executive (HSE), Bootle, Great Britain, 2014.
- [6]. Moraru R.I., Băbuț G.B., Cioca L.I., *Rationale and Criteria Development for Risk Assessment Tool Selection in Work Environments*, Environmental Engineering and Management Journal, Vol. 13, No. 6, pp.1371 – 1376, 2014.
- [7]. Moraru R.I., Băbuț G.B., Cioca L.I., *Drawbacks and traps in risk assessment: examples in Romania*, Proceedings of the 5th International Conference on Manufacturing Science and Educations - MSE 2011, Volume 2, pp. 363-366, Sibiu, Romania, 2011.
- [8]. Joy J., Griffiths D., *National minerals industry safety and health risk assessment guideline*, version 3, March 2008.
- [9]. Kokangül A., Polat U., Dağsuyu C., *A new approximation for risk assessment using the AHP and Fine Kinney methodologies*. Saf Sci 91:24–32, 2017.
- [10]. Cioca L.I., Moraru R.I., Băbuț G.B., *A Framework for Organisational Characteristic Assessment and their Influences on Safety and Health At Work*, 15th Int. Conf. on Knowledge-Based Organization: Management, Conference Proceedings, Sibiu, Romania, Vol. 2 pp. 43-48, 2009.
- [11]. Romanian Parliament, Law no. 319 regarding occupational safety and health (in Romanian), *The Official Journal of Romania*, part I, no. 646/26.07.2006, Bucharest, Romania, 2006.
- [12]. Paman, H.J., *Learning from the past and knowledge management: Are we making progress?*, *Journal of Loss Prevention in the Process Industries*, Vol 22, pp 672-679, 2009.
- [13]. Labour Inspection, *Verifying how employers comply with legal requirements for professional risk assessment. Guidance for inspectors* (in Romanian), Labour Inspection, Bucharest, Romania, 2015.
- [14]. European Commission, *Guidance on risk assessment at work* (Directive 89/391/EEC), European Commission, Directorate General V Employment, Industrial Relations and Social Affairs, Office for Official Publications of the European Communities, Luxembourg, 1996.
- [15]. HSE, *The health and safety toolbox: How to reduce risks at work*, HSG268, Health and Safety Executive (HSE), Bootle, Great Britain, 2014.
- [16]. Ispășoiu A., Moraru R.I., Popescu-Stelea M., Băbuț G.B., *Study on the potential of artificial intelligence application in industrial ergonomics performance improvement*, Acta Technica Napocensis - Series: Applied Mathematics, Mechanics and Engineering, [S.I.], v. 64, n. 1-S1, Pages: 45-54 , feb. 2021. ISSN 2393–2988.; IDS Number: QL6ZK, Accession Number: WOS 000621232900006, 2021.
- [17]. Romanian Government, Government Decision no. 1048 regarding the minimum safety and health requirements for the use by workers of personal protective equipment at the workplace (in Romanian), *The Official Journal of Romania*, part I, no. 722/23.08.2006, Bucharest, Romania, 2006.

- [18]. **Romanian Government**, Government Decision no. 1425 for approval of Methodological Norms for applying occupational safety and health Law no. 319/2006 (in Romanian), *The Official Journal of Romania*, part I, no. 882/30.10.2006, Bucharest, Romania, 2006.
- [19]. **Romanian Government**, Government Decision no. 1029 regarding the conditions for placing machines on the market (in Romanian), *The Official Journal of Romania*, Part I, no. 674/30.09.2008.
- [20]. **Romanian Government**, Government Decision no. 517 for amending and supplementing Government Decision no. 1029/2008 regarding the conditions for placing machines on the market (in Romanian), *The Official Journal of Romania*, Part I, no. 373/27.05.2011.
- [21]. **Romanian Government**, Government Decision no. 191 for the approval of the National Strategy on Safety and Health at Work for the period 2018-2020 (in Romanian), *The Official Journal of Romania*, Part I, no. 331/16.04.2018.
- [22]. **Moraru R.I., Băbuț G.B., Popescu-Stelea M.**, Approaching occupational safety and health emerging risks categories and prevention, *Quality - Access to Success*, Volume 15, Issue 139, pp. 104-108, 2014.
- [23]. **Niskanen T., Naumanen P., Hirvonen M.L.**, An evaluation of EU legislation concerning risk assessment and preventive measures in occupational safety and health, *Applied Ergonomics*, Volume 43, Issue 5, pp. 829-842, 2012.
- [24]. **Stanton N.A., Harvey C.**, *Beyond human error taxonomies in assessment of risk in sociotechnical systems: a new paradigm with the EAST 'broken-links' approach*. *Ergonomics* 60(2):221–233, 2017.
- [25]. **U.S. Department of Army**, *Safety Mishap Risk Management*, DA-PAM 385-30, Retrieved August, 2011 from http://www.apd.army.mil/pdffiles/p385_30.pdf, 2010.
- [26]. **Băbuț G.B., Moraru R.I.**, *Critical analysis and ways to improve the I.N.C.D.P.M. Bucharest for the assessment of the risks of accidents and occupational diseases*, "Quality - access to success", vol. 14, no. 137, pp. 55-66 2013.
- [27]. **Petrilean D.C., Stanilă S., Dosa I.**, *A mathematical model for determining the dimensionless heat flux with application in mine environment*, *Environmental Engineering and Management Journal*, Vol.16, No. 6, 1249-1414, 2017.
- [28]. **Petrilean D.C.**, *Compresoare eliciodale*, Editura Tehnica-Info, 2006
- [29]. **Petrilean D.C.**, *Termodinamica tehnica si masini termice*, Editura A.G.I.R., 2010.
- [30]. **Petrilean D.C.**, *Mathematical model for the determination of the non-stationary coefficient of heat transfer in mine works*, The 19th American Conference on Applied Mathematics (AMERICAN-MATH '13), Cambridge, MA, USA.2013.
- [31]. **Petrilean D. C.**, *Transmiterea căldurii*, Editura Universitas, 2016.
- [32]. **Handra A.D., Popescu F.G., Păsculescu D.**, *Utilizarea energiei electrice: lucrări de laborator*, Editura Universitas, 2020.
- [33]. **Popescu F.G., Păsculescu D., Păsculescu V.M.**, *Modern methods for analysis and reduction of current and voltage harmonics*, LAP LAMBERT Academic Publishing, pp. 233, 2020.
- [34]. **Fîță N. D., Lazăr T., Popescu F. G., Păsculescu D., Pupăză C., Grigorie E.**, *400 kV power substation fire and explosion hazard assessment to prevent a power black-out*, International Conference on Electrical, Computer Communications and Mechatronics Engineering-ICECCME, pp. 16-18, 2022.

MANAGING THE RISKS OF INJURY AND OCCUPATIONAL DISEASE IN THE MAINTENANCE ACTIVITY OF WIND FARMS

GEORGETA BUICĂ¹, ANCA ELENA ANTONOV², CONSTANTIN
BEIU³, DRAGOS PASCULESCU⁴, MIRCEA RISTEIU⁵

Abstract: In the context of climate change and through the lens of the objectives set at the EU level regarding climate neutrality, through the Integrated National Plan in the field of Energy and Climate Change 2021-2030, Romania proposed to increase the share of sources to 55.8% in 2030 of renewable energy in the electricity sector. For this purpose, one of the targets established at the national level is related to the construction and commissioning of new electricity production capacities from wind and solar sources. The paper aims to present a synthesis of the research carried out regarding the assessment of accident risks and professional improvement in the exploitation and maintenance of wind farms. Considering the new regulations regarding the safety of machines, in the category of which wind turbines fall, taking into account the European and national strategies regarding digitalization, the implementation of software systems for monitoring, control and data acquisition in the integrated management systems of electricity producers led to the reduction over time of the risks of occupational injury and disease.

The paper considers new research regarding the risks that may appear as a result of the aging of the workforce and its fluctuation/migration in the activity of exploitation and maintenance of wind farms in order to establish some measures to prevent the risks of accidents and occupational diseases determined by the introduction of new digital production technologies.

Key words: risk, evaluation, safety, wind turbine.

1. INTRODUCTION

Romania attaches great importance to developing internal sources of electricity production, pursuing two aspects: their diversification and reducing greenhouse gas emissions.

The national policies regarding the fulfilment of the European Union's energy targets for 2030-2050 emphasize the integration of localized renewables by increasing

¹ Ph.D., Eng., *georgiana_buica@yahoo.com*

² Ph.D., Eng.

³ Ph.D., Eng.

⁴ Ph.D., Eng.

⁵ Ph.D., Eng.

wind and solar potential. Through the Integrated National Plan in the field of Energy and Climate Change 2021-2030 from April 2020, updated in 2023, Romania proposed as a target for 2050 the achievement of an installed capacity of 30.4 GW, of which 76% would come from renewable sources of energy [1], [22], [24], [27].

After 2010, wind farms registered rapid growth in Romania, with wind energy becoming an integral part of the national energy system. According to the data reported by the Ministry of Energy, the share of electricity produced from renewable sources (wind, solar, biomass, biogas and geothermal) in 2023 was a significant 18% of the total electricity produced [2]. This achievement is a testament to Romania's commitment to renewable energy.

The data reported on the Transelectrica website show that in June 2024, 116 wind energy farms with a net power of 2966.439 MW provided electricity in the NES [3 - 5]. This specific data provides a clear picture of the current state of wind energy production in Romania.

Figure 1 shows the electricity production from 07.05.2024, by types of energy, graphically presented.

On 07/05/2024, the net production of electrical energy was 5923 MW, of which the average wind energy production was 566 MW [3 - 5].

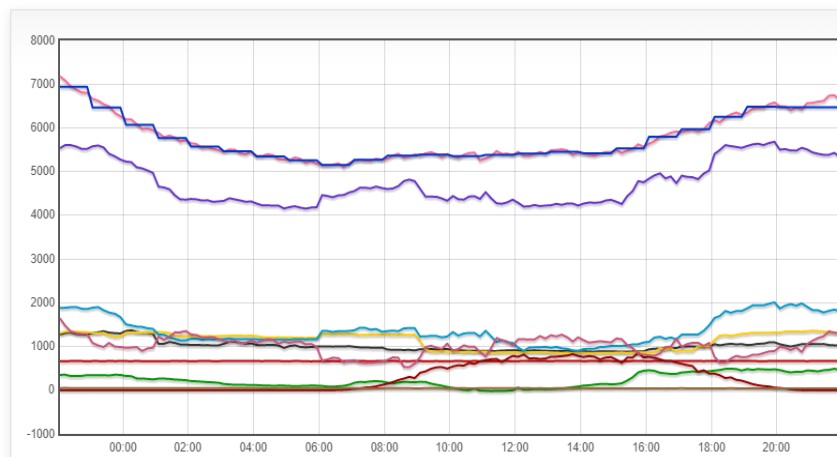


Fig.1. Electricity production from 07/05/2024 by types of energy [5]

In order to reach the targets proposed by Romania, it must build and implement new electricity production capacities from renewable wind, solar, biomass, biogas and geothermal sources.

Although wind energy is considered environmentally friendly, at the European and national levels, dangerous working conditions both during construction and during exploitation have generated events. The paper presents the results of the research carried out regarding the assessment of the risks of accidents and professional improvement in the exploitation and maintenance of wind farms.

The research was carried out within the framework of three contracts signed with economic agents, producers, and distributors of electricity from 2010 to 2022, with the

aim of identifying and evaluating the risks of accidents and occupational diseases, analyzing them, and proposing security measures to comply with technical conditions and security and health requirements and ensure safe and healthy workplaces.

One hundred thirty-nine wind turbines, with an installed capacity of 2.5 MW each, 4 110/33 kV electrical substations, a 400/110/20 kV electrical transformer station and the 33 kV and 110 kV cable networks were evaluated and diagnosed. kV, the 33 kV and 110 kV cable networks, but also in the ensemble as a workplace for maintenance and repair operators [6, 7].

The evaluated and diagnosed wind turbines are installed onshore and mainly consist of a foundation that also contains the grounding installation, the metal tower, three vertical blades, the turbine nacelle/housing, the shaft, the rotor, the kinematic chain, the electrical part/electrical system (generator, converter system, MV transformer, medium voltage distribution installation, control systems) batteries for energy storage, azimuth system and wind measurement devices, control, monitoring, measurement and data acquisition systems [6 - 8].

2. ASPECTS REGARDING THE OCCUPATIONAL HEALTH AND SAFETY REQUIREMENTS APPLICABLE TO WIND TURBINES

The main components of wind farms, wind turbines, must guarantee the essential safety and health requirements applicable provided by Directive 2006/42/EC, respectively HG no. 1029/2008 regarding the conditions for placing machines on the market, Directive 2009/104/EC, respectively HG no. 1146/2006 regarding the minimum safety and health requirements for the use of work equipment by workers, as well as Directive 2014/35 /EU, respectively HG no. 409/2016 regarding the establishment of the conditions for making low-voltage electrical equipment available on the market, the applicable European and national standards, national technical regulations and codes of good practice [6, 9 - 14].

Since maintenance activities usually occur at high heights, wind turbines must guarantee the safety and health requirements regarding access/work at high heights. Thus, the work equipment for access and work at height must guarantee the applicable safety and health requirements provided by Directive 2009/104/EC regarding the minimum safety and health requirements for the use of work equipment by workers at work and the harmonized European standards. The stairs for access to each level of the turbine and the platforms/walkways at each level must comply with the clauses of the SR EN ISO 14122 Machine Safety series of standards — permanent means of access to machines. The climbing stairs must have a protective basket and fall protection equipment/s - anchor points, safety lines or "lifeline" as the utility climbers call them and, if necessary, a fall arrester [23], [25].

Anchorage points and protective equipment against falling from a height (e.g. a sliding fall arrester on a flexible support equipped with an energy absorber or a retractable fall arrester) must guarantee the essential safety and health requirements applicable under the Regulation (EU) 2016/425 of the European Parliament and the Council regarding personal protective equipment and applicable standards.

Also, the wind turbines must be equipped with an emergency descent system with a friction braking system, which must meet the essential safety and health requirements mentioned above [26], [28].

Wind turbines must meet the safety and health requirements for workplaces from Directive 89/654/EEC regarding access, working spaces, ventilation, lighting, ergonomic principles, vibrations, Wind turbines must meet the safety and health requirements for workplaces work from Directive 89/654/EEC regarding access, platforms, workspaces, ventilation, lighting, noise and vibrations and principles, respectively the provisions of HG no. 1091/2006 regarding minimum safety and health requirements for the workplace.

Wind turbines must also meet the minimum safety and health requirements regarding the exposure of workers to the risks generated by physical agents - noise provided by Directive 2003/10/EC, respectively HG no. 493/12.04.2006 regarding the minimum safety and health requirements in work related to the exposure of workers to the risks generated by noise [6, 9].

3. EVALUATION OF WORK ACCIDENTS AND OCCUPATIONAL DISEASES

The wind energy industry registers many professional risks identified in each phase of the technological process. From the testing and production of components necessary for wind turbines to the transportation, installation, and maintenance of the turbines, the safety and health risks at the workplace can be quantified in each phase.

Improving the reliability of wind turbine manufacturing technology, transportation, installation, and maintenance directly impacts their safety in use.

Also, improving diagnostic methods through the intelligent use of data can further reduce breakdowns, so as to limit the severity of defects when they occur, which actually leads to a reduction in the duration of maintenance/service interventions and fewer accidents of work, under the conditions of compliance with operational procedures.

The final goal resulting from improvements in the reliability of wind turbine manufacturing technology, as well as transportation, installation and maintenance, leads to operations that become much more efficient and thus reduce the need for workers to be in a dangerous work environment.

The purpose of the research study was to identify and analyze the professional risks generated by the components of the wind farm, taking into account the applicable safety and health requirements, the technical documents that are the basis of their design, operation and maintenance, respectively the OSH management documents and the history of the events generated by them in use.

The research methodology carried out in order to identify and analyze the risks of occupational injury and illness at the wind farm had in mind compliance with:

- the safety and health requirements stipulated by the regulations regarding the safety of cars, in the category of which wind turbines fall;
- the safety and health requirements provided by the regulations regarding low-voltage electrical equipment, in the category of which the electrical part of the wind

turbines and the low-voltage electrical equipment in the power station and substations fall.

- the provisions of the technical regulations for the design and execution of electrical installations (electrical stations, electrical cable networks, etc.);
- the safety and health requirements stipulated by the regulations regarding the work equipment.

As regards the operation and maintenance activity, it must be carried out in safety and health conditions, which ensure compliance with the safety and health requirements provided by the regulations regarding workplaces, considering the permanent safe access (stairs, platforms, anchor points, lighting, etc.) to reach the locations for inspection and maintenance activities and to carry out these activities safely.

Risk assessment involves identifying all risk factors in the analyzed system and quantifying their size based on the combination of two parameters: the severity and frequency of the maximum possible consequence on the human body [15, 16].

The identification of the professional risks generated by the components of the wind farm was carried out taking into account the applicable safety and health requirements, the technical documents that are the basis of their design, operation and maintenance, respectively the OSH management documents and the history of the events generated by them in use, for which applicable security requirements sheets were drawn up in the first phase of the studies.

The operation and maintenance activity must be carried out in safety and health conditions by the safety and health requirements provided by the workplace regulations, with the specifications from the internal documents of integrated management, and those from the organizational forms of work, in the case of electricians.

In establishing the security and health requirements, the aging and fluctuating workforce and, more recently, the integration of workers of other nationalities, especially those who emigrated from Asian countries, into the maintenance teams of Elolian parks were taken into account.

Based on the security and health requirements established for wind turbines, non-conformities were identified with regard to [6, 7].

- The lighting system. Following the visual examination and the technical documents, it was found that the lighting circuit was provided with a single switch located on level 1 of the wind turbine. No other switches were identified on the other levels. Also, the reserve power source with the lighting system ensures 30 minutes of operation.

- Elevator. It was found that the door could open during boarding/descent. Also, no stops were identified at any level of the wind turbine.

- The door of the fence of the "elevator gap." The fence door of the "elevator void." From level x, it was found that it is not equipped with a mechanical lock.

- The anchoring points: It was found that the anchoring points on the upper part of the turbine/nacelle were mounted at a distance of more than 1 m between them, a fact that implies difficulties, especially for the small operating personnel (e.g. for workers originating from Asian countries. Given that at the national level, there is an increase in

the number of workers from Asian countries in the field of construction but also the field of electricity and utility climbing);

- Detection and signalling in case of fire. It was found that the wind tower did not have a fire detection and signalling system.

- The communication system. There was a lack of a communication system with the operating staff in the control room or between the maintenance staff;

- Access. At level x of the turbine, it was found that the space between the turbine wall and the elevator is narrow, forcing the staff to pass (crouch) under the electrical cables.

It was also found that:

- the markings and order labels were in English and other international languages and not in the user's language;

- the warnings regarding the residual risks of the work equipment were in English and other languages of international circulation and not in the language of the user;

- missing emergency number 112 on the information posters regarding providing first aid.

Nonconformities identified in the station and electrical substations [6, 7]:

- the 33 kV electrical cell access doors in all substations were provided with mechanical locking devices, but when they are opened, the installation remains under tension. According to art. 3.3.8 from annexe no. 1 of HG no. 1146/2006, the doors of the high voltage electrical cells must be provided with an optoacoustic voltage warning system in the respective cell [10, 13 - 14].

- several protection conductors connected to the single protection terminal in the low-voltage electrical cabinets (identified H1, F1 and D3);

- protective conductors that were not provided at the ends of the shoes (the area of the cable trunks in substation three and at the internal services in the power station).

The maintenance and upkeep of wind turbines offer challenges regarding safe work, especially in winter conditions and/or with strong winds.

The maintenance operators ensure the proper functioning of the work equipment in the station, substations, and wind turbines and perform specific activities.

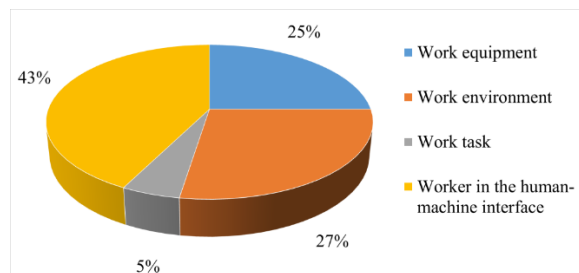


Fig.2. The weight of the identified risk factors on the four elements of the work system for maintenance

Figure 2 shows the weight of the risk factors identified on the four work system elements for the maintenance activity. It was found that the risk factors generated by the

operator in the interface with the work equipment and risk factors generated by the work equipment have the highest weight, 68%.

Figure 3 shows the weight of the risk factors in the interface between the contractor and the work equipment for the activity to be maintained. The contractor has the largest weight in the interface with the work equipment through the wrong actions and omissions due in large part to the residual risks of the equipment for work.

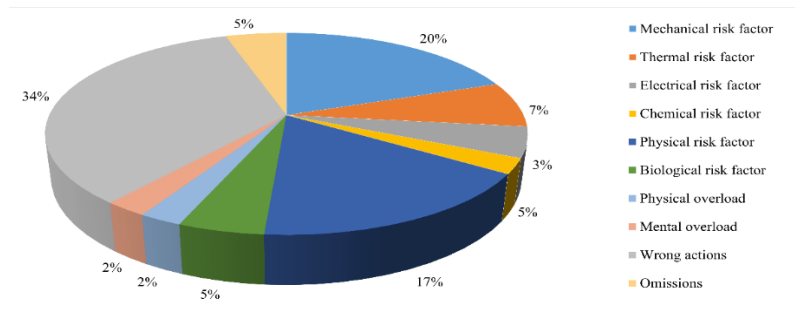


Fig.3. The weight of the risk factors for maintenance

The risk factors generated by work equipment are of a mechanical and thermal nature, such as burns caused by flames or explosions, of an electrical nature, such as contact with live parts, and of a chemical and physical nature, such as noise, and lighting.

The mechanical risk factors are mainly generated by falling from a height due to the specifics of maintenance work at height and the non-conformities identified at the anchoring points and the lift. These factors have been reduced by the security measures proposed and generated by the fall of pieces of ice during the winter from the metal structure of the wind turbine. In the maintenance activity, the chemical risk is generated by working with solvents, degreasing and greasing substances for the rotor, generator, and generator motors, and oil samples from transformers. The chemical risk assessment was carried out using two criteria: the classification of substances from the point of view of danger and, respectively, the quantitative threshold at which the presence of the substance can lead to accidents, the weakening/deterioration of the protective quality of work equipment and protection [17, 18].

The introduction of new digital monitoring production technologies through the implementation of monitoring, control and data acquisition software systems has led to a reduction in risk exposure time, to a decrease in the number of wrong actions and omissions generated by executors. Some of the electrical risks and thermal risks identified during the execution of the manoeuvres in the electrical installations and/or the operations of stopping and de-energizing the work equipment on which maintenance operations are carried out have been eliminated. The implementation of monitoring, control and data acquisition software systems regarding the operating parameters of work equipment has reduced the time to identify defects and exposure to unfavourable work conditions due to the work environment: strong winds and dust, varying temperatures from low to very high and less, lately, of snowfall, due to climate changes.

The new digital technologies are designed to provide a useful tool for assessing the technical condition of wind turbines, to overcome the specific problems of

monitoring, control and data acquisition, and to find a solution that best meets the technical requirements and customers [19].

The data produced from the application of risk analysis can be used to ensure safe equipment and methods of protection and strike a balance between technical and safety needs, dependability, and economic requirements [20].

The research conducted on operational wind turbines has led to the development of a robust methodology. This methodology is designed to effectively identify, assess, and monitor occupational risk factors, particularly those associated with work equipment. It serves as a practical tool for predicting and preventing technical events and work accidents, with a specific focus on the human-equipment interface.

The INCDPM method, a scientifically rigorous approach to assessing the risks of occupational injury and illness at work, played a pivotal role in our research. It allowed us to evaluate the ratio of factors determined by work equipment and other components of the work system. This evaluation focused on the effects on workload, work environment, and the executor, who is the primary interface with the work equipment.

The developed methodology focuses on evaluating the professional risk factors determined by the work equipment, their effects on the work environment, and the activity carried out by the operator.

Their implementation's opportunity, aim and necessity resulted from the present occupational safety and health (OSH) law requirements. [21].

The research carried out highlighted the need to evaluate the conformity in the use of this category of work equipment, considering the high level of work accidents recorded in the energy sector, taking into account the new digital technologies used at the European level, respectively safety devices, safety tools access and control equipment, which make the work safer, such as the drones used when inspecting a wind turbine. This solution eliminates the need to climb the wind turbine.

The studies highlighted the need to evaluate the level of noise generated by the wind turbines to determine the risks for the workers exposed in the activities carried out, respectively, the population in the areas where these wind farms are located.

Another aspect resulting from the research studies carried out refers to the need to develop standards of professional training, improvement, and training of workers in this sector, mainly from the operation and maintenance services, where a large number of accidents are recorded.

Professional training is an important element in reducing costs and professional risks in the wind sector to ensure a safe and healthy work environment. It must be adapted to consider the risks specific to the wind sector and new risks that may appear determined by the introduction of digital technologies.

5. CONCLUSIONS

Risk assessment, based on the principles established by Directive 2006/42/EC, Directive 2009/104/EC, and the applicable security standards, is essential to prevent dangers and guarantee the safety of work equipment in use, considering the new technological challenges regarding digitization.

The research resulted in the identification of new approaches regarding the assessment of occupational risks at the workplace, determined by the introduction of new digital technologies. It also highlighted the need to comply with and certify the fulfilment of the safety and health requirements applicable to this category of work equipment, both from the point of view of the use as well as of the preparation and training of the serving personnel.

Following the results of the analysis of the causative factors of the production of electric arcs, the diagnosis of the existing protection measures in use corroborated with the established technical and security requirements; it was found the need to develop a specific methodology for the evaluation and control of the risks and dangers generated by the electric arc in the installations electrical.

The research studies carried out aimed at evaluating and eliminating the risks that can lead to the occurrence of technological or human events and identified the need to develop new technical diagnostic tools for work equipment, as well as through new professional training methods in the wind energy sector that taking into account all technological operations from manufacturing, construction per wind farm location, use and maintenance of this category of machines, in the digitization decade.

The tools to be developed will be made available to companies to increase their market competitiveness and ensure a high level of safety for the people who carry out these activities in the wind energy sector.

REFERENCES

- [1]. <https://www.mmediu.ro/categorie/pnisc-revizuit/467> The National Integrated Plan in the Field of Energy and Climate Change 2021-2030-revised.
- [2]. <https://energie.gov.ro/2023-un-an-bun-pentru-investitiile-in-sectorul-energetic-in-romania-2024-se-anunta-si-mai-bun/>
- [3]. <https://www.transelectrica.ro/ro/web/tel/productie>, "The situation of installed capacity at the SEN level as of 01.04.2024"
- [4]. <https://www.sistemulenergetic.ro/>
- [5]. https://www.transelectrica.ro/widget/web/tel/sen-grafic/-/SENGrafic_WAR_SENGraficportlet
- [6]. INCDPM, Contract no. 1201, *Accident risk assessment services in the Wind Park*, 2010.
- [7]. INCDPM, *Study on the identification of occupational hazards in electrical installations in order to ensure the safety and health of workers for 35 workplaces*, 2021.
- [8]. INCDPM, *Project POC Partnership for the transfer of knowledge and the development of research related to the assessment and prevention of occupational risks that can lead to disasters (PROC)*, ID/Cod SMIS 2014+: POC P_40_182/111954, 2022-2023.
- [9]. Antonov A.E., Buica G., Beiu C., Remus D., *Risk assessment of work equipment in use - principle of compliance with the requirements of Directive 2009/104/EC*, 8th Edition International Symposium on Occupational Health and Safety Bucharest, Romania, 2017.
- [10]. INCDPM, *Guide for the application of GD No.1146/2006 regarding the minimum safety and health requirements for the use of work equipment by workers (in Romanian)*, National Institute of Research and Development for Occupational Safety Alexandru Darabont, Bucharest, Romania. Available on : <http://www.inpm.ro/files/publicatii/2013-05.01-ghid-t.pdf>, 2013.
- [11]. GD nr. 409/2016 - *Laying down the conditions for making available on the market of low-voltage electrical equipment*, 2016.

- [12]. *Directive 2014/35/UE on the harmonisation of the laws of the Member States relating to the making available on the market of electrical equipment designed for use within certain voltage limits (recast)*, 2014.
- [13]. *GD 1146/2006 concerning the minimum safety and health requirements for the use of work equipment by workers at work*, 2006.
- [14]. *Directive 89/655/CEE concerning the minimum safety and health requirements for the use of work equipment by workers at work*, 1989.
- [15]. **Pece S.**, *Risk assessment in work system*, Rubin, Bucharest, pp. 170-226, 2010.
- [16]. **G. Buică**, *Contributions of diagnostic methods of safety and health at work in electrical installations*, PhD Thesis, Universitas Petroșani, pp.70 – 149, 2010.
- [17]. **Petrilean D.C.**, *The study of Energy Losses through Case Helical Screw Compressor*, Bulletin of the Transilvania University of Brasov, Proceedings of the internationally attended national conference on thermodynamics, 2009.
- [18]. **Andras A., Popescu F.D., Radu S.M., Pasculescu D., Brinas I., Radu M.A., Peagu D.**, *Numerical Simulation and Modeling of Mechano–Electro–Thermal Behavior of Electrical Contact Using COMSOL Multiphysics*. Applied Sciences, 14(10):4026, 2024.
- [19]. **Leba M., Ionica A., Dobra R., Pasculescu V.M.**, *Quality function deployment (QFD) based expert system for renewable energy structures. A wind turbine case study*, Environmental Engineering and Management Journal, 3 (6), pp. 1365 – 1369, 2014.
- [20]. **Leba M., Ionica A., R. Dovleac, Dobra R.**, *Waste Management System for Batteries Sustainability*, Sustainability, 10 (2), 332, 2018. <https://www.mdpi.com/2071-1050/10/2/332>.
- [21]. **R. M. Iordache, D. Mihăilă, D. C, Darabont, V. Petreanu**, *Analysis of mental effort and its subjective and psychophysiological indicators for gas transport dispatchers*, Human Systems Management, 42(3), pp. 1-9, 2022.
- [22]. **Handra A.D., Popescu F.G., Păsculescu D.**, *Utilizarea energiei electrice: lucrări de laborator*, Editura Universitas, 2020.
- [23]. **Fîță N.D., Radu S.M., Păsculescu D., Popescu F.G.**, *Using the primary energetic resources or electrical energy as a possible energetical tool or pressure tool*, In International conference KNOWLEDGE-BASED ORGANIZATION, vol. 27, no. 3, pp. 21-26. 2021.
- [24]. **Popescu F.G., Păsculescu D., Păsculescu V.M.**, *Modern methods for analysis and reduction of current and voltage harmonics*, LAP LAMBERT Academic Publishing, ISBN 978-620-0-56941-7, pp. 233, 2020.
- [25]. **Păsculescu D., Romanescu A., Păsculescu V., Tătar A., Fotău I., Vajai Gh.**, *Presentation and simulation of a modern distance protection from the national energy system*, 10th International Conference on Environment and Electrical Engineering, pp. 1-4. IEEE, 2011.
- [26]. **Pasculescu D., Dobra R., Ahmad M.A.**, *Dosimetric Quantity System for Electromagnetic Fields Bio-effects*, International Journal of Scientific Research (IJSR) 5, no. 2, pp. 28-32, 2016.
- [27]. **Dobra R., Buica G., Pasculescu D., Leba M.**, *Safety management diagnostic method regarding work cost accidents from electrical power installations*. Proc. 1st Int. Conf. on Industrial and Manufacturing Technologies (INMAT), Vouliagmeni, Athens, Greece. 2013.
- [28]. **Petrilean D.C.**, *Mathematical model for the determination of the non-stationary coefficient of heat transfer in mine works*, The 19th American Conference on Applied Mathematics (AMERICAN-MATH '13), Cambridge, MA, USA.2013.

This article was reviewed and accepted for presentation and publication within the 11th edition of the International Multidisciplinary Symposium "UNIVERSITARIA SIMPRO 2024".

ASPECTS REGARDING THE USAGE OF THE HIGH VOLTAGE IMPULSE GENERATOR IN ORDER TO VERIFY THE INSULATION SYSTEMS OF ELECTRIC MOTORS USED IN POTENTIALLY EXPLOSIVE ATMOSPHERE

DRAGOȘ FOTĂU¹, MARCEL RAD², DIANA SĂLĂȘAN³, VALENTIN SÎRBU⁴

Abstract: The purpose of this paper is to present the importance of the specific tests for electric motors with type of protection increased safety „e” designed to be used in explosive atmosphere. This paper presents the voltage impulse ignition test applicable to electric motors with increased safety protection type.

Due to the fact that electric motors with type of protection Increased Safety, whose supply voltage exceeds 1000 V, presents a high risk of sparks occurring in windings, it is necessary to perform tests to verify that the insulation of the windings is adequate and does not lead to electric discharge (through electric springs or sparks) at winding levels. Evaluation of explosion-proof protected electrical equipment in scope of certification is extremely important considering the risk of explosion that has to be minimized in order to ensure life safety and health of workers and to prevent damaging of property and the environment, as well as free movement of goods when they meet the essential safety requirements at European level.

The standard SR EN 60079-0 (Explosive atmospheres Part 0: General requirements) and one or more of the standards containing the specific requirements for the type(s) of protection applied to equipment (ex. SR EN 60079-7 for the type of protection increased safety "e"), are used to perform the assessment.

Key words: electrical equipment, increased safety, explosive atmosphere.

1. INTRODUCTION

Explosive atmospheres are defined as a mixture with air, under atmospheric conditions, of flammable substances in the form of flammable gases, mist vapors or combustible dusts, in which, after ignition, combustion is spread throughout the unburned mixture. To generate an explosive atmosphere, the flammable substance

¹ Ph.D., Eng., INSEMEX Petroșani, dragos.fotau@insemex.ro

² Ph.D., Eng.

³ Ph.D., Eng.

⁴ Ph.D., Eng.

must be present in certain concentrations, between the lower explosive limit (lel) and upper explosive limit (uel). Explosion limits of the substance may depend on pressure, oxygen concentration in the air and temperature. The mechanism of an explosion generated by a mixture of flammable gas, vapor or mist with air can be expressed by the well-known explosion triangle [8], [10], [12], [14]. Thus, the occurrence of an explosion is conditioned by the simultaneous presence of the following three factors:

1. fuel (flammable gases, vapours, mists);
2. oxygen (oxygen, oxidizing substances);
3. efficient ignition source for ensuring the activation of molecules in order to ignite and propagate the fast combustion reaction [4], [9], [11], [13], [15], [17].

Using electric equipment in potentially explosive atmospheres brings forward several particularities therefore the problems that appear during the design, construction and operation of electrical devices and installations brings forward numerous difficulties, their approach requiring special attention considering all the technical, economical and labor safety aspects. Due to this fact, it is very important that the equipment is properly tested during the certification process [5], [16], [19], [21].

Even if electric motors for explosive atmospheres are designed and manufactured following some of the same principles as the ones used for other electric machinery, they have certain particularities related to their field of use. Thus, a series of specific restrictions and tests are required to be considered in their case.

The risk of explosion may appear in all the fields of activity in which flammable substances are involved, such as gases, vapours, dusts, mists, which mixed with air may result in potentially explosive atmospheres [6], [18], [20], [22], [27].

To prevent the ignition of explosive atmospheres, the electrical equipment used in such areas must be made with different types of protection so that it can not ignite the explosive mixture surrounding the electrical equipment [1], [4], [31].

The type of protection means the specific measures applied to electrical equipment to avoid ignition of a surrounding explosive atmosphere [2], [23], [25], [28].

For each type of protection applied to electrical equipment used in potentially explosive atmosphere, a wide range of type tests have been developed so that they can be used safely [2], [32].

In order to verify explosion protection, the representative samples made available by explosion-protected equipment manufacturers are tested under the most unfavorable conditions that may occur in operation [4], [6], [33].

Most of the equipment used in technical installations in potentially explosive atmospheres (refineries, fuel depots, gas stations, dyestuffs, etc.) are electric motors, which in most situations act on various other elements [4], [24], [26], [30].

2. ELECTRICAL TESTS CARRIED OUT ON ELECTRIC MOTORS WITH TYPE OF PROTECTION INCREASED SAFETY

Explosion-proof characteristics of electrical equipment, are assessed mainly according the provisions of harmonized standards from the SR EN 60079 series. The standards SR EN 60079-0 and one or more of the standards containing the specific

ASPECTS REGARDING THE USAGE OF THE HIGH VOLTAGE IMPULSE GENERATOR IN ORDER TO VERIFY THE INSULATION SYSTEMS OF ELECTRIC MOTORS USED IN POTENTIALLY EXPLOSIVE ATMOSPHERE

requirements for the type(s) of protection applied to equipment (also from the SR EN 60079 series) are used for performing the assessment [2].

Most of the equipment operating in potentially explosive atmospheres (chemical compounds, refineries, fuel depots, dyestuffs, etc.) are electric motors, which in most situations act on various other elements (pumps, vibrating sites, conveyors, etc.).

The "e" increased safety type of protection implies equipment that does not produce electric arcs, sparks or excessive temperatures on any of the interior or exterior parts of the equipment, because of that it is necessary that these phenomena to be avoided.

Electrical equipment and Ex Components of type of protection increased safety "e" are either: Level of Protection "eb" (EPL 'Mb' or 'Gb'); or Level of Protection "ec" (EPL 'Gc') [3]

Level of Protection "eb" applies to connections, conductors, windings, lamps, and batteries; but not including semiconductors or electrolytic capacitors [3].

Level of protection "ec" applies to connections, conductors, windings, lamps, and batteries; including semiconductors or electrolytic capacitors.

Electric motors with type of protection increased safety usually works in zone 1, when the electric motor is stopped, inside the casing explosive mixture may enter. When starting the motor, overvoltage can be generated, much higher than the nominal voltage, and if windings are not properly insulated, sparking may occur between windings.

According to standardized requirements, in addition to the tests specified by SR EN 60079-0, the electric motors with type of protection increased safety are subject to additional specific tests (for electric motors) as specified in SR EN 60079-7: [3]

- a) Determination of starting current ratio I_A / I_N and the time t_E
- b) Mounting of machine for test
- c) Stator winding insulation system (impulse ignition test for "eb" stator insulation systems and steady state ignition test for "eb" and "ec" stator insulation systems)

Because electric motors with increased safety type of protection (eb), whose supply voltage exceeds 1000 V, pose a high risk of sparks occurring in windings (due to the choice of an inadequate method of winding insulation), it is necessary to perform tests to verify that winding insulation is adequate and does not lead to electric discharge (by electric arcs or sparks) at winding levels [6], [29].

This sparking risk in the winding occurs at weak insulation spots when the charge in the weak spot becomes too high. This weak spot is excessively stressed during the operation of the electric motor or during the high-voltage test. This weak spot cannot resist this increased stress. As a result there is a partial breakdown in this location. This partial breakdown is referred to as partial discharge. However, the remaining insulation can still resist the increased voltage stress so that there is not a complete breakdown [7].

The tests by which these aspects are tested are the impulse ignition test and the overvoltage-ignition test, applicable to electric motors with type of protection increased safety [3].

Insulation systems and connecting cables shall be tested in an explosive test mixture as presented in Table 1. They shall be subjected to 10 voltage impulses of not less than three times peak phase to earth voltage and with a voltage rise time between 0,2 μ s and 0,5 μ s and with a time to half value which is at least. No ignition of the explosive test mixture shall occur [3].

Table 1. Explosion test mixtures

Equipment group	Test mixture in air v/v
II C	(21 \pm 5) % hydrogen
II B	(7,8 \pm 1) % ethylene
II A	(5,25 \pm 0,5) % propane

In the National Institute for Research and Development in Mine Safety and Protection to Explosion – laboratories were performed impulse ignition test for stator insulation systems on electric motors used in potentially explosive atmosphere. To carry out these tests were used specific testing equipment like: Oxygen analyser SERVOMEX 2200, Baker (Megger) Fig. 1, surge tester D12R, PP24 -impulse generator. The tests were carried out with an explosive mixture whose characteristics correspond to the requirements (concentration-22% hydrogen, test temperature - 22°C) [6].

Pre-start purge may be adopted for Ex e, N or n motors at risk of incendive sparking, and is designed to purge clean air through the motor enclosure to remove any residual potentially flammable gas. Its purpose is to prevent the risk of explosions due to rotor sparking during starting; air flow sensors and pre-start timers may monitor this purge process before allowing the application of the HV electrical supply, or control may be achieved by procedures. Once the motor is started, no further pre-purge flow is provided.

A suitable purge connection point should be provided by the manufacturer. The purge gas supply is provided by the user, from a fixed supply or from portable gas bottles. (Nitrogen is sometimes used instead of using clean air) [6].

Ignition risks owing to stator sparking may also occur when the motor is running; this phenomenon has only been acknowledged relatively recently. Note that pre-start purge does not offer any protection, but suitable special measure might be to pressurise the motor enclosure continuously in order to prevent the ingress of a potentially flammable atmosphere; this arrangement should be interlocked with pre-start and post shut-down timers and pressure/flow measurement, but may not fully comply with the standard for Ex p apparatus[7].

After performing the test in explosive mixtures, it turned out that the windings of the motor correspond to the requirements of the type of protection increased safety.

ASPECTS REGARDING THE USAGE OF THE HIGH VOLTAGE IMPULSE GENERATOR
IN ORDER TO VERIFY THE INSULATION SYSTEMS OF ELECTRIC MOTORS USED IN
POTENTIALLY EXPLOSIVE ATMOSPHERE



Fig.1. High voltage pulse generator



Fig.2. Electric motor windings prepared to be tester in explosive mixtures



Fig.3. High voltage pulse generator display

5. CONCLUSIONS

Medium voltage electric motors with increased safety type of protection present a fairly high risk of explosion, also because of the sparking phenomenon that can occur in the stator windings (including partial discharges). These phenomena shall

be avoided by the construction of the motor and especially of the insulation system of the stator winding.

Motors with type of protection increased safety “eb” can work in zone 1, and when the motor is stopped, inside the housing explosive mixture may enter. When starting the motor, overvoltage can be generated, much higher than the rated voltage, and if windings are not properly insulated, sparking may occur. For this reason it is important that the motors are tested in accordance with the requirements in force.

To prevent the risk of explosions, due to rotor sparking during starting, the motor can be purge with clean air or with a gas which is not explosive as it is done on the pressurised electric motors.

Motors with type of protection increased safety “eb” can work in zone 1, and when the motor is stopped, inside the housing explosive mixture may enter. When starting the motor, overvoltage can be generated, much higher than the rated voltage, and if windings are not properly insulated, sparking may occur. For this reason it is important that the motors are tested in accordance with the requirements in force.

To prevent the risk of explosions due to rotor sparking during starting the motor can be purge with clean air or with a gas which is not explosive as it is done on the pressurised electric motors.

In this paper was revealed the importance of the tests carried out on electric motors used in potentially explosive atmosphere and the aspects that should be considered when starting the motors. With the high voltage pulse generator we can perform more accurate tests, in explosive mixtures.

In order to protect people who work in explosive environments, it is important that equipment operating in such areas to comply with the requirements in force, and be properly maintained by personnel who know the principles of explosion protection.

REFERENCES

- [1]. Directive 2014/34/EU of the European Parliament and of the Council of 26 February 2014 on the harmonization of the laws of the Member States relating to equipment and protective systems intended for use in potentially explosive atmospheres (recast) Text with EEA relevance, 2014.
- [2]. Standard IEC 60079-0 - *Explosive atmospheres - Part 0: General requirements*, 2018.
- [3]. Standard IEC 60079-7 - *Explosive atmospheres - Part 7: Equipment protection by increased safety "e"*, 2016.
- [4]. **Fotău D.**, *Researches regarding the increase of operational safety of electrical-mechanical equipment used in potentially explosive atmospheres*, Doctoral thesis, University of Petroșani, Romania, 2016.
- [5]. **Ghicioi. E., Gaman. G., Vlasin. N., Păsculescu. V., Gabor. D.**, *Prevention of accidental pollution with combustion gases after the occurrence of explosion*, Environmental Engineering and Management Journal, Romania, vol. 16, pp 1289-1294, 2017.
- [6]. *Partial discharge test to evaluate windings of low-voltage electric motors with regard to frequency converter capability as well as general insulation strength, Partial discharge brochure.*

ASPECTS REGARDING THE USAGE OF THE HIGH VOLTAGE IMPULSE GENERATOR
IN ORDER TO VERIFY THE INSULATION SYSTEMS OF ELECTRIC MOTORS USED IN
POTENTIALLY EXPLOSIVE ATMOSPHERE

- [7]. <http://www.hse.gov.uk/offshore/infosheets/is3-2010.htm>
- [8]. **Handra A.D., Popescu F.G., Păsculescu D.,** *Utilizarea energiei electrice: lucrări de laborator*, Editura Universitas, 2020.
- [9]. **Fîță N.D., Radu S.M., Păsculescu D., Popescu F.G.,** *Using the primary energetic resources or electrical energy as a possible energetical tool or pressure tool*, In International conference KNOWLEDGE-BASED ORGANIZATION, vol. 27, no. 3, pp. 21-26. 2021.
- [10]. **Lazar T., Marcu M.D., Utu I., Popescu F. G., Păsculescu D.,** *Mașini electrice - culegere de probleme*, Editura Universitas, Petroșani, pp. 197, 2023.
- [11]. **Csaszar T., Păsculescu D., Darie M., Ionescu J., Burian S.,** *Method for assessing energy limited supply sources, designed for use in potentially explosive atmospheres*, Environmental Engineering and Management Journal 11, no. 7, 1281-1285, 2012.
- [12]. **Marcu M., Niculescu T., Slusariuc R. I., Popescu, F. G.,** *Modeling and simulation of temperature effect in polycrystalline silicon PV cells*, IOP Conference Series: Materials Science and Engineering, Vol. 133, No. 1, pp. 012005, 2016.
- [13]. **Popescu F.G., Arad S., Marcu M.D., Pana L.,** *Reducing energy consumption by modernizing drives of high capacity equipment used to extract lignite*, Papers SGEM2013/Conference Proceedings, Vol. Energy and clean technologies, pp. 183 - 190, Albena., Bulgaria, 2013.
- [14]. **Păsculescu D., Romanescu A., Păsculescu V., Tătar A., Fotău I., Vajai Gh.,** *Presentation and simulation of a modern distance protection from the national energy system*, 10th International Conference on Environment and Electrical Engineering, pp. 1-4. IEEE, 2011.
- [15]. **Păsculescu D., Dobra R., Ahmad M.A.,** *Dosimetric Quantity System for Electromagnetic Fields Bio-effects*, International Journal of Scientific Research (IJSR) 5, no. 2, pp. 28-32, 2016.
- [16]. **Popescu F.G., Păsculescu D., Păsculescu V.M.,** *Modern methods for analysis and reduction of current and voltage harmonics*, LAP LAMBERT Academic Publishing, ISBN 978-620-0-56941-7, pp. 233, 2020.
- [17]. **Păsculescu D., Niculescu T.,** *Study of transient inductive-capacitive circuits using data acquisition systems.* International Multidisciplinary Scientific GeoConference: SGEM 2, no. 1, 323-329, 2015.
- [18]. **Pana L., Janusz G., Păsculescu D., Păsculescu V. M., Moraru R. I.,** *Optimal quality management algorithm for assessing the usage capacity level of mining transformers*, Polish Journal of Management Studies 18, no. 2, 233-244, 2018.
- [19]. **Dobra R., Buica G., Păsculescu D., Leba M.,** *Safety management diagnostic method regarding work cost accidents from electrical power installations.* Proc. 1st Int. Conf. on Industrial and Manufacturing Technologies (INMAT), Vouliagmeni, Athens, Greece. 2013.
- [20]. **Andras A., Popescu F.D., Radu S.M., Păsculescu D., Brinas I., Radu M.A., Peagu D.,** *Numerical Simulation and modeling of mechano-electro-thermal behavior of electrical contact using comsol multiphysics.* Applied Sciences, 14(10), 4026, 2024.
- [21]. **Stepanescu, S., Rehtanz, C., Arad, S., Fotau, I., Marcu, M., Popescu, F.** *Implementation of small water power plants regarding future virtual power plants* 10th International Conference on Environment and Electrical Engineering, pp. 1-4, IEEE, 2011.

- [22]. **Fîță N. D., Lazăr T., Popescu F. G., Pasculescu D., Pupăză C., Grigorie E.**, *400 kV power substation fire and explosion hazard assessment to prevent a power black-out*, International Conference on Electrical, Computer Communications and Mechatronics Engineering-ICECCME, pp. 16-18, 2022.
- [23]. **Fita N.D., Obretenova M.I., Pasculescu D., Tatar A., Popescu F.G., Lazar T.**, *Structure and analysis of the power subsector within the national energy sector on ensuring and stability of energy security*, Annals of „Constantin Brâncuși” University of Târgu Jiu, ENGINEERING SERIES, Issue 2/2022, pp.177-186, 2022.
- [24]. **Petrilean, D. C. ;Irimie, S. I.**, *Solutions for the capitalisation of the energetic potential of sludge collected in Danutoni wastewater treatment plant*, Journal of Environmental Protection and Ecology, Vol.16 No.3 pp.1203-1211, 2015.
- [25]. **Petrilean D.C.**, *Elaborating and Analysing the Real Balance of Heat for the Steam Generator RGL 10/DD* Annals of the University of Petrosani, Mechanical Engineering, Volume 10, 155-160, 2008.
- [26]. **Petrilean, D.C., Preda, L., Marinescu, D.C.**, *Real and optimum exergetic balance sheet of helical screw compressor ATLAS COPCO GA 30 CF to reduce energy consumption*, 15th International Multidisciplinary Scientific, GeoConference SGEM 2015, SGEM2015 Conference Proceedings, June 18-24, Book 4, pp. 425-432, Albena, Bulgaria, 2015.
- [27]. **Petrilean D.C., Stanilă S., Dosa I.**, *A mathematical model for determining the dimensionless heat flux with application in mine environment*, Environmental Engineering and Management Journal, Vol.16, No. 6, 1249-1414, 2017.
- [28]. **Petrilean D.C., Stănilă S., Irimie S.I.**, *Study of variable heat exchange between a thickness limited cylindrical pipe and the rock massif for application in mine environment*, Environmental Engineering and Management Journal June 2014, Vol.13, No. 6, 1523-1531.
- [29]. **Irimie S.I., Dan Codruț Petrilean D.C.**, *Environmental Impact Assessment for Dismantling an Energetic Complex Using Thermodynamic Concepts*, 9th International Conference on ENERGY, ENVIRONMENT, ECOSYSTEMS and SUSTAINABLE DEVELOPMENT" (EEESD '13), Lemesos, Cyprus, March 21-23, pp. 76-81, 2013.
- [30]. **Petrilean D.C.**, *Compresoare eliciodale*, Editura Tehnica-Info, 2006
- [31]. **Petrilean D.C.**, *Termodinamica tehnica si masini termice*, Editura A.G.I.R., 2010.
- [32]. **Vasilescu G.D., Petrilean C.D., Kovacs A., Vasilescu G.V., Pasculescu D., Ilcea G.I., Burduhos-Nergis D.P., Bejinariu C.**, *Methodology for assessing the degree of occupational safety specific to hydrotechnical construction activities, in order to increase their sustainability*, Sustainability, Jan 21;13(3):1105, 2021.
- [33]. **Petrilean D. C.**, *Transmiterea căldurii*, Editura Universitas, 2016.

This article was reviewed and accepted for presentation and publication within the 11th edition of the International Multidisciplinary Symposium "UNIVERSITARIA SIMPRO 2024".

THE MODERN TECHNOLOGY IMPLEMENTATION FOR SAFE ENERGY TRANSITION

MARIA DANIELA STOCHITOIU¹, ILIE UTU²

Abstract: The role of electrical energy becomes more important with the progress in transitioning towards clean energy and thus increases the importance of electric power networks for society and economy. The need of electrification and of renewable sources is growing. The risk that can appear is that the transition to clean energy may stagnate if the networks are not sufficiently updated for connecting the new supplies of electricity on consumer demand. This paper emphasises the theoretical aspects and the importance of the static power-electronic devices installed in AC transmission (where static synchronous series compensator SSSC device is considered as one of the active power control facilities) as an essential features to avoid technical problems in the power networks, for increasing the transmission capacity and assuring efficiently the stability of the system.

Key words: active power control, series compensator, voltage compensation.

1. INTRODUCTION

The electric network is the main element of energetic systems, sustaining the economic activity through supplying necessary electrical energy to domestic, commercial and industrial customers. As the transition to clean energy advances, the role of electrical energy is increasing, and the energy systems becomes more important. With wider use of electrification and of renewable sources, the development of electric transmission network has a major role in mitigating the risks that may affect transition to clean energy [1], [2].

The electrical network is characterized by:

- grid infrastructure;
- interruptions costs;
- network congestions;
- output diminution;
- contraction of network development deadlines.

It has been noticed that sometimes the networks become an obstacle in transition phase to clean energy and there are risks arising if the development and

¹ Ph.D., Associate Prof. Eng., University of Petroșani, danielastochitoiu@upet.ro

² Ph.D., Associate Prof. Eng., University of Petroșani, ilieutu@yahoo.com

improvements of network are not advancing fast enough. A delayed reform of the electrical network means extending dependence to fossil fuel and determine increase of gases emissions and , in the long run, increased costs to society.

The electric network is major infrastructure element including a lot of components with a high-tech degree of complexity. To understand the present state of network development is not easy due to the difficulties of data availability even with the infrastructure and the technology currently used in their operation and management.

The total length of electrical networks infrastructure has been constantly growing in the last fifty years. The fast growth of use of variable renewable sources and distributed sources creates new challenges and require a large flexibility for electric networks. In the emerging markets and developing economies, significant progress has been made by increasing access to electricity at the same time with the growing demand. The supply chain for the distribution networks has already presented constrains, which generate possible risks for the future of network development.

The flexible AC transmission system (FACTS) provides an important role in the increase of the level of implementation of renewable energy resources, making possible continuous control of active and reactive power in the network [3].

Static Synchronous Series Compensator represents the scheme of series compensation which uses a power converter as synchronous voltage source (SVC) to supply a controllable voltage phased forward in quadrature of current. The SSSC includes a synchronous voltage source (SVS) connected to power network through a transformer. This transformer is connected in series with the transmission line, as the SSSC represents an improvement from compensation based on using series line capacitors. This is an advantageous because when using SSSC the serial compensation becomes independent of the line current.

2. IDENTIFY THE DIFFERENCES AS PATH TO THE FUTURE NETWORKS

In order to be a reliable instrument that enables a safe energetic transition, they networks must fulfil three conditions: to be low maintenance, to be up to date and to answer to the future needs of the energetic system.

The growth of electrical energy demand represents one of the three key factors in driving network expansion in all counties together with the growth of renewable sources and replacement of the obsolete components of the networks [3], [4]. The growth in energy demand is also dependent of some factors such as growing number of people as well as earnings and economy growth. These lead to increasing the use of electrical energy in traditional applications, for example heating and colling devices, communications and industrial applications. In addition, new applications of electricity are evolving rapidly, like for example transportation (electric vehicles), heating (electric heat pumps) and hydrogen production (electrolyze).

Modernization is further made based on a list of criteria analysis which includes technical stage, age, importance, perspective of implementation of telecontrol in conjunction with maintenance work on power transmission networks [5], [1]:

- interconnection with neighbouring power networks;
- zonal system connections or between main power stations;
- release of power from main power plants;
- supplying important consumption areas.

Regarding the implementation of modern technologies in power transmission network, a National Project refers to installation a SSSC device in the 220kV axis Urechesi -Târgu Jiu Nord - Pârâşeni – Baru Mare – Hasdat [6], [5].

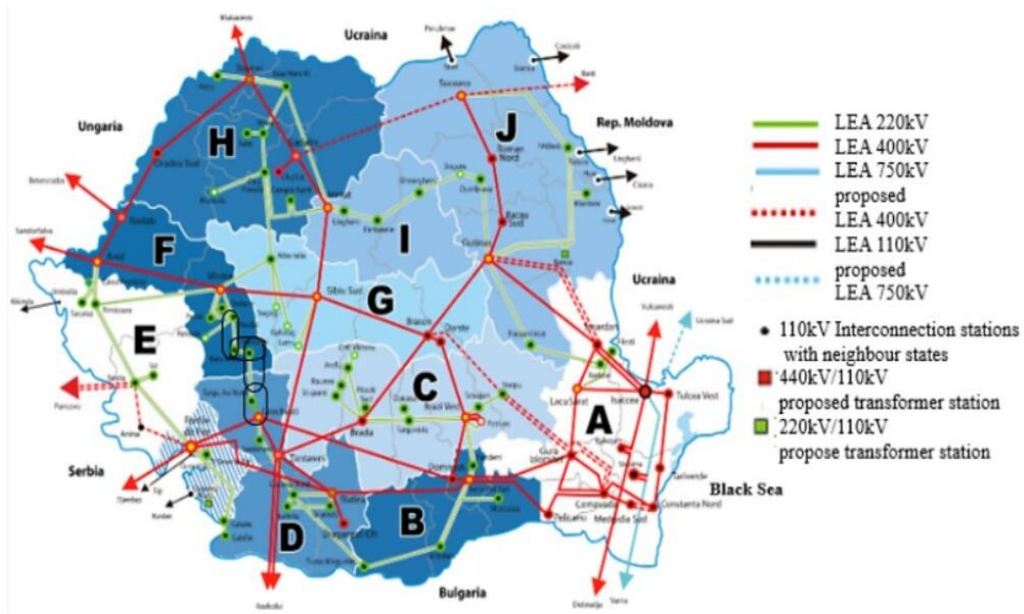


Fig. 1. The available capacity for transmission network connection and possibility of SSSC implementation; Source: www.transelectrica.ro

2.1. Static synchronous series compensator

The SSSC device consists a synchronous voltage source in series transmission line using a transformer between m , n nodes. For supplying the storage capacitor and for power compensation a power source is necessary in the inverter. Taking into account that the longitudinal resistance and the transversal admittance are negligible, the lines reactance is considered (X_{l1} , X_{l2}).

Parameters P_{ref} and Q_{ref} control the amplitude VSSSC of the voltage supplied at the output of VSC that is necessary for exchange of the reactive and active power with the power grid. The P_{ref} will be set to zero value if the VSC is used only for exchange of reactive power [7], [1]. Since VSC is used for series compensation and runs only for established fundamental frequency, the sub-synchronous resonance is avoided because the impedance for different frequencies will be practical zero. This feature of the SSSC sets it apart of series capacitor method whose impedance is depending on frequency and can generate resonances for various reactive impedances from the power network.

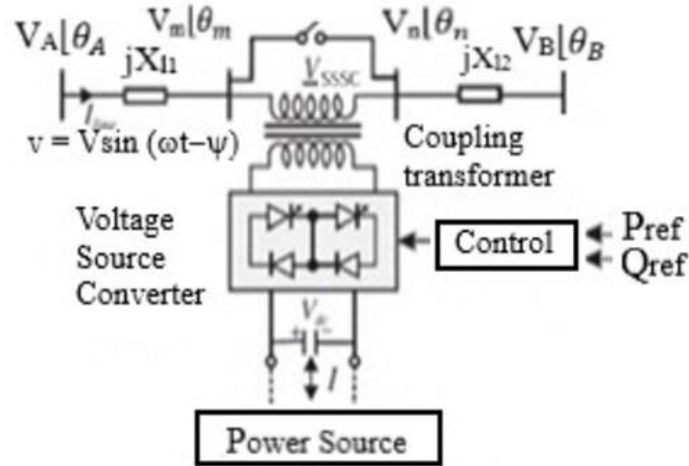


Fig. 2. Components structure of SSSC

2.2. The operation structure

Up to its designated voltage rating, the SSSC can deliver capacitive or inductive compensatory voltage independent of line current because of the independent voltage source characteristic of the VSC. The two operating modes are: voltage compensation and reactance compensation [7], [3].

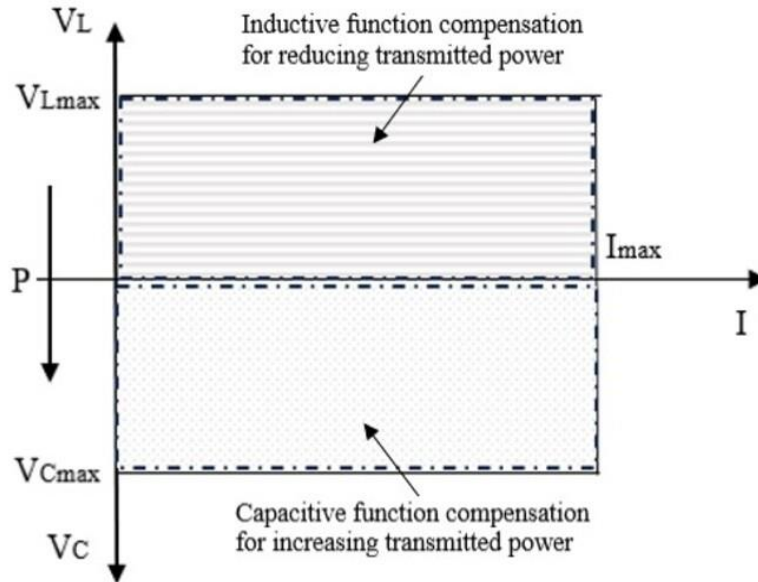


Fig. 3. Design of dependence compensation voltage and line current

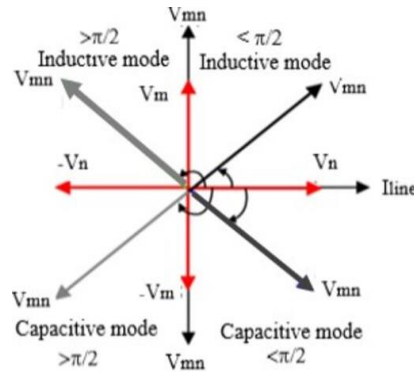


Fig. 4. Types of SSSC operating

If there is no difference of quadrature between the phase of injected voltage (V_{mn}) and the line current I_{line} , an exchange of real power between the SSSC and line will appear. Replacing the DC Capacitor from the input with an energy storage solution the real power exchange is assured. The above figure explains that SSSC can operate in all four quadrants to supply active power and to provide reactive power compensation to the ac system [8].

An ideal synchronous generator which can supply a set of three sinusoidal voltages at fundamental frequency can be replaced with Voltage Source Converter (VSC) as a synchronous voltage source. This component can supply or absorb reactive power when is connected to power network same as a synchronous compensator.

The VSC also can exchange active power with power system when is connected to a corresponding energy source or to an energy storage battery. The transmitted power is depending on supplied voltage through controlling the complex argument of the voltage, the SSSC can exchange even active power or reactive power with the power network where is connected [3], [7], [9].

The transformer located on the secondary side can be connected in triangle or star, while the primary windings are connected in series on the transmission lines. The reference values of P_{ref} and Q_{ref} are representing the imposed values of power controlled by SSSC device.

Using a three phase VSC for SSSC has the advantage that there is a lower number of semiconductors necessary. There is a disadvantage with respect of the output voltages and their harmonics if the reference voltages are unbalanced.

The currents through semiconductors devices for triangle connection are multiplied 1.73 times when the transformer is in star connection but the compensation voltage through transformer in star connection is divided by 1.73.

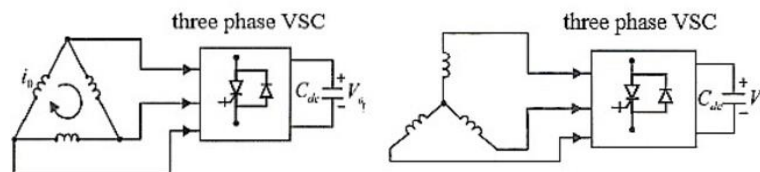


Fig. 5. Triangle and star connection of VSC transformer

3. COMPARATION BETWEEN SERIES CAPACITORS COMPENSATION AND SSSC

In comparison with series capacitor, the SSSC device is more efficient respect to control of power circulation and improved stability [8], [10], [11].

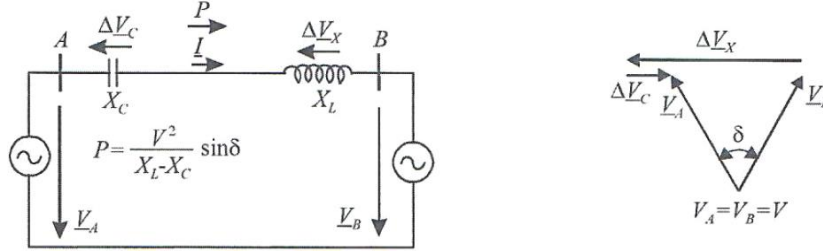


Fig. 6. Basic compensation using series capacitors

Where: ΔV_C – represents the phasor of the compensation voltage produced when the current passes the capacitor and the compensation voltage is proportional with the I line, but the opposite polarity as inductive drop voltage;

$X_L = X_{L1} + X_{L2}$ – represents the line inductive reactance;

X_C – represents the capacitor reactance, producing the same compensation effect as synchronous voltage source;

Series capacitor compensation assures an indirectly reduction of equivalent line impedance and increases the line transmitted active power [11], [13], [15].

$$P = \frac{V_A \cdot V_B}{X_L - X_C} \cdot \sin \delta \quad (1)$$

Assuming $V_A = V_B = V$, the above relation becomes:

$$P = \frac{V^2}{X_L - X_C} \cdot \sin \delta \quad (2)$$

The same transmitted power on network line can be established with series compensation using a voltage synchronous source (the below figure) which supplies the same voltage with the voltage supplied at the terminals of the series capacitor. Due to use of the controllable series voltage source at fundamental frequency instead of the series capacitor, it can be obtained a voltage amplitude proportional with the line current phased with $\pm\pi/2$ and keep this voltage constant even when the current I is varying, or can be controlled independent of the current amplitude. Usually, for capacitor compensation, the voltage is phased behind the current in quadrature, but through a simple control, the voltage it can be phased forward the current, emulating an inductive compensation, having the same effect with an increase of line inductive reactance. [12], [16], [17], [18].



Where, γ – is a parameter;
 $V_s(\gamma)$ – the compensation voltage amplitude injected in series with the line.

Where, γ – is a parameter;
 $V_s(\gamma)$ – the compensation voltage amplitude injected in series with the line.

$V_s(\gamma)$ – the compensation voltage amplitude injected in series with the line.

The implementation of modern components replacing of obsolete electrical equipment is driven by the faster technological evolution which ensures the operation to high level of today's technology. by replacing the worn-out elements and adding additional features and benefits of new technologies. The SSSC devices are primary active power control facilities designed to increase the transmission capacity for important parts of the power system.

REFERENCES

- [1]. **Musatescu V., s.a.**, *Bazele tehnice si economice ale pietelor de energie electrica*, Ed. Agir, Bucuresti, 2019.
- [2]. <https://www.library.abb.com/> A matter of FACTS – Deliver more high quality power, 2015
- [3]. **Eremia M., Sanduleac M., s.a.**, *Dispozitive FACTS. Concepte și aplicații în energetică*, Ed. Agir, Academia de Stiinte Tehnice din România, 2017.
- [4]. **Golovanov N., s.a.**, *Surse regenerabile de energie in sistemul electroenergetic*, Ed. Agir, Bucuresti, 2015.
- [5]. <https://www.economica.net/transelectrica-consum-productie>
- [6]. **Vatra F., Postolache P., Vatra C.A., Poida A.**, *Smart grids- Introducere pentru profesioniști*, Ed. SIER, Bucuresti, 2014.

- [7]. **Saurabh P., Mahevas A., s.a** *An overview of static synchronous series compensator*, Journal of Research in Engineering and Applied Sciences, vol.05, 2020.
- [8]. **Gyugyi L., Edris A., Eremia M.,** *Static Synchronous Series Compensator (SSSC)*. In *Advanced Solutions in Power Systems: HVDC, FACTS, and Artificial Intelligence* (eds M. Eremia, C.-C. Liu and A.-A. Edris), 2016.
- [9]. **Piyasinghe L., Zhixin M., Khazaei J., Lingling F.,** *Impedance model-based ssr analysis for tcsc compen-sated type-3 wind energy delivery systems*, IEEE Transactions on Sustainable Energy Volume: 6, 2015.
- [10]. **Sen K. K.,** *SSSC-static synchronous series compensator: theory, modeling, and application*, IEEE Transactions on Power Delivery, 1998.
- [11]. **Hingorani N., Gyugyi L.,** *Understanding FACTS: Concepts and Technology of Flexible AC Transmission Systems*. IEEE Press, New York, 2000.
- [12]. **Chimirel C., Sanduleac M., Mohani V.,** *New technologies promoted within CNTEE Transelectrica, STATCOM and Electric Valves*, Mesagerul energetic nr.230, 2023.
- [13]. **Stochitoiu M.D., Utu I.,** *The role of STATCOM in dynamic compensation of electrical networks*, Annals of University of Petrosani, Electrical Engineering, vol.24, 2022.
- [14]. **Kumar A., s.a,** *Power system stability Enhancement using FACTS controllers*, International Conference on Emerging Trends in Electrical Engineering and Energy Management (ICETEEEM), 2012.
- [15]. **Alvira D., Torre M., Bola J., Burdalo U., Marquez M.,** *The use of a static synchronous series compensator (SSSC) for power flow control in the 220 kV Spanish transmission network*, CIGRE, 2010.
- [16]. **Edris A. A., (Convener), Chow J., Watanabe E., s.a.** *Static synchronous series compensator (SSSC)*. CIGRE Working Group B4-40, Technical Brochure no. 371, January 2008.
- [17]. **Yunkai L., Ting L., Quan T., Yunling W., Chuan Y., Xiaoxi Y., Yang L.,** *Comparison of upfc, svc and statcom in improving commutation failure immunity of lcc-hvdc systems*, Open Access Journal Special section on key enabling technologies for prosumer energy management, 2020.
- [18]. **Gupt S., Dixit A., Mishra N., Singh S.P.,** *Custom power devices for power quality improvement*, International Journal of Research in Engineering & Applied Science, vol.2, 2012.

This article was reviewed and accepted for presentation and publication within the 11th edition of the International Multidisciplinary Symposium "UNIVERSITARIA SIMPRO 2024".

HEALTH AND SAFETY RISK ASSESSMENT FOR THREE REPRESENTATIVE WORKSTATIONS FROM A LOCAL COMPANY THAT MANUFACTURES ELECTRICAL LIGHTING EQUIPMENT

FLORIN MUREȘAN-GRECU¹, ROLAND IOSIF MORARU²

Abstract: In the current context of accelerated developments towards a VUCA (Volatile-Uncertain-Complex and Ambiguous) world, more and more industrial companies are trying to adjust their management systems and associated procedures from the perspective of an effective - but always perfectible - risk management for the business, including here the quality, safety, security, financial risks and more. Attempts to optimize industrial and occupational safety are based on the basic principle of risk assessment and - from this perspective - this article presents the procedure applied and the results obtained in a systematic process of assessing the risks of occupational accidents for workplaces within a local company that manufactures electrical lighting equipment. The results obtained were the prerequisites for establishing the measures to minimize the identified and ranked risks, thus substantiating the prevention and protection plan of the investigated company, in accordance with the provisions of the national legislation in force.

Key words: electrical equipment manufacturing, accident at work, occupational risk assessment and management, hazard mitigation.

1. INTRODUCTION

Starting from the legislative, normative and methodological requirements, it can be stated that the occupational risk assessment is the systematic study of all aspects of the work process that are likely to generate unwanted events, of the means of eliminating hazards and applicable prevention and protection measures to control the associated risks [1], [2], [3]. As established in previous studies, businesses that have the ability to devote resources to these issues are more likely to report higher levels of implementation of good OSH practices and to understand that OSH is fundamental to business success their [4], [5]. As long as one of the first individual instinctive needs is that of safety, according to Maslow's pyramid model, and the new trend of addressing the issue of occupational safety and health (OSH) is centered on workers, they are the

¹ *Ph.D. Student, University of Petroșani, flomavon2002@yahoo.com*

² *Professor., Ph.D. Eng., University of Petroșani, roland_moraru@yahoo.com*

optimal resource for solving these problems [6], [7], [8]. In order to successfully involve each worker in the management system, as a component part of it, all those involved must have a level of knowledge and awareness with similar and unified values, embodied in a safety culture. Understanding, shared and individual acceptance of the safety culture is the starting point of this study. As these prerogatives are fulfilled, they naturally contribute to the efficient operation of a work safety management system. Similarly, management, in general, deals with problems in a unitary way, in common and not individually, in isolation. Only for the identification of the cause-effect connection of the management system is necessary in the first stage the isolation for the individual study of the problem [9], [10], [26], [28], [31], [35].

The proposed approach allows to a certain company to define and implement a risk control tactic starting from the top management level and being integrated into usual, routine activities and operations of the company. In every working places and workstations the manager has the overall mission – imposed by the legal framework - to protect the life, safety integrity, health and wellbeing of every employee against accidental risks that may appear in the occupational environmentand, providing work conditions designed to ensure their complete physical, psychological and –nevertheless - social comfort. A certain company, developing his operations in a concrete environment that raise potential hazards will also create –simultaneously – a general context that establishes quite clearly the boundaries within which hazard prevention and must and should be controlled [11], [12]. The implementation by the top – level management, within its responsibilities/and considering his liabilities, of prevention/protection measures/solutions targeting the mitigation of accidental hazards, information/training/awareness raising of workers and confirming the organizational framework and means required imposes to perform an effective occupational hazard/risk evaluation [13]. The above mentioned considerations are quite a sound basis for stating that the main target of occupational risk assessment is always prevention of occupational risks, even if this objective is not really and completely always achievable in day – to – day practice [14]. Always when it is not indeed feasible to eliminate hazards, risks should be diminished in such a way that the residual risks are kept bellow a predetermined level [15]. In later stages and under a rigorous control program, residual risks will be reassessed, considering rationally the opportunity to further /minimize/eliminate/reduce them, following the latest developments in scientific and technical knowledge [16], [27], [29], [30], [37], [40].

Any approach of hazard/risk assessment should cover the work injury risks that are reasonably foreseeable and manageable. All the specific risks resulting from routine activities are normally considered insignificant, requiring no special attention unless professional activity implies their significant, fast increasing aggravation and the occurrence of fast developing worse-case scenarios [17], [18], [19], [20], [32], [39].

The methodology for assessing professional hazards should be defined according to the scope, and nature to ensure they effective and are used in a systematic way [21], [22]. Companies do employ various and differently complex risk assessment tools part of their global strategy to deal with various hazards or activities. The complexity of the risk assessment method does not depend on the size of the organization but on the hazards associated with the organization's activities. Figure 1

shows schematically a simplified, but not simplistic, version of the basic elements of the stage of assessing the risks of injury and illness at work, together with some methodological benchmarks of occupational risk management [23], [33], [36], [38].

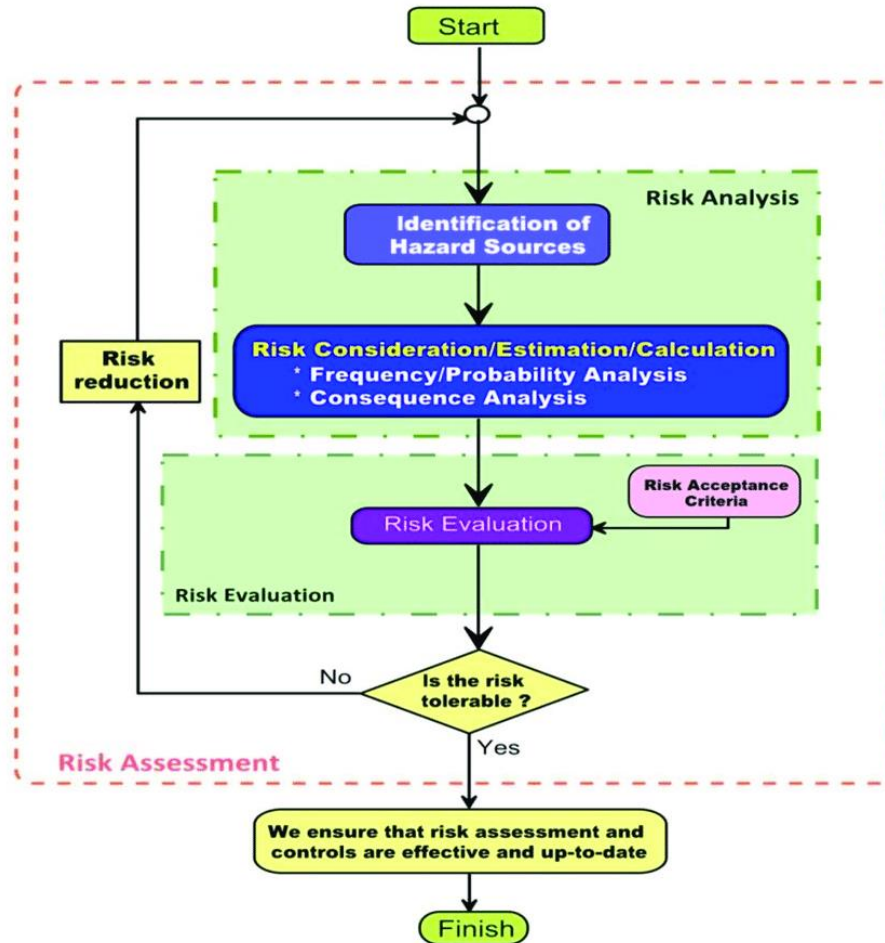


Fig.1. General schematic representation of the risks assessment/management process concerning work injuries and occupational illnesses (adapted after [23])

To be effective, coherent, systematic and sustainable, the risk assessment process should be not unnecessarily complicated, kept sufficiently practical, and easy to understand by all the involved stakeholders. The process must be put in practice only by experts, people with adequate skills, supported by proper technology that is correctly selected and sized for the particular working task. Risk assessment should always and in any circumstances be part of a larger, consolidated framework that resorts to the use of the information gathered to make decisions about risk responses and monitoring, and returns information back into the overall strategic planning process [24], [34], [41].

HEALTH AND SAFETY RISK ASSESSMENT FOR THREE REPRESENTATIVE WORKSTATIONS FROM A LOCAL COMPANY THAT MANUFACTURES ELECTRICAL LIGHTING EQUIPMENT

In accordance with the provisions of art. 15, para. 1, point 1 of H.G. no. 1425/2006 for the approval of the Methodological Norms for the application of the provisions of the Occupational Health and Safety Law no. 319/2006, the first of the prevention and protection activities carried out within the enterprise and/or unit is represented by *"the identification of hazards and the assessment of risks for each component of the respective work system, work load, means of work/work equipment and the work environment at jobs/work stations"*. To facilitate the fulfillment of employers' legal obligations in the field of occupational injury and disease risk assessment, a relatively large number of methods have been designed and are currently being used. In the first part of the article, a brief description of the analyzed company and the method developed by I.N.C.D.P.M. Bucharest (purpose, principle, users, stages, method of application, work procedure and application conditions), as well as work tools (risk factor identification list, list of consequences, severity and frequency rating scale, risk level classification grid, etc.). The second part is dedicated to presenting the concrete way of using the method developed by I.N.C.D.P.M. Bucharest for the assessment of occupational injury and illness risks at the company that was the object of the research.

2. MATERIAL AND METHOD

2.1. Overall presentation of the company subject of the research

Electrical Lighting Equipment Manufacturing LLC (general view given in Figure 2), with its 25 years of experience in the field, has become one of the important manufacturers of high-brightness LED lighting systems. In addition to the professional systems it produces and sells all over the world (lighting for potentially explosive environments, lighting for airports and beaconing), the company has developed a range of street, ambient and architectural lighting products. With extensive experience in the design, manufacture and testing of high-intensity LED products, the company offers high-quality products designed and built specifically with LED requirements in mind, not just a replacement for other lighting systems with LEDs. Due to the design and manufacture of these lighting fixtures, customers benefit from technical support at the highest level, system integration or even lighting fixtures designed and manufactured according to the customer's requirements.



Fig.2. General view of the company's headquarters and manufacturing location

The company uses the latest technologies for design, production and testing of products and systems. The high-tech LEDs (the company being certified by OSRAM™) together with very good quality materials (polycarbonate, stainless steel, anodized aluminum, etc.) give the products a special appearance and durability even in difficult operating conditions.

The total number of employees is 46, and the main activity falls under CAEN code 2740 *Manufacture of electrical lighting equipment*. The manufactured products fall under "*Lighting fixtures and systems with high intensity LEDs*". They can be divided into several groups depending on the final destination.

a. High-intensity LED lighting fixtures - here are several fixtures for:

- safety and evacuation lighting;
- exterior lighting (architectural);
- interior lighting;
- street lighting (also in the ATEX version);
- lighting with dynamic color control;
- commercial lighting;
- industrial lighting.

b. Luminaires for airfields

Used in the aviation field for ground lighting, they represent the last group (in order of achievement and concern). Within this group we mention:

- bodies to signal obstacles, of low intensity (type A and B beacons - in several variants);
- obstacle lighting fixtures, of medium intensity;
- runway lighting system for small airports, with several lighting fixtures plus 1.4 A DC power supply system;
- runway access lighting fixture (Figure 3);
- naval lighting fixture.



Fig.3. PAPI – Precision Approach Path Indicator

HEALTH AND SAFETY RISK ASSESSMENT FOR THREE REPRESENTATIVE
WORKSTATIONS FROM A LOCAL COMPANY THAT MANUFACTURES ELECTRICAL
LIGHTING EQUIPMENT

The resources owned and valued by the company can be summarized as follows:

Buildings:

1. Administrative Building (Ground + Floor + Attic)
 - a) Administration offices
 - b) Show-room
 - c) Electronics laboratory
 - d) Photometry laboratory
 - e) Changing room 1
 - f) Sanitary groups (for each level)
 - f) Annexes
2. Production hall (ground floor + partial E) composed of:
 - a) Space for production activities
 - b) Production offices, warehouse management and quality control
 - c) Warehouse
 - d) Locker room 2
3. Dyeing hall
4. Production hall (ground floor + first floor)
5. Storehouse

Quality control equipment:

1. Electronics laboratory – 1 pc
2. Photometry laboratory – 1 pc

Machinery, installations, equipments, devices used in the activity:

1. Universal lathe – 2 pcs
2. Hydraulic press – 1 pc
3. Drilling machine – 3 pcs
4. Equipment for cutting metal material - 3 pcs
5. Cutter – 1 pc
6. Welding machine with stored energy - 3 pcs
7. Portable electric welding station – 1 pc
8. Ultrasonic welding machine – 1 pc
9. Compressor – 2 pcs
10. Ecological soldering station (lead-free flux) – 10 pcs
11. Conductor slipper machine – 1 pc
12. Conductor cutting machine – 1 pc
13. Oven - 2 pcs
14. Power source, grates – 6 pcs
15. Metal cutting machine with numerical control (CNC), Figure 4 – 2 pcs
16. Engraving and cutting equipment (Laser), figures 5 – 1 pc
17. Equipment for cutting metal landmarks (Guillotine) – 1 pc
18. Band-cutting machine – 2 pcs
19. Polishing machine with disc - 1 pc
20. Water jet cutting equipment – 1 pc
21. SMD planting line – 1 pc
22. MIG MAG welding equipment – 1 pc

- 23. Painting installation in the field - 2 pcs
- 24. CNC machining center – 1 pc
- 25. Foil application line – 1 pc
- 26. Electric forklift – 1 pc
- 27. Gas thermal power plants



Fig.4. Metal cutting machine with numerical control (CNC)

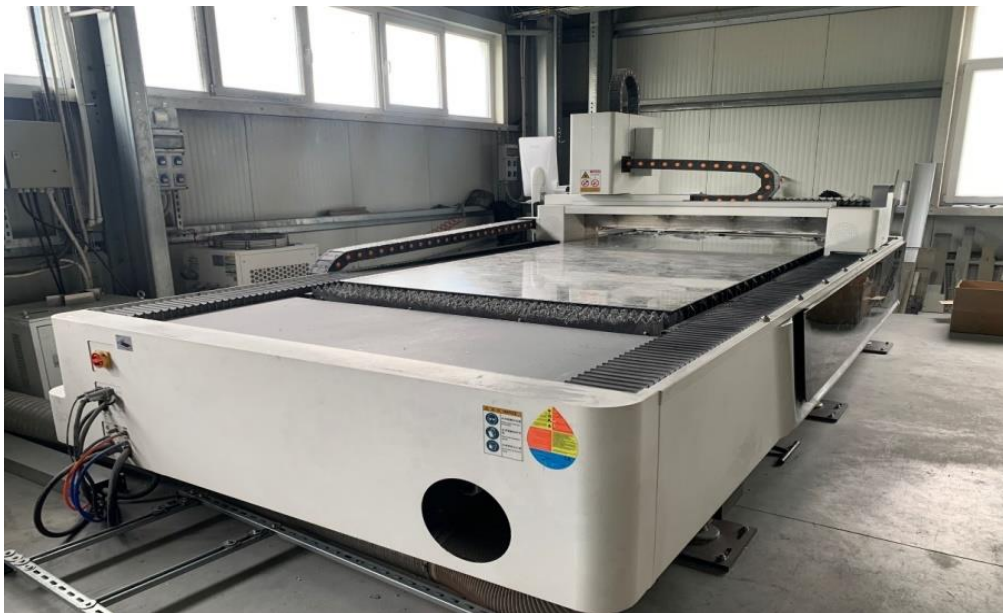


Fig. 5. Engraving and cutting equipment (Laser)

The distribution of workers by workstations/jobs is summarized in table 1.

HEALTH AND SAFETY RISK ASSESSMENT FOR THREE REPRESENTATIVE
WORKSTATIONS FROM A LOCAL COMPANY THAT MANUFACTURES ELECTRICAL
LIGHTING EQUIPMENT

Table 1. List of workplaces for which the risk assessment was carried out

Crt. No.	Job/workstation	Number of workers
1.	Numerically Controlled (CNC) Metal Cutting Machine Operator	2
2.	Engraving and cutting equipment operator (Laser)	2
3.	Assembler of electronic subassemblies	6
	Other categories of staff members	36
	TOTAL	46

2.2. Brief description of the I.N.C.D.P.M. Bucharest tool for assessing the risks of occupational accidents and illnesses

The method includes the following mandatory **steps**: i) *defining the system to be analyzed (workplace)*; ii) *identification of risk factors in the system*; iii) *assessment of occupational injury and illness risks*; iv) *the ranking of risks and the establishment of prevention priorities*; v) *proposing preventive measures*.

The **work tools used**: the stages necessary for the assessment of work safety in a system, described previously, are carried out using the following work tools:

- a. *List of identification of risk factors*;
- b. *List of possible consequences of the action of risk factors on the human body*;
- c. *Rating scale of severity and probability of consequences*;
- d. *The risk assessment grid*;
- e. *The classification scale of the risk levels, respectively of the security levels*;
- f. *Job sheet - centralized document*;
- g. *List of proposed measures*.

The stages of application of the method:

- a. *Setting up the analysis and evaluation team*;
- b. *Description of the system to be analyzed*;
- c. *Identification of risk factors in the system*;
- d. *Risk assessment and ranking*;

The formula for calculating the global risk level is as follows :

$$N_r = \frac{\sum_{i=1}^n r_i \cdot R_i}{\sum_{i=1}^n r_i} \quad (1)$$

where:

N_r is the global risk level at the workplace;

r_i – rank of risk factor “I”;

R_i – risk level for risk factor “I”;

n – the number of risk factors identified at the workplace.

In the case of the evaluation of some macrosystems (sector, section, enterprise), the weighted average of the average safety levels determined for each job analyzed from the composition of the macrosystem is calculated (similar jobs are considered as a single job), in order to obtain the global level of work safety for the workshop/section/sector or the investigated enterprise – N_g :

$$N_g = \frac{\sum_{p=1}^n r_p \cdot N_{sp}}{\sum_{p=1}^n r_p} \quad (2)$$

where:

r_p is the rank of the job "p" (equal in value to the risk level of the job);

n - the number of analyzed jobs;

N_{sp} - average level of job security for job "p".

e. Establishing preventive measures

The application of the method ends with the drafting of the analysis report. This is an informal instrument that must contain, clearly and succinctly, the following:

- the manner of carrying out the analysis;
- the persons involved;
- the results of the assessment, respectively job sheets with risk levels;
- interpretation of the evaluation results;
- prevention measures sheets.

3. ASSESSMENT OF ACCIDENTAL RISKS FOR THE WORKPLACE: OPERATOR METAL CUTTING MACHINE WITH NUMERICAL CONTROL (CNC) FROM ELECTRICAL LIGHTING EQUIPMENT MANUFACTURING LLC

The working process: making unique pieces and small series for different industrial fields, made of metal according to drawings, models or prototypes.

The components of the evaluated work system

a. Working equipments: machine with numerical control (CNC); chucks, drills, reamers, cutters, chamfers, taps for different types of threads; fixed keys, adjustable keys; hydraulic printing press; clamping vise and clamps for material; measuring equipment: subler, micrometers, gauges; 3D coordinate measuring machine and 2D coordinate measuring machine; storage shelves for raw material and finished parts; platform cart for transporting goods; emulsion (lubricating and cooling fluid); compressor and compressed air storage cylinder at 8 bar.

b. Working task: preparation of the semi-finished product for the machining operation by chipping; running the CNC program on the numerical control machine according to the operating instructions and technical specifications; measuring and checking the parts using the measuring instruments, according to the requirements and technical specifications; loading and handling components using lifting and/or transport equipment in safe conditions; ensures that all products executed in the process meet the

HEALTH AND SAFETY RISK ASSESSMENT FOR THREE REPRESENTATIVE
WORKSTATIONS FROM A LOCAL COMPANY THAT MANUFACTURES ELECTRICAL
LIGHTING EQUIPMENT

quality conditions and technical specifications; participate in daily start-of-shift meetings; periodically checks the condition of the tools, devices and verifiers used, prepares them for the processing of the next benchmark and performs their cleaning before storing them in the specially designed space; ensures the change of tools and inserts; keeps both the CNC machine he operates and the tools, devices and equipment he uses in good working order; performs and maintains the cleanliness of the CNC machine, including the periodic removal of chips to ensure its proper operation; ensures the maintenance of the CNC machine according to the work instructions;

c. Working environment: natural and artificial lighting; natural and artificial ventilation; adjustable temperature in the cold season. The premises are heated with radiant panels; air currents on the work route; electromagnetic radiation near electrical equipment; natural calamities; pneumoconionogenic dusts - metal and graphite dusts (from milling, polishing and polishing activities); toxic vapors, toxic gases.

Applying the tools and the procedure specific to the INCDPM Bucharest method [25], the specific risks factors present in the working system were identified, the severity and the probability classes related to each of the identified risks were assigned, and then the partial risk levels were set. The results obtained are centralized in Table 2. The meaning of the notations in table 3 is as follows: *WSE* - Work system element; *IR* - identified risk; *RF* – risk factor; *MC* - Maximum consequence; *S* - Severity; *Likelihood*; *RL* - Risk level; *WE* - Working equipment; *OE* - Occupational environment; *WT* - Working task; *HF* - Human factor; *N*-negligible; *LTI 3-45* – Lost Time Injury from 3 to 35 days; *LTI 45-180* – Lost Time Injury from 45 to 180 days; *INV I* – first degree invalidity; *INV II* – second degree invalidity; *INV III* – third degree invalidity; *D* – death.

Table 2. The evaluation form of the analyzed workplace

ELEM LLC		EVALUATION FORM	Exposed workers: 2			
			Exposure length: 8 hours			
Work station: Operator metal cutting machine with numerical control			Assessors: Risk assessor Tehchnical staff/engineer Occupational physician Worker/operator			
WSE	IR	Risk Factors	MC	S	L	R L
WE	Mech. RF	1. Moving machine parts - crushing - the human body is caught between two moving pieces of equipment (F1)	Death	7	3	5
		2. Machine parts in motion - shearing - when a part of the human body (especially fingers) is caught between two machine components, one fixed and one moving, the result leads to amputation (F2)	INV III	4	2	3

		3. Moving machine parts - getting clothes or hair caught in the rotating parts of the machine, this can lead to the person being pulled into the machine (F3)	Death	7	2	4
		4. Machine parts in motion - projecting metal chips and tools during CNC operation, these materials can enter the human body. (F4).	INV III	4	1	2
		5. Unbalance/rolling/falling of heavy metal parts (F5)	LTI 3-45	2	2	2
		6. Free fall of incorrectly positioned parts, tools, materials or during manual handling (F6)	LTI 3-45	2	3	2
		7. Direct contact with dangerous surfaces (cutting, stinging) (F7)	LTI 3-45	2	6	3
	Thermal RF	8. Contact with hot surfaces of metal parts or cutters immediately after processing, if cooling was not adequate during processing (F8)	LTI 3-45	2	2	2
	Electrical RF	9. Electrocution by direct contact with uninsulated cables (F9)	Death	7	1	3
	Chemical RF	10. Working with flammable substances - transmission oil (F10)	Death	7	1	3
11. Working with emulsion - which can cause an allergic skin reaction (F11)		LTI 3-45	2	6	3	
OE	Physical RF	12. Noise from work equipment. (F12)	LTI 3-45	2	6	3
		13. Natural calamities - earthquakes, storms, lightning (F13)	Death	7	1	3
		14. Low lighting level, especially when working in dark areas and during the evening (F14)	LTI 3-45	2	3	2
		15. Slipping on wet or frozen surfaces, when moving outside the hall (F15)	LTI 3-45	2	3	2
	Chemical RF	16. Pneumoconogenic dusts in the atmosphere of the workplace (metallic dusts or hazardous fog formed from fine powder from the processed material or metal powder from tools and emulsion vapors during the operation of the equipment CNC) (F16)	Death	7	3	5
WT	Unadequate content	17. Wrong sequence of CNC power on/off operations (F17)	Death	7	1	3
		18. Wrong operations, rules, procedures - the absence of operations indispensable to work safety (F18)	Death	7	2	4
		19. Storing materials on shelves improperly, exceeding the safety factor given by the shelf manufacturer (F19)	LTI 3-45	2	3	2

HEALTH AND SAFETY RISK ASSESSMENT FOR THREE REPRESENTATIVE
WORKSTATIONS FROM A LOCAL COMPANY THAT MANUFACTURES ELECTRICAL
LIGHTING EQUIPMENT

	Mental overload	20. Monotony of work - repetitive operations (F20)	LTI 3-45	2	3	2
HF	Wrong actions	21. Improper fixation of workpieces (F21)	LTI 3-45	2	3	2
		22. Hand grip - improper finger positioning between the chuck and CNC main shaft or improper finger positioning between the workpiece and the hydraulic press (F22)	INV gr.III	4	4	4
		23. Working without protective devices (LEXAN windows) (F23)	LTI 3-45	3	2	2
		24. Carrying out maintenance operations on CNC machines without disconnecting the machine from the power source (F24)	Death	7	3	5
		25. Falling to the same level by slipping, tripping, unbalancing (F25)	LTI 3-45	3	3	3
	Omissions	26. Wearing inadequate personal protective equipment or not wearing protective equipment (F26)	Death	7	1	3

The overall risk level of the job is:

$$N_{rg} = \frac{\sum_{i=1}^{26} r_i \cdot R_i}{\sum_{i=1}^{26} r_i} = \frac{3 \cdot (5 \times 5) + 3 \cdot (4 \times 4) + 10 \cdot (3 \times 3) + 10 \cdot (2 \times 2)}{3 \times 5 + 3 \times 4 + 10 \times 3 + 10 \times 2} = \frac{223}{77} = 2,89 \quad (3)$$

The ranking of the identified risks is summarized in the histogram shown in fig. 6, and the proposed measures for the prevention of risks and the protection of exposed workers, in table 3.

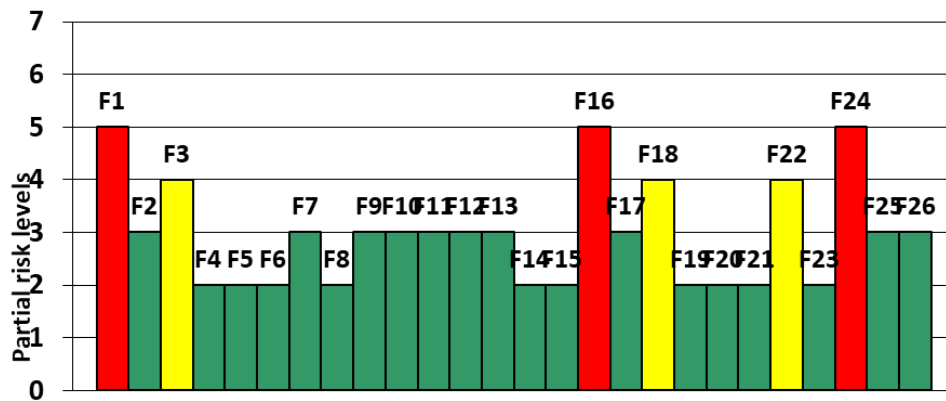


Fig.6. Partial risk levels by risk factors: „Operator metal cutting machine with numerical control (CNC)”

Table. 3. The list of proposed measures: „Operator metal cutting machine with numerical control (CNC)”

Crt. no.	Risk factor identified, assessed and ranked	Risk level	Prevention/protection measures
1.	F1: Moving machine parts - crushing - the human body is caught between two moving pieces of equipment	5	Organizational measures: <ul style="list-style-type: none"> daily visual inspection of the car enclosure to check that all panels are in place. visually inspect the enclosure and safety glass for any signs of warping, cracking or other damage. prohibiting the start or continuation of work if the absence, damage or incorrect placement of protective devices is found. training workers and checking how safety rules are respected. testing the door safety lock:
2.	F16: Pneumoconogenic dusts in the atmosphere of the workplace (metal dusts or hazardous fog formed from fine powder from the processed material or metal powder from tools and emulsion vapors during the operation of CNC equipment)	5	Technical measures: <ul style="list-style-type: none"> purchase of a fog evacuation system Organizational measures: <ul style="list-style-type: none"> training on the need to use protective glasses or a breathing mask periodic ventilation of the production hall every 2 hours.
3.	F24: Carrying out maintenance operations on CNC machines without disconnecting the machine from the power source	5	Organizational measures: <ul style="list-style-type: none"> • training workers regarding the Lock out procedure - tag out;
4.	F3: Moving machine parts - getting clothes or hair caught in the rotating parts of the machine can lead to the person being pulled into the machine.	4	Organizational measures: <ul style="list-style-type: none"> training workers on the importance of not coming close with any part of the body to moving machine components or when movements may occur. ensure casual clothing and make sure all staff have their hair tied up.
5.	F18: Wrong operations, rules, procedures - the absence of operations indispensable to work safety	4	Organizational measures: <ul style="list-style-type: none"> training workers regarding the consequences of non-compliance with safety restrictions - non-use or incomplete use of protective

HEALTH AND SAFETY RISK ASSESSMENT FOR THREE REPRESENTATIVE
WORKSTATIONS FROM A LOCAL COMPANY THAT MANUFACTURES ELECTRICAL
LIGHTING EQUIPMENT

			equipment, etc. <ul style="list-style-type: none"> • verification by permanent control, from the head of the formation, and/or by survey, from the hierarchically superior bosses.
6.	F22: Hand grip - improper finger positioning between the chuck and CNC main shaft or improper finger positioning between the workpiece and the hydraulic press	4	Organizational measures: <ul style="list-style-type: none"> • training workers on hand positioning; • installation of warning icons

Interpretation of assessment results

The global risk level calculated for the job "*Operator metal cutting machine with numerical control (CNC)*" is equal to 2.89, a value that places it in the category of jobs with a low to medium level of risk, not exceeding the maximum acceptable limit (3.5).

The result is supported by the "Assessment Sheet", from which it can be seen that out of the total of 26 risk factors identified, only 6 exceed, as a partial level of risk, the value of 3.5 falling into the category of high risk factors, and 3 falling into -are in the category of medium risk factors. To reduce or eliminate the 6 risk factors (which are in the unacceptable range), the generic measures presented in the "*Proposed measures sheet*" are necessary.

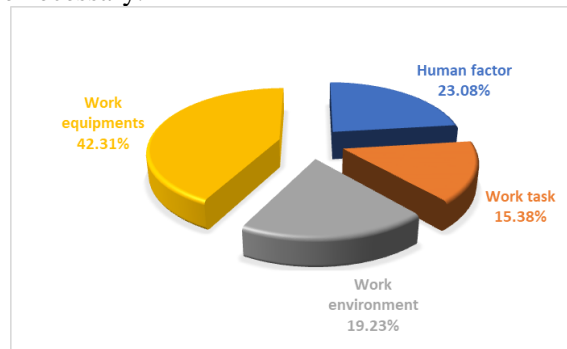


Fig.7. The share of risk factors identified by the elements of the work system „Operator metal cutting machine with numerical control (CNC)”

Regarding the distribution of risk factors by generating sources, the situation is as follows (fig.7):

- 41.31%, factors specific to the means of production/work equipment;
- 15.38%, factors specific to the work environment;
- 19.23%, factors specific to the workload;
- 23.08%, human factor related risks.

From the analysis of the *Evaluation Form*, it is found that 13 (50%) of the identified risk factors can have irreversible consequences on the performer (death or disability).

4. CONCLUSIONS

This study aimed at assessing the risks and developing the prevention and protection plan for Electrical Lighting Equipment Manufacturing LLC, in accordance with the provisions of art. 7, para. 4, lit. b, art. 12, para. 1, lit. and art. 13 of Law no. 319/2006 and art. 15, para. 1, points 1 and 2 of H.G. no. 1425/2006. The results of the risk assessment are presented in the "Job Evaluation Sheet" and the "Proposed Measures Sheet" related to each analyzed workplace. The list of jobs evaluated and the primary results obtained is presented in table 4.

Table 4. Risk assessment overall results

Nr. crt	File no.	Workplace/job	Overall risk level for each job
1	F01	Operator metal cutting machine with numerical control (CNC)	2.89
2	F02	Assembler of electronic subassemblies	3.20
3	F03	Engraving and cutting equipment operator (Laser)	2.94

The overall risk level for the three jobs is:

$$N_{gs} = \frac{\sum_{i=1}^3 r_i \cdot N_{gi}}{\sum_{i=1}^3 r_i} = 2,98 \quad (4)$$

The ranking of places, depending on the global level of risk, is shown in table 5.

Table 5. Hierarchy of risks on the workstations where the evaluation was carried out

Nr. crt	File no.	Workplace/job	Ranked overall risk level for each job
1	F02	Assembler of electronic subassemblies	3.20
2	F03	Engraving and cutting equipment operator (Laser)	2.94
3	F01	Operator "metal cutting machine with numerical control (CNC)"	2.89

According to the ranking, it is found that all workplaces have a global risk level below the allowed limit (3.5) they fall into the category of those with a low to medium risk level. The value of the aggregate global risk level per company $N_{gs} = 2.98$, determines its inclusion in the category of those with a low to medium risk level. As a rule, the action of a risk factor is eliminated / diminished by several measures, one of which is mandatory of an organizational nature (OSH training). In the same way, a measure can act on several risk factors. Depending on the result, the measures can be:

- organizational measures for the worker and the work load;
- technical measures for the means of production and the work environment.

The development of the prevention and protection plan requires ensuring a significant consultation on the part of the employees. The specialized literature in the field of OSH emphasizes the need to use as a management tool the active involvement of all employees in the adoption of decisions that directly concern them. Prevention and protection measures primarily impact workers. Therefore, a realistic plan of measures is based on the widest possible consultation of the employees of the respective organization. The selection of measures will be made not only depending on the level of risks they will eliminate or reduce, but also on the cost-benefit ratio.

The proposed measures (technical, organizational, hygienic-sanitary, others) together with the deadline and the responsible person make up the mitigation-elimination systems. These measures will be taken for each identified factor. Even if all the proposed preventive measures are taken, there are risk factors that cannot be eliminated, called residual risk factors in the specialized literature. These risk factors can be kept under control through organizational measures. Statistics show that most accidents are related to non-observance of OSH instructions. As a result, there will be an emphasis on the professional training of workers for the formation of the security culture at the workplace and the awareness of professional risks, if they do not respect the work procedures.

REFERENCES

- [1]. **Aven T., Zio E.**, *Some considerations on the treatment of uncertainties in risk assessment for practical decision making*, Reliability Engineering & System Safety, Volume 96, Issue 1, Pages 64-74, 2011.
- [2]. **Azadeh-Fard N., Schuh A., Rashedi E., Camelio J.A.**, *Risk assessment of occupational injuries using accident severity grade*. Saf Sci **76**:160–167, 2015.
- [3]. **Bedford T., Cooke R.**, *Probabilistic risk analysis: foundations and methods*. Cambridge: Cambridge University Press, 2001.
- [4]. **Cioca L.-I., Ivascu, L.**, *Risk Indicators and Road Accident Analysis for the Period 2012–2016*. Sustainability, 9, 1530., 2017.
- [5]. **HSE**, *Risk assessment: A brief guide to controlling risks in the workplace*, Leaflet INDG163 (rev4), Health and Safety Executive (HSE), Bootle, Great Britain, 2014.
- [6]. **Moraru R.I., Băbuț G.B., Cioca L.I.**, *Rationale and Criteria Development for Risk Assessment Tool Selection in Work Environments*, Environmental Engineering and Management Journal, Vol. 13, No. 6, pp.1371 – 1376, 2014.
- [7]. **Moraru R.I., Băbuț G.B., Cioca L.I.**, *Drawbacks and traps in risk assessment: examples in Romania*, Proceedings of the 5th International Conference on Manufacturing Science and Educations - MSE 2011, Volume 2, pp. 363-366, Sibiu, Romania, 2011.
- [8]. **Joy J., Griffiths D.**, *National minerals industry safety and health risk assessment guideline*, version 3, March 2008.
- [9]. **Kokangül A., Polat U., Dağsuyu C.**, *A new approximation for risk assessment using the AHP and Fine Kinney methodologies*. Saf Sci 91:24–32, 2017.
- [10]. **Cioca L.I., Moraru R.I., Băbuț G.B.**, *A Framework for Organisational Characteristic Assessment and their Influences on Safety and Health At Work*, 15th Int. Conf. on Knowledge-Based Organization: Management, Conference Proceedings, Sibiu, Romania, Vol. 2 pp. 43-48, 2009.

- [11]. **Romanian Parliament**, Law no. 319 regarding occupational safety and health (in Romanian), *The Official Journal of Romania*, part I, no. 646/26.07.2006, Bucharest, Romania, 2006.
- [12]. **Pasman, H.J.**, Learning from the past and knowledge management: Are we making progress?", *Journal of Loss Prevention in the Process Industries*, Vol 22, pp 672-679, 2009.
- [13]. **Labour Inspection**, *Verifying how employers comply with legal requirements for professional risk assessment. Guidance for inspectors* (in Romanian), Labour Inspection, Bucharest, Romania, 2015.
- [14]. **European Commission**, *Guidance on risk assessment at work* (Directive 89/391/EEC), European Commission, Directorate General V Employment, Industrial Relations and Social Affairs, Office for Official Publications of the European Communities, Luxembourg, 1996.
- [15]. **HSE**, *The health and safety toolbox: How to reduce risks at work*, HSG268, Health and Safety Executive (HSE), Bootle, Great Britain, 2014.
- [16]. **Ispășoiu A., Moraru R.I., Popescu-Stelea M., Băbuț G.B.**, *Study on the potential of artificial intelligence application in industrial ergonomics performance improvement*, Acta Technica Napocensis - Series: Applied Mathematics, Mechanics and Engineering, [S.l.], v. 64, n. 1-S1, Pages: 45-54 , feb. 2021. ISSN 2393–2988.; IDS Number: QL6ZK, Accession Number: WOS 000621232900006, 2021.
- [17]. **Romanian Government**, Government Decision no. 1048 regarding the minimum safety and health requirements for the use by workers of personal protective equipment at the workplace (in Romanian), *The Official Journal of Romania*, part I, no. 722/23.08.2006, Bucharest, Romania, 2006.
- [18]. **Romanian Government**, Government Decision no. 1425 for approval of Methodological Norms for applying occupational safety and health Law no. 319/2006 (in Romanian), *The Official Journal of Romania*, part I, no. 882/30.10.2006, Bucharest, Romania, 2006.
- [19]. **Romanian Government**, Government Decision no. 1029 regarding the conditions for placing machines on the market (in Romanian), *The Official Journal of Romania*, Part I, no. 674/30.09.2008.
- [20]. **Romanian Government**, Government Decision no. 517 for amending and supplementing Government Decision no. 1029/2008 regarding the conditions for placing machines on the market (in Romanian), *The Official Journal of Romania*, Part I, no. 373/27.05.2011.
- [21]. **Romanian Government**, Government Decision no. 191 for the approval of the National Strategy on Safety and Health at Work for the period 2018-2020 (in Romanian), *The Official Journal of Romania*, Part I, no. 331/16.04.2018.
- [22]. **Moraru R.I., Băbuț G.B., Popescu-Stelea M.**, Approaching occupational safety and health emerging risks categories and prevention, *Quality - Access to Success*, Volume 15, Issue 139, pp. 104-108, 2014.
- [23]. **Niskanen T., Naumanen P., Hirvonen M.L.**, An evaluation of EU legislation concerning risk assessment and preventive measures in occupational safety and health, *Applied Ergonomics*, Volume 43, Issue 5, pp. 829-842, 2012.
- [24]. **Stanton N.A., Harvey C.**, *Beyond human error taxonomies in assessment of risk in sociotechnical systems: a new paradigm with the EAST 'broken-links' approach*. *Ergonomics* 60(2):221–233, 2017.
- [25]. **Băbuț G.B., Moraru R.I.**, *Critical analysis and ways to improve the I.N.C.D.P.M. Bucharest for the assessment of the risks of accidents and occupational diseases*, "Quality - access to success", vol. 14, no. 137, pp. 55-66 2013.

- [26]. **Petrilean D.C., Stanilă S., Dosa I.**, *A mathematical model for determining the dimensionless heat flux with application in mine environment*, Environmental Engineering and Management Journal, Vol.16, No. 6, 1249-1414, 2017.
- [27]. **Petrilean D.C.**, *Compresoare eliciodale*, Editura Tehnica-Info, 2006
- [28]. **Petrilean D.C.**, *Termodinamica tehnica si masini termice*, Editura A.G.I.R., 2010.
- [29]. **Petrilean D.C.**, *Mathematical model for the determination of the non-stationary coefficient of heat transfer in mine works*, The 19th American Conference on Applied Mathematics (AMERICAN-MATH '13), Cambridge, MA, USA.2013.
- [30]. **Petrilean D. C.**, *Transmiterea căldurii*, Editura Universitat, 2016.
- [31]. **Handra A.D., Popescu F.G., Păsculescu D.**, *Utilizarea energiei electrice: lucrări de laborator*, Editura Universitat, 2020.
- [32]. **Fîță N.D., Radu S.M., Păsculescu D., Popescu F.G.**, *Using the primary energetic resources or electrical energy as a possible energetical tool or pressure tool*, In International conference KNOWLEDGE-BASED ORGANIZATION, vol. 27, no. 3, pp. 21-26. 2021.
- [33]. **Pasculescu D., Dobra R., Ahmad M.A.**, *Dosimetric Quantity System for Electromagnetic Fields Bio-effects*, International Journal of Scientific Research (IJSR) 5, no. 2, pp. 28-32, 2016.
- [34]. **Popescu F.G., Păsculescu D., Păsculescu V.M.**, *Modern methods for analysis and reduction of current and voltage harmonics*, LAP LAMBERT Academic Publishing, ISBN 978-620-0-56941-7, pp. 233, 2020.
- [35]. **Pasculescu D., Niculescu T.**, *Study of transient inductive-capacitive circuits using data acquisition systems.* International Multidisciplinary Scientific GeoConference: SGEM 2, no. 1, 323-329, 2015.
- [36]. **Pana L., Janusz G., Pasculescu D., Pasculescu V. M., Moraru R. I.**, *Optimal quality management algorithm for assessing the usage capacity level of mining transformers*, Polish Journal of Management Studies 18, no. 2, 233-244, 2018.
- [37]. **Dobra R., Buica G., Pasculescu D., Leba M.**, *Safety management diagnostic method regarding work cost accidents from electrical power installations*. Proc. 1st Int. Conf. on Industrial and Manufacturing Technologies (INMAT), Vouliagmeni, Athens, Greece. 2013.
- [38]. **Stepanescu, S., Rehtanz, C., Arad, S., Fotau, I., Marcu, M., Popescu, F.** *Implementation of small water power plants regarding future virtual power plants* 10th International Conference on Environment and Electrical Engineering, pp. 1-4, IEEE, 2011.
- [39]. **Fîță N. D., Lazăr T., Popescu F. G., Pasculescu D., Pupăză C., Grigorie E.**, *400 kV power substation fire and explosion hazard assessment to prevent a power black-out*, International Conference on Electrical, Computer Communications and Mechatronics Engineering-ICECCME, pp. 16-18, 2022.
- [40]. **Marcu M., Niculescu T., Slusariuc R. I., Popescu, F. G.**, *Modeling and simulation of temperature effect in polycrystalline silicon PV cells*, IOP Conference Series: Materials Science and Engineering, Vol. 133, No. 1, pp. 012005, 2016.
- [41]. **Popescu F.G., Arad S., Marcu M.D., Pana L.**, *Reducing energy consumption by modernizing drives of high capacity equipment used to extract lignite*, Papers SGEM2013/Conference Proceedings, Vol. Energy and clean technologies, pp. 183 - 190, Albena., Bulgaria, 2013.

THE IMPACT OF MEDITATION IN A VIDEO GAME BASED ON BCI

SEBASTIAN DANIEL ROSCA¹, MARIUS MARCU², MONICA LEBA³,
DANIEL IOAN DINEA⁴, DUMITRU CRISTIAN IACOBESCU DINEA⁵

Abstract: This study explores the impact of meditation-induced non-task related states on brain activity in a motor imagery paradigm for brain-computer interfaces (BCI). Using a wearable EEG device, the research analyzes theta (θ) and alpha (α) wave patterns during relaxation and meditation states. Three healthy subjects participated on an EEG recording session using the Emotiv Insight neural headset, maintaining a defocused eye gaze while viewing a static image of a BCI-controlled pool game. In this paper we developed an algorithm to preprocess EEG data that focus on frequency-specific signal extraction and peak-to peak amplitude computing for all channels in interest frequencies domain. The analysis aims to reveal distinct theta and alpha wave activity patterns across brain regions for each subject.

Key words: BCI, EEG, peak-to-peak, relaxation, MATLAB.

1. INTRODUCTION

The main worldwide problem that generates more than 23 million deaths per year is represented by mental stress. This is a health epidemic caused by cognitive disorders of the hippocampal region of the brain that affects memory and learning [1]. A possible solution to solve this major problem it represents by the practice of meditation, which is known to reduce the experience of anxiety, while improving both the level of consciousness and attention. Embracing this behavior can touch on key factors involving to driving the brain-computer interface, known as BCI, using the power of concentration as input to induce different states of consciousness [2], [16]. So, we investigate the effects of meditation induced by a non-task related state as part of motor imagery paradigm [3]. In this way, the user must maintain a totally mental state of relaxation based on the focus of not managing a task, freeing his mind, and keeping the eye gaze defocused, [17], [18], [20], [23], [25], [29].

¹ Ph.D Student Eng., at the University of Petrosani, sebastianrosca91@gmail.com

² Prof. Ph.D Eng, at the University of Petrosani, mariusmarcu@upet.ro

³ Prof. Ph.D Eng., at the University of Petrosani, monicaleba@yahoo.com

⁴ Ph.D. Student, University of Petroșani, danieldinea@yahoo.com

⁵ Ph.D. Student, University of Petroșani, iacdinea@gmail.com

2. THE STUDY OF THE PROBLEM

Both relaxation and meditation state can be captured from brain signals using a wearable electroencephalogram (EEG) equipment with minimal contact with the subject's scalp area. As the specialized literature presents, the electrical signals of the brain have an amplitude related to the order of microvolts and a classification within frequency bands. Among these of interest are Theta waves (θ) predominant in meditation activities and Alpha waves (α) that dominate the resting and relaxing conditions [4], [19], [21], [24], [27], [31].

The θ waves are characterized by frequencies between: 4-8 Hz and amplitudes between: 100-150 μ V. Some studies associate them with the installation of the state of relaxation, but also with the processes of working memory load [5], [6], [7]. The waveform of θ rhythm and brain areas localization are presented in Fig.1.

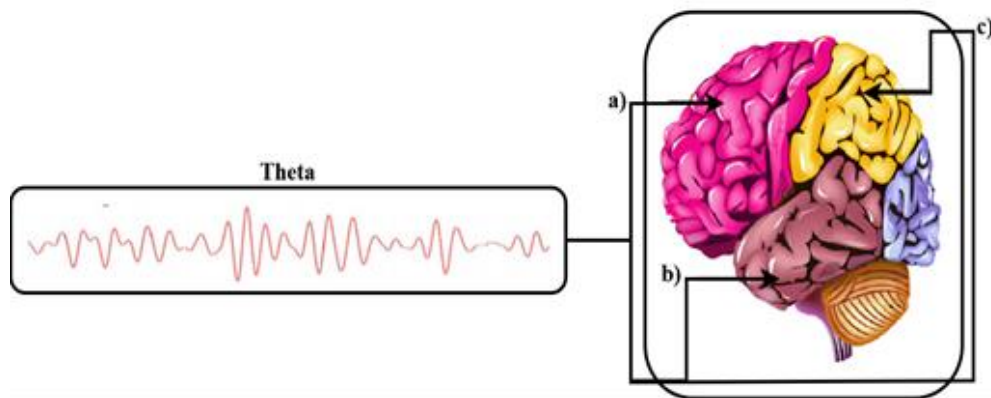


Fig.1. Theta rhythm waveform [5]

Theta rhythm appear on the frontal midline of the brain as presented in Fig.1 a) triggered by positive emotion evoked. The EEG signal from this brain region can be captured using a channel montage that is placed on proximal of the upper of forehead in left and right brain hemisphere on prefrontal cortex location [5], [8], [9], [22], [26].

The temporal and parietal lobes, presented in Fig.1 b), c), are linked to encoding and retrieval process in which theta rhythm present a higher activation and also an indicator of stress, anxiety and emotions regulation modulated by amygdala and hippocampus through temporo-parietal area [10], [11], [12], [28], [33], [35].

The α waves are characterized by frequencies between: 8-13 Hz and amplitudes between: 20-100 μ V [5]. This rhythm presents a localization and a waveform as presented in Fig. 2.

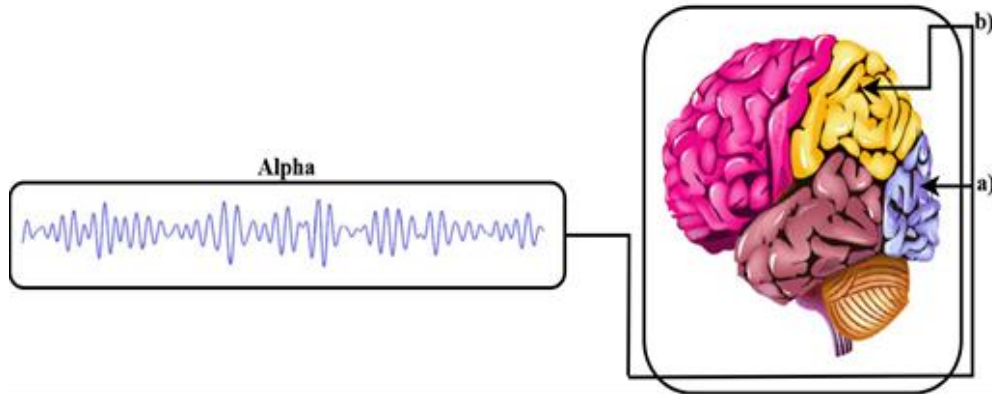


Fig.2. Alpha rhythm waveform [5]

Alpha rhythm occurs both on occipital lobe, as presented in Fig. 2 a), and on somatosensory cortex as part of parietal lobe, as presented in Fig. 2 b). The presence on occipital lobe is related to induce the mental relaxation process. Alpha rhythm prominence is higher on all brain regions, except the frontal lobe at rest condition [4], [5], [13], [30], [32], [36].

3. EXPERIMENT METHODOLOGY

For experiment study three healthy subject was chosen to participate to a brain EEG signal recording session. Each subject was trained to maintain a defocused eye gaze during the session and their brain activity was measured with same EEG device represented by Emotiv Insight neural headset with five EEG semidry electrodes. Each EEG session was record with Emotiv Xavier TestBench software in laboratory condition without external noise presence. This BCI solution was chosen for its capability to measure and visualize 3D brain activity using EEG electrodes placed according to the 10-20 International Standardized system, complemented by software for real-time analysis and offline data export [14], [34].

During one unique trial, each subject maintains a non-task related state based on how he was trained, during which he does not have to speak. Brain signal recording is performed based on a static image of each subject in a BCI-controlled pool game previously developed by us in Unity3D called "Mental Pool Game" [15]. The BCI interface of this video game is presented in Fig. 3.

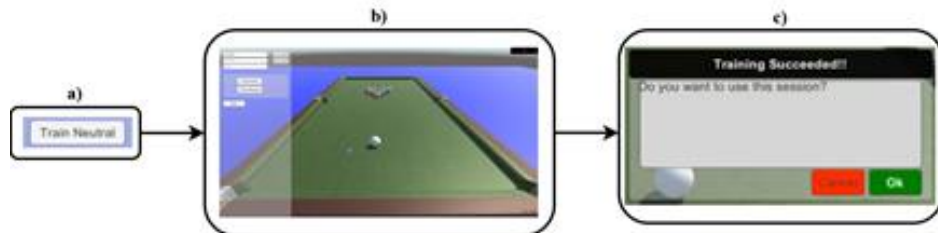


Fig.3. Mental Pool Game GUI [14]

The electrical potential activity of each subject's brain is recorded for a 9 second interval, once the BCI instructor presses the neutral state recording start button presented in Fig.3 a). During this interval the subject follows the established scenario, being presented a static image of the game interface, as presented in Fig.3 b), to induce a state of relaxation through meditation. Successful training of this state is signaled by a pop-up window, as presented in Fig.3 c).

4. EEG DATA RECORDED ANALYSIS

To study each recorded EEG session, we developed a three-step algorithm that prepare the data to be analyzed in-depth related the alpha and theta brainwave contributions for the specified time interval, which is to be integrated by code written in MATLAB programming language, as presented in Fig. 4.

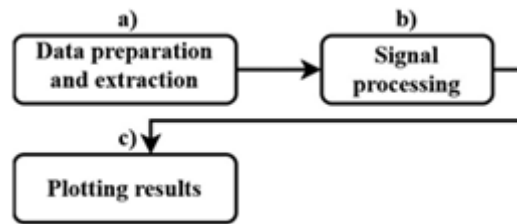


Fig.4. EEG data analyzation algorithm

The first step, presented in Fig.4. a), aim to load EEG data from CSV file exported by Emotiv software, obtained by extracting the specific EEG channels data for the 9 second interval, at a 128 Hz sampling rate, related to the data collection rate provided by the Emotiv Insight neural headset. Also, we implement instructions to eliminate the mean from each channel to eliminate DC offset, to center the signals around zero with the scope to enhance the signal-to-noise ratio for accurate frequency analysis.

The second step, presented in Fig.4 b), it focusses on frequency-specific signal extraction using a fourth-order Butterworth bandpass filter in order to isolate theta and alpha waves from the preprocessed EEG data. The `filtfilt()` MATLAB function as implemented to allow the zero-phase digital filtering to be applied so that the temporal properties of these frequency bands are preserved. A detailed time vector is created so that the time aligns with the extracted signals for further analysis and to prepare the results visualization.

The Third step, presented in Fig. 4 c), implement a way of visualization and interpretation of the analyzed EEG data by showing the results in terms of different plots. This represents the original plot of EEG data composed by raw EEG signals for the interest extracting time interval, as shown below, representative for subject S1, depicting the variation of amplitude with time for all channels, which helps in identifying general trends and potential artifacts, as presented in Fig. 5.

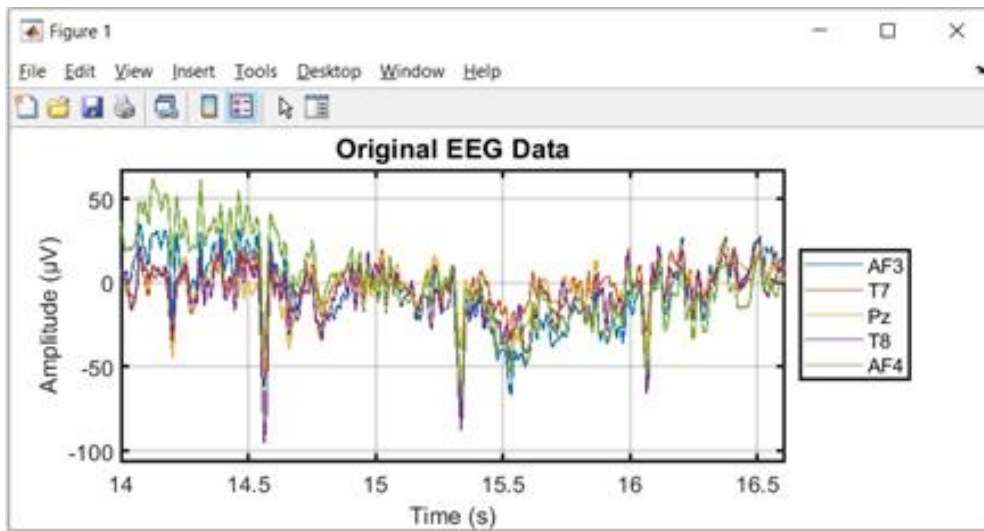


Fig.5. Sample of approximatively 2,5 second of raw EEG data from subject S1 recording

Next, the theta band activity is plotted with fixed spacing between the channels, which enables a clear representation of the filtered low-frequency brain activity associated with relaxation and cognitive states. The resulted plot for subject S1 is presented in Fig. 6.

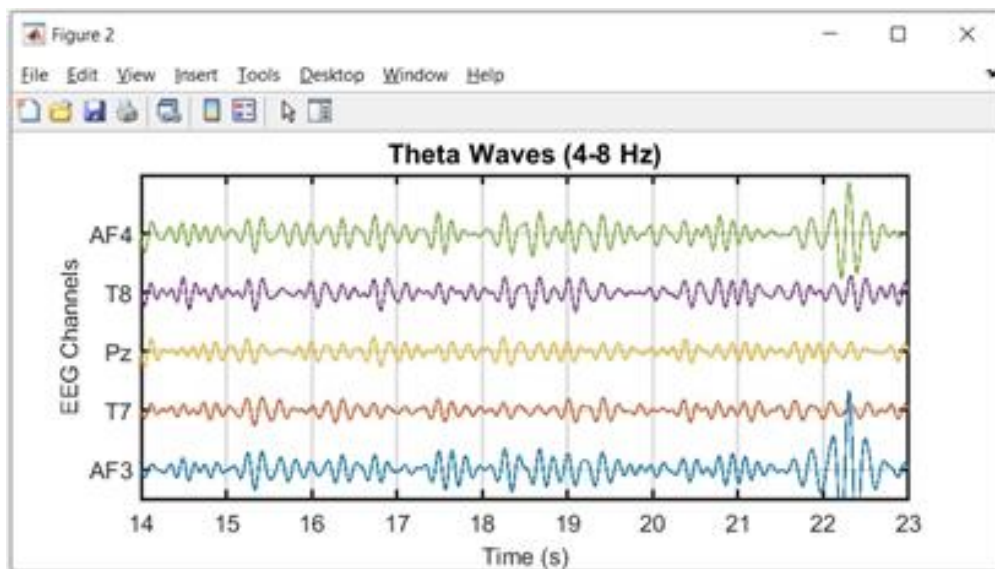


Fig.6. S1 Theta waves activity

Alpha band activity similarly shows mid-frequency oscillations linked to states of calmness and attentiveness as depicted from S1 resulted plot, presented in Fig. 7.

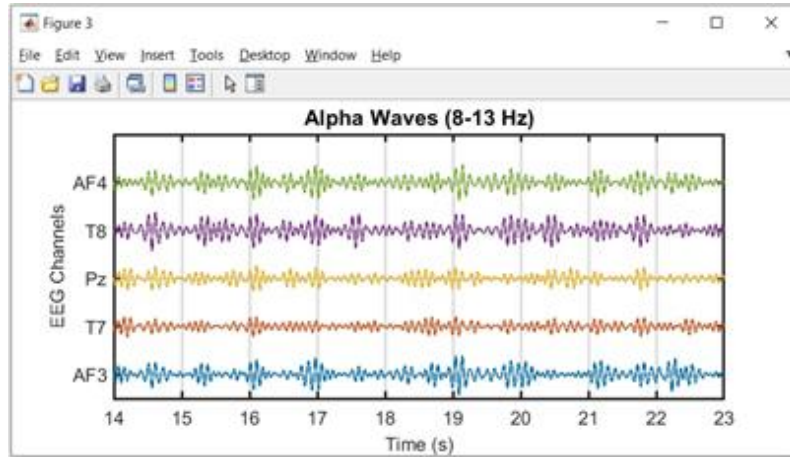


Fig.7. S1 alpha waves activity

Next, for each channel we calculate the maximum (max) and minimum (min) values for the filtered EEG data, separately for theta waves, then for alpha waves to compute the peak-to-peak amplitudes for all channels, based on the relation:

$$\text{Peak to Peak Amplitude} = \max(\text{signal}) - \min(\text{signal}) \quad (1)$$

where:

signal - refers to electroencephalogram (EEG) data gathered for each of the frequency bands (theta and alpha) across all channels.

Next, based on the result obtained by calculus, we generate a comparative bar plot, to display each peak-to-peak amplitudes of theta and alpha waves across all channels, in order to understand the relative strengths of these frequency bands, as shown for subject S1 plot in Fig.8.

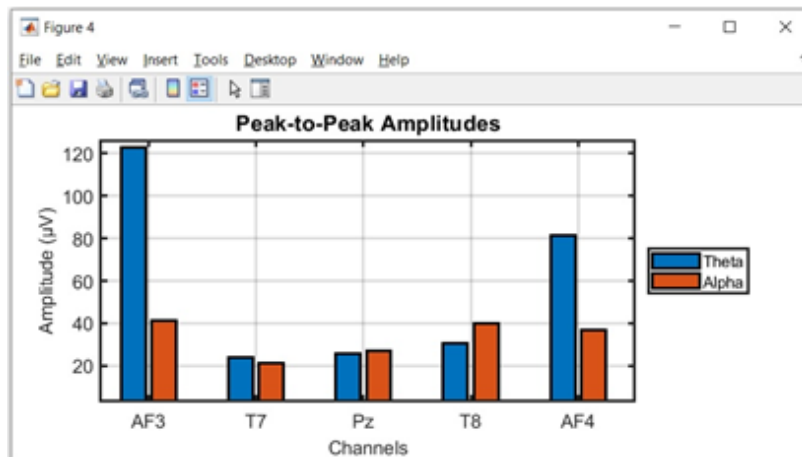


Fig.8. S1 Peak-to-peak amplitudes

Applying the same algorithm was obtained the comparative bar plot of peak-to-peak amplitudes of theta and alpha waves across all channels for the subject S2 EEG dataset, as presented in Fig. 9.

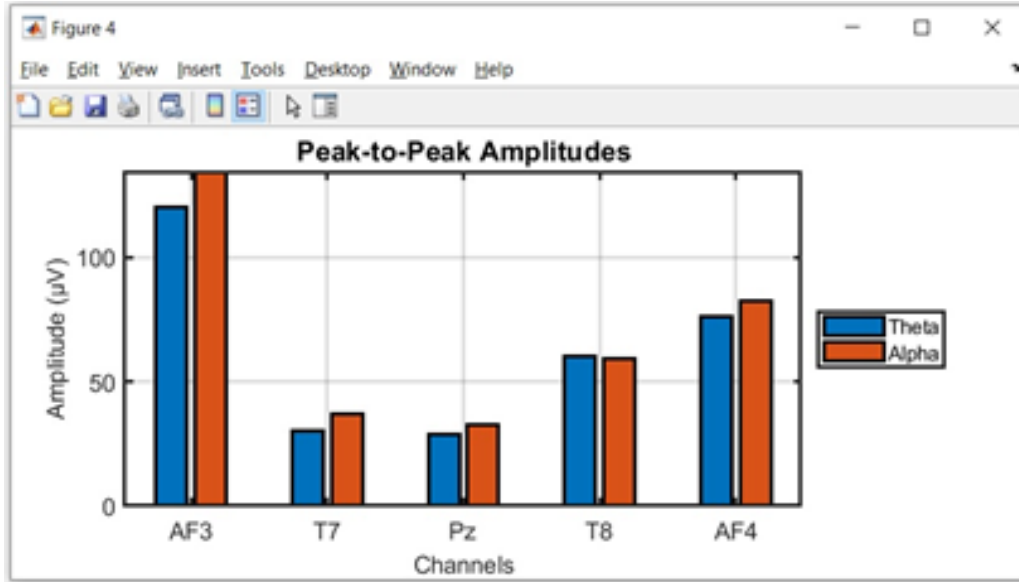


Fig.9. S2 Peak-to-peak amplitudes

Similar was obtained the peak-to-peak amplitudes plot for subject S3 dataset, as presented in Fig. 10.

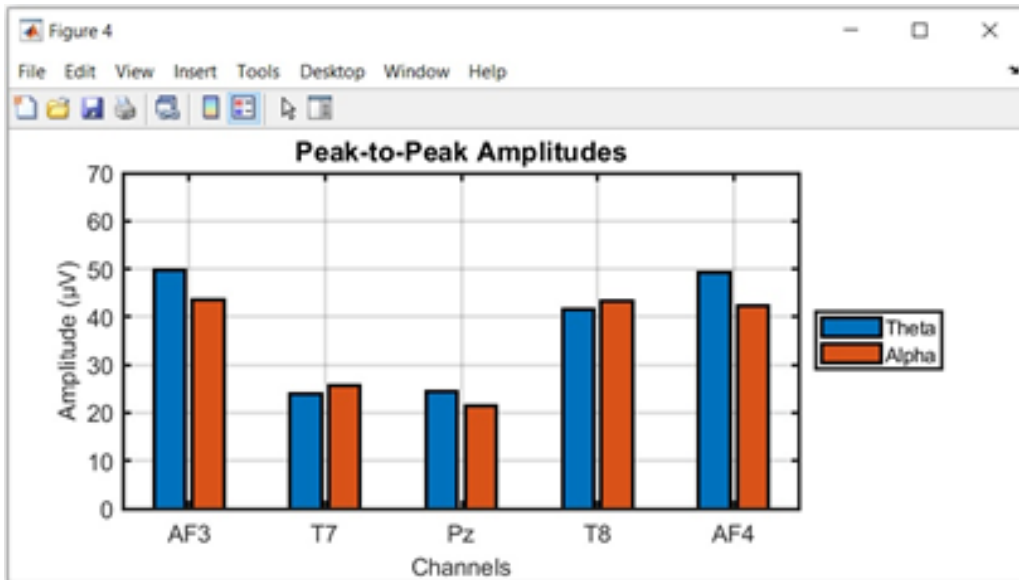


Fig.10. S3 Peak-to-peak amplitudes

5. COMPARATIVE RESULTS

The comparative analysis of theta and alpha wave patterns from each subject's dataset reveals some key findings:

- The frontal midline theta activity is most prominent on S1 and S2 dataset, indicating potentially stronger emotional processing and working memory engagement;
- The right temporal dominance across all subjects suggests consistent asymmetry in temporal lobe processing;
- The parietal activity shows lower than expected theta amplitudes, which might indicate reduced relaxation state during the open-eyes condition;
- The S2 dataset present high alpha activity in the frontal region, which differs from typical patterns where alpha should be less prominent in frontal areas.

6. CONCLUSIONS

The experimental setup using the Emotiv Insight neural headset succeeded in recording recognizable theta and alpha wave patterns. The defocused gaze protocol successfully elicited quantifiable alterations in markers associated with relaxation as well as cognitive processing. The defocused gaze protocol effectively induced measurable changes in both relaxation and cognitive processing markers.

The findings support the potential use of minimal-contact EEG devices for monitoring relaxation states. The clear differentiation between subjects suggests possible applications in personalized neurofeedback protocols.

Further study needs to be implemented to validate the result, as implementation of analysis of Signal-to-Noise Ratio (SNR), comparison across EEG channels, application of ICA decomposition to identify the neural sources and complete separate the artifactual component.

REFERENCES

- [1]. Stapleton P., Dispenza J., McGill S., Sabot D., Peach M., Raynor D., *Large effects of brief meditation intervention on EEG spectra in meditation novices*, IBRO Reports, vol. 9, pp. 290-301, 2020.
- [2]. Papanastasiou G., Drigas A., Skianis C., Lytras M., *Brain computer interface-based applications for training and rehabilitation of students with neurodevelopmental disorders. A literature review*, Heliyon, 6(9), e04250, 2020.
- [3]. Ahn M., Cho H., Ahn S., Jun S. C., *High theta and low alpha powers may be indicative of BCI-illiteracy in motor imagery*, PloS one, vol.8, no. 11, e80886, 2013.
- [4]. Rosca S.D., Leba M., Sibisanu R.C., Panaite A.F., *Brain controlled lego NXT mindstorms 2.0 platform*, In 2021 International Seminar on Intelligent Technology and Its Applications (ISITIA), pp. 325-330, 2021.
- [5]. Houssein E. H., Hammad A., Ali, A. A., *Human emotion recognition from EEG-based brain-computer interface using machine learning: a comprehensive review*, Neural Computing and Applications, vol. 34, no. 15, pp. 12527-12557, 2022.

- [6]. Nyhus E., Engel W. A., Pitfield T. D., Vakkur, I.M.W., *Increases in theta oscillatory activity during episodic memory retrieval following mindfulness meditation training*, Frontiers in human neuroscience, vol.13, 311, 2019.
- [7]. Addante R.J., Yousif M., Valencia R., Greenwood C., Marino, R., *Boosting brain waves improves memory*, Front. Young Minds, 9(605677), 2021.
- [8]. Nakamura-Palacios E.M., Façoni Júnior A.T., Anders Q.S., de Paula L. D.S.P., Zottele M.Z., Ronchete C.F., Lirio P.H.C., *Would frontal midline theta indicate cognitive changes induced by non-invasive brain stimulation? A mini review*, Frontiers in Human Neuroscience, vol. 17, 1116890, 2023.
- [9]. Pratama S.H., Rahmadhani A., Bramana A., Oktivasari P., Handayani N., Haryanto F., Khotimah S.N., *Signal comparison of developed EEG device and emotiv insight based on brainwave characteristics analysis*, In Journal of Physics: Conference Series, Vol. 1505, No. 1, pp. 012071, IOP Publishing, 2020.
- [10]. Rudoler J. H., Herweg N.A., Kahana M.J., *Hippocampal theta and episodic memory*, Journal of Neuroscience, vol. 43, no.4, pp. 613-620, 2023.
- [11]. Xie Y., Li Y., Duan H., Xu X., Zhang W., Fang P., *Theta oscillations and source connectivity during complex audiovisual object encoding in working memory*, Frontiers in Human Neuroscience, vol. 15, 614950, 2021.
- [12]. Lazarou I., Oikonomou V.P., Mpaltadoros L., Grammatikopoulou M., Alepopoulos V., Stavropoulos T.G., Bezerianos A., Nikolopoulos S., Kompatsiaris I., Tsolaki M., RADAR-AD Consortium, *Eliciting brain waves of people with cognitive impairment during meditation exercises using portable electroencephalography in a smart-home environment: a pilot study*, Frontiers in Aging Neuroscience, vol. 15, 1167410, 2023.
- [13]. Xavier G., Su Ting A., Fauzan, N., *Exploratory study of brain waves and corresponding brain regions of fatigue on-call doctors using quantitative electroencephalogram*, Journal of occupational health, vol. 62, no. 1, e12121, 2020.
- [14]. Rosca S., Leba M., Ionica A., Gamulescu, O., *Quadcopter control using a BCI*, In IOP Conference Series: Materials Science and Engineering, Vol. 294, No. 1, pp. 012048, IOP Publishing, 2018.
- [15]. Rosca S.D., Leba M., *Design of a brain-controlled video game based on a BCI system*, In MATEC Web of Conferences, Vol. 290, pp. 01019, EDP Sciences, 2019.
- [16]. Handra A.D., Popescu F.G., Păsculescu D., *Utilizarea energiei electrice: lucrări de laborator*, Editura Universitas, 2020.
- [17]. Fiță N.D., Radu S.M., Păsculescu D., Popescu F.G., *Using the primary energetic resources or electrical energy as a possible energetical tool or pressure tool*, In International conference KNOWLEDGE-BASED ORGANIZATION, vol. 27, no. 3, pp. 21-26, 2021.
- [18]. Csaszar T., Pasculescu D., Darie M., Ionescu J., Burian S., *Method for assessing energy limited supply sources, designed for use in potentially explosive atmospheres*, Environmental Engineering and Management Journal 11, no. 7, 1281-1285, 2012.
- [19]. Păsculescu D., Romanescu A., Păsculescu V., Tătar A., Fotău I., Vajai Gh., *Presentation and simulation of a modern distance protection from the national energy system*, 10th International Conference on Environment and Electrical Engineering, pp. 1-4. IEEE, 2011.
- [20]. Pasculescu D., Dobra R., Ahmad M.A., *Dosimetric Quantity System for Electromagnetic Fields Bio-effects*, International Journal of Scientific Research (IJSR) 5, no. 2, pp. 28-32, 2016.

- [21]. Popescu F.G., Păsculescu D., Păsculescu V.M., *Modern methods for analysis and reduction of current and voltage harmonics*, LAP LAMBERT Academic Publishing, ISBN 978-620-0-56941-7, pp. 233, 2020.
- [22]. Pasculescu D., Niculescu T., *Study of transient inductive-capacitive circuits using data acquisition systems.*" International Multidisciplinary Scientific GeoConference: SGEM 2, no. 1, 323-329, 2015.
- [23]. Pana L., Janusz G., Pasculescu D., Pasculescu V. M., Moraru R. I., *Optimal quality management algorithm for assessing the usage capacity level of mining transformers*, Polish Journal of Management Studies 18, no. 2, 233-244, 2018.
- [24]. Dobra R., Buica G., Pasculescu D., Leba M., *Safety management diagnostic method regarding work cost accidents from electrical power installations*. Proc. 1st Int. Conf. on Industrial and Manufacturing Technologies (INMAT), Vouliagmeni, Athens, Greece. 2013.
- [25]. Andras A., Popescu F.D., Radu S.M., Pasculescu D., Brinas I., Radu M.A., Peagu D., *Numerical simulation and modeling of mechano-electro-thermal behavior of electrical contact using comsol multiphysics*. Applied Sciences, 14(10), 4026, 2024.
- [26]. Stepanescu, S., Rehtanz, C., Arad, S., Fotau, I., Marcu, M., Popescu, F. *Implementation of small water power plants regarding future virtual power plants* 10th International Conference on Environment and Electrical Engineering, pp. 1-4, IEEE, 2011.
- [27]. Fiță N. D., Lazăr T., Popescu F. G., Pasculescu D., Pupăză C., Grigorie E., *400 kV power substation fire and explosion hazard assessment to prevent a power black-out*, International Conference on Electrical, Computer Communications and Mechatronics Engineering-ICECCME, pp. 16-18, 2022.
- [28]. Fita N.D., Obretenova M.I., Pasculescu D., Tatar A., Popescu F.G., Lazar T., *Structure and analysis of the power subsector within the national energy sector on ensuring and stability of energy security*, Annals of „Constantin Brâncuși” University of Târgu Jiu, ENGINEERING SERIES, Issue 2/2022, pp.177-186, 2022.
- [29]. Marcu M., Niculescu T., Slusariuc R. I., Popescu, F. G., *Modeling and simulation of temperature effect in polycrystalline silicon PV cells*, IOP Conference Series: Materials Science and Engineering, Vol. 133, No. 1, pp. 012005, 2016.
- [30]. Popescu F.G., Arad S., Marcu M.D., Pana L., *Reducing energy consumption by modernizing drives of high capacity equipment used to extract lignite*, Papers SGEM2013/Conference Proceedings, Vol. Energy and clean technologies, pp. 183 - 190, Albena., Bulgaria, 2013.
- [31]. Lazar T., Marcu M.D., Utu I., Popescu F. G., Pasculescu D., *Mașini electrice - culegere de probleme*, Editura Universitat, Petroșani, pp. 197, 2023.
- [32]. Petrilean D.C., Stanilă S., Dosa I., *A mathematical model for determining the dimensionless heat flux with application in mine environment*, Environmental Engineering and Management Journal, Vol.16, No. 6, 1249-1414, 2017.
- [33]. Petrilean D.C., *Compresoare eliciodale*, Editura Tehnica-Info, 2006
- [34]. Petrilean D.C., *Termodinamica tehnica si masini termice*, Editura A.G.I.R., 2010.
- [35]. Petrilean D.C., *Mathematical model for the determination of the non-stationary coefficient of heat transfer in mine works*, The 19th American Conference on Applied Mathematics (AMERICAN-MATH '13), Cambridge, MA, USA.2013.
- [36]. Petrilean D. C., *Transmiterea căldurii*, Editura Universitat, 2016.

ARC FLASH DETECTION ON PHOTOVOLTAIC SYSTEMS

CONSTANTIN BEIU¹, GEORGETA BUICĂ², ANTONOV ANCA
ELENA³, DRAGOS PASCULESCU⁴, REMUS DOBRA⁵, MIRCEA
RISTEIU⁶

Abstract: Photovoltaic (PV) systems are increasingly being used. Because of ageing and the trend toward higher DC voltage levels, incidents of DC arc faults in PV systems are becoming more common, which seriously impacts system stability and human safety. Parallel arcs draw a higher current than series arc faults, so detecting the latter is more challenging. The undetected arc faults pose a severe fire hazard to residential, commercial, and utility-scale PV systems. Such a dangerous event must be detected early to deliver electricity safely and reliably. This paper comprehensively reviews the state-of-the-art techniques for DC arc fault detection in photovoltaic systems (PV). Different methods and the features used for detection are discussed and compared in detail. This paper also emphasizes the importance of DC arc fault simulation for characteristics study and fault diagnosis purposes. Several DC arc fault models have been reviewed and compared.

Key words: risk, evaluation, safety, solar panel.

1. INTRODUCTION

With the advancement of technology and increasing realization of pollution in the environment, clean, renewable sources such as solar energy are gradually replacing traditional fossil fuels. Solar power installation is increasing throughout the world. Residential rooftop solar panels and grid-connected photovoltaic (PV) generation will support the main utility networks and microgrids. The increasing amount of PV systems and the trend toward increasing DC voltage levels can create DC arc faults. Because of the deterioration of cables, connectors, conductors, and other system components caused

¹ Eng., cbeiu@protectiamuncii.ro

² Ph.D., Eng.

³ Ph.D., Eng.

⁴ Ph.D., Eng.

⁵ Ph.D., Eng.

⁶ Ph.D., Eng.

by long-time weathering and ageing effects, without adequate and proper maintenance, the possibility of DC arc occurrence is expected to increase sharply[1,4].. It should also be stressed that, unlike AC arcing, the absence of current zero-crossing makes DC arcs more sustainable [21], [23], [26], [29], [31].

An example of a PV system and different types of arc faults are shown in Fig.1.

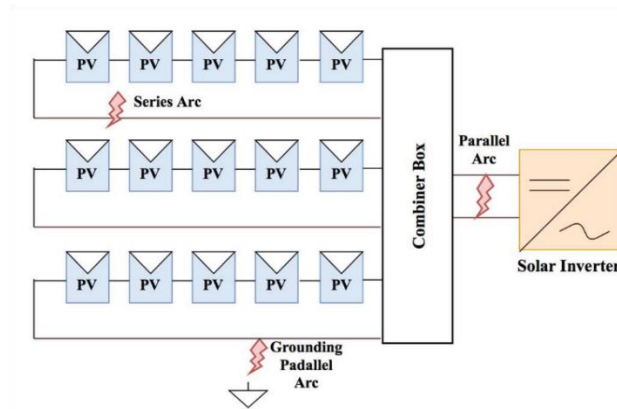


Fig.1. An example of PV systems and arc fault types

DC arcing occurs across small gaps in connections. Bad joints decrease the cross-section's contact area, effectively increasing the resistance and, thus, the heat loss. The higher operating temperature accelerates the deterioration process of the connecting point, which leads to a loose connection [5]. Subsequently, the point of discontinuity forms a tiny gap that the current could keep flowing. When the electric field between two electrodes exceeds about (in normal conditions), air starts to ionize and plasma is developed, which will finally form a series arc [37]. Due to the extra impedance contributed by the arc, the fault current (lower than the standard operating current level) will not be sufficient to melt the fuse or activate the overcurrent protection devices [6], [7], [38]. Specifically, the series arc fault will not draw an inverse current like a parallel arc fault [8], and the average load current contributes to the total fault current. With the increased impedance injected by arc fault, the current level will go down and thus cannot reach the level to melt the fuse [9], [22], [24], [28], [32].

Furthermore, the current level will return to normal because the inverter operates for maximum Power Point Tracking (MPPT). At the same time, the arcing fault still exists, presenting more challenges to DC arcing fault detection. As a result, the heat energy generated by the arc over a long duration could damage system components severely, seriously threatening system stability and human safety [10], [25], [27], [30].

2. ELECTRIC SHOCK AND ARC FLASH HAZARDS

There is a real danger of electric shock to anyone entering any of the electrical cabinets, such as combiner boxes, disconnect switches, inverters, or transformers, or

otherwise coming in contact with voltages over 50 Volts. Another electrical hazard is an arc flash, an energy explosion that can occur in a short circuit situation. This explosive release of energy causes a flash of heat and a shockwave, both of which can cause severe injury or death. Properly trained and equipped technicians and electricians know how to install, test, and repair PV systems safely. However, there is always some risk of injury when hazardous voltages and/or currents are present. Untrained individuals should not attempt to inspect, test, or repair any aspect of a PV system due to the potential for injury or death due to electric shock and arc flash [33], [35], [36].

The possibility of fires resulting from or intensified by PV systems may trigger concern among the general public and firefighters. However, concern over solar fire hazards should be limited because only a tiny portion of materials in the panels are flammable, and those components cannot self-support a significant fire. Flammable components of PV panels include the thin layers of polymer encapsulates surrounding the PV cells, polymer backsheets (framed panels only), plastic junction boxes on the rear of the panel, and insulation on wiring. The rest of the panel comprises non-flammable components, notably including one or two layers of protective glass that comprise over three-quarters of the panel's weight [34].

The heat from a small flame is inadequate to ignite a PV panel, but the heat from a more intense fire or energy from an electrical fault can ignite a PV panel [11]. Improving understanding of the PV-specific risks, safer system designs, and updated fire-related codes and standards will continue to reduce the fire risk caused by PV systems.

3. CHARACTERISTICS OF DC ARC

Understanding and studying the characteristics of an electric arc is very important. DC arc exhibits nonlinear features, and their characteristics vary with arc length, electrode material, electrode geometry, and current level [12]. The quasi-static arcing V-I characteristic with a fixed arc length is shown in Fig. 2. It can be seen that in the lower current region, the smaller the current, the larger the voltage, where the power of the arc ($P_{arc} = V_{arc}I_{arc}$) tends to remain the same; while in the higher current region, with the increasing current, the voltage remains approximately unchanged. The red line identifies those two regions, which is the so-called current transition point line. Stokes and Oppenlander carried out the most exhaustive experiment that covered a wide range of current levels and arc lengths with series electrodes. The transition current is then defined by (1).

Furthermore, based on the huge data set, the V-I characteristic in the “constant voltage” region is defined in (2) [13].

$$I_{arc} = 10 + 0.2L \quad (1)$$

$$P_{arc} = (20 + 0.534L)I_{arc}^{1.12} \quad (2)$$

where L is arc length in mm. It should be noted that the arc gap width is not equal to actual arc length, and the additional impedance injected into the circuit is contributed by arc length.

The current level in the PV string is not high, whereas it is much higher in the combiner box and the DC side of the inverter (the current level at the DC side of the inverter could go up to several thousand amps in large PV utilities).

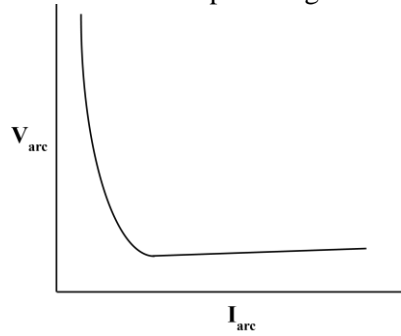


Fig.2. Arcing voltage and current characteristic

Figure 2 shows the quasi-static $V-I$ characteristic for a “fixed” length arc. In the low-current region (identified by the dotted line), the arc voltage drops as the arc current increases; as a result, the arc power ($P = V I$) tends to remain relatively constant in this region. For “larger” currents, the arc voltage increases slightly with increasing arc current. (A transition current, which defines the boundaries between the low- and high-current regions, is presented later). With wall-stabilized arcs, the arc plasma is only partially ionized in the low-current region, whereas the plasma becomes fully ionized above some threshold current [14]. A similar transition in the level of ionization is observed for free burning arcs.

4. DC ARC FLASH HAZARD CALCULATIONS

At the present time, methods for calculating the DC arc flash hazard are not directly addressed in any standard. IEEE 1584 2018 IEEE Guide for Arc Flash Hazard Calculations [15] only addresses the ac arc flash hazards.

Other few important technical papers were published that began to change the understanding of dc arc flash [16 - 19]. These papers provide a theoretical approach to DC incident energy calculations.

Calculating the incident energy for a dc arc flash begins with application of Ohm’s law:

$$I = \frac{U}{R} \quad (3)$$

Where:

I = Current in amperes

U = Voltage in volts

R = Resistance in ohms

By including the dc arc resistance as part of the dc circuit model illustrated in Figure 3, the arcing current can easily be determined. This circuit diagram is of a battery string and includes the DC voltage, DC battery resistance, conductor resistance and dc arc resistance. As part of the overall process, the DC arc resistance must also be calculated since it is usually not known.

Once all of the resistance values have been determined, the dc arcing current, $I_{dc\ arc}$ can be calculated by [12]:

$$R_{arc} = [(20 + 0.534 \times L)] / I_{dc\ arc}^{0.88} \quad (4)$$

Where:

R_{arc} = resistance of the arc in ohms

L = conductor gap distance in millimeters

$I_{dc\ arc}$ = dc arcing current

In order to calculate the arc resistance using this equation, the conductor gap distance L and the dc arcing current must be known. The gap distance is specified by the user however, in order to determine the dc arcing current, the arc resistance must already be known. To solve this problem, an iterative solution is used. This requires making an initial assumption of the dc arcing current. A the initial assumption is that the dc arcing short circuit current is 50% of the dc bolted short circuit current.

Once this initial assumption is made, the dc arc resistance can be calculated which is then used to re calculate the dc arcing current. The “new” dc arcing current can then be used to re calculate the dc arc resistance. This process continues until the dc resistance and dc arcing current values no longer change significantly and converge to a final answer.

Figure 3 illustrates the circuit that is used as an example for calculating the dc arc resistance and the dc arcing current. The calculation process begins by determining the dc bolted short circuit current first. This requires taking the dc voltage (V_{dc}) and dividing by the known impedances of the conductor and battery string.

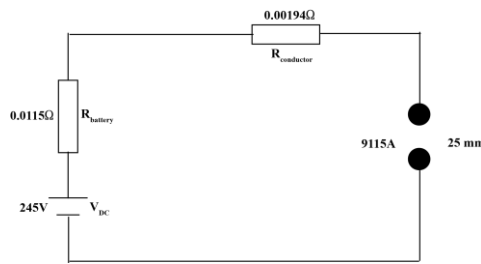


Fig.3. DC Arc Flash Example

First iteration is for the bolted dc short circuit current using the values from Figure 3. For the bolted case, R_{arc} and the conductor gap distance are ignored and only the resistance of the battery string and conductor are used.

$$I_{dc\ bolted} = U_{DC} / (R_{battery} + R_{conductor}) \quad (5)$$

$$I_{dc\ bolted} = 245 / (0.0115 + 0.00194) = 18229A \quad (6)$$

$$I_{arc} = 0.5 \times 18229A = 9115A \quad (7)$$

To calculate R_{arc} , equation 4 is used. For the first iteration, $R_{arc} = 0.01051$
For the next iteration, equation 5 becomes:

$$I_{dc\ arc} = U_{DC} / (R_{battery} + R_{conductor} + R_{arc}) \quad (8)$$

Table 1 shows the results for ten iterations.

Table 1. Results of $I_{dc\ arc}$ and R_{arc}

Iteration	$I_{dc\ arc}$ (A)	R_{arc} (Ω)
1	9115	0,010927667
2	10054	0,010023651
3	10442	0,00969567
4	10590	0,009576304
5	10645	0,009532811
6	10665	0,009516958
7	10672	0,009511178
8	10675	0,00950907
9	10676	0,009508302
10	10676	0,009508022

Figure 4 illustrates the final results.

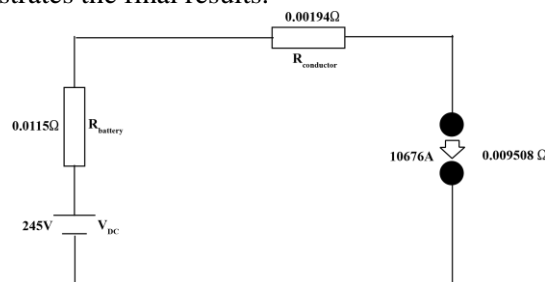


Fig.4. Final results of the iteration

Once the dc arcing current and dc arc resistance have been determined, the power in the arc can be calculated by:

$$P_{arc} = I_{dc\ arc}^2 \times R_{arc} \quad (9)$$

$$P_{arc} = 1.084 \text{ kW} \quad (10)$$

Where:

P_{arc} = power in the arc in watts

$I_{dc\ arc}$ = dc arcing circuit current in amperes

R_{arc} = dc arc resistance in ohms

The energy in the arc is a function of power and time. Therefore the energy in the arc can be calculated by:

$$E_{arc} = P_{arc} \times t_{arc} \quad (11)$$

Where:

E_{arc} = arc energy in watt x seconds or Joules

t_{arc} = arc duration in seconds

The duration of the arc flash will either be dependent on the clearing time of an upstream protective device operating or the reaction time of a person jumping away from the hazard. IEEE 1584 presently suggests that a maximum time of 2 seconds may be used based on the reaction time and assuming there are reasonable conditions for a person to escape. Thus, for arc duration of 0.3 s, the arc energy is 325 kJ.

4.1. DC Incident Energy Calculations in open air

Similar to the IEEE 1584 calculation methods, consideration must be given to whether the dc arc flash occurs in open air or in an enclosure/box. If the dc arc flash occurs in open air, the energy will radiate spherically in all directions and the person would be exposed to a smaller portion of the energy. If the event occurs in an enclosure, the incident energy exposure will be greater since it is focused out of the box opening.

According to [12], the incident energy for an arc flash in open air at a specific distance can be calculated based on the following equation:

$$E_{i\ air} = E_{arc} / (4\pi \times d^2) \quad (12)$$

Where d is distance from the arc in mm

Using the dc arcing short circuit current and arc resistance that was previously calculated, the incident energy can be calculated. This requires knowing the working distance from the prospective arcing location to the worker as well as knowing the duration of the arc flash. For this calculation, a maximum arc duration of 0.3 seconds was used. This value would normally be defined by the characteristic of an upstream protective device. A working distance of 18 inches (457 mm) was used which is a “typical” value obtained from IEEE 1584 [19]. In case of open air, the incident energy is 0.1238 J/mm² or 2.96 cal/cm².

4.2. DC arc flash in an enclosure / box

If the dc arc flash occurs in an equipment enclosure, the energy will be directed out of the open end of the box. For this calculation, the DC arc models defined in [20] are used.

According to this paper, the equation for determining the incident energy from a dc arc flash being focused out of an enclosure is:

$$E_{i\ box} = k \times E_{arc} / (a^2 + d^2) \quad (13)$$

Where:

$E_{i\ box}$ = incident energy from an arc flash in a box at distance d in J/mm²

E_{arc} = arc energy in Joules

d = distance from the arc source in mm

a and k are obtained from optimal values defined in [20].

For a panel board, a = 100 and k = 0.127.

Using values that were previously calculated for $I_{dc\ arc}$ and R_{arc} , the incident energy will now be calculated based on the arc flash occurring in a box/enclosure. The enclosure is assumed to be a panelboard and the same working distance and arc duration from the earlier example are used.

In case of a panel board, the incident energy is 0.189 J/mm² or 4.50 cal/cm².

5. CONCLUSION

The models presented in this paper have been based on tests conducted over time by researchers in different countries and under very different protocols. The V –I characteristic is inversely proportional and nonlinear at low current levels. At high arcing-current levels, the analysis in this paper has shown that the arc-resistance voltage drop approaches a constant value. A method has been presented to estimate the incident energy levels possible during an arcing fault to quantify the risks associated with high-current DC systems. Results from a case study demonstrated that the risks associated with high current dc systems may be significant.

Arcing behaviour is highly variable, and the existing DC arc models cannot accurately and reliably assess all the characteristics of DC arcs. Additional arc testing is needed to develop more accurate V –I characteristics and better DC-arc resistance models. Extensive testing in a controlled environment is needed to study the incident energy levels associated with DC arcing faults. A hazard risk assessment is needed to identify where dc arcing faults might be initiated in industrial power systems. The relative severity of the arc flash hazard posed by different types of DC power equipment must be identified.

REFERENCES

- [1]. Lu S., Phung B. T., Zhang D., *Study on DC Series Arc Fault in Photovoltaic Systems for Condition Monitoring Purpose*, Australasian Universities Power Engineering Conference (AUPEC), Melbourne, VIC, Australia, November, 2017.
- [2]. <https://www.mrs.org/spring-2018-symposium-sessions-detail?code=EN16>
- [3]. Lu S., Phung, B., Zhang, D., *Study on DC series arc fault in photovoltaic systems for condition monitoring purpose*, 2017.
- [4]. Lu S., Phung B. T., Zhang D., *A comprehensive review on DC arc faults and their diagnosis methods in photovoltaic systems*, Renewable and Sustainable Energy Reviews, 89, 2018.
- [5]. Umar A. S., Khalid Hamid Y., *Summaries of Causes, Effects and Prevention of Solar Electric Fire Incidents*, International Journal of Engineering and Applied Physics, 3, 2023.

- [6]. **Pana L., Janusz G., Pasculescu D., Pasculescu V. M., Moraru R. I.,** *Optimal quality management algorithm for assessing the usage capacity level of mining transformers*, Polish Journal of Management Studies 18, no. 2, 233-244, 2018.
- [7]. **Umar A. S., Khalid Hamid Y.,** *Summaries of Causes, Effects and Prevention of Solar Electric Fire Incidents*, International Journal of Engineering and Applied Physics (IJEAP) 3, 2023.
- [8]. **Strobl C., Meckler P.,** *Arc faults in photovoltaic systems*. Proceedings of the 56th IEEE Holm Conference on Electrical Contacts, 2010.
- [9]. **Earley M. W., Sargent J. S.,** *National Electrical Code 2011 Handbook, 12th ed.* National Fire Protection Association, 2010.
- [10]. **Wang Z., McConnell S., Balog R. S., Johnson J.,** *Arc Fault Signal Detection-Fourier Transformation vs. Wavelet Decomposition Techniques using Synthesized Data*. IEEE 40th Photovolt. Spec. Conf., 2014.
- [11]. **Yang H.Y., Zhou X.D., Yang L.Z., Zhang T.L.,** *Experimental Studies on the Flammability and Fire Hazards of Photovoltaic Modules*, Materials 8(7), 4210-4225, 2015.
- [12]. **Ammerman R. F., Gammon, T., Pankaj K.,** *Models and Incident-Energy Calculations*, IEEE Trans. Ind. Appl., 46, 1810-1819, 2010.
- [13]. **Stokes A. D., Oppenlander W. T.,** *Electric arcs in open air*, J. Phys. D, Appl. Phys., 24, 26–35, 1991.
- [14]. **Jones G. R.,** *High Pressure Arcs in Industrial Devices*. Cambridge Univ. Press: London, 1988.
- [15]. **IEEE 1584** *Guide for Arc Flash Hazard Calculations*, 2018.
- [16]. **Doan D. R.,** *Arc Flash Calculations for Exposures to DC Systems*, IEEE Transactions on Industry Applications, 46, 6, 2299-2302, 2010.
- [17]. **Das J. C.,** *Arc-Flash Hazard Calculations in LV and MV DC Systems—Part I: Short-Circuit Calculations*, IEEE Transactions on Industry Applications, 50, 3, 1687–1697, 2014.
- [18]. **Das J. C.,** *Arc-Flash Hazard Calculations in LV and MV DC Systems Part—II: Analysis*, IEEE Transactions on Industry Applications, 50, 3, 1698–1705, 2014.
- [19]. **Klement K.,** *DC Arc Flash Studies for Solar Photovoltaic Systems: Challenges and Recommendations*, IEEE Transactions on Industry Applications, 51, 5, 4239–4244, 2015.
- [20]. **R. Wilkins, M. Allison, Lang M.,** *Improved method for arc flash hazard analysis*, IEEE Industrial and Commercial Power Systems Technical, 2004.
- [21]. **Petrilean D.C.,** *Mathematical model for the determination of the non-stationary coefficient of heat transfer in mine works*, The 19th American Conference on Applied Mathematics (AMERICAN-MATH '13), Cambridge, MA, USA.2013.
- [22]. **Petrilean D.C.,** *The study of energy losses through case helical screw compressor*, Bulletin of the Transilvania University of Brasov, Proceedings of the internationally attended national conference on thermodynamics, 2009.
- [23]. **Petrilean D.C., Irimie. S.I.,** *Carrying out and analysing the real and optimum energetic balance of thermal consumers issuing from the outline of the balance SC SEWS Romania SRL Alba Iulia*, Research Scientific Report, University of Petroșani, 2013.
- [24]. **Petrilean D.C., Irimie. S.I.,** *Solutions to increase the energetic efficiency of pneumatic mining distribution networks*, 9 th International Conference on Energy, Environment, Ecosystems and Sustainable Development (EEESD'13), Lemesos, Cyprus, 2013.
- [25]. **Lazar T., Marcu M.D., Utu I., Popescu F. G., Pasculescu D.,** *Mașini electrice - culegere de probleme*, Editura Universitat, Petroșani, pp. 197, 2023.

[26]. **Petrilean D.C., Popescu D.F.**, *Temperature Determination in Hydrotechnical Works as a Variable of the Energy Change Between Air and Environment*, WSEAS TRANSACTIONS on HEAT and MASS TRANSFER, 2008.

[27]. **Dosa I., Anutoiu S., Petrilean D.C., Urdea G.**, *Influence of ambient temperature on the efficiency of underground spot cooling system*, MATEC Web of Conferences, Volume 354, 2022

[28]. **Arad, S., Marcu, M., Pasculescu D., Petrilean D.C.** *Aspects of the electric arc furnace control*, Proceeding. of international symposium advanced engineering & applied management, Faculty of Engineering Hunedoara, 2010.

[29]. **Petrilean D.C.**, *Cercetări privind îmbunătățirea eficienței producerii și utilizării energiei pneumatice în industria minieră*, Investigation regarding the improving of efficiency for producing and using the pneumatic energy in the mining industry), PhD thesis, University of Petroșani, 2005.

[30]. **Andras A., Popescu F.D., Radu S.M., Pasculescu D., Brinas I., Radu M.A., Peagu D.**, *Numerical Simulation and modeling of mechano–electro–thermal behavior of electrical contact using comsol multiphysics*. Applied Sciences, 14(10), 4026, 2024.

[31]. **Marcu M., Niculescu T., Slusariuc R. I., Popescu, F. G.**, *Modeling and simulation of temperature effect in polycrystalline silicon PV cells*, IOP Conference Series: Materials Science and Engineering, Vol. 133, No. 1, pp. 012005, 2016.

[32]. **Stepanescu, S., Rehtanz, C., Arad, S., Fotau, I., Marcu, M., Popescu, F.** *Implementation of small water power plants regarding future virtual power plants* 10th International Conference on Environment and Electrical Engineering, pp. 1-4, IEEE, 2011.

[33]. **Fîță N. D., Lazăr T., Popescu F. G., Pasculescu D., Pupăză C., Grigorie E.**, *400 kV power substation fire and explosion hazard assessment to prevent a power black-out*, International Conference on Electrical, Computer Communications and Mechatronics Engineering-ICECCME, pp. 16-18, 2022.

[34]. **Fita N.D., Obretenova M.I., Pasculescu D., Tatar A., Popescu F.G., Lazar T.**, *Structure and analysis of the power subsector within the national energy sector on ensuring and stability of energy security*, Annals of „Constantin Brâncuși” University of Târgu Jiu, ENGINEERING SERIES, Issue 2/2022, pp.177-186, 2022.

[35]. **Handra A.D., Popescu F.G., Păsculescu D.**, *Utilizarea energiei electrice: lucrări de laborator*, Editura Universitas, 2020.

[36]. **Fîță N.D., Radu S.M., Păsculescu D., Popescu F.G.**, *Using the primary energetic resources or electrical energy as a possible energetical tool or pressure tool*, In International conference KNOWLEDGE-BASED ORGANIZATION, vol. 27, no. 3, pp. 21-26. 2021.

[37]. **Popescu F.G., Păsculescu D., Păsculescu V.M.**, *Modern methods for analysis and reduction of current and voltage harmonics*, LAP LAMBERT Academic Publishing, ISBN 978-620-0-56941-7, pp. 233, 2020.

[38]. **Pasculescu D., Niculescu T.**, *Study of transient inductive-capacitive circuits using data acquisition systems.* International Multidisciplinary Scientific GeoConference: SGEM 2, no. 1, 323-329, 2015.

This article was reviewed and accepted for presentation and publication within the 11th edition of the International Multidisciplinary Symposium "UNIVERSITARIA SIMPRO 2024".

APPLICATION OF ALTERA PROGRAMMED LOGIC INTEGRATED CIRCUIT IN EFFICIENT ASYNCHRONOUS DRIVE SYSTEM

VALERY BORODAY¹, OLGA NESTEROVA², VLADYSLAV NAIDA³

Abstract: The work is a logical continuation of the development of an energy-efficient asynchronous drive [11], which is based on previous theoretical studies. A practical implementation based on the ALTERA programmable logic circuit (PLC) is proposed, which will contribute to the spread of energy-saving and energy-saving technologies under the condition of a deep change in the load of mechanisms of long-term operation and minimal costs for control equipment.

Key words: asynchronous drive, system of energy-efficient application, adjustable AC drive, ALTERA programmable logic integrated circuits.

1. INTRODUCTION

It is known that most electromechanical installations of mechanisms of long-term operation operate at full voltage of the power supply network without the use of regulation devices. This is accompanied by significant energy consumption, especially in unloaded modes, which may occur due to chaotic load changes. Today's conditions are such that they do not allow significant consumption of electricity due to its significant cost [1].

The best way to save energy is to use industrial frequency converters. Analysis of the cost of such equipment, especially of the world's leading manufacturers, shows its significant value, which is not always acceptable for average consumers.

The purpose of the paper is to find simple and reliable methods and to propose hardware and software solutions for the power regulation system of asynchronous drives of mechanisms of long-term operation, which will ensure greater efficiency in the use of electricity with a significant reduction in capital costs for regulatory equipment.

¹ *Ph.D., Assoc. Prof. Eng., Dnipro University of Technology, boroday_va2@ukr.net*

² *Ph.D., Assoc. Prof. Eng., Dnipro University of Technology, olnesterova1@rambler.ru*

³ *Ph.D., Assoc. Prof. Eng., Dnipro University of Technology*

2. LITERATURE REVIEW

The authors of the source [2] prove that the maximum energy efficiency of asynchronous drives of S1 operating mode mechanisms can be achieved due to a comprehensive approach in solving the set goal. Therefore, it makes sense to analyse the entire range of component of electromechanical systems of this type.

High-efficiency motors [3], despite their obvious energy advantages, are also endowed with disadvantages: significant costs in technological units; the method of frugality takes place only with a small variable load and an average moment of resistance close to the nominal one; the efficiency of the electric drive system is typical with a properly adjusted power channel.

Energy saving in network lines and power transformers involves the absence of the circulation of reactive currents that arise as a result of powering electric motors. Currently, the best compensation result is provided by the presence of RC local circuits, which additionally improve the switching modes of the control keys [4-6]. The disadvantage of systems of this type is a significant initial cost.

The use of converters with different topologies of the power part or power correctors gives a good effect of energy efficiency. At the same time, systems of this type have a significant level of capital investment [7], [8].

An evaluation of the efficiency of the frequency converter and the softstarter [9] found that their joint operation with pumping units provides a ratio of indicators of 12 to 3. It should be noted that the cost of the frequency converter exceeds the price of the parametric converter by about two times.

A system [10] that provides the desired steady-state energy efficiency can be a full-fledged substitute for the frequency converter. Its advantage is simplicity and affordable cost while simultaneously maintaining high values of power coefficients and useful system performance.

Control systems [1], [11] are a complete device for correcting the consumed power depending on the amount of load. They have desirable properties in terms of cost and technical characteristics, but the proposed system is implemented in a design form and is not adapted to conventional circuit technology. Thus, the task of the publication is to show the practical possibility of implementing the idea [1], [11] on the basis of modern FPGA schemes.

3. THE MAIN PART

The idea underlying the work is presented in the source [11]. Its essence is in the organization of the power supply of the electric machine according to the principle - at each moment of time, the amount of power that does not exceed the amount necessary to overcome the current load is supplied to the motor. At the same time, the proposed system provides two main modes: nominal, for a load close to the nominal, and efficient, for a load less than 60% of the nominal. In addition, transitional modes (start-up and transitions from mode to mode) are carried out from the intensity selector, which helps to avoid dynamic overloads, both in the mechanical and electrical parts of the electric drive. The effective mode uses the method of simultaneous reduction of voltage and frequency to the level of 0.5 nominal and at the same time maintains the

sinusoidal form of the voltage, which is an important factor in the operation of the converter for an active-inductive load.

Let's consider the scheme of practical implementation of the regulation system, which is built based on the ALTERA PLC of the EMR 7032 LS-44-6 series (Fig. 1).

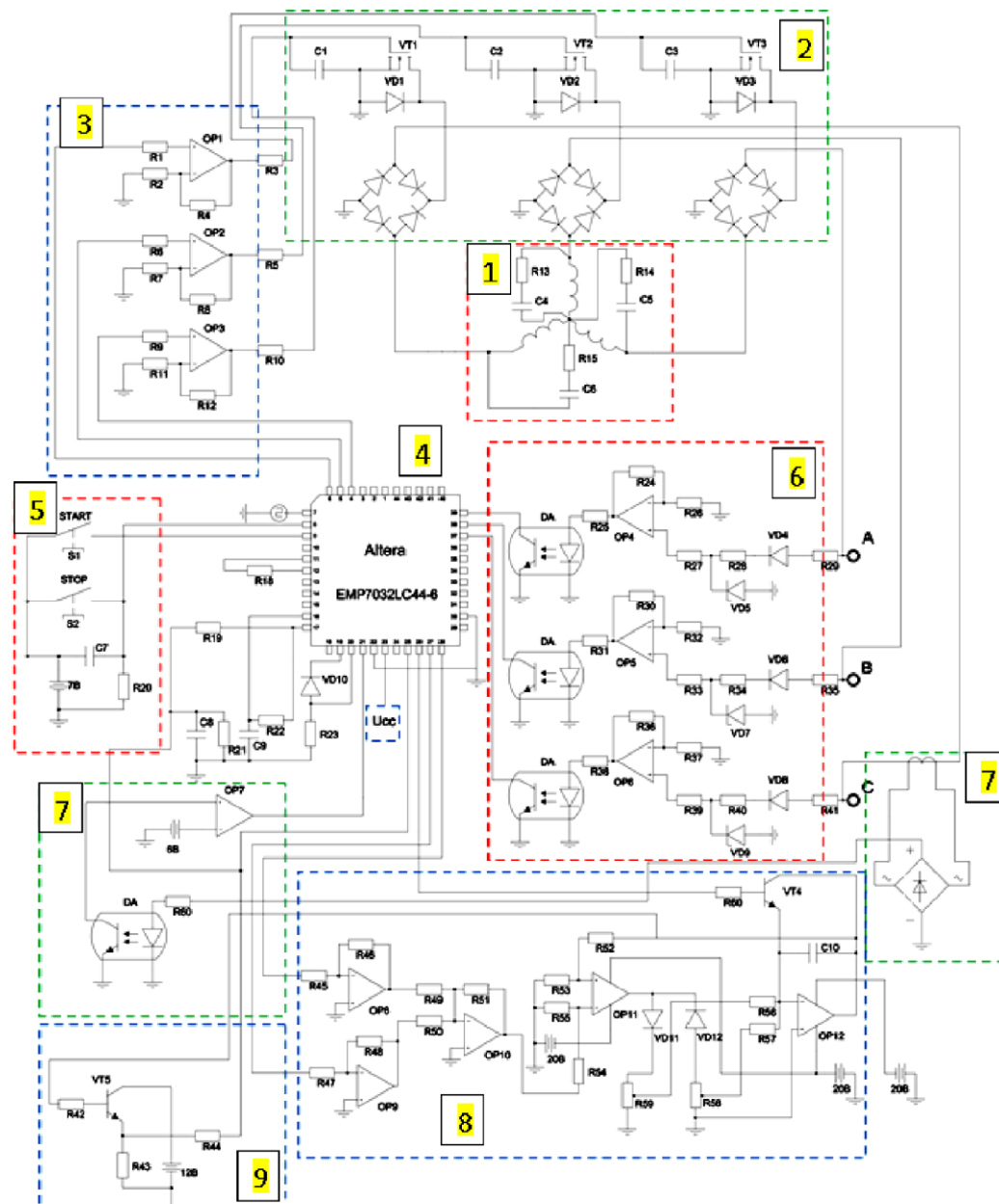


Fig. 1. Scheme of the control machine

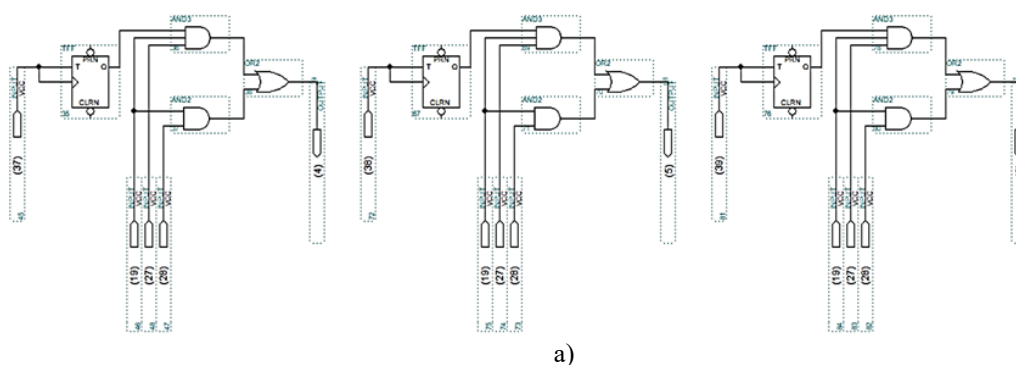
It includes a three-phase power supply marked with the letters ABC; asynchronous motor 1 with circuits of local reactive power compensation; voltage conversion link 2; power amplifiers 3; PLC 4, push-button post with forced shutdown system 5, synchronization unit of effective mode with optical solutions 6; continuous load control system 7; the voltage level matching system and the intensity setter 8 and the signal amplifier for the task of changing the spacing 9. The operation of the efficient power supply system is ensured by an algorithm that performs the soft start function every time the start button is turned on. Control of the degree of load is carried out by continuous measurement of the phase current and its comparison with the value of the limit-determined level, after which the nominal mode is automatically switched to the effective mode and vice versa. Such transitions are limited to the corresponding time intervals, which reduces the dynamics of the system. At the same time, in the mode, the effective frequency is regulated by passing every second period of the mains voltage, and the voltage level is regulated by the PWM method. Stopping the system - pressing the stop button.

A feature of the design of the ALTERA FPGA of the EMR 7032 LS-44-6 series is the need to configure it according to a previously developed electronic circuit project, which is built on the basis of separate logical elements. The FPGA configuration program is shown in Fig. 2. It includes three independent fragments of schemes. Their development and research was carried out on the basis of the electronic laboratory Multisim. This approach was adopted in order to clearly and reliably make sure of performance of the designed circuit, and the final check of the FPGA project is performed in the MAX+II software shell.

The fragment of Fig. 2, a) provides for the formation of pulses of permission to skip every second period of the mains voltage depending on the synchronization signal of Fig. 1, module 6 of the "effective" mode. In addition, this system is the performing element of switching between "nominal-effective" modes.

The auxiliary elements of the circuit in Fig. 2, b) are components of the generator of controlled splicing, which is designed to regulate the voltage level at start-up and change modes depending on the continuous control of the current sensor of the motor load.

The general control system of Fig. 2, c) communicates the operator through the button post of Fig. 1, module 5 with the modules that were described above.



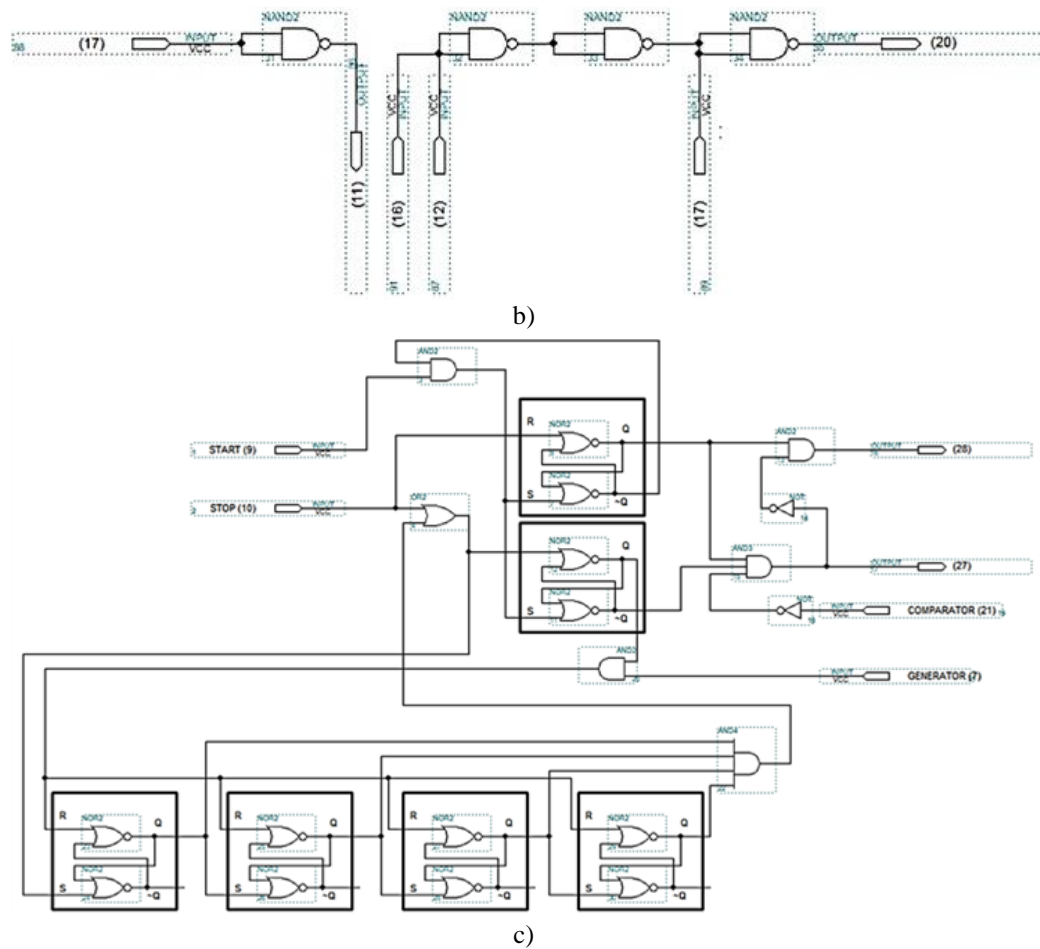
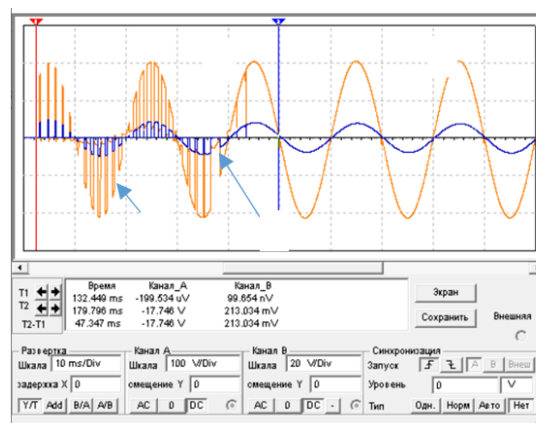
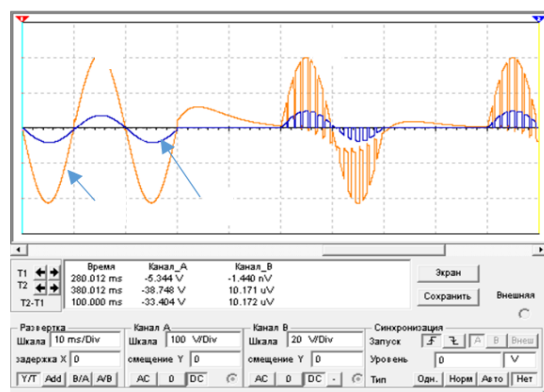


Fig. 2. ALTERA FPGA configuration program of the EMR 7032 LS-44-6 series



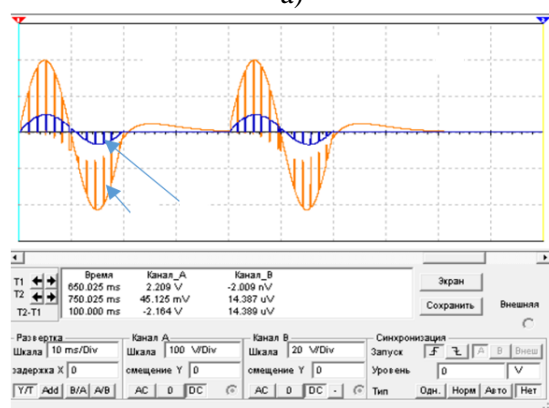
A – smooth start; B is nominal

APPLICATION OF ALTERA PROGRAMMED LOGIC INTEGRATED CIRCUIT IN EFFICIENT ASYNCHRONOUS DRIVE SYSTEM

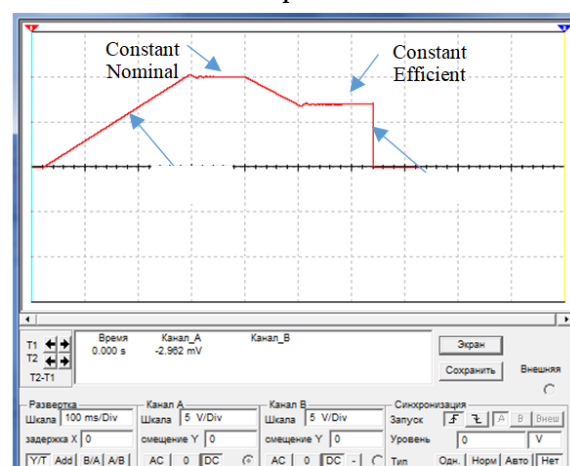


B – efficient

a)



Γ – Stop mode



Intensity selector output

b)

1 - voltage (scale 100 V/div); 2 – current (scale 20 A/division)

Fig. 3. Modeling modes [1]: a) – startup, nominal and efficient; b) –turned off.

The effective drive control system was tested on models in the Multisim environment, Fig. 3. Its ability to obtain a positive effect is confirmed by time diagrams and control of power consumption for different load levels. With a deep load change, the consumption of active power can be saved up to 40%, and reactive power can be saved up to 51%.

The scientific novelty of the work consists in proving the fundamental possibility of practical implementation of the declared control principle by means of PLSS, which will ensure rational energy consumption under the condition of the minimum cost of the control equipment.

4. CONCLUSIONS

The proposed schematic implementation of the automaton of efficient energy consumption will allow to significantly reduce losses, both for industrialists, housing, and communal services, and for any ordinary citizen, which is especially relevant during martial law.

REFERENCES

- [1]. **Kovaliov O., Nesterova O., Borodai V.**, *Automatic control of the efficiency of an asynchronous drive with a soft start function*. Microsyst Electron Acoust, vol. 26, no. 2 2021.
- [2]. **Kozjaruk A.E., Vasil'ev B.Ju.**, *Methods and means of increasing the energy efficiency of machines and technologies with asynchronous electric drives*, "Bulletin of SUSU. Series "Energy", vol 15, no 1, pp. 47–53. 2015.
- [3]. **Bespalov V.Ja.**, *New high-performance series of 7AVE asynchronous motors, its modifications and specialized versions*, In Trudy VIII Mezhdunar. (HIH Vseros.) nauch.-tehn. konf. po avtomatizir. elektroprivodu. pp. 239-243, 2014.
- [4]. **Mugalimov R.G.**, *Modeling of energy efficiency indicators of electric drive options of industrial plants based on the use of traditional and compensated asynchronous motors*, Bulletin of MSTU. G. I. Nosova, vol 2 (34), pp. 59-64, 2011.
- [5]. **Kapitonov O. A., Tret'jakov A.S., Lenevskij G.S.**, *Soft starter with pulse voltage regulation and compensated reactive power*. Vestnik Belorussko-Rossijskogo Universiteta, vol 4(61), pp. 39-48, 2018.
- [6]. **Parfenovich O. N., Kapitonov O. A.**, *Transistor pulse-width voltage regulator for asynchronous electric motors*, Vestnik Belorussko-Rossijskogo Universiteta, vol 3(28), pp.119-127, 2010.
- [7]. **Ushkov A.S., Kolganov A.R.**, *Energy efficiency analysis of an asynchronous electric drive with a power factor corrector*, VestnikIGJeU, vol 6, pp.1-5, 2013.
- [8]. **Ushkov A.S., Kolganov A.R.**, *Research of modern methods of energy-saving control of asynchronous electric drive*. VestnikIGJeU, vol 2, pp.1-8, 2012.
- [9]. **Belousov V.Yu., Nedorezova Ye. V.**, *Energy saving and application of frequency converters and soft start devices*. IzvestijaTulGU. Tehnicheskienauki, vol 6, Ch. 1, pp. 148-151, 2011.
- [10]. **Borodai V.A.**, *Parametric control of asynchronous drive efficiency by means of the converter with the increased power factor*, Elektrotehnika ta elektroenergetyka, vol 2, pp. 8-16, 2020.

APPLICATION OF ALTERA PROGRAMMED LOGIC INTEGRATED CIRCUIT IN
EFFICIENT ASYNCHRONOUS DRIVE SYSTEM

[11]. UA 151636 U Ukraine, MIIK (2022) H02K 19/36. (Utility model patent) Method of controlling an asynchronous machine / O. Nesterova, V. Borodai; applicant and patent holder of Dniprovskaya Polytechnic National Technical University; Application No. u 2021 06874 dated December 2, 2021; published Bull No. 34 dated 08/25/2022.

This article was reviewed and accepted for presentation and publication within the 11th edition of the International Multidisciplinary Symposium "UNIVERSITARIA SIMPRO 2024".

A LITERATURE REVIEW ON INTEGRATING AI AND BLOCKCHAIN TECHNOLOGIES IN ANIMATRONICS FOR CHILDREN'S ENTERTAINMENT AND EDUCATION

ALINA STEPANEK¹, FABIAN ARUN PANAIT²

Abstract: This paper presents a comprehensive literature review on the integration of animatronics for children, AI systems applicable to animatronics, and blockchain in IoT for animatronics. It begins with an overview of the historical context and evolution of animatronics in children's entertainment and education, highlighting key milestones and safety considerations. The review explores various AI systems used in animatronics, including machine learning, computer vision, natural language processing, and behavioral AI, discussing their implementation and associated challenges.

The study further investigates the role of blockchain technology in animatronics, focusing on critical aspects such as data security, supply chain management, and operational transparency. Blockchain ensures secure data transmission between animatronics and control systems, enhances the traceability and verification of components and materials used in animatronics, and maintains transparent and immutable records of maintenance logs and operational data.

The paper provides a comprehensive analysis of the integrated role of AI and blockchain in advancing animatronic technologies, aiming to offer valuable insights for designers, developers, and educators involved in the field of animatronics.

Key words: animatronics, AI systems, blockchain, internet of things (IoT), children's entertainment, educational technology, machine learning, data security.

1. INTRODUCTION AND STATE OF THE ART

The integration of advanced technologies such as Artificial Intelligence (AI) and blockchain with animatronics is revolutionizing children's entertainment and education. Animatronics, which combines the precision of electronics with the creativity of animation, has long fascinated young audiences with lifelike, interactive characters. This literature review explores the cutting-edge convergence of AI and blockchain technologies with animatronics, offering new dimensions of interactivity, security, and educational potential.

¹ Ph.D., Student Eng., University of Petroșani, alinasoltoianu@upet.ro

² Ph.D., Eng., University of Petroșani, fabianpanaite@upet.ro

AI enhances animatronics by enabling more sophisticated behaviors and interactions. Through machine learning, computer vision, and natural language processing, animatronic characters can now recognize faces, understand speech, and respond to gestures in real-time.

This makes them not only more engaging as toys but also powerful tools for personalized learning and therapeutic applications. For instance, educational robots equipped with AI can adapt to a child's learning pace and style, making complex subjects more accessible and enjoyable.

Blockchain technology, on the other hand, offers robust solutions for data security and operational transparency in animatronics. By utilizing decentralized, immutable ledgers, blockchain can ensure the secure transmission of data between animatronic devices and control systems. This is crucial in safeguarding the privacy of children interacting with these devices and maintaining the integrity of the data collected. Moreover, blockchain can enhance supply chain management for animatronic components, ensuring the authenticity and quality of materials used.

This review will delve into the historical context of animatronics, highlighting key technological advancements and their applications in children's entertainment and education. It will examine the roles of AI and blockchain in enhancing the functionality, safety, and educational value of animatronic devices. By synthesizing current research and case studies, we aim to provide a comprehensive understanding of how these technologies can be integrated to create innovative, secure, and effective animatronic solutions for children. The potential of integrating AI and blockchain in animatronics is vast, promising to transform how children engage with educational content and entertainment. This literature review aims to map out the current landscape, identify the benefits and challenges, and explore future directions for research and development in this exciting interdisciplinary field.

2. ANIMATRONIX FOR CHILDREN

Historical Context

The evolution of animatronics in children's entertainment can be traced back to early theme park attractions and mechanical toys. One of the pioneering uses of animatronics in entertainment was Walt Disney's Enchanted Tiki Room, which debuted in 1963. This attraction featured lifelike birds, flowers, and tikis that could sing and talk, marking a significant advancement in the field of animatronics. "The Audio-Animatronics technology that powers the show was introduced to the world when Walt Disney's Enchanted Tiki Room debuted in 1963 at Disneyland Park. This groundbreaking technology allowed animators to synchronize movement, audio and visual effects, paving the way for other classic attractions like "it's a small world", Pirates of the Caribbean and Haunted Mansion." [1]

Key milestones in the development of animatronic technology include the integration of computer controls and more sophisticated sensors. These advancements have allowed for greater precision and interactivity, which have been particularly influential in the development of animatronic toys and educational tools. For example, the Furby toy, introduced by Tiger Electronics in 1998, was a groundbreaking product

that combined animatronics and artificial intelligence to create an interactive play experience. “Equipped with rudimentary sensors, it could respond to touch, sound, and even light” [2], making the toys seem almost lifelike. They could communicate using a language called “Furbish” when first activated, which gradually evolved into English as they interacted with their owners. This ability to learn and adapt language made them unique among toys of the time. The Furby used a combination of motors, cams, and gears to create movements such as blinking eyes, moving mouths, and wiggling ears, adding to the perception of lifelike behavior. “In the case of Furbies, the child’s caretaking responsibility is centered on teaching. Like Tamagotchis,

Furbies are presented as visitors from another planet. This explains why they only speak Furbish when they are first brought to life: it is the mother language of their planet. In the course of play, Furbies “learn” to speak English. In fact, this learning reflects the unfolding of a program that evolves Furby language to a set of simple English phrases. For most children 5-9, the illusion works: children believe that they are teaching their Furby by interacting with it. As in the case of Tamagotchis, Furbies demand attention; children understand that a lack of attention will have a negative impact on the toy’s inner “state.””.[3]

Design and Features

Characteristics and Features of Animatronics Designed Specifically for Children

Animatronics designed for children often prioritizes safety, durability, and interactivity. Key characteristics include soft and rounded edges to prevent injuries, materials that are safe and non-toxic, and robust construction to withstand rough handling. This animatronics are also typically designed to be highly engaging, with features such as responsive facial expressions, voice recognition, and interactive storytelling capabilities. “The animatronic figures must identify the guests and recognize their status in dynamic interactions for enhanced acceptance and effectiveness as socially interactive agents, in the general framework of human-robot interactions.” [4] Safety considerations and regulatory standards are crucial in the design of animatronics for children. Manufacturers must adhere to stringent guidelines to ensure that these products are safe for use. This includes compliance with regulations such as the ASTM F963 standard, which specifies safety requirements for toys, and the European EN71 standard, which covers various safety aspects of toys.

Examples of Popular Animatronic Characters and Their Impact

Popular animatronic characters such as those found in theme parks or produced as standalone toys have had a significant impact on children's entertainment. Characters like the animatronic dinosaurs in the Jurassic Park theme parks have captivated children's imaginations, blending education with entertainment.” “The Jurassic Park River Adventure.” Advertisements promise that visitors to this “world of T-Rex” can “pet a living, breathing dinosaur.” [5] Additionally, animatronic characters like the interactive Elmo dolls from the Sesame Street franchise have become beloved figures, providing both comfort and educational value to children. These dolls, particularly the “Tickle Me Elmo” series, blend simple animatronic elements with interactive features to engage and educate young children.

Educational and Therapeutic Uses

Use of Animatronics in Educational Settings

In educational settings, animatronics are used to create engaging and interactive learning experiences. Museums and science centers often employ animatronic displays to teach children about history, biology, and technology in an immersive and memorable way. For example, animatronic dinosaurs in natural history museums help to bring prehistoric eras to life, providing children with a tangible connection to the past. In classrooms, animatronic tools like programmable robots are used to teach coding and robotics, fostering STEM skills from a young age.” Children are natural inventors and digital savvies, and are easily inspired by creative content. Research has highlighted how extra-curricular robotics programs can foster these natural skills through robotic challenges that integrate computational thinking (CT) and science, technology, engineering, and mathematics (STEM)”[6] These educational animatronics can make complex concepts more accessible and enjoyable for children, thereby enhancing their learning experience.

Therapeutic Applications of Animatronics for Children with Special Needs

Animatronics also have therapeutic applications for children with special needs. Therapeutic robots, as the “artificial pets such as the baby seal Paro”[7] robot, which resembles a baby seal, have been used to provide comfort and emotional support to children with autism and other developmental disorders. These robots can respond to touch and sound, providing a sense of companionship and helping to reduce anxiety. “Resources for children with autism and their families are usually rare and costly. Therefore, a robot that could help them to learn and acquire new developmental skills while having fun would be appreciated by teachers and parents as well as enriching for the children.”[7]. Moreover, animatronics can be used in therapy sessions to improve social skills and communication. Interactive animatronic devices can encourage children to engage in social interactions and practice speech, providing a controlled and supportive environment for therapeutic progress. “a robot companion tailored towards becoming a social mediator, empowering children with disabilities to discover the range of play styles from solitary to social and cooperative play.”[8].

3. AI SYSTEMS APPLICABLE TO ANIMATRONICS

Types of AI Systems

Machine Learning and Computer Vision

Machine learning and computer vision (CV) are pivotal in advancing animatronics “CV should enable the system to recognize different worldly objects, like pencil, notebook, bottle, etc., and memorize human faces exhibiting memory better than any other human.”[9], particularly in gesture recognition, facial recognition, and movement coordination. Gesture recognition enables animatronic characters to interpret and respond to human body movements, enhancing interactive experiences. For instance, systems utilizing convolutional neural networks (CNNs) can accurately identify and track gestures in real time. “CNNs are also useful for combining multi-modal data inputs, a technique which has proved useful for gesture recognition in challenging lighting conditions” [10]. Facial recognition technology allows animatronics

to identify and respond to individual users, personalizing interactions. This technology employs deep learning algorithms to analyze facial features and expressions, thereby enabling characters to mirror human emotions. Movement coordination, facilitated by machine learning, ensures that animatronics can perform complex motions smoothly and realistically. Techniques such as reinforcement learning are used to optimize these movements, ensuring they are both natural and synchronized with the environment.

Natural Language Processing (NLP)

Natural Language Processing (NLP) plays a crucial role in enabling animatronics to engage in interactive dialogues and perform speech recognition. NLP allows animatronic characters to understand and generate human language, making conversations with users more natural and meaningful. This involves sophisticated algorithms for language modeling and understanding context, enabling characters to provide relevant responses. “NLP researchers aim to gather knowledge on how human beings understand and use language so that appropriate tools and techniques can be developed to make computer systems understand and manipulate natural languages to perform the desired tasks.”[11] Speech recognition, a subset of NLP, allows animatronics to comprehend spoken language, facilitating seamless communication with users. Advanced speech recognition systems, powered by deep learning, can accurately transcribe speech into text, even in noisy environments. This capability is crucial for interactive toys and educational robots that rely on voice commands.

Behavioral AI

Behavioral AI is essential for developing personality traits and adaptive behaviors in animatronics. This type of AI involves creating algorithms that allow animatronics to exhibit distinct personalities and adapt their behavior based on interactions. For example, through the use of reinforcement learning and neural networks, animatronics can learn from user interactions and modify their responses to appear more lifelike and engaging. Behavioral AI enables animatronics to develop complex emotional responses and social behaviors, making them more relatable and appealing to users. This technology is particularly important in therapeutic and educational applications, where animatronics must engage users effectively and empathetically. “there is a growing necessity for developing behavioral models for social robots to have a high-quality interaction and level of acceptability in providing useful and efficient services”[12].

Implementation and Challenges

Technical Challenges in Integrating AI with Animatronic Hardware

Integrating AI with animatronic hardware presents several technical challenges. One significant challenge is ensuring real-time processing and response, which requires powerful computing resources and efficient algorithms. Additionally, synchronizing AI-driven software with the mechanical components of animatronics demands precise control systems and robust communication protocols. Another challenge is managing power consumption, as AI algorithms and complex movements can be energy-intensive. This necessitates innovative solutions in power management and battery technology to ensure that animatronics can operate for extended periods without frequent recharging.

Case Studies of AI-Powered Animatronics in Commercial and Experimental Projects

AI-powered animatronics have been implemented in various commercial and experimental projects, showcasing their potential and versatility. One notable example is Disney's A1000 series animatronics, which use advanced AI to perform intricate gestures and facial expressions, creating highly realistic characters for theme park attractions. In the experimental realm, MIT's Media Lab has developed animatronic robots like Kismet “often considered the first so ciable robot”[13], which uses AI to interact with humans through expressive facial features and vocalizations. Kismet's AI system allows it to perceive and respond to social cues, demonstrating the potential for AI to enhance human-robot interactions.

Ethical Considerations and Public Perception

The integration of AI into animatronics raises several ethical considerations and affects public perception. Privacy concerns are paramount, particularly with animatronics that use facial recognition and data collection. Ensuring that user data is securely stored and managed is critical to maintaining public trust.

Moreover, the ethical implications of creating lifelike animatronics that can influence human behavior and emotions must be carefully considered. There is a risk of dependency, especially in therapeutic contexts, where users might form emotional attachments to animatronic characters. Public perception of AI-powered animatronics can vary, with some viewing them as innovative and beneficial, while others may express concerns about privacy and the potential for misuse. “most common visions of the impact of AI elicit significant anxiety. Only two of the eight narratives elicited more excitement than concern (AI making life easier, and extending life).”[14].

4. BLOCKCHAIN IN IOT FOR ANIMATRONICS

Overview of Blockchain Technology

Basic Principles of Blockchain and Its Functionalities

Blockchain technology is a decentralized digital ledger that securely records transactions across a network of computers. This ledger is immutable, meaning once a transaction is recorded, it cannot be altered. The fundamental principles of blockchain include decentralization, transparency, immutability, and enhanced security. Each block in the chain contains a cryptographic hash of the previous block, a timestamp, and transaction data, ensuring that data is tamper-proof and verifiable. “This chain grows as new blocks are appended to it continuously.”[15]

Relevance of Blockchain to IoT

Blockchain technology is highly relevant to IoT due to its ability to provide a secure framework for data exchange between interconnected devices. IoT ecosystems involve a multitude of devices communicating with each other, often transmitting sensitive data. Blockchain ensures that these interactions are secure and trustworthy by recording them in an immutable ledger, thereby preventing unauthorized access and tampering. “Blockchains give us resilient, truly distributed peer-to-peer systems and the ability to interact with peers in a trustless, auditable manner. Smart contracts allow us to

automate complex multi-step processes. The devices in the IoT ecosystem are the points of contact with the physical world. When all of them are combined we get to automate time-consuming workflows in new and unique ways, achieving cryptographic verifiability, as well as significant cost and time savings in the process.”[16].

Applications in Animatronics

Data Security and Privacy

Blockchain technology can be used to ensure secure data transmission between animatronics and control systems. By encrypting data and distributing it across a decentralized network, blockchain minimizes the risk of data breaches and unauthorized access. This is crucial for animatronics, which rely on real-time data to function correctly. An example of an application of blockchain with IoT is the framework described in the article “Original Research Article An efficient framework for secure data transmission using blockchain in IoT environment”[17] for secure data transmission. “This paper presents a framework for secure data transmission using blockchain (SDTUB) for blockchain-based IoT systems, with a focus on enhancing data security”[17]. This framework leverages blockchain technology to enhance data security in IoT-enabled smart systems. By using blockchain, the system ensures that data transmitted between IoT devices is protected against unauthorized access and security breaches. The framework employs authentication and access control techniques, using digital certificates and both regional and central blockchains, to verify the authenticity of IoT devices and manage their authorization. Additionally, the proposed mechanism addresses scalability and efficiency, ensuring that even lightweight IoT devices can securely transmit data with low energy consumption. The integration of this framework with existing network infrastructure maintains a secure and immutable record of all transactions and configurations, ultimately improving the performance and security of IoT systems.

Supply Chain Management

In animatronics, blockchain can track and verify the components and materials used. Each step in the supply chain can be recorded on the blockchain, providing a transparent and immutable record of the origin, authenticity, and journey of each component. This reduces the risk of counterfeit parts and ensures that all materials meet the required standards. An example of blockchain application in supply chain management involves tracking the provenance of goods described in “Toward an ontology-driven blockchain design for supply-chain provenance”[18]. In a complex supply chain, goods are often produced and transported across multiple organizations and countries, making it challenging to trace the origin and authenticity of items. By integrating IoT with blockchain technology, each step in the supply chain can be recorded in a secure and immutable ledger. “Internet-aware sensors capture finely granular real-time data about product and environment characteristics as well as location and timestamps throughout the supply chain. So lack of a digital footprint may no longer be an issue. Furthermore, distributed, shared databases using Blockchain technologies promise to offer highly secure and immutable access to supply chain data”[18]

Operational Transparency

Blockchain can maintain immutable logs of the operational and maintenance data of animatronics. This includes performance metrics, maintenance schedules, and repair histories. By having a transparent and tamper-proof record, stakeholders can ensure that animatronic systems are operating optimally and address any issues promptly. The paper "Blockchain and The Value of Operational Transparency"[19] explores how blockchain technology enhances verifiability of inventory transactions, which is crucial for signaling a firm's operational capabilities to lenders. It presents a new theory that signaling through verifiable inventory transactions is more efficient and less costly than through loan requests, leading to less operational distortion. The authors introduce *b_verify*, an open-source blockchain system demonstrating practical implementation in supply chains to maintain transparent and tamper-proof records. The paper emphasizes that blockchain adoption increases operational transparency, making it harder for low-quality firms to imitate high-quality ones, thereby securing favorable financing terms at lower signaling costs. This technology is particularly beneficial in environments with prevalent trust and fraud issues, where traditional monitoring mechanisms are either too costly or ineffective.

"Our paper identifies an important benefit of blockchain adoption—by opening a window of transparency into a firm's operations, blockchain technology furnishes the ability to secure favorable financing terms at lower signaling costs"[19].

Potential Benefits and Limitations

The integration of blockchain in animatronics will have several benefits, including enhanced security, improved transparency, and more efficient supply chain management. However, challenges remain, such as the high computational resources required and the complexity of integrating blockchain with existing systems.

5. CONCLUSIONS

The journey through this literature review has been illuminating, revealing the profound impact that AI and blockchain technologies can have on animatronics for children's entertainment and education. The fusion of these advanced technologies not only enhances the capabilities of animatronic devices but also opens up new avenues for learning, engagement, and security. One of the most exciting insights from this review is how AI transforms animatronics into interactive and adaptive companions for children. The ability of AI to recognize faces, understand speech, and respond to gestures creates a level of engagement that traditional toys simply cannot match. Personally, I am fascinated by how these intelligent systems can tailor educational experiences to each child's unique learning style, making complex subjects more accessible and fun. Imagine a world where learning is seamlessly integrated into play, where children are not just entertained but also educated in ways that adapt to their needs.

Blockchain's role in enhancing data security and transparency is another crucial aspect. In an age where data privacy is paramount, blockchain offers a solution that ensures children's interactions with animatronics are safe and secure. The immutability and decentralized nature of blockchain not only protect sensitive information but also provide transparency in the supply chain, ensuring that every component used in

animatronics is authentic and safe. This level of security is reassuring, knowing that children can interact with these advanced devices without compromising their privacy.

Of course, integrating these technologies is not without its challenges. The technical hurdles of real-time processing, power management, and system synchronization are significant. Yet, these challenges also present opportunities for innovation. Overcoming these obstacles will require creative solutions and interdisciplinary collaboration. Moreover, the ethical implications, particularly concerning data privacy and emotional dependency, cannot be overlooked. It's essential to navigate these issues thoughtfully to ensure that the benefits of these technologies are realized without unintended negative consequences.

Reflecting on the ethical dimensions, it becomes clear that we must approach the development of AI and blockchain-integrated animatronics with caution and responsibility. Public perception will play a crucial role in the acceptance of these technologies. Transparency in how data is managed and addressing ethical concerns head-on will be vital in building trust. Personally, I believe that with careful consideration and proactive measures, we can mitigate these risks and create a positive impact.

Looking to the future, the potential for AI and blockchain in animatronics is vast and exciting. Continued research and development will be key to overcoming current limitations and pushing the boundaries of what is possible. Collaboration between technologists, educators, and policymakers will be essential to ensure that these innovations are used responsibly and effectively.

REFERENCES

- [1]. **Marcus R., Rus C., Leba M., Risteiu M.**, *Electric vehicles between recycling and sustainable development-@. ro*, International Conference on Computers Communications and Control, pp. 47-62, Cham: Springer International Publishing, 2022.
- [2]. **Ajao Q., Sadeeq L.**, *Overview analysis of recent developments on self-driving electric vehicles*, arXiv preprint arXiv:2307.00016, 2023.
- [3]. **Wang R., Sell R., Rassolkin A., Otto T., Malayjerdi E.**, *Intelligent functions development on autonomous electric vehicle platform*, Journal of Machine Engineering, Vol. 20, 2020.
- [4]. **Parekh D., Poddar N., Rajpurkar A., Chahal M., Kumar N., Joshi G. P., Cho W.**, *A review on autonomous vehicles: Progress, methods and challenges*, Electronics, Vol. 11, No. 14, p. 2162, 2022.
- [5]. **Rus C., Leba M., Risteiu M., Marcus R.**, *Vehicle control modeling and simulation for small electric car case*, 24th International Carpathian Control Conference, Miskolc-Szilvásvárad, Hungary, pp. 388-393, 2023.
- [6]. **Rus C., Leba M., Negru N., Marcus R., Risteiu M.**, *Electric vehicles in smart grid and smart city for Petroșani case*, MATEC Web of Conferences, Vol. 342, p. 05002, 2021.
- [7]. **Disneyland**, *Enchanted Tiki Room*, <https://disneyland.disney.go.com/attractions/disneyland/enchanted-tiki-room/>.
- [8]. **Global Toy News**, *Behind an Interactive Toy Phenomenon: What Makes Furbies Tick*, June 26, 2023, <https://globaltoynews.com/2023/06/26/behind-an-interactive-toy-phenomenon-what-makes-furbies-tick/>.

- [9]. **Turkle S., et al.**, *Encounters with kismet and cog: Children respond to relational artifacts*, Digital Media: Transformations in Human Communication, p. 120, 2006.
- [10]. **Burns, B., Samanta, B.**, *Mechanical Design and Control Calibration for an Interactive Animatronic System*, Volume 4B: Dynamics, Vibration, and Control, 2015.
- [11]. **Desmond J.**, *Displaying Death, Animating Life: Changing Fictions of 'Liveness' from Taxidermy to Animatronics*, "Representing Animals", pp. 159-179, 2002.
- [12]. **Newley A., et al.**, *Animatronic lions, and tigers, and bears, oh my!*, *Sci Child*, Vol. 56, p. 64-71, 2019.
- [13]. **Ferrari E., Robins B., Dautenhahn K.**, *Therapeutic and educational objectives in robot assisted play for children with autism*, RO-MAN 2009 - The 18th IEEE International Symposium on Robot and Human Interactive Communication, Toyama, Japan, 2009, pp. 108-114.
- [14]. **Patrizia M., Claudio M., Leonardo G., Alessandro P.**, *A robotic toy for children with special needs: From requirements to design*, IEEE International Conference on Rehabilitation Robotics, Kyoto, Japan, pp. 918-923, 2009.
- [15]. **Verma, Jatin, Hemant Singh, Akshay Kumar, Shubham Tripathi**, "A Smart Animatronic Human Face," 2017.
- [16]. **Molchanov, Pavlo, et al.**, "Online detection and classification of dynamic hand gestures with recurrent 3D convolutional neural network," *Proceedings of the IEEE Conference on Computer Vision and Pattern Recognition*, 2016.
- [17]. **Chowdhary K. R.**, "Natural Language Processing," *Fundamentals of Artificial Intelligence*, pp. 603-649, 2020.
- [18]. **Nocentini, Olivia, Laura Fiorini, Giorgia Acerbi, Alessandra Sorrentino, Gianmaria Mancioffi, Filippo Cavallo**, *A survey of behavioral models for social robots*, Robotics, Vol. 8, No. 3, p. 54, 2019.
- [19]. **Kidd, Cory David**, "Engagement in long-term human-robot interaction," *PhD Thesis in Media Arts & Sciences*, MIT, Cambridge, MA, 2007.
- [20]. **Cave, Stephen, Kate Coughlan, Kanta Dihal**, "Scary Robots," *Examining Public Responses to AI, Proceedings of the 2019 AAAI/ACM Conference on AI, Ethics, and Society (AIES '19)*, Association for Computing Machinery, New York, NY, USA, pp. 331-337, 2019, DOI: <https://doi.org/10.1145/3306618.3314232>.
- [21]. **Zheng, Z., Xie, S., Dai, H., Chen, X., Wang, H.**, "An Overview of Blockchain Technology: Architecture, Consensus, and Future Trends," *2017 IEEE International Congress on Big Data (BigData Congress)*, Honolulu, HI, USA, 2017, pp. 557-564, DOI: 10.1109/BigDataCongress.2017.85.
- [22]. **Christidis, K., Devetsikiotis, M.**, "Blockchains and Smart Contracts for the Internet of Things," *IEEE Access*, Vol. 4, pp. 2292-2303, 2016, DOI: 10.1109/ACCESS.2016.2566339.
- [23]. **Bhattacharjee, Shyama Barna, et al.**, "An efficient framework for secure data transmission using blockchain in IoT environment," *Journal of Autonomous Intelligence*, Vol. 7, No. 2, 2024.
- [24]. **Kim, H. M., Laskowski, M.**, *Toward an ontology-driven blockchain design for supply-chain provenance*, Intelligent Systems in Accounting, Finance and Management, Vol. 25, pp. 18-27, 2018.
- [25]. **Chod, Jiri, Nikolaos Trichakis, Gerry Tsoukalas, Henry Aspegren, Mark Weber**, *Blockchain and the value of operational transparency for supply chain finance*, SSRN Electronic Journal, 2018.

This article was reviewed and accepted for presentation and publication within the 11th edition of the International Multidisciplinary Symposium "UNIVERSITARIA SIMPRO 2024".

ATEX THERMISTOR MOTOR PROTECTION RELAYS IN ON BOARD ELECTRICAL INSTALLATIONS

**LEON PANĂ¹, FLORIN GABRIEL POPESCU², SEBASTIAN DANIEL
ROSCA³**

Abstract: Protecting electric motors in ATEX areas is very important to prevent the risk of explosion and ensure the safety of personnel and equipment in the area. To ensure adequate protection, a number of safety factors must be considered, including the design and construction of electric motors, electrical connections, and the qualification and training of personnel who install and maintain them. In this context, the protection of the electric motors within these on board installations is necessary, even mandatory, as the ships have potentially explosive areas. Most protection relays protect electrical motors against overheating in the windings and overloads or inadequate cooling and the basic size is determined by the intensity of the electric current. The disadvantage of these relays is that they do not detect the real temperature of the motor windings. Along with the evolution of electronics, ATEX certified protection relays have also developed significantly. This paper aims to present the technical solution of the protection of electric motors in HVAC installations on board ships with explosive potential. At the end of the paper a CAD application is presented to simulate the operation of the ATEX thermistor motor protection relay.

Key words: ATEX, CAD, PTC thermistor relay, overload, short-circuits.

1. INTRODUCTION

A multitude of electric motors, of different sizes and types, are found on board ships. No ship, whether commercial or military, is without HVAC installations. In this context, the protection of electric motors within these installations is necessary, even mandatory, as ships have potentially explosive areas [1], [3], [12], [14], [17], [20].

Protecting electric motors in ATEX areas is extremely important to prevent the risk of explosion and ensure the safety of personnel and equipment in the area. [5], [9], [25]. To ensure adequate protection, a number of safety factors must be taken into account, including the design and construction of the electric motors, the electrical

¹ *Ph.D., Lecturer, Eng., Mircea cel Batran Naval Academy, leon_pana@yahoo.com*

² *Ph.D., Associate Prof. Eng., University of Petroșani, floringabriel82@yahoo.com*

³ *Ph.D Student Eng., at the University of Petrosani, sebastianrosca91@gmail.com*

connections and the qualification and training of the personnel who install and maintain them [2], [8], [11], [13], [15], [16], [19].

2. PTC-THERMISTOR RELAY TYPE U-EK230E FOR ATEX ELECTRIC MOTOR PROTECTION

The relay protects electrical equipment against excessive warming and thermal overload. If this is used in combination with adequate temperature sensors (e.g. thermistors) tripping temperatures from 60 °C up to 180 °C can be realized [7]. The relay is conform to EN 60947-8 and temperature sensors (thermistors) according to DIN VDE V 0898-1-401 (ATEX) or equivalent detail specification (UKEX) shall be connected. The temperature sensors are suitable for mounting into windings of electric motors or power transformers, bearings and heatsinks as well as to monitor the temperature of liquid media, airflow and gases. With ATEX approval, equipment in explosive gas atmospheres Zone 1 and 2 (marking G: gas) or in areas with combustible dust Zone 21 and 22 (marking D: dust) can be protected.

All protection functions of this thermistor relay serve to protect non-explosive-protected equipment and explosive-protected equipment in regular operation and in case of failure [4], [6], [10], [18], [21], [24].

Figure 1 shows the circuit diagram for the single-phase or three-phase connection [11].

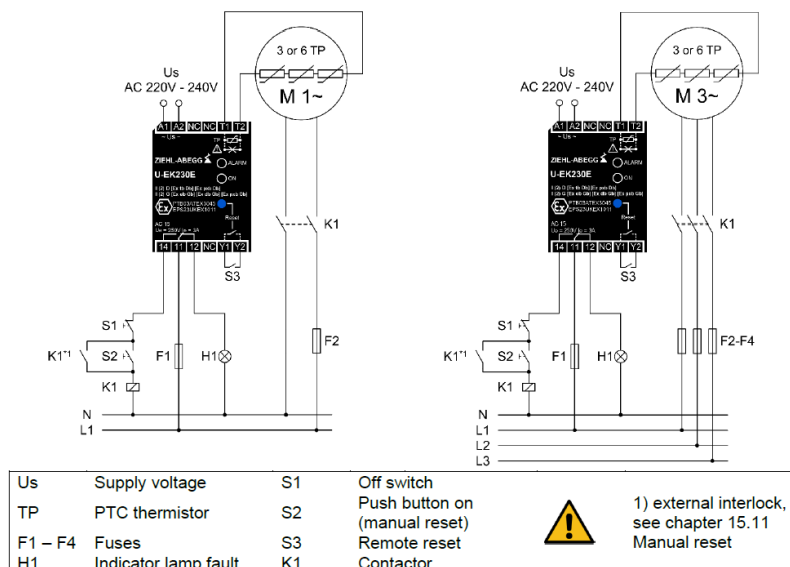


Fig.1. Single phase and three phase circuit diagram

The principal features of relay are:

- 1 thermistor circuit for 1 (not allowed for explosive atmospheres), 3 or 6 PTC thermistors “TP” connected in series.
- Short-circuit detection within the thermistor circuit.

ATEX THERMISTOR MOTOR PROTECTION RELAYS IN ON BOARD ELECTRICAL INSTALLATIONS

- Output relay with 1 change-over contact (co).
- Operating status display

The principle of the relay operation is simple. A current monitors continuously the resistance of the thermistor circuit. In cold state, the resistance is $\leq 250 \Omega$ per thermistor (thermistor circuit $\leq 1.5 \text{ k}\Omega$). The relay is switched on his contacts 11, 14 are closed. The resistance of the thermistors rises rapidly at sensor operating temperature TNF. The relay switches off at a resistance of $3 \dots 4 \text{ k}\Omega$ and his contacts 11, 12 close. The relay also switches off in the case of detector or line short-circuit ($< \text{approx. } 20 \Omega$) or detector or line interruption. The relay remains switched off until the build in or an external reset button is pressed. Power-on is recognized as reset action. With bridged terminals Y1, Y2, the reclosing lock function is disabled [22], [23], [26].

Function diagram of the relay is presented in fig.2. The device switches on automatically in case of a supply voltage dip

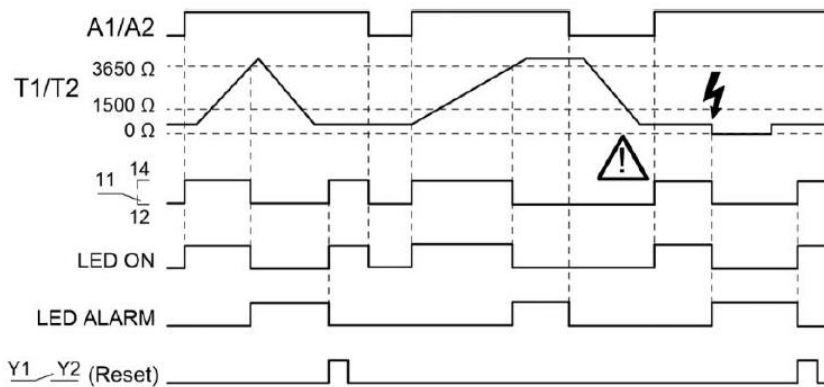


Fig.2. Basic function diagram

Figure 3 shows the connection mode with a bridge at the reset input relay (Y1/Y2) the reclosing lock is out of operation. In this case the relay switches back automatically, when the temperature of the thermistor circuit has fallen below the switchback value.

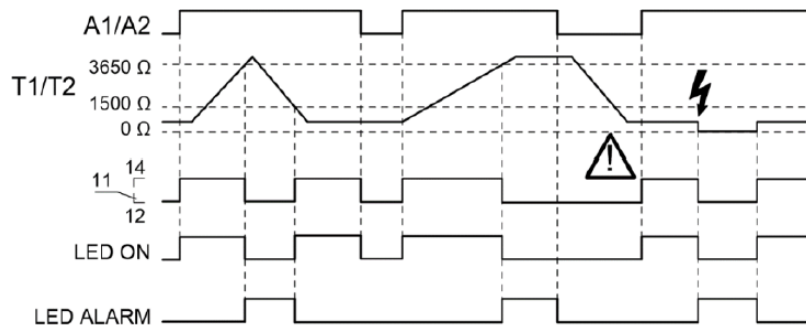


Fig.3 Inputs (Y1 and Y2) bridge connection mode

The relay must be installed outside ATEX area (gas area Zone 0, 1 and 2) unless the device is protected by a suitable ignition protection type (pressurized enclosures or flameproof enclosures).

3. CAD SIMULATION

The CAD simulation created in Matlab, using App Designer, aims to present a simplified simulation of the principle operation of the U-EK230E PTC Thermistor assembly. The application has two components: the code and the design. Both can be easily accessed from the main App designer window.

Initially, the design was created, according to fig. 4. It contains the following elements: the system tripping device, an integrated circuit breaker (motor starter) and the electric motor.

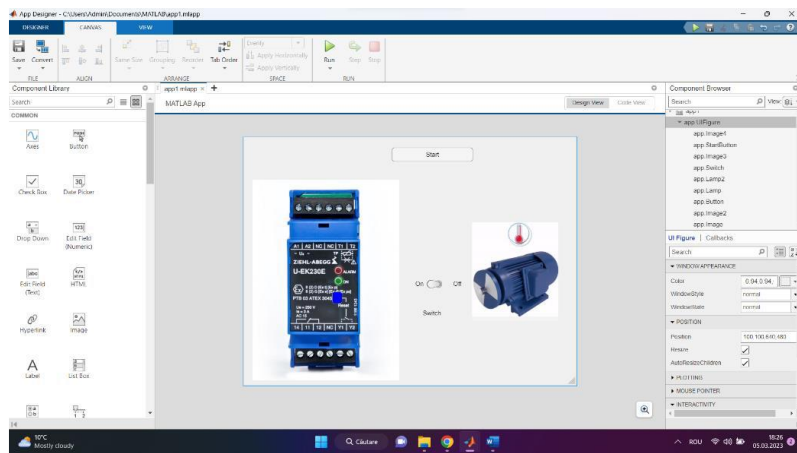


Fig.4. Graphical components of the CAD application

After finalizing the CAD configuration, the code was written, using callbacks for each element, as can be seen in fig.5.

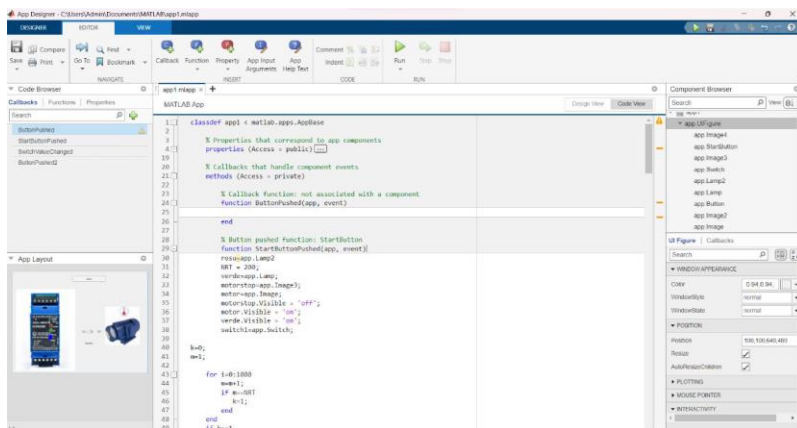


Fig.5. Graphical simulation code program

ATEX THERMISTOR MOTOR PROTECTION RELAYS IN ON BOARD ELECTRICAL INSTALLATIONS

The steps to simulate the application are:

1. Press the START button. The electric motor starts and a green LED comes on to indicate this (fig.6).
2. Using the temperature sensor that is mounted on the stator windings of the motor, the temperature is monitored, and when it reaches the preset value (insulation class temperature), an integrated switch opens, thus stopping the motor. and the red LED of the relay lights up (fig.7).

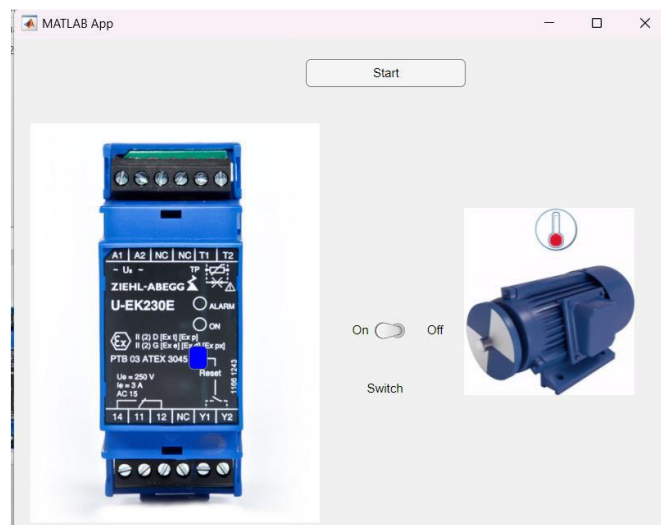


Fig.6. Start (run) electric motor

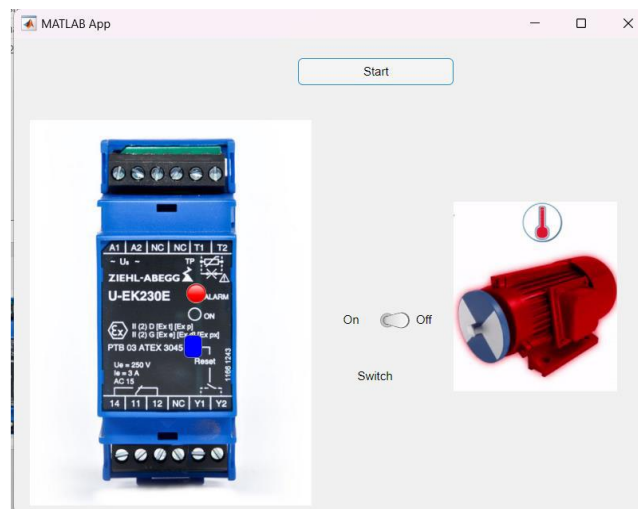


Fig.7. Protection tripping (motor stop)

3. When the temperature drops enough for the motor to operate safely, the red LED of the relay lights up. At this point, the RESET button can be pressed to restart the motor safely (fig.8).

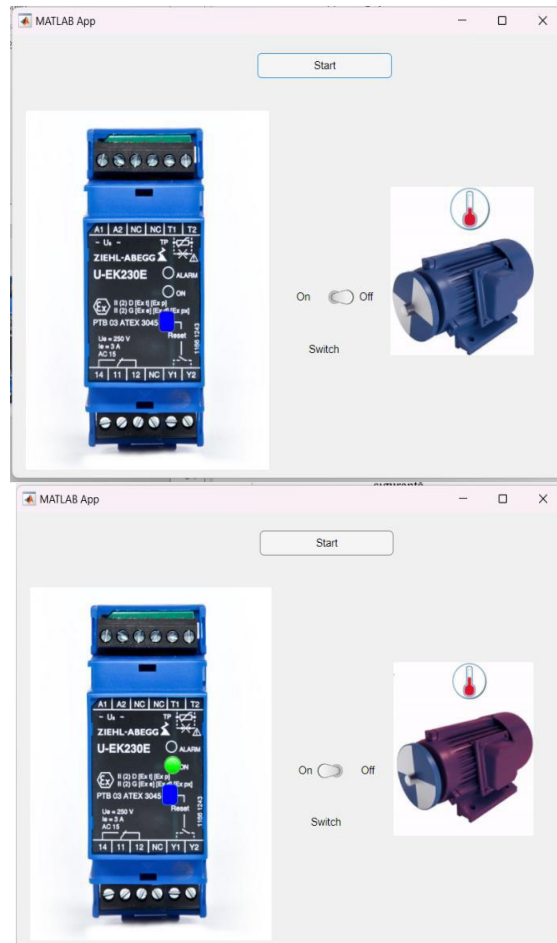


Fig.8. Relay reset mode

4. CONCLUSIONS

PTC thermistors are used in a wide range of applications, such as temperature control, overload protection, liquid level detection, and more. For example, a PTC thermistor can be used to monitor the temperature of an electric motor. If the temperature exceeds a specified value, the thermistor's resistance increases sharply, which can trigger a protective device to stop the motor and prevent overheating.

Some of the advantages of the PTC thermistor include:

- High sensitivity to temperature changes: PTC thermistors are very sensitive to temperature variations, making them ideal for applications that require precise temperature monitoring.
- High electrical resistance at high temperatures: Once the temperature exceeds a specified value, the resistance of the PTC thermistor increases sharply, making it useful for protecting circuits from overloads.

- Reliable operation: PTC thermistors are reliable and robust, and because they have no moving or mechanical parts, they have a longer lifespan than other types of temperature sensors.
- Low cost: The cost of PTC thermistors is relatively low compared to other types of temperature sensors, making them a popular choice for industrial and commercial applications.
- Compact size: PTC thermistors are small and compact, making them ideal for applications where space is limited.

REFERENCES

- [1]. **Borstlap R., Katen H.T.**, *Ship Electrical Systems – 2nd Edition*, Dokmar Maritime Publisher B.V, 2022
- [2]. **Marcu M.D., Popescu F.G., Pana L.**, *Modeling and simulation of power active filter for reducing harmonic pollution using the instantaneous reactive power theory*. Environmental Engineering and Management Journal, June, Vol.13, No. 6, Pages: 1377-1382, 2014.
- [3]. **Pana L., Deliu F., Rosca S.D.**, *Measurement and analysis of vibrations of electric motors on board container ships*, Scientific Bulletin "Mircea cel Batran" Naval Academy Constanta, vol.24(1), pp. 145-156, 2021.
- [4]. **Pana L., Dobref V., Delhi F.**, *Simulation of protection functions in LV shipboard electrical power systems*, Scientific Bulletin "Mircea cel Batran" Naval Academy Constanta, vol.25, (1), pp. 8-15, 2022.
- [5]. **Pana L., Dragomir E., Eni M.**, *ETAP simulation of short circuit currents in on board HV power plants*, Scientific Bulletin "Mircea Cel Batran" Naval Academy, vol. 27, (1), pp. 164-174,164A, 2024.
- [6]. **Pană L. Popescu F.G.**, *Analytical modeling of protection relays*, Annals of University of Petrosani, Electrical Engineering, Vol. 17, pag. 61-68, Petroșani, 2015.
- [7]. **Pană L. Popescu F.G.**, *Evaluation of the moments load and maximum allowable voltage drop for overhead and underground power lines*, Annals of University of Petrosani, Electrical Engineering, Vol. 19, pag.15-27, Petroșani, 2017.
- [8]. **Pana L., Stochitoiu M.D.**, *The influence of the deforming regime on the losses of power and energy in the electrical transformers on board the cruise ships*, Scientific Bulletin "Mircea Cel Batran" Naval Academy, vol. 24, (1), pp. 157-166, 2021.
- [9]. **Popescu F.G., Marcu M.D.**, *Metode moderne de analiză și reducere a armonicilor de curent și tensiune*, Editura Universitas, Petroșani, 2016.
- [10]. **Popescu F.G., Marcu M.D.**, *Electronică de putere*, Editura Universitas, Petroșani, 2021.
- [11]. *** Operating Instructions. Type U-EK230E Part.-No. 382008 *Releasing unit for motors with temperature sensors "TP" (thermistors)*.
- [12]. **Fita N.D., Obretenova M.I., Pasculescu D., Tatar A., Popescu F.G., Lazar T.**, *Structure and analysis of the power subsector within the national energy sector on ensuring and stability of energy security*, Annals of „Constantin Brâncuși” University of Târgu Jiu, ENGINEERING SERIES, Issue 2/2022, pp.177-186, 2022.

- [13]. **Marcu M., Niculescu T., Slusariuc R. I., Popescu, F. G.,** *Modeling and simulation of temperature effect in polycrystalline silicon PV cells*, IOP Conference Series: Materials Science and Engineering, Vol. 133, No. 1, pp. 012005, 2016.
- [14]. **Handra A.D., Popescu F.G., Păsculescu D.,** *Utilizarea energiei electrice: lucrări de laborator*, Editura Universitas, 2020.
- [15]. **Păsculescu D., Dobra R., Ahmad M.A.,** *Dosimetric Quantity System for Electromagnetic Fields Bio-effects*, International Journal of Scientific Research (IJSR) 5, no. 2, pp. 28-32, 2016.
- [16]. **Popescu F.G., Păsculescu D., Păsculescu V.M.,** *Modern methods for analysis and reduction of current and voltage harmonics*, LAP LAMBERT Academic Publishing, ISBN 978-620-0-56941-7, pp. 233, 2020.
- [17]. **Păsculescu D., Niculescu T.,** *Study of transient inductive-capacitive circuits using data acquisition systems.* International Multidisciplinary Scientific GeoConference: SGEM 2, no. 1, 323-329, 2015.
- [18]. **Pana L., Janusz G., Păsculescu D., Păsculescu V. M., Moraru R. I.,** *Optimal quality management algorithm for assessing the usage capacity level of mining transformers*, Polish Journal of Management Studies 18, no. 2, 233-244, 2018.
- [19]. **Dobra R., Buica G., Păsculescu D., Leba M.,** *Safety management diagnostic method regarding work cost accidents from electrical power installations.* Proc. 1st Int. Conf. on Industrial and Manufacturing Technologies (INMAT), Vouliagmeni, Athens, Greece. 2013.
- [20]. **Fîță N. D., Lazăr T., Popescu F. G., Păsculescu D., Pupăză C., Grigorie E.,** *400 kV power substation fire and explosion hazard assessment to prevent a power black-out*, International Conference on Electrical, Computer Communications and Mechatronics Engineering-ICECCME, pp. 16-18, 2022.
- [21]. **Popescu F.G., Arad S., Marcu M.D., Pana L.,** *Reducing energy consumption by modernizing drives of high capacity equipment used to extract lignite*, Papers SGEM2013/Conference Proceedings, Vol. Energy and clean technologies, pp. 183 - 190, Albena., Bulgaria, 2013.
- [22]. **Fîță N.D., Radu S.M., Păsculescu D., Popescu F.G.,** *Using the primary energetic resources or electrical energy as a possible energetical tool or pressure tool*, In International conference KNOWLEDGE-BASED ORGANIZATION, vol. 27, no. 3, pp. 21-26. 2021.
- [23]. **Csaszar T., Păsculescu D., Darie M., Ionescu J., Burian S.,** *Method for assessing energy limited supply sources, designed for use in potentially explosive atmospheres*, Environmental Engineering and Management Journal 11, no. 7, 1281-1285, 2012.
- [24]. **Andras A., Popescu F.D., Radu S.M., Păsculescu D., Brinas I., Radu M.A., Peagu D.,** *Numerical simulation and modeling of mechano–electro–thermal behavior of electrical contact using comsol multiphysics.* Applied Sciences, 14(10), 4026, 2024.
- [25]. **Stepanescu, S., Rehtanz, C., Arad, S., Fotau, I., Marcu, M., Popescu, F.** *Implementation of small water power plants regarding future virtual power plants* 10th International Conference on Environment and Electrical Engineering, pp. 1-4, IEEE, 2011.
- [26]. **Păsculescu D., Romanescu A., Păsculescu V., Tătar A., Fotău I., Vajai Gh.,** *Presentation and simulation of a modern distance protection from the national energy system*, 10th International Conference on Environment and Electrical Engineering, pp. 1-4. IEEE, 2011.

DEVELOPMENT OF A MOBILE PLATFORM WITH A MANIPULATOR ROBOT

STANISLAV SHYKHOV¹, VLADYSLAV KNYSH², OLEKSII
PLAHUNOV³

Abstract: Traditional manufacturing production lines are characterized by static and rigid configurations, resulting in significant idle time during reconfigurations for new products or processes. This inflexibility not only decreases productivity but also limits the ability to respond quickly to market demands. With the advent of Industry 4.0, mobile robotic units have leveraged the Internet of Things and Artificial Intelligence to significantly enhance their capabilities and application fields. By integrating sensors, actuators, and machine-to-machine communication, mobile manipulators have become essential components of modern smart industry. These systems combine the capabilities of a mobile platform with a robotic arm, making them versatile tools in production, science, military, construction, medical care, and business sectors. This paper introduces the development and implementation of the "CuRoK" mobile robot manipulator at the Dnipro University of Technology. The CuRoK features a robust hardware architecture, including a mobile platform and a multi-link manipulator arm with five degrees of motion. Critical components such as actuators, sensors, controllers, and human-machine interfaces are discussed in details. The paper addresses challenges encountered during the development process, such as mechanical vibrations and electrical interference, and presents solutions to mitigate these issues. Emphasis is placed on improving part machining quality, reducing tolerances, and enhancing electrical isolation. The successful deployment of CuRoK underscores the importance of integrating mobile manipulators in modern education and industry, highlighting their role in fostering skills essential for the next generation of engineers and technicians.

Key words: service robotics, mobile manipulation, modern manufacturing, Industry 4.0, education.

1. INTRODUCTION

Production lines in traditional manufacturing are static and rigid, which often leads to significant idle time during reconfiguration for new products or production process. This inflexibility not only decreases productivity but also limits the ability to

¹ *Ph.D. Student Eng., Dnipro University of Technology, shykhov.stan.k@nmu.one*

² *Ph.D. Student Eng., Dnipro University of Technology*

³ *Ph.D. Student Eng., Dnipro University of Technology*

react quickly to market needs. As part of Industry 4.0, mobile robotic units entered the era of Internet of Things and Artificial Intelligence, which significantly increased their capabilities and application fields. Using combination of sensors, actuators and machine-to-machine communication, mobile manipulators became essential part of modern smart industry [1].

Robot manipulator in traditional form [2], [3] consists of an articulated mechanical arm that is installed in a desired location and used for handling heavy or dangerous materials. They became the current manifestation of the third industrial revolution in automation, and they have been developing today to meet the dynamic demands of the industry. Modern requirement in intelligent human-machine collaboration pushed traditional manipulator robots further to mobile robot units or mobile manipulators.

Mobile manipulators are multipurpose robotic systems which combine the capabilities of a mobile platform and a robotic arm. Throughout last decades, mobile robots rapidly evolved from first mobile robot arm prototype MORO (1984, Fraunhofer IPA, Stuttgart) [4] to modern intelligent solutions, having been provided by world known organizations such as Boston Dynamics, KUKA, Fetch Robotics and Stanford [5]. They are actively used in various fields such as production, science, military, construction, medical care and business [6].

Therefore, modern education also needs to pay attention to studying and mastering the skills of working with mobile robots, which have already become an integral part of the production process. As a part of this idea, many educational facilities establish their own mobile robot projects [7] and participate in different robotics competitions [8] in order to promote robotics all over educational system and interest students and university staff.

2. MOBILE MANIPULATOR “CUROK”

The hardware architecture of the vast majority of mobile manipulators consists of several blocks that can be divided by functionality [9]: actuators, sensors, controllers and human machine interface. Actuators consist of manipulator arm, which can perform different tasks, and mobile platform on which the manipulator is mounted. In order to provide safe and precise movement, robots require information about environment, which is provided from different types of sensors. Controllers are used to process sensor data and control actuators. The interaction with the human-operator is carried out through the human-machine interface.

On the basis of the Dnipro University of Technology Hardware Lab, a general-purpose mobile robot manipulator "CuRoK" was developed (Fig. 1).

The frame, made of aluminum profile, serves as a foundation for the mobile platform. With dimensions of 43x70x24 mm, the frame has the form of a parallelepiped and provides the construction with necessary rigidity, stability and reliability. The upper and bottom faces of the platform are secured with screws and are made of 2 mm steel sheets onto which the mobile robot's equipment is fixed.



Fig. 1. CuRoK general view

The next set of hardware is fixed and closed off from the surroundings on the lower platform, in the center of the frame (Fig. 2):

1. A 24-volt battery pack that consists of three electric car battery modules;
2. A Battery Management System that is dedicated to the oversight of a battery pack and maintains conditions for long-term uninterrupted operation of the autonomous power source;
3. An inverter to supply the power to the manipulator from the battery pack;
4. Twowheel hub motors;
5. An STM32-based motor-wheel control board;
6. An ESP32-based communication module.

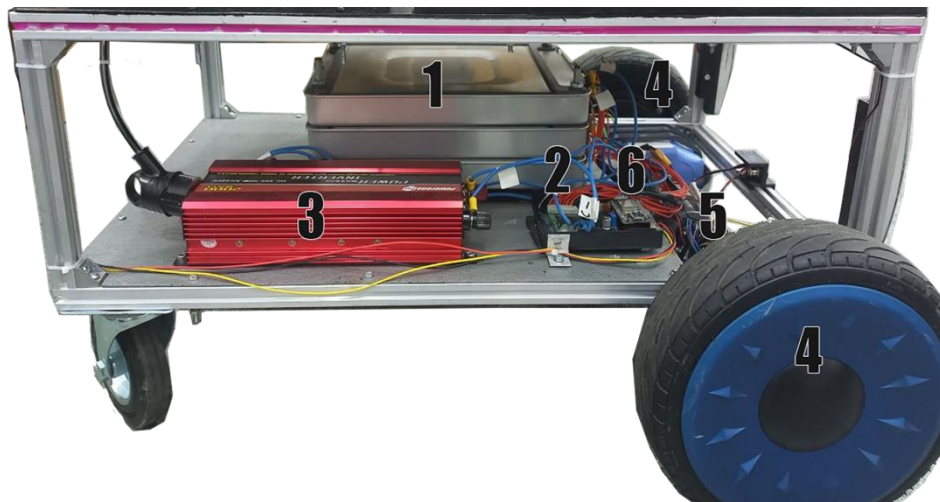


Fig. 2. Mobile platform structure

The main components of the manipulator are fixed on the upper platform, namely: executive, in the form of a manipulator arm, and control, in the form of a control unit. Robot manipulator (Fig. 3) is the multi-link mechanism that has five degrees of motion and all rotational joints, which provide flexibility and repeatability of movement [10]. Its end effector is a gripper.

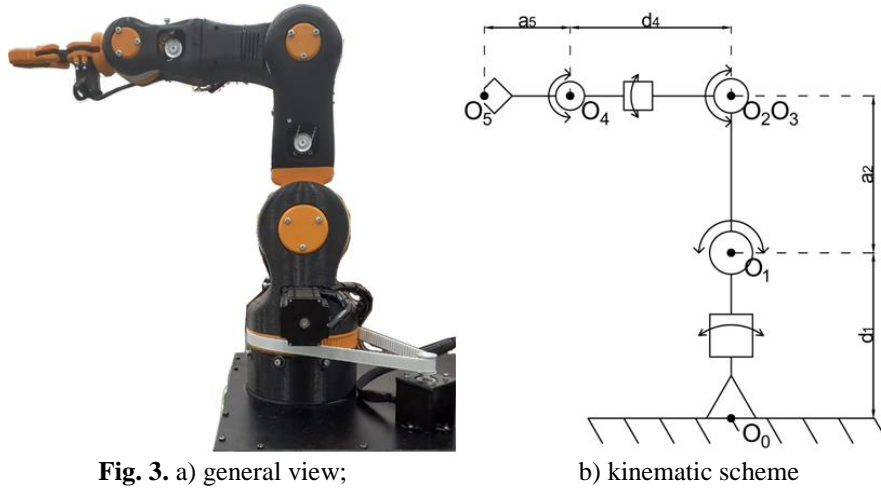


Fig. 3. a) general view;

b) kinematic scheme

It consists of the following main nodes:

- supporting structures;
- drives (stepper motors);
- transmission mechanisms;
- executive mechanisms;
- capturer (capturing device).

The control unit is encased and positioned adjacent to the manipulator. The following hardware is situated inside (Fig. 4):



Fig. 4. Control unit

1. Stepper motor drivers, 6 pcs.;
2. Arduino Mega 2560 with RAMPS 1.4 expansion module;
3. Rectifier AC/DC 350 W, 24 V;
4. DC/DC converter for 12 V;
5. DC/DC converter for 6 V;
6. Cooling fan.

The diagram of electrical connections is shown in Fig. 5. The presence of separate inverter and rectifier is due to the need to maintain the ability to separate the mobile robot into two independent stands.

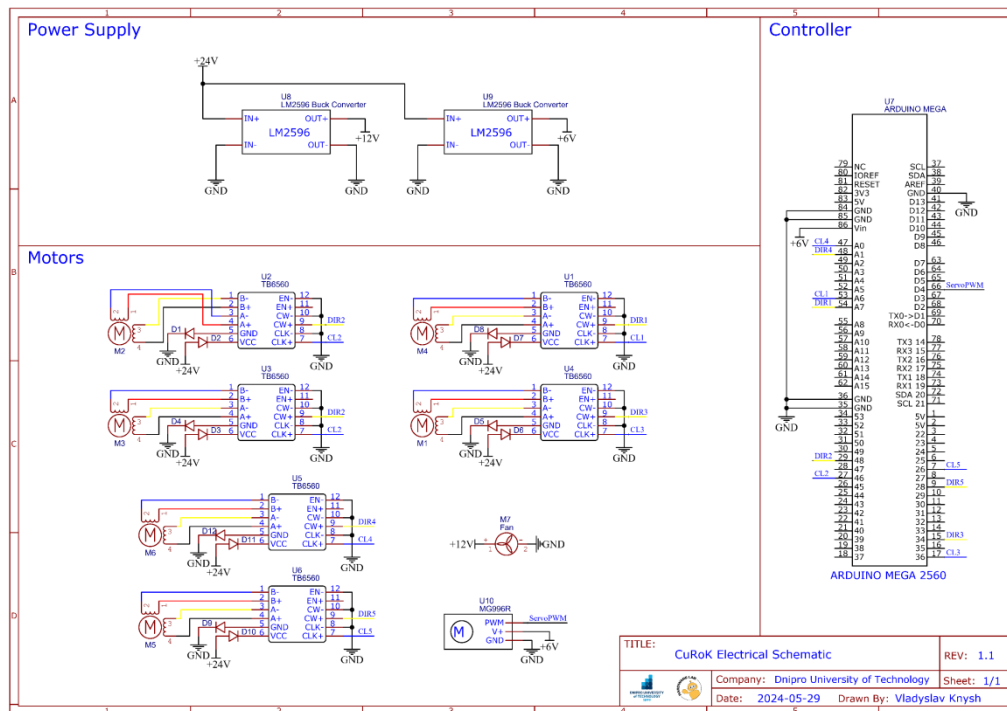


Fig. 5. Electrical Schematic

3. RESULTS AND DISCUSSION

The development of the CuRoK mobile robot manipulator at the Dnipro University of Technology Hardware Lab provided significant challenges. After the successful implementation of the system, it became possible to see the following key outcomes:

Mechanical design stability and ergonomics

The aluminum profile frame provides the necessary rigidity and reliability together with protection of inner components. Despite the robust design, challenges such as mechanical vibrations due to imperfections in the mechanical power transmission system and surface abrasives were encountered. Solutions included

improving machining quality, reducing tolerances, and using dampers to minimize vibrations.

Another source of vibration is the use of a stepper motor with a significant discreteness of the rotation angle. In other words, the movement of manipulator was too fast, which is expressed in the form of vibrations, that damage joints of mobile manipulator. These mechanical vibrations were mitigated by switching motor drivers to micro-stepping mode and additional post-treatment of friction surfaces.

Electrical System and Control

The electrical system featured a 24-volt battery pack, controlled by Battery Management System (BMS), and an inverter for power supply. In order to maintain stable operation some changes in design was implemented, such as galvanic isolation of connection ports, use of separate power sources for each driver. Issues with electrical interference and back EMF from stepper motors were mitigated by redesigning the electrical circuit of motor drivers by including protection diodes.

Motion Control

Motor wheels used for mobile platform was originally designed for gyroscooter, which does require high manufacturing precision. The integration of vector control algorithms with speed feedback compensated for different wheel speeds, enhancing the overall stability and control of the mobile robot.

Discussion

The successful deployment of the CuRoK mobile robot manipulator highlights the critical role of mobile manipulators in modern education and industry. Several key insights emerged from the development process:

- Importance of Mechanical Precision: the mechanical design's precision directly impacts the robot's performance. Mitigating mechanical vibrations through better machining practices and using damping materials proved essential for stable operation.

- Electrical Isolation and Power Management: ensuring electrical isolation and proper power management is crucial to prevent interference and maintain system stability. The use of high-speed stepper motors and separate power sources for drivers were effective solutions.

- Educational Impact: The project provided valuable practical experience for students and highlighted the necessity of integrating mobile robotic systems into educational curricula. The practical skills gained are essential for preparing the next generation of engineers and technicians.

- Industrial Relevance: mobile manipulators like CuRoK are versatile tools for modern smart industries. Their ability to adapt to different tasks and environments makes them valuable assets in production, construction, medical care, and other fields.

Future Work

The development of CuRoK is important step forward for Hardware Lab team, but there are areas for further improvement:

- Enhancing the mechanical design to further reduce vibrations and improve precision.

- Integrating more advanced sensors and control algorithms to enhance the robot's autonomy and adaptability.

- Developing intuitive means of remote control of the robot.
- Chassis redesign for outdoor driving.
- Expanding the application fields of CuRoK to explore its capabilities in more diverse industrial and educational environments.

4. CONCLUSIONS

The development of the CuRoK mobile robot manipulator by the Dnipro University of Technology's Hardware Lab highlights the significant advancements in robotic technology and its applications in various fields. In the process of developing the CuRoK mobile robot manipulator, the Hardware Lab team faced a number of challenges and difficulties of various origins, both mechanical and electrical. A number of measures were taken to eliminate the identified problems, including: additional post-treatment of friction surfaces, the use of damping materials, switching drivers to micro-stepping mode, redesigning the electrical circuit of the manipulator control unit to ensure reliable and safe power supply to the modules, mandatory use of protective galvanic isolation at all times, as well as analysis and selection of the optimal wheel control algorithm. These measures ensured stable and precise operation of the manipulator. The project not only provided valuable theoretical and practical skills for the team but also emphasized the crucial role of mobile manipulators in modern education and industry. CuRoK's success underscores the necessity of integrating mobile robotic systems into educational curricula and industrial processes to foster innovation and meet dynamic market demands. This work serves as a model for future developments in mobile robotics, promoting versatility, efficiency, and collaboration in smart industry environments.

REFERENCES

- [1]. Ghodsian N., Benfriha K., Olabi A., Gopinath V., Arnou A., *Mobile Manipulators in Industry 4.0: A Review of Developments for Industrial Applications*. Sensors Basel, Switzerland, 23(19), 8026. 2023.
- [2]. Nazarova O., *Mechatronic automatic control system of electropneumatic manipulator* / V. Osadchyy, T. Hutsol, Sz. Glowacki, T. Nurek, V. Hulevskyi, I. Horetska // Scientific Reports, 2024.
- [3]. Nazarova O., Osadchyy V., Shulzhenko S., Olieinikov M., *Software and Hardware Complex for The Study of Electropneumatic Mechatronic Systems*, 2022 IEEE 4th International Conference on Modern Electrical and Energy System (MEES), Kremenichuk, Ukraine, pp. 1-6, 2022.
- [4]. Hägele, Martin & Nilsson, Klas & Pires, J. Norberto. *Industrial Robotics*. doi: 10.1007/978-3-540-30301-5_43, 2007.
- [5]. Roy N., Posner I., Barfoot T., Beaudoin P., Bengio Y., Bohg J., et al. *From Machine Learning to Robotics: Challenges and Opportunities for Embodied Intelligence*. Mach. Learn. arXiv preprint arXiv:2110.15245. 2021.
- [6]. Liao, Jianfeng & Huang, Fanghao & Chen, Zheng & Yao, Bin. *Optimization-based motion planning of mobile manipulator with high degree of kinematic redundancy*. International Journal of Intelligent Robotics and Applications. 3, 2019.

[7]. **Srinivasa, Siddhartha & Berenson, Dmitry & Cakmak, Maya & Collet, Alvaro & Dogar, Mehmet & Dragan, Anca & Knepper, Ross & Niemueller, Tim & Strabala, Kyle & Weghe, Mike & Ziegler, Julius.** HERB 2.0: Lessons Learned From Developing a Mobile Manipulator for the Home. Proceedings of the IEEE, 2012.

[8]. **Sereinig, Martin & Werth, Wolfgang & Faller, Lisa-Marie.**, *A review of the challenges in mobile manipulation: systems design and RoboCup challenges.* e & i Elektrotechnik und Informationstechnik. 137, pp. 1-12. 2020.

[9]. **Dömel A., Kriegel S., Kaßecker M., Brucker M., Bodenmüller T., Suppa M.**, *Toward fully autonomous mobile manipulation for industrial environments.* International Journal of Advanced Robotic Systems, 2017.

[10]. **Buschhaus, Arnd & Grünsteudel, H. & Franke, Jörg.** *Geometry-based 6D-pose visual servoing system enabling accuracy improvements of industrial robots*, pp. 195-200, 2016.

This article was reviewed and accepted for presentation and publication within the 11th edition of the International Multidisciplinary Symposium "UNIVERSITARIA SIMPRO 2024".

MIMICKING HUMANOID ROBOT GAIT USING HUMAN MOTION DATA FROM IMU

EMANUEL MUNTEAN¹, MONICA LEBA²

Abstract: This paper presents a new method for mimicking the gait of a humanoid robot using data obtained from Inertial Measurement Unit (IMU) sensors placed on a human body. The proposed framework benefits from the capabilities of IMU sensors to capture detailed motion data, including acceleration and angular velocity from various parts of the human body. The IMU sensors are strategically placed on the both feet to ensure comprehensive gait analysis. The collected data is processed using 2 Arduino UNO that send PWM signals to control the robot's Servo Motors in order to replicate human-like walking patterns. The methodology involves several key steps: data acquisition, preprocessing, feature extraction, and gait synthesis. During data acquisition, IMU sensors record the human subject's gait in real-time. The effectiveness of the proposed method is validated through a series of experiments, where the humanoid robot successfully mimics the human gait on flat surfaces. The results demonstrate that the IMU-based gait imitation framework achieves high fidelity in replicating human walking patterns, offering significant improvements in the robot's stability and adaptability. This research contributes to the field of humanoid robotics by providing a robust and efficient approach to gait imitation, with potential applications in rehabilitation, assistive robotics, and human-robot interaction. Future work will focus on refining the control algorithms and exploring the integration of additional sensory data to further enhance the robot's gait performance.

Key words: Humanoid robot, IMU sensors, gait imitation, signal processing, gait analysis, human-robot interaction.

1. INTRODUCTION

In recent years, the field of humanoid robotics has seen significant advancements, particularly in the development of bipedal locomotion systems. Mimicking human gait in humanoid robots is a complex task that requires precise control and coordination of multiple joints and actuators. This paper presents a new method to replicate the gait of a bipedal humanoid robot using data from four IMU sensors strategically placed on the human's legs. Specifically, two IMU sensors are mounted on the thigh and tibia of each leg, providing comprehensive motion data. The IMU sensors capture critical gait parameters such as acceleration, angular velocity, and orientation, which are essential for accurate gait analysis and replication. The data collected from

¹ Ph.D., Student Eng., emanuelmuntean@upet.ro

² Ph.D., Eng.

these sensors are processed by two Arduino Uno microcontrollers, which serve as the central processing units for the system. The Arduino Uno microcontrollers analyze the sensor data in real-time and generate control signals for the servomotors. To achieve precise control of the servomotors, the system employs two PCA9685 16-channel 12-bit PWM Servo Drivers. These drivers are capable of controlling up to 16 servomotors each, allowing for scalable and flexible motor control. In this setup, four servomotors are used to actuate the joints of the humanoid robot, enabling it to perform bipedal walking motions.

The integration of IMU sensors with Arduino microcontrollers and PCA9685 servo drivers provides a robust and cost-effective solution for humanoid gait replication. This method not only enhances the robot's ability to navigate complex environments but also improves its interaction with human tools and surroundings. The proposed system demonstrates the potential for advanced humanoid robots to achieve more natural and efficient bipedal locomotion, paving the way for future developments in humanoid robotics.

This paper will detail the design, implementation, and testing of the proposed gait replication system, highlighting the advantages and challenges associated with using IMU sensors and Arduino-based control for humanoid robots.

2. LITERATURE REVIEW

The main focus of paper [1] is to generate stable gaits for small-sized humanoid robots using geometric methods for kinematic analysis. The paper employs a 3D linear inverted pendulum model to determine the trajectory of the robot's center of mass, which, combined with foot positions, is used to solve the Denavit-Hartenberg (D-H) matrix. The goal is to find a computationally efficient solution to the inverse kinematics problem, enabling the robot to walk forward, turn left, and turn right in a stable manner. The paper also discusses the implementation and testing of these gaits on a 17-degree-of-freedom humanoid robot named TONY.

Paper [2] is focused on overcoming the sim2real gap for humanoid robots, specifically the HRP-5P humanoid robot, by utilizing current feedback from actuators and training policies in a simulation environment with degraded torque-tracking. The authors propose a method to address the discrepancies between simulated and real-world environments, which often result in poor performance when transferring policies trained in simulation to real hardware. They achieve this by simulating poor torque-tracking during training and incorporating current feedback from the actuators into the observation space of the reinforcement learning policy. This approach allows the policy to compensate for inaccuracies in torque application, leading to successful deployment of bipedal locomotion policies on the real HRP-5P robot.

The work [3] presents an intelligent motion attitude control algorithm for humanoid robots. This algorithm leverages deep reinforcement learning (DRL) to address issues related to the precision of motion manipulation control and the balance of humanoid robots. The paper proposes an offline pre-training approach for the attitude controller using an identification model as prior knowledge, which helps to overcome

the challenges of limited physical training samples and low training efficiency. The effectiveness of the proposed intelligent attitude controller is demonstrated through experiments, showing significant improvements in tracking accuracy and stability compared to traditional control methods like PID, PID + MPC, and MPC + DOB controllers.

Paper [4] improves the walking behavior of a humanoid robot to enable it to walk faster while ensuring safety during the learning process. The paper proposes the use of Safe Reinforcement Learning (Safe RL), specifically the Policy Reuse for Safe Reinforcement Learning (PR-SRL) algorithm, which leverages a safe baseline policy to guide the learning process. This approach aims to achieve fast convergence to near-optimal walking policies while minimizing the risk of falls and potential damage to the robot during training.

Authors of [5] propose and analyze robust control strategies for different models of the linear inverted pendulum, which represent the upper, middle, and lower body of a bipedal walking robot. The paper investigates the performance of one mass, two masses, and three masses linear inverted pendulum models in terms of stability, noise rejection, and set-point tracking to the zero-moment point (ZMP). The study aims to improve the stability and control of bipedal walking robots by using robust control methods and comparing the effectiveness of these models through simulations and experimental setups using an Arduino microcontroller and MATLAB Simulink system.

Paper [6] proposes a trajectory-planning method for biped robots that enhances walking stability and flexibility. The method combines the Linear Inverted Pendulum Model (LIPM) for the Single Support Phase (SSP) and the Linear Pendulum Model (LPM) for the Double Support Phase (DSP). The paper addresses the limitations of existing models that often ignore the DSP, leading to discontinuities in the acceleration of the center of mass (CoM) and negatively impacting walking stability. By incorporating both LIPM and LPM, the proposed method aims to achieve smoother CoM acceleration transitions, improve walking stability, and enable real-time trajectory planning for various walking scenarios, including periodic walking, speed adjustments, disturbance recovery, and walking on uneven terrain.

The work [7] analyzes and compares the optimal control of the zero-moment point (ZMP) for a bipedal walking robot. The study involves both experimental and theoretical approaches to determine the ZMP during the single support phase of the robot's gait cycle. The research utilizes a 17 degrees of freedom bipedal robot made of hard aluminum sheets and employs MATLAB Simulink for simulation. The paper aims to achieve optimal balance control by minimizing the performance index through optimal feedback control gains, and it discusses the principles of ZMP, the methodology for measuring ZMP, and the application of optimal control methods to ensure the stability of the bipedal robot.

Paper [8] is developing a dynamic gait planning method for the NAO humanoid robot to effectively climb and descend stairs. The method involves modeling the NAO robot's kinematics, analyzing its gait characteristics, and planning its movements using a first-order linear inverted pendulum model. The paper also introduces the zero-moment point (ZMP) stability judgment and supporting polygons control to ensure the robot's stability during stair navigation. The feasibility of the proposed gait planning method is

verified through simulations and real-world experiments using the Webots platform and the NAO robot.

The work [9] proposes an improved model predictive control (MPC) method incorporating an extended Kalman filter (EKF) to enhance the robustness of humanoid robots' walking capabilities by using a simplified finite-sized foot-pendulum model for gait planning in both single-support and double-support phases, ensuring the robot's center of mass (CoM) converges to the divergent component of motion (DCM), thereby simplifying feedback control and enabling the robot to adjust its step duration to compensate for CoM trajectory errors caused by disturbances, as demonstrated through simulations on flat surfaces, under impact disturbances, and on uneven terrain.

Authors of [10] develop a highly efficient motion planner that generates stable center-of-mass (CoM) trajectories for legged robots, specifically for walking, running, and jumping motions, by leveraging the 3D-Divergent Component of Motion (3D-DCM) framework, which was previously used for walking, and extending its application to include running and jumping; the key contributions of the paper include: introducing a unified formulation for the CoM and DCM waypoints at the start and end of each motion phase, making the framework extensible and enabling efficient waypoint computation, proposing a highly efficient algorithm for computing DCM and CoM waypoints for a general sequence of motion phases, including stance, flight, and transition phases, implementing transitions between different modes of motion (standing, walking, running, and jumping) within the 3D-DCM framework, and demonstrating the feasibility of the generated reference trajectories through extensive whole-body simulations with the humanoid robot TORO, aiming to show that the 3D-DCM framework retains its validity and coherence during flight phases and can be used for planning complex locomotion tasks involving arbitrary contact sequences and time parametrizations.

Research from [11] improves the fast and stable walking ability of humanoid robots by proposing a gait optimization method using a Parallel Comprehensive Learning Particle Swarm Optimizer (PCLPSO) algorithm, with key aspects including the selection of key parameters affecting walking gait based on the natural zero-moment point (ZMP) trajectory planning method, decomposing gait training tasks in a parallel distributed multi-robot environment using the RoboCup3D simulation platform, employing a layered learning approach to enhance turning ability, and experimentally validating that the PCLPSO algorithm achieves quick, optimal solutions for a fast, steady gait and flexible steering, emphasizing the use of intelligent algorithms to balance speed, stability, and flexibility in humanoid robot walking.

In paper [12] is developed a robust and efficient gait controller for the humanoid robot NAO by integrating a Particle Swarm Optimization (PSO) technique with a Proportional-Integral-Derivative (PID) controller to enhance the robot's stability and navigation capabilities [13], emphasizing gait planning and stability using the Linear Inverted Pendulum Model (LIPM), implementing a PSO-tuned PID controller to optimize the parameters for better obstacle avoidance and stability, validating the approach through simulations and real-world experiments, and demonstrating through comparative analysis that the PSO-tuned PID controller significantly outperforms other techniques in terms of stability and efficiency.

3. MATERIALS AND METHODS

To develop a method to imitate the walking of a bipedal humanoid robot, we used a robot created by Youbionic [Figure 1], 3D printed from PetG material. The robot, named Ionut, has the appearance of a kindergarten child but with the personality of a teenager. He is 110 cm tall and weighs around 40 kg. The robot is equipped with various servomotors, which allows it to easily perform various tasks, including walking on a straight surface, at the request of the user. We focused on making the movement on both legs of the robot.

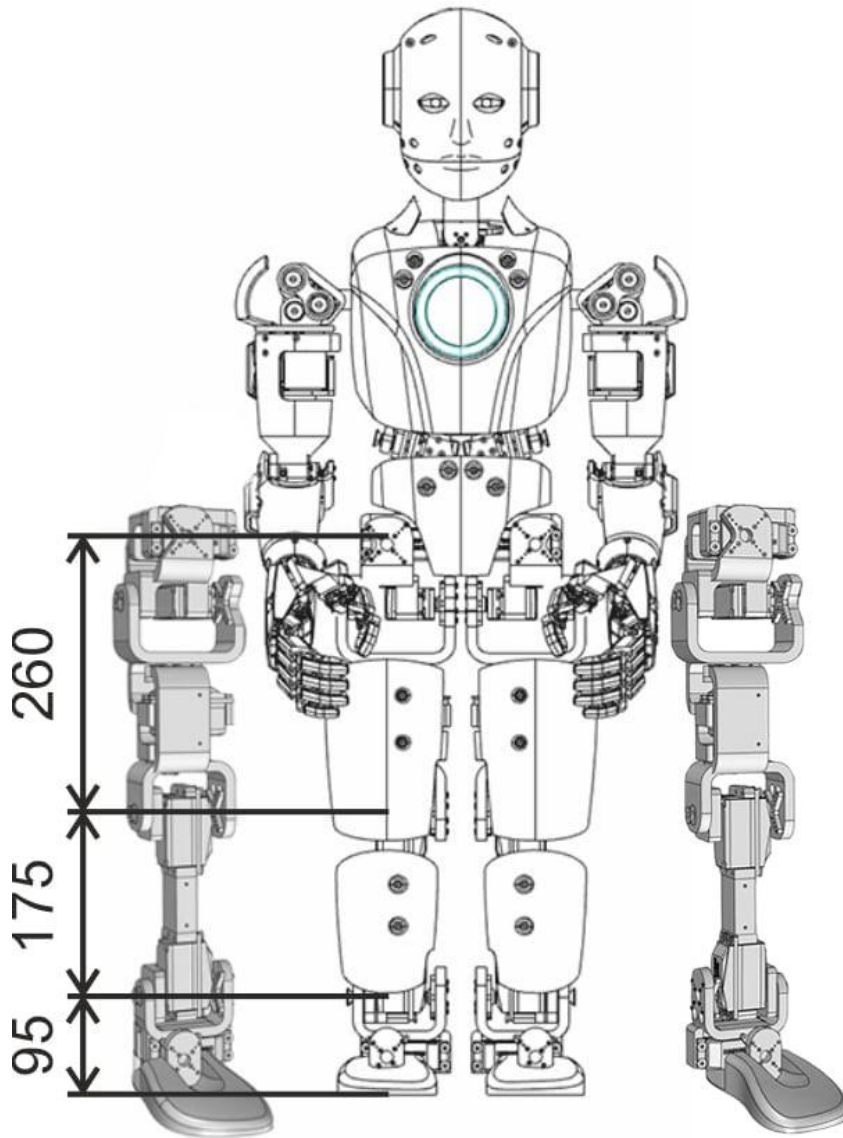


Fig.1. Humanoid robot scheme with accent on both legs (reproduced with written approval from Youbionic)

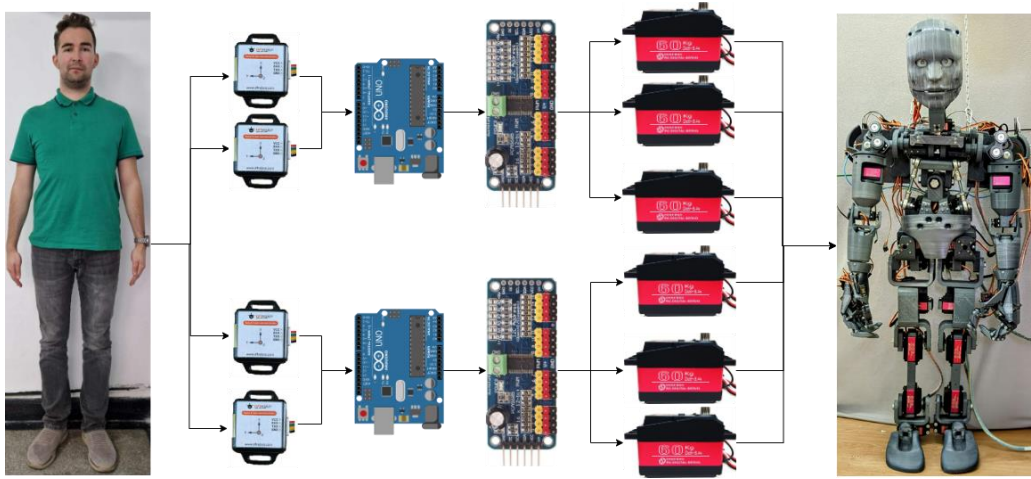


Fig.2. Hardware Block Diagram of the humanoid robot legs control system

To build the physical system, we used four IMU [14] sensors distributed two on each leg, located on the calf and leg bone. As the main microcontrollers, we used two independent Arduino UNO boards, along with two PCA9685 PWM motor drivers and six servo motors, each capable of a power of 60 kg depending on the received supply voltage, as seen in Figure 2.

4. EXPERIMENTAL RESULTS

To improve lower limb coordination during walking you have to stand tall with good posture by keeping the head up, eyes forward, shoulders back and down, and core engaged; start with a heel-to-toe step, striking the ground with the heel first, rolling through to the toes and pushing off to start the next step; take appropriately sized steps, avoiding overly long strides and letting the back leg provide power; keep the hips level to avoid swaying side-to-side; swing arms naturally in opposition to the legs with slightly bent elbows; maintain a steady rhythm with evenly timed steps at a comfortable pace; practice on different surfaces, starting on flat ground and progressing to uneven terrain; focus on balance by keeping the body centered.

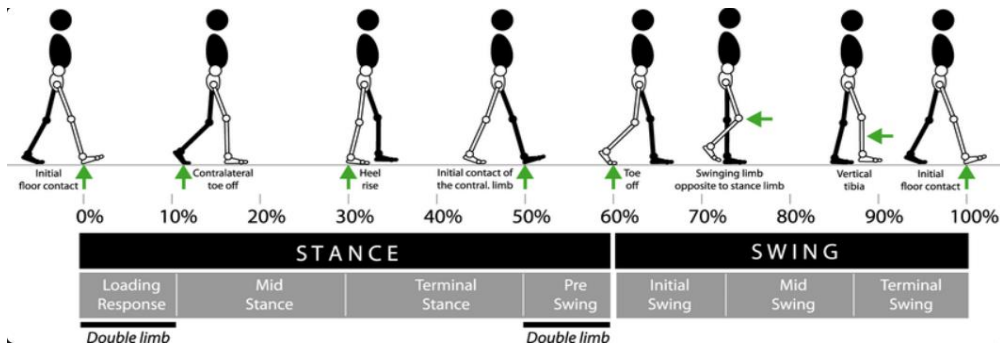


Fig.3. How to make a step [15]

In humans' case, bipedalism is a mode of terrestrial locomotion in which an organism moves using its two hind limbs or legs. This is a distinctive feature of the human species and its ancestors, which involves walking and running on two legs. To realize a locomotion of the biped robot, we used four IMU sensors, two placed on each leg. We started the first movement with the right foot, focusing on the X-axis. In Figure 4 the left leg serves as the pivot. In this image, a flexion/extension movement is observed: the yellow line represents the sensor located on the knee, which indicates an angle of about 90 degrees and the purple line corresponds to the sensor on the hip leg, which shows an angle of about 40 degrees then when the right leg is tense. The gray and blue lines represent the Y-axis, with values between 0 and 5 degrees. The pivot leg in this case is represented by left leg and the yellow line is 95 degrees, the purple line 90 degrees and the gray and blue line has 0 and 5 degrees.

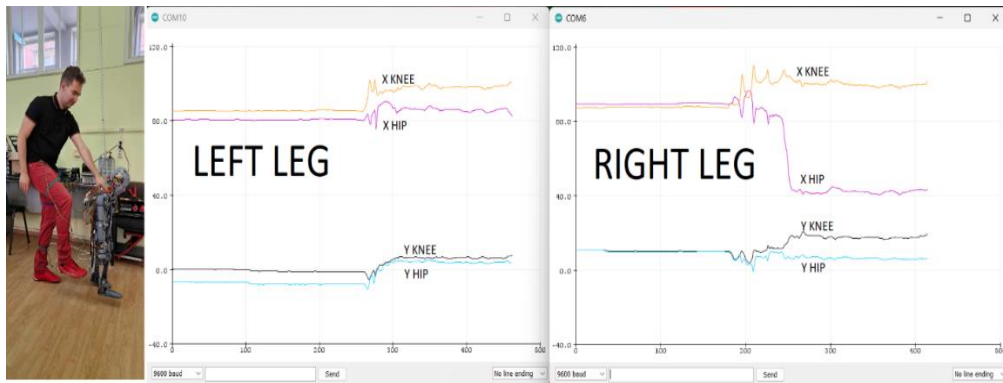


Fig.4. Left leg pivot position and right leg raised

In Figure 5 the left leg is ready to perform the movement on the X axis. The yellow line represents the sensor located on the knee, which indicates an angle of approximately 95 degrees, and the purple line corresponds to the sensor on the hip leg, which indicates an angle of approximately 80 degrees when the right leg is support for movement. The gray and blue lines represent the Y-axis, with values between 0 and -10 degrees. The pivot leg in this case is represented by right leg and the yellow line is 100 degrees, the purple line 80 degrees and the gray and blue line has 5 and 0 degrees.

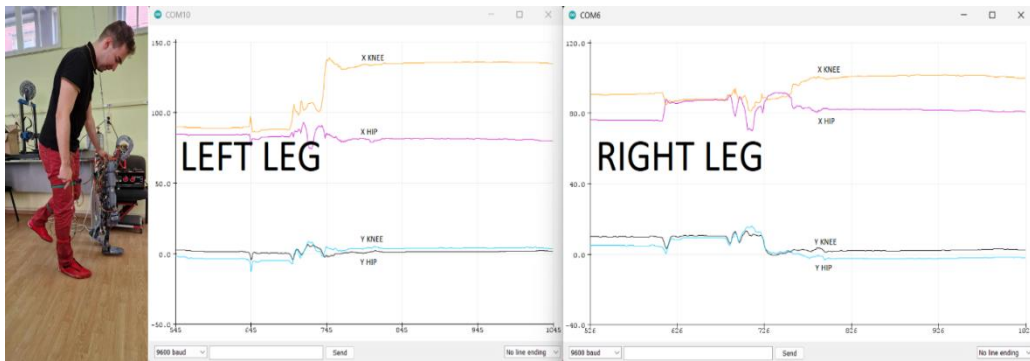


Fig.5. The right leg pivot and the left foot perform the movement

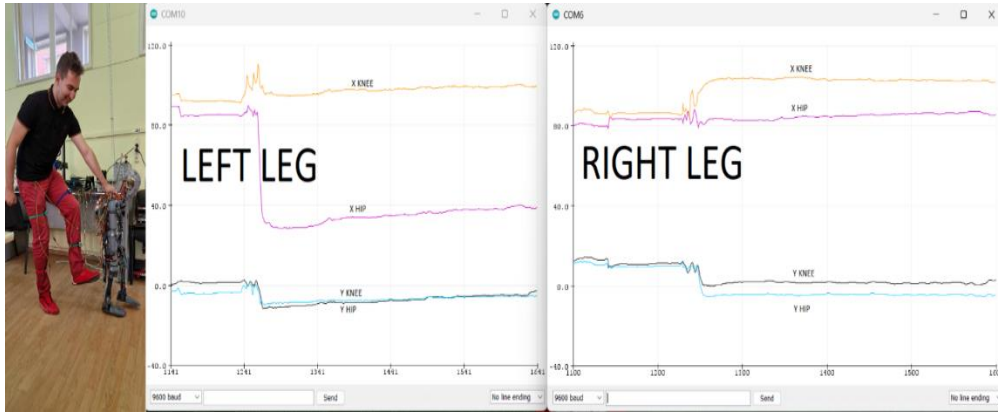


Fig.6. Right leg pivot position and left leg raised

Finally, I finished the movement with the right leg according to Figure 6 as the pivot and the left leg making the final movement on the X axis. The yellow line represents the sensor located on the knee, which indicates an angle of approximately 90 degrees and the purple line corresponds to the sensor on the hip leg, which indicates an angle of approximately 40 degrees.

The gray and blue lines represent the Y-axis, with values between 0 and -10 degrees. The pivot leg in this case is represented by right leg and the yellow line at the shin of 95 degrees, the purple line 90 degrees and the gray and blue line has 5 and - 5 degrees.

5. CONCLUSIONS

In this paper, we have presented a new method for mimicking the gait of a bipedal humanoid robot using data from four IMU sensors strategically placed on the robot's legs. By positioning two IMU sensors on the thigh and tibia of each leg, we were able to capture detailed motion data essential for accurate gait analysis.

The data collected from these sensors were processed in real-time by two Arduino Uno microcontrollers, which generated the necessary control signals for the servomotors.

Our experimental results demonstrate that the proposed system can successfully replicate the gait of a bipedal humanoid robot, enabling it to navigate complex environments and interact more naturally with its surroundings.

This method not only enhances the robot's mobility but also opens up new possibilities for its application in various fields, including assistive robotics, human-robot interaction, and autonomous navigation. While the current system shows promising results, there are still challenges to be addressed, such as improving the robustness of the gait under different terrains and conditions, and optimizing the real-time processing capabilities of the microcontrollers.

Future work will focus on refining the control algorithms, integrating additional sensors for enhanced feedback, and exploring machine learning techniques to further improve the robot's gait adaptation and performance.

In conclusion, the proposed method provides a solid foundation for advancing bipedal locomotion in humanoid robots, contributing to the ongoing development of more capable and versatile robotic systems. The insights gained from this research will be instrumental in driving future innovations in the field of humanoid robotics.

REFERENCES

- [1]. **Sriganesh P., Mahendrakar P. R., Mohan R.,** *Solving inverse kinematics using geometric analysis for gait generation in small-sized humanoid robots*, In 2020 IEEE/SICE International Symposium on System Integration (SII), pp. 384-389, IEEE, January 2020, DOI: <https://doi.org/10.1109/SII46433.2020.9025944>.
- [2]. **Pratap Singh, R., Xie Z., Gergondet P., Kanehiro F.,** *Learning Bipedal Walking for Humanoids with Current Feedback*, arXiv e-prints, arXiv-2303, 2023, DOI: <https://doi.org/10.48550/arXiv.2303.03724>.
- [3]. **Shi Q., Ying W., Lv L., Xie J.,** *Deep reinforcement learning-based attitude motion control for humanoid robots with stability constraints*, Industrial Robot: the international journal of robotics research and application, Vol. 47, No. 3, pp. 335-347, 2020, DOI: <https://doi.org/10.1108/IR-11-2019-0240>.
- [4]. **García J., Shafie D.,** *Teaching a humanoid robot to walk faster through Safe Reinforcement Learning*, Engineering Applications of Artificial Intelligence, Vol. 88, p. 103360, 2020, DOI: <https://doi.org/10.1016/j.engappai.2019.103360>.
- [5]. **Kareem, A. F. A., Ali, A. A. H.,** *Robust stability control of inverted pendulum model for bipedal walking robot*, Al-Nahrain Journal for Engineering Sciences, Vol. 23, No. 1, pp. 81-88, 2020, DOI: <http://doi.org/10.29194/NJES.23010081>.
- [6]. **Li L., Xie Z., Luo X., Li J.,** *Trajectory planning of flexible walking for biped robots using linear inverted pendulum model and linear pendulum model*, Sensors, Vol. 21, No. 4, p. 1082, 2021, DOI: <https://doi.org/10.3390/s21041082>.
- [7]. **Kareem A. F. A., Ali A. A. H.,** *Experimental and theoretical optimal regulator control of balance zero moment point for bipedal robot*, Journal of Engineering and Sustainable Development, Vol. 24, No. 6, pp. 68-82, 2020, DOI: <https://doi.org/10.31272/jeasd.24.6.6>.
- [8]. **Juang L. H.,** *Humanoid robot runs up-down stairs using zero-moment with supporting polygons control*, Multimedia Tools and Applications, Vol. 82, No. 9, pp. 13275-13305, 2023, DOI: <https://doi.org/10.1007/s11042-022-13723-0>.
- [9]. **Zhang Z., Zhang L., Xin S., Xiao N., Wen X.,** *Robust walking for humanoid robot based on divergent component of motion*, Micromachines, Vol. 13, No. 7, p. 1095, 2022, DOI: <https://doi.org/10.3390/mi13071095>.
- [10]. **Mesanan G., Schuller R., Engelsberger J., Ott C., Albu-Schäffer A.,** *Unified Motion Planner for Walking, Running, and Jumping Using the Three-Dimensional Divergent Component of Motion*, IEEE Transactions on Robotics, 2023, DOI: <https://doi.org/10.1109/TRO.2023.3321396>.
- [11]. **Tao C., Xue J., Zhang Z., Cao F., Li C., Gao H.,** *Gait optimization method for humanoid robots based on parallel comprehensive learning particle swarm optimizer algorithm*, Frontiers in Neurorobotics, Vol. 14, p. 600885, 2021, DOI: <https://doi.org/10.3389/fnbot.2020.600885>.
- [12]. **Kashyap A. K., Parhi D. R.,** *Particle Swarm Optimization aided PID gait controller design for a humanoid robot*, ISA Transactions, Vol. 114, pp. 306-330, 2021, DOI: <https://doi.org/10.1016/j.isatra.2020.12.033>.
- [13]. **Rus C., Lupulescu E., Leba M., Risteiu, M.,** *Advanced Mathematical Modeling and Control Strategies for Autonomous Drone Systems*, 25th International Carpathian Control Conference (ICCC), pp. 1-6, IEEE, May 2024.

[14]. **Rus C., Leba M., Sibisanu R.,** *SOS-My Grandparents: Using the Concepts of IoT, AI and ML for the Detection of Falls in the Elderly*, In World Conference on Information Systems and Technologies, pp. 164-173, Cham: Springer Nature Switzerland, March 2024.

[15]. *Phases of human locomotion and related biomechanical events*, ResearchGate, https://www.researchgate.net/figure/Phases-of-human-locomotion-and-related-biomechanical-events-According-to-the-reciprocal_fig7_306359098/actions#reference.

This article was reviewed and accepted for presentation and publication within the 11th edition of the International Multidisciplinary Symposium "UNIVERSITARIA SIMPRO 2024".

PARTICULARITIES REGARDING THE DETERMINATION OF MAXIMUM SURFACE TEMPERATURE OF JUNCTION BOXES WITH TYPE OF PROTECTION INCREASED SAFETY “E” DESIGNED FOR USE IN GASEOUS EXPLOSIVE ATMOSPHERES

LUCIAN MOLDOVAN¹, MIHAI MAGYARI², CLEMENTINA MOLDOVAN³, SORIN RÂȘNOVEANU⁴

Abstract. Increased safety “e” represents a type of protection applied to electrical equipment or Ex Components designed for use in potentially explosive atmospheres generated by the presence of flammable substances in the form of gases, vapours or mists. According to this type of protection, additional measures are applied so as to exclude the possibility of occurrence of arcs, sparks and excessive temperatures even in case of abnormal operation. This type of protection cannot be applied to equipment producing electrical arcs and sparks in normal operation. This paper underlines some specific aspects regarding the determination of maximum surface temperature (such as the preparation of the test sample, determination of the hottest points and the maximum surface temperature), considering the requirements of the specific standards, in case of increased safety junction boxes designed for use in gaseous explosive atmospheres (including hydrogen).

Key words: increased safety, junction box, type of protection, maximum surface temperature.

1. GENERALITIES

Considering that increased safety “e” [[1]] can only be applied to equipment that is not producing electrical arcs and sparks in normal operation (and in specific abnormal operation), one of its’ main applications is related to junction boxes. By the supplementary measures taken in the designing and construction of such equipment, even in specific abnormal operating conditions excessive temperatures, arcs and sparks are prevented to occur [[1]], [8], [11], [13].

¹ *Ph.D., Eng.*, INCD INSEMEX, lucian.moldovan@insemex.ro

² *Ph.D., Eng.*

³ *Ph.D., Eng.*

⁴ *Ph.D., Eng.*

In the specific case of junction boxes, protected by increased safety “e”, the proper selection of insulating materials (used in the construction of enclosures and terminals), a suitable ingress protection IP for the enclosure and provision of adequate insulation distances (clearances and creepage distances) between the conductive parts subjected to electrical voltages represents the main aspects on which the explosion protection is based [[1]].

In case of increased safety equipment one of the ignition sources is represented by hot surfaces. Identification of the hottest points on the equipment is made by thermal tests. The temperatures of the hottest points are determined both on the external and internal parts of the equipment (considering that the explosive atmosphere can come in contact with the internal parts of the equipment) [[2]], [9], [10], [12], [15].

Determination of maximum surface temperature [[3], [4]], in case of increased safety junction boxes, is made in the conditions provided by SR EN IEC 60079-0 [[3]] and SR EN 60079-7 [[1]].

The specific standards considered, under the ATEX Directive [[5]], for assessment of electrical equipment with type of protection increased safety “e”, are SR EN IEC 60079-0 (providing the general requirements for equipment designed for use in explosive atmospheres) and SR EN 60079-7 (providing the specific requirements for the type of protection increased safety “e”) [1, 3].

2. SPECIFIC REQUIREMENTS FOR DETERMINATION OF MAXIMUM SURFACE TEMPERATURE IN CASE OF JUNCTION BOXES WITH TYPE OF PROTECTION INCREASED SAFETY “E”

The junction (connection) boxes, when tested to determine the maximum surface temperature are fitted with a number of terminals (considering the 'worst case' terminal). The terminals are wired using conductors of the maximum size (as specified for the particular terminal). The length of conductor connected to each terminal and contained within the enclosure shall be equal to the maximum internal dimension (three-dimensional diagonal) of the enclosure. The wiring (terminals and conductors) are so arranged that the test current is passed through each terminal and its wiring in series. In order to represent the thermal effects of bunching of conductors and also other effects of typical installations, the conductors have to be arranged in groups (of six), each with a length outside the box of at least 0,5 m. The 'worst case' terminal is that which has been found to exhibit the highest temperature rise [[1]].

A current equal to the rated current of the terminal for the application shall be passed through the series circuit. The temperature of the hottest part shall be measured when steady state conditions have been reached [[1]], [14], [17], [19], [24].

The test to determine maximum surface temperature shall be performed under the most adverse ratings with an input voltage of 90 % of the rated voltage or at 110 % of the rated voltage of the electrical equipment whichever gives the maximum surface temperature. Where the input voltage does not directly affect the temperature rise of the equipment or Ex Component, such as a terminal or a switch, the test current shall be increased to 110 % of the rated current [[3]], [20], [22].

The results can be affected by the conductor size, conductor entry location, terminal location / geometry, and terminal size [[3]]. For equipment which can normally be used in different positions, the temperature in each position shall be considered [[3]], [26].

The temperature measuring devices (thermometers, thermocouples, etc.) and the connecting cables must be selected and installed so that they do not significantly affect the thermal behaviour of the equipment [[3]], [21].

The final temperature is considered to have been reached when the rate of temperature rise does not exceed a rate of 2 K/h (in case of equipment designed for use in gaseous explosive atmospheres – including hydrogen) [[3]], [16], [18], [23], [25].

The measured maximum surface temperature shall not exceed for Group II equipment, temperature class T6, the temperature class, less 5 K (80°C) [[3]].

3. EXPERIMENTAL PART

To perform the testing, a sample junction box was used, with the outer approximate dimensions of 27 cm x 27 cm x 13,5 cm (L x W x H). The junction box was equipped with 36 feed-through terminals of 2,5 mm² installed on a mounting rail with two end clamps. Conductors with a cross section of 2.5 mm² were used (according to the terminal specifications) – this was the maximum cross section of a flexible conductor with a ferrule. The length of the conductors connected to each terminal and contained within the enclosure was equal to the maximum internal dimension - three-dimensional diagonal [[6]].

For the tests, a DC constant current power source TTi QPX1200S was used. To measure the current a high definition oscilloscope Lecroy HDO9304 and a current clamp CP031A were used. For the measurement of voltage, a specific channel of the multimeter Agilent 34972A (equipped with two 34901A multiplexers) was used.

The terminals were tightened at a torque of 0,55 Nm (according the terminal datasheet) with the help of a digital torque screwdriver BMS MS500S.

Type K thermocouples, with 0.25 mm diameter were used to measure the temperatures. The method for fixing the thermocouples was with mechanical pressure. Also, thermal conductive paste was used to create a better contact between the measured surface and the thermoelement. These were connected to an Agilent 34972A multimeter (equipped with 34901A multiplexers). A number of 9 thermocouples were used to measure the temperature during the tests. Also, a thermal vision camera was used, at first (in a pre-test phase) to identify the hottest areas (hottest points) so that thermocouples to be placed there.

The arrangement used for testing is presented in figure 1.

The indicated temperature class of the equipment was T6, and the test sample was tested with different currents to find the maximum current that complies with the limiting temperature of temperature class T6 (in this case 80 °C).

The junction box was placed in vertical position with free air movement (not being in contact with a wall). The testing of the junction box was made using DC in two steps:

1. Testing of the “worst case terminals” scenario

The testing was made with the junction box equipped with all the 36 terminals. The terminals were connected in series so as the testing current to pass through all the terminals. The conductors were bundled in groups of 6 [[1], [6]].



Fig.1. Testing arrangement to determine the hottest point

A specific current of 12 A was first used to determine the hotspot [[6]]. Also, to determine the maximum current for temperature class T6 (at a maximum ambient temperature of + 40 °C) the junction box was supplied to different currents (6 A, 8 A, 10 A, 13,89 A, 14,67A) and the maximum current associated to temperature class T6 was calculated.

2. Testing with the rated current scenario

Testing was made on 6 terminals (the 6 terminals mounted in the middle of the 36 terminals). The other 30 terminals were not removed. The test current was set to 21 A (according to the terminal datasheet) and the hotspot was also determined [[6]].

4. RESULTS AND DISCUSSIONS

The following results were obtained after performing the specified tests.

1. Testing of the “worst case terminals” scenario

When testing at 12 A, the hotspot was determined to be at the second (middle) group of six conductors inside the junction box (top part). The ambient temperature considered was 22,5 °C. The final temperature at the hotspot was 53,1°C (30,6 K increase of temperature) (Figure 2). Similar values were recorded when the test was performed with an AC power source.

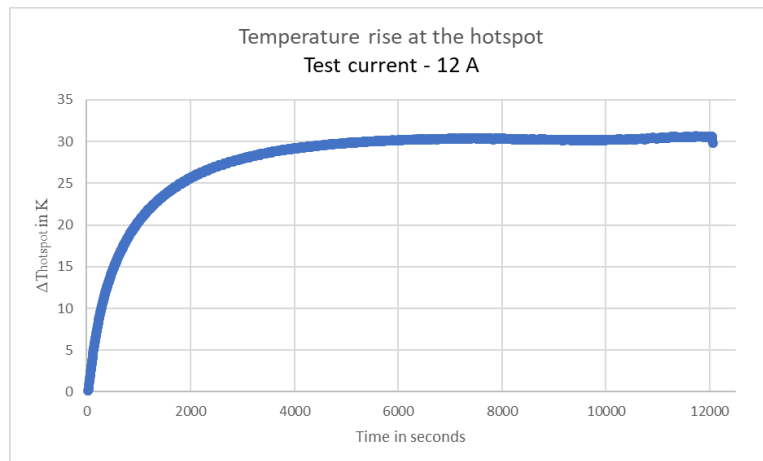


Fig.2. Temperature rise at the hotspot

PARTICULARITIES REGARDING THE DETERMINATION OF MAXIMUM SURFACE
TEMPERATURE OF JUNCTION BOXES WITH TYPE OF PROTECTION INCREASED
SAFETY “E” DESIGNED FOR USE IN GASEOUS EXPLOSIVE ATMOSPHERES

Also, in the second part of the test, the temperature rise was determined for different currents in order to determine the maximum current associated to temperature class T6 as specified in Table 1. The maximum increase of temperature, according the temperature class, must also consider the safety margins associated to the temperature classes together with the maximum ambient temperature at which the product can be used (for example, in case of temperature class T6, for a maximum ambient temperature of 40°C, the safety margin is 5 K, resulting a maximum temperature increase of 40 K – the temperature shall not exceed 80°C) [[3], [5]].

Table 1. Temperature rise function of the testing current

Crt. No.	Test current [A]	Ambient temperature [°C]	Temperature rise at the hotspot [K]
1.	6	22,5	8,0
2.	8	21,9	14,3
3.	10	22,8	21,7
4.	12	22,5	30,6
5.	13,89	22,5	39,7
6.	14,67	22,9	44,4

The maximum current for the temperature class T6 was calculated and found to be 13,91A (considering the maximum ambient temperature of 40°C). For calculation, the regression line (trendline) was used as a polynomial function of the fourth order (Figure 3). In order to have a better estimation of the heating effect induced by the electric current, the squared values of the current were used in correspondence with the temperature rise at the hotspot.

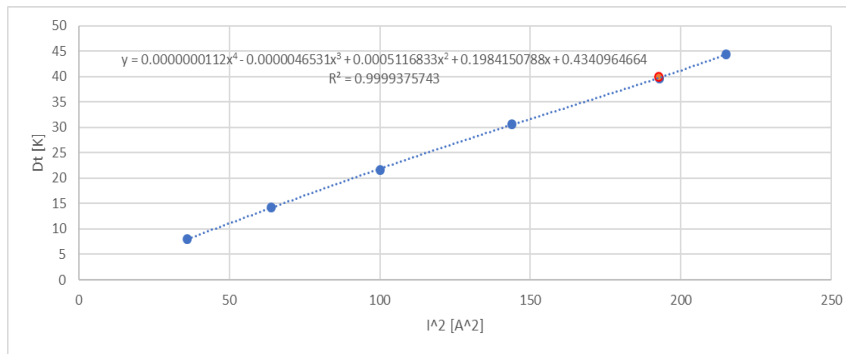


Fig.3. Polynomial regression line dependency on the squared current

2. Testing with the rated current scenario

When testing at 21 A, having only 6 terminals connected in series, the maximum temperature (hotspot) was found to be in the second (middle) group of six conductors inside the junction box (top part). The ambient temperature was 22,9 °C and the final temperature was measured as 61,6 °C (giving an increase of temperature of 38,7 °C). Also, a high temperature was measured on the internal metallic surfaces of the 2 terminals placed in the middle of the 6 terminals group (having a temperature of 60,81 °C) and giving an increase of temperature of 37,95 °C (Figure 4).

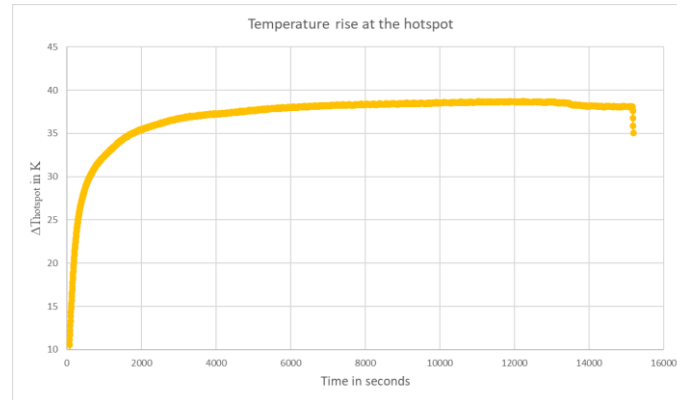


Fig.4. Temperature rise at the hotspot

When performing the tests to determine the maximum surface temperature in case of connection (junction) boxes with the type of protection increased safety, the hotspot might be found on the metallic part of the terminals or on the cables connected to the terminals under test. Even if the connection boxes are certified without the connecting cables (these are chosen by the installer according the criteria provided in the specific standard EN 60079-14 [[7]]) the hottest point might be found on the cables (conductors) inside the junction box.

When a certain temperature class is required for a junction box, equipped with a specific number of terminals, the maximum permitted current is calculated. One method used for the calculation is based on the temperature increase as a function of the squared current and using the polynomial regression (regression trendline). Also, specific software (like Microsoft Excel) can be use to identify the regression trendline and the maximum permitted value of the current.

The preparation of the test sample is very important and must consider the standard requirements for preparation (grouping the conductors in bundles of six, tightening the terminal screws at a specific torque given by the manufacturer, using thermal conductive paste to provide a more intimate thermal contact between the thermocouples and the measuring surface/point etc.).

5. CONCLUSIONS

In the beginning of the paper were analysed the required conditions to perform the determination of the maximum surface temperature in case of junction boxes with type of protection increased safety “e”.

For a certain temperature class (T6) the maximum surface temperature (maximum temperature rise) was determined together with the maximum admitted current for the “worst case terminal scenario”. The testing method and determination by calculus of the maximum admitted current were presented.

The maximum surface temperature was determined also in the case of maximum rated current scenario. In order to find the hottest point, in case of junction boxes with type of protection increased safety, temperature must be monitored both on the terminals and on the cables inside the enclosure.

The factors influencing the determination of the maximum surface temperature related to the preparation of the test sample were also presented.

This paper is important for those performing the tests for determination of maximum surface temperatures (testing laboratories and manufacturers of explosion proof junction boxes with type of protection increased safety “e” designed for use in explosive gaseous atmospheres) in order to consider the factors influencing the determination of maximum surface temperature and of the hottest points inside the enclosure.

6. ACKNOWLEDGEMENTS

This work was carried out through the “Nucleu” program of the National Research, Development and Innovation Plan 2022-2027, supported by MCID, project no. PN23320102.

REFERENCES

- [1]. *** SR EN 60079-7:2016, *Explosive atmospheres - Part 7: Equipment protection by increased safety "e"*, ASRO, 2016.
- [2]. Moldovan L., Burian, S.; Magyari, M.; Darie, M.; Fotău, D., *Factors influencing the determination of maximum surface temperature for explosion-proof luminaires*, Environmental Engineering and Management Journal, Vol.16, No.6, June, Pg. 1309-1316, 2017. <https://doi.org/10.30638/eemj.2017.139>
- [3]. *** SR EN IEC 60079-0, *Explosive atmospheres - Part 0: Equipment – General requirements*, ASRO, 2018.
- [4]. *** SR EN 1127-1, *Explosive atmospheres. Explosion prevention and protection Basic concepts and methodology*, ASRO, 2019.
- [5]. *** Directive 2014/34/EU *on the harmonisation of the laws of the Member States relating to equipment and protective systems intended for use in potentially explosive atmospheres (recast)*, Official Journal of the European Union, no.96, 2014.
- [6]. Wu J., Krause T., *Procedure Instruction Connection and Junction Boxes (“CJB”) Test Round*, Physikalisch-Technische Bundesanstalt, Document-ID: PI-CJB2023-01, 2023.
- [7]. *** SR EN 60079-14, *Explosive atmospheres – Part 14: Electrical installations design, selection and erection*, ASRO, 2014.
- [8]. Stepanescu, S., Rehtanz, C., Arad, S., Fotău, I., Marcu, M., Popescu, F. *Implementation of small water power plants regarding future virtual power plants* 10th International Conference on Environment and Electrical Engineering, pp. 1-4, IEEE, 2011.
- [9]. Fîță N. D., Lazăr T., Popescu F. G., Pasculescu D., Pupăză C., Grigorie E., *400 kV power substation fire and explosion hazard assessment to prevent a power black-out*, International Conference on Electrical, Computer Communications and Mechatronics Engineering-ICECCME, pp. 16-18, 2022.
- [10]. Fita N.D., Obretenova M.I., Pasculescu D., Tatar A., Popescu F.G., Lazar T., *Structure and analysis of the power subsector within the national energy sector on ensuring and stability of energy security*, Annals of „Constantin Brâncuși” University of Târgu Jiu, ENGINEERING SERIES, Issue 2/2022, pp.177-186, 2022.
- [11]. Handra A.D., Popescu F.G., Pasculescu D., *Utilizarea energiei electrice: lucrări de laborator*, Editura Universitas, 2020.
- [12]. Fîță N.D., Radu S.M., Pasculescu D., Popescu F.G., *Using the primary energetic resources or electrical energy as a possible energetical tool or pressure tool*, In International conference KNOWLEDGE-BASED ORGANIZATION, vol. 27, no. 3, pp. 21-26. 2021.

- [13]. **Lazar T., Marcu M.D., Utu I., Popescu F. G., Pasculescu D.,** *Mașini electrice - culegere de probleme*, Editura Universitas, Petroșani, pp. 197, 2023.
- [14]. **Popescu F.G., Păsculescu D., Păsculescu V.M.,** *Modern methods for analysis and reduction of current and voltage harmonics*, LAP LAMBERT Academic Publishing, ISBN 978-620-0-56941-7, pp. 233, 2020.
- [15]. **Pasculescu D., Niculescu T.,** *Study of transient inductive-capacitive circuits using data acquisition systems.*" International Multidisciplinary Scientific GeoConference: SGEM 2, no. 1, 323-329, 2015.
- [16]. **Pana L., Janusz G., Pasculescu D., Pasculescu V. M., Moraru R. I.,** *Optimal quality management algorithm for assessing the usage capacity level of mining transformers*, Polish Journal of Management Studies 18, no. 2, 233-244, 2018.
- [17]. **Andras A., Popescu F.D., Radu S.M., Pasculescu D., Brinas I., Radu M.A., Peagu D.,** *Numerical simulation and modeling of mechano-electro-thermal behavior of electrical contact using comsol multiphysics*. Applied Sciences, 14(10), 4026, 2024.
- [18]. **Petrilean D.C., Racz M.D.,** *The influence of humidity on air temperature in underground mines as a factor of air quality assessment*, Romanian Society for Quality Assurance, Journal Calitatea, 2019.
- [19]. **Petrilean D.C., Racz M.D., Gaita B.I.,** *Determination of the energy performance of the CHP Danutoni installation*, International Multidisciplinary Scientific GeoConference: SGEM, Surveying Geology & Mining Ecology Management (SGEM). 2018.
- [20]. **Radu S.M., Petrilean D.C., Irimie S.I., Gaita B.I., Racz M.D.,** *Energetic and environmental efficiency of the cogeneration of a baking plant*, 2018.
- [21]. **Petrilean D.C.,** - *Method of calculus for the power input of the helical screw compressor*, Journal Sci. Bull. Series D, University of Politehnica Bucharest, 2009.
- [22]. **Petrilean D.C., Jitea P.C., Suciu A.,** *Energetic efficiency of pneumatic installation with polytropic compression*, University of Petrosani, 2009.
- [23]. **Gaita B.I., Mortoiu D., Petrilean D.C, Tataru A.C. Danci M.,** *Special lifting and transport solutions for heavy and complex loads in the design of the lifting frame*, MATEC Web Conf. Volume 373, 10th edition of the International Multidisciplinary Symposium "UNIVERSITARIA SIMPRO 2022": Quality and Innovation in Education, Research and Industry – the Success Triangle for a Sustainable Economic, Social and Environmental Development, 2022.
- [24]. **Vasilescu G.D., Petrilean C.D., Kovacs A., Vasilescu G.V., Pasculescu D., Ilcea G.I., Burduhos-Nergis D.P., Bejinariu C.,** *Methodology for assessing the degree of occupational safety specific to hydrotechnical construction activities, in order to increase their sustainability*, Sustainability, Jan 21;13(3):1105, 2021.
- [25]. **Marcu M., Niculescu T., Slusariuc R. I., Popescu, F. G.,** *Modeling and simulation of temperature effect in polycrystalline silicon PV cells*, IOP Conference Series: Materials Science and Engineering, Vol. 133, No. 1, pp. 012005, 2016.
- [26]. **Popescu F.G., Arad S., Marcu M.D., Pana L.,** *Reducing energy consumption by modernizing drives of high capacity equipment used to extract lignite*, Papers SGEM2013/Conference Proceedings, Vol. Energy and clean technologies, pp. 183 - 190, Albena., Bulgaria, 2013.

This article was reviewed and accepted for presentation and publication within the 11th edition of the International Multidisciplinary Symposium "UNIVERSITARIA SIMPRO 2024".

AUTONOMOUS INDOOR NAVIGATION SYSTEM CONCEPT: HARDWARE AND SOFTWARE INTEGRATION FOR ELECTRIC VEHICLES

COSMIN RUS¹, LEBA MONICA²

Abstract: This paper presents a comprehensive investigation into the development of an autonomous electric vehicle specifically designed for indoor use. The research focuses on two critical aspects: the hardware-based steering system and the software algorithm for autonomous navigation. The steering system integrates a set of sensors and a closed-loop control algorithm to accurately determine the wheel positions relative to the steering wheel, utilizing a microcontroller and a LiDAR sensor for precise directional control. Concurrently, an interactive dashboard was developed, using Python and Qt, to display real-time data including motor temperature, battery voltage, and current consumption. The autonomous navigation algorithm, implemented and tested in MATLAB Simulink, uses LiDAR-generated maps to define the vehicle's trajectory within a physical space. The algorithm guides the vehicle through predefined coordinates, adapting to environmental changes and obstacles. The integration of these hardware and software components aims to achieve reliable autonomous navigation in confined indoor spaces, enhancing the vehicle's performance and safety. This research contributes significantly to the field of intelligent electric vehicles, promoting advancements in autonomous mobility solutions for industrial, commercial, and residential applications.

Key words: navigation, closed space, Simulink, Lidar, dashboard, monitoring.

1. INTRODUCTION AND STATE OF THE ART

In the age of technological advancement and the push for sustainable transport, the development of autonomous electric vehicle prototypes is increasingly gaining interest across various sectors. The creation of these vehicles hinges on several critical components, including the architecture and control system, environmental perception, navigation, energy efficiency, and specific hardware like BLDC and servo motors. These elements are crucial for the vehicles' safe and efficient operation, requiring seamless integration and coordination. Key aspects include flexible and modular design for easy updates, real-time decision-making capabilities through advanced algorithms, and the use of sensors and machine learning for environmental understanding. Additionally, precise navigation and localization technologies, alongside energy optimization and

¹ *Ph.D., Eng., cosminrus@upet.ro*

² *Ph.D., Eng.*

storage solutions, are essential. The synergy and optimization of these components are vital for achieving reliable autonomous driving, underscoring the importance of comprehensive studies and research in the field for the successful realization of autonomous electric vehicle prototypes [1].

Ajao and Sadeeq [2] provide a detailed overview of recent advances in autonomous electric vehicles. The paper begins by highlighting the importance of the development of autonomous electric vehicles and how it can revolutionize the way we move and transport goods, providing safer and more efficient solutions for our transportation needs. The authors then analyze the various subsystems that make up an autonomous electric vehicle, including energy storage systems, battery management systems, vehicle charging systems, electric motor mechanisms, and braking systems. Within each subsystem, the authors provide a detailed overview of recent advances and comparisons with other similar technologies. The paper also presents several prototypes of autonomous electric vehicles, providing an overview of how these technologies are implemented in practice.

In the paper done by Wang et al. (2020) [3], the authors focus on the development of intelligent functions on autonomous electric vehicle platforms and explore the fascinating world of autonomous driving and the challenges it presents for safety engineering and human-vehicle interaction. In the paper, the authors present an experimental study on human-autonomous vehicle interaction, which was carried out on a robot platform. Also, theoretical models for the analysis of human-autonomous vehicle interaction are presented and the main challenges and objectives of the development of autonomous driving technology are discussed. In addition, the paper addresses policy and societal issues such as user information and acceptance, as well as the regulatory adaptations needed to ensure the safety and efficiency of autonomous vehicles.

The paper done by Parekh et al. [4] presents a review of the progress, methods and challenges encountered in the development of autonomous vehicles. The authors performed a bibliometric and scientific analysis of the existing literature, examining previous studies and research in the field. They identified a number of challenges, such as safety, regulation and public acceptance, but also a number of potential benefits, such as reducing road accidents and improving mobility. In addition, the authors examined the various methods used to develop autonomous vehicles, including sensor technology, artificial intelligence, and navigation systems. Overall, this paper provides a comprehensive insight into autonomous vehicles and how they could change the way we get around in the future.

The paper by Rus, Leba, Risteiu, and Marcus (2023) [5] aims to investigate the development of intelligent electric vehicles that possess the potential for transformation into autonomous counterparts. A crucial aspect of this research involves the formulation of a robust and intuitive mathematical model, which serves as the foundation for a dedicated cruise control system designed for small electric vehicles. The proposed control system is intended for deployment in both outdoor and indoor industrial environments, in alignment with the principles of sustainable development. To achieve this objective, the researchers engaged in extensive simulations and mathematical modeling of a small electric vehicle. The primary focus of the modeling process encompassed the dynamic behavior of the vehicle and its core components. These

components comprise the powertrain, suspension system, tires, and the human driver. The powertrain model intricately incorporated the electrical and mechanical characteristics of the electric motor, the behavior of the controller, and the state of charge of the battery. Additionally, the suspension system model accounted for the unique attributes of dampers, springs, and the vehicle's mass and moment of inertia. On the other hand, the tire model encompassed essential features such as tire-road contact, lateral and longitudinal forces, and slip angle. Furthermore, the driver model captured the inputs from the accelerator and brake pedals, as well as the steering wheel. The various component models were meticulously combined in a comprehensive simulation framework to facilitate the examination of the small electric vehicle's dynamic behavior under diverse operating conditions. Moreover, this integrated simulation environment served as an effective platform for rigorous testing of various control algorithms. Among the control algorithms studied were those pertaining to regenerative braking systems, energy management, and battery charging. The researchers relied on the powerful MATLAB Simulink software platform to implement the numerous vehicle component models and conduct the control algorithm assessments. MATLAB Simulink provides a versatile and user-friendly block-based modeling environment, which is ideally suited for this type of complex system modeling. Moreover, the software's support for real-time hardware-in-the-loop simulation enabled the researchers to execute the control algorithms on a real-time platform. As a result, they could send inputs to the physical vehicle components and receive outputs, facilitating the evaluation and validation of the control strategies in a real-world context.

In summary, the investigation undertaken by Rus, Leba, Risteiu, and Marcus (2023) [5] constitutes a significant advancement in the development of intelligent electric vehicles that can eventually transition into fully autonomous entities. The establishment of a reliable mathematical model and the utilization of the MATLAB Simulink software platform have been pivotal in simulating and testing control algorithms critical to the performance and autonomy of these vehicles. By embracing these technological advancements, the automotive industry moves closer to realizing a greener, safer, and more efficient future for sustainable transportation. This provides the ability to test control algorithms in a real environment to verify their performance and ensure that they meet the desired specifications. The literature review reveals that there is a wide variety of research related to the development of electric vehicles, especially regarding the extension of their autonomy, energy efficiency and the implementation of advanced control systems [6, 7]. Based on the developed mathematical model [5], the researchers demonstrated its use for sizing electric motors for various types of electric vehicles, including off-road vehicles such as the electric buggy and electric ATV [8].

Using the mathematical model as an inverse model, they were able to determine the minimum moment required for the vehicles to climb slopes of varying degrees. These results allowed the appropriate selection of electric motors for the vehicles in question, thus ensuring the reliable and efficient operation of the propulsion systems. The study emphasizes the importance of continued research in the field of electric vehicles, especially for the development and implementation of autonomous driving algorithms. Advances in this area promise to bring significant improvements in the efficiency, safety and performance of electric vehicles. The integration of advanced technologies, such as

artificial intelligence, into electric vehicles will make them more intelligent, autonomous and easy to use, contributing to sustainable development and reducing the impact on the environment [9].

The study by Rus and Leba (2023) [10] provides a succinct but insightful exploration of the progress made in the development of an intelligent electric vehicle with autonomous driving capabilities. This revolutionary vehicle demonstrates outstanding adaptability, seamlessly integrating into the next-generation concepts of Smart Grid and Smart City, also contributing as a prosumer element in electricity supply networks. The research provides a brief but informative outline of the complicated process involved in creating a small electric vehicle, which is achieved by converting a thermal engine into a highly efficient electric motor. Additionally, the study highlights the successful incorporation of state-of-the-art communication systems based on the LoRa network, improving vehicle connectivity and data exchange capabilities. In particular, the integration of LiDAR sensors adds a remarkable dimension to the vehicle's functionality, enabling precise mapping of specific areas of interest. Furthermore, the research introduces a future concept for establishing an innovative power supply system. Combining cutting-edge technologies, innovative design concepts and sustainability principles, this study presents the potential for significant advances in the field of intelligent electric vehicles, thus contributing to a more efficient and environmentally conscious future of transport. A noteworthy aspect is that this vehicle's environmental impact is genuinely 100% non-polluting, as its batteries are entirely powered by renewable energy sources [10].

Within our university, there are several achievements regarding the development of autonomous electric vehicles, one such outstanding example is the prototype of a mini autonomous electric vehicle made on the functional platform of a Buggy-type vehicle, an innovation that promises to revolutionize the way we move in the urban environment as well as on off-road terrain. This prototype represents a compact and intelligent version of an electric vehicle, designed to offer an efficient and environmentally friendly transport solution. It is proposed to equip it with advanced technologies, such as sensors, video cameras and artificial intelligence algorithms, which allow it to navigate autonomously through traffic, without requiring human intervention. The mini autonomous electric vehicle is designed to meet urban mobility needs, with small dimensions that allow it to easily slip through dense traffic and park in small spaces.

Thus, it becomes a practical and efficient option for traveling short distances, such as the daily commute to work or shopping. Another remarkable aspect of this prototype is its exclusive use of electricity. The vehicle is equipped with an advanced electric propulsion system based on a BLDC brushless motor, powered by a high-performance battery. This sustainable approach not only reduces carbon emissions and the noise produced by vehicles with conventional engines, but also provides a smooth driving experience, without unpleasant vibrations or noises. Also, this mini autonomous electric vehicle comes with a modern and intuitive interface that allows users to access different functions of the vehicle, turning it into a viable solution for public and shared transportation. In the future, through a mobile application, users can request the vehicle, check availability and even monitor the route and status of the vehicle in real time.

The prototype of this mini autonomous electric vehicle represents an important step in the direction of smart and sustainable mobility. The integration of autonomous technology in electric vehicles opens new horizons for urban transport, increasing the safety, efficiency and comfort of passengers, while reducing the negative impact on the environment [5].

2. IMPLEMENTED METHODS AND SYSTEMS

This work presents two system prototypes that are the basis of the construction of a mini autonomous electric vehicle. The first system prototype is a hardware type developed to manage the direction of travel of the mini autonomous electric vehicle, while the second system is a software type that allowed the creation of a dashboard for this type of vehicle. Regarding the development of the autonomous steering hardware prototype, in the first stage, a system was created using a control algorithm in a closed loop with the help of sensors that can be used to determine the position of the vehicle's wheels in relation to the steering wheel's position (Figure 1). This is just a concept; at this stage of research, it has not been realized from a hardware point of view.

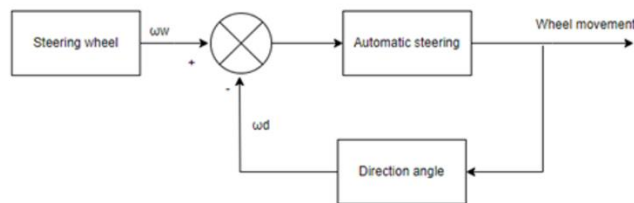


Fig.1. System block diagram

The vehicle's physical steering wheel can be replaced with a trajectory function whose output values can control the direction change system via a microcontroller. To do this, a Raspberry Pi-type development board, a Lidar sensor, a speed sensor, a temperature sensor, a touchscreen and a voltage and current sensor were used, so that a dashboard for this type of vehicle was created. In Figure 2 shows the connection of the Lidar sensor to the Raspberry Pi development board which was also connected to the touchscreen.

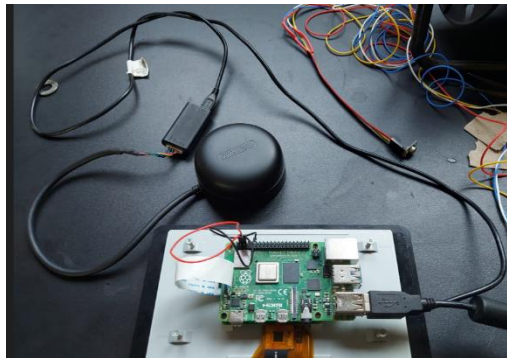


Fig.2. Hardware connections

This dashboard has the ability to display various essential vehicle data, including engine temperature, battery terminal voltage, battery capacity and current consumption, allowing drivers and technicians to monitor vehicle performance in real time. In the initial stage, the development environment was set up, ensuring that there was Python installed on the working system and the necessary libraries were included to program the GUI using Qt. To design the interface, QtDesigner was used, thus allowing the development of an ergonomic and intuitive design for users. Our dashboard features a set of information panels, each providing essential vehicle data (Figure 3).

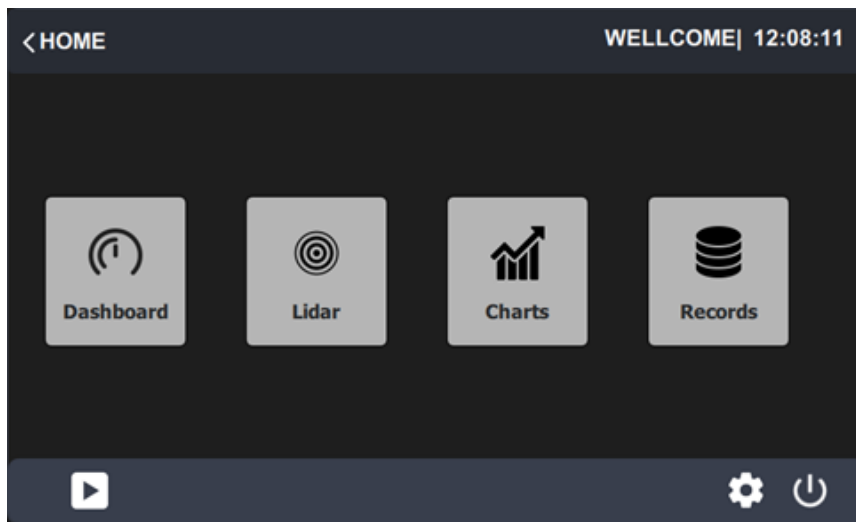


Fig.3. Main dashboard screen

The main panel displays data related to engine temperature, battery terminal voltage, battery capacity and current consumed (Figure 4 and Figure 5).

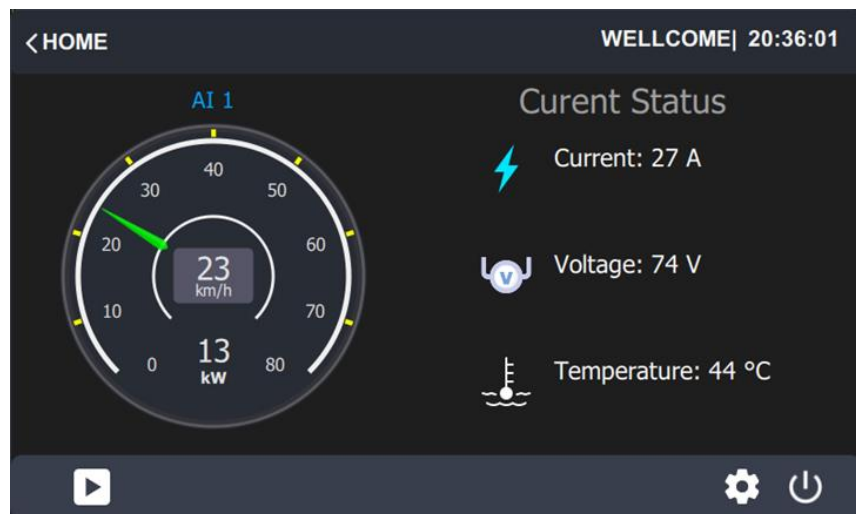


Fig.4. Screen for viewing speed, battery voltage, current consumed and engine temperature

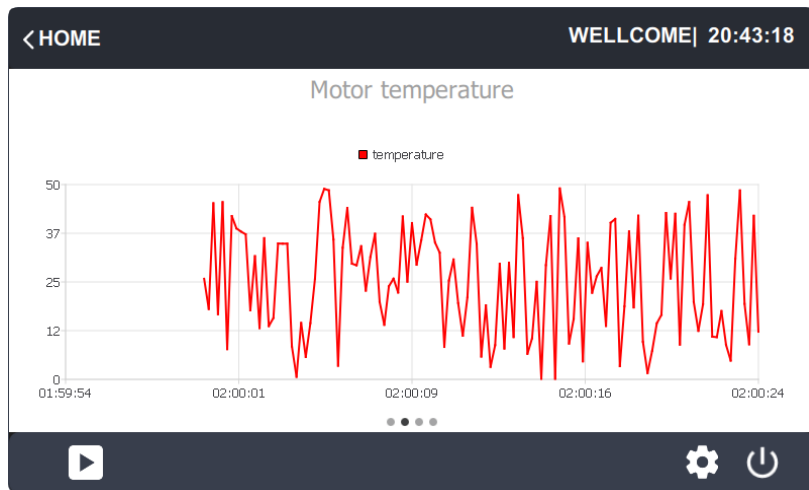


Fig.5. Graphic representation of the engine temperature evolution

This critical information is updated in real time, allowing users to monitor the condition of the vehicle throughout its life. An innovative element of this dashboard is the integration with the Lidar sensor. This sensor plays a crucial role in creating an efficient and safe autonomous navigation system. Through the Lidar sensor, the dashboard can retrieve relevant data about the vehicle's environment and provide a graphic representation of the route followed by it (Figure 6).

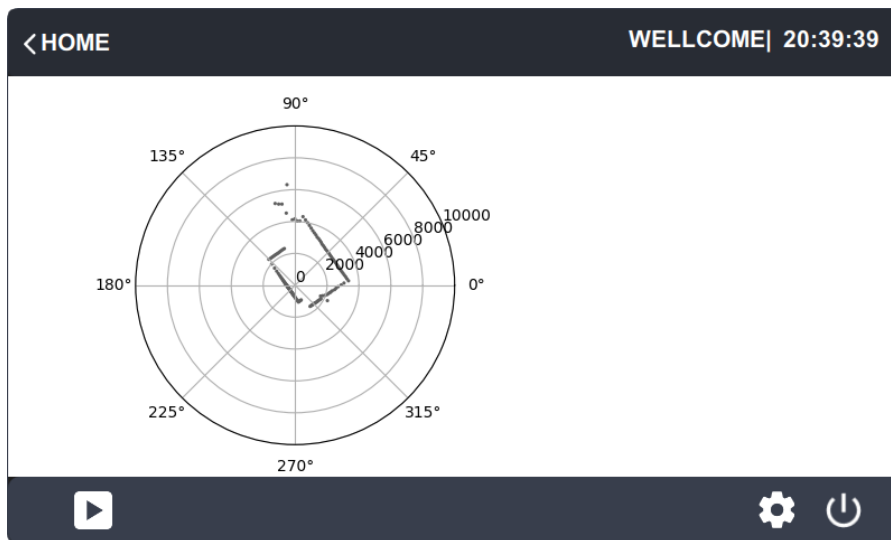


Fig.6. The map generated using the Lidar sensor

Through this route map, users can observe in real time how the vehicle plans its movements and adapts to different traffic situations. This advanced functionality significantly improves user confidence and safety in self-driving systems.

3. RESULTS AND DISCUSSION

Until now, the hardware structure of the entire system has been successfully implemented and relatively good results have been obtained in a simulation of the entire autonomous driving algorithm made in Matlab Simulink. The algorithm is structured into 9 main design and simulation steps as follows. Making a map of the physical space where the electric vehicle will follow a route, this being done with the Lidar sensor, as can be seen in Figure 7.

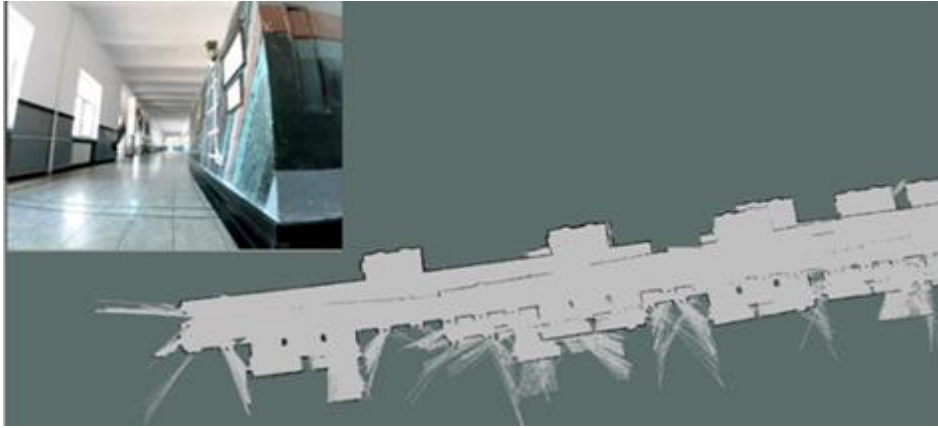


Fig.7. Map resulting from the use of the system based on the LiDAR sensor [11]

Then based on a part of the map of the studied premises, a simple algorithm was implemented in the Matlab Simulink simulation environment that generated the trajectory of the autonomous electric vehicle in the form of a sequence of coordinate points (x, y) in the plane. The generated trajectory is shown in Figure 8 [11].

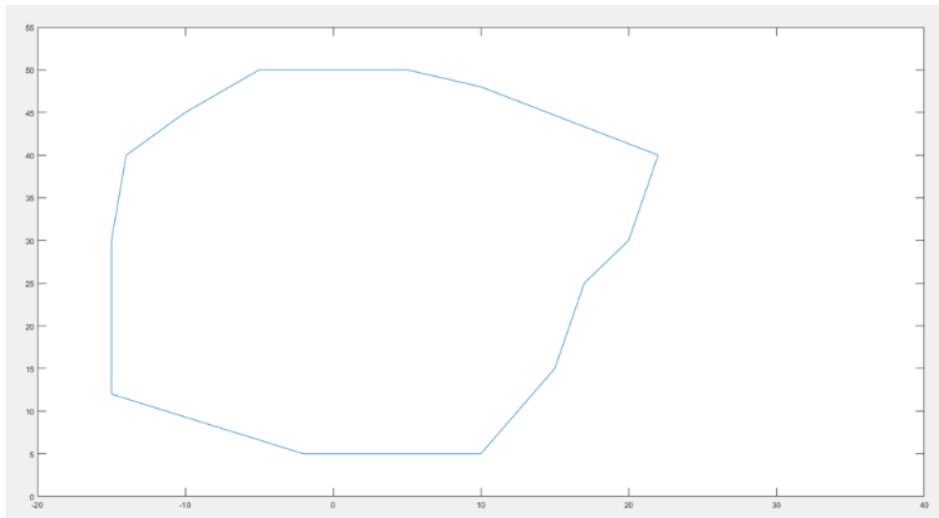


Fig.8. The map generated using the Lidar sensor

The entire process of driving an autonomous electric vehicle was thought to follow the following steps: checking the position of the electric vehicle in relation to the trajectory, reading the position of the electric vehicle with the help of a localization system, orienting the electric vehicle to the desired trajectory, imposing the necessary position on the proposed trajectory, determining the direction angle of the electric vehicle, actuating the servomotor coupled to the steering as well as the drive motor and last but not least avoiding obstacles.

In order to simplify the simulation model made in Matlab, it was considered that when encountering an unforeseen obstacle while traveling an imposed route, the electric vehicle will stop. In the first sequences of the realized Matlab program, the number of points on the imposed trajectory represented in a 2D plane (16 points) were defined, then the x,y pairs related to each point and the starting point of the electric vehicle were defined. The speed of the electric vehicle was considered to be 3 m/s, approximately 10 km/h. With the help of a minimum algorithm, the closest point on the imposed trajectory and the distance from the initial position of the electric vehicle were determined. The angle α was determined, which represents the angle of movement of the electric vehicle's steering wheel required to reach a certain point on the imposed route, as well as the time required to move from one point to another on the defined trajectory. The simulation results for an imposed route represented in Figure 9 are satisfactory and can be taken into account when implementing an autonomous navigation system on an electric vehicle [11].

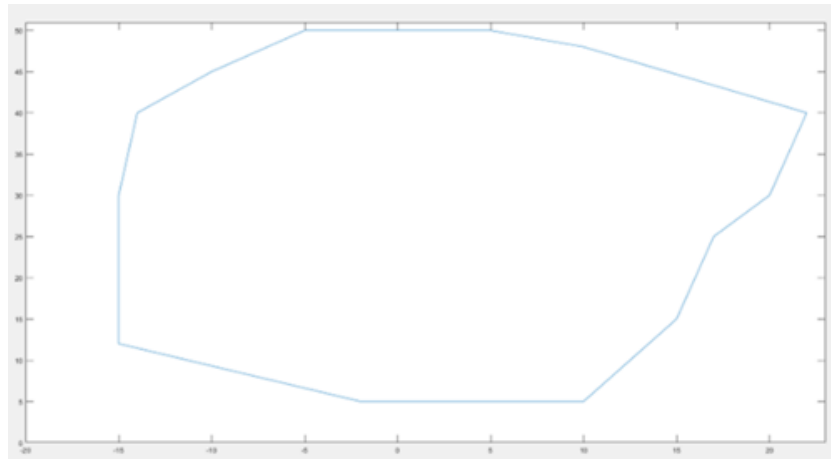


Fig.9. Navigation route imposed

Figure 10 shows the graph of the change in angle α for each pair of points separately, as well as the graph showing the time required to travel a distance between two points on the imposed trajectory. It is thus possible to carefully analyze the evolution of angle α according to each distinct point on the trajectory, highlighting the differences between its values for various pairs of points. The graph reveals how the angle α varies depending on the route taken, allowing a deeper understanding of the vehicle's behavior on the predetermined trajectory. In addition to this aspect, the time required to cover the distances between the points on the trajectory can also be seen in the graph. This graph

shows the relationship between the distance traveled and the time required to perform this operation, providing an insight into the vehicle's performance on the required route. By combining these two aspects, a comprehensive approach is proposed to evaluate the behavior and performance of the autonomous electric vehicle on the set trajectory. Thus, possible deficiencies or optimizations that can be brought to the control system and the navigation algorithm can be identified to ensure a more precise, safe and efficient movement. These results make significant contributions to the field of autonomous vehicles, where a good understanding of the interaction between angle α and travel time between trajectory points is crucial for optimizing the autonomous driving experience.

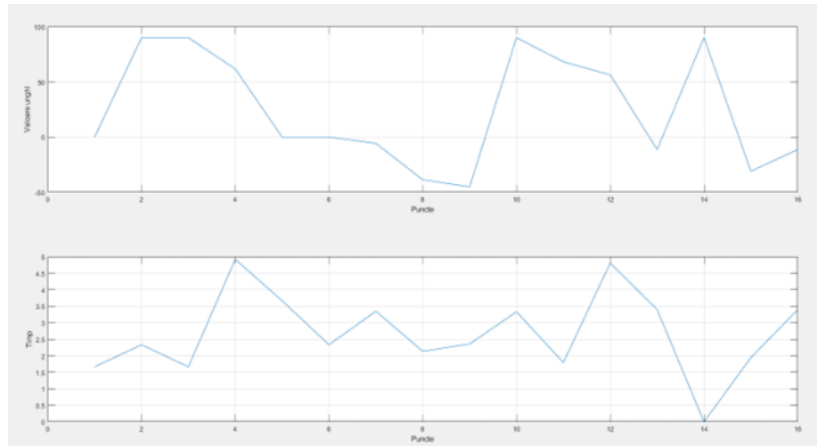


Fig.10. Graph of angle α and graph of travel time distance between two points

In Figure 11, we present the simulation system that plays a crucial role in our study. This system actually acquires the steering angle from the workspace, where it is meticulously calculated based on the desired trajectory. Afterwards, this calculated steering angle is skillfully translated into the precise direction of the vehicle's wheels. The integration of this simulation system marks an essential step in our research, as it allows us to analyze and optimize the steering behavior of the vehicle in relation to the desired trajectory. By accurately translating the calculated steering angle into actual wheel movements, we can assess the vehicle's ability to follow the intended path and make the necessary adjustments to improve its overall performance. This simple simulation system is an indispensable tool in our quest to develop and refine cutting-edge self-driving capabilities for the smart electric vehicle.

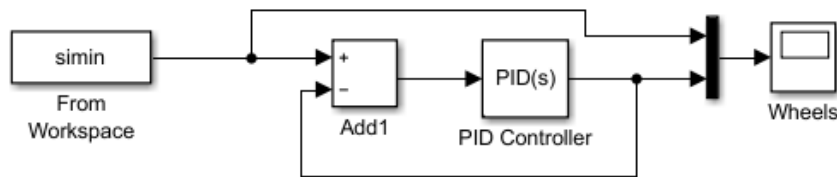


Fig.11. Simulation diagram for steering system

In Figure 12, we illustrate a vital aspect of our research, where the comparison between calculated and actual steering angles is shown. The blue curve represents the steering angle values meticulously calculated based on the imposed trajectory, while the red curve describes the real-time steering movements of the vehicle's wheels. This representation allows us to closely observe the alignment between the desired steering angles and the actual response of the vehicle during operation. Analyzing this data enables us to obtain valuable information about the accuracy and effectiveness of our steering control system.

Discrepancies or variations between calculated and actual steering angles can provide critical feedback for further refinement and optimization of our self-driving capabilities. By striving to minimize the gaps between the two curves, we aim to increase the precision and reliability of the vehicle's direction, consequently improving its ability to faithfully follow the imposed trajectory.

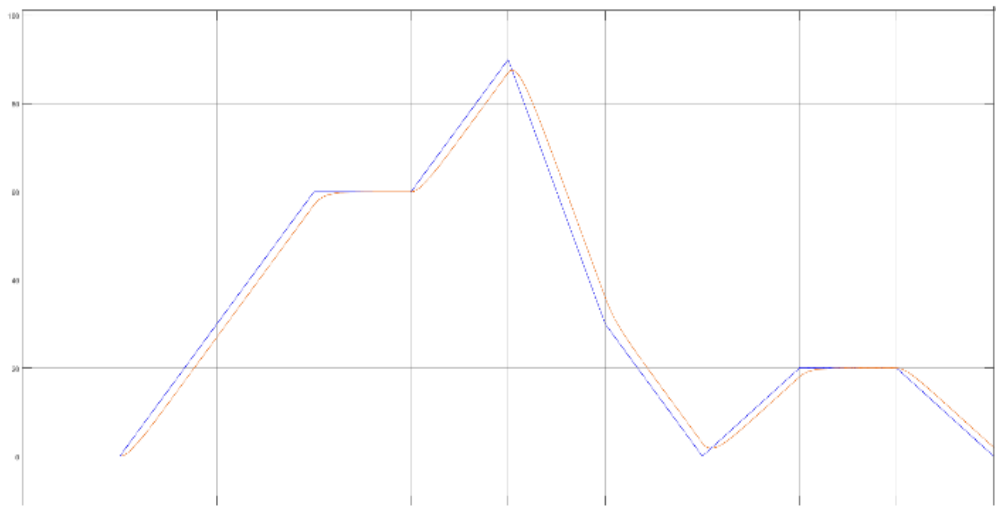


Fig.12. Steering simulation results

Figure 13 and Figure 14 show the difference between the imposed trajectory and the trajectory achieved by the autonomous electric vehicle if its starting point is inside the imposed trajectory and if the initial position is outside the imposed trajectory. Satisfactory results are observed even if the two curves do not overlap perfectly, the algorithm presenting some errors, something that can be improved by choosing more points to define the imposed trajectory. The curve of the trajectory made on the basis of the trajectory imposed using this algorithm is then superimposed over a certain area on the map of the studied space obtained with the help of the system based on LiDAR mapping and after it is established that the simulated route falls perfectly over the mapped area considering also a certain safety zone in relation to its proximities (the safety space in the industrial environment is usually considered 10%), the algorithm can be implemented in the software structure of the system thus obtaining an autonomous driving system.

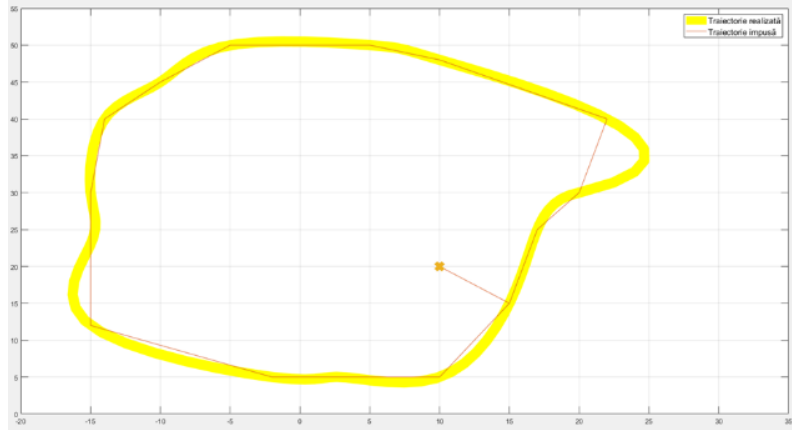


Fig.13. The result of the simulation of the autonomous driving algorithm for the case where the initial position of the vehicle is inside the imposed trajectory [11]

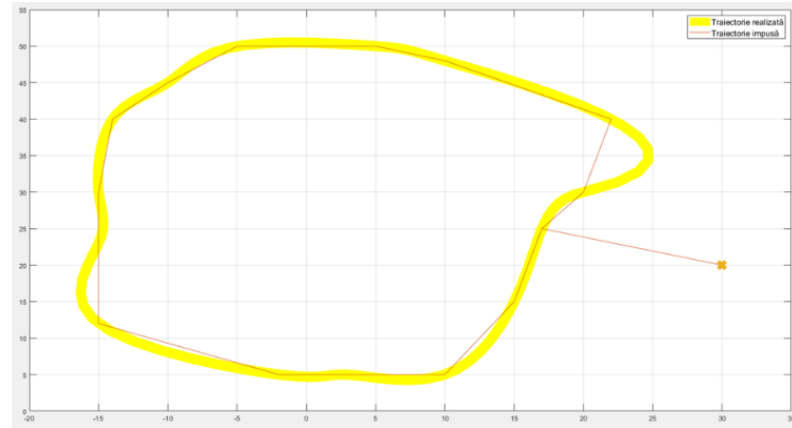


Fig14. The result of the simulation of the autonomous driving algorithm for the case where the initial position of the vehicle is outside the imposed trajectory [11]

Undoubtedly, the algorithm used in our study presents some errors when it comes to accurately achieving an imposed trajectory. However, it is important to note that despite these challenges, the algorithm remains a valuable asset that can be effectively integrated into the functional system of an electric vehicle. This integration is made possible by incorporating a sophisticated communication and location system along with a state-of-the-art LiDAR mapping system [12, 13]. As a result of this comprehensive integration, we successfully transform the electric vehicle into an autonomous entity.

The use of this algorithm in the functional system of our electric vehicle represents a significant step in this stage of research and development [14]. It lays the foundation for a fully autonomous electric vehicle that can navigate any type of environment with far above average precision and safety. Although some errors persist, they serve as valuable learning opportunities to refine and optimize the algorithm. Continuous improvement, guided by real-world data and feedback, is essential to

enhance vehicle autonomy and ensure smooth tracking of the imposed trajectory. With the convergence of advanced communication, localization and mapping technologies, we can achieve an autonomous electric vehicle. The culmination of these efforts will ultimately lead to greener, safer and more efficient transport, revolutionizing the way we travel and shaping a sustainable future for generations to come [15].

4. CONCLUSIONS

This paper stands out for its dual focus on developing a precise steering control system, enhanced by a suite of sensors and a closed-loop algorithm, and a sophisticated software algorithm for autonomous navigation, underpinned by Matlab Simulink simulations and Lidar sensor data for environmental mapping. The cornerstone of this research is the hardware prototype, which employs a microcontroller and Lidar sensor to achieve exact steering control, crucial for the vehicle's precise maneuvering. This system's flexibility and modularity are highlighted, allowing for upgrades and adaptations as technology progresses. The integration of an interactive dashboard that displays vital performance metrics such as motor temperature, battery voltage, and current consumption in real-time further exemplifies the hardware's role in enhancing vehicle monitoring and safety. Parallely, the software component's innovation lies in its algorithm for autonomous navigation. The algorithm, validated through simulations, utilizes Lidar-generated maps and defined coordinates to navigate the vehicle autonomously within a predefined trajectory, showcasing adaptability to environmental changes. The research illustrates the algorithm's capability to guide the vehicle efficiently, marking a significant step towards autonomous indoor mobility. The paper's findings contribute significantly to the field by demonstrating the successful integration of hardware and software systems for autonomous electric vehicles. It underscores the importance of a harmonized approach to vehicle design, where steering systems, navigation algorithms, and real-time monitoring coalesce to create a vehicle capable of intelligent autonomous operation in indoor environments. This research's implications extend beyond academic interest, offering insights into practical applications for autonomous electric vehicles in industrial, commercial, and residential settings. It lays a foundation for future advancements in autonomous mobility, emphasizing the need for continuous innovation in hardware and software development. The study serves as a testament to the potential of integrated technologies in transforming transportation, making strides towards safer, more efficient, and environmentally friendly autonomous vehicles.

REFERENCES

- [1]. **Marcus R., Rus C., Leba M., Risteiu M.,** *Electric vehicles between recycling and sustainable development-@. ro*, In International Conference on Computers Communications and Control, pp. 47-62, Cham: Springer International Publishing, 2022.
- [2]. **Ajao Q., Sadeeq L.,** *Overview analysis of recent developments on self-driving electric vehicles*, arXiv preprint arXiv:2307.00016, 2023.
- [3]. **Wang R., Sell R., Rassolkin A., Otto T., Malayjerdi E.,** *Intelligent functions development on autonomous electric vehicle platform*, Journal of Machine Engineering, Vol. 20, 2020.

- [4]. Parekh D., Poddar N., Rajpurkar A., Chahal M., Kumar N., Joshi G. P., Cho W., *A review on autonomous vehicles: Progress, methods and challenges*, Electronics, Vol. 11, No. 14, p. 2162, 2022.
- [5]. Rus C., Leba M., Risteiu M., Marcus R., *Vehicle control modeling and simulation for small electric car case*, In 24th International Carpathian Control Conference, Miskolc-Szilvásvárad, Hungary, pp. 388-393, 2023.
- [6]. Rus C., Leba M., Negru N., Marcus R., Risteiu M., *Electric vehicles in smart grid and smart city for Petroșani case*, MATEC Web of Conferences, Vol. 342, p. 05002, EDP Sciences, 2021.
- [7]. Leba M., Ionica A., Dovleac R., Dobra R., *Waste management system for batteries*, Sustainability, Vol. 10, No. 2, p. 332, 2018.
- [8]. Rus C., Leba M., Negru N., Marcus R., Costandoiu A., *Autonomous control system for an electric ATV*, In MATEC Web of Conferences, Vol. 343, p. 06003, EDP Sciences, 2021.
- [9]. Rus C., Mija N., Leba M., *Autonomous electric ATV using IPM based inverter control and deep learning*, In Trends and Innovations in Information Systems and Technologies, Vol. 1, pp. 746-755, Springer International Publishing, 2020.
- [10]. Rus C., Leba M., *Autonomous smart electric vehicle integrated into a smart grid type system*, In Benítez-Andrades, J.A., García-Llamas, P., Taboada, Á., Estévez-Mauriz, L., Baelo, R. (eds) Global Challenges for a Sustainable Society. EURECA-PRO 2022, Springer Proceedings in Earth and Environmental Sciences, Springer, Cham, 2023.
- [11]. Rus C., Leba M., *Use of electric vehicles in closed spaces*, Universitas Publishing House, Petrosani, Romania, ISBN: 978-973-741-862-3, 2022.
- [12]. Real-Moreno O., Rodríguez-Quíñonez J. C., Ramírez-Hernández L. R., Trujillo-Hernández G., Flores-Fuentes W., Castro-Toscano M. J., Sergiyenko, O., *Scanning Systems for Environment Perception in Autonomous Navigation*, In Scanning Technologies for Autonomous Systems, pp. 33-66, Cham: Springer Nature Switzerland, 2024.
- [13]. Silva E., Soares F., Souza W., Freitas, H., *A Systematic Mapping of Autonomous Vehicle Prototypes: Trends and Opportunities*, IEEE Transactions on Intelligent Vehicles, 2024.
- [14]. Berceanu A., Leba M., Risteiu M., Mija N., Ionica A., *Simulation of an autonomous car drive scenario*, In 7th International Conference on Mathematics and Computers in Sciences and Industry (MCSI), pp. 170-174, IEEE, 2022.
- [15]. Ferreira M. A., Moreira L. C., Lopes A. M., *Autonomous Navigation System for a Differential Drive Mobile Robot*, Journal of Testing and Evaluation, Vol. 52, No. 2, pp. 841-852, 2024.

This article was reviewed and accepted for presentation and publication within the 11th edition of the International Multidisciplinary Symposium "UNIVERSITARIA SIMPRO 2024".

PREBUNKING, AN EFFECTIVE DEFENSE MECHANISM TO STRENGTHEN CONSUMERS' CYBER AWARENESS

SIMONA RIUREAN¹, TATIANA ANTIPOVA²

Abstract: In today's digital age, especially with generative AI, several significant cyber threats exploit the consumers' vulnerabilities. Prebunking, a proactive strategy aiming to protect consumers from misinformation and cyber attacks, can serve as an effective defense mechanism by exposing them to milder versions of deceptive content. Traditional reactive approaches, such as post-incident responses and debunking misinformation, often fall short. Prebunking, on the other hand, poses a proactive alternative, aiming to preemptively arm consumers with the knowledge and skills needed to recognize and resist both cyber threats, and misinformation. This paper explores various prebunking methods aiming to enhance consumers' cyber defense. Different approaches to prebunking methods and strategies are developed in this paper, aiming to raise consumers' ability to create a stronger, more instinctive defense against cyber threats and deep fake news, contributing to a more informed and secure digital environment for us.

Key words: cybersecurity, cyber resilience, cyber hygiene, deep fake, misinformation, ethical phishing simulation

1. INTRODUCTION

In this increasingly interconnected world, where the internet forms the foundation of modern life, cybersecurity has never been more critical. In today's digital landscape, businesses, as well as consumers, are increasingly targeted by a range of cyber threats, including phishing, malware, identity theft, and fake news by cyber manipulation using extended misinformation and ethical phishing campaigns. The sophistication and frequency of these attacks require innovative defense mechanisms beyond traditional reactive measures [1].

Just as the body can be vulnerable to physical pathogens, so too are consumers susceptible to the "viruses" such as deception, scams, stealing of sensible personal data, identity theft, and misrepresentation. To combat these, the principles of inoculation theory, as prebunking, are viable to be applied to cybersecurity as reliable proactive measures. The goal of prebunking techniques applied in cybersecurity is to strengthen consumers' psychological defenses against these attacks, making them more resistant to manipulation by malicious actors seeking to exploit human trust and weaknesses [2].

¹ Ph.D., Eng., sriurean@yahoo.com

² Ph.D., Eng.

The research of behavioral scientists such as William McGuire has revealed the potential power of a preventative technique, referred to as prebunking [3]. This approach, grounded in social psychology, seeks to inoculate consumers against the persuasive tactics of misinformation by exposing them to the methods often employed by those who spread disinformation, thereby rendering them more resistant to manipulation.

The concept of prebunking involves proactive efforts to prevent misinformation from spreading by exposing individuals to a weakened form of the argument and refuting it in advance. As a proactive approach, it should anticipate misinformation and phishing attacks before it can do the aimed damage. It can also be better understood as a "psychological vaccine" against misinformation.

Rather than trying to correct false beliefs after the fact (which can be notoriously difficult), prebunking aims to educate individuals (aka users or consumers) about common misinformation techniques, phishing attacks and fake websites, such as cherry-picking facts or using emotional appeals so that they are more likely to spot and question misinformation when they encounter it [4].

Research in the psychology area has demonstrated that prebunking is an effective counter-disinformation strategy [5]. Prebunking concept has also been already used in various other contexts resurch such as health domain (during Covid-19 pandemic) [6,7], biotechnology [8], climate change [9, 10], energy transitions (Geothermal Energy Systems) [11], theology field [12], earthquake predictions [13] or public relations [14]. Also *"in 2020, Twitter launched a new strategy dubbed 'prebunking' in hopes of pre-emptively countering false information about voting by mail and election results. Prebunking was touted as a potential solution."* [14].

Since prebunking has been proven in many studies and different areas to reduce susceptibility to misinformation, it can also be implemented as an effective measure to increase consumers' resilience against social engineering attacks. By preparing consumers with simulated "mild" and ethical cyber threats and misinformation, prebunking can strengthen their critical thinking skills and awareness, making them less susceptible to real attacks. This proactive approach should help consumers to recognize and resist more effectively to varios types of cyber threats.

A commonly used technique in misinformation cases is debunking. Debunking corrects false information after it has already spread, but it is less effective in preventing initial belief in disinformation. Despite the indispensable role played by debunking and fact-checking in the battle against disinformation on various digital platforms, these strategies possess certain limitations. The power of information to stick in our memories and shape our beliefs can be strong, rendering the falsity we encounter stubbornly resistant to correction, even after being presented with reliable, verifiable facts. Once a false claim has taken root in our minds, debunking alone may not be sufficient to eject it, leaving the door open for the continued propagation of misinformation [16]. In the ongoing struggle against online misinformation, above common debunking methods, Google implemented innovative solutions for prebunking. Jigsaw, a division within Google focused on counteracting threats to open societies, has joined forces with leading scholars from the Universities of Cambridge, Bristol, and American University to explore the effectiveness of this approach. By addressing the problem at its source, this

technique offers a glimmer of hope in combating the pervasive influence of deep fake and disinformation campaigns. The effectiveness of prebunking in various contexts (as demonstrated by research [5-14]), serves as an encouraging result that decreases the impact of online disinformation and, in turn, shields those consumers that are most susceptible to its negative effects [15].

Within this paper we define the general concept of prebunking, explore the applicability of the prebunking in cybersecurity, discuss cyber threats and AI-generated disinformation, cyber-defense measures and deep fake detector tools as well as proactive strategies of prebunking and its application in enhancing consumers' cyber hygiene and best practices. We also explore its theoretical foundation, as well as various proactive instruments as effective defense mechanisms against disinformation, fake news, and cyber threats. Within this paper, we also aim to explore how prebunking can be used to improve consumers' cyber hygiene by attending culturally tailored cyber awareness training classes, ethical phishing simulations, and extended national campaigns.

2. CYBERSECURITY AND AI-GENERATED THREATS

Cybersecurity threats have grown increasingly sophisticated and widespread. Among the most common threats are phishing, malware, identity theft, and the spread of fake news.

2.1. Cybersecurity threats

Phishing is a subcategory of the social engineering attack that uses deceptive messages (sent by email, SMS, voice calls, WhatsApp, QR codes) or websites to deceive consumers into divulging sensitive personal data. It is a ubiquitous and continually evolving threat that exploits human psychology to steal sensitive information. By understanding its characteristics and implementing comprehensive security measures, consumers can reduce the hazard of falling victim to such attacks. Malware, is another prevalent threat, as malicious software can infect computers or smart devices to steal data or disrupt system functions by compromising data integrity and system functionality. Identity theft represents stealing and exploiting personal information for financial gain or to commit other crimes. Identity theft causes significant financial and reputational damage to victims.

Fake news is intentionally false or misleading material presented as news to manipulate public opinion. It is created to influence public opinion, deceive readers, or generate financial gain through advertising revenue [17,18].

2.2. AI-generated digital content as potential threats

As AI continues to advance at a fast speed, the specter of AI-generated disinformation has emerged as a genuine cause for concern among researchers and experts. AI models can now generate massive content with little to no human involvement, posing a grave threat to the integrity of information online. AI-generated disinformation (text, audio, images, or video - figure 1) is a rising and worrying trend

that must be under continuous surveillance and closely monitored before it becomes a significant part of the disinformation landscape. There have been several alarming instances that serve as a reminder of the growing potential for AI to be weaponized by malicious actors in the disinformation arena. [15].

Private AI-generated text, that is not examined based on a reliable external verification tool, poses a risk of directly exposing consumers to incorrect or misleading information. This danger is especially acute when Large Language Models (LLMs) rely on controversial datasets and lack strong safety guard mechanisms.



Fig.1. Examples of Copilot AI generated images

On the other hand, public disinformation that is publicly shared AI-generated text poses a more traditional disinformation threat. As the European Digital Media Observatory (EDMO) underlined [19], there is a particular risk, since consumers tend to believe that answers from chatbots based on LLMs are the most correct ones, and not just a convincing one. Just like any technology, LLMs can be exploited for harmful purposes. Cybercriminals could manipulate them to spread misinformation or create toxic content, therefore, storing LLM queries online could lead to accidental exposure or hacking, potentially compromising sensitive information.

In AI-generated images, some common evidence points to the images being not real but created with AI technology because of the details of the image itself: hands with fingers and nails not well undefined, both eyes even and perfectly shaped, other body parts and objects' shapes, and shades that are often weird, if not completely unreal [20]. The most common AI-generated images are old images that are altered to mislead consumers in a way to get the impression of being related to current events. Because of their quality, AI-generated images should be relatively easy to spot for experts, but also for consumers to allow quick and effective detection and debunking, especially when an advanced method like prebunking is used as a proactive measure. AI-generated audio poses a scary challenge in the fight against disinformation[21]. Without the visual signs that often aid in discerning synthetic content, it becomes increasingly difficult for the average consumer to differentiate between human and AI-generated audio. Even advanced detection tools struggle to identify the synthetic nature of such content. This growing capability of AI-generated audio to seamlessly balance in with genuine human-generated audio presents a significant threat to the integrity of data and threatens to exacerbate the already pervasive issue of disinformation [22]. The rapid advancement of AI-generated video technology has led to the creation of tools that produce increasingly realistic and convincing videos. A notable example is the upcoming Sora by OpenAI, which can generate videos from simple text prompts [23].

This development raises significant concerns about the misuse of AI-generated videos for spreading misinformation. The difficulty for average consumers in

distinguishing between AI-generated and real videos further intensifies the threat posed by this evolving technology.

3. CYBER-DEFENSE MEASURES AND DEEP FAKE DETECTOR TOOLS

Traditional cybersecurity measures, play critical roles in protecting against cyber threats, being essential to protect networks, systems, and data from cyber-attacks. The most effective cybersecurity measures are Security Information Event Management (SIEM), firewalls, antivirus, and anti-malware software, multi-factor authentication (MFA), strong passwords, encryption, Intrusion Detection and Prevention Systems (IDPS), operation system updates (OS updates), and regular software updates. This classification of cybersecurity measures are presented in Figure 2.

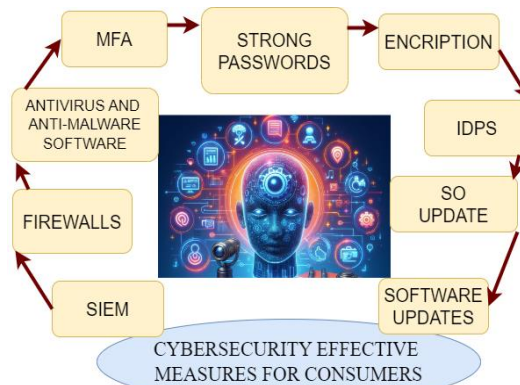


Fig.2. Cybersecurity measures for consumers

SIEM systems offer real-time analysis of security alerts generated by applications and network hardware. They collect and analyze data from various sources to detect suspicious activity. Splunk, IBM QRadar, and Microsoft Azure Sentinel are a few examples of SIEM solutions for monitoring, searching, and analyzing machine-generated big data, integrating security intelligence and event monitoring to provide real-time visibility and actionable insights. Firewalls are network security means (software and/or hardware) that monitor In/Out network traffic based on security rules. They act as a barrier between a trusted internal network and untrusted external networks, such as the Internet. For example, network-based firewalls protect entire networks by filtering traffic at the network perimeter and host-based firewalls protect individual devices by filtering incoming and outgoing traffic. Antivirus and anti-malware software are programs designed to detect, prevent, and remove malicious software. They regularly scan systems for known malware and provide real-time protection. Norton Antivirus offers extensive protection against viruses, malware, spyware, and phishing attacks and Malwarebytes provides advanced protection against malware, ransomware, and other online threats. MFA enhances security by requiring two or more verification methods to gain access to resources. This often includes something the user *knows* (password), something the user *has* (security token), and something the user *is* (biometric

verification). Google Authenticator generates Time-based One-Time Passwords (TOTP) for MFA and Duo Security provides two-factor authentication with a second factor delivered via mobile devices [24].

Strong passwords are essential for defending accounts and personal data from unauthorized access. A strong password should be at least 12-16 characters long (since longer passwords are more secure), and use a mix of uppercase and lowercase letters, numbers, and special characters (e.g., !, @, #, \$, %).

Consumers should use different passwords for different accounts to prevent a security breach on one account from compromising others and avoid using easily guessable information such as names, birthdays, common words, or simple patterns (e.g., 123456, admin, qwerty). Using a paraphrase, which is a sequence of random words or a sentence that is easy to remember but hard to guess is also a good idea. Consumers should use a password manager to generate, store, and manage passwords securely such as LastPass, 1Password, and Dashlane.

Encryption is converting data into a coded format to prevent unauthorized access. It ensures that only authorized parties can read the data. Advanced Encryption Standard (AES) is widely used as a symmetric encryption algorithm for securing data and Secure Sockets Layer/Transport Layer Security (SSL/TLS) are protocols for encrypting data transmitted over the internet. IDPS are systems that monitor network and system activities for malicious activities or policy violations and can take action to prevent or mitigate attacks.

Snort is an open-source intrusion detection and prevention system (IDPS) that analyzes network traffic for signs of attacks and Palo Alto Networks offers integrated IDPS capabilities within its next-generation firewalls. Keeping operating systems (OS) and software updated with the latest patches helps protect against known vulnerabilities that attackers can exploit. Windows update automatically delivers security patches and updates to Microsoft operating systems and patch management solutions are tools like Ivanti and ManageEngine help automate the patching process across various platforms [25].

Natural language processing NLP are tools that analyze and understand the sentiment, context, and semantic structure of text. They can be used to identify potential misinformation in text content. AI fast-checking tools cross-reference the information in the text with a database of verified facts to identify potential misinformation. Fast-checking tools that allow to testing of different types of digital content (text, image, audio, and video), is a proactive defense method against cyber threats and fake news. Audio analysis tools refer to speech-to-text conversion and speaker recognition. Speech-to-text converts spoken words into written text that can then be analyzed using NLP and fact-checking tools. Speaker recognition tools can identify the speaker based on their unique vocal characteristics, being used to verify the authenticity of the audio content. Deep fake audio detectors are tools designed to identify and mitigate the impact of synthetic audio created using artificial intelligence techniques. These detectors are increasingly crucial as deep fake technology becomes more sophisticated and widely accessible.

Popular deep fake audio detection tools are Resemble AI [26] which detects deep fake audio by analyzing the characteristics of the audio files, Pindrop which uses machine learning and signal processing techniques to analyze the audio and identify fake or tampered files.

Video analysis tools consist of video recognition and deep fake detection. Video Recognition can analyze video content to identify objects, people, text, scenes, and activities. They can also detect any modifications made to the video. Deep fake video detectors are tools and technologies designed to identify and mitigate the impact of synthetic videos created using artificial intelligence techniques. As deep fake video technology becomes more sophisticated, the importance of these detectors is growing in fields such as media, security, and public safety. Deepfake Detection uses AI to detect deep fakes - manipulated videos that are often used to spread misinformation [27].

Various tools are very helpful in identifying and debunking misinformation. Deepware Scanner is an app that can detect deep fake audio and video by analyzing digital media for signs of manipulation and FakeCatcher, developed by Intel, detects deep fakes by analyzing subtle changes in facial blood flow that are not present in synthetic media, applicable to both audio and video [28].

FaceForensics++ is a large-scale dataset and benchmark for detecting manipulated facial imagery, which can be used to train and evaluate detection models [29]. DeepFaceLab while primarily a tool for creating deep fakes, it includes features that can help identify synthetic videos by analyzing the artifacts left by its own generation process. TruePic provides solutions for authenticating images and videos, ensuring they have not been tampered with. Sensity AI (formerly Deepttrace) offers a deep fake detection platform that leverages machine learning to identify manipulated videos across various media [30].

Several platforms adhere to the International Fact-Checking Network's codes of principles that examine all parties and sides, examine discrete claims and reach conclusions, track political promises, are transparent about sources and methods, disclose funding/affiliations and their primary mission is news and information. Snopes is one of the most popular fact-checking platforms and PolitiFact is a fact-checking website that rates the accuracy of claims by elected officials and others.

These useful platforms are: Annenberg Public Policy Center, which consistently produces high-rated articles, Reuters Fact Check operated by the international media agency Reuters, the Washington Post's dedicated fact-checking platform, the fact-checking platform by the Associated Press, the international media agency France-Presse, Africa's first independent fact-checking organization with offices in Kenya, Nigeria, South Africa, Senegal, and the UK, a West African independent verification and fact-checking project and the first fact-checking platform in Catalonia [31].

4. PREBUNKING PROACTIVE STRATEGY

The "prebunking" approach comprises three main key stages (figure 3). First, a warning is issued to inform consumers of potential attempts to manipulate them and their information ecosystem. Next, a "microdose" of the false narrative is administered, similar to a vaccine, allowing consumers to recognize and identify similar narratives in the future. Finally, a comprehensive repudiation of the false claims, debunking them with factual information, completes the process. This three-pronged approach seeks to create a psychological "immunity" against the spread of disinformation [32].

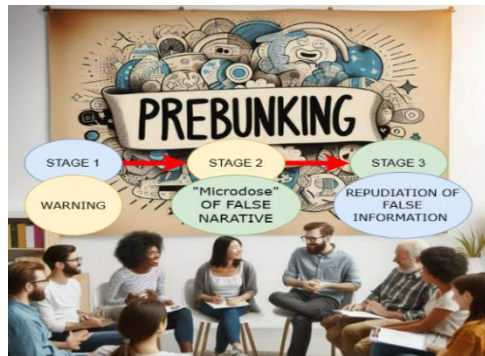


Fig.3. Key stages of prebunking approach

Education has always been a proactive tool for solid preparation in any area, therefore, consumers participating in cybersecurity threats awareness training sessions is one of the most effective tools for a reliable, consistent result. Therefore, consumers who are exposed to prebunking interventions can be better equipped to identify and resist phishing attempts and misinformation. For example, a study revealed that prebunking messages significantly improved participants' ability to discern fake news [33, 34]. These findings recommend prebunking as an effective tool for enhancing cyber awareness among consumers.

The most common threats used for simulation can be ethical phishing and fake websites. Instead of waiting for users to fall for phishing scams, prebunking can involve showing them examples of how phishing emails look and explaining the tactics attackers use (such as urgency or fake links). By learning these tactics in advance, users are better prepared to identify phishing attempts in real-world situations. Consumers can also visit fake websites examples as fraudulent websites or pages designed to steal personal information. The training sessions must cover detailed explanations of how attackers create legitimate-looking sites and offer tips to spot inconsistencies or red flags.

Several companies provide applications (free or by subscription) that can be customized to mimic real-world attack scenarios, with some sophisticated tools that offer phishing, and smishing simulations, as well as employee progress evaluation reports. Some of the most advanced examples are Infosec IQ's, Gophish, LUCY – a social engineering platform, SpeedPhish Framework (SPF), TrustedSec with the Social-Engineer Toolkit, Phishing Frenzy with penetration testing tools, Usecure with the uPhish platform that provides detailed analytics and reports to quantify employee progress, Sophos Phish Threat, and so on [24]. Ethical phishing simulations prove highly effective, particularly when organizations deploy these tests to employees regularly. With consistent phishing simulations, employees become better at identifying the indicators of phishing attempts and are more likely to report them to the organization, thereby reducing the probability of successful attacks (Figure 4). Regular campaigns, as a prebunking method of cybersecurity awareness training, must be consistently effective for both consumers and employees.

Cybercriminals often exploit psychological triggers, like fear, greed, or urgency. Prebunking can teach users about social engineering techniques (e.g., phishing, baiting, and pretesting) by explaining how attackers use these tactics to manipulate behavior. By

knowing these strategies in advance, users are more likely to think critically when confronted with suspicious requests. Consumers can be exposed to interactive, realistic simulations where they encounter cyber threats in a controlled environment. They would be taught how attackers might try to deceive them and how to respond before facing the actual risks. This training could simulate ransomware attacks, malware downloads, and credential theft attempts, building users' defenses against these threats. Prebunking can debunk common cybersecurity myths (e.g., "*I'm not important enough to be hacked*," or "*I have antivirus software, so I'm safe*") before these misconceptions lead to risky behavior. By addressing these beliefs ahead of time, users are more likely to adopt safer practices online. Similar to how prebunking combats misinformation, it can inoculate consumers against common scams, such as tech support fraud or online shopping scams. Training could expose consumers to typical scam formats and show how scammers operate. The core of prebunking is providing consumers with the tools to detect threats on their own. By educating them about the evolving tactics of cybercriminals, they become more resilient to attacks and can make smarter decisions without having to rely on constant updates or reminders.

Prebunking proactive strategies consists of nine blocks: Educational Games; Videos and Infographics; Browser Extensions; Social Media Campaigns; Interactive workshops; Automated Alerts and Fact-Checking Bots; Media-Literacy Programs; Prebunking Newsletters as presented in Figure 4.

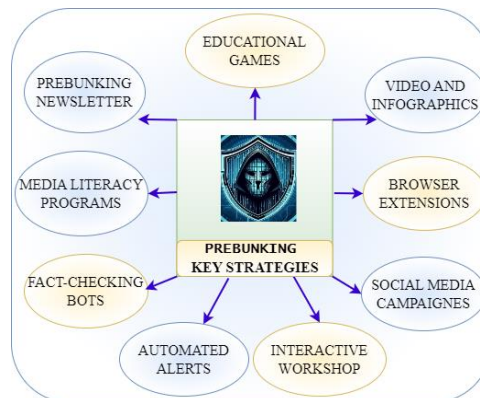


Fig.4. Prebunking proactive key strategies

Educational Games

By interactively engaging consumers, games like "Bad News" [36] and "Go Viral!" [37] build awareness of common deception strategies and improve critical thinking skills [35]. They simulate the experience of creating fake news, helping players recognize common manipulation tactics, and allowing consumers to experience how misinformation is created and spread. Education lays the foundation for effective adult behavior in any field, and prebunking, as well [38].

Videos and Infographics

Prebunking infographics are visual representations that combine text and graphics to convey information about misinformation and how to identify and counteract it. Visual and easily digestible content can quickly educate a broad audience, making

complex concepts more understandable and unforgettable. Therefore, engaging videos and infographics that explain how to recognize phishing emails, fake news, and other forms of cyber deception is some of the most effective methods used in prebunking. In February 2024, The Federal Trade Commission (FTC), USA, proposed an amendment to the Impersonation Rule to protect consumers against deep fake scams that leverage AI technology. This amendment underscores the FTC's dedication to safeguarding consumers from the potentially devastating consequences of AI-enabled impersonations. By holding parties accountable for the misuse of their products and services, the FTC aims to discourage future acts of deep fake fraud and maintain the integrity of digital identities [39].

Browser Extensions

By alerting consumers to potentially misleading content as they browse, these extensions offer immediate, practical guidance to help consumers avoid cyber traps. Tools like "NewsGuard" and "Fakey" help consumers identify credible sources and understand the reliability of the information they encounter online by providing real-time information about the credibility of websites and news articles. These extensions allow real-time prebunking by alerting consumers to potentially misleading content before they engage with it.

NewsGuard is a service that assesses the credibility of news and information sources to help consumers navigate the digital landscape and avoid misinformation. It monitors and flags misinformation trends, including AI-generated content and false narratives. For example, it has identified over 950 websites that produce content with little to no human oversight, which are often prone to spreading misinformation. They also maintain databases like the Misinformation Fingerprints catalog, which tracks provably false narratives circulating online [40].

Fakey is an interactive news literacy game developed by Indiana University to help consumers identify and debunk fake news on social media platforms. The game simulates a social media news feed, presenting players with a mix of legitimate news articles and those that are false or misleading. Consumers are invited to decide whether to share, like, or fact-check each post, receiving immediate feedback on their choices to help them learn from their mistakes and improve their media literacy skills. The game is designed to be engaging and fun, making the process of learning about news literacy enjoyable. Players receive feedback on their decisions, which helps them understand the nuances of identifying credible sources versus misleading ones. It represents an innovative approach to combating misinformation by combining education with gamification, making it an effective tool for improving news literacy in an engaging manner [41]. Platforms can integrate prebunking into their content moderation systems. For example, YouTube has experimented with displaying information panels from authoritative sources when consumers search for topics prone to misinformation, like vaccines or climate change.

Social Media Campaigns

Leveraging the extensive reach of social media, these campaigns can quickly disseminate prebunking information to large and diverse audiences. Social media platforms can run targeted prebunking campaigns, displaying posts or ads that educate consumers about common misinformation tactics. Social platforms like Meta, Instagram,

or Twitter can push prebunking messages or educational content to consumers based on their activity and the type of information they are likely to encounter.

The BBC launched the campaign "Get Your Facts Straight" to educate consumers on how to spot fake news through infographics, articles, and videos. The campaign included tips on verifying sources, checking for biases, and understanding the difference between opinion and fact [42]. Google's "Be Internet Awesome" initiative primarily focused on internet safety for kids; this campaign includes modules on recognizing misinformation. It uses interactive games and activities shared on social media to teach critical thinking skills [43]. The "Pause " Initiative by the United Nations uses social media platforms to spread awareness about misinformation related to COVID-19. It includes myth-busting posts, educational videos, and collaborations with influencers to reach a broader audience [44]. The campaign "Think Before You Share" by the European Commission focuses on the importance of verifying information before sharing it online. It uses a mix of videos, infographics, and interactive content to educate consumers on common misinformation tactics [45].

Interactive workshops

Prebunking interactive workshops are an effective method to educate consumers about the tactics and strategies used in misinformation and build their resilience against such content. These workshops aim to provide participants with the skills to recognize and critically evaluate information, making them less susceptible to false information.

Automated Alerts and Fact-Checking Bots

Bots like "Botometer" and various fact-checking bots can analyze social media posts in real-time, providing messages or flagging misleading content before it spreads widely, being powerful tools in the fight against misinformation. They leverage artificial intelligence (AI) and NLP to identify and counter false information in real time [46]. Being a proactive strategy that aims to inoculate people against harmful actions by exposing them to the techniques used to deceive them "in advance", prebunking can be applied in cybersecurity awareness training for consumers. This concept, when applied to cybersecurity domain, can help consumers better recognize and avoid threats.

5. CONCLUSIONS

This Prebunking, a proactive strategy based on inoculation theory, has solid grounds to emerge as a promising approach to enhance cyber awareness and resilience among digital consumers. By inoculating consumers against potential cyber threats, prebunking can reduce the possibility of efficacious cyber-attacks. Prebunking can be integrated into existing cybersecurity awareness training programs and extended campaigns, providing consumers with the tools to identify and resist proactively to different forms of cyber threats. Organizations deploy simulated ethical phishing campaigns and misinformation exercises regularly to reinforce these skills and maintain high levels of cyber awareness. Such training awareness strategies and campaigns should be conceived for consumers, as well. As cyber threats continue to evolve, innovative strategies like prebunking are essential in safeguarding consumers and maintaining trust in the digital ecosystem. There are several methods and tools that can assist consumers in testing, identifying, recognizing, and defending against cyber misinformation and

cyber threats, ultimately creating a more informed and resilient digital community. As a result of this study, we have defined the key stages of the prebunking approach. We also designed the prebunking proactive most effective strategies that consist of nine blocks: Educational Games; Videos and Infographics; Browser Extensions; Social Media Campaigns; Interactive workshops; Automated Alerts and Fact-Checking Bots; Media-Literacy Programs; Prebunking Newsletters. The positive impact of prebunking on consumer cyber awareness can have several implications. Organizations and policymakers should consider incorporating prebunking strategies into their cybersecurity education programs. By proactively equipping consumers with the skills to identify and resist cyber threats and misinformation, prebunking can enhance overall cybersecurity.

We also concluded that the impact of misinformation, and phishing attacks can be efficiently reduced by adapting content to specific audiences, using clear language, and engaging consumers across multiple platforms therefore, future studies will investigate the scalability of prebunking interventions and their effectiveness across different cultural and demographic contexts.

REFERENCES

- [1]. **Rains T., Youngblood T.**, *Cybersecurity Threats, Malware Trends, and Strategies: Discover Risk Mitigation Strategies for Modern Threats to Your Organization*, Packt Publishing, 2023.
- [2]. **Treglia J., Delia M.**, *Cyber Security Inoculation*, NYS Cyber Security Conference, Empire State Plaza Convention Center, Albany, NY, June 3-4, 2017.
- [3]. **McGuire W. J.**, *Resistance to persuasion conferred by active and passive prior refutation of same and alternative counterarguments*, *Journal of Abnormal Psychology*, Vol. 63, No. 2, pp. 326–332, 1961.
- [4]. **Lewandowsky S., Van Der Linden S.**, *Countering Misinformation and Fake News Through Inoculation and Prebunking*, *European Review of Social Psychology*, Vol. 32, No. 2, pp. 348–384, 2021.
- [5]. **Van Der Linden S., Roozenbeek J., Maertens R., et al.**, *How Can Psychological Science Help Counter the Spread of Fake News?*, *The Spanish Journal of Psychology*, Vol. 24, 2021.
- [6]. Bertolotti M., Catellani P., *Counterfactual Thinking as a Prebunking Strategy to Contrast Misinformation on COVID-19*, *Journal of Experimental Social Psychology*, Vol. 104, 2022.
- [7]. **Basol M., Roozenbeek J., Berriche M., Uenal F., McClanahan W. P., Van Der Linden S.**, *Towards Psychological Herd Immunity: Cross-Cultural Evidence for Two Prebunking Interventions Against COVID-19 Misinformation*, *Big Data & Society*, Vol. 8, No. 1, 2021.
- [8]. **Overton H. K., Yang F.**, *Do Information Disputes Work: The Effect of Perceived Risk, News Disputes, and Credibility on Consumer Attitudes and Trust Toward Biotechnology Companies*, *Journal of Communication Management*, Vol. ahead-of-print, 2023.
- [9]. **Christner C., Merz P., Barkela B., Jungkunst H., Von Sikorski C.**, *Combating Climate Disinformation: Comparing the Effectiveness of Correction Placement and Type*, *Environmental Communication: A Journal of Nature and Culture*, 2024.

- [10]. **Van Der Linden S., Leiserowitz A., Rosenthal S., Maibach E.,** *Inoculating the Public Against Misinformation About Climate Change*, Global Challenges, Vol. 1, No. 2, 2017.
- [11]. **Spampatti T., Brosch T., Trutnevyte E., Hahnel U. J. J.,** *A Preregistered Field Study of the Trust Inoculation Against a Negative Event Involving Geothermal Energy Systems*, Collabra: Psychology, Vol. 9, No. 1, 2023.
- [12]. **Peters T.,** *Prebunking Disinformation in Science, Skepticism, and Theology*, Theology and Science, Vol. 20, No. 4, pp. 381–385, 2022.
- [13]. **Fallou L., Bossu R., Cheny J. M.,** *Prebunking Earthquake Predictions on Social Media*, Frontiers in Communication, Vol. 9, 2024.
- [14]. **Boman C. D.,** *Examining Characteristics of Prebunking Strategies to Overcome PR Disinformation Attacks*, Public Relations Review, Vol. 47, No. 5, 2021.
- [15]. **Korshunov P., Jain A., Marcel S.,** *Custom Attribution Loss for Improving Generalization and Interpretability of Deepfake Detection*, ICASSP 2022 - IEEE International Conference on Acoustics, Speech and Signal Processing, Singapore, 2022.
- [16]. **Petrov A.,** *Countering Fake News with Contagious Inoculation and Debunking: A Mathematical Model*, 15th International Conference Management of Large-Scale System Development (MLSD), Moscow, 2022.
- [17]. **Moldovan D., Riurean S.,** *Cyber-Security Attacks, Prevention and Malware Detection Application*, J. Digit. Sci., Vol. 4, No. 2, pp. 3–23, 2022.
- [18]. **Manukyan L., Gevorgyan M.,** *Social Engineering Attacks: How to Prevent*, J. Digit. Sci., Vol. 6, No. 1, pp. 28–35, 2024.
- [19]. *Generative AI and Disinformation: White Paper*, EDMO, 2023, <https://edmo.eu/wp-content/uploads/2023/12/Generative-AI-and-Disinformation-White-Paper-v8.pdf>.
- [20]. **Stepanov A.,** *A Brief Overview of Existing Neural Network Solutions and Services for Photographers*, J. Digit. Sci., Vol. 5, No. 1, pp. 31–47, 2024.
- [21]. **Chauhan R., Popli R., Kansal I.,** *A Systematic Review on Fake Image Creation Techniques*, 10th International Conference on Computing for Sustainable Global Development (INDIACom), New Delhi, India, pp. 779–783, 2023.
- [22]. **Khanjani Z., Watson G., Janeja V. P.,** *Audio Deepfakes: A Survey*, Frontiers in Big Data, Vol. 5, 2023, DOI: 10.3389/fdata.2022.1001063.
- [23]. **Waisberg E., Ong J., Masalkhi M., et al.,** *Concerns with OpenAI's Sora in Medicine*, Annals of Biomedical Engineering, Vol. 52, pp. 1932–1934, 2024.
- [24]. **Riurean S.,** *Concepte și Tehnologii Noi de Comunicații în Arhitecturi de Rețele / Novel Communications Concepts and Technologies in Network Architectures*, Ed. Universitas Petroșani, 2023.
- [25]. **Riurean S., Leba M., Crivoi L.,** *Enhanced Security Level for Sensitive Medical Data Transmitted Through Visible Light*, 2021 International Symposium on Networks, Computers, and Communications (ISNCC), Dubai, UAE, 2021.
- [26]. **Kamuni N., Chintala S., Kunchakuri N., Narasimharaju J. S. A., Kumar V.,** *Advancing Audio Fingerprinting Accuracy with AI and ML: Addressing Background Noise and Distortion Challenges*, IEEE 18th International Conference on Semantic Computing (ICSC), Laguna Hills, CA, USA, pp. 341–345, 2024.
- [27]. **Muppalla S., Jia S., Lyu S.,** *Integrating Audio-Visual Features for Multimodal Deepfake Detection*, IEEE MIT Undergraduate Research Technology Conference (URTC), Cambridge, MA, USA, pp. 1–5, 2023.
- [28]. **Ganfure G. O., Wu C.-F., Chang Y.-H., Shih W.-K.,** *DeepWare: Imaging Performance Counters with Deep Learning to Detect Ransomware*, IEEE Transactions on Computers, Vol. 72, No. 3, pp. 600–613, 2023.

- [29]. Rössler A., Cozzolino D., Verdoliva L., Riess C., Thies J., Niessner M., *FaceForensics++: Learning to Detect Manipulated Facial Images*, IEEE/CVF International Conference on Computer Vision (ICCV), Seoul, Korea, pp. 1–11, 2019.
- [30]. Chauhan R., Popli R., Kansal I., *A Systematic Review on Fake Image Creation Techniques*, 10th International Conference on Computing for Sustainable Global Development (INDIACom), New Delhi, India, pp. 779–783, 2023.
- [31]. Shristi T., Kaur T., Verma A., Kaushal R., *Towards Automated Claim Detection in Fact-Checking*, 14th International Conference on Computing, Communication, and Networking Technologies (ICCCNT), Delhi, India, pp. 1–5, 2023.
- [32]. Lewandowsky S., Van Der Linden S., *Countering Misinformation and Fake News Through Inoculation and Prebunking*, European Review of Social Psychology, Vol. 32, No. 2, pp. 348–384, 2021.
- [33]. Marche C., Cabiddu I., Castangia C. G., Serreli L., Nitti M., *Implementation of a Multi-Approach Fake News Detector and of a Trust Management Model for News Sources*, IEEE Transactions on Services Computing, Vol. 16, No. 6, pp. 4288–4301, 2023.
- [34]. Caramancion K. M., *An Interdisciplinary Assessment of the Prophylactic Educational Treatments to Misinformation and Disinformation*, State University of New York at Albany, ProQuest Dissertations & Theses, 2022.
- [35]. Roozenbeek J., Van Der Linden S., *Fake News Game Confers Psychological Resistance Against Online Misinformation*, Palgrave Communications, Vol. 5, No. 65, 2019.
- [36]. *Get Bad News: A Game to Build Misinformation Resilience*, <https://www.getbadnews.com/books/english/>
- [37]. *Go Viral Game: Fighting Misinformation*, <https://www.goviralgame.com/books/go-viral/>
- [38]. Rosca S., Riurean S., Leba M., Ionica A., *An Educational Model of Graduation Project for Students at Automation and Computer Engineering*, J. Digit. Sci., Vol. 1, No. 1, pp. 34–42, 2019.
- [39]. *FTC Targets AI and Impersonation Fraud Rulemaking*, Wiley Law, 2024, <https://www.wiley.law/alert-FTC-Targets-AI-and-Potentially-More-in-Impersonation-Fraud-Rulemaking>
- [40]. *NewsGuard: Reports on Misinformation Trends*, <https://www.newsguardtech.com/reports/>
- [41]. Khalil A. A., Rahman M. A., Kholidy H. A., *FAKEY, Fake Hashed Key Attack on Payment Channel Networks*, IEEE Conference on Communications and Network Security (CNS), Orlando, FL, USA, pp. 1–9, 2023.
- [42]. *Get Your Facts Straight Toolkit for Educators and Training Providers*, ALL DIGITAL, 2024, <https://all-digital.org/resources/get-your-facts-straight-toolkit-for-educators-and-training-providers/>
- [43]. *Be Internet Awesome: Google's Digital Safety Curriculum*, Google, https://beinternetawesome.withgoogle.com/ro_ro
- [44]. *UN Calls for Stronger Efforts to Combat Misinformation*, United Nations, 2021, <https://news.un.org/en/story/2021/07/1095222>
- [45]. Kartal Y. S., Kutlu M., *Re-Think Before You Share: A Comprehensive Study on Prioritizing Check-Worthy Claims*, IEEE Transactions on Computational Social Systems, Vol. 10, No. 1, pp. 362–375, 2023.
- [46]. Torusdağ M. B., Kutlu M., Selçuk A. A., *Are We Secure from Bots? Investigating Vulnerabilities of Botometer*, 5th International Conference on Computer Science and Engineering (UBMK), Diyarbakir, Turkey, pp. 343–348, 2020.

This article was reviewed and accepted for presentation and publication within the 11th edition of the International Multidisciplinary Symposium "UNIVERSITARIA SIMPRO 2024".

PUBLIC OPINION ABOUT THE IMPACT OF RENEWABLE ENERGY SOURCES ON THE ENVIRONMENT OF JIU VALLEY

**ALEXANDRA SOICA¹, NICOLETA NEGRU²,
RAZVAN BOGDAN ITU³, SUSANA APOSTU⁴**

Abstract: This study examines public opinion on the environmental impact of renewable energy sources, focusing on a comprehensive survey conducted in 2023 involving 10,000 residents aged 18 to 60. The survey consisted of 20 questions designed to gauge opinions on energy sources and their application in both private households and public spaces. The findings reveal that while a majority of residents are in favor of adopting renewable energy sources, they perceive the associated costs as prohibitive. The study concludes that significant governmental support is essential to make the transition to renewable energy viable for the community. The research employs a structured questionnaire to collect quantitative and qualitative data, highlighting the substantial potential for renewable energy adoption in regions traditionally dependent on coal mining.

Key words: adoption, coal mining, energy sources, environment, renewable energy.

1. INTRODUCTION

The Jiu Valley, nestled between the Retezat and Parâng Mountains in southwestern Transylvania, Romania, is a region with a deep-rooted industrial heritage, primarily driven by coal mining. For over a century, the valley has been synonymous with coal extraction, with cities such as Petroșani, Vulcan, Lupeni, and Petrila serving as the epicenters of this industry. The region's coal mines, including Lonea, Lupeni, Livezeni, and Vulcan, have not only shaped its economic structure but also its cultural identity and social fabric. The coal industry provided livelihoods for thousands of families, and the towns in the Jiu Valley grew and developed around this vital economic activity.

¹ *Ph.D., Assistant Prof. Eng., University of Petroșani, alexandra_valynikalay@yahoo.com*

² *Ph.D., Student, Eng., University of Petroșani, negru.ioanamicoleta@yahoo.ro*

³ *Ph.D., Lecturer Eng., University of Petroșani, razvanitu@upet.ro*

⁴ *Ph.D., Lecturer Eng., University of Petroșani, apostu_susana@yahoo.com*

However, the coal industry in the Jiu Valley has been in decline for several decades, facing numerous challenges such as depleted coal reserves, rising operational costs, and increasing environmental concerns. The European Union's stringent environmental regulations and the global shift towards reducing carbon emissions have accelerated the closure of many coal mines in the region. This decline has led to significant economic hardships, including job losses, population decline, and social unrest, as the region grapples with the need to reinvent itself in a post-coal economy.

Despite these challenges, the Jiu Valley holds untapped potential for transitioning towards a more sustainable energy future. The region's geographical characteristics, such as its mountainous terrain and the Jiu River, present opportunities for the development of renewable energy sources, including hydropower, wind, and solar energy. Additionally, the transition to green energy in the Jiu Valley is not only a necessity driven by environmental concerns but also a strategic opportunity to revitalize the local economy, create new jobs, and improve the quality of life for its residents.

Green energy, or renewable energy, is derived from natural processes such as solar, wind, and hydropower, and it plays a crucial role in reducing greenhouse gas emissions and combating climate change. The importance of this transition is underscored by its potential to provide significant socio-economic benefits, including job creation, enhanced energy security, and economic diversification, as supported by previous research [1], [2], [9], [11]. Despite these advantages, the implementation of green technologies often faces resistance due to economic, logistical and social factors, including the high initial costs and the need for substantial infrastructure changes.

This study seeks to explore public opinion on renewable energy in the Jiu Valley, focusing on the critical need for governmental support and active community engagement to facilitate this transition. The research is framed within the broader context of the 2030 Sustainable Development Agenda, which emphasizes the importance of clean energy and the creation of sustainable communities as key global objectives [4], [10], [12].

The adoption of renewable energy sources in the Jiu Valley offers significant potential for mitigating the environmental impacts traditionally associated with coal mining, such as air pollution and water contamination. Transitioning to renewable energy could lead to improvements in local air quality, conservation of water resources, and the promotion of sustainable economic development. These changes align with global efforts to reduce carbon emissions and achieve sustainable development goals [3], [13]. However, realizing this potential requires overcoming the socio-economic challenges and addressing the perceptions and concerns prevalent among the local population. This study aims to provide insights into these challenges and offer recommendations for fostering a successful energy transition in the region.

2. MATERIALS AND METHODS

The study employed a structured survey method to comprehensively assess public attitudes towards renewable energy in the Jiu Valley. Recognizing the region's historical dependence on coal mining and the growing importance of transitioning to

sustainable energy sources, the survey was meticulously designed to capture a wide range of data relevant to this transition. The survey aimed to gather insights into not only the public's attitudes towards renewable energy but also the socio-economic and demographic factors that influence these attitudes.

The survey was structured into 20 questions, strategically divided into four main categories to provide a holistic view of the public's perceptions:

Residence Characteristics and Energy Consumption: This section focused on gathering detailed information about the respondents' living conditions, including the type of residence, size of the household, and patterns of energy consumption. Questions in this category aimed to establish a baseline understanding of how energy is used within households, which is critical for assessing the potential impact of adopting renewable energy sources.

Expenditures: This category sought to understand the financial aspects of energy consumption, including monthly energy bills, expenditures on heating, and any investments made in energy efficiency measures. Understanding the economic burden of energy costs on households is essential for evaluating the feasibility of transitioning to more sustainable energy options.

Green Energy Adoption: Questions in this section explored the respondents' awareness of and attitudes towards green energy technologies, such as solar panels, wind turbines, and energy-efficient appliances. The survey also investigated the extent to which residents have already adopted or are willing to adopt these technologies in their homes.

Perceptions of Cost and Feasibility: This final category delved into the perceived barriers to adopting renewable energy, focusing on the costs associated with green technologies and the perceived ease or difficulty of implementing these solutions. This section aimed to identify the key factors that may hinder or promote the adoption of renewable energy in the Jiu Valley.

Data was collected from a large sample of 10,000 residents across the Jiu Valley, achieving a valid response rate of 85.6%, which resulted in 8,562 responses. The survey population was carefully stratified to ensure that the sample was representative of the Jiu Valley's diverse demographics. Stratification was based on key variables such as age, gender, household size, and employment status. This approach ensured that the findings could be generalized to the broader population of the Jiu Valley.

The demographic breakdown of the respondents included a balanced representation of men and women, a range of age groups, and varied household sizes. Employment status was also considered, reflecting the economic diversity of the region, which includes both employed individuals and those who are unemployed, retired, or students. This comprehensive sampling approach provided a robust dataset for analyzing public attitudes towards renewable energy.

The structured survey method was chosen for its ability to collect large amounts of data from a broad population efficiently. This approach is particularly advantageous in a region like the Jiu Valley, where diverse opinions and experiences with energy consumption need to be captured to inform effective policy and decision-

making. The standardized format of the survey ensured consistency in data collection, allowing for a clear comparison of responses across different demographic groups.

However, the method is not without its limitations. One potential drawback is the reliance on self-reported data, which can introduce biases, such as the tendency of respondents to provide socially desirable answers rather than fully accurate ones. Additionally, while the survey was designed to capture a wide range of opinions, the standardized nature of the questions may not fully capture the complexity and nuance of individual attitudes towards renewable energy.

To mitigate these limitations, the survey design incorporated best practices from similar studies on public attitudes towards renewable energy [5], [6], [13] ensuring that the questions were both relevant and clear to the respondents.

Overall, the survey method provided valuable insights into the current state of public opinion on renewable energy in the Jiu Valley, offering a solid foundation for understanding the challenges and opportunities associated with transitioning to a more sustainable energy model in the region.

3. RESULTS AND DISCUSSION

The study yielded important insights into the acceptance and adoption of renewable energy sources in the Jiu Valley, revealing both the challenges and opportunities that exist within this historically coal-dependent region.

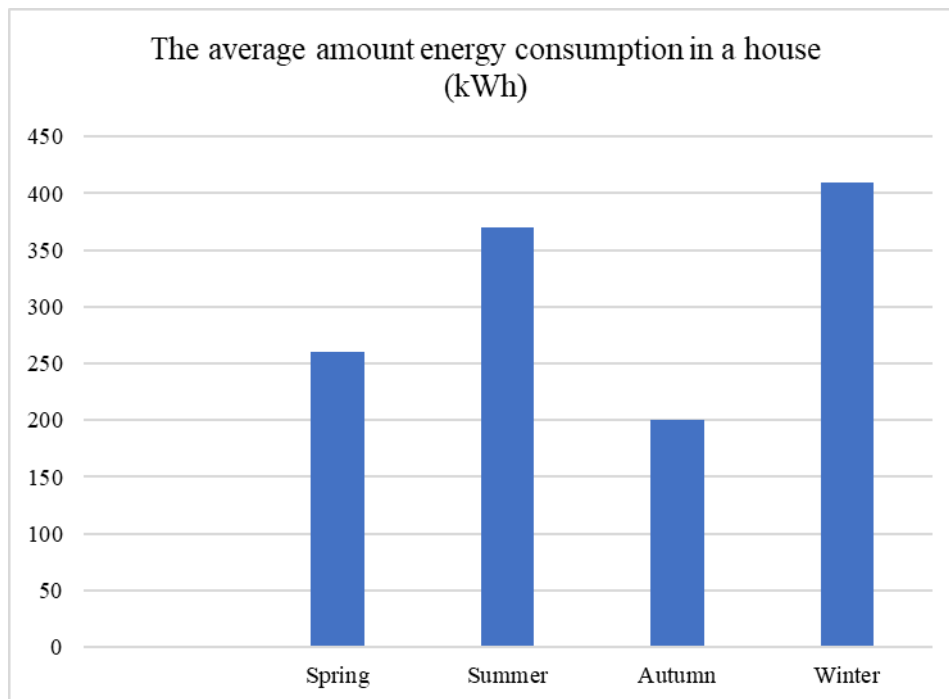


Fig. 1. The energy consumption in a house

The demographic analysis of the survey respondents provided a snapshot of the Jiu Valley's population. The survey revealed a slightly higher proportion of men (51%) than women, reflecting the gender dynamics of a region historically shaped by its coal mining industry. The majority of residents live in apartment buildings (89.8%), with 70% concentrated in central urban areas such as Petroșani, Vulcan, and Lupeni. This urban concentration suggests a population accustomed to centralized infrastructure, which can both aid and complicate the transition to decentralized renewable energy systems.

One of the most significant findings was the low implementation rate of energy-saving measures among the population. Despite the region's harsh winters and the rising costs of energy, 70% of households reported lacking basic energy efficiency upgrades, such as thermal insulation and energy-efficient windows.

This gap in energy efficiency highlights a major barrier to reducing energy consumption and transitioning to renewable energy sources. The primary reasons cited for this lack of adoption were the high costs associated with retrofitting existing buildings and the logistical challenges posed by the region's aging infrastructure. These findings echo concerns raised in earlier studies [2] about the financial and practical hurdles of improving energy efficiency in established urban environments.

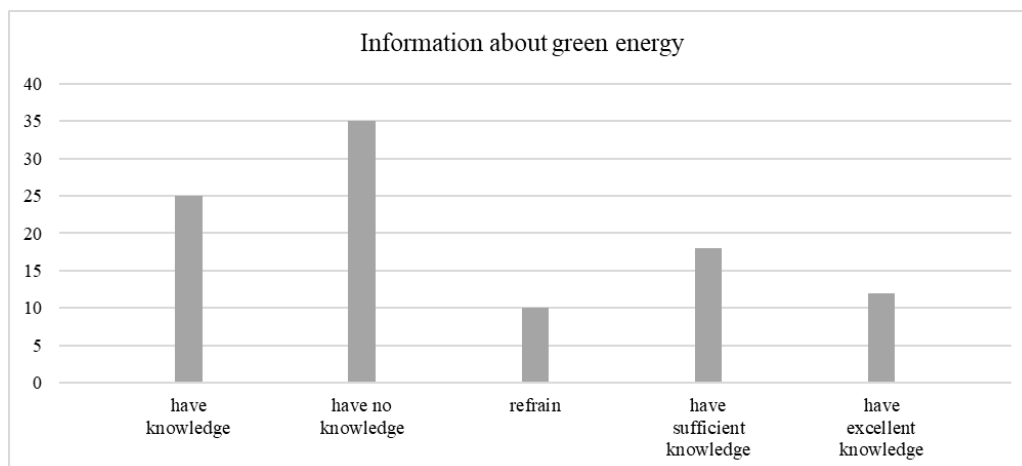


Fig. 2. Information about green energy

While there is a general awareness of the environmental benefits associated with green energy, the study uncovered significant resistance to its adoption. Notably, 60% of respondents expressed opposition to implementing renewable energy technologies, such as solar panels or wind turbines. The primary reason for this opposition was the perceived high cost of these technologies, which many residents felt was beyond their financial reach. This resistance is indicative of a broader challenge in the Jiu Valley: while the concept of green energy is recognized and even supported in theory, the practicalities of adoption—especially the upfront costs—present a formidable obstacle.

The findings underscore the critical need for targeted policies and financial incentives to overcome the barriers to energy efficiency and renewable energy adoption in the Jiu Valley. The high costs and logistical difficulties associated with

retrofitting existing buildings are significant challenges that must be addressed if the region is to successfully transition to a more sustainable energy model. Additionally, the opposition to green energy adoption due to cost concerns suggests that there is a need for greater public education and engagement, particularly around the long-term economic benefits of renewable energy, such as reduced energy bills and increased energy independence.

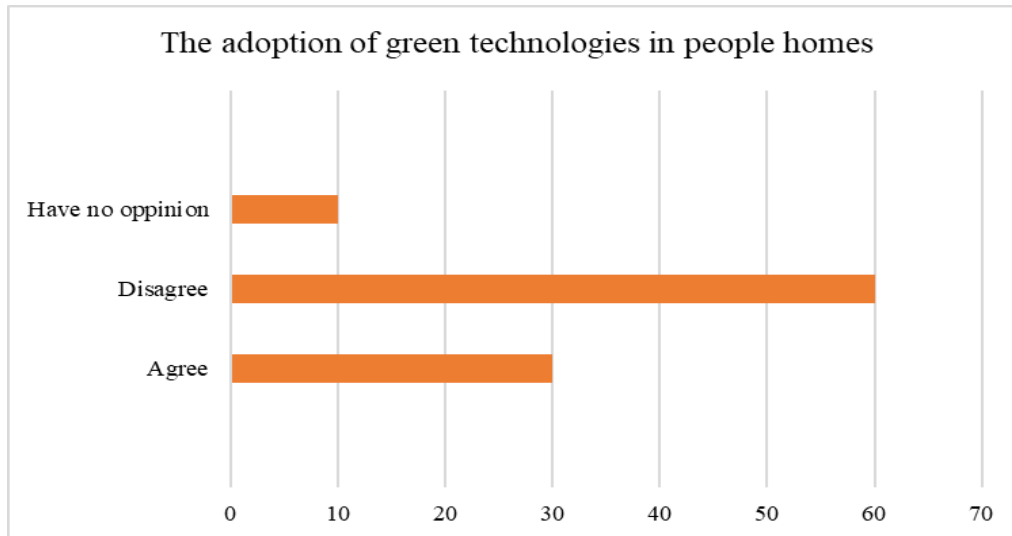


Fig. 3. The adoption of green technologies in people homes

The study also revealed a "not in my backyard" (NIMBY) attitude among some residents, who acknowledge the need for renewable energy but resist its implementation near their homes. This resistance is often fueled by misinformation and skepticism about the feasibility and benefits of green technologies [1]. The lack of widespread adoption of energy-saving measures indicates a need for more effective public education campaigns and financial incentives to overcome these barriers.

Furthermore, the finding that 1 in 3 citizens selectively heat parts of their homes to manage energy costs underscores the potential for targeted interventions to promote energy efficiency. Financial incentives, combined with community-based education initiatives, could play a critical role in shifting public opinion and behavior towards more sustainable energy practices.

4. CONCLUSIONS

The findings from the study reveal both the potential for renewable energy adoption in the Jiu Valley and the significant barriers that must be addressed to realize this potential. While the region is well-positioned to transition to a more sustainable energy model, several challenges stand in the way, including the high costs of implementation, a lack of comprehensive information, and socio-economic factors that shape public attitudes towards renewable energy.

The study highlights that the financial burden associated with adopting renewable energy technologies is one of the most significant obstacles for residents of the Jiu Valley. The initial costs for installing solar panels, wind turbines, or other green energy systems are perceived as prohibitively high by many households, particularly in a region that has historically relied on coal and where economic conditions are often constrained. This financial barrier underscores the need for targeted interventions such as government subsidies, low-interest loans, or other financial incentives that can lower the entry cost for households and businesses.

Another critical barrier identified is the lack of comprehensive information available to residents regarding the benefits and feasibility of renewable energy technologies. The study suggests that many residents are not fully aware of the long-term savings and environmental benefits associated with green energy, leading to skepticism and resistance. This gap in knowledge contributes to the prevalence of misconceptions and a lack of enthusiasm for renewable energy projects. To overcome this, there is a clear need for educational campaigns and outreach programs that provide accurate, accessible information about renewable energy and its potential benefits for the Jiu Valley.

The study also identifies socio-economic factors, including the prevalence of NIMBY (Not In My Backyard) attitudes, as a significant challenge. These attitudes reflect a resistance to the implementation of renewable energy projects in the immediate vicinity of residents, often due to concerns about property values, aesthetics, or perceived inconveniences. Additionally, the demographic profile of the population, which includes a high proportion of residents living in older apartment buildings, further complicates the widespread adoption of renewable energy technologies. The combination of these socio-economic factors and the physical infrastructure of the region necessitates a tailored approach that considers the specific needs and concerns of the local population.

To address these challenges and enhance the acceptance and implementation of renewable energy technologies, the study suggests a multi-faceted approach. This approach should involve:

Government Support: Active governmental involvement is crucial in creating a supportive policy environment that incentivizes renewable energy adoption. This could include financial subsidies, tax breaks, and regulatory support for both individuals and businesses investing in green energy.

Targeted Financial Incentives: Specific financial programs tailored to the needs of the Jiu Valley's residents are necessary to overcome the cost barriers. These could include grants, low-interest loans, or even direct financial assistance for lower-income households to make renewable energy technologies more accessible.

Community Engagement: Engaging the community through public consultations, educational campaigns, and participatory planning processes is essential to build trust and address the socio-economic factors that contribute to resistance. By involving residents in the decision-making process and addressing their concerns directly, it is possible to mitigate NIMBY attitudes and foster a more positive outlook towards renewable energy projects.

In conclusion, while the Jiu Valley has substantial potential for adopting renewable energy, realizing this potential requires addressing significant barriers related to cost, information, and socio-economic factors. A comprehensive, multi-faceted approach that includes strong government support, targeted financial incentives, and robust community engagement is essential for overcoming these challenges. By addressing these specific issues, there is considerable potential to enhance the acceptance and implementation of renewable energy technologies in the Jiu Valley, contributing to the broader goals of sustainable development and the transition to a low-carbon economy.

REFERENCES

- [1]. **Assefa G., Frostell B.**, *Social sustainability and social acceptance in technology assessment: A case study of energy technologies*. *Technology in Society*, 29 (1), pp. 63-78, 2007.
- [2]. **Bang H.K., Ellinger A.E., Hadjimarcou J., Traichal P.A.**, *Consumer concern, knowledge, belief, and attitude toward renewable energy: An application of the reasoned action theory*. *Psychology & Marketing*, 17(6), pp. 449-468, 2000.
- [3]. **Delucchi M.A., Jacobson, M.Z.**, *Renewable energy sources: Their global potential for the first half of the 21st century at a global level: An integrated approach*. *Energy Policy*, 2010.
- [4]. **European Commission**, *European Green Deal*, 2020, Retrieved from https://ec.europa.eu/info/strategy/priorities-2019-2024/european-green-deal_en
- [5]. **Nnaji C.C., Chibueze C., Afangideh C.B.**, *The menace and mitigation of air pollution in the built environment: A review*. *Nigerian Journal of Technology*, 42(1), pp. 12-29, 2023.
- [6]. **Zhou S., He H., Zhang L., Zhao W., Wang F.**, *A Data - Driven Method to Monitor Carbon Dioxide Emissions of Coal-Fired Power Plants*. *Energies*, 16(4), 2023.
- [7]. **Itu R.B., Șoica A.**, *The Reintegration of The Surfaces Affected by the Phenomenon of Subsidence through the Cultivation of Trees with High Energy Value*. *Revista De Gestão Social E Ambiental*, 18(3), 2024.
- [8]. **U.S. Department of Energy**, *Energy Efficiency and Renewable Energy*, 2021. <https://www.energy.gov/eere/>
- [9]. **Arad, S., Marcu, M., Pasculescu D., Petrilean D.C.** *Aspects of the electric arc furnace control*, Proceeding. of international symposium advanced engineering & applied management, Faculty of Engineering Hunedoara, 2010.
- [10]. **Petrilean D.C., Popescu D.F.**, *Temperature Determination in Hydrotechnical Works as a Variable of the Energy Change Between Air and Environment*, WSEAS TRANSACTIONS on HEAT and MASS TRANSFER, 2008.
- [11]. **Petrilean D.C.**, *The study of energy losses through case helical screw compressor*, Bulletin of the Transilvania University of Brasov, Proceedings of the internationally attended national conference on thermodynamics, 2009.
- [12]. **Petrilean D.C.**, *Compresoare eliciodale*, Editura Tehnica-Info, 2006.
- [13]. **Petrilean D.C.**, *Termodinamica tehnica si masini termice*, Editura A.G.I.R., 2010.
- [14]. **Petrilean D. C.**, *Transmiterea căldurii*, Editura Universitas, 2016.

This article was reviewed and accepted for presentation and publication within the 11th edition of the International Multidisciplinary Symposium "UNIVERSITARIA SIMPRO 2024".

MODERNIZATION OF ELECTRICAL INSTALLATIONS FOR LIGHTING AND POWER IN THE ELECTROENERGETICS LABORATORY OF THE UNIVERSITY OF PETROȘANI

FLORIN MUREȘAN-GRECU¹, FLORIN GABRIEL POPESCU²,
MARIUS DANIEL MARCU³, DRAGOS PASCULESCU⁴,
MIRCEA RISTEIU⁵, TEODORA LAZAR⁶

Abstract: Creating an interior electrical installation for lighting and sockets is a rigorous endeavor that must comply with current regulations and standards in the field. For this, it is necessary to draft a technical project that includes the designed situation and calculation briefs to determine the parameters of the installation. This paper succinctly presents the realization of interior electrical installations for lighting and outlets in the Electroenergetics Laboratory ("Laboratory L1") in Building A of the University of Petroșani and its adjacent rooms.

Keywords: electrical installation, modernization, standards, calculations, protections.

1. INTRODUCTION

The discovery of electrical energy and the ways it can be utilized have represented essential turning points in the progress and development of human civilization. Today, electrical energy is indispensable in all aspects of life and human activities, offering a series of advantages compared to other forms of energy [1], [23]:

- production under economically favorable conditions in power plants;
- rapid—practically instantaneous—and economical transmission of energy over long distances through overhead and underground transmission lines;
- economical distribution to a large number of consumers with different power requirements;

¹ Assist. Prof. Ph.D. Student Eng., University of Petroșani, flomavon2002@yahoo.com

² Associate Prof. Ph.D. Eng., University of Petroșani, floringabriel82@yahoo.com

³ Professor Ph.D. Eng., University of Petroșani, marisumarcu66@yahoo.com

⁴ Associate Prof. Ph.D. Eng., University of Petroșani, pdragos_74@yahoo.com

⁵ Associate Prof. Ph.D. Eng., 1 Decembrie 1918 University of Alba Iulia, mristeiu@uab.ro

⁶ Lecturer Ph.D. Eng, University of Petroșani, teomititica@yahoo.com

- efficient and advantageous transformation possibilities of electrical energy into other forms of energy (mechanical, thermal, etc.), even at the consumption site, with high efficiency.

Regarding the specific provisions for the design and execution of low voltage electrical installations in Romania, these are generally legislated through the technical regulation *"Norm for the design, execution, and operation of electrical installations related to buildings"*, indicated as I7. The most recent edition of this norm was approved in 2011 by an Order of the Minister of Regional Development and Tourism, published in the Official Gazette of Romania No. 802 bis on 14.11.2011, and was modified and supplemented by the Order of the Minister of Development, Public Works and Administration No. 959/18.05.2023, published in the Official Gazette of Romania No. 512 on 12.06.2023 [2]. The I7-2011 norm was mainly developed based on the SR HD 60364 series of standards. Additionally, in the design and execution of lighting electrical installations, the provisions of the technical regulation *"Norm for the design and execution of artificial lighting systems in buildings"*, indicated as NP-061-02, are also taken into account [3], [24], [25], [29].

2. EXISTING SITUATION

The main building of the University of Petroșani, known as "Building A," was constructed between 1949 and 1952. The internal electrical installations were designed and executed according to the technical regulations valid at that time, which are now technically outdated.



Fig. 1. Electrical panel from the years 1949-52, in an open construction

The electrical circuits were made with cables and conductors insulated with rubber and jute, lacking fire-resistant properties, and in some cases, with smaller cross-sections than those specified by current regulations. Most of the electrical panels were built in an open construction on marble supports, equipped with fuses and switches that are also in open construction and unprotected (see fig. 1) [4]. The installations were sized

for the electrical energy consumption of that period when the number of electrical devices was much lower than it is today. Considering the need for the electrical installations to support the state-of-the-art laboratory equipment intended to be acquired for the modernization of the educational spaces, the urgency of replacing the old electrical installations of the Laboratory L1 complex becomes fully justified [26], [28].

The L1 Laboratory complex includes the following rooms:

- the main laboratory;
- the office of the teaching staff;
- the office of the laboratory staff;
- the technical annex.

3. PROJECTED SITUATION

3.1. Specifications document

The first step in modernizing the electrical installations of Laboratory L1 and its associated rooms is the preparation of a project for the new electrical installations for lighting and power. For this purpose, a specifications document has been prepared, outlining a series of requirements, such as: determining the number and placement of electrical panels, lighting and power electrical receptors, as well as their installed power and their mode of operation and usage. The main provisions of the specifications document are summarized in the following paragraphs [27], [30].

3.1.1. Electric power supply

For the electric power supply, the two existing electrical panels in the old installation will be used: the main electrical panel (MEP), located in the basement technical hallway, and the secondary electrical panel, located in the laboratory hallway, which will be renamed SEP-1. The two old electrical panels at the mentioned locations will be decommissioned, and new panels equipped with modern protection devices, chosen in accordance with current technical regulations, will be installed in their places. In addition to these two panels, a new secondary electrical panel, named SEP-2, will be installed in the laboratory. The secondary electrical panels SEP-1 and SEP-2 will be powered from the main electrical panel MEP through two three-phase electrical columns with 5 conductors (L1, L2, L3, N, PE), appropriately sized and installed underground in the existing cable ducts [5], [31].

3.1.2. Lighting electrical installations

Both normal and emergency lighting installations will be implemented. For the normal lighting installations, the placement of existing lighting fixtures will be maintained. Within the laboratory room, lighting will be supplemented with 8 wall-mounted sconce-type fixtures, installed on the eastern and western side walls.

MODERNIZATION OF ELECTRICAL INSTALLATIONS FOR LIGHTING AND POWER
IN THE ELECTROENERGETICS LABORATORY OF THE UNIVERSITY OF PETROȘANI

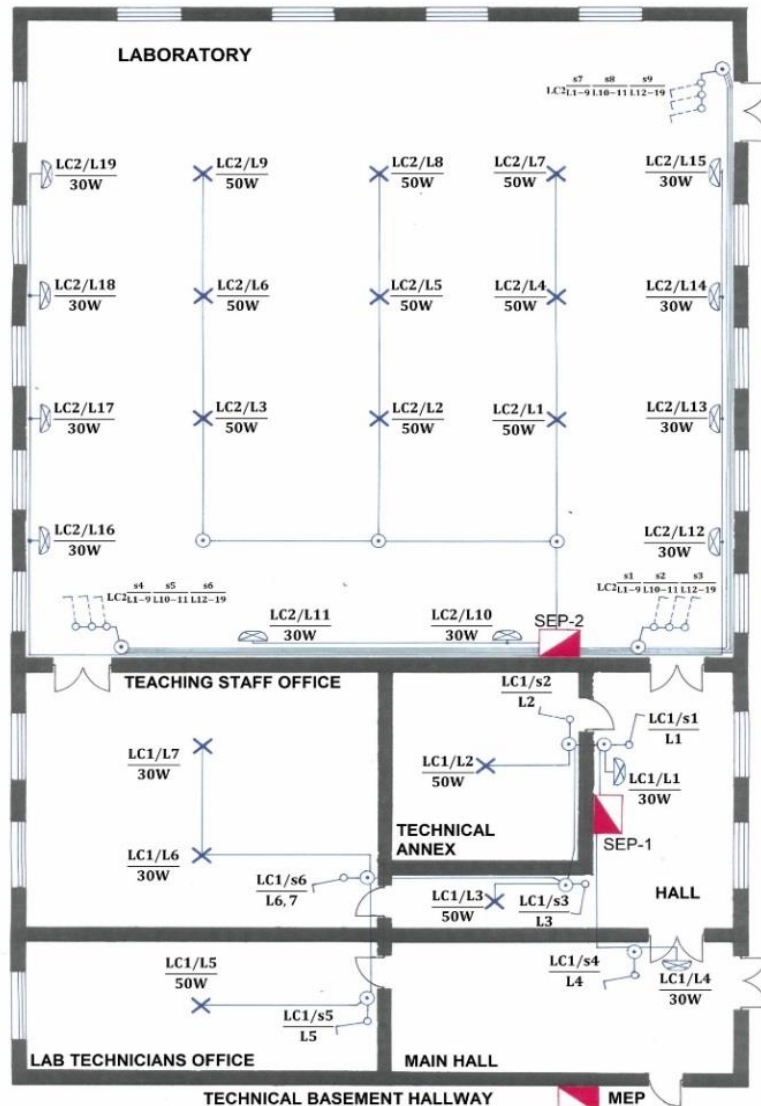


Fig. 2. The electrical plan for normal lighting installations

The normal lighting installation will consist of two circuits:

- lighting circuit LC-1, containing the lighting fixtures in the laboratory's annex rooms;
- lighting circuit LC-2, containing the lighting fixtures in the laboratory.

The lighting fixtures will be LED, point-type, chandelier and/or sconce-type, mounted on ceilings and/or walls.

The emergency lighting installation will consist of one emergency lighting circuit LC-3 and will include emergency lighting fixtures with local battery for evacuation, signaling, and panic [6].

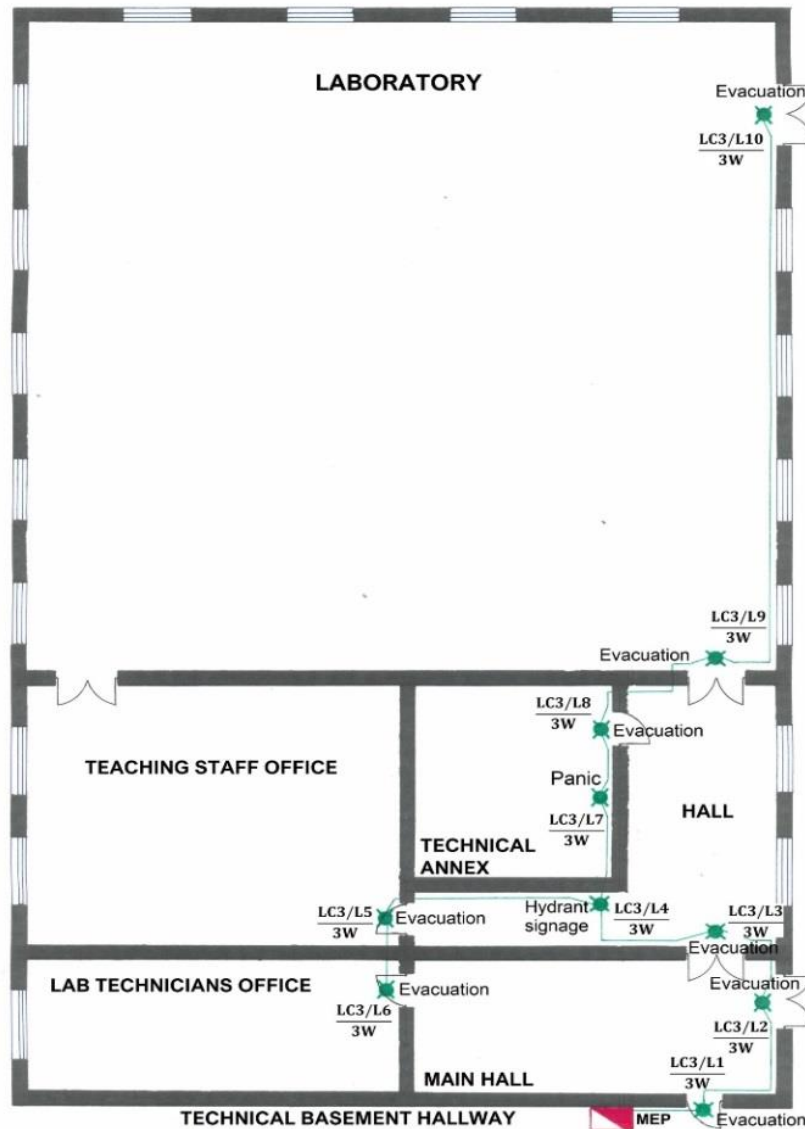


Fig. 3. The electric plan for emergency lighting installation

3.1.3. Electrical installations for single-phase sockets

To supply power to the electrical appliances and devices, several socket outlet circuits will be implemented as follows:

- circuit SC-1 in the laboratory staff office;
- circuit SC-2 in the technical annex;
- circuit SC-3 in the teaching staff office;
- circuits SC-4 and SC-5 in the laboratory.

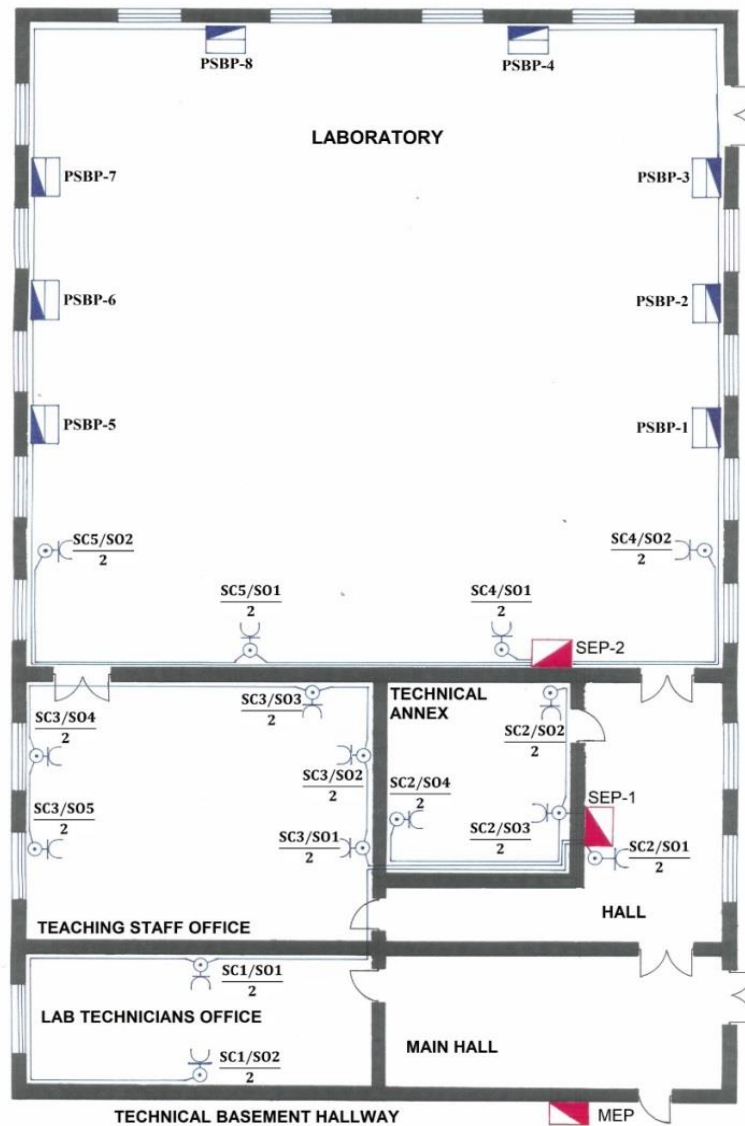


Fig. 4. The electrical plan for single-phase socket outlets installations

3.1.4. Electrical installations for powering specific teaching equipment in the Electroenergetics Laboratory

In order to power the educational apparatus and equipment that will be acquired and installed in Laboratory L1, a total of 8 power supply blocks with protection (PSBPs) will be provided. These will essentially function as capsulated type electrical panels, each equipped with two three-phase sockets outlets and three single-phase sockets outlets. Each socket outlet will be locally protected by miniature circuit breakers (MCBs).

3.2. Preparations for electrical plans

The preliminary stage for preparing the electrical plans consisted of creating the survey drawing. The electrical plans were developed by tracing the electrical circuits and positioning the distribution boards, lighting fixtures, and terminal equipment on the survey drawing. Three electrical plans were prepared [7]:

- electrical plan for normal lighting installations (Fig. 2);
- electrical plan for emergency lighting installation [8] (Fig. 3);
- electrical plan for single-phase socket outlets installations (Fig. 4).

The symbols used in the electrical plans are explained in Fig. 5, and the legend of abbreviations used in the electrical plans and the purpose of each circuit are detailed in Table 1 [9].

	Electric panel
	Single-phase socket with protective earth
	Three-phase socket with protective earth
	Switch
	Push-switch
	LED lamp for mounting on/under the ceiling
	Wall mounted LED lamp
	Power supply block with protection PSBP
	Junction box and/or appliance box
	Emergency LED lamp

Fig. 5. Symbols used in the preparation of electrical plans

Table 1. Legend of abbreviations and the purpose of electrical circuit destinations

Abbreviation	Component element of the electrical installation
MEP	Main Electric Panel
SEP-1	Secondary electric panel no. 1
SEP-2	Secondary electric panel no. 2
$\frac{SC3/SO4}{2}$	Example notation: unit of 2 modular socket outlets no.4, mounted in a common device box, connected in socket circuit SC-3
$\frac{LC3/L8}{3W}$ Evacuation	Example notation: Emergency evacuation lighting fixture no. 8 from emergency lighting circuit LC-3, with a nominal power of 3W
$\frac{LC3/L7}{3W}$ Panic	Example notation: Emergency panic lighting fixture no. 7 from emergency lighting circuit LC-3, with a nominal power of 3W
$\frac{LC3/L4}{3W}$ Hydrant signage	Example notation: Emergency hydrant signage lighting fixture no. 4 from emergency lighting circuit LC-3, with a nominal power of 3W

$LC2 \frac{s1}{L1-9} \frac{s2}{L10-11} \frac{s3}{L12-19}$	Example notation: unit of 3 modular push-button switches, mounted in a common device box, connected in lighting circuit LC-2: - s1, for controlling lighting fixtures L1...L9 - s2, for controlling lighting fixtures L10-L11 - s3, for controlling lighting fixtures L12...L19
$\frac{LC1/L7}{30W}$	Example notation: Lighting fixture number 7 from normal lighting circuit LC-2, with a nominal power of 30W.
$\frac{LC1/s5}{L6,7}$	Example notation: Modular toggle switch no. s5, for controlling lighting fixtures L6 and L7, mounted in normal lighting circuit LC-1.
PSBP-2	Three-phase power supply block with protection no. 2

4. TECHNICAL MEMORANDUM

4.1. Preparing the calculation summary and configuring the electrical Installation

4.1.1. Normal Lighting Installation

In the case of lighting installations, the illumination level on the work plane is determined by NP-061-02 [3].

To determine the characteristics of lighting installations, the following data will be used:

- h_a - height of suspension of lighting fixtures (m);
- h_u - height of the working plane (m);
- H - room height (m);
- h - free height (m);
- L - room length (m);
- l - room width (m);
- i - room index;
- Φ - luminous flux falling on a reflecting surface (walls or ceiling) (lm);
- Φ_r - reflected luminous flux inside the room (lm);
- ρ - reflection factor;
- u - utilization factor, provided in the technical sheets of lighting fixtures;
- M_F - maintenance factor;
- E_m - average illuminance of the room;
- Φ_{req} - luminous flux required for a room;
- Φ_{lamp} - luminous flux of a lighting fixture. In the case of LED fixtures with a matte cover, if the value of Φ_{lamp} is not provided in the product's technical specifications, it is determined by multiplying the nominal power of the lamp by 80;
- s - area of the room (m²);
- n - number of light sources;

Free height is calculated using the equation (1):

$$h = H - h_u - h_a \quad (1)$$

Room index is calculated using the equation (2):

$$i = \frac{L * l}{h(L+l)} \quad (2)$$

Reflected luminous flux inside the room is calculated using the equation (3):

$$\Phi_r = \Phi * \rho \quad (3)$$

Luminous flux required for a room is calculated using the equation (4):

$$\Phi_{req} = \frac{Em * s}{MF * u} \quad (4)$$

Number of light sources is calculated using the equation (5):

$$n = \frac{\Phi_{req}}{\Phi_{lamp}} \quad (5)$$

For this project, a working plane height of $h_u=0.7$ m was adopted, specific to room where intellectual activities are conducted.

The reflection factors considered for this project are:

- for educational rooms: $\rho_{ceiling} = 0.7$; $\rho_{walls} = 0.5$;
- for the technical annex: $\rho_{ceiling} = 0.5$; $\rho_{walls} = 0.3$.

The maintenance factors considered for this project are:

- for educational rooms: $M_F = 0.8$;
- for the technical annex: $M_F = 0.7$.

Regarding the average illuminance level Em , the rooms in this project are considered to have visual tasks with specific visual requirements, and the Em value considered is 1000 lx, according to Table 7.1 of NP-061-02 [3].

The light sources used will be LED technology, requiring the selection of a light color appropriate to the type of activities performed. In terms of emitted color, there are three groups of light sources [10, 11]:

- the group of light sources that emit warm light, with a yellowish-white hue, having a color temperature of less than 3000K (typically $T_k = 2700K$);
- the group of light sources that emit neutral light (sometimes called "natural light"), with a white hue, having a color temperature between 3000-4000K;
- the group of light sources that emit cool light, with a bluish-white hue, having a color temperature of $T_k = 6000K$.

For the educational activities specific to the spaces covered by this project, it is recommended to use lighting fixtures with a color temperature of $T_k=4000K$. Additionally, these lighting fixtures must ensure visual protection for the users.

The data resulting from the calculations are synthesized in Table 2 [12, 13].

Table 2. Calculation of normal lighting installation

Circuit abrevia- tion	Room	Lighting fixtures					
		Ceiling-mounted			Wall-mounted		
		Number	Nominal power	Total nominal power	Number	Nominal power	Total nominal power
LC-1	Main hall	-	-	-	1	30	30
LC-1	Hol	1	50	50	1	30	30
LC-1	Technical annex	1	50	50	-	-	-
LC-1	Lab technicians office	1	50	50	-	-	-
LC-1	Teaching staff office	2	30	60	-	-	-
LC-2	Laboratory	9	50	450	10	30	300

4.1.2. Emergency lighting installation

For emergency lighting, the option chosen is to use LED luminous block-type fixtures with continuous operation, equipped with local batteries and having a nominal power of 3W. The lighting fixtures will be intended for:

- emergency evacuation lighting, for fixtures installed above access ways and/or evacuation routes;
- panic emergency lighting, in the technical annex, which lacks natural lighting;
- emergency lighting for the interior fire hydrant signage, located in the hallway.

Connection to the network and protection of the lighting fixtures will be done in the MEP.

4.1.3. Determining the electrical parameters of the installation

Within the calculation summary, the following data were used [12]:

- U_l - line voltage = 400 V AC;
- U_f - phase voltage = 230 V AC;
- $\cos \varphi$ - power factor; for this project, a value of $\cos \varphi = 0.92$ was considered [13];
- L - circuit length (m);
- s - conductor cross-section (mm²);
- P_i - installed power (W);
- k_s - simultaneity coefficient;
- k_u - utilization coefficient;
- P_r - instantaneous absorbed (required) power (W);
- I_n - nominal current of the circuit breaker;
- I_r - instantaneous absorbed (required) current (A);
- I_z - permissible current according to the chosen reference mounting method (B2) (from Annex 5.10 of I7-2011) [2];

- k_1 - ambient temperature factor, from Annex 5.18 of I7-2011 [2]. For this project, an ambient temperature of 25°C was considered, which corresponds to a value of $k_1 = 1.06$;
- k_2 - group reduction factor, from Annex 5.19 of I7-2011 [2]. In this project, the most unfavorable situation is with 3 grouped circuits, which corresponds to a k_2 factor value of 0.7;
- I_a - maximum permissible current in continuous operation (A);
- Δ_U - voltage drop expressed as a percentage;
- ρ_{Cu} - electrical resistivity of copper = 0.0175 $\Omega\text{mm}^2/\text{m}$;
- Z_{L-N} - direct fault loop impedance phase-neutral L-N (Ω);
- Z_{L-PE} - direct fault loop impedance phase-earth L-PE (Ω);
- I_{SC-L-N} - direct short-circuit current phase-neutral L-N (A);
- $I_{SC-L-PE}$ - direct short-circuit current phase-earth L-PE (A);
- R_p - dispersion resistance of the local ground electrode, presumed to be 4 Ω .

The requested power P_r was determined using the equation (6):

$$P_r = P_i * k_s * k_u \quad (6)$$

The sizing of the circuits was done based on the required current I_r , ensuring that the equation (7) is satisfied:

$$I_r \leq I_n \leq I_a \quad (7)$$

The maximum permissible current in continuous operation was determined using the equation (8):

$$I_a = I_z * k_1 * k_2 \quad (8)$$

The minimum cross-section of copper conductors is 1.5 mm² for lighting circuits and 2.5 mm² for socket circuits, even if calculations suggest the possibility of choosing smaller cross-sections [2]. The reference installation method for the circuits in this project, determined from Annex 5.6 of I7-2011, is B2. From Annex 5.10, the values of the maximum permissible currents were determined, taking into account the most unfavorable conditions [2].

The required current I_r was determined for each circuit using equation (9) and (10):

For one-phase circuits:

$$I_r = \frac{P_r}{U_f \cdot \cos \varphi} \quad (9)$$

For three-phase circuits:

$$I_r = \frac{P_r}{\sqrt{3} \cdot U_L \cdot \cos \varphi} \quad (10)$$

For the protection of the circuits were selected circuit breakers with standardized nominal current values I_n , each immediately higher than the corresponding I_r values, ensuring that these values satisfy equation (7) for each circuit [14].

The voltage drops expressed as a percentage were calculated for the longest circuits. For single-phase socket circuits, circuit SC-3 has the biggest length of 15 m, between panel SEP-1 and socket outlet SC3/SO5. For normal lighting circuits, the

section with the biggest length of 20 m is in circuit LC-2, between panel SEP-2 and lamp LC2/L19. Regarding three-phase circuits, the section between panel SEP-2 and PSBP-8 is the longest, measuring 19 m.

The maximum permissible voltage drops expressed as a percentage are 3% for lighting circuits and 5% for socket circuits [2, 15, 16]. The calculation of the voltage drops expressed as a percentage was carried out using equations (11) and (12):

For one-phase circuits:

$$\Delta U_f = \frac{2 \cdot 100 \cdot I_n \cdot L \cdot \cos \varphi \cdot \rho_{Cu}}{U_f \cdot s} \quad (11)$$

For three-phase circuits:

$$\Delta U_l = \frac{\sqrt{3} \cdot 100 \cdot I_n \cdot L \cdot \cos \varphi \cdot \rho_{Cu}}{U_l \cdot s} \quad (12)$$

The values determined by calculations using equations (11) and (12) for voltage drops are: 1.87% for the lighting circuit; 1.3% for single-phase socket circuits and 0.93% for three-phase socket circuits. These values are below the maximum limits provided by I7-2011 [2, 17].

For the correct selection of the type of miniature circuit breakers (MCBs) in the electrical panels, in addition to their nominal current, it is necessary to determine the time-current characteristics of each circuit breaker. These characteristics, also known as tripping curves, show the time in which a circuit breaker trips depending on the value of the overload current it is subjected to. The most common tripping curves of circuit breakers used in residential areas are as follows (fig. 6) [10, 18, 19]:

- curve B, where the circuit breaker trips when a current between (3-5) * I_n passes;
- curve C, where the circuit breaker trips when a current between (5-10) * I_n passes;
- curve D, where the circuit breaker trips when a current between (10-20) * I_n passes.

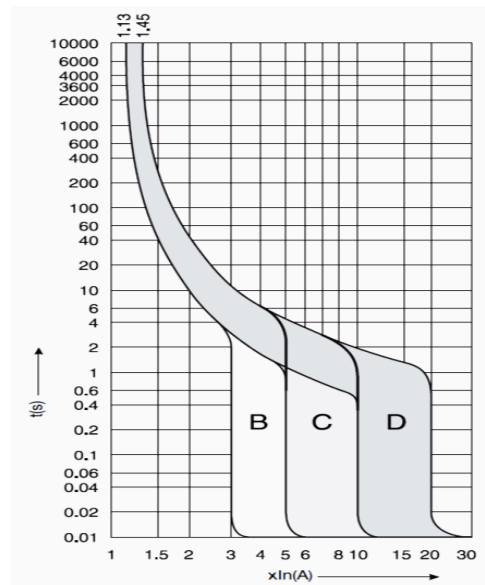


Fig. 6. Tripping curves of the MCBs

Manufacturers generally recommend using circuit breakers with tripping curve B for the protection of circuits with long lengths (which implicitly have a higher fault loop impedance), those with tripping curve C for the protection of general-purpose circuits in all types of installations, and those with tripping curve D for the protection of circuits supplying devices that draw high currents upon connection to the network (e.g., electric motors or high-power lighting installations equipped with LED luminaires that switch on simultaneously, where the inrush current has a high value for a very short period) [14, 20].

In order to correctly determine the fault currents and make the appropriate choice of circuit breaker type, it is necessary to know the values of the phase-neutral and phase-earth fault loop impedances, calculated for the longest circuits or circuit sections. These impedances are calculated using equations (13) and (14) [15, 21]:

$$Z_{L-N} = 2 \cdot \frac{\rho_{Cu} \cdot L}{s} \quad (13)$$

$$Z_{L-PE} = \frac{(\rho_{Cu} \cdot L) + R_p}{s} \quad (14)$$

Knowing the values of the fault loop impedances, the presumed values of short-circuit currents were determined using equations (15) and (16):

$$I_{SC-L-N} = \frac{U_f}{Z_{L-N}} \quad (15)$$

$$I_{SC-L-PE} = \frac{U_f}{Z_{L-PE}} \quad (16)$$

The results of the calculations have been summarized in Table 3.

The next step in designing the electrical installation involves configuring the electrical panels based on the previously calculated data and parameters. Figure 7 depicts the single-line diagram of the main electrical panel MEP.

Table 3. Electrical installation parameters

Circuit Simbol	Destination	P _r (W)	I _r (A)	Material	I _n (A)	S (mm ²)	I _z (A)	I _a (A)	Z _{L-N} (Ω)	Z _{L-PE} (Ω)	I _{sc-L-N} (A)	I _{sc-L-PE} (A)	Tripp. curve	k _s	k _u
LC-1	Normal lighting circuit	270	1,28	Cu	6	1,5	16,5	12,99	0,47	2,90	489,36	79,30	C	1	1
LC-2	Normal lighting circuit	750	3,54	Cu	6	1,5	16,5	12,99	0,47	2,90	489,36	79,30	C	1	1
LC-3	Emergency lighting circuit	30	0,14	Cu	6	1,5	16,5	12,99	0,47	2,90	489,36	79,30	C	1	1
SC-1	One-phase socket outlets in laboratory staff office	2000	9,45	Cu	10	2,5	23	17,89	0,21	1,70	1095	135,30	C	1	1
SC-2	One-phase socket outlets in technical annex	2000	9,45	Cu	10	2,5	23	17,89	0,21	1,70	1095	135,30	C	1	1
SC-3	One-phase socket outlets in teaching staff office	2000	9,45	Cu	10	2,5	23	17,98	0,21	1,70	1095	135,30	C	1	1
SC-4	One-phase socket outlets in laboratory	2000	6,05	Cu	10	2,5	23	17,98	0,21	1,70	1095	135,30	C	0,8	0,8
SC-5	One-phase socket outlets in laboratory	2000	6,05	Cu	10	2,5	23	17,98	0,21	1,70	1095	135,30	C	0,8	0,8
PSBP 1...4	Three-phase Power Supply Block with Protection	12000	12,06	Cu	20	6	34	25,23	0,11	0,72	3636	555,56	C	0,6	0,6
PSBP 5...8	Three-phase Power Supply Block with Protection	12000	12,06	Cu	20	6	34	25,23	0,11	0,72	3636	555,56	C	0,6	0,6

MODERNIZATION OF ELECTRICAL INSTALLATIONS FOR LIGHTING AND POWER
IN THE ELECTROENERGETICS LABORATORY OF THE UNIVERSITY OF PETROȘANI

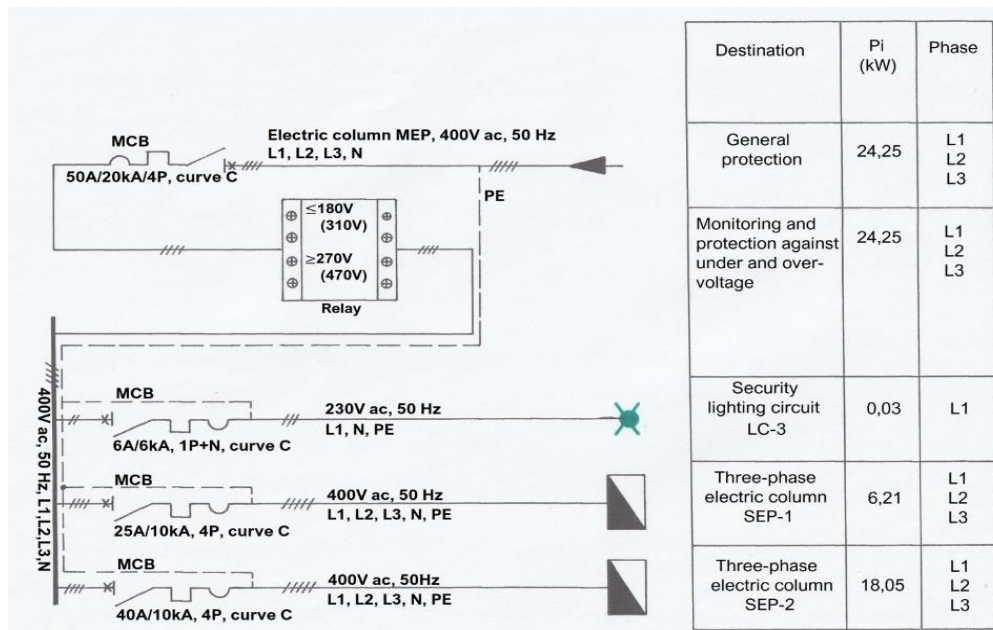


Fig. 7. The single-line electrical diagram of the main electric panel MEP

For monitoring and protecting the entire electrical installation against network over/undervoltages, a three-phase monitoring and protection relay with a nominal current of 63A will be installed in the MEP (main electrical panel) (see figure 7).

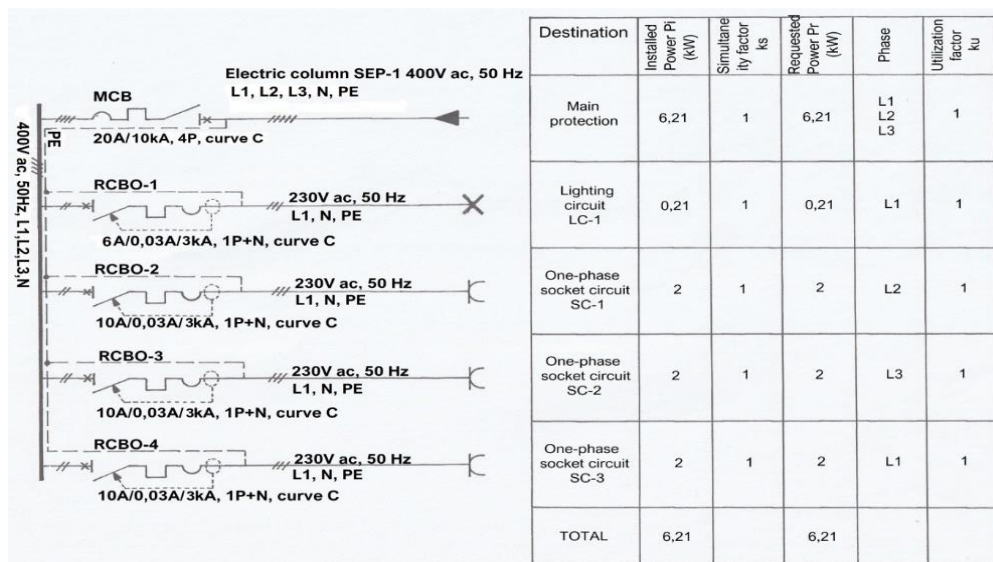


Fig. 8. The single-line electrical diagram of the secondary electric panel SEP-1

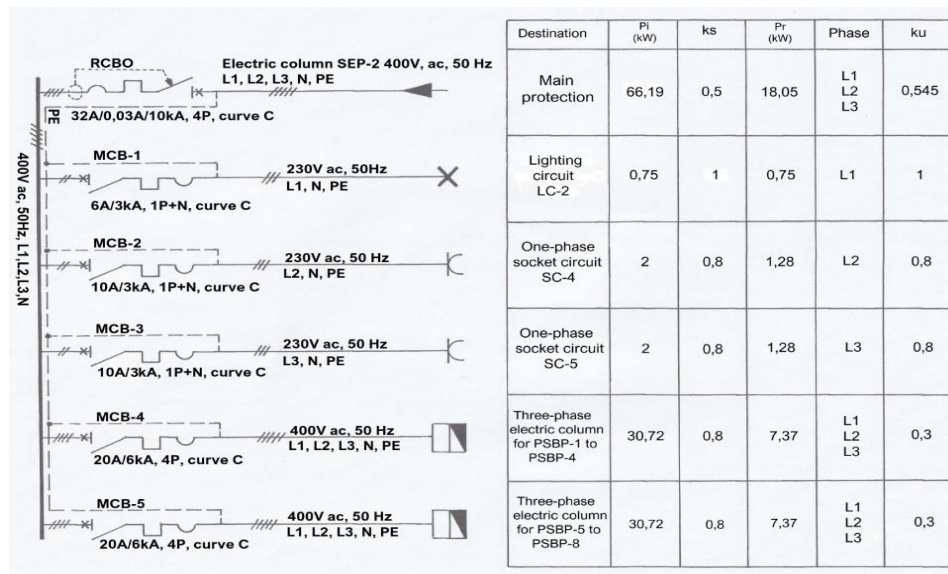


Fig. 9. The single-line electrical diagram of the secondary electric panel SEP-2

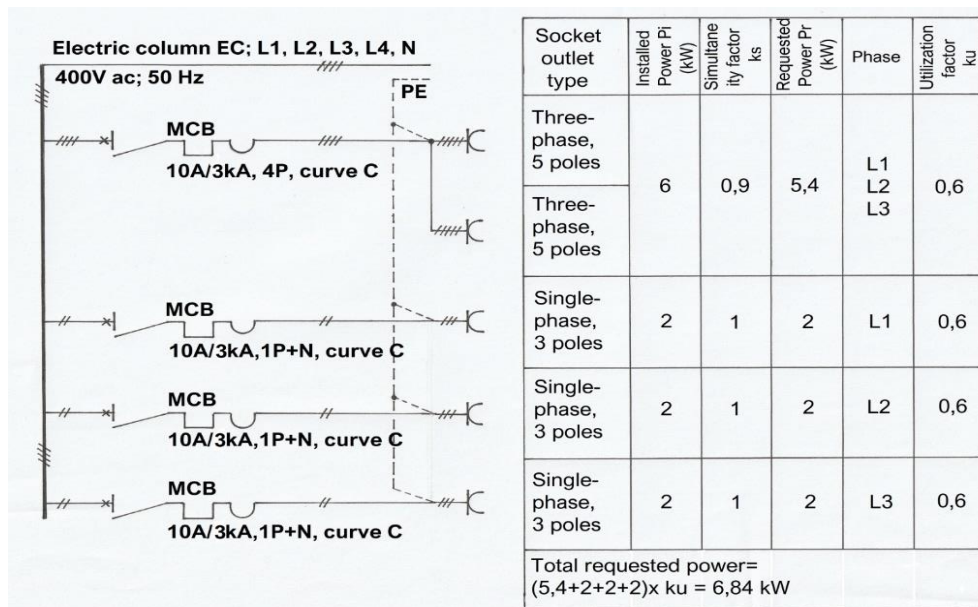


Fig. 10. The single-line electric diagram of the power supply block with protection PSBP

Upon analyzing the single-line diagrams in figures 8-10, it is observed that all final circuits of the installation are protected against residual currents by bipolar (1P+N) or four-pole (4P) high-sensitivity RCBO (Residual Current Breaker with Overcurrent protection) devices, with a nominal residual current of 30 mA. These are installed either as the main protection for the entire panel or as individual protections for the final circuits [16].

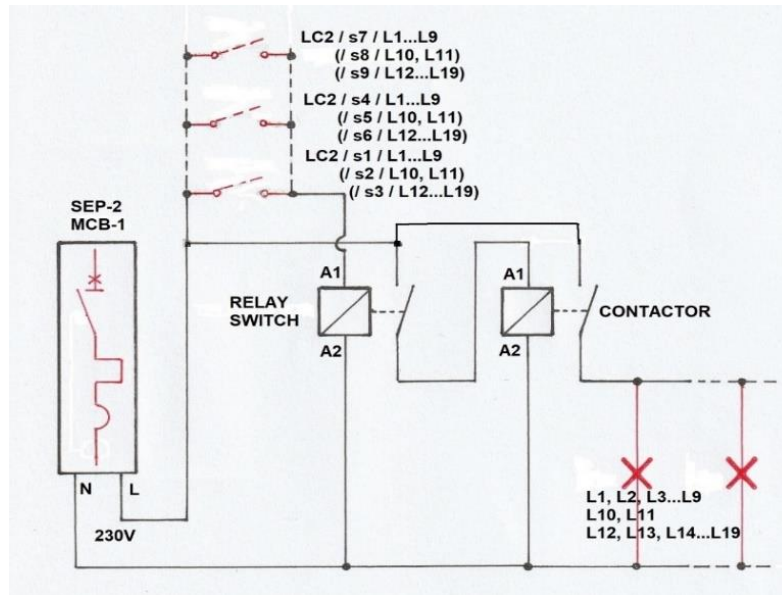


Fig. 11. The electrical control diagram for the lighting in the laboratory, utilizing a 3-point control system with step relays and contactor setup

Regarding the lighting fixtures in the laboratory, it is necessary that these can be controlled from each of the 3 access points into the laboratory. Control needs to be distinct for the ceiling lights, the lights on the side walls, and the lights on the front wall above the smart board. To achieve this, in the secondary panel SEP-2, 3 relay switches (step relays) and 3 contactors have been installed, one for each grouping of lights. Each of the 3 step relays is controlled from the 3 control points via a momentary push-button switch (see figure 11).

The operation of the control scheme is as follows: when one of the momentary push-button switches S1...S3, S4...S6, or S7...S9 is pressed, the corresponding step relay coil receives a voltage pulse, causing the internal cam-driven mechanism to rotate one step and close the corresponding contact. This energizes the coil of the corresponding contactor. By closing the normally open (NO) contact of the contactor, the power circuit to the corresponding lighting line is completed [9, 10].

Upon pressing the corresponding push-button switches again, the step relay coil receives a new pulse and rotates the cam-driven mechanism again, opening the relay contact. This interrupts the coil circuit of the contactor, causing it to de-energize and thereby stopping the power supply to the lighting line.

5. THE PRACTICAL IMPLEMENTATION OF THE ELECTRICAL INSTALLATION

After completing the project, the next steps in the practical implementation of the interior electrical installations in laboratory L1 and its annexes involved selecting materials and equipment, and executing the installation.

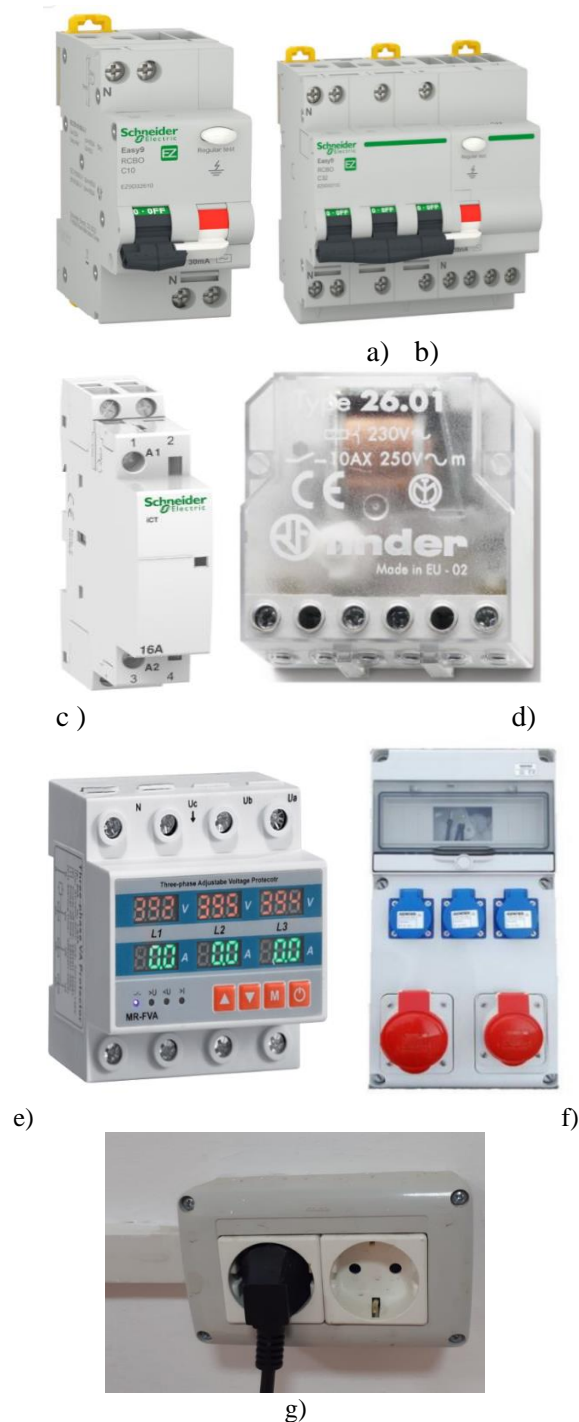


Fig. 12. Examples of the electrical equipment and devices used in the installation:
a) Bipolar RCBO; b) Four-pole RCBO; c) DIN rail-mounted contactor; d) Step relay; e) Three-phase monitoring and protection relay; f) PSBP; g) Unit of 2 modular socket outlets installed in surface-mounted box

The electrical columns supplying the secondary panels SEP-1 and SEP-2 were executed using multi-strand copper conductors with PVC insulation having enhanced resistance to flame propagation, type HO7V-K, of flexibility class 5, with a cross-section of 16 mm². These were protected in corrugated flexible PVC conduit type FK15 with a diameter of 40 mm, capable of withstanding a compression resistance of 750 N [5, 22].

For equipping the electrical panels, protective and control equipment from renowned European manufacturers such as Schneider Electric, Legrand, and Finder was used. Regarding terminal equipment (single-phase socket outlets, toggle-switches and push-button switches), we opted for products from the Italian manufacturer Gewiss - modular equipment from the System range installed in surface-mounted boxes from the 27 Combi series. From the same manufacturer, Gewiss, we also selected the power supply blocks with protection PSBPs which are to be installed in the laboratory [14, 17].

The lighting fixtures are LED, wall or ceiling-mounted sconces with a matte diffuser, featuring a color temperature of 4000K. The electrical circuits were installed with PVC-insulated single-core copper conductors and flame-retardant sheathing type CYY-F, with cross-sections of 1.5, 2.5, and 6 mm², surface-mounted on the non-combustible structural elements of the building (masonry walls) and protected in 40 x 60 mm PVC ducts. Penetrations between rooms for routing electrical circuits were made through masonry walls, without compromising the structural integrity of the building. Within-room transitions were protected with PVC conduits. Minimum distances from other installations (water, gas) as per Norm I7-2011 were adhered to.

In Figure 12 are some photographs and illustrations of various types of equipment used in the installation.

6. CONCLUSIONS

Over its 75 years of existence, the University of Petroșani has earned a well-deserved reputation within the scientific and technical community of Romania and beyond. The university's educational facilities have primarily served the training of specialists in the field of mining, equipped specifically for this purpose. With the evolution of society and the gradual shift away from coal for electricity generation, the University is now facing the necessity to "reinvent" itself in order to remain a significant player in today's competitive university environment, where attracting new students at all academic levels is crucial.

With the gradual disappearance of strictly mining-related specializations and the emergence of new fields of study, it is natural to consider the discontinuation of many of the old equipment and facilities in the university laboratories that no longer serve their purpose in the current context. Over the coming years, there is a plan to replace these outdated facilities with state-of-the-art teaching materials and equipment.

It is obvious that the electrical installations that have served the university's educational spaces for seven decades no longer meet the requirements to support modern laboratory equipment. Additionally, they do not align with the safety and operational standards mandated by current regulations and industry standards. Therefore, there is a need to upgrade these installations to ensure they can support the new laboratory equipment effectively and comply with the latest safety regulations.

In the context outlined above, the initiative to design and implement modern and safe electrical installations to serve the entirety of the rooms comprising Laboratory of Electrical Engineering (Laboratory No. 1) in Building A of the university, as the subject of this project, is entirely normal. Its culmination can only be positive, with the aim to extend similar initiatives to other educational spaces across the campus.

Furthermore, this project underscores once again that the design and implementation of internal electrical installations must be approached professionally by specialists and industry professionals. Not only is this a legal requirement, but it also ensures rigorous handling of all issues and aspects, leading to excellent results.

REFERENCES

- [1]. **Dromereschi, R., Gavril, V., Ionescu, L.,** „*Instalații electrice*”, M.A.S.T. Publishing House: Bucharest, Romania, 2008.
- [2]. <https://migs.ro/wp-content/uploads/2023/06/Normativ-pentru-proiectarea-executia-si-exploatarea-instalatiilor-electrice-afereente-cladirilor-indicativ-I-7%E2%80%94942011.pdf> (accessed on 17 June 2024).
- [3]. <https://www.scribd.com/document/21770873/NP-061-02-NORMATIV-PENTRU-PROIECTAREA-%C5%9E-EXECUTAREA-SISTEMELOR-DE-ILUMINAT-ARTIFICIAL-DIN-CL%C4%82DIRI> (accessed on 17 June 2024).
- [4]. **Fîță, N.D., Diodiu, I.L., Vișan, R.N., Olteanu, C.R., Mureșan-Grecu, F., Pinte, D.M.,** „*Evaluarea riscurilor electrice*”, Focus Publishing House, Petroșani, 2023.
- [5]. **A.S.R.O. SR 234:2008** *Standard român. Branșamente electrice. Prescripții generale de proiectare și executare.*
- [6]. **Fîță, N.D., Diodiu, I.L., Vișan, R.N., Olteanu, C.R., Mureșan-Grecu, F., Pinte, D.M.,** „*Noțiuni de electrosecuritate*”, Focus Publishing House, Petroșani, 2023.
- [7]. **Fitero, L., Bizadea, S., Popa, M., Nicoară, P.,** „*Desen tehnic industrial: Curs pentru facultatea de electrotehnică*”, Litografia Institutului Politehnic, Timișoara, 1989.
- [8]. **I.N.C.D. „URBAN INCERC”,** „*Ghid de bună practică pentru proiectarea instalațiilor de iluminat/protecție în clădiri*”, Bucharest, 2012.
- [9]. **Pietrăreanu, E.,** „*Agenda electricianului*”, Technical Publishing House, Bucharest, 1986.
- [10]. **Niculescu, T.,** „*Fundamente teoretice de electrotehnică*”, Focus Publishing House, Petroșani, 2018.
- [11]. **Petrilean, D. C., Irimie, S. I.,** „*Solutions for the capitalisation of the energetic potential of sludge collected in Danutoni wastewater treatment plant*”, Journal of Environmental Protection and Ecology, Vol.16, No.3, pp.1203-1211, 2015.
- [12]. **Racoți, E.,** „*Dimensionarea rețelelor electrice cu ajutorul tabelelor și nomogramelor*”, Technical Publishing House, Bucharest, 1988.
- [13]. **Costinaș, S., Niculescu, T.,** „*Electrotehnică. Circuite electrice*”, The Litography of The University of Petroșani, 2000.
- [14]. **Petrilean, D.C.,** „*Elaborating and Analysing the Real Balance of Heat for the Steam Generator RGL 10/DD 2008*”, Annals of the University of Petroșani, Mechanical Engineering, Volume 10, 155-160, 2008.
- [15]. **Buta, A., ș.a.,** „*Calitatea energiei*”, AGIR Publishing House, 2001.
- [16]. **Schneider Electric,** „*Manualul instalațiilor electrice*”, 2007.
- [17]. **Handra A.D., Popescu F.G., Păsculescu D.,** *Utilizarea energiei electrice: lucrări de laborator*, Editura Universitas, 2020.
- [18]. **Delesega, I.,** „*Aparate electrice*”, Universitatea tehnică, Timișoara, 1993.

[19]. Mureșan-Grecu, F., Fiță, N.D., Popescu, F.G., Păsculescu, D., Marcu, M.D., Moraru, R.I., „The identification and application of solutions to increase energy efficiency in an agro-food market”, Annals of University of Petroșani, Electrical Engineering, Vol. 25, pp. 95-104, Petroșani, 2023.

[20]. Petrilean, D.C., Preda, L., Marinescu, D.C., „Real and optimum exergetic balance sheet of helical screw compressor ATLAS COPCO GA 30 CF to reduce energy consumption”, 15th International Multidisciplinary Scientific, GeoConference SGEM 2015, SGEM2015 Conference Proceedings, June 18-24, Book 4, pp. 425-432, Albena, Bulgaria, 2015.

[21]. Petrilean, D.C., Stanilă S., Dosa, I., „A mathematical model for determining the dimensionless heat flux with application in mine environment”, Environmental Engineering and Management Journal, Vol.16, No. 6, 1249-1414, 2017.

[22]. Petrilean, D.C., „Compresoare elicoidale”, Tehnica-info, Chisinau, 2006.

[23]. Marcu M., Niculescu T., Slusariuc R. I., Popescu, F. G., Modeling and simulation of temperature effect in polycrystalline silicon PV cells, IOP Conference Series: Materials Science and Engineering, Vol. 133, No. 1, pp. 012005, 2016.

[24]. Popescu F.G., Arad S., Marcu M.D., Pana L., Reducing energy consumption by modernizing drives of high capacity equipment used to extract lignite, Papers SGEM2013/Conference Proceedings, Vol. Energy and clean technologies, pp. 183 - 190, Albena., Bulgaria, 2013.

[25]. Andras A., Popescu F.D., Radu S.M., Pasculescu D., Brinas I., Radu M.A., Peagu D., Numerical simulation and modeling of mechano-electro-thermal behavior of electrical contact using comsol multiphysics. Applied Sciences, 14(10), 4026, 2024.

[26]. Fiță N.D., Radu S.M., Păsculescu D., Popescu F.G., Using the primary energetic resources or electrical energy as a possible energetical tool or pressure tool, In International conference KNOWLEDGE-BASED ORGANIZATION, vol. 27, no. 3, pp. 21-26. 2021.

[27]. Popescu F.G., Păsculescu D., Păsculescu V.M., Modern methods for analysis and reduction of current and voltage harmonics, LAP LAMBERT Academic Publishing, ISBN 978-620-0-56941-7, pp. 233, 2020.

[28]. Pasculescu D., Niculescu T., Study of transient inductive-capacitive circuits using data acquisition systems." International Multidisciplinary Scientific GeoConference: SGEM 2, no. 1, 323-329, 2015.

[29]. Stepanescu, S., Rehtanz, C., Arad, S., Fotau, I., Marcu, M., Popescu, F. Implementation of small water power plants regarding future virtual power plants 10th International Conference on Environment and Electrical Engineering, pp. 1-4, IEEE, 2011.

[30]. Fiță N. D., Lazăr T., Popescu F. G., Pasculescu D., Pupăză C., Grigorie E., 400 kV power substation fire and explosion hazard assessment to prevent a power black-out, International Conference on Electrical, Computer Communications and Mechatronics Engineering-ICECCME, pp. 16-18, 2022.

[31]. Fita N.D., Obretenova M.I., Pasculescu D., Tatar A., Popescu F.G., Lazar T., Structure and analysis of the power subsector within the national energy sector on ensuring and stability of energy security, Annals of „Constantin Brâncuși” University of Târgu Jiu, ENGINEERING SERIES, Issue 2/2022, pp.177-186, 2022.

This article was reviewed and accepted for presentation and publication within the 11th edition of the International Multidisciplinary Symposium "UNIVERSITARIA SIMPRO 2024".

HARDWARE AND SOFTWARE USED FOR THE STUDY OF ANGULAR MOTION BY REMOTE CONTROL

NICOLAE PATRASCOIU¹

Abstract: This work is part of a project that includes methods for studying automation elements' functionality. From this project, I chose to present, in this paper, the hardware and software structure used for the study of angular motion. The generation of movement in the sense of controlling the spinning direction and amplitude is achieved by a DC motor. The Discovery Studio module, a Digilent product, controls the motor through the L298N DC motor driver module. The movement parameters are measured through an experimental incremental transducer through a National Instruments data acquisition module. The software created in LabVIEW allows both the control of the motor and the determination of the spinning direction and amplitude. The user has an interface with movement control elements and visualization of measurement results, for various operating conditions.

Key words: incremental sensors, DC motor control, LabVIEW, DiscoveryStudio, remote control

1. INTRODUCTION

The development of virtual tools like virtual instruments that can be used in education processes or in research activities offer a number of advantages over hardware structures based on measuring devices with manual data logging, including:

- the generation of signals with very precise shapes and amplitudes and at very well-determined moments of time,
- automatic data retrieval and processing,
- graphical interfaces that allow users to effectively control the computer or device they interact with,
- virtual instruments through their interfaces offer the user:
 - ✓ clarity, that's means recognizable features and elements that are intuitive to interact with,
 - ✓ consistency which helps the users feel at ease and in control of their actions,
 - ✓ accessibility which makes all users feel comfortable, at ease, and in control when using a software product.

¹ Ph.D. Eng., University of Petroșani, nicolaepatrascoiu@upet.ro

LabView is a graphical programming language that allows users in various fields to develop and implement interactive programs that will enable the acquisition of data from different technical equipment and also analysis and data processing and then displaying the obtained results in different forms like reports, graphs, or charts. The LabView programming environment provides the user with many functions, programming structures, libraries, and routines that allow the creation of virtual tools that can be used in many branches of engineering [1]. The facilities offered by the LabVIEW software by generating virtual laboratory instruments along with the corresponding hardware enable the development of student's abilities to conduct experiments with dynamic systems to study their responses [2], [3].

Motion can be defined as a physical quantity of a mechanical change that can provide information about the position of a material point or mobile against a reference system. Quantities derived from this, which may be considered, are: position, distance or speed [4]. In many applications, all these quantities are considered vectors, so measuring both size and direction for this quantity is necessary.

The usual procedure for obtaining the size of these quantities is by counting the pulses acquired from an incremental sensor that generates a pulse train [5]. The same incremental sensors can be used to detect the direction of movement if it provides two trains of pulses shifted by one quarter of the period, in which case it is named quadrature encoder. A quadrature encoder can have up to three channels – channels A, B, and Z.

In order to understand the operation and use of incremental sensors, it is necessary to use a rotation mechanism whose angular displacement and rotation speed can be set. The DC motor can fulfill this role if it is possible to control the supply voltage.

2. THE HARDWARE STRUCTURE OF THE LABORATORY STAND

The purpose of this paper is to present the physical structure and virtual instrument that allows automatic control and acquisition from the experiments in the study of angular motion. This hardware structure and virtual instrument are part of interactive and low-cost tools used for students' training systems.

The following elements were used to create the laboratory stand:

1. DC motor $U_n=9V$;
2. Interface L298N DC Motor Driver Module;
3. Incremental encoder with 4 slits and $D=80$ mm, necessary choice to be able to visually observe the rotation movement and its sense;
4. Two transmissive optical sensors with phototransistor output TCST1103 (Vishay Semiconductors);
5. A trigger-type signal adapter module made with the Hex Non-Inverting Buffer CD4050 integrated circuit;
6. Analog Discovery Studio module (Digilent);
7. USB-6008 data acquisition module (National Instruments);

The block diagram of the entire system is shown in Figure 1

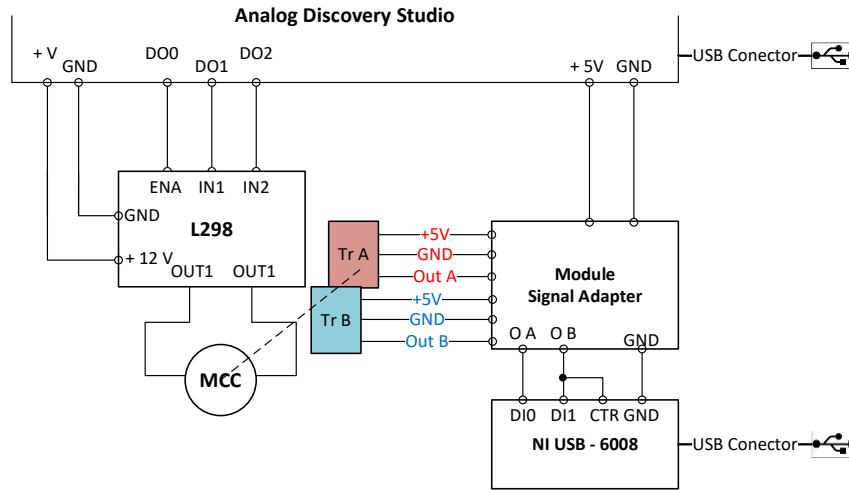


Fig.1. Laboratory stand block diagram

The elements component of the of this system are arranged like shown in Figure 2. The generation of the values of the rotation speed as well as its direction is carried out by means of the Analog Discovery Studio and L298N DC Motor Driver modules respectively.

The Analog Discovery Studio is a fully functional, portable test and measurement device that can turn any cross-functional space into a pop-up electronics laboratory. This equipment includes the Power Suppliers and other 13 instruments including 16 channels digital I/O lines with input logic standard: LVCMOS (1.8/3.3 V, 5 V tolerant) and output logic standard: LVCMOS (3.3 V, 12 mA). From this device is used the Variable Power Supply for which the generation, with a resolution of 12 bits, of a programmable voltage in the range (0 ... 5) V, the 5 V Fixed Power Supply, and digital channels D0 to D2 like output lines [6].

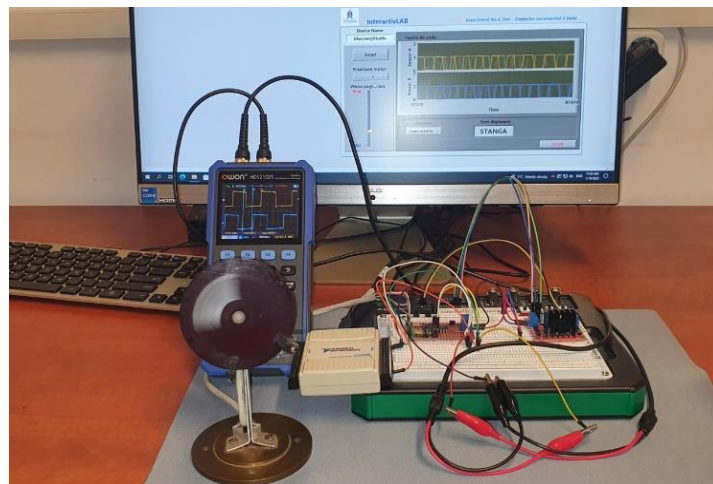


Fig.2. Setting up the laboratory stand

The Variable Power Supply and the three digital channels are used to control the angular movement of the DC motor through the L298N DC Motor Driver. Thus, the output lines DO1 and DO2 are connected to motor A input pins IN1 and IN2 which are used to control the spinning direction of the DC motor. Line DO0 is connected to the ENA pin that enables the PWM signal for the DC motor. The Variable Power Supply is connected to input from DC power Source at the L298N module and the 5 V Fixed Power Supply is used to supply power for the switching logic circuitry inside L298N integrated circuit.

The DC motor is connected to the output OUT1 and OUT2 pins.

The two transmissive optical sensors TrA and TrB with phototransistor output TCST1103 are mechanically fixed relative to the incremental encoder such the output signals of these must be two pulse trains Out A and Out B in quadrature. By using a relatively large encoder disk together with the two optical sensors, students are given the opportunity to observe and understand the operation of incremental rotary transducers as well.

The Out A and Out B signals taken from the transducers are processed in order to improve the transitions between their logical levels by using two gates from the CD4050B CMOS Noninverting Buffer and Converter. This operation is performed by the Signal Adapter Module.

The two pulse trains Out A and Out B in quadrature are used to measure the DC motor spinning value and direction. These signals are connected to the digital I/O lines and also to the counter input line on the N USB-6008 data acquisition module. Thus, are used the digital inputs DI0 and DI1 for the spinning direction identification, and the PFI0 for spinning value measurement.

The NI USB-6008 is a low-cost, bus-powered, all-in-one data acquisition (DAQ) module with a USB connection. Along with the functionalities related to the acquisition or generation of voltages, as analog quantities, this module also includes two ports with 12 digital I/O lines and a 32-bit counter. Each of these digital channels can be individually programmed as input or output and is compatible with TTL, LVTTTL, and CMOS logic levels. The counter is a 32-bit resolution up-counter, which counts the falling-edges of pulses with frequencies up to 5 Mhz [7].

3. VIRTUAL INSTRUMENT IMPLEMENTATION

The virtual instrument that is proposed in this paper is built in the LabVIEW graphical programming environment. This virtual instrument consists of the front panel which is the user interface and the diagram block which is the actual program for controlling the laboratory stand.

3.1 Front panels of the virtual instrument

The front panel of the virtual instrument, shown in Figure 3 include two sections.

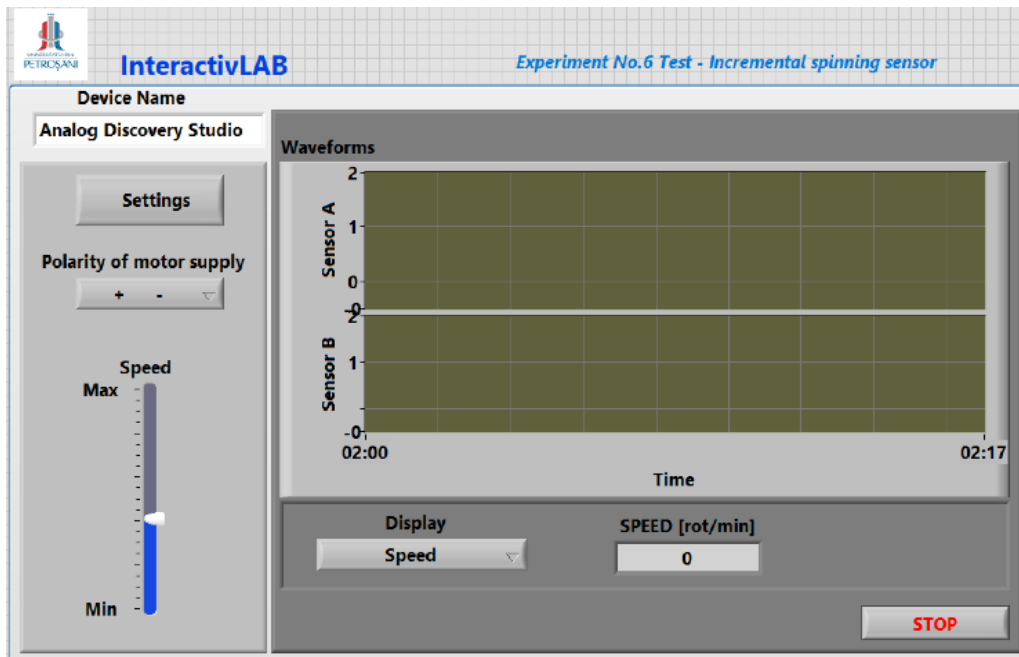


Fig.3. Front panel of the virtual instrument

The first section is used to set the movement parameters, thus from the controls here the user can set the polarity (Polarity of the motor supply) and the value (Speed) of the power supply for the DC motors. For both input type elements that generate the rotation movement (polarity of the DC motor supply voltage and its PWM control) the parameters used to set this movement are not measured and are not available on the front panel to the user.

The second section is used to display the waveforms of the Out A and Out B signals taken from the transducers and also to display direction of motor spinning or speed value. The information that will be displayed about spinning direction or speed (in rev/min) can be selected through the selector control, Display, placed on this section.

3.2. Block diagrams of the virtual instrument

The block diagram of the virtual instrument, which represents its operating program, consists of two While loops that work independently, their only common element being the STOP command to stop the program. Block diagram used to read electrical values.

The loop used to control the movement of the DC motor is shown in Figure 4.

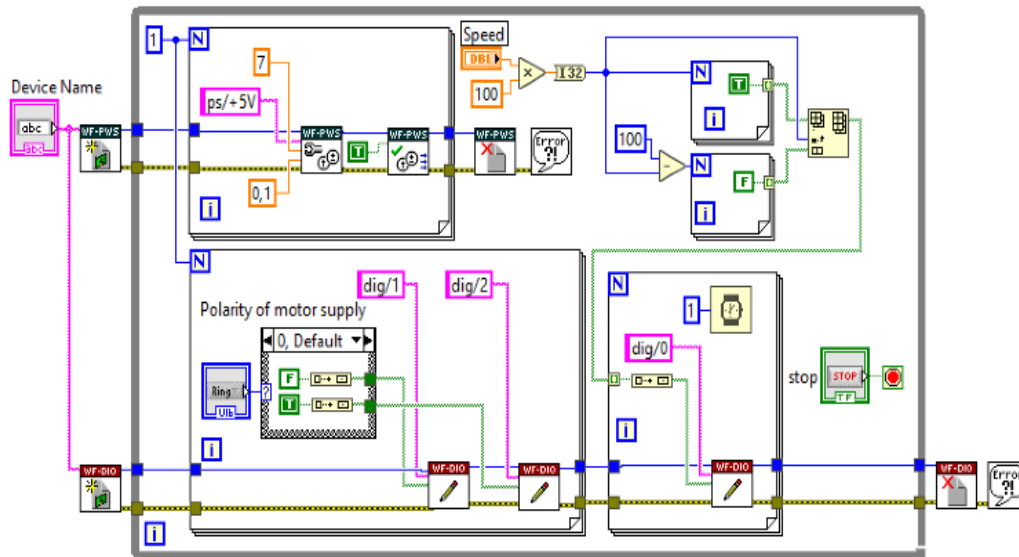


Fig4. The part of the block diagram used for control

This contains, in addition to typical LabVIEW programming functions and structures, functions from the Digilent WF VIs library used for DC motor power supply and setting its spinning direction.

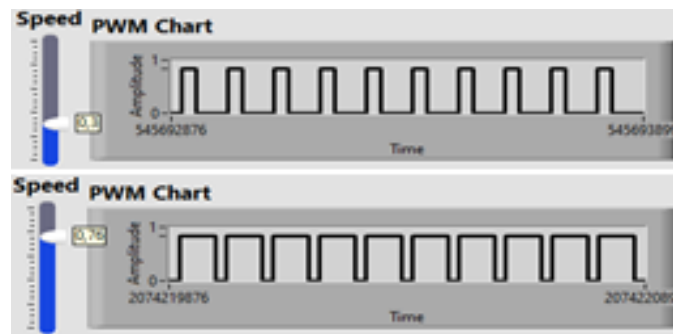


Fig.5. PWM waveform generation

Thus, the function DWF PS Configure Voltage Output is used to configure a voltage output on the +5 channel for a max 7 V voltage and max 100 mA current. The validation of this function is performed through the DWF PS Enable function which enables or disables all outputs on all channels of the instrument. By means of two For loops whose number of cycles is controlled by the Speed control, a PWM type waveform is generated, Figure 5. The width of the pulses is determined in relation to the unitary value of 100% by setting the value N and respectively 100-N of the number of loops of the two For structures.

The PWM signal is obtained at the digital output DO0 of the Analog Discovery Studio module and it is applied to the ENA input of the L298N driver and for this the DWF Dig Write function is used. This function writes data to the specified lines.

Bidirectional control of the motor is established by the logical combination of inputs IN1 and IN2 of the L298N as follows [8]:

Table 1. L298 motor control

	Inputs	Function
ENA=H	IN1=H ; IN2=L	Forward
	IN1=L ; IN2=H	Reverse
	IN1= IN2	Fast motor stop
ENA=L	IN1=x; IN2=x	Free running

The logic levels are transmitted, by selection with the Polarity of motor supply control, to the outputs DO1 and DO2 of the Analog Discovery module using the same DWF Dig Write function with the arguments dig/1 and dig/2.

The second While loop is used to display the spinning direction or the speed of rotation. The choice of one of the two options is made from the front panel through the Display control and a Case structure.

In the case of selecting the display of the direction of rotation, which corresponds to case 0 which is shown in Figure 6, the signals from the DI0 and DI1 inputs of port 0 of the NI USB-6008 low cost data acquisition module are read through the DAQ Assistant function.

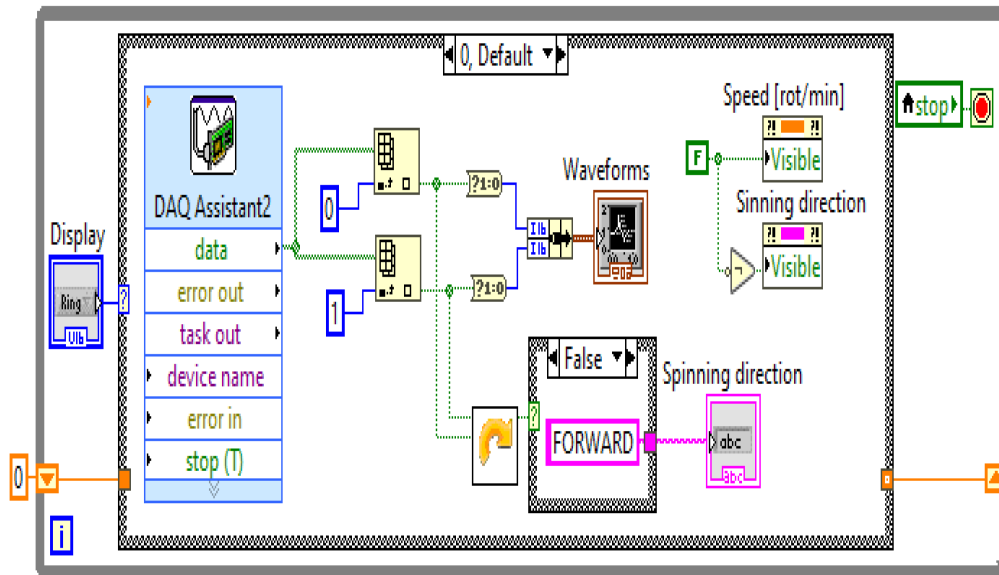


Fig.6. The part of the block diagram used for display spinning direction

These signals are displayed in their dynamic development on the Waveforms chart indicator. These also represent the input variables of a SubVI which is a representation in LabVIEW of a sequential logic circuit through which the logic functions necessary to identify the spinning direction are implemented [9]. In Figure 7 is shown the logic configuration of this SubVI.

where N represents the counted number of pulses between two successive cycles of the While loop and the resolution is $PPR=4$.

Thus, the duration of the measurement is reduced to 250 msec, which means that the number N of pulses by multiplying by 60 will represent the rotation speed expressed in rev/min.

The simultaneous stopping of the two While loops and implicitly of the motor control program and measurement of the movement parameters is done by the STOP button on the front panel.

4. CONCLUSIONS

This paper presents one of the applications created in LabView that allows the realization of several experiments related to different topics from the educational plan of electrical engineering students. The other experiments are used to study force sensors (strain bridge) or temperature sensors (RTD, thermistor) or semiconductor devices like diode and transistor.

This laboratory stand and the experiment is used to verify the operation of both a direct current motor whose control is achieved through the rotor circuit and angular motion incremental transducers. Students are given the opportunity, on the one hand, to study the principles of control (direction and speed) of a direct current motor and, on the other hand, to study the operating principle of an incremental transducer.

The experiment benefits from its own command and control panel and both the hardware configuration and the virtual tool proposed in this work were made and tested in the laboratory.

I consider this application can be the starting point for creating a system based on virtual laboratories that can be accessed via an internet connection from anywhere in the world. In this sense, we intend to complete the tools created with G Web Development Software interfaces. The G Web programming environment helps programmers to create web-based user interfaces for test and measurement applications.

Acknowledgment

This work is part of the CNFIS-FDI-2022-0160 project which provides for the development of an interactive laboratory for the control through virtual instrumentation of the students' practical training activities.

REFERENCES

- [1]. **Pătrășcoiu N., Rus C., Negru N., Roșulescu C.**, *Using virtual instrumentation in the application study of electronic devices*, MATEC Web of Conferences, 2022.
- [2]. **Rana K.P.S, Vineet K.**, Mendiratta J., *An educational laboratory virtual instrumentation suite assisted experiment for studying fundamentals of series resistance–inductance–capacitance circuit*, European Journal of Engineering Education, Vol. 42, No. 6, pp. 1220-1239, 2017.
- [3]. **Magana A., Lovan J., Gomez R., Marulanda D., Dyke J.**, *Virtual, local and remote laboratories for conceptual understanding of dynamic systems*, The International Journal of Engineering Education, Vol. 33, No. 1, pp. 91-105, 2017.

- [4]. **Webster G.J.**, *The Measurement, Instrumentation and Sensors Handbook*, CRC Press LLC, 2000.
- [5]. **Bentley P.J.**, *Measurement Systems*, Fourth Edition, Pearson Prentice Hall, 2005.
- [6]. Digilent Reference, <https://digilent.com/reference/test-and-measurement/analog-discovery-studio/start>.
- [7]. National Instruments Corporation, *NI USB-6008/6009 User Guide and Specifications*, 2012, <https://www.ni.com/docs/en-US/bundle/usb-6008-6009-oem-features/resource/371728b.pdf>.
- [8]. Octopart, *Datasheet L298 DUAL FULL-BRIDGE DRIVER*, STMicroelectronics, 2000, <https://www.st.com/resource/en/datasheet/l298.pdf>.
- [9]. **Patrascoiu N., Poanta A., Tomus A., Sochirca B.**, *Virtual Instrumentation used for Displacement and Angular Speed*, International Journal of Circuits, Systems and Signal Processing, Vol. 5, Issue 1, pp. 168-175, 2011, <https://www.naun.org/main/NAUN/circuitssystemssignal/19-726.pdf>.

This article was reviewed and accepted for presentation and publication within the 11th edition of the International Multidisciplinary Symposium "UNIVERSITARIA SIMPRO 2024".

DEVELOPING A PROGRAMMABLE ELECTRONIC CIRCUIT FOR THE CONTROLLED IGNITION OF EXPLOSIVE MIXTURES

ZOLTAN VASS¹, MARIUS ȘUVAR², BOGDAN ȘIMON-MARINICĂ³,
LAURENȚIU MUNTEAN⁴

Abstract: The research performed in the domain of explosive gaseous mixtures, in particular of hydrogen-oxygen gaseous mixtures, is gaining ground due to their applications in various fields, such as power generation, propulsion systems and safety engineering. Due to the current realities of environmental and political considerations it is necessary to transition away from conventional carbon based sources of energy, to more clean sources of energy. In order to accomplish this goal, research is needed in the field of clean energy, in particular in the research of hydrogen. These research activities are performed under a strict laboratory environment where the conditions and requirements of the ignition of these gaseous mixtures are critical. In this context, the design and development of programmable electronic control circuit for the controlled ignition of explosive gaseous mixtures represents a significant advance. The objective is to create a system that not only is reliable, but also cost-effective and simple to use. In this paper we present a design and development of a digital electronic circuit.

Key words: hydrogen, mixture, ignition, control circuit.

1. INTRODUCTION

With the beginning of the first industrial revolution, which necessitated the rapid extraction and burning of fossil fuels, which in turn lead to the release of greenhouse gases into the atmosphere in quantities never seen before, global temperatures begin to rise, leading to increase in a number of negative effects, such as drought, high intensity storms, rise of the sea level, melting of glaciers. In order to mitigate these negative effects of global warming it is necessary to transition the economy from the consumption of fossil fuels to other, more cleaner forms of energy.

Energy is the basic element for human survival and human consumption of energy has increased dramatically due to the rapid development and progress of

¹ Sc. Res., Ph.D.Eng., INCD-INSEMEX Petroșani, vass.zoltan@insemex.ro

² Sc. Res., Ph.D.Eng., INCD-INSEMEX Petroșani, marius.suvar@insemex.ro

³ Sc. Res., Ph.D.Eng., INCD-INSEMEX Petroșani, bogdan.simon@insemex.ro

⁴ Sc. Res., Ph.D.Eng., INCD-INSEMEX Petroșani, laurentiu.muntean@insemex.ro

society. In particular, the consumption of large amounts of non renewable fossil energy has aggravated environmental degradation and energy crisis. Therefore, the development and construction of a clean, efficient, and renew-able new energy carrier is of great significance to achieving the goal of carbon neutrality. As a globally recognized clean energy carrier, hydrogen energy has the advantages of wide sources, high energy density, and stable properties at room temperature [1].

In the current political, social and political climate, where the governments of the countries of the world promote clean energy sources, hydrogen is one of the alternatives proposed to replace fossil fuels. Due to the different thermal, chemical properties of hydrogen, compared to fossil fuels, it is necessary to conduct research to determine the behavior and potential risks the use of hydrogen presents in the ordinary activities.

In the research on gas explosions, the emphasis has been and continues to be primarily on physical experiments conducted on various scaled-down models. Building models at actual size is often a resource-intensive task in terms of materials, time, and human resources. The rapid advancement of computational techniques has allowed, among other things, the transfer of gas explosion research into the virtual environment. For validating computerized simulations of this kind, physical experiments and specialized literature are still considered fundamental. However, one of the challenges posed by the virtualization process is the limitation of conducting simulations in fully or partially enclosed spaces, under initially imposed conditions, without the possibility of dynamically modifying these conditions based on the development of over-pressures generated by the virtual explosion. This paper details a computerized experiment where the boundary conditions were successfully transformed into predefined pressure threshold surfaces, transitioning from rigid surfaces to surfaces capable of releasing the over-pressures developed in fully or partially enclosed spaces. This approach aligns the results of these simulations with the real dynamic effects of gas explosion events [1].

The dangers associated with hydrogen mainly come from its wide flammability range, it's extremely fast burning rate (having much more aggressive explosive properties than methane gas) and the considerable amount of energy released when it burns or explode. The development of new applications that use hydrogen as clean energy is constantly increasing, thus, hydrogen can be used on a large scale. This paper presents the use of computational fluid dynamics techniques, regarding the linear propagation of the explosion of air and hydrogen mixture in closed spaces, the main purpose being the determination of the over-pressures to which a test stand of this processes is subjected [2].

These research activities are performed under a strict laboratory environment where the conditions and requirements of the ignition of these gaseous mixtures are critical. In this context, the design and development of programmable electronic control circuit for the controlled ignition of explosive gaseous mixtures represents a significant advance. The objective is to create a system that not only is reliable, but also cost-effective and simple to use [3].

Hydrogen will become a key player in transitioning toward a net-zero energy system. However, a clear pathway toward a unified European hydrogen infrastructure to support the rapid scale up of hydrogen production is still under discussion. This

study explores plausible pathways using a fully sector-coupled energy system model [4].

Hydrogen together with methane, is one of the most common gaseous fuels that also exist in nature as the main part of the natural gas, the flammable part of bio-gas or as part of the reaction products from biomass pyrolysis. In this respect, the bio-gas and biomass installations are always subjected to explosion hazards due to methane. Simple methods for evaluating the explosion hazards are of great importance, at least in the preliminary stage [5].

2. COMPONENT ELEMENTS OF THE CIRCUIT

Due to the type of laboratory experiment performed, which consists of igniting gaseous mixtures of hydrogen and oxygen, it is necessary to employ the use of an electronic circuit that can provide a controlled and reliable way of igniting of these gaseous mixtures [6].

This electronic device is a digital programmable electronic circuit, with a custom instruction set.

The circuit is composed of multiple modules. These communicate with each other using a central bus.

Table 1. Component elements of the circuit

1	Program memory
2	Instruction Decoder
3	Arithmetic and Logic Unit
4	Register file
5	Program Counter
6	IO Module

The program memory holds the instructions than will be executed by the electronic circuit.

There are two types of memory available. volatile memory which will lose all data when the memory is disconnected from the power source, and non-volatile memory, which will preserve the data stored in it even when is disconnected from the power source.

The instruction decoder is responsible with decomposing the instructions read from program memory and generating control signals for enable or disable different components of the circuit. This is necessary in order to avoid conflicting scenarios that could rise during the functioning of the electronic circuit.

Every computer has a word length that is characteristic of that machine. A computer's word length is usually determined by the size of its internal storage elements and interconnecting paths (referred to as buses), for example, a computer whose registers and buses can store and transfer 8 to 32 bits. The characteristic 8-bit field is referred to as a byte. Each operation that the processor can perform is identified by a unique binary number known as an instruction code or operation code (OP code). An 8-bit word used as an instruction code can distinguish among 256 alternative actions, more than adequate for most processors.

The processor fetches an instruction in two distinct operations. In the first, it transmits the address in its program counter to the memory. In the second, the memory returns the addressed byte to the processor. The CPU stores this instruction byte in a register known as the instruction register and uses it to direct activities during the remainder of the instruction execution. The mechanism by which the processor translates an instruction code into specific processing actions requires more elaboration than we can afford here. The data stored in the instruction register can be decoded and used to selectively activate one of a number of output lines, in this case up to 256 lines. Each line represents a set of activities associated with execution of a particular instruction code. The enabled line can be combined coincidentally with selected timing pulses, to develop electrical signals that can then be used to initiate specific actions. This translation of code into action is performed by the instruction decoder and by the associated control circuitry [7].

In computing, an arithmetic logic unit is a combinatorial digital circuit that performs arithmetic and bit-wise operations on integer binary numbers. This is in contrast to a floating-point unit, which operates on floating point numbers. It is a fundamental building block of many types of computing circuits, including the central processing unit of computers, floating-point unit, and graphics processing units.

The inputs to an Arithmetic and Logic Unit are the data to be operated on, called operands, and a code indicating the operation to be performed; the Arithmetic and Logic Unit's output is the result of the performed operation. In many designs, the Arithmetic and Logic Unit also has status inputs or outputs, or both, which convey information about a previous operation or the current operation, respectively, between the Arithmetic and Logic Unit and external status registers [8].

The arithmetic and logic unit is responsible with performing logic and arithmetic operations such as logic operations and arithmetic operations. Taking into account the purpose and the intended use of this electronic circuit, the implementation of logic operations was deemed as not necessary.

The register file is the component part of the electronic circuit that consists of a number of fast memory modules, which are used to store data. The data stored in these memory modules can be accessed by using control signals that allow us to use one or multiple registers simultaneously.

A register file is an array of processor registers in a central processing unit. The instruction set architecture of a central processing unit will almost always define a set of registers which are used to stage data between memory and the functional units on the chip. The register file is part of the architecture and visible to the programmer.

In simpler central processing units, these architectural registers correspond one-for-one to the entries in a physical register file within the central processing unit. More complicated processors use register renaming, so that the mapping of which physical entry stores a particular architectural register changes dynamically during execution.

Modern integrated circuit-based register files are usually implemented by way of fast static RAMs with multiple ports. Such RAM memories are distinguished by having dedicated read and write ports, whereas ordinary multi-ported S-RAM memory will usually read and write through the same ports. Register banking is the method of

using a single name to access multiple different physical registers depending on the operating mode [9].

The program counter is a component part of the electronic circuit which ensures that the instructions are loaded from program memory into the decoder sequentially. This module is also responsible for the execution of jump instructions, using a number of control signals provided by the decoder module.

The output module is used to allow for the circuit to communicate with other devices. The output module, is designed in such a way that allow multiple ignition devices to be controlled simultaneously.

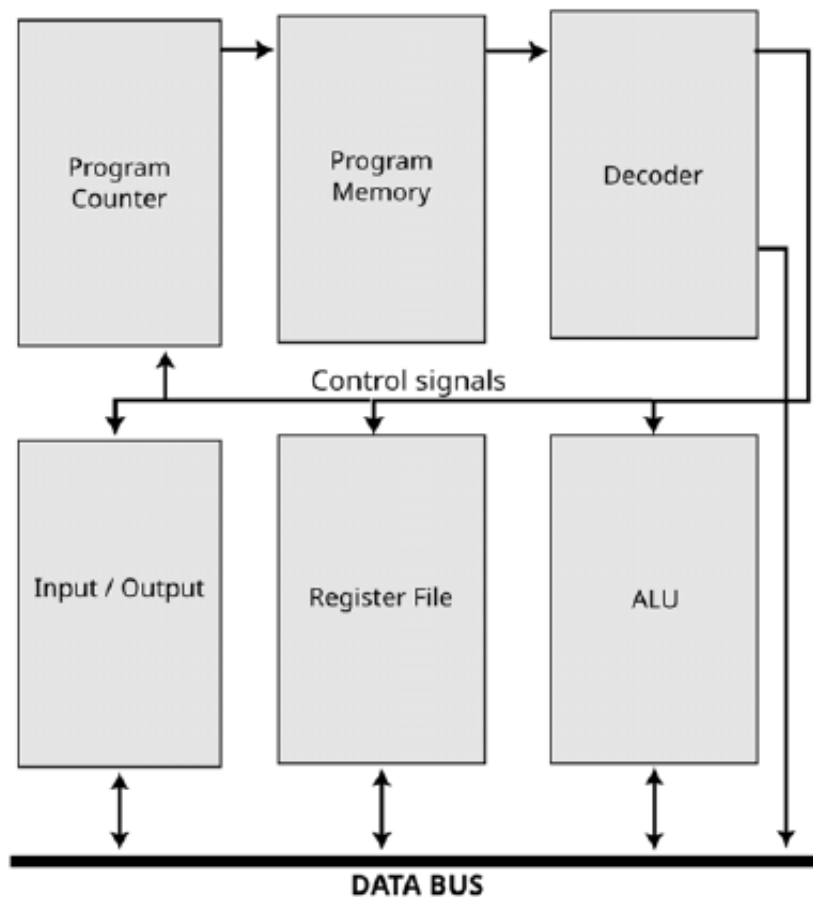


Fig. 1. Block diagram of the electronic circuit

The Input / Output module of can be used to control a number if external devices, such as:

- Data acquisition systems: i/o module can be used in data acquisition systems to acquire and process data from various sensors and input devices. the i/o processor can handle high-speed data transfer and perform real-time processing of the acquired data.

- Industrial control systems: i/o module can be used in industrial control systems to interface with various control devices and sensors. the i/o processor can provide precise timing and control signals, and can also perform local processing of the input data.

- Multimedia applications: i/o module can be used in multimedia applications to handle the input and output of multimedia data, such as audio and video. the i/o processor can perform real-time processing of multimedia data, including decoding, encoding, and compression.

- Network communication systems: i/o module can be used in network communication systems to handle the input and output of data packets. the i/o processor can perform packet routing, filtering, and processing, and can also perform encryption and decryption of the data.

- Storage systems: i/o processors can be used in storage systems to handle the input and output of data to and from storage devices. the i/o processor can handle high-speed data transfer and perform data caching and pre-fetching operations. [10]

3. INSTRUCTION SET

In order to be useful, a programmable electronic circuit must have a set of instructions that will allow to perform useful tasks.

The number of instructions a processor is capable of executing, varies depending on the environment in which this processor will be used. Therefore if the programmable electronic circuit is used in a special circumstance that require only a limited functionality, it is not necessary to implement a full set of instructions. However if the programmable circuit is used in a more complex environment, implementing a full set of instructions may be necessary.

All processors carry out their require operations by executing sequences of instructions. Each instruction defines a simple operation, for example, simple Arithmetic and Logic Unit operation, data access to the memory system, program branch operation, etc.

For the processor, it takes instructions in form of binary code and decodes them in internal hardware (instruction decoder), then passes on the information about the decoded instruction to the execution stage. In simple processor designs, for minimum the following types of instructions are required:

- Data processing(arithmetic and / or logic operations);
- Memory access operations(read from memory, write to memory);
- Program flow control instructions(branches, conditional jump instructions, function calls);
- Access to registers;
- Other operations [11].

In our case, the programmable circuit is used in a laboratory setup, to control the ignition of explosive gaseous mixtures, therefore it is not necessary for us to implement a large set of instructions.

In the table below are listed all the instructions that our programmable circuit can execute.

Table 2. List of instructions of the programmable circuit

Opcode	Instruction name:	Instruction binary map
00000	NOP	0000000000000000
11111	HLT	-----00000
00001	JR	mmmmmmmm---00000
00010	JA	mmmmmmmm---00000
00011	JC	mmmmmmmmfffooooo
00011	JZ	mmmmmmmmfffooooo
00011	JE	mmmmmmmmfffooooo
00011	JL	mmmmmmmmfffooooo
00011	JG	mmmmmmmmfffooooo
01001	ADD	--bbbaadddooooo
11001	SUB	--bbbaadddooooo
01011	INC	-----aaadddooooo
11011	DEC	-----aaadddooooo
11000	CMP	--bbbaaa---00000
10110	MOV	-----aaadddooooo
10101	LDI	iiiiiiiddooooo

Legend:

o – opcode

m – memory address

a – first operand register address

b – second operand register address

d – destination register address

i – immediate value

f – function select

3.1. NOP instruction

The purpose NOP instruction its to allow for the processor to pause execution for a limited amount of time. This time can be controlled by executing one or more NOP instructions sequentially.

Table 3. Binary representation of the NOP instruction

15	5	4	0
		0	0
		0	0
		0	0
		0	0

The fields from 0 to 4 is used to encode the binary representation of the NOP instruction. As it can be observed from the table above, this instruction is encoded with zero values.

The rest of the fields from 5 to 15 are unused.

3.2. HLT instruction

The The purpose of the HLT (halt) instruction is to terminate execution of the program. This instruction is very important. Without this instruction the programmable circuit will continue to run out of control, which could lead to errors.

Table 4. Binary representation of the HLT instruction

15	5	4	0
		1	1

From the table above, the binary encoding of the HLT instruction can be observed.

The fields ranging from 0 to 4 is used to encode the binary representation of the HLT instruction.

The fields from 5 to 15 are unused.

3.3. JUMP instructions

Our programmable circuit is capable to execute special instructions that allow it to load instructions from the program memory from any arbitrary memory address. These instructions can be used to provide a greater flexibility to our programmable circuit. Our circuit that we develop is capable of a number of seven jump instruction: relative jump, absolute jump and five conditional jump instructions.

In the table below are presented the binary representation of the jump instructions.

Table 5. Binary representation of the relative and absolute jump instruction

15	8	7	5	4	0
m m m m m m m m	f f f	o o o o o			

From From table 5 above can be observed the binary encoding of the jump instructions.

The fields ranging from 0 to 4 is reserved for encoding of the jump instruction.

The fields ranging from 5 to 7 is reserved to encode the type of the jump instruction.

The fiends ranging from 8 to 15 is reserved to encode the memory location of the jump instruction.

It can be observed from the above table that in fact the HLT instruction is a special case of the absolute jump instruction.

3.4. Arithmetic instructions

Arithmetic instructions are an important part of the functioning of the programmable circuit that we design. These instruction allow us to perform simple arithmetic instructions such ad adding or subtracting two values, incrementing or decrementing a value, and store the result in a specified registry location.

Table 6. Binary representation of the arithmetic instructions

Table 3: Binary Representation of the arithmetic instructions																									
15		13			11			10			8			7			5			4			0		
-	-	b	b	b	a	a	a	d	d	d	o	o	o	o	o	o	o	o	o	o	o	o	o		

In table above we can observe the binary encoding of the addition and subtract instructions.

The fields ranging from 0 to 4 is used to encode the binary code of the instruction.

The fields ranging from 5 to 7 id used to encode the address of the registry where the result of the instruction will be stored.

The fields ranging from 8 to 10 is used to encode the address of the registry where the value of the first operand is stored.

The fields ranging from 11 to 13 is used to encode the address of the registry where the value of the second operand is stored.

Table 7. Binary representation of the arithmetic instructions

15	10	8	7	5	4	0
	a	a	a	d	d	d

In table above we can observe the binary encoding of the increment and decrement instructions.

The fields ranging from 0 to 4 is used to encode the binary code of the instruction.

The fields ranging from 5 to 7 id used to encode the address of the registry where the result of the instruction will be stored.

The fields ranging from 8 to 10 is used to encode the address of the registry where the value of the operand is stored.

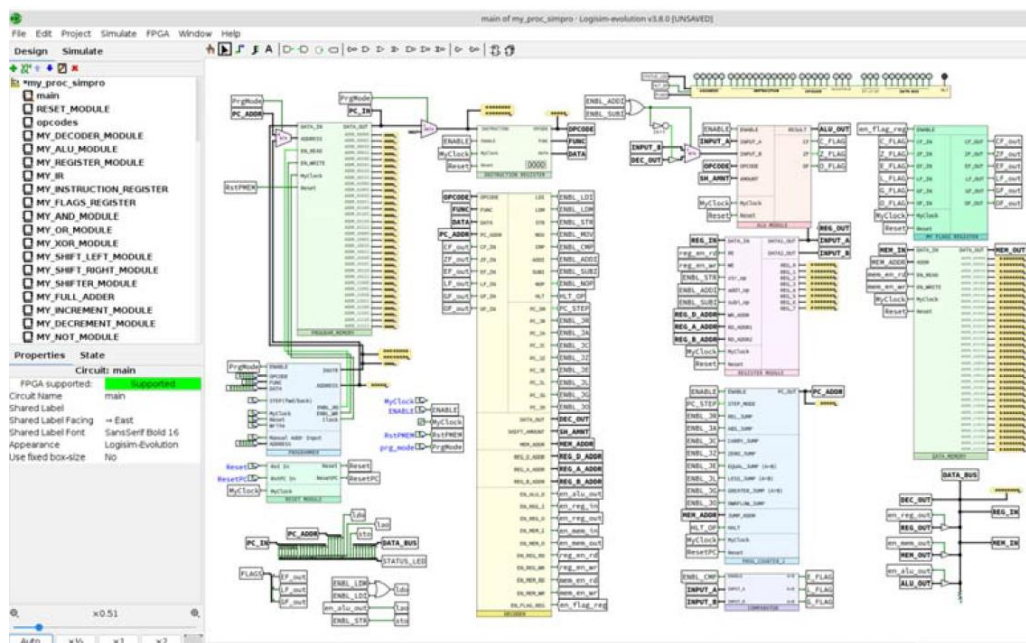


Fig. 2. Screen capture of the simulation of the electronic circuit

This work was carried out through the "Nucleu" Program within the National Plan for Research, Development and Innovation 2022-2027, with the support of the Romanian Ministry of Research, Innovation and Digitalization, project no PN-23 32 02 01., title: Development of the knowledge level of the explosion parameters of gaseous and hybrid mixtures based on hydrogen, involved in the processes of obtaining and storage in order to reduce the explosion risk.

4. CONCLUSIONS

The development of a programmable electronic circuit, for the ignition of explosive gaseous mixtures, can lead to an increased accuracy of the experiments, and also to the improvement on the field of safety. Using a programmable electronic circuit allow us to use ignition patterns that are unavailable or are difficult to implement using traditional technologies.

REFERENCES

- [1]. Long J.J., Wu H-C., Liu Y-T., Ding Y-Y., Yao Q-L., Metin O., Lu Z-H., *Hydrogen production from chemical hydrogen storage materials over copper-based catalysts*, Youke Publishing Co., Ltd., 2024.
- [2]. Florea G., Petrilean D., *Computational Simulation of Methane Ignition in Enclosed Spaces*. Mining Revue, 30(1), pp. 58-67., 2024.
- [3]. Şimon-Marinică A.B., Manea F., Vass Z., Păsculescu V.M., *Virtual experiments about hydrogen explosions with linear propagation*, MATEC Web of Conferences 2024.
- [4]. Şimon-Marinică A.B., Manea F., Gaman G.A., s.a. *Development of a Programmable System Used for the Preparation of a Mixture of Flammable/Explosive Gases*. Automation 5, pp. 246 -258, 2024.
- [5]. Kountouris I., B Ramstoft R., Theis Madsen T., Gea-Bermúdez J., s.a. *A unified European hydrogen infrastructure planning to support the rapid scale-up of hydrogen production*, Nature Communications, vol. 15, 2024.
- [6]. Prodan M., Ghiciei E., Laszlo R., s.a. *Experimental and Numerical Study of Ignition and Flame Propagation for Methane–Air Mixtures in Small Vessels*, MDPI, 2021.
- [7]. Samuel C. L., *Encyclopedia of Physical Science and Technology*, Third Edition, 2003.
- [8]. https://en.wikipedia.org/wiki/Arithmetic_logic_unit
- [9]. https://en.wikipedia.org/wiki/Register_file
- [10]. <https://www.geeksforgeeks.org/introduction-of-input-output-processor/>
- [11]. Yiu J., *The Definitive Guide to Arm® Cortex®-M0 and Cortex-M0+ Processors* (Second Edition), 2015.
- [12]. Malvino A. P., Ph.D. Jerald A. Brown – *Digital Computer Electronics* – 3rd Edition, 1994.

This article was reviewed and accepted for presentation and publication within the 11th edition of the International Multidisciplinary Symposium "UNIVERSITARIA SIMPRO 2024".

ENERGY CONSUMPTION AND RESOURCE ALLOCATION MADE MORE EFFICIENT THROUGH ARTIFICIAL INTELLIGENCE: AI-DRIVEN DESIGN OPTIMIZATION FOR HVAC (HEATING, VENTILATION, AND AIR CONDITIONING) SYSTEM

MARIA-ISABELA GHICAJANU (CAȘOTĂ)¹,
DAN CODRUȚ PETRILEAN²

Abstract: In contemporary industrial and commercial settings, Heating, Ventilation, and Air Conditioning (HVAC) systems are critical for maintaining optimal indoor environments. However, the efficient operation of these systems is often challenged by varying external and internal conditions, leading to suboptimal energy consumption and increased operational costs.

This paper explores the integration of Artificial Intelligence (AI) to enhance the performance and efficiency of HVAC systems. Using Brain.js, a JavaScript-based neural network library, we train a model using multiple input parameters, including indoor temperature, outdoor temperature, humidity, airflow rate, operating hours, and occupancy levels, to predict optimal setpoints and energy consumption.

To facilitate practical application and user interaction, I developed a Vue.js-based web interface. This interface allows users to input real-time environmental and operational data, which is then processed by the trained neural network to provide actionable predictions for optimizing HVAC performance.

Future work will focus on enhancing the model's accuracy by incorporating additional data sources, such as weather forecasts, real-time energy prices, and more occupancy data. I also plan to implement adaptive learning algorithms to allow the system to continuously improve its predictions based on new data.

Furthermore, expanding the system's capabilities to include predictive maintenance alerts and integrating with IoT sensors for more precise data collection may be key areas of development. By pursuing these improvements, I aim to create a more robust, intelligent, and comprehensive solution for HVAC system optimization, ultimately contributing to smarter and more sustainable building management practices.

Key words: Artificial Intelligence, HVAC, predictive, improvement, intelligence, system optimization, programming, data modelling, energy saving.

¹ Ph.D., Student Eng., ghicajanumaria@gmail.com

² Ph.D., Eng.

1. INTRODUCTION

The findings indicate that AI-driven optimization can significantly enhance the efficiency of HVAC systems, leading to substantial energy savings and improved environmental sustainability. The user-friendly interface ensures ease of use, enabling facility managers and operators to make informed decisions in real time [8], [10], [12], [15], [18].

It is obvious that carbon neutrality has become the most important issue and challenge of this century for humanity to respond to climate change.

However, the global target for greenhouse gas emissions commitments would need to be six times higher to keep the global temperature rise below 2°C above pre-industrial levels and seven times higher to limit warming to 1.5°C. This points to failure to respond to extreme weather and climate change as the greatest risk to humanity [1], [3], [14], [16], [22].

Insufficient global participation and carbon price signals are currently the most pressing challenges in the global response to climate change.

Thus, broadening participation and strengthening carbon price signals are crucial tasks for addressing climate change.

2. ABOUT HVAC

The title is set in bold 14 pt Times New Roman (TNR), centered. First letter of the title should be capitalised with the rest in lower case. You should leave 2 space (12 pt) below the title.

Heating, Ventilation, and Air Conditioning (HVAC) systems are essential for keeping us comfortable and healthy every day. With the latest advancements in technology, especially Artificial Intelligence (AI), the HVAC industry is seeing a major transformation. AI algorithms and machine learning are making HVAC systems smarter and more efficient, helping to optimize energy use [9], [11], [13], [17], [20].

Buildings are complicated and ever-changing environments where the thermal flow shifts due to varying occupancy and weather conditions. To optimize an HVAC system's performance, it's important to understand energy flow and predict its changes. The huge amount of data and complex equations needed to ensure optimal HVAC performance can be overwhelming for traditional energy management systems.

Did you know that HVAC systems are responsible for 40% of a building's energy use, with about 30% of that energy usually going to waste?

AI helps improve HVAC systems primarily through smart data analysis. These AI algorithms can sort and analyze tons of data to spot patterns, including temperature, humidity, occupancy, and weather conditions. Since energy costs fluctuate throughout the day, this is another factor considered. The data processing can happen on-site, in cloud data centers, near the system sensors, or using a mix of these methods [2], [5], [19], [21].

The following diagram shows the simplified setup of a typical HVAC system.

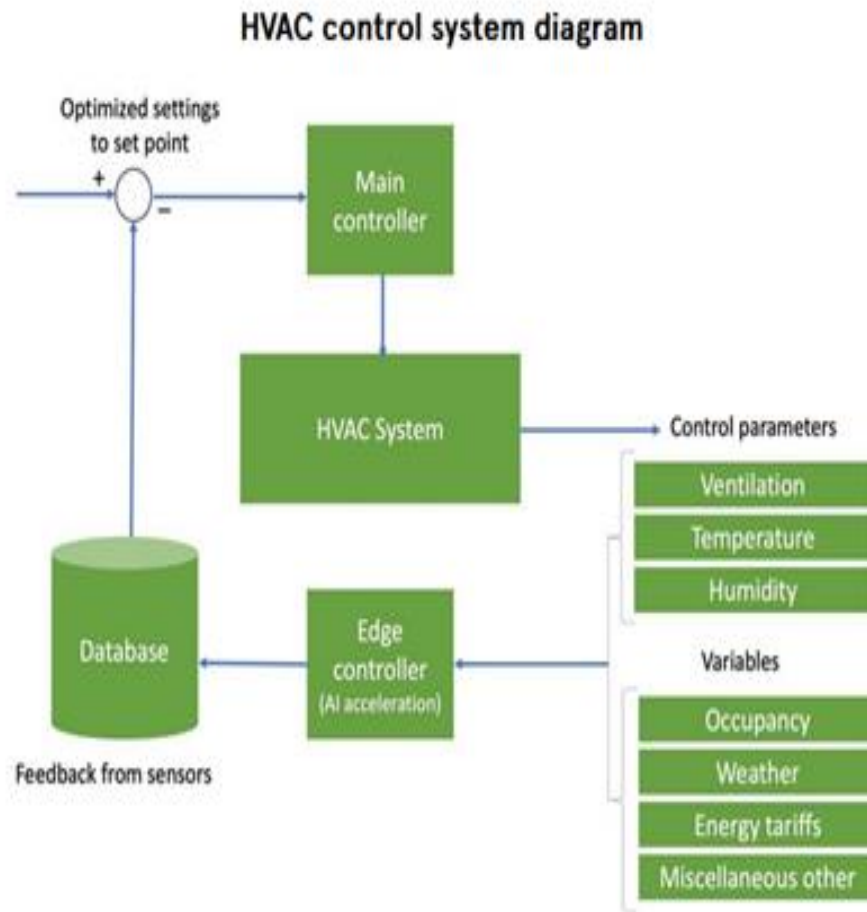


Fig.1. HVAC system

3. REAL-WORLD OUTCOMES OF AI IN HVAC IMPLEMENTATIONS

Although using AI in HVAC systems is still relatively new, there are already some real-world success stories.

For example, in 2020, Yokogawa used AI to cut energy use at its semiconductor sensor manufacturing plant in Miyada-mura, Japan. According to the International Society of Automation, the AI model used a reinforcement learning algorithm to run the HVAC system in the company's clean room fabrication environment.

The goal was to keep the environment tightly controlled while using as little energy as possible. Clean rooms at the facility used liquefied petroleum gas and accounted for 30% of the plant's total energy consumption. Yokogawa's AI system worked alongside the existing HVAC setup and conventional controls, requiring

minimal capital investment. After several months of self-driven model refinement, energy consumption dropped by 3.6%.

In another case, BrainBox AI, an HVAC company in Montreal, Canada, showcased its AI technology in a 509,612-square-foot shopping center. They converted the traditional HVAC system into an autonomous one using custom algorithms running in the cloud [4], [6], [7].

These algorithms combined building data collected over several weeks with external weather and energy-tariff data to optimize the system's operation. After a year, electricity savings reached 21% (205,214 kWh), with the AI ensuring the required building-zone temperatures were maintained while significantly reducing the HVAC equipment's runtimes.

4. HOW AI IS REVOLUTIONIZING HVAC SYSTEMS

Current HVAC systems are part of the problem. “Inefficient HVAC systems consume excessive energy, often derived from fossil fuels, to heat, cool, and ventilate assets, contributing to 4% of greenhouse gas emissions globally,” says Mateusz Lukasiewicz, digital projects manager at KEO International Consultants. This firm specializes in planning, architecture, engineering, sustainability, project and construction management, and digital advisory services. “The increased resource usage results in higher emissions of carbon dioxide, methane, chlorofluorocarbons, and other greenhouse gases, intensifying climate change and environmental degradation,” he explains.

As building managers look to improve HVAC performance with new technologies, integrating AI and machine learning is a promising approach. These advancements can optimize building operations and help address sustainability concerns.

4.1. Enhanced Comfort and Personalization

AI-powered HVAC systems can learn what people like and adjust settings accordingly. By analyzing patterns and user behavior, AI algorithms can create personalized comfort profiles, ensuring individualized temperature and airflow control in different areas of a building. This personalized approach enhances occupant comfort and satisfaction.

4.2. Energy Efficiency and Cost Savings

AI algorithms optimize HVAC system operation by continuously analyzing and adapting to real-time conditions. By considering factors like outdoor temperature, occupancy patterns, and thermal loads, AI-powered systems adjust settings dynamically, maximizing energy efficiency. This results in reduced energy consumption, lower utility bills, and a smaller carbon footprint.

4.3. Predictive Maintenance and Fault Detection

AI algorithms also enable predictive maintenance for HVAC systems. By analyzing performance data, AI can spot early signs of equipment wear or potential issues. This proactive approach allows for timely maintenance, reducing downtime and improving system reliability. AI also helps with fault detection and diagnostics, quickly identifying the root cause of problems for prompt resolution.

4.4. Smart Load Management and Demand Response

AI algorithms optimize energy usage by managing HVAC loads intelligently. During peak demand periods, AI-powered systems can automatically adjust temperature settings or activate load-shedding strategies to reduce energy consumption without compromising comfort. This smart load management helps stabilize the grid and lowers overall energy costs.

5. MACHINE LEARNING WITH BRAIN.JS

Machine learning is one of the hottest topics in the tech world right now. It is the science of making computers learn from data and perform tasks that normally require human intelligence, such as image recognition, natural language processing, recommendation systems, and more.

Brain.js is a JavaScript library that allows you to create and train neural networks using GPU and fallback to pure JavaScript when GPU is not available. You can export and import trained models, use cross validation, stream training and more features with Brain.js. It is simple, fast and easy to use, and provides multiple neural network implementations as different neural nets can be trained to do different things well.

A neural network is a computational model that mimics the structure and function of the human brain. It consists of layers of nodes called neurons connected by weights. The weights determine how much influence each neuron has on the next layer. The neural network learns by adjusting the weights based on the input and output data.

This is an example of data related to an HVAC system for AI optimization. This data includes various parameters such as temperature, humidity, airflow rates, and energy consumption, which can be used to train and optimize AI models for HVAC system optimization:

Timestamp, Indoor Temperature (°C), Outdoor Temperature (°C), Humidity (%), Airflow Rate (m³/s), HVAC Setpoint (°C), Energy Consumption (kWh)

Table 1. Example of data related to an HVAC system for AI optimization

Timestamp	Indoor Temperature (°C)	Outdoor Temperature (°C)	Humidity (%)	Airflow Rate (m ³ /s)	HVAC Setpoint (°C)	Energy Consumption (kWh)
2022-01-01 08:00:00	22	5	50	0.5	20	10
2022-01-01 09:00:00	23	6	48	0.6	21	11
2022-01-01 10:00:00	24	7	47	0.7	22	12
2022-01-01 11:00:00	25	8	45	0.8	23	13
2022-01-01 12:00:00	26	9	44	0.9	24	14
2022-01-01 13:00:00	27	10	42	0.8	25	13
2022-01-01 14:00:00	28	11	41	0.7	26	12
2022-01-01 15:00:00	29	12	40	0.6	27	11
2022-01-01 16:00:00	30	13	39	0.5	28	10
2022-01-01 17:00:00	31	14	38	0.4	29	8

This data includes timestamps representing hourly intervals, along with corresponding values for indoor and outdoor temperature, humidity, airflow rate, HVAC setpoint, and energy consumption.

In this Brain.js starter program, the prediction refers to the output generated by the neural network based on the input data provided.

In the provided example, the neural network is trained using dummy data where each data point consists of input values representing indoor temperature, outdoor temperature, humidity, and airflow rate, and corresponding output values representing HVAC setpoint and energy consumption.

After training the neural network with this data, the program makes a prediction by providing a dummy input object { indoorTemp: 27, outdoorTemp: 10, humidity: 42, airflowRate: 0.8 } to the neural network using the net.run() method.

The output of the prediction is then logged to the console using console.log('Prediction:', output);.

The specific output of the prediction will vary based on the trained neural network's learned patterns and relationships between the input and output data. It could include predicted values for HVAC setpoint and energy consumption based on the provided input data.

ENERGY CONSUMPTION AND RESOURCE ALLOCATION MADE MORE EFFICIENT THROUGH ARTIFICIAL INTELLIGENCE: AI-DRIVEN DESIGN OPTIMIZATION FOR HVAC (HEATING, VENTILATION, AND AIR CONDITIONING) SYSTEM

```
1  const brain = require('brain.js');
2
3  // Dummy data
4  const data = [
5    { input: { indoorTemp: 22, outdoorTemp: 5, humidity: 50, airflowRate: 0.5 }, output: { setpoint: 20, energyConsumption: 10 } },
6    { input: { indoorTemp: 23, outdoorTemp: 6, humidity: 48, airflowRate: 0.6 }, output: { setpoint: 21, energyConsumption: 11 } },
7    { input: { indoorTemp: 24, outdoorTemp: 7, humidity: 47, airflowRate: 0.7 }, output: { setpoint: 22, energyConsumption: 12 } },
8    { input: { indoorTemp: 25, outdoorTemp: 8, humidity: 45, airflowRate: 0.8 }, output: { setpoint: 23, energyConsumption: 13 } },
9    { input: { indoorTemp: 26, outdoorTemp: 9, humidity: 44, airflowRate: 0.9 }, output: { setpoint: 24, energyConsumption: 14 } },
10   // Add more data here...
11 ];
12
13 // Create a neural network
14 const net = new brain.NeuralNetwork();
15
16 // Train the neural network
17 net.train(data);
18
19 // Dummy input for prediction
20 const input = { indoorTemp: 27, outdoorTemp: 10, humidity: 42, airflowRate: 0.8 };
21
22 // Make a prediction
23 const output = net.run(input);
24
25 // Output the prediction
26 console.log('Prediction:', output);
```

Fig.2. Brain.js Starter Program

After running the program, it gave the result Prediction: {setpoint: 0.9999996423721313, energyConsumption: 0.9999992847442627}.

The output {setpoint: 0.9999996423721313, energyConsumption: 0.9999992847442627} signifies the predicted values for the HVAC setpoint and energy consumption based on the input data provided to the trained neural network.

In Brain.js, the output values are normalized between 0 and 1 by default during the training process. Therefore, the predicted values are also within this range after running the neural network.

For the specific prediction provided:

- setpoint: 0.9999996423721313: This indicates that the neural network predicts the HVAC setpoint to be very close to 1, which is likely the maximum or optimal setpoint value. The actual value would need to be denormalized back to its original scale (e.g., degrees Celsius) based on the range used during training.
- energyConsumption: 0.9999992847442627: Similarly, this indicates that the neural network predicts the energy consumption to be very close to 1, which could suggest high energy consumption. As with the setpoint, the actual value would need to be denormalized back to its original scale (e.g., kWh) based on the range used during training.

Here's a more complex version of the starter program that includes additional layers and neurons in the neural network, as well as more sophisticated preprocessing of the input data:

```

14 const normalizedData = data.map(({ input, output }) => ({
23   output: {
25     energyConsumption: output.energyConsumption / 20, // Normalize energy consumption (assuming maximum value of 20)
26   },
27 }));
28
29 // Create a more complex neural network with hidden layers
30 const net = new brain.NeuralNetwork({
31   hiddenLayers: [8, 8], // Two hidden layers with 8 neurons each
32 });
33
34 // Train the neural network with normalized data
35 net.train(normalizedData);
36
37 // Dummy input for prediction (normalized)
38 const input = {
39   indoorTemp: 27 / 100, // Normalize indoor temperature
40   outdoorTemp: 10 / 50, // Normalize outdoor temperature
41   humidity: 42 / 100, // Normalize humidity
42   airflowRate: 0.8 / 1, // Normalize airflow rate
43   operatingHours: 8 / 24, // Normalize operating hours
44   occupancy: 1, // Occupancy (binary value)
45 };
46
47 // Make a prediction
48 const output = net.run(input);
49
50 // Denormalize the predicted output values
51 const denormalizedOutput = {
52   setpoint: output.setpoint * 30, // Denormalize setpoint
53   energyConsumption: output.energyConsumption * 20, // Denormalize energy consumption
54 };
55
56 // Output the denormalized prediction
57 console.log('Prediction:', denormalizedOutput);

```

PROBLEMS OUTPUT DEBUG CONSOLE **TERMINAL** PORTS

```

PS C:\Users\ghica\Desktop\hvac-yarn> node hvac-improved.js
Prediction: { setpoint: 20.91543138027191,
  energyConsumption: 11.712839603424072 }
PS C:\Users\ghica\Desktop\hvac-yarn> node hvac-improved.js
Prediction: { setpoint: 21.011354327201843,
  energyConsumption: 11.767369508743286 }
PS C:\Users\ghica\Desktop\hvac-yarn>

```

Fig.3. Brain.js Starter Program

In this updated version of the program:

- Additional input data, such as operating hours and occupancy status, are included in the training data and the prediction input.
- The input and output values are normalized before training the neural network to improve convergence and stability during training.
- The neural network architecture includes two hidden layers with 8 neurons each, making the network more complex and capable of capturing nonlinear relationships in the data.
- After making a prediction, the output values are denormalized to obtain the predicted setpoint and energy consumption values in their original scales.

ENERGY CONSUMPTION AND RESOURCE ALLOCATION MADE MORE EFFICIENT THROUGH ARTIFICIAL INTELLIGENCE: AI-DRIVEN DESIGN OPTIMIZATION FOR HVAC (HEATING, VENTILATION, AND AIR CONDITIONING) SYSTEM

The result {setpoint: 21.011354327201843, energyConsumption: 11.767369508743286} signifies the predicted values for the HVAC setpoint and energy consumption after denormalizing the output of the neural network.

In this version of the program, the prediction output values are denormalized to obtain the predicted values in their original scales. These values represent the neural network's predictions for the HVAC system based on the input data provided. Specifically:

- setpoint: 21.011354327201843: This indicates that the neural network predicts the HVAC setpoint to be approximately 21.01 units, which could represent the optimal setpoint value for the given input conditions

- energyConsumption: 11.767369508743286: Similarly, this indicates that the neural network predicts the energy consumption to be approximately 11.77 units, which could represent the expected energy consumption level for the HVAC system under the given input conditions.

5. CONCLUSIONS

The integration of Artificial Intelligence (AI) in HVAC systems is an ongoing process with exciting future trends.

Artificial Intelligence is revolutionizing HVAC industry, empowering systems to deliver personalized comfort, maximize energy efficiency, and reduce costs. Through the integration of AI algorithms and machine learning, HVAC systems can adapt to changing conditions, optimize energy consumption, and proactively address maintenance needs.

Future AI-powered HVAC systems will have enhanced capabilities to optimize energy efficiency further. AI algorithms will leverage advanced machine learning techniques to continuously learn and adapt to building dynamics, occupant behaviors, and weather conditions. This will result in more precise and dynamic energy management, reducing waste and maximizing energy savings.

REFERENCES

- [1]. Dasheng, L., Shang-Tse, L., *Artificial intelligence enabled energy-efficient heating, ventilation and air conditioning system: Design, analysis and necessary hardware upgrades*, Applied Thermal Engineering, 235, 121253, 2023. <https://doi.org/10.1016/j.applthermaleng.2023.121253>
- [2]. Fundamentals of HVAC Controls - Course content, <https://people.eecs.berkeley.edu/~culler/cs294-f09/m197content.pdf>
- [3]. Kanokogi H., Case Study: AI-Based Autonomous Control, By, PhD - <https://www.isa.org/intech-home/2022/october-2022/features/case-study-ai-based-autonomous-control>
- [4]. <https://medium.com/@bacdmessung/how-artificial-intelligence-is-revolutionizing-hvac-systems-226a9194e311>
- [5]. <https://my.avnet.com/silica/resources/article/ai-takes-on-growing-role-in-hvac-system-efficiencies/>
- [6]. <https://www.w3schools.com/ai/default.asp>

- [7]. **Handra A.D., Popescu F.G., Păsculescu D.**, *Utilizarea energiei electrice: lucrări de laborator*, Editura Universitas, 2020.
- [8]. **Fîță N.D., Radu S.M., Păsculescu D., Popescu F.G.**, *Using the primary energetic resources or electrical energy as a possible energetical tool or pressure tool*, In International conference KNOWLEDGE-BASED ORGANIZATION, vol. 27, no. 3, pp. 21-26. 2021.
- [9]. **Popescu F.G., Păsculescu D., Păsculescu V.M.**, *Modern methods for analysis and reduction of current and voltage harmonics*, LAP LAMBERT Academic Publishing, ISBN 978-620-0-56941-7, pp. 233, 2020.
- [10]. **Păsculescu D., Niculescu T.**, *Study of transient inductive-capacitive circuits using data acquisition systems.* International Multidisciplinary Scientific GeoConference: SGEM 2, no. 1, 323-329, 2015.
- [11]. **Andras A., Popescu F.D., Radu S.M., Păsculescu D., Brinas I., Radu M.A., Peagu D.**, *Numerical simulation and modeling of mechano-electro-thermal behavior of electrical contact using comsol multiphysics*. Applied Sciences, 14(10), 4026, 2024.
- [12]. **Marcu M., Niculescu T., Slusariuc R. I., Popescu, F. G.**, *Modeling and simulation of temperature effect in polycrystalline silicon PV cells*, IOP Conference Series: Materials Science and Engineering, Vol. 133, No. 1, pp. 012005, 2016.
- [13]. **Popescu F.G., Arad S., Marcu M.D., Pana L.**, *Reducing energy consumption by modernizing drives of high capacity equipment used to extract lignite*, Papers SGEM2013/Conference Proceedings, Vol. Energy and clean technologies, pp. 183 - 190, Albena., Bulgaria, 2013.
- [14]. **Petrilean, D. C. ;Irimie, S. I.**, *Solutions for the capitalisation of the energetic potential of sludge collected in Danutoni wastewater treatment plant*, Journal of Environmental Protection and Ecology, Vol.16 No.3 pp.1203-1211, 2015.
- [15]. **Petrilean D.C.**, *Compresoare eliciodale*, Editura Tehnica-Info, 2006
- [16]. **Petrilean D.C.**, *Termodinamica tehnica si masini termice*, Editura A.G.I.R., 2010.
- [17]. **Petrilean D.C.**, *The study of energy losses through case helical screw compressor*, Bulletin of the Transilvania University of Brasov, Proceedings of the internationally attended national conference on thermodynamics, 2009.
- [18]. **Petrilean D.C., Popescu D.F.**, *Temperature Determination in Hydrotechnical Works as a Variable of the Energy Change Between Air and Environment*, WSEAS TRANSACTIONS on HEAT and MASS TRANSFER, 2008.
- [19]. **Petrilean D.C.**, *Method of calculus for the power input of the helical screw compressor*, Journal Sci. Bull. Series D, University of Politehnica Bucharest, 2009.
- [20]. **Petrilean D. C.**, *Transmiterea căldurii*, Editura Universitas, 2016.
- [21]. **Petrilean D.C., Irimie. S.I.**, *Solutions to increase the energetic efficiency of pneumatic mining distribution networks*, 9 th International Conference on Energy, Environment, Ecosystems and Sustainable Development (EEESD'13), Lemesos, Cyprus, 2013.
- [22]. **Petrilean D.C.**, *Mathematical model for the determination of the non-stationary coefficient of heat transfer in mine works*, The 19th American Conference on Applied Mathematics (AMERICAN-MATH '13), Cambridge, MA, USA.2013.

This article was reviewed and accepted for presentation and publication within the 11th edition of the International Multidisciplinary Symposium "UNIVERSITARIA SIMPRO 2024".

IS THE EUROPEAN INFRASTRUCTURE READY FOR LONG HAUL ELECTRIC TRANSPORTATION? AN ANALYSIS OF A FREIGHT TRANSPORT FROM ROMANIA TO GERMANY USING AN ELECTRIC SEMI-TRAILER TRUCK

ALINA PANCIU¹, MIHAI VICTOR ZERBES², LUCIAN LOBONT³

Abstract: The heavy-duty vehicle sector is responsible for over 25% of the greenhouse gas emissions generated by road transport in the EU. In order to achieve their ambitious objectives stated in the "Fit for 55" Package, the European Institutions have to provide the legal framework, that will compel the member states to assure the infrastructure to support the transition towards more sustainable modes of transport, and to put the Union on track for the full decarbonization of the transport sector by 2050. Thus, the new Alternative Fuels Infrastructure Regulation (AFIR) – part of "Fit for 55" Package, has to ensure there is sufficient public charging infrastructure to follow the deployment of zero emission cars and semi-trailer trucks. Accordingly, the top ranked European semi-trailer truck makers have to align their industrial plans and business activity to fully transition to zero-emission semi-trailer truck sales. The purpose of this analysis is to evaluate the possibility of a heavy-duty electric semi-trailer truck to carry out a trip on a frequent commercial route between Romania and Germany. The scientific paper is based on an analysis in the form of a case study generated on the basis of a theoretical requirement. The results will show to what extent electric vehicles and infrastructure are ready for this type of transport. After results examination, we found that our findings overlap with the literature and that there is still much room for improvement in this area. Major changes are needed, namely additional investments in infrastructure and subsequent detailed analyses of the opportunity to develop the use of electric vehicles..

Key words: battery electric trucks, European infrastructure, electric long-haul trips, AFIR regulation, zero emission vehicles, electric charging stations.

1. INTRODUCTION

The heavy-duty vehicle (HDV) sector is responsible for over 25% of the greenhouse gas emissions from road transport in the EU. CO₂ emission standards for

¹ Ph.D. Student, Eng., University of Sibiu, alina.panciu@ulbsibiu.ro

² Ph.D., Lecturer Eng., University of Sibiu, mihai.zerbes@ulbsibiu.ro

³ Ph.D., Associate Prof. Eng., University of Sibiu, lucian.lobont@ulbsibiu.ro

certain heavy-duty vehicles were first set in 2019, with targets for the period 2025-2029 and for the period after 2030, with a provision to review these regulations by 2022 [1].

On the 14th of February 2023, the Commission presented a proposal to revise the CO₂ emission standards for heavy-duty vehicles. Although the proposal is not part of the "Fit for 55" legislative package, it is closely linked to it as it contributes to the EU's target of reducing its net greenhouse gas emissions by at least 55% by 2030 compared to levels of 1990 and to achieve climate neutrality by 2050. The main proposed changes relate to the extension of the scope of the regulation to include buses and trailers, the definition of the term "zero emission vehicle" and the new EU emission reduction targets for 2030, 2035 and 2040 [1].

Even though, from an economic point of view, road transport is indispensable, acting as a backbone of trade, facilitating the movement of goods within and outside the EU (European Union), its environmental footprint is substantial: heavy vehicles account for less than 5% of on European roads, but are responsible for around 25% of carbon dioxide (CO₂) emissions from road transport and around 2–4% of total EU emissions. Despite the overall decrease in CO₂ emissions in various sectors in the EU, semi-trailer truck emissions have increased steadily over the last three decades (1990-2020), except for a short decrease in 2020 due to the COVID-19 pandemic. The sector's considerable greenhouse gas emissions underline its dual role as an economic catalyst and significant environmental threat [2].

Electrification quickly emerged as a potential solution to this challenge. Although there is no clear technological method for electrifying road freight transport to date, potential solutions include the direct use of electricity in battery-powered semi-trailer trucks and fuel cell semi-trailer trucks powered by green hydrogen from renewable electricity [3].

The EU supports the electrification of the transport sector through the "Fit for 55" legislative package, which aims to implement legal provisions, mandatory for the member states, which have the effect of reducing greenhouse gas emissions by at least 55% by 2030 [4]. By transitioning from predominantly diesel-powered semi-trailer trucks to electric ones, the aim is to significantly reduce direct emissions. In addition, as electricity grids continue to go green – thanks to the growing share of renewable energy – the estimated emissions reductions from electrified road freight transport continues to grow. While the conversion rates to electric semi-trailer trucks currently available on the commercial market in the EU is less than 1% of total vehicle sales, as indicated by the sales figures of heavy vehicle manufacturers, according to the standards of existing CO₂, there could be more than 600,000 such vehicles on European roads by 2030 [5].

Semi-trailer trucks deliver essential goods to consumers and keep society moving. They provide most of our daily needs, such as food or medical supplies. In addition, they support essential public services such as construction, garbage collection and firefighting and rescue services. Semi-trailer trucks are also the foundation of the European logistics and transport system. The demand for freight transport is increasing and all modes of transport will need to continuously improve to meet the needs of the future. Road transport is expected to remain the most used mode of goods transport [6].

Why would it be more important to switch from semi-trailer trucks that use conventional fuels (diesel and petrol) to electric semi-trailer trucks? While cars are parked most of the time, semi-trailer trucks are mostly in motion. A semi-trailer truck can easily drive up to 150,000 kilometers per year – 12 times more than a passenger car [7]. For this reason, the scope of this paper is to analyze the sustainability of carrying out a transport of goods with an electric semi-trailer truck, in order to observe the existing advantages and disadvantages and to provide future improvement solutions.

2. METHODS AND SELECTION METHODOLOGY

In order to identify the current readiness of the long-haulroad freight with an electric semi-trailer truck, we designed a theoretical transport on an important commercial corridor from the industrial area of Sibiu to the industrial area of Munich, in Dingolfing. To reach the purpose of our study, we followed these steps: we selected a specific commercial road corridor in Europe, then we settled upon an electric semi-trailer truck, researched the legislation that regulates road freight transport, documented the charging stations and their capability to charge, on this specific route and the approximate costs to carry out this transport. This study tries to point out from both an economical and technical perspective the advantages and disadvantages of a battery electric semi-trailer truck. The same methodology was used for a diesel semi-trailer truck to establish a comparison in terms of route travel time and economic point of view.

2.1. Selecting the route

In order to achieve its the zero emission policies, the European Commission issued a regulation called AFIR -Alternative Fuels Infrastructure Regulation [4]. In accordance with the provisions of this regulation, a plan is established for the development of charging points so that semi-trailer trucks charging infrastructure will be located along the Trans-European Transport Network (TEN-T), which spans over 108,000 km of road network across the EU [8].

The TEN-T road network, as provided for in Article 9 of Decision 661/2010/EU, consists of existing, new or to be adapted high-quality motorways and roads, which:

- play an important role in long-distance traffic;
- bypass the main urban centers on the routes identified by the network;
- ensures interconnection with other modes of transport;
- connects the landlocked and peripheral regions with the central regions of the

Union [8].

In addition to those listed above, the network should guarantee users a high, uniform and continuous level of service, comfort and safety. It also includes infrastructure for traffic management, user information, incident and emergency handling and management, electronic toll collection, or such infrastructure being based on active cooperation between European, national and regional traffic management systems [5]. Thus, we considered that choosing a route on the TEN-T core network,

will be highly relevant for our study. As shown in figure 1 (Corridor 9-Rhine-Danube of TEN-T – light blue color on figure), our transport will start in Cristian (Sibiu) – Arad – Budapest – Vienna – Passau and will end in Dingolfing (Munich) – 1.160 km [8].

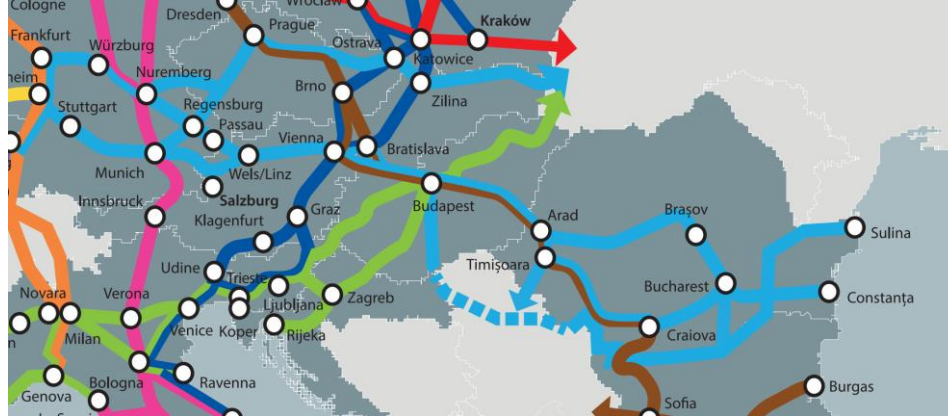


Fig. 1. The selected route integrated in the Corridor 9-Rhine-Danube of TEN-T[8]

2.2. Selecting the means of transport

The latest report of the expert group within [9] declared that Scania, Mercedes-Benz and Man semi-trailer trucks, are the three European frontrunners based on their announced ambition, strategy and readiness. All three aim for 100% new zero-emission semi-trailer truck (ZET) sales by 2040 or earlier. Volvo semi-trailer trucks is the current market leader in battery-electric semi-trailer truck sales in Europe and the manufacturer with the most ambitious 2030 target (70% ZET sales share). Renault semi-trailer trucks and IVECO Group are lagging behind in the transition. DAF closes the ranks with a very weak score, having no public ZET target for 2030. We selected four of these manufacturers, namely, Scania [10], Mercedes-Benz [11], Volvo semi-trailer trucks [12] and Renault semi-trailer trucks [13] and formally, requested the technical data and price offers through their official Romanian dealers, in order to decide which electric semi-trailer truck trailer is more suitable for the long haul between our point of departure and destination. First, we singled out the essential features presented in the technical data sheets as shown in the table 1 and secondly, a criterion analysis was carried out, taking into consideration the lowest purchase price, the highest range, the shortest time of charge and the longest period of warranty. Therefore, the best option for the task was Mercedes-Benz eActros 600 LS.

2.3. Identifying long-haul semi-trailer truck trips

In this study, we focus on BETs that use public chargers to reach their destination, including a single charge at the point of departure, e.g., depots [14]. We must consider the fact that [15] define HDVs long-haul, if they have a travel period of around 333 km using average travel speed on German roads and a buffer distance, resulting in 4.5 hours. In another paper, [16] use 350 km as a distance threshold and

[17] define a trip as being long-haul, if it exceeds distances over 400 km. In our study, we follow the frequently used distance-based definition of “long-haul operation” that considers point of origin and destination with travel times over 4.5 h or 360 km distance traveled using the typical average speed of semi-trailer trucks of about 80 km/h [14].

Table 1. Criterion analysis for the selection of an electric semi-trailer truck trailer

Brand Features	Mercedes eActros 600 LS	Scania R400E	Volvo FH 42	Renault E-tech T
Year of production	2024	2023	2023	2023
Purchase price *	320.000	365.000	392.000	350.000
Maintenance interval(km)	120.000	120.000	120.000	120.000
Range(km)	500	320	300	300
Charging time from 20-80% **	1 h	2 h	2 h and 30'	1 h and 20 '

*The prices are Euro and do not include VAT (value added tax).

** At direct current (DC) stations with a charging power of at least 135 kWh (kilowatt-hour).

2.4. Break and rest assumptions

We try to estimate the remaining range of the electric semi-trailer truck batteries on each main segment of the road, in order to recharge on time, before the batteries run lower than 20%, meanwhile we also applied the provisions of Regulation (EC) No 561/2006 of the European Union, which states that the daily driving period must not exceed 9 hours and drivers should stop driving at least 45 minutes, after a 4.5-hour continuous drive. Those two periods of time charging/driver's break did not, always, overlap.

2.5. Charging infrastructure

The selected electric semi-trailer truck has a charging capacity of 400 kW per hour at an average CCS Type 2 (Type 2 is standard for European and Asian vehicles from 2018 onwards, it's a triple-phase plug and can charge at a level of up to 43 kW; Combined Charging System is a version of type 2 with two additional power contacts allowing fast charging) charging point, resulting an approximate 60 minutes time frame to charge from 20% to 80% [18] and a 4-hour charging time, if the charging point has a 100-kW output socket. Therefore, it is imperative to plan and indicate in advance, the stations, which will mandatory meet two conditions simultaneously:

- A loading power of at least 100 kw per hour;
- Access to the charging station as a semi-trailer truck.

2.6. Charging infrastructure

The average energy consumption rate for BETs varies significantly depending on a variety of factors. ICCT [19] and Suzan & Mathieu [17] consider that the energy

IS THE EUROPEAN INFRASTRUCTURE READY FOR LONG HAUL ELECTRIC
TRANSPORTATION? AN ANALYSIS OF A FREIGHT TRANSPORT FROM ROMANIA
TO GERMANY USING AN ELECTRIC SEMI-TRAILER TRUCK

efficiency of new semi-trailer trucks entering the fleet will reach 1.2–1.23 kWh/km in 2030. Speth [15] notes an energy consumption of 1.23 kWh/km. In their study, Lin and Zhou [20] use real-world driving data of energy consumption from 18 electric semi-trailer trucks and found energy consumption of 0.80–1.20 kWh/km on urban roads and 1.30–1.80 kWh/km on highways. Mareev [16] also find that real-world BET energy consumption rates are between 1.23 kWh/km and 1.94 kWh/km, depending on speed limits and road type and Al-Hanahi [21] pointed out the energy consumption of the BETs is between 1 and 1.75 kWh/km. The manufacturer Mercedes-Benz technical data report a 500 km range and 600 kWh of usable battery capacity, resulting a 1.2 kWh/km consumption, for our selected semi-trailer truck.

Table 2. The structure of the selected route and the consumption of the electric semi-trailer truck

No.	Road Category	Road Segment	Dist. [km]	Time [h and min]	Consumption [kWh]	Remained range [km]/ Capacity [kW]		Elapsed Time from departure [min]
1.	National Road DN1 /DN7H	Cristian – Calea Șurii Mici	13.7	12'	16.44	500	600	12'
						486.3	583.5	
2.	Highway A1	Calea Șurii Mici – Coșevița	142	1h 46'	170.4	344.3	413.1	118'
3.	National Road DN68A	Coșevița - Margina	15	18'	18	329.3	395.1	136'
4.	Highway A1	Margina - Nădlac	157	1h 56'	188.4	172.3	206.7	252'+60'=312'
						297	356.7	
5.	Highway M43	Nădlac - Szeged	57	43'	68.4	240	288.3	369'
6.	Highway M5	Szeged - Gyál	137	1h 43'	164.4	103	123.9	472'***
7.	Highway M0	Gyál-Törökbálint	30	20'	36	400	480	492'+60'=(charging)= 552
						370	344	
8.	Highway M1	Törökbálint-Nickelsdorf	157	1h 57'	188.4	213	155.6	552'+60'+660'=1272***
9.	Highway A4	Nickelsdorf-Mannsworth	57	43'	68.4	156	87.2	1351'*****+ 120'=1471'
						400	480	
10.	Express road S1	Mannsworth Vosendorf	18	13'	21.6	482	458.4	1484'
11.	Highway A21	Vosendorf-Hinterleiten	38	28'	45.6	444	412.8	1522'

12.	Highway A1 - A25	Hinterleiten- Passau	162	2h	194.4	282 416	218.4 500	1642***** +60' (charging)= 1702'
13.	Highway A8 – A3	Passau- Deggendorf	128	1h 36'	153.6	288	346.4	1798'
14	Highway A92	Deggendorf- Dingolfing	45	32'	67.5	243	278.9	1830' = 1 day 6h 30'

At the point of origin, Cristian (Sibiu), the electric semi-trailer truck trailer will be fully charged, according with the Romanian provider tariffs, which are calculated depending on consumption thresholds as in equation 1 [22].

$$C_0 = 0,26 \text{ Euros} \times 500 \text{ kW} = 130 \text{ Euros} \quad (1)$$

where C represents the charging cost, calculated according to each transitcountry/provider.

On the chosen route, we will pass through Hungary, Austria with the final destination Germany, so we will calculate the rate for 1 kWh, as we will find it on the Plugshare application - for Romania and Hungary and the Smatrics application[23] - for Austria and Charge Finder [24] in Germany.

* a stop is mandatory for the driver to take his mandatory 45-minute break, after crossing the border at Nădlac. At the MOL Magyarcsanak filling station, right after entering Hungary on the M43, there is a high-power charging station (equipped with CCSType 2, power output = 11-150 kW, DC charging costs – 309 Ft/ 1kWh + 1 Ft/ 1kWh after 30 minutes), where Ft represent the abbreviation for Forint, which is the Hungarian official currency.

During the break, for efficiency reasons, it will last for an hour, so the driver can rest and the semi-trailer truckcan charge.

SoC₁ = 206.7kW, we will charge the batteries with 150 kW, where SoC – state of charge.

$$C_1 = (309 \times 150) + (1 \times 30) = 46,350 + 30 = 46,380 \text{ Ft.} = 117 \text{ Euros} \quad (2)$$

** another battery charge will be necessary, immediately after entering the M0, because, we haveat our disposal, the Shell Szigetszentmiklós, high-power station (equipped with CCS Type 2, a power output of 350 kW, DC charging cost 280 Ft/kWh), where it also accepts trailers, a fact clearly mentioned in the application:

SoC₂=120 kw, charging time – 1 h, to achieve a 480 kW

$$C_2 = 360 \text{ Ft} \times 280 \text{ kW} = 100,800 \text{ Ft.} = 254 \text{ Euros} \quad (3)$$

*** after one hour of driving, the driver will perform the mandatory 11-hour rest period in the first parking place arranged for this purpose, after which, at the end of this period, he will continue the journey to the border with Austria, without loading.

IS THE EUROPEAN INFRASTRUCTURE READY FOR LONG HAUL ELECTRIC
TRANSPORTATION? AN ANALYSIS OF A FREIGHT TRANSPORT FROM ROMANIA
TO GERMANY USING AN ELECTRIC SEMI-TRAILER TRUCK

*Charging is required, we have a high-power station (equipped with CCS Type 2, power output = 200kW) near Lidl, before entering the Vienna ring road, where we will charge up to 80%, DC charging cost:

SoC₃= 87.2 kW, we will also correlate the mandatory 45-minute driver break with the 2-hour charging period.

$$C_3 = 9.90 \text{ Eur. (pass/month)} + 392,8 \text{ kW} \times 0,65 \text{ Eur.} + 29' \times 0,15 \text{ Eur.} = 270 \text{ Eur.} \quad (4)$$

**** When entering Passau we will charge, at OMV, at a high-power station (equipped with CCS Type 2, power output = 350kW, DC cost = 0.69 Euro/kWh, where we will charge up to 80%, SoC₄=218.4 kW, after one hour of charging we will reach almost 500 kw.

$$C_4 = 281 \text{ kW} \times 0.69 \text{ Euros} = 194 \text{ Euros} \quad (5)$$

$$\text{Total cost with charging (on route)} = 117 + 254 + 270 + 194 = 835 \text{ Euros} \quad (6)$$

$$\text{Total cost with charging per transport} = 130 \text{ Euros} + 835 \text{ Euros} = 965 \text{ Euros} \quad (7)$$

Meanwhile, for the diesel HDV, applying the same methodology, on the exact, same route, we have the following results: a) after 4 hours and 12 minutes of driving, the semi-trailer truck driver will take the mandatory break, provided by the law; b) upon entering Austria, at Nickelsdorf, the driver must take the mandatory 11 hours of rest after the 9 hours of driving; c) upon entering Germany, in Passau, the driver will have a 15-minute break, after which he will continue the route to the destination.

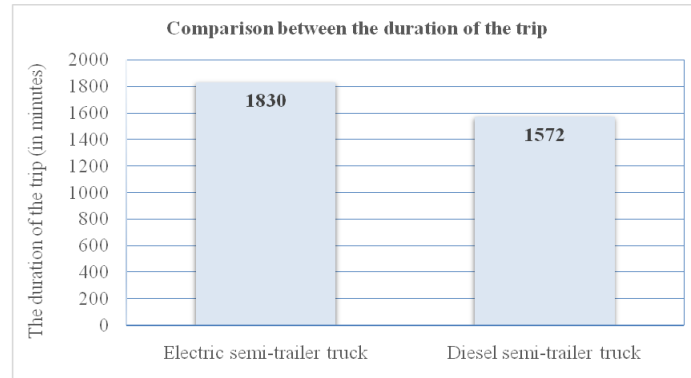


Fig. 2. The duration of the trip with the electric semi-trailer truck and with the diesel semi-trailer truck

The diesel semi-trailer truck was fueled at the point of departure, in Cristian, at the OMV Station, [25], where a liter of diesel costs 1.44 Euros/liter and the total cost for the fuel supply was 1.600 Euros (the tank has a 1.110 diesel liters capacity). Taking into consideration that the consumption of Mercedes Actros 5 LFHS 1848 is 27 liters/100 km, as stated in the technical data sheet, and the consumption estimated for the 1.160 km of is 300 liters, the total cost with fuel per transport is 432 Euros.

The duration of the trip with an electric semi-trailer truck trailer was 1 day, 6 hours and 30 minutes, while the duration of the trip with a diesel semi-trailer truck trailer lasted 1 day, 2 hours and 12 minutes. The difference is not that big as shown in figure 2, but that is a relative fact, due to the fact that the research had its limitation as regards to the period of the trip.

4. DISCUSSIONS

The analysis of long-haul freight transport with an electric semi-trailer truck has highlighted several weaknesses of this mean of transport, but above all, deficiencies in the high-power charging infrastructure and legislative loopholes, which will discourage hauliers from converting their diesel semi-trailer truck fleets to electric propulsion. Reducing the negative effects of these problems and improving them would make electric freight transport cost-effective and sustainable.

4.1. Lack of high-power charging stations

There are two key factors for the widespread use of battery electric commercial vehicles: increased range and shorter charging times. Charging time, which can be quantified as distance per unit of time charged, should be considered for the whole fleet and should also take into account lost charging time due to late charging or even problems related to charging equipment (i.e., long queues, overheating, faulty errors). The implementation of the MCS (Megawatt Charging System – very fast high power charging system) provides the charging rate needed to achieve widespread adoption of battery electrification in the commercial vehicle market by increasing driving range gained per minute spent charging [26]. Commercial vehicle customers have very specific driving patterns. The increased charging rate offered by MCS will allow customers to cover as much distance as possible per day, using the mandatory break time in the hours-of-service regulations.

These regulations require drivers to take an occasional break during their driving cycle; the exact amount varies by location, but it is well understood that reducing charging times to fit within normal duty cycle breaks is an enabler for improved electrification for commercial vehicles. This is just one specific example of how the MCS charging rate can activate the market [26]. We must note the lack of any MCS along the analyzed route (neither charging application indicated the MCS).

4.2. The small number of special places for charging a semi-trailer truck semi-trailer at existing stations

Another challenge an electric semi-trailer truck driver faces is the space required at the charging point, when driving a semi-trailer truck. Given that the length of an assembly is approximately 15 meters or more, it is important to choose a charging station that allows access and has the necessary space, without inconveniencing the other vehicles, located in the perimeter. So, it is imperative to plan the transport route in detail and indicate the stations ahead, which will have to meet

IS THE EUROPEAN INFRASTRUCTURE READY FOR LONG HAUL ELECTRIC TRANSPORTATION? AN ANALYSIS OF A FREIGHT TRANSPORT FROM ROMANIA TO GERMANY USING AN ELECTRIC SEMI-TRAILER TRUCK

two conditions cumulatively: charging power of at least 100 kWh and access for a semi-trailer truck.

In our case, we identified only 14 stations that meet these conditions (as in figure 3), with the help of the Plug Share application, which facilitates the location of the charging stations, the application of filters, according to the requirements of the situation. These stations, are not evenly spread, a fact that discourages electric road freight. Of course, there are other types of charging points, with less output power, but they are neither next to the highway, nor they allow semi-trailer trucks. Transport managers must calculate the stopping points for the drivers to charge both exactly and preventively. Still at this moment in time, there is not an electric semi-trailer truck with enough range that could cross this road segment without having to charge [27].

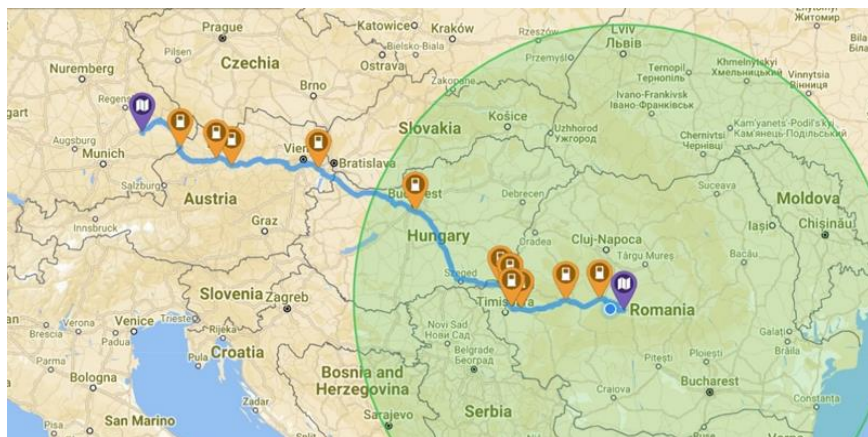


Fig. 3. Fast charging stations on the selected route

4.3. Unpredictability of charging station prices depending on ownership

As shown in figure 4, the charging cost with electricity is twice as high as the fuel supply cost for a transport, i.e., Cristian-Dingolfing, these costs will be doubled, when returning Dingolfing-Cristian.

If the price of diesel is somewhat predictable, with little fluctuation from one country to another (in our case study, there was no need to refuel, due to the tank large capacity), the price of electricity is calculated differently, depending on several factors:

- The state, on whose territory the charging station is located and the rates regulated per kWh;
- The owner of the charging station;
- Effective charging time; there are stations, where, after a determined period of time, every minute spent at the charging point will be reflected in the final cost, aside the price of the kWh;
- The existence or not of a subscription; the tariffs without a subscription, are not profitable, at all.

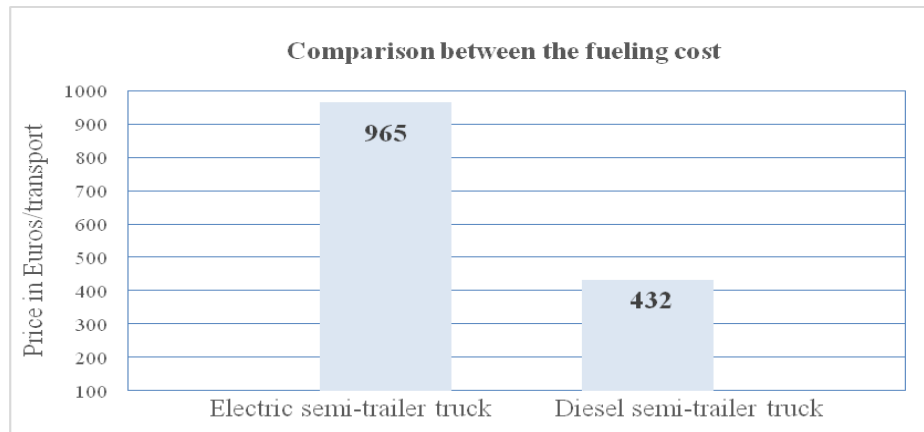


Fig. 4. The difference between fueling costs

As a solution to improve and encourage the use of electric semi-trailer trucks, we propose the development of a common kWh pricing policy at the level of the European Union, so that the carrier has, to a certain extent, the highest possible predictability and stability of the current price.

4.4. Lack of regulations on road tolls and property taxes

In order to encourage the purchase of electric passenger vehicles, the EU member states have granted various facilities, such as exemption from taxes and duties due to local authorities or special parking spaces or even the freeparking spaces.

At the level of HDV, there is not, at this moment, in Romania, nor at the European level, a clear policy that provides facilities for them. There was, at one point, a debate at the level of the decision-making forums of the EU, to eliminate road taxes (vignette, toll collection) for electric semi-trailer trucks, but it did not materialize, in a legislative act, to regulate this field, at the European level, so for the moment, there no road toll exemptions.

Also, the property taxes, which are quite high, in Romania, HDVs remained without a special regulation, so that, for now, at least on the Romanian territory, the law does not distinguish between an electric semi-trailer truck and a conventional fuel semi-trailer truck. Considering the other disadvantages that arise from the purchase of an electric semi-trailer truck, we can conclude that they are not a cost-effective solution, neither for the transporter nor for the end customer, who will feel all these additional costs in the final price of the product.

4.5. The inefficiency of purchase incentives, considering electric HDVs high prices

In Many European countries offer tax support to stimulate the market uptake of electric commercial vehicles, but these tax advantages and purchase incentives differ greatly from one member state to another [28].

IS THE EUROPEAN INFRASTRUCTURE READY FOR LONG HAUL ELECTRIC TRANSPORTATION? AN ANALYSIS OF A FREIGHT TRANSPORT FROM ROMANIA TO GERMANY USING AN ELECTRIC SEMI-TRAILER TRUCK

Some states grant these benefits for the purchase of passenger vehicles, for the purchase of electric semi-trailer trucks or electric buses, or for the development of charging infrastructure. Of course, there are states that grant benefits for all sectors, but there are states that do not grant benefits at all for the electrification of road transport, among them we list: Hungary, Lithuania, Slovenia. Among the states with the biggest incentives for the purchase of an electric semi-trailer truck, we can mention: Austria, England, Belgium, Croatia, Cyprus, Finland, Germany, Iceland, Malta, Spain and Sweden [28].

As we can see in figure 5, an electric semi-trailer truck is 3 times more expensive than a diesel semi-trailer truck. Without the support of government funds or non-reimbursable funds granted by the European Commission, through its various programs or support packages, it will be impossible to convert heavy commercial vehicle fleets to the zero-emission restriction.

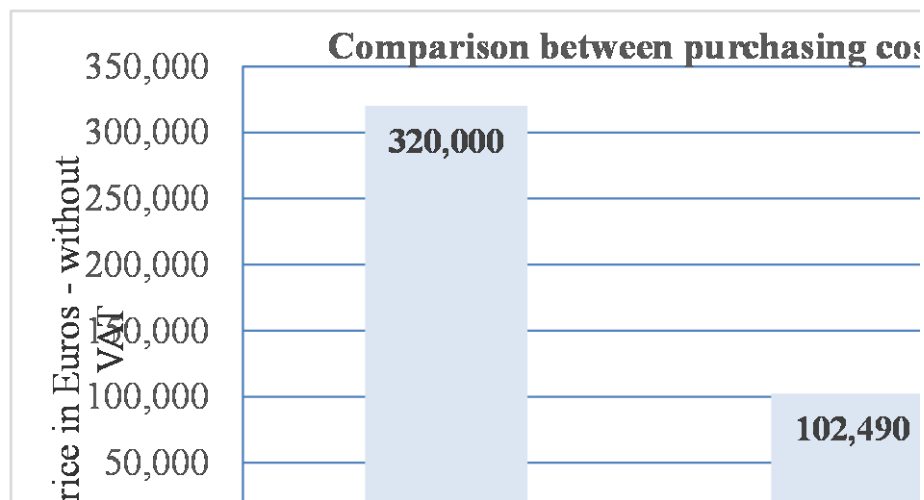


Fig. 4. The difference between purchasing costs

4.6. Unpredictability of trip duration due to a number of factors

Time plays a crucial role in the road transport of goods, being essential in the following aspects:

- **Delivery efficiency:** road freight must ensure pre-arranged deliveries, according to chosen deadlines. Thus, the consignee does not need to create safety stocks. This aspect eliminates excessive storage, the possible depreciation of goods during storage and the immobilization of financial resources for stocks.
- **Cost reduction:** Freight companies are looking for solutions to reduce costs and time to deliver goods.
- **Influence on the cost of transportation:** When referring to time as a factor influencing the cost of freight transportation, one must consider the transportation time, order time, delivery schedule, punctuality and frequency of runs.

- Legal regulations: there are legal regulations that control driving and rest time in the road transport of goods, legislated at the level of the member states. These are intended to ensure road safety and prevent driver burnout.

4.7. Limitations of the research

In conclusion, effective time management in road freight transport can lead to a number of benefits, including cost reduction, improved efficiency and compliance with legal regulations.

Given the vital importance of time in transport, our analysis could not identify to a scientific level of precision, the following issues that will cause unexpected delays, during a trip:

- The periods in which the mandatory breaks of the driver cannot be correlated with the battery charging period. In this situation, the transport time will increase, because at the moment, there is no regulation, which considers the charging period as a break and deducts it from the driver's service time.

- Waiting periods for performing customs formalities at state borders. The study carried out did not take into account the waiting time at the borders. It is known that there are queues, customs controls, which will cause delays, but the autonomy of the electric semi-trailer truck will be affected by these queues and therefore, most likely, at least one additional charge caused by these delays will be needed. An additional charge will result in higher costs and increased travel time.

- Battery charging time below 20% and above 80%. Electric semi-trailer truck manufacturers cannot estimate either the charging time, if the state of charge of the batteries drops below 20%, or the charging time required for the batteries to be fully charged. Therefore, if for various reasons, the driver lets the batteries drop below the 20% threshold, it will increase the charging time, which will generate additional costs and delivery delays.

- Route topography and weather conditions. Thermal extremes (too hot or too cold), as well as the differences in slope of the route, will play an important role on the state of charge of the battery, with direct effects on the transport time and charging costs. It is important to know these factors because they influence the range of the batteries to a great extent.

- Other types of costs such as: tires costs, tolls and insurance costs, drivers' salaries, miscellaneous other transport costs were not taken into consideration, although they were calculated, due to the fact their values are the same at some point or they differ slightly.

5. CONCLUSIONS

In the European Union, 732 electric semi-trailer trucks were sold in 2022 and 2,486 electric semi-trailer trucks in 2023 [6]. The number is not large, but it is a start. The models of electric semi-trailer trucks are neither various, nor their autonomy is, on average, greater than 400 km, but the semi-trailer truck manufacturers have sensed the electrification trend of this sector and evaluate the necessary improvement solutions.

IS THE EUROPEAN INFRASTRUCTURE READY FOR LONG HAUL ELECTRIC TRANSPORTATION? AN ANALYSIS OF A FREIGHT TRANSPORT FROM ROMANIA TO GERMANY USING AN ELECTRIC SEMI-TRAILER TRUCK

According to the data and analysis carried out in this study, it is not cost-sustainable to transport a certain quantity of goods on a major trade route with an electric semi-trailer truck at this moment in time. As presented in figures 3 and 4, the most important cost differences: the purchase cost and the supply cost for the two semi-trailer trucks are so great, that a transport company could not endanger their profits/survival by converting its diesel fleet, for decarbonization sake.

Considering that all the costs presented above and the delaying time risks will be reflected in the price of the product reaching the final customer, it is reasonable to conclude that any product transported, at this moment, with an electric semi-trailer truck will not be able to be competitive or sustainable, due to the economical component of the sustainability.

Most certainly, technological developments at the level of charging infrastructure, diversity of models of semi-trailer truck heads, but also the development of legislation related to this new field, will change the balance in favor of electric semi-trailer trucks in the future.

Acknowledgements: This work was supported by the Learn.Inc 2021-1-RO01-KA220-HED-000031136 project.

REFERENCES

- [1]. **Consiliul European**, *Comunicate de presă*, 18 January 2024 Available: <https://www.consilium.europa.eu/ro/press/press-releases/2024/01/18/heavy-duty-vehicles-council-and-parliament-reach-a-deal-to-lower-co2-emissions-from-trucks-buses-and-trailers/> (accessed on 30 March 2024).
- [2]. **Ertelt, S.-M.**, *Beyond predict and provide: Embracing sufficiency synergies in road freight electrification across the European Union*. Energy Res. Soc. Sci., pp. 111, 2024.
- [3]. **Plötz P., Wachsmuth J., Sprei F., Gnann T., Speth D., Neuner F., Link S.**, *Greenhouse gas emission budgets and policies for zero-Carbon road transport in Europe*. Clim. Policy, 23/3, 2023.
- [4]. **European Commission**, *Alternative fuels infrastructure*, 2024, Available: https://transport.ec.europa.eu/transport-themes/clean-transport/alternative-fuels-sustainable-mobility-europe/alternative-fuels-infrastructure_en (accessed on 10 June 2024).
- [5]. **European Federation for Transport and Environment**, *Fully charged for 2030 - Enough infrastructure for more electric trucks in 2030*, <https://www.transportenvironment.org/articles/fully-charged-for-2030> (accessed on 23 March 2024).
- [6]. **ACEA**, *New commercial vehicle registrations in Q1 2024*, Available: <https://www.acea.auto/cv-registrations/new-commercial-vehicle-registrations-vans-12-6-trucks-4-buses-23-3-in-q1-2024/> (accessed on 1 June 2024).
- [7]. **ACEA**, *New commercial vehicle registrations in 2023*, Available: https://www.acea.auto/files/Press_release_commercial_vehicle_registrations_2023.pdf (accessed on 31 March 2024).
- [8]. **European Commission**, *Mobility and Transport - CORE NETWORK CORRIDORS ON THE TEN-T*, Available: <https://ec.europa.eu/transport/infrastructure/tentec/tentec-portal/site/en/maps.html> (accessed on 13 June 2024).

- [9]. **Transport & Environment**, *Who are the frontrunners in the global race to clean up trucks and gain technology leadership?*, Available: https://www.transportenvironment.org/wp-content/uploads/2023/06/2023_06_truckmakers_ZE_readiness_report.pdf (accessed on 31 March 2024).
- [10]. **Scania**, *Vehicul electric cu baterii*, Available: <https://www.scania.com/ro/ro/home/products/trucks/battery-electric-truck.html> (accessed on 07 May 2024).
- [11]. **Mercedes Benz**, Available: <https://hub.mercedes-benz-trucks.com/ro/ro/trucks/eactros-600.html> (accessed on 2 April 2024).
- [12]. **Volvo**, **Volvo FH Electric**, Available: <https://www.volvotrucks.ro/ro/ro/trucks/electric/volvofh-electric.html> (accessed on 7 May 2024).
- [13]. **Renault Trucks**, *Conducerea camioanelor electrice*, Available: <https://www.renault-trucks.ro/static/conducerea-camioanelor-electrice> (accessed on 8 May 2024).
- [14]. **Shoman W., Yeh S., Sprei F., Plötz P., Speth D.**, *Battery electric long-haul trucks in Europe: Public charging, energy, and power requirements*, *Transp. Res. D*, pp. 121, 2023.
- [15]. **Speth D., Plötz P., Funke S., Vallarella E.**, *Public fast charging infrastructure for battery electric trucks – a model-based network for Germany*, *Environ. Res.: Infrastruct. Sustain.*, 2022.
- [16]. **Mareev I., Becker J., Sauer D.U.**, *Battery Dimensioning and Life Cycle Costs Analysis for a Heavy-Duty Truck Considering the Requirements of Long-Haul Transportation*, *Energies*, 2017.
- [17]. **Suzan S., Mathieu L.**, *Unlocking Electric Trucking in the EU: long-haul trucks: long-haul trucks: recharging along highways*, Available: https://te-cdn.ams3.digitaloceanspaces.com/files/202102_pathways_report_final.pdf (accessed on 20 June 2024).
- [18]. **Mercedes-Benz Trucks**, *Modelul eACTROS 600 în detaliu*, 2024. Available: https://hub.mercedes-benz-trucks.com/ro/ro/trucks/eactros-600.html#eactros600_technical-data (accessed on 2 April 2024).
- [19]. **ICCT**, *Estimating the infrastructure needs and costs for the launch of zero-emission trucks*, *International Council on Clean Transportation*, Available: <https://theicct.org/publication/estimating-the-infrastructure-needs-and-costs-for-the-launch-of-zero-emission-trucks/> (accessed on 20 April 2024).
- [20]. **Lin J., Zhou W.**, *Important factors to daily vehicle routing cost of battery electric delivery trucks*, *Int. J. Sustain. Transp.*, 2020.
- [21]. **Al-Hanahi B., Ahmad I., Habibi D., Masoum M.**, *Charging Infrastructure for Commercial Electric Vehicles: Challenges and Future Works*, *IEEE Access*, 2021.
- [22]. **Avest**, *Pretul energiei consumul casnic 2024*, Available: <https://www.avest.ro/blog/?pretul-energiei-consumul-casnic-2024> (accessed on 12 June 2024).
- [23]. **SMATRICS**, *Tariffs*, 2024. Available: <https://smatrics.com/en-AT/charging/tariffs> (accessed on 24 April 2024).
- [24]. **Charge Finder**, *Charging stations*, Available: <https://chargefinder.com/en/charging-station-taufkirchen-omv-taufkirchen/r38x3p> (accessed on 24 April 2024).
- [25]. **OMV**, *Pret statie de distributie*, Available: <https://www.omv.ro/ro-ro/statii-de-distributie-carburant/localizare-statii-omv> (accessed on 15 June 2024).

IS THE EUROPEAN INFRASTRUCTURE READY FOR LONG HAUL ELECTRIC
TRANSPORTATION? AN ANALYSIS OF A FREIGHT TRANSPORT FROM ROMANIA
TO GERMANY USING AN ELECTRIC SEMI-TRAILER TRUCK

- [26]. **CharIN Association**, *Recommendations and requirements for MCS related standards bodies and solution suppliers*, Available: https://www.charin.global/media/pages/technology/knowledge-base/c708ba3361-1670238823/whitepaper_megawatt_charging_system_1.0.pdf (accessed on 15 March 2024).
- [27]. **MacDonnell O., Wang X., Qiu Y., Song S.**, *The Zero-Emission Truck and Bus Market*, Available: https://globaldrivetozero.org/site/wp-content/uploads/2023/06/Final_ZETI-Report-June-2023_Final.pdf (accessed on 2 May 2024).
- [28]. **ACEA**, *Electric commercial vehicles-Tax benefits and purchase incentives 2023*, Available: <https://www.acea.auto/fact/electric-commercial-vehicles-tax-benefits-and-purchase-incentives-2023/> (accessed on 2 June 2024).
- [29]. **PlugShare**, <https://www.plugshare.com/>, Available: <https://www.plugshare.com/> (accessed on 3 May 2024).
- [30]. **ACEA**, *New passenger car registrations, European Union Report, 2023*, Available: <https://www.acea.auto/pc-registrations/new-car-registrations-13-9-in-2023-battery-electric-14-6-market-share/> (accessed on 2 June 2024).

This article was reviewed and accepted for presentation and publication within the 11th edition of the International Multidisciplinary Symposium "UNIVERSITARIA SIMPRO 2024".

RELIABILITY OF BLASTING MACHINES USED TO INITIATE ELECTRICAL DETONATORS

DAN GABOR¹, MIHAELA PĂRĂIAN², ANCA TĂZLĂUANU³

Abstract: In underground or surface mining operations in Romania, blasting machines manufactured before 1990 are still used to initiate electric detonators. These blasting machines have a long or very long operating life and certain operating parameters have changed over time. On the basis of the data collected during the periodic inspections, the data contained in the test reports issued by the Laboratory of Non-Electrical Ex Equipment, Electrostatic Materials and Personal Protective Equipment of INCD Insemex Petroșani, an analysis was made in this paper of the parameters that change in a blasting machine over time, the possible causes and the consequences of these changes. Data from test reports from 2003 to 2023, i.e., over a period of 20 years, performed on blasting machines manufactured in Romania and the former German Democratic Republic was used for the analysis. According to the analysis carried out for the preparation of this paper, it was found that the blast machines with the longest service life were those produced in the former GDR, i.e., Vopil M514 blast machines, and that most of them were inductor and capacitor blast machines. The parameters that changed as a result of long use were the output voltage value, the pulse power and, in the case of blasting machines intended for coal mining, the pulse duration.

Key words: blasting machines, electric detonators, mining.

1. INTRODUCTION

Blasting machines, also known as blasting caps, detonators or initiators, are devices used to initiate explosive charges in mining operations. Advanced technologies in this field include the use of capacitors to provide the energy required to initiate explosions.

These devices are preferred for their accuracy and reliability, as they are capable of delivering highly controlled pulses of energy. These devices are vital in various applications including mining, construction and demolition.

Here's an overview of blasting machines for initiating electrical detonators:

¹ Ph.D., Eng., INSEMEX dan.gabor@insemex.ro

² Ph.D., Eng.

³ Ph.D., Student Eng.

1.1. Types of Blasting Machines

1.1.1. Hand-Operated Blasting Machines

- These are manual devices that generate an electric charge when a handle is turned or a plunger is pushed.
- They are typically used in smaller operations where portability and simplicity are important.
- Example: Crank-operated or push-down blasting machines.

1.1.2 Battery-Powered Blasting Machines

- These machines use batteries to provide the necessary electrical current to initiate detonators.
- They offer greater convenience and reliability compared to manual devices.
- Example: Digital or electronic blasting machines with rechargeable batteries.

1.1.3 Capacitor-Discharge Blasting Machines

- These machines store electrical energy in capacitors and release it in a sudden, controlled burst to initiate detonators.
- They are known for their precision and ability to generate a high current pulse.
- Example: CD (capacitor discharge) blasting machines.

1.1.4 Electronic Blasting Systems

- Advanced systems that use microprocessors to control the initiation sequence.
- They offer features like programmable delay sequences and enhanced safety mechanisms.
- Example: Electronic detonators with programmable delay options.

1.2. Operation and Safety

1.2.1 Initiation Process

- The blasting machine generates an electric current.
- The current travels through wires to the detonators.
- The detonators then initiate the explosive material.

1.2.2 Safety Measures

- Ensuring all personnel are at a safe distance before initiation.
- Using proper insulation and handling techniques to avoid accidental discharge.
- Regular maintenance and testing of blasting machines to ensure reliability.

1.3. Applications

- Mining: Used for breaking rock and ore to access mineral deposits.
- Construction: Demolition of buildings, road construction, and tunnelling.
- Military: Controlled explosions for clearing obstacles or demolitions. [1]

Capacitors used in the manufacture of mining blasting machines are capable of storing large amounts of electrical energy and releasing it rapidly to initiate a controlled explosion. Types of capacitors used include:

- Electrolytic capacitors. Commonly used because of their large capacity and relatively low cost. They can store a large amount of energy and release it quickly. They have a fairly short lifetime (especially those produced in the past).
- Metallized polypropylene capacitors. These capacitors are used because of their stability and ability to withstand high voltages. They have a long life and are reliable in harsh conditions.
- Ceramic capacitors. They are used in applications that require high thermal stability and good reliability. Their capacitance is small and they are rarely used as energy storage capacitors in the production of mining blasters.

These types of capacitors are selected according to their working (operating) voltage, energy storage capacity, physical size and reliability under extreme environmental conditions.

The mining blasting machines that were analysed in this paper used high-voltage (1000 ... 2000V) electrolytic capacitors with a large electrical energy storage capacity (2 ... 20 μ F).

The reliability of capacitor-based blasting machines depends on several factors, including the type and quality of capacitors used, circuit design and operating conditions.

Four types of mining blasting machines from different manufacturers were chosen for the analysis. The analysis was carried out on a total of 775 blasters. Most were of the Vopil M514 type (614 pieces). Vopil M514 are mining blasting machines with capacitor, inductor and gas tube trigger and were produced in the former German Democratic Republic since the 1960s.

2. CAPACITOR-BASED BLASTING MACHINES

2.1. Principle of operation

Capacitor-based blasting machines work by storing electrical energy in a capacitor. When this capacitor is charged to the required capacity, the stored energy is suddenly discharged to an electrical detonator, triggering the blast. [2]

2.2. Advantages of using capacitors

- Accuracy and control: Capacitor-based blasting machines can deliver accurate and controlled electrical pulses, essential for the safe initiation of explosive charges.

- Reliability: Compared to other types of blasting equipment, these machines are less prone to failure.

- Safety: Because the energy is not permanently available in the circuit, the use of capacitors reduces the risk of inadvertent triggering of the explosion. [3]

2.3. Main components

- Capacitor: Energy storage device.

- Charging circuit: The mechanism that charges the capacitor. The capacitor can be charged by an inductor or by a voltage boosting electronic circuit.

- Detonator: The device activated by the electrical impulse supplied by the capacitor to trigger the explosion, in other words the electrical fuse. [4]

2.4. Applicability

These blasting machines are widely used in mining, quarrying and other industries where controlled explosions are required to fragment rock or other materials. [5]

3. RELIABILITY OF CAPACITOR-BASED BLASTING MACHINES

Their reliability depends on several factors, including the type and quality of capacitors used, circuit design and operating conditions. Here are some key points:

3.1. Capacitor quality

The use of high-quality capacitors from recognised manufacturers contributes significantly to the reliability of blasters. Capacitors must be able to store and release the required energy consistently and reliably. Poor quality capacitors can lead to major failures and risks in mining operations. [6]

4. THE LIFESPAN OF HIGH-VOLTAGE ELECTROLYTIC CAPACITORS

The lifespan of high-voltage electrolytic capacitors varies significantly based on several factors, including operating temperature, voltage, and ripple current. Typically, high-quality electrolytic capacitors have a base lifespan of around 5,000 to 10,000 hours at their maximum rated temperature, usually 105°C. However, this lifespan can be extended by operating the capacitor under less demanding conditions.

A common rule of thumb is that for every 10°C reduction in operating temperature, the lifespan of an electrolytic capacitor doubles. For instance, if a capacitor rated for 5,000 hours at 105°C is operated at 85°C, its lifespan could extend to around 20,000 hours. [7, 8]

RELIABILITY OF BLASTING MACHINES USED TO INITIATE ELECTRICAL DETONATORS

Additionally, operating the capacitor at a lower voltage than its maximum rating can also improve its lifespan. For example, running a capacitor at 50% of its rated voltage can approximately double its lifespan. [9]

The ripple current also impacts the lifespan. High ripple currents generate more internal heat, which can shorten the capacitor's life. Operating at 50% of the rated ripple current can potentially increase the lifespan by about 23%. [9]

For a precise calculation of the expected lifespan under specific operating conditions, you can use the de-rating formula (Equations 1):

$$Life_{actual} = life_{base} \cdot temperatureFactor \cdot voltageFactor \cdot currentFactor \quad (1)$$

where each factor adjusts for operating conditions relative to rated conditions. [7, 8]

5. ANALYSIS OF DATA COLLECTED FOR THE STUDY OF RELIABILITY OF CAPACITOR-BASED BLASTING MACHINES

The data analysed and studied were taken from the certification reports issued after the periodic tests carried out at the Laboratory for Non-Electrical Ex Equipment, Electrostatics, Materials and PPE of INCD Insemex Petroșani. Data were collected from 775 certification reports over a period of 20 years (Table 1).

Table 1. Situation regarding the type of blasting machines and the number of inspections carried out at INCD Insemex Petroșani over a period of 20 years.

Year	Type and number of blasting machines checked			
	VOPIL M514	AICmI	EI-200D	ECI-100
2003	169	1	-	8
2004	55	4	5	7
2005	9	4	5	10
2006	146	10	6	2
2007	26	6	3	2
2008	97	10	3	2
2009	77	8	4	3
2010	18	3	-	-
2011	-	3	2	-
2012	-	-	-	-
2013	-	1	2	-
2014	2	3	2	-

2015	4	3	-	2
2016	-	-	-	2
2017	2	1	2	-
2018	-	-	-	1
2019	4	-	8	-
2020	2	-	2	-
2021	-	1	-	1
2022	1	4	5	-
2023	2	4	5	1
TOTAL	614	66	54	41

As can be seen from Table 1, most of the periodically inspected blasting machines were of the Vopil M514 type (Figure 1), 614 certification reports.



Fig.1. Vopil M514 Blaster machine

RELIABILITY OF BLASTING MACHINES USED TO INITIATE ELECTRICAL DETONATORS

The Vopil M 514 mining blaster is designed to trigger low-intensity electric detonators connected in series for carrying out blasting operations with explosives in mines with a risk of explosive atmosphere (coal mines).

The procedure for working with Vopil M 514 blasters is as follows:

- Connect the ends of the main ignition cable to the terminals on the blaster;
- Mount the operating crank and turn it clockwise at a speed of more than 4 revolutions per second until the "charged" signal lamp lights up and then until the explosion starts.

Technical data of Vopil M514:

- Rated voltage: 1800 V d.c.
- Capacity of the charging capacitor: 2 μ F
- Maximum number of low-current electrical detonators connected in series: 100 pieces
- Maximum circuit resistance: 510 Ω
- Type of detonator: low-current electric detonator
- Detonators must be connected in series only.

Since the analysis followed the behaviour of a mining capacitor-based blasting machine over time, and the data on Vopil M514 blasters was much more extensive than that on other types of blasters (EI-200D and ECI-100), only the behaviour of Vopil M514-type blasters was followed.

The AICmI type mining blasters are of a different generation, they are electronically triggered blasters, with firing circuit control, etc. They were not included in this analysis.

The analysis was carried out on data from 18 blasting machines over a period of 7 years (2003 ... 2010). Of the 169 Vopil M514 blasters from 2003, only 18 were still undergoing verification in 2010.

In the year 2023 only two blasting machines that had not been verified at INCD Insemex Petroşani and therefore were not taken in the study, arrived to be verified.

Data were available for 6 repairs. Repairs were made by replacing the storage capacitors in all cases, replacing the discharge tubes in 2 cases and re-magnetising the inductor stator in one case.

It was also found that in 2 blasting machines the stored energy had increased at some point which implies that they were repaired.

The study period was limited to only 7 years and to a set of 18 Vopil M514 blasters. It was found that 8 blasters were repaired during this period and therefore these were also removed from the analysis. In the end, only 10 blasters were analysed over a period of 7 years (2003 ... 2010).

The aim of the analysis was to determine the existence of a decrease in energy output over the life of the blasting machines and the possible causes of this decrease.

Data was collected from test reports which included records of output voltage and output energy.

The blasting machine shall be capable of reliably delivering sufficient ignition energy (kRe) to reliably ignite the maximum number of electrical detonators with the permissible ignition lead resistance in the circuit. [10]

The value of the output pulse is plotted over the seven years for the 10 blasting machines. (Figure 2).

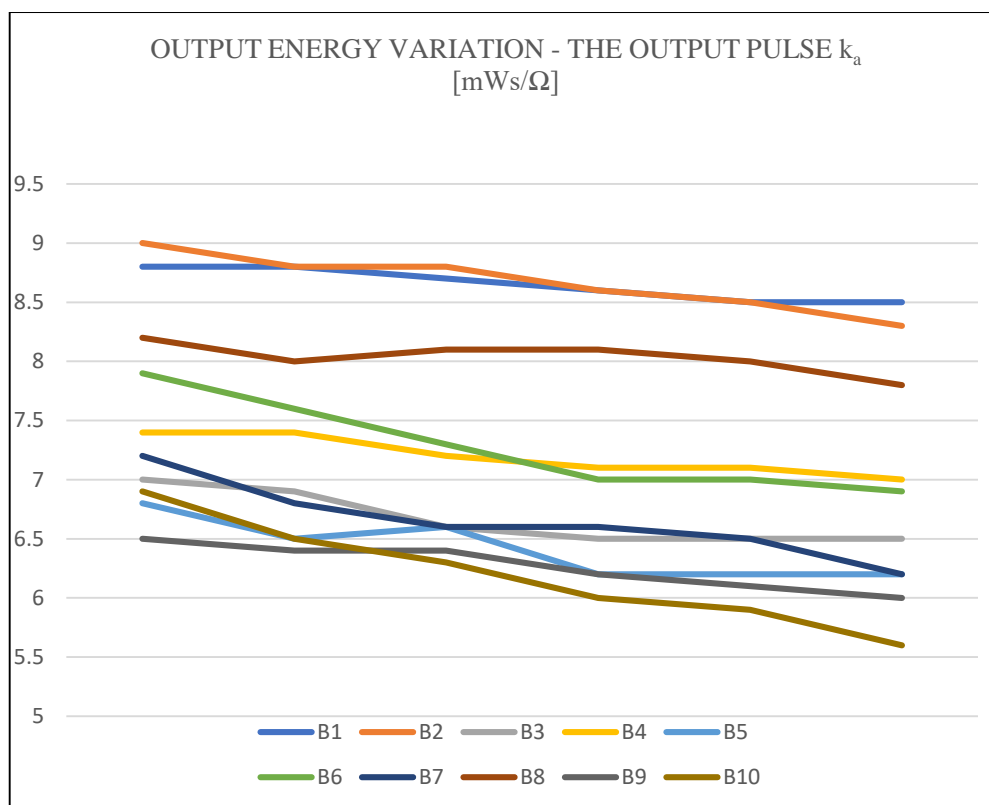


Fig.2. The output pulse variation

6. CONCLUSIONS

The analysis of the data collected over a period of 10 years from the certification reports issued by INCD Insemex Petroșani revealed the following:

- Table 1 shows a sharp decrease in the number of units inspected in 2010. This sharp reduction is due to the decline in the mining industry, particularly in the Jiu Valley. Financial problems and reduced production caused mining units to abandon many of the blasters they had previously used. Another explanation would be that they have started to carry out their own periodic checks.

- The longest-lived capacitor-based blasting machines were those produced in the GDR - Vopil M514.

- Vopil M514 blasters have electrolytic capacitors for energy storage, the required voltage is supplied by an electromagnetic inductor and the triggering is done by a gas tube.

- The graph in Figure 2 shows that there are variations in the energy released by the blaster, in the sense of a decrease, but the decrease is small and does not pose a

RELIABILITY OF BLASTING MACHINES USED TO INITIATE ELECTRICAL DETONATORS

problem, even though the blasters are very old (blasters produced from the 1960s to 1987 were studied).

- Reducing the output voltage and/or reducing the capacity of the energy storage capacitors can reduce the output energy.
- The drop in output voltage may be due to failure of the discharge tube (which sets the voltage at which the discharge occurs).
- The drop in energy may also be due to a reduction over time in the capacity of the capacitors that store electrical energy.
- A drop in the output voltage of the electromagnetic inductor causes the detonator to stop working as it is unable to charge the capacitor to a voltage sufficient to trigger it.
- Most repairs have been carried out by replacing the storage capacitors. The inductor stators were also re-magnetised and the gas discharge tubes replaced.
- It was found that users of Vopil M514 blasters were gradually replacing them with more modern, safer and more reliable electronic capacitor-based blasters, inductor-charged blasters or battery-charged blasters.
- Vopil blasters were very reliable blasters, simple in design, robust and well suited to the harsh working environment in which they were used.
- It was also found that the correct choice of components, robust circuit design and regular and careful maintenance are essential to ensure the reliability of mining blasters.
- The study would be more conclusive if data from more blasters could be collected. Many of the blasting machines verified at INCD Insemex in 2003, although still in use, have not been sent for verification and therefore traceability could not be achieved for them.
- A future comparative analysis of electronic and induction mining blasting machines can identify the advantages and disadvantages of the two types of mining blasting machines. Also, by collecting and analysing data from electronic mining blasting machines currently in use in mines, potential problems that may arise from long-term use can be identified.

REFERENCES

- [1]. **Bureau of Mines** *Explosives and Blasting Procedures Manual*. A comprehensive guide covering various aspects of blasting and explosives handling. <https://www.cdc.gov/niosh/mining/works/cover-sheet1510.html>
- [2]. **Bailey P.**, *Advancements in Mining Explosives and Detonator Technologies*. Mining Engineering Journal, vol. 70, no. 4, pp. 34-42, 2018.
- [3]. **Chen, Z., Wang, L.**, *Capacitor-based Blasting Systems in Modern Mining*. International Journal of Rock Mechanics and Mining Sciences, vol. 75, pp. 12-20, 2015.
- [4]. **Murray R.**, *Innovations in Blasting Technology*. Mining Technology, vol. 125, no. 3, pp. 50-58, 2016.
- [5]. **Roberts J.**, *Safety and Efficiency in Modern Blasting Practices*. Journal of Mining Safety, vol. 11, no. 2, pp. 22-30, 2017.
- [6]. <https://electronics360.globalspec.com/article/17742/factors-affecting-capacitor-reliability>

- [7]. <https://www.allaboutcircuits.com/news/calculating-the-lifespan-of-electrolytic-capacitors-with-de-rating/>
- [8]. <https://electrowebs.com/electrolytic-capacitor-info/>
- [9]. <https://resources.altium.com/p/electrolytic-capacitor-lifespan>
- [10]. SR EN 13763-26:2005 *Explozivi pentru uz civil. Capse detonante și relele întârziatoare. Partea 26: Definiții, metode și cerințe referitoare la dispozitivele și elementele necesare pentru fiabilitatea și siguranța în funcționarea a capselor detonante și a releelor întârziatoare*, 2005.

This article was reviewed and accepted for presentation and publication within the 11th edition of the International Multidisciplinary Symposium "UNIVERSITARIA SIMPRO 2024".

ASPECTS REGARDING THE USE OF VARIABLE SPEED DRIVES IN THE CASE OF EXPLOSION PROTECTED ELECTRIC MOTORS USED IN EXPLOSIVE ENVIRONMENTS

MIHAI MAGYARI¹, DRAGOȘ FOTĂU², SORIN ZSIDO³

Abstract: This paper presents some of the most important aspects that have to be considered regarding the functioning of variable speed explosionproof electric motors designed for use in explosive mixtures of gases and vapors, highlighting some of the most important technical issues which can occur in practice, as well as some practical solutions in terms of designing these types of electrical drives in order to overcome some of the short comes which can arise while functioning in various technical installations of operators in the oil and gas industry.

Key words: variable speed drive, explosionproof electric motor, explosive atmosphere.

1. GENERAL CONSIDERATIONS REGARDING VARIABLE SPEED DRIVES

Explosion protected electric motors, designed to operate safely in hazardous areas, such as oil and gas as well as chemical industry play a crucial role in preventing accidents. Variable speed drives (VSDs) have been developed in order to enhance both the safety and efficiency of these motors.

The reasons for a rotor cage three phase asynchronous electric motor to be supplied by a static frequency converter, instead of a sinusoidal supply, is to reduce the energetic consumption and to optimize the technological processes, improving the reliability and safety in operation. Equipment consisting of rotor cage three phase asynchronous electric motor supplied by a static frequency converter are designed to enhance the performances in exploitation, in the sense of reducing the energetic consumption, optimization of the technological processes, enhancing the reliability and safety in operation, simplification of the installation and reducing of the costs for the maintenance and repair of the overall equipment.

¹ Ph.D., Eng., mihai.magyari@insemex.ro

² Ph.D., Eng.

³ Ph.D., Eng.

Explosion protected electric motors are designed to prevent the ignition of surrounding explosive gases, vapors or dust. These motors have to be manufactured according to explosion protection standards they and have to comply with certain rules of certification, such as ATEX in Europe [1, 2] and IECEx globally, ensuring they can operate safely in classified hazardous areas.

The combination of an electric motor supplied via a frequency converter can be used in a wide range of power drives systems in which the variation of speed ensures the regulating of certain technological parameters (pressure, flow, etc.).

1.1. The Power Drive System

The concept of a power drive system (PDS) is used to describe an electric motor drive system within an overall installation. The terminology is used throughout IEC and EN standards relating to electrical variable speed drives to describe a combination of components, including a power converter and motor. The conventional illustration of a PDS and its component parts is shown in Figure 1 [3], [9], [11].

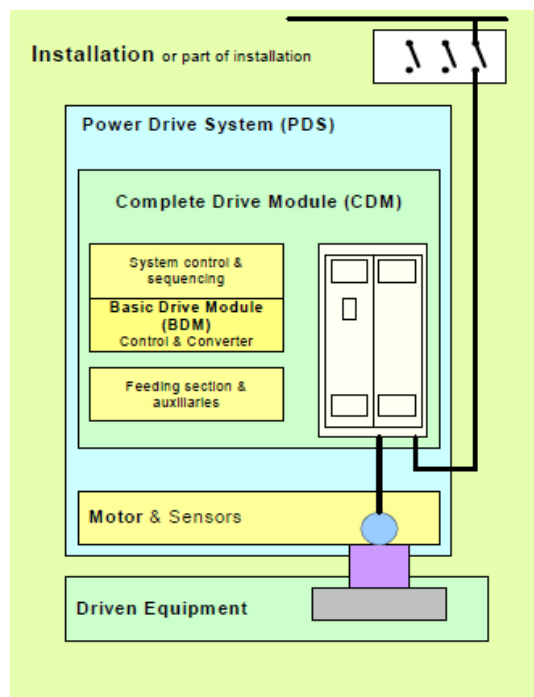


Fig.1. The Power Drive System

Where:

- BDM – Basic drive module consisting of power input, control and power output selections;
- CDM – Complete drive module consisting of BDM and auxiliary sections, but excluding the motor and motor – coupled sensors.
- PDS – Power Drive System, comprising CDM, motor and sensors.

2. POWER DRIVE SYSTEMS (PDS) USED IN POTENTIALLY EXPLOSIVE ATMOSPHERES

2.1. Operating conditions of the PDS

Usually only the motor and driven load will be installed in the potentially explosive atmosphere, with the converter supply operating in a safe area.

Compared to a motor connected directly to a mains supply, the motor manufacturer must take account of a converter supply changing the operation conditions mostly due to:

- reduced cooling for self-ventilated motors at reduced speed, due to reduced airflow;
- increased losses due to non-sinusoidal supply at the motor's terminals leading to increased temperature rise, compared to sinusoidal supply;
- specific additional heat generation, particularly in the rotor cage and supporting structure as a result of harmonic currents;
- induced voltages in the rotor, which can lead to currents through the bearings (due to PWM technology and high switching frequency);
- dielectric heating due to high frequency / voltages.

For these reasons the application of the ATEX Directive calls for an extra attention to be paid when an Ex-motor is used with a frequency converter (CDM), and may require them to be tested together for certification [1, 3], [10], [12].

2.2. Selection of Ex-motor and BDM/CDM for PDS applications

2.2.1. General

The safety aspects include ensuring that:

- no additional risks exist of sparks due to premature insulation failure or to shaft voltages / bearing currents;
- no additional risks exist of exceeding the temperature class due to extra losses and possibly lower cooling.

2.2.2. Risk management of sparks

The motor and converter manufacturers will ensure that bearing currents are limited and sparks are prevented using techniques including:

- suitable stator insulation materials and techniques;
- reduction of voltage transients, by use of electrical filters.
- prevention of excessive bearing currents, by use of insulated bearings or bearing houses, usually at the non drive-end of the motor, reduced or optimized switching frequency, or by the use of electrical filters.

2.2.3. Risk management of excess temperature

The temperature class of the motor shall be checked by calculation or by testing as required by the appropriate standard concerning the type of protection of the motor [5, 8].

There are two main methods for diminishing the risks of excess surface temperature:

- a) to have a physical feedback signal from the motor (thermal sensing element) and use this signal to initiate shut down in the case of excess temperature;
- b) to control and limit the heat (temperature) which can be generated by the motor.

Temperature sensing technique uses thermostats, thermistors or RTD devices embedded in the stator windings, with the appropriate controls to ensure that the temperatures are within the permitted limits.

This does not always control any additional temperature rise within the rotating element, and for high power motors the manufacturer / Notified Body may stipulate the use of additional thermal detectors at the bearings.

It is also mandatory that the protection used in conjunction with the temperature detectors is suitable for the purpose (including any intrinsic safety barriers where appropriate). As the correct functioning of the protection is critical to the safety of the overall system, the functional safety of the protection should be assessed and approved in accordance with the appropriate standards [5, 8], [13].

Control of heating is achieved by limiting the current passing through the motor at a specific frequency. As the torque generated is directly related to current, a loadability curve may be established, which gives the maximum continuously available torque at a particular speed or frequency. The curve is dependent on the motor design, and can be advised by the manufacturer. The loadability curves must take into account the CDM technology, the surface temperature class of the motor and the type of Ex protection (flameproof enclosure, increased safety, etc.).

In many cases a manufacturer will publish the loadability curves for his products to allow users to check that the load characteristics fall within the PDS capability. Figure 2 shows an example of a loadability curve for a cage induction motor, fed by an inverter. This shows the reduction in torque capability at low speeds due mainly to the reduction in ventilation, a reduction in torque at base speed to allow a sufficient margin for safety, and a reduction above base speed due to the application of a constant voltage (field weakening) [3, 6, 7].

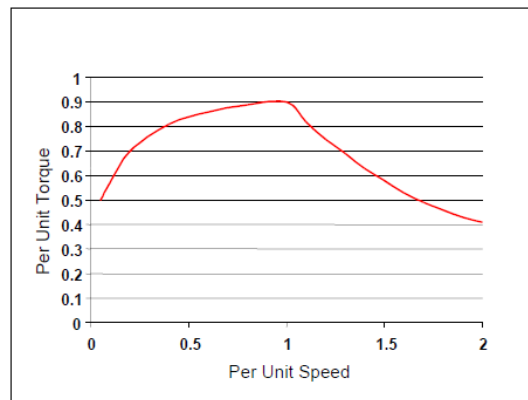


Fig.2. Example of loadability curve established by test for induction motor for PDS use

2.3. Specific requirements for flameproof “Ex d” and increased safety “Ex e” electric motors

In the case of flameproof Ex d electric motors, the following requirements apply [8]:

Flameproof electric motors Ex d supplied at variable frequencies and voltages require either:

a) means (or equipment) for direct temperature control with the help of imbedded sensors, which are specified in the technical documentation of the motor, or other effective means for the limiting of maximum surface temperature of the motor enclosure. The action of the protective device must lead to the disconnection of the motor supply. In this case, it is not mandatory to test the combination between the motor and the converter together; or

b) the motor to have been submitted to a type test, for this kind of service, as an assembly together with the converter, specified according to the provisions of the standard CEI 60079-0 and with the protective device provided.

The user must also observe that in some cases, the highest temperature occurs on the motor shaft and for motors with type of protection increased safety Ex e terminal boxes, when using converters with high frequency pulses in the output, care should be taken to ensure that any overvoltage spikes and higher temperatures which may be produced in the terminal box are taken into consideration.

As regards the type of protection increased safety Ex e, electric motors which use this type of protection and which are supplied at varying frequency and voltage by a converter, have to be type tested for this duty in association with the converter and the protective device. The motors should be used within their electrical rating and the converter configuration should be set to match the motor rating information with respect to frequency range and any other specified parameters such as minimum carrier frequency. The converter configuration shall enable to adjust the parameter [8].

The user shall also take into account that permanent magnet motors operate as a generator while coasting after the power is removed. In the case of Level of protection “eb” where the voltage can be greater than the rated voltage, the motor-converter system will need to be suitable for the voltages that will result [8].

3. PARTICULAR REQUIREMENTS IN THE CASE OF EXPLOSION PROTECTED ELECTRIC MOTORS SUPPLIED BY STATIC FREQUENCY CONVERTERS IN HAZARDOUS AREAS

3.1. Constructive characteristics

The electric motor has to be designed in such a way that the maximum surface temperature of the enclosure of the motor is less (with a certain safety margin) than the minimum ignition temperature of the gases and vapors which are specific to the application in which it will be used.

In order to check and measure the external temperature of the motor running at rated load, heating tests have to be carried out [5, 6].

Most electric motors which are normally rated in T4 temperature class are being tested by supplying via static frequency converter using a load characteristic according to Figure 3.

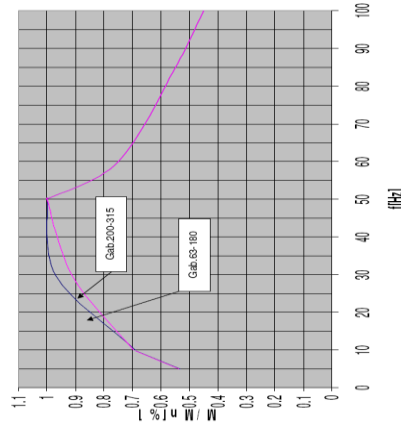


Fig.3. Loading characteristics [4]

3.2. Life expectancy of winding insulation

When the motor is supplied via a static frequency converter, the winding insulation system will be submitted to higher dielectric stresses, as compared to supplying the motor with sinusoidal voltages. When a current source converter is used, voltage peaks are likely to occur in the motor, especially during the commuting phase, voltage peaks which can lead to high stresses in the winding insulation system.

The dielectric stress of the winding insulation is caused by the peak voltage, the rise time and the frequency of the impulses produced by the converter, the characteristics and the length of the connections between the converter and the motor, the winding construction, as well as other parameters of the entire system.

In order to deal with this issue, filters are sometimes required to be used at the output of the converters [6, 7].

Due to the complex inter conditionings, it is necessary to have a careful design of the entire electric power drive. This requires sometimes the use of filters at the output of the converter [6, 7].

3.3. Thermal protection of the insulation

Usually, thermistors with positive temperature coefficient (PTC code), which are imbedded in the windings of the motor, are used for the temperature control of electric motors which are supplied by static frequency converters. These thermistors are connected to the protective device of the static converter, through the terminal box of the motor, thus ensuring that the motor can be disconnected safely from the electric power supply, in case of overloading conditions, so that the maximum temperature of the motor will not exceed the maximum admitted limits. The entire system comprising the electric motor and the frequency converter, for explosive atmospheres has to ATEX certified [1, 2,

8]. The motors are tested when supplied by the converter and the temperature of the motor is determined in order to predict the temperature evolution and to prevent the overheating of the motor [6, 7].

3.4. Bearing currents

Several situations can cause bearing currents and, in all cases, the bearing current will flow when the voltage is developed across the bearing sufficient to break down the insulating capacity of the lubricant.

The main sources for this voltage are:

- Asymmetry in the magnetic circuit of a motor creates a situation that causes slow frequency bearing currents (usually for motors with power greater than 400 kW);
- Electrostatic build up on the shaft of the motor due to the driven load such as an ionized filter fan;
- High frequency common mode voltage at the motor terminals generates common mode currents parts of which can flow through the bearings of the motor or of the driven equipment. The common mode currents may also generate a voltage across the bearings by transformer action. These effects result from the use of fast switching semiconductor devices and can cause bearing problems, due to different effects, in motors of all ratings.

In the case of generation of high frequency bearing currents, the most important factors that define which mechanism is prominent are the size of the motor and how the motor frame and the shaft are grounded. The electrical installation, meaning a suitable cable type and proper bonding of the earthing conductors and the electrical shield, also plays an important role, as well as the rated converter input voltage and the rate of rise of the converter output voltage. The source of bearing currents is the voltage across the bearing. There are three types of high frequency bearing currents: circulating, shaft earthing and capacitive discharge [7].

3.5. Supply cables and the distance motor – converter

Several parameters have to be considered for the determination of the cross section of the cable as well as the distance between the converter and the motor: the value of the current, the maximum diameter of the sealing gasket of the cable gland entry of the terminal box of the motor, the drop voltage across the cable, which can affect the motor parameters. By using frequency converters, it is possible to compensate the voltage drop across the supply conductors of motors which are located at great distances from the converter [6, 7].

3.6. Frequency/speed variation field and maximum safety speed in operation

Function of the design of the motor, operation at higher speeds can be allowed, but this possibility has to be checked by appropriate testing.

In the case of operation at speeds higher than the rated speed, the noise levels and the vibrations increase. It may be necessary to re-balance the rotor in order to operate at speeds higher than the rated speed.

Long term operation at speeds close to the maximum safety operation speed can lead to a considerable life shortening of the bearings.

This may also affect the sealing of the shaft and / or the lubrication intervals of the bearings [6].

4 CONSTRUCTIONAL AND FUNCTIONAL REQUIREMENTS IN THE CASE OF EXPLOSION PROTECTED (FOR EXAMPLE FLAMEPROOF ELECTRIC MOTORS „EX D”, SUPPLIED BY STATIC FREQUENCY CONVERTERS

Electrical motors which endorse the type of protection “flameproof enclosure” have to be designed and manufactured according to the specific standards EN 60079 – 0 and EN 60079 – 1, and have to be certified by a Notified Body in the European Union. The Notified Body will issue an ATEX certificate for the electric motor. The static converter is normally located outside the Ex classified area (see also subchapter 2.3).

The most important subassemblies of flameproof enclosure motors that endorse this type of protection are: stator casing, shields, rotor, fan and fan hood, terminal box, terminal box cover, as shown in Fig.4.

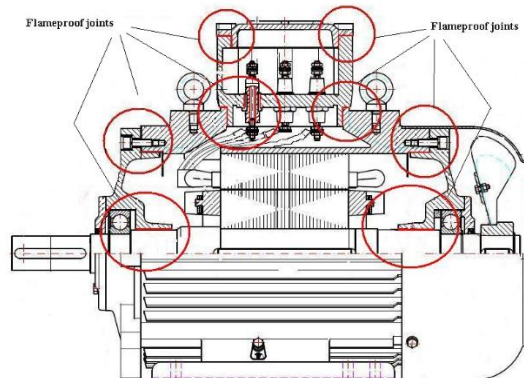


Fig.4. Flameproof enclosure motor assembly

In order to be ATEX certified, the electric motors designed with type of protection flameproof have to be submitted to certain tests and verification in explosive mixtures, according to the explosion group (or groups) for which the certification is sought. The enclosure of the motor (as well as the terminal box enclosure) have to withstand the following type tests and verifications [5]:

- reference pressure determination and overpressure test;
- test for non-transmission of an internal ignition.

In the case of reference pressure determination, each test consists of igniting an explosive mixture inside the enclosure and measuring the pressure developed by the explosion.

ASPECTS REGARDING THE USE OF VARIABLE SPEED DRIVES
IN THE CASE OF EXPLOSION PROTECTED ELECTRIC MOTORS
USED IN EXPLOSIVE ENVIRONMENTS

The explosive mixture is ignited by one or more ignition sources. The location of the ignition sources, as well as of the pressure recording devices is left at the discretion of the testing laboratory, based on its experience to find the combination that produces the highest explosion pressure. After that, the enclosure will also be tested for the ability to withstand 1.5 times this highest explosion pressure during the so called overpressure test, so that the manufacturer of the motor will have to design the enclosure for this new increased pressure of 1.5 times the reference pressure.

For the test for non-transmission of an internal ignition, which is normally carried out in a so called explosion chamber, in which the enclosure of the motor is placed, both the enclosure of the motor, as well as the explosion chamber are filled with the same explosive mixture, at the concentration required by the specific standard (EN 60079-1).

The explosive mixture in the enclosure of the motor is then ignited using an ignition device and it is observed whether the explosion inside the enclosure is transmitted to the explosive mixture outside the enclosure (explosion chamber). This is a yes / no test (a qualitative test), the only result that matters is whether the internal ignition of the explosive mixture has been transmitted or not, to the external surrounding atmosphere.

The electric motors are normally designed for use in hazardous gases and vapors related to explosion groups IIB or IIC (which contains the most dangerous gases, in terms of their explosion potential). The temperature class of these motors (that is the maximum external surface temperature that can be obtained in normal operation, including any abnormal operation, such as overloads, which are admitted by the manufacturer) is normally rated T3, T4, T5, or in some cases even T6, depending on the maximum ambient temperature and rated power of the motor as well as the frame size of the motor involved.

The terminal box (or terminal boxes) of the motor is normally also designed with type of protection flameproof enclosure, but it can also endorse other types of protection, such as increased safety Ex e, which can easily be used in association with the flameproof type of protection of the stator frame of the electric motor.

As far as the environmental conditions are concerned, most electric motors are manufactured for operating and transport in areas with temperate climate, but of course, on request, they can be designed for use in other areas, as well.

5. LEGAL REQUIREMENTS REGARDING THE SAFETY IN OPERATION FOR EXPLOSION PROTECTED ELECTRIC MOTORS SUPPLIED BY STATIC FREQUENCY CONVERTERS

5.1. Classification of environment and equipment according to the ATEX Directives

The European Union has adopted two major Directives covering all equipment used in a potentially explosive atmosphere:

- the Product Directive ATEX (officially known as the product Directive 2014/34/EU,) concentrates on the responsibilities of the equipment manufacturer and It defines the Essential Health and Safety Requirements (EHSRs) of equipment;

- the Worker Protection Directive ATEX 137 (officially known as the Worker Protection Directive 1999/92/EC).

This Directive is concerned specifically with Worker Protection, and concentrates on the responsibilities of the end user. It classifies the environment into Zones and states which Category of equipment must be used in each Zone.

5.2. The product Directive 2014/34/EU

This “Product Directive” is required to be implemented by the product manufacturer before a product may be placed on the European market for use in a potentially explosive atmosphere. This Directive constitutes a real “new approach” compared to previous directives. According to this “new approach” the ATEX Directive introduces the EHSRs needed for all equipment installed in potentially explosive atmospheres instead of prescriptive solutions given in previous directives. Directive ATEX 2014/34/EU applies consistently throughout the EU and the EEA [1].

All equipment shall be delivered with instructions for safe:

- assembling, installation and taking into service;
- operation, adjustment and maintenance;
- dismantling.

The manufacturer shall, in most cases, use a quality management system for production quality or product quality assurance that has been assessed and approved by a Notified Body, chosen by the manufacturer.

5.3. The Working Protection Directive 1999/92

Among different articles, this Directive specifies:

- places where explosive atmospheres may occur (Zones);
- category of equipment according to the Zone.

The users of all equipment used in potentially explosive atmospheres (Ex – equipment) are responsible for the application of this Directive.

For the first time, the Directive contains requirements for equipment and for worker protection in locations having atmospheres with potentially combustible dust.

The safety of an installation in a potentially explosive atmosphere is the result of a cooperation between the equipment manufacturer, the installer and the end user. This directive concentrates on the duties of the end user, which are [2]:

· explosion protection measures should be taken and an Explosion Protection Document (EPD) must be established;

- zone 0 or zone 20 requires category 1 equipment;
- zone 1 or zone 21 requires category 1 or category 2 equipment;
- zone 2 or zone 22 requires category 1 or category 2 or category 3 equipment;

The most important PDS related responsibilities are:

- the employer should train workers on potentially explosive atmosphere issues;
- authorisation should be delivered to each employee who is working in a potentially explosive atmosphere;

ASPECTS REGARDING THE USE OF VARIABLE SPEED DRIVES
IN THE CASE OF EXPLOSION PROTECTED ELECTRIC MOTORS
USED IN EXPLOSIVE ENVIRONMENTS

- explosion protection measures shall be taken and an Explosion Protection Document (EPD) shall be established;
- the employer should initiate a co-ordination procedure in the case of maintenance of equipment from different 'origins' in potentially explosive atmospheres. When equipment has to be repaired, the end user has the responsibility to select a competent repair shop and, where spare parts are used, to ensure they comply with the legislation where relevant;
- the employer shall implement the following equipment selection principles:
 - zone 0 or zone 20 requires category 1 equipment;
 - zone 1 or zone 21 requires category 1 or category 2 equipment;
 - zone 2 or zone 22 requires category 1 or category 2 or category 3 equipment.

Compliance with the ATEX Directives provides improved safety aspects, first of all by simplicity, because there are only two fields of responsibility. Third parties are responsible either to the manufacturers or by default to the end users, and the duties of each party are clearly defined in the specific standards (Figure 5) [3].

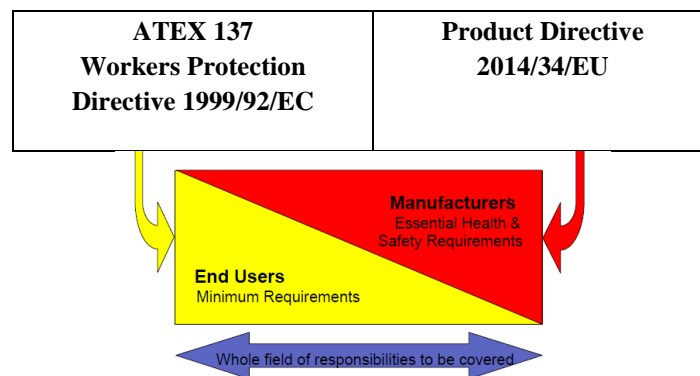


Fig.5. Responsibilities

6. CONCLUSIONS

Variable Speed Drives represent a significant advancement in the operation of explosion protected electric motors in hazardous environments. By enhancing safety, improving energy efficiency and offering greater operational flexibility, VSDs contribute to the reliable and efficient performance of critical industrial processes.

As industries continue to prioritize safety and efficiency, the adoption of VSDs in explosion protected motors is set to become increasingly prevalent, driving further innovations and improvements in this vital field.

The aim of this paper is to give the user of such a system, made up of a motor supplied by a converter designed for use in potentially explosive atmosphere an overview of what the implications are, when such a system is used in a hazardous location, specific to refineries, chemical and petrochemical industries. The most important aspects that have to be observed are the following:

- Particular requirements in the case of explosion protected electric motors supplied by static frequency converters in hazardous areas;

- Constructional and functional requirements in the case of explosion protected (for example flameproof electric motors Ex d, supplied by static frequency converters, as well as the requirements concerning the ability to function of variable speed explosion protected electric motors in potentially explosive atmospheres;
- Legal requirements regarding the safety in operation, of variable speed electric motors, used in hazardous locations, according to the European Directives which regulate this field of activity.

REFERENCES

- [1]. *** Directive 2014/34/EU of the European Parliament and of the Council of 26 February 2014. Official Journal of the European Union, no. 96, 2014.
- [2]. *** Directive 1999/92/EC (ATEX 137) of the European Parliament and the Council of 16 th December 1999 on the minimum requirements for improving the health and safety protection of workers potentially at risk from explosive atmospheres, 1999.
- [3]. *** CEMEP European Directives – Application of the ATEX Directives to Power Drive Systems (PDS), 2006.
- [4]. *** Technical specification S.C. UMEB S.A. ST 45: Flameproof three phase induction cage asynchronous motors for potentially explosive atmospheres of group IIC. Ex d / de, framesizes 63 – 315 with variable speed, 2007.
- [5]. *** IEC 60079-1 Edition 7.0 Explosive atmospheres. Part 1: Equipment protection by flameproof enclosures “d”, 2014.
- [6]. *** SR CEI 60034-17, Rotating electrical machines. Partea 17: Cage induction motors when fed from converters. Application guide, 2003.
- [7]. *** SANS 60034-25, Rotating electrical machines. Part 25: Guide for the design and performance of cage induction motors specifically designed for converter supply, 2007.
- [8]. *** IEC 60079-14 Explosive atmospheres. Part 14: Electrical installations design, selection and erection, 2013.
- [9]. **Pana L., Janusz G., Pasculescu D., Pasculescu V. M., Moraru R. I.**, Optimal quality management algorithm for assessing the usage capacity level of mining transformers, Polish Journal of Management Studies 18, no. 2, 233-244, 2018.
- [10]. **Marcu M., Niculescu T., Slusariuc R. I., Popescu, F. G.**, Modeling and simulation of temperature effect in polycrystalline silicon PV cells, IOP Conference Series: Materials Science and Engineering, Vol. 133, No. 1, pp. 012005, 2016.
- [11]. **Petrilean, D. C. ;Irimie, S. I.**, Solutions for the capitalisation of the energetic potential of sludge collected in Danutoni wastewater treatment plant, Journal of Environmental Protection and Ecology, Vol.16 No.3 pp.1203-1211, 2015.
- [12]. **Handra A.D., Popescu F.G., Păsculescu D.**, Utilizarea energiei electrice: lucrări de laborator, Editura Universitas, 2020.
- [13]. **Arad, S., Marcu, M., Pasculescu D., Petrilean D.C.** Aspects of the electric arc furnace control, Proceeding. of international symposium advanced engineering & applied management, Faculty of Engineering Hunedoara, 2010.

This article was reviewed and accepted for presentation and publication within the 11th edition of the International Multidisciplinary Symposium "UNIVERSITARIA SIMPRO 2024".

ASPECTS OF EARTHING OF INSTALLATIONS IN ENVIRONMENTS WITH POTENTIALLY EXPLOSIVE ATMOSPHERES

MIRELA ANCUȚA RADU¹, CĂTĂLIN MIHAI POPA², ANA PETRINA PĂUN³

Abstract: In environments with potentially explosive atmospheres, earthing protection covers three aspects: protection against electric shock, prevention of electrostatic discharges from equipment/facilities, processed materials or people, and protection against atmospheric discharges. The paper presents some aspects regarding the specific requirements for earthing protection in atmospheres with the risk of explosive atmospheres that must be taken into account when evaluating the risk of explosions. Norms and reference standards are also highlighted, which are constantly changing in step with the latest scientific achievements, emphasizing the importance of updating them with the latest information.

Key words: potentially explosive atmospheres, earthing protection, grounding.

1. INTRODUCTION

In general, the protective earthing system is designed for protection against electric shocks – standards SR HD 60364-4-41:2017/A12:2020/IEC 60364-4-41 and protection against lightning – standards series SR EN 62305-x/ IEC 62305. In addition, in installations in environments with potentially explosive atmospheres, earthing systems (earthing protection) must provide protection against static electricity.

In this work, some particular aspects are highlighted for the protection against electrostatic discharges by grounding installations in Ex environments.

2. PREVENTING DANGEROUS STATIC ELECTRICITY BY GROUNDING

In industrial environments where potentially explosive atmospheres exist, there are many conductors that, if not properly grounded, can become charged to a

¹ Sc. Res.Assist, PhD. Stud. Eng., INCD-INSEMEX Petroșani, mirela.radu@insemex.ro

² Sc. Res., Ph.D.Eng., INCD-INSEMEX Petroșani, mihai.popa@insemex.ro

³ Ph.D., Lecturer Ec., University of Petroșani, stanciu.anapetrina@yahoo.com

dangerous level. Some of these are component parts of the plant or equipment used and include: plant structure, reaction vessels, pipes, valves, storage tanks and drums. Other parts are there only by accident or carelessness, for example: pieces of wire that are no longer needed, metal containers floating in medium or weakly conductive liquids, or tools accumulating conductive liquids on the surface of insulating materials.

Charges built up on one conductor can then be discharged to earth or to another conductor with the release of all stored energy as a single spark which may be sufficient to ignite the explosive mixture as in Fig 1.

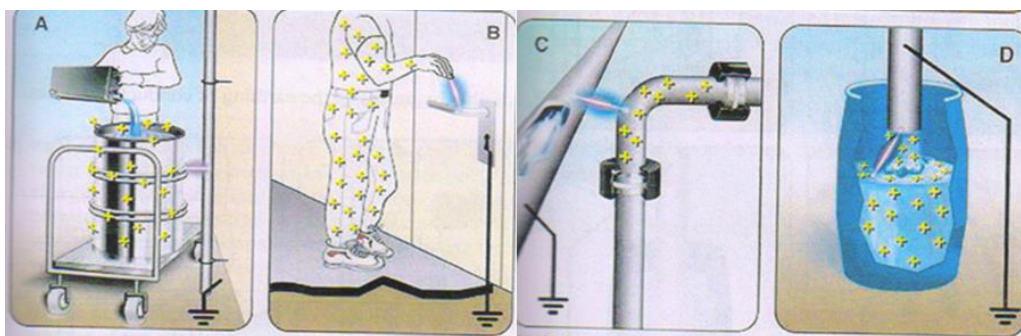


Fig. 1. Electrostatic spark discharges

The most effective way to avoid the dangers of static electricity is to bond all conductors together and then to ground. Bonding the components together is used to minimize the potential difference between conductive objects to an insignificant level, even when the resulting system is not grounded. Grounding, on the other hand, equalizes the potential differences between objects and the ground.

Examples of connecting the components to each other and grounding are shown in Fig 2.

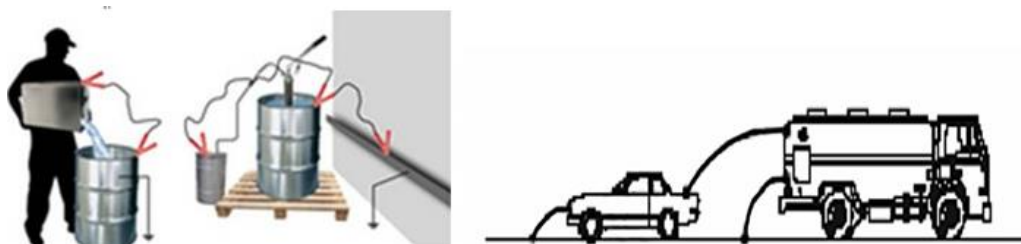


Fig. 2. Earthing and Bonding

A conductive object can be grounded by a direct conductive path to earth or by bonding it to another conductive object that is already grounded. Certain objects are inherently bound to others or inherently grounded due to their contact with the ground. The total resistance between an object and ground is the sum of the individual resistances of the grounding conductor, its connectors, other conductive materials along the desired grounding path, and the resistance of the grounding electrode (i.e. the grounding rod).

3. DISSIPATION CRITERIA OF STATIC ELECTRICITY FROM A CONDUCTOR

The resistances of the electrical paths must be low enough to allow the relaxation of the load and to prevent potential build-up on the conductor to a dangerous level. If this potential is V , the maximum allowed value of the resistance R depends on the rate at which the conductor receives charges, i.e. the charging current I . Because of this principle, the total resistance to earth must not exceed the acceptable level given by the equation:

$$V = I \cdot R \quad (1)$$

To prevent all incendiary discharges it is necessary to ensure that the conductor does not reach the potential necessary to initiate an incendiary discharge. For normal industrial operations this potential is at least 300 V. Using the value of 100 V as the limit value for safe dissipation of static electricity, the value of the total earth resistance R , can be calculated as follows:

$$R = \frac{100}{I} \quad (2)$$

where : R is in ohms

I is in amps

When specifying grounding requirements, each concrete situation must be taken into account, i.e. each individual value of the load current I . Since it is known that the charging currents are in the range between 10 pA and 100 μ A, the corresponding values of R are between 10 T Ω and 10 M Ω . For a maximum value of I , a ground resistance of 1 M Ω will ensure safe dissipation of static electricity under all conditions.

However, in most industrial operations I does not exceed 1 μ A and the conductor capacitance C does not exceed 100 pF. In this case the ground resistance of 100 M Ω is appropriate.

Conductors that have good contact with the ground have a ground resistance of less than 10 Ω . Although a value of up to 1 M Ω is acceptable for static dissipation, values greater than 10 Ω may give an early indication of developing problems (eg corrosion or a poor connection) and should be investigated. It is important that all connections are reliable, permanent and not damaged.

A clear distinction must be made between a value chosen for convenience when monitoring metal-to-metal connections and the 1 MW value which represents the upper limit of the ground resistance of a conductor in all situations. What is most important, however, is that all connections are reliable, permanent and not subject to damage.

Mobile metal elements require special grounding connections, which must have a resistance of less than 1 MW.

In IEC 60079-32-1 TS [1] maximum grounding resistances are given for static electricity control for specific applications.

In some cases values up to $10^8 \Omega$ are acceptable, especially when the conductor capacitance does not exceed 100 pF.

If the common bonding/earthing system is all metal, typically the resistance of the paths to earth is less than 10Ω . Such systems include those with multiple components. Higher resistance usually indicates that the metal path is not continuous, usually due to corrosion and loose connections. A grounding system that is acceptable for power circuits or for lightning protection will be more than adequate for static electricity grounding.

An important element of protective earthing installations is the earthing socket. The requirements for the resistance of the earth plug are given in the norms I7 and NP 099 [2], [3] [12], [13], [16].

According to point 5.5.7.11. from the standard I7:2011, the resistance of the earth socket can be:

- not more than 4 ohms when used only for protection against electric shock
- not more than 1 ohm when it is shared with the earthing socket for the lightning protection installation of the building.

According to point 12.3.6. from the norm NP 099, the earth socket of the lightning arrester installation is designed according to the provisions of I 20. The dispersion resistance value of the artificial earth plug that is used exclusively for the lightning arrester installation must be a maximum of 5 ohms for installations mounted on the construction and a maximum of 10 ohms for independent lightning arrester installations.

Normative I7 from 2011 with updates from 2023 applies to the design, execution and operation of electrical installations related to buildings, regardless of the form of ownership, including electrical equipment located in environments with a risk of explosion, to which the provisions of NP 099- 04. The regulation NP 099-04 (revision of ID 17-1986) for the design, execution, verification and operation of electrical installations in areas with explosion hazard was developed in 2005 and was not updated with the requirements of the new regulations and standards. With regard to protection by grounding for protection against dangerous static electricity and against atmospheric discharges, reference is made to standard I 20, which, however, is canceled and included in standard I7.

Since the rules and standards in force (latest editions) must be respected when designing and implementing earthing protection systems, they must be updated whenever changes occur in order not to create confusion or contradictions.

4. ASPECTS OF GROUNDING OF MOBILE EQUIPMENT

The grounding requirements of mobile equipment in potentially explosive atmospheres to prevent electrostatic spark discharges are revealed in many studies, in norms and standards, but in practical activity it is found that there are many aspects that are not well managed and that could be a source of danger of ignition of explosive atmosphere by electrostatic discharges. The grounding of fixed equipment is somewhat

easier to achieve and control with technical means. A more sensible approach is to make temporary connections to mobile equipment which can be made using pressure type earth clamps or other special clamps. Temporary grounding connections of movable elements can be made with screws, pressure-type earthing clamps or other special clamps. Pressure clamps must have sufficient pressure to penetrate any coating of paint, rust or spilled material to ensure contact with the metal base.

When flammable or combustible products are handled and processed in hazardous areas, it is essential to use certified equipment to protect personnel from electrostatic ignition sources. Certification of equipment for explosive atmospheres requires compliance with the requirements of the ATEX Directive [4], [14], [15], [17].

The question is asked: Earthing clamp shall it be Ex or not? Does the earthing clamp fall within the scope of the directive or not?


Electrostatic discharge, as a source of ignition, is often within the control of the design of the installation, rather than the equipment, and comes within the scope of the ATEX "workplace" Directive 1999/92/EC [5], backed up by standards providing appropriate detailed information.

However, the design of equipment can help to mitigate such risks and appropriate requirements are detailed in European harmonized standards.

Where equipment is otherwise outside the scope of Directive 2014/34/EU, the potential for a static discharge in use does not bring it into scope.

The answer to the question is given in Borderline list – ATEX products from **ATEX 2014/34/EU Guidelines-5th Edition**

Table 1. Timers configuration and executed sequences

Products	Scope of 2014/34/EU	Examples of products	Comments
Simple earthing clamps with and without cord	No		"Simple earth clamps" are clamps with a single earth connection. The clamp shall provide evidence that it is actually making contact. No own source of ignition, and for additional considerations, see note 2.
Complex earthing clamps with and without cord	Yes (Electrical)		The clamp shall provide evidence that it is actually making contact. Potential ignition sources cannot be excluded according to the ignition hazard assessment.

Note 2: Equipment, protective systems, Ex components, safety, controlling, regulating devices and/or other products indicated as not falling within the scope of the ATEX Directive 2014/34/EU, ignition sources and explosion hazards related to the use shall be considered. Friction impacts and abrasion processes involving rust and light metals (e.g. aluminum and magnesium) and their alloys may initiate an aluminothermic (thermite) reaction, which can give rise to particularly incensive sparking.

Although European directives, transposed into national legislation, require employers to assess the risk of explosions and take all measures to prevent ignition sources by using equipment that complies with ATEX requirements, there is a weak application of them in the case of pliers grounding, in many applications using classic clamps for which there are no documents attesting the technical and security performances.

Both IEC 60079-32-1 [1], 13.4.1 and NFPA 77 [6], 7.4.1.6 & 7.4.1.4 state: temporary connections can be made using bolts, pressure-type earth (ground) clamps, or other special clamps. Pressure-type clamps should have sufficient pressure to penetrate any protective coating, rust, or spilled material to ensure contact with the base metal with an interface resistance of less than 10 Ω .

Where wire conductors are used, the minimum size of the bonding or earthing wire is dictated by mechanical strength, not by its current-carrying capacity. Stranded or braided wires should be used for bonding wires that will be connected and disconnected frequently.

However, suppliers have appeared on the market that guarantee these performances, sometimes even through certification of compliance with the ATEX Directive and the applicable standards [IEC 60079-32-1, NFPA 77, SR EN 80079-36, SR EN 80079-37] [1], [6], [7], [8].

Some static earth clamps on the market combine ATEX certification with Factory Mutual approvals, being rigorously tested and certified to ensure they are capable of dissipating static charges from potentially loaded equipment. This is especially important when the equipment may be covered with product deposits or rust that are capable of preventing the clamp from making low-resistance electrical contact with the equipment to be grounded. Establishing a solid electrical connection can only be achieved by penetrating any connection inhibitors such as coatings, product deposits and rust. Factors such as these will prevent the dissipation of static charges from the object to ground if the clamp is not able to penetrate them and make a connection to the base metal of the container or vessel. Once a strong connection is established, it is vital that this connection remains constant throughout the operation of the process. Factory Mutual approved clamps undergo a series of mechanical and electrical tests to ensure they can perform as reliable static grounding clamps in EX/HAZLOC areas. ATEX certification ensures that there are no sources of mechanical sparks such as thermosetting materials or aluminum, or sources of stored mechanical energy, present in the construction of the clamp.

There are four good reasons to use FM approved clamps:

- Clamp Pressure Testing ensures the grounding clamp is capable of establishing and maintaining low resistance electrical contact with equipment
- Electrical Continuity Testing ensures the electrical continuity from the teeth throughout the grounding clamp is less than 1 ohm
- High Frequency Vibration Testing ensures the grounding clamp is capable of maintaining positive contact when attached to vibrating equipment
- Mechanical Pull Testing ensures the grounding clamp cannot be pulled off the equipment without an intentional application of force.

Also using certified ATEX certified clamps ensures that no sources of mechanical sparks are present in the clamp.



Fig. 3. Static Grounding Clamp capable of breaking through coatings, product deposits and rust to ensure a good electrical connection to process equipment

A wide range of ATEX certified clamps are available on the market - simple clamps (Fig 3) as well as self-testing clamps with LED indication or Grounding Clamp With Visible & Audible Alarms (Fig 4), as well as ground monitoring systems with interlocking control.



Fig. 4. Grounding Clamp With Visible & Audible Alarms [9,10]

A good example of ground monitoring systems with interlock control are grounding installations that not only provide a grounding solution but also monitors earth resistance, like battery operated clamps for hazardous environments and specialized earthing systems for road tankers, which designed to break the flow of flammable liquid using relays (figure 5)

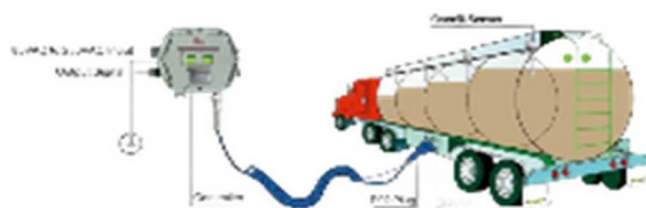


Fig. 5. Grounding Clamp With monitoring system with interlocking control

5. ENSURING SAFETY AND RELIABILITY IN MODERN INFRASTRUCTURES WITH GROUND RESISTANCES DETECTOR

5.1. Detecting corrosion and other issues

Grounding systems are susceptible to various forms of degradation over time. Ground Resistances Detector are designed to detect issues such as chemical corrosion, metal oxidation, galvanic corrosion, lightning-induced damage, and natural dissolution. By identifying these problems early, the detector helps prevent serious safety hazards and costly repairs.

Corrosion and other forms of degradation can significantly impact the performance of grounding systems. Chemical corrosion occurs when grounding electrodes react with soil chemicals, leading to material loss and increased resistance. Metal oxidation, a common issue in moist environments, results in the formation of non-conductive oxide layers on the electrodes. Galvanic corrosion happens when different metals in the grounding system come into contact, causing one metal to corrode faster than the other. Lightning-induced damage can alter the physical properties of grounding conductors, compromising their effectiveness.

Using the Ground Resistances Detector ensures that these problems are detected early, allowing for timely maintenance and repairs. The most modern Ground Resistances Detector are ground resistance online detector (Fig 6). Through remote monitoring and management of the grounding system, problems can be discovered and handled in time to ensure the safety of production facilities and personnel.



Fig. 6. Ground resistance online detector [11]

A ground resistance online detector is a device designed to continuously monitor the resistance of grounding systems. Unlike traditional methods that require periodic manual testing, these detectors offer real-time data, enabling prompt detection of any issues. This technology is particularly valuable for buried grounding networks, which are often out of sight and difficult to inspect manually.

Ground resistance online detectors utilize advanced sensing techniques to measure the resistance between grounding electrodes and the earth. These devices typically can detect minute changes in resistance, indicative of potential issues within the grounding system. By providing continuous data, ground resistance online detectors allow for early detection of problems such as corrosion or disconnection of grounding conductors. This proactive approach enables maintenance teams to address issues before they escalate, ensuring the integrity and safety of electrical installations.

6. VERIFICATION/MONITORING OF GROUNDING SYSTEMS

Checking earthing as protection against static electricity should be recognized as different from checks made for other purposes such as: maintenance of earthing systems associated with electrical power supply systems and lightning protection installations. Checks must be made both before the plant is put into operation and periodically, and the check documents must be available.

It is desirable to implement automatic monitoring systems that can not only monitor the resistances but also warn about their changes.

It is recommended that employers who, according to Directive 1999/92/Ce, are obliged to take all measures to prevent and protect against explosions, including protection by grounding, treat the grounding installation in the chapter on the assessment of the risk of explosions generated by electricity static from the Explosion Protection Document, in accordance with the requirements of applicable norms and standards. In addition, it must ensure the compliance of the equipment used with the requirements of the ATEX Directive (certificates of conformity) as well as the verification of the installation by competent persons (documents, records). Is recommended **Ensuring Safety and Reliability in Modern Infrastructures whit special devices such as** Grounding Clamp With monitoring system with interlocking control and **Ground Resistances Detector**.

7. CONCLUSIONS

Grounding protection installations in environments with potentially explosive atmospheres must ensure, in addition to electrical protection, protection against atmospheric discharges and protection against dangerous static electricity.

The most effective way to avoid the dangers of static electricity is to bond all conductors together and then to earth, thus preventing electrostatic spark discharges that could ignite the explosive atmosphere.

The methods and means of grounding, protection against dangerous static electricity, must correspond to the norms and standards in force in the electrical field and ATEX.

The paper highlights the importance of certifying the compliance of Static Grounding Clamp with the requirements of the ATEX directive but also with the mechanical requirements, to ensure the necessary pressure so that they are capable of breaking through coatings, product deposits and rust to ensure a good electrical connection to process equipment.

Employers responsible for the explosion protection of installations in environments with potentially explosive atmospheres must apply the best solutions for protection. Therefore, it is recommended that employers responsible for ensuring the security and reliability of grounding protection systems use modern devices that can not only monitor the resistances, but also warn of changes in the resistance.

It is recommended that employers who, according to Directive 1999/92/Ce, are obliged to take all measures to prevent and protect against explosion, treat the earthing installation in the chapter on the assessment of the risk of explosions generated by

static electricity in the Explosion Protection Document in compliance with the requirements of applicable norms and standards. In addition, it must ensure the compliance of the equipment used with the requirements of the ATEX Directive (certificates of conformity) as well as the verification of the installation by competent persons (documents, records).

The paper also presents some inconsistencies in the rules in force that are not updated with the new standards and that must be revised in order to be used correctly in the design, installation, maintenance and verification of earthing protection installations.

REFERENCES

- [1]. Ghid IEC **60079-32-1**
- [2]. Normativ **I7** (2011)
- [3]. Normativ **NP 099** (2004)
- [4]. Directive **2014/34/EU** (2014)
- [5]. **HG 1058** (2006)
- [6]. Ghid **NFPA 77** (2024)
- [7]. Standard **SR EN ISO 80079-36**(2016)
- [8]. Standard **SR EN ISO 80079-37** (2016)
- [9]. <https://cmctechnologies.net.au/solutions/explosion-prevention-protection/static-earthing/alptec-grounding-clamps/>
- [10]. <https://cmctechnologies.net.au/solutions/explosion-prevention-protection/static-earthing/alptec-grounding-reels/>
- [11]. <https://www.sltup.com/Ground-Resistance-Online-Detector-Ensuring-Safety-and-Reliability-in-Modern.html>
- [12]. **Andras A., Popescu F.D., Radu S.M., Pasculescu D., Brinas I., Radu M.A., Peagu D.**, *Numerical simulation and modeling of mechano–electro–thermal behavior of electrical contact using comsol multiphysics*. Applied Sciences, 14(10), 4026, 2024.
- [13]. **Handra A.D., Popescu F.G., Păsculescu D.**, *Utilizarea energiei electrice: lucrări de laborator*, Editura Universitas, 2020.
- [14]. **Fîță N.D., Radu S.M., Păsculescu D., Popescu F.G.**, *Using the primary energetic resources or electrical energy as a possible energetical tool or pressure tool*, In International conference KNOWLEDGE-BASED ORGANIZATION, vol. 27, no. 3, pp. 21-26. 2021.
- [15]. **Petrilean D.C., Popescu D.F.**, *Temperature Determination in Hydrotechnical Works as a Variable of the Energy Change Between Air and Environment*, WSEAS TRANSACTIONS on HEAT and MASS TRANSFER, 2008.
- [16]. **Irimie S.I., Radu S.M., Petrilean D.C., Andras A.**, *Reducing the environmental impact of a gas operated cogeneration installation*, MATEC Web Conf. Volume 121, 8th International Conference on Manufacturing Science and Education – MSE “Trends in New Industrial Revolution” Environmental Engineering, 2017.
- [17]. **Petrilean D. C.**, *Transmiterea căldurii*, Editura Universitas, 2016.

This article was reviewed and accepted for presentation and publication within the 11th edition of the International Multidisciplinary Symposium "UNIVERSITARIA SIMPRO 2024".

DEVELOPING AN AUTONOMOUS DRONE FOR EARLY DETECTION OF FOREST FIRES

REMUS SIBIŞANU¹, TUDOR MANOLE², COSMIN RUS³

Abstract: This research aims to develop an autonomous drone system for early detection of forest fires. By integrating specialized sensors with AI algorithms, the drone can quickly identify fire outbreaks in remote areas, enabling prompt responses to potential threats. The study provides a detailed analysis of sensor capabilities and data collection methods to optimize detection accuracy. Advanced AI algorithms, such as machine learning and computer vision techniques, are utilized to enhance real-time data processing and decision-making. The system architecture is robust and scalable, allowing deployment in diverse forest environments. The focus is on ensuring the drone's autonomy for navigating challenging terrains and performing continuous monitoring without human intervention. Regulatory compliance is addressed by thoroughly examining current aviation and environmental laws, ensuring the drone operates within legal frameworks while maximizing efficacy. Field trials in various forest regions demonstrate the system's effectiveness in early fire detection, with case studies showing its success in preventing fire escalation. The research highlights the potential for integrating this technology into existing forest management practices, offering a cost-effective and sustainable solution for fire prevention.

Key words: AI, sensors, autonomy, machine learning, environmental monitoring.

1. INTRODUCTION AND LITERATURE REVIEW

Forest fires are among the greatest natural hazards we face, with devastating consequences for the environment, including the destruction of vast forest areas, natural habitats, and various species of plants and animals. These disasters also pose a direct threat to human life and well-being. Consequently, early detection of these fires is essential for the effective prevention and management of such emergencies, enabling rapid intervention and limiting the spread of flames. Traditional detection methods, such as human observations and reports from residents, are often inefficient and can lead to significant delays in reporting fires. Therefore, a technological and innovative approach is necessary to improve the efficiency of the detection process and reduce response time.

¹ Ph.D., Student Eng.

² Ph.D., Student Eng.

³ Ph.D., Eng., cosminrus@upet.ro

Protecting human life is a critical reason for the early detection of forest fires. These fires can endanger the lives of people, both those directly involved in firefighting and residents of affected areas. Early detection allows for the rapid initiation of intervention operations and the preventive evacuation of people from threatened areas, thereby reducing the risk of loss of human life. Furthermore, early detection is vital for saving natural habitats and biodiversity. Forests are invaluable ecosystems that house a wide variety of plant and animal species. Forest fires can irreversibly destroy these habitats and cause a loss of biodiversity. Detecting fires in their early stages allows for swift and effective intervention to limit the spread of the fire and protect the forest's flora and fauna.

In addition to protecting life and biodiversity, early detection helps in conserving natural resources. Forests play an essential role in conserving soil, water, and air. Forest fires can lead to soil erosion, pollution of water sources, and degradation of air quality. Early detection enables the implementation of preventive and intervention measures to minimize the impact on natural resources and facilitate ecosystem regeneration. Moreover, reducing material losses is another significant benefit of early detection. Forest fires can cause substantial damage to private properties, infrastructure, and the local economy. Quick detection allows for the rapid intervention of firefighting teams and the implementation of adequate protection measures, thereby reducing material losses and the costs associated with reconstruction and recovery.

Efficiency in emergency management is also greatly enhanced by early detection of forest fires. It provides the opportunity to efficiently coordinate intervention operations by directing human and material resources to affected areas. The use of autonomous drones for fire detection can cover large areas in a short time, providing real-time information and images to intervention teams, facilitating appropriate decision-making and actions. In conclusion, early detection of forest fires is crucial for protecting human life, saving natural habitats and biodiversity, conserving natural resources, reducing material losses, and improving efficiency in emergency management.

The paper by Chahil Choudhary, Anurag, and Pranjal Shukla [1], aims to develop a robust ML model for detecting forest fires using drone imagery. The primary objective is to leverage the capabilities of machine learning to process and analyse the vast amounts of data generated by drones, thereby identifying patterns and anomalies indicative of forest fires. The proposed model is intended to improve the speed and accuracy of forest fire detection, thus enabling quicker response and mitigation efforts.

The primary objective of the FireFly Project [2] is to develop an automated system that addresses the limitations of existing UAV technologies, which often struggle with early fire detection due to the limited resolution and sensitivity of thermal cameras. By combining UAVs with ground-based IoT sensors, the project aims to detect forest fires at their inception, even when obscured by dense tree canopies. This hybrid approach leverages the strengths of both aerial and ground-based systems to provide a more comprehensive and effective solution for forest fire monitoring and prevention. Another important paper is [3] by Sergey Filist et al., which demonstrates how a methodology and algorithm for autonomous UAV flight trajectory planning can improve the early detection of ignition sources. The proposed method involves three distinct flight plans covering area surveillance, navigation to the fire source, and return to the departure

point. The mathematical modelling of the UAV flight control algorithm, executed using MATLAB® R2019b, demonstrated control stability and accelerated identification of the ignition source coordinates, exceeding the set goals by 1.5 to 2 times. The paper [4] by Rodrigo De la Fuente, Maichel M. Aguayo and Carlos Contreras-Bolton, demonstrates how an integrated forest fire monitoring system can be optimized using a combination of surveillance towers, monitoring balloons, and drones. The authors develop a mixed-integer linear programming (MILP) model that optimizes the location of these monitoring technologies and the routing of drones to ensure extensive terrain coverage while minimizing costs. The proposed algorithm includes six components: a solution procedure, perturbation procedures, local search procedures, a call to a general-purpose solver for the MILP model, a global reset strategy, a local reset strategy, and an acceptance criterion.

The research tests the model and algorithm on both random instances and a real-life case study in Chile, showing that while the MILP model can solve small instances, the algorithm can find good-quality solutions for all instances. This study provides valuable insights for the government and private sector in designing an integrated fire monitoring system that leverages the strengths of watchtowers, monitoring balloons, and drones, aiming to enhance early detection and response to forest fires.

2. PROBLEM CONTEXT

Forests face threats from various factors, both abiotic and biotic. Non-living factors include fires, drought, storms, and air pollution, while living factors encompass animals, insects, and diseases. Fires, a common abiotic threat in the Mediterranean region, have been increasing alongside major storms, averaging two per year over the last six decades. Air pollution, primarily from vehicles and factories, also endangers forests. Additionally, the expansion of transportation infrastructure fragments forests, posing a significant threat to biodiversity. Overall, approximately 6% of forested areas are impacted by at least one of these factors [5, 6].

European forests are significantly affected by climate change, which varies across different regions, influencing forest growth rates, forested areas, and species diversity. These changes also affect the spread of living organisms, such as parasites, and the frequency and intensity of extreme weather events. Key challenges include the forests' ability to adapt to these changes and their role in mitigating them, such as using wood instead of non-renewable resources for energy and materials [7].

Historically, forest fire detection relied on human observations and reports from residents or observation towers, which had several drawbacks: delays in reporting, difficulty accessing remote areas, and reliance on weather conditions for visibility.

Recently, unprecedented and devastating fires have occurred globally, affecting areas from the United States to Australia, Indonesia, Africa, the Amazon, and even the Arctic. In Europe alone, over 400,000 hectares of land are burned annually by vegetation fires, causing severe damage to protected areas. In 2023, over 48% of forest fires occurred in designated conservation zones. Variations in rainfall, frequency of lightning strikes, and temperature fluctuations contribute to the frequent and severe wildfires in various ecosystems, from boreal peatlands to tropical forests. Climate models predict

worsening weather conditions in most European regions under high-emission scenarios, leading to an increase in fire-prone areas and an extended fire season [5], [7].

3. PROPOSED SOLUTION

The current trend across all sectors is towards automating systems and providing autonomous tools to ease human labour. For the efficient early detection of forest fires, the proposed solution is an autonomous drone equipped with artificial intelligence for image processing.

Designing the architecture of an autonomous drone for forest fire detection must consider the specific environmental requirements and the tasks the drone needs to perform. This involves careful planning and evaluation of available hardware and software components, as well as integration and communication with other systems and teams [8], [9]. A well-designed architecture ensures the efficient and reliable functionality of the autonomous drone, enabling early detection and effective management of forest fires.

Key characteristics in drone design include:

- Flight platform: selecting a suitable drone capable of carrying necessary equipment and sensors, with enough autonomy to cover large areas.
- Specialized sensors: integrating appropriate sensors, such as thermal cameras, smoke sensors, gas sensors, and localization systems, to provide essential data for fire detection and monitoring.
- Power system: ensuring a reliable power system, which may include batteries, additional power sources, or energy management systems to maximize the drone's autonomy during missions.
- Automatic control system: developing an automatic control system that enables the drone to perform necessary tasks autonomously. This involves navigation and route planning algorithms, allowing the drone to follow predefined routes and avoid obstacles.
- Fire detection algorithms: designing and implementing specialized algorithms for forest fire detection. These algorithms may use image analysis techniques, artificial intelligence, or other methods to identify specific signs and patterns of forest fires in collected images and data.

To detect fires, the drone uses an OV7675 camera for continuous image capture, and artificial intelligence analyses the smoke's movements and path. Future enhancements include a module with a thermal camera and a visual spectrum camera to transmit images to a fire monitoring center and analyse the damage. The thermal imaging device measures the thermal radiation emitted by objects, identifying temperature changes specific to forest fires. Autonomous drones can use thermal cameras to detect and pinpoint heat sources related to fires, producing thermal images to highlight the affected regions. The self-flying drone also comes with communication and navigation equipment. It can send data and information immediately to the intervention team or a command centre using communication equipment, allowing for effective organization and a quick response to the wildfire. GPS technology enables the drone to track its location in real-time, making it easier to plan routes and closely observe the fire-stricken

region. To manage and control the drone, the H743 WING V3 with an ARM Cortex-M7 processor is used, providing the computational power necessary for executing complex flight control algorithms. This ensures improved stability and accuracy while flying and offers advanced features like GPS navigation, waypoints, and automatic stabilization. The controller includes a gyroscope, a barometric altimeter, a MicroSD card slot as a black box, along with a current regulator and a voltmeter. To incorporate all features, two additional companion computers are used: an Arduino Nano 33 BLE and an Arduino Nano. The Nano model controller is a compact microcontroller, ideal for fitting into a drone without taking up too much space. Its small size allows for flexible positioning and installation within the drone's layout, and it can be programmed using the Arduino language, which is simple and user-friendly.

4. MATHEMATICAL MODEL OF THE AUTONOMOUS DRONE

In this chapter, we will detail the mathematical model of an autonomous drone, covering the equations of motion, the forces and moments generated by the rotors, as well as the control model. These components are essential for understanding and simulating the behaviour of an autonomous drone.

4.1 The equations of motion

The equations of motion describe the translational and rotational dynamics of the drone. These are fundamental to understanding how the drone responds to various control inputs.

The translational motion of the drone is governed by Newton's second law (1):

$$m \frac{d^2 \vec{x}}{dt^2} = \vec{F} - m \vec{g} \quad (1)$$

where:

- m is the mass of the drone.
- $\vec{x} = [x, y, z]^T$ represents the drone's position in Cartesian coordinates.
- \vec{F} is the total force generated by the rotors.
- $\vec{g} = [0, 0, -g]^T$ is the gravitational acceleration, with g being the gravitational acceleration.

This equation shows how the drone's acceleration depends on applied forces and gravitational force.

The rotational motion is described by the moment equation:

$$I \frac{d\vec{\omega}}{dt} = \vec{\tau} - \vec{\omega} \times (I\vec{\omega}) \quad (2)$$

where:

- I is the inertia tensor of the drone.
- $\vec{\omega} = [p, q, r]^T$ is the angular velocity.
- $\vec{\tau}$ is the total moment generated by the rotors.

These equations (1), (2) describes how angular velocity changes over time based on applied moments and drone inertia properties.

4.2 Forces and moments generated by rotors

Forces and moments generated by rotors are essential for controlling drone motion. Each rotor contributes to lift force generation and control moments. The force generated by a rotor can be modelled as:

$$F_i = k_f \omega_i^2 \quad (3)$$

where:

- F_i is the force generated by rotor i .
- k_f is a thrust coefficient.
- ω_i is the angular velocity of rotor i .

The moment generated by a rotor is given by:

$$\tau_i = k_m \omega_i^2 \quad (4)$$

where:

- τ_i is the moment generated by rotor i .
- k_m is a moment coefficient.

Typically, a quadcopter has four rotors arranged in a square. Opposite rotors spin in opposite directions to stabilize the drone and allow control over yaw movements (rotation around the vertical axis).

4.3 Control model

Drone control involves adjusting rotor speeds to achieve desired position and orientation. A PID (Proportional-Integral-Derivative) controller is often used for this purpose. The PID controller is defined by:

$$u(t) = K_p e(t) + K_i \int_0^t e(\tau) d\tau + K_d \frac{de(t)}{dt} \quad (5)$$

where:

- $u(t)$ is the control signal.
- $e(t)$ is the error, the difference between desired and current position.
- K_p, K_i, K_d are the PID constants that adjust the proportional, integral, and derivative response.

The PID control minimizes position and orientation errors, ensuring a stable and precise trajectory for the drone.

The graphs (Figure 1) illustrate the dynamic behaviour of the drone as it attempts to reach and stabilize at a target position using a PID controller. The position graph indicates that the drone achieves significant vertical movement while maintaining relatively stable horizontal positions [10]. The velocity graph shows an initial acceleration followed by a deceleration, aligning with the position control strategy. The angular velocity graph reveals active rotational control, with oscillations in the x and y directions and a steady increase in the z direction, demonstrating the effect of applied moments for stability and orientation control.

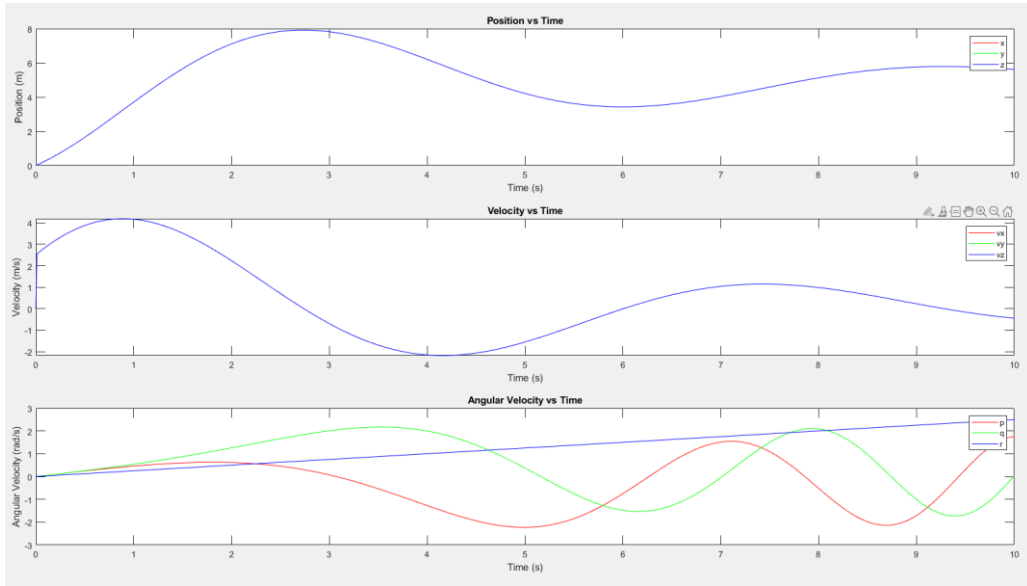


Fig.1. Simulation of drone motion: position, velocity, and angular velocity over time

Overall, the simulation results indicate effective control of the drone's position and orientation, achieved through the combined use of PID control for translation and constant moments for rotation.

5. NAVIGATION AND TRAJECTORY PLANNING

Navigation and trajectory planning are essential components in developing the software system of an autonomous drone, enabling it to move through a complex environment and perform specific tasks without human intervention. The navigation of an autonomous drone involves determining its position and orientation in space and calculating an optimal trajectory to reach a destination.

Navigation algorithms rely on various techniques and sensors to ensure accuracy and reliability. The basic navigation system is satellite-based (GPS), which is frequently used for locating the drone in space. GPS provides precise coordinates of the drone's position, allowing it to move along predefined trajectories. For cases when the GPS signal is lost, I have created a Lua script for an inertial navigation system (INS), which uses accelerometers and gyroscopes to measure the drone's accelerations and angular velocities. These measurements are integrated to estimate position and orientation in real-time. I have also implemented a GSM module, allowing access to and viewing of the drone's telemetry at any time with Ardupilot software (Figure 2).

DEVELOPING AN AUTONOMOUS DRONE FOR EARLY DETECTION OF FOREST FIRES

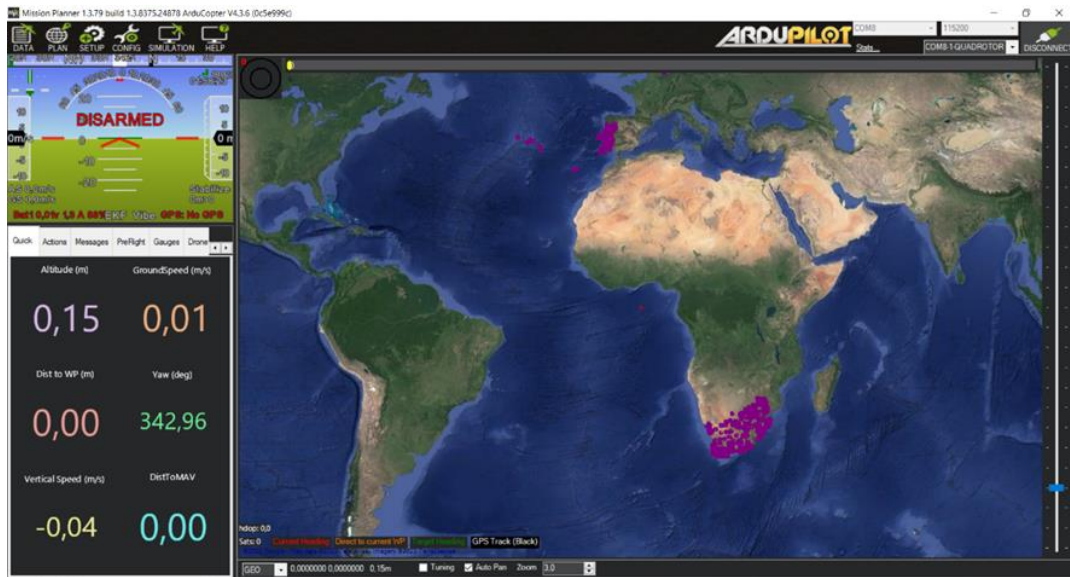


Fig.2. Ardupilot GUI

6. AI SYSTEM FOR FIRE DETECTION

To develop a robust AI system for fire detection [11], the Edge Impulse platform was utilized. This section outlines the comprehensive process of training the AI, from data collection to configuring the neural network structure.

The first step in training the AI system involves collecting relevant data. For this purpose, the camera on a smartphone was used to capture images.

These images were taken in various conditions to ensure a diverse dataset, which is crucial for the model to learn to recognize fires in different scenarios and environments. Using the smartphone camera, a substantial amount of image data was acquired. This step is critical as the quality and diversity of the data directly impact the performance of the AI model. Images were captured in different lighting conditions, from various angles, and in multiple settings to cover a wide range of potential fire appearances.

Once a sufficient number of images were collected, the next step was to label the data. This involved identifying and marking the presence of fire in each image. Accurate labelling is essential as it teaches the model what to look for when detecting fires. Each image was carefully reviewed and annotated to ensure high-quality labelled data.

After labelling the data, the next step was configuring the training blocks on the Edge Impulse platform.

The image size was standardized to 96x96 pixels (Figure 3). This size was chosen to balance the need for detail with the computational efficiency required for training the model. Smaller images are quicker to process, but they must still be large enough to capture the necessary features for fire detection.

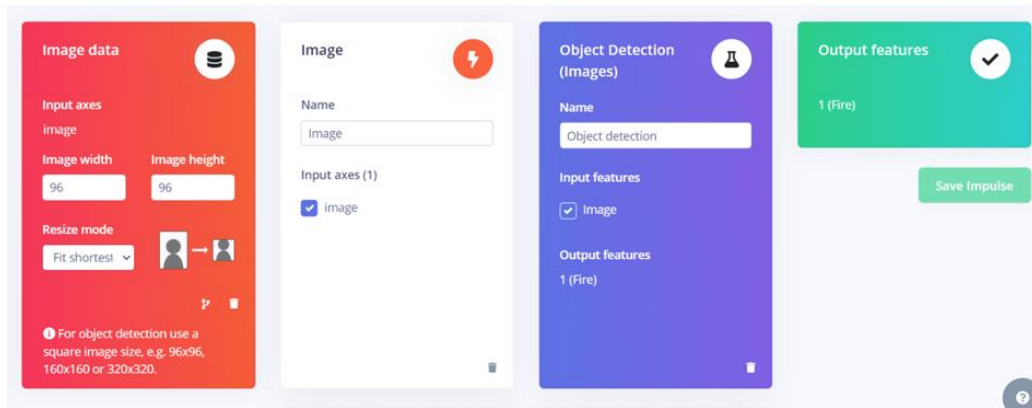


Fig.3. Configuring image data and object detection settings on Edge Impulse platform

The next step was to define the labels that would be used during training. In this case, the primary label was "fire," indicating the presence of fire in the image. This label is crucial for the supervised learning process, where the model learns to associate specific features in the images with the labelled categories.

With the image size and labels set, the neural network structure was configured. The Edge Impulse platform provides various options for building and customizing neural networks. For fire detection, a Convolutional Neural Network (CNN) was chosen due to its effectiveness in image recognition tasks [12]. The CNN architecture was designed to include multiple convolutional layers, pooling layers, and fully connected layers to extract and learn features from the images efficiently (Figure 4).

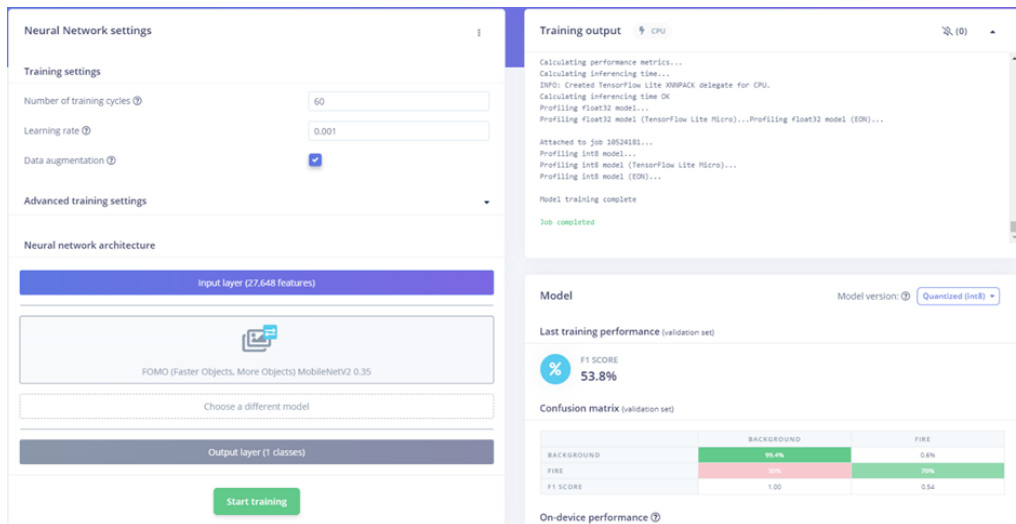


Fig.4. Neural network training and performance metrics for fire detection on Edge Impulse platform

After completing the rigorous training process using the Edge Impulse platform, the AI model for fire detection was successfully developed. The model underwent extensive training, as detailed in the previous steps, which included collecting a diverse dataset of images, accurately labeling them, and configuring the neural network structure. The training settings were meticulously chosen, with 60 training cycles, a learning rate of 0.001, and data augmentation to enhance the model's robustness.

The neural network architecture was carefully designed, incorporating multiple layers to effectively learn and extract features necessary for accurate fire detection. The model's performance was evaluated, showing an F1 score of 53.8%, indicating a balanced precision and recall rate. The confusion matrix provided insights into the model's accuracy, with a high rate of correct classifications for both fire and non-fire images.

Upon completion of the training, the AI model was deployed and tested on new data. The accompanying image illustrates the successful identification of a fire, with the model confidently detecting a flame with a high confidence score of 1.00 (Figure 5).



Fig.5. Fire detection AI model identifying a flame with high confidence

This result showcases the model's effectiveness in recognizing fire, even in varying conditions and settings, as captured in the diverse training dataset. This successful detection is a testament to the robustness of the AI model developed through a comprehensive training process. The precise identification of the fire in the image highlights the potential applications of this model in real-world scenarios, offering a reliable tool for early fire detection and prevention. The deployment of such an AI system can significantly enhance safety measures, providing timely alerts and enabling prompt responses to fire incidents.

7. CONCLUSION

The research into developing an autonomous drone for early detection of forest fires has yielded promising and impactful results, showcasing a significant step forward in the realm of environmental monitoring and disaster prevention. The meticulous design process and integration of advanced technologies have demonstrated the feasibility and effectiveness of employing drones equipped with artificial intelligence for fire detection.

The core of this study lies in enhancing early detection capabilities, a crucial factor in initiating timely responses and preventing the devastating spread of forest fires. By leveraging specialized sensors and state-of-the-art AI algorithms, the autonomous drone system is able to promptly identify fire outbreaks. This not only helps in safeguarding vast forest ecosystems but also plays a vital role in protecting human lives and property in adjacent communities. The ability of the drone to detect fires early significantly mitigates the risks and potential damage, highlighting the system's importance in contemporary forest management strategies.

The integration of artificial intelligence into the drone's functionality, particularly through the use of the Edge Impulse platform, has been a pivotal aspect of this research. The AI model was rigorously trained using a diverse dataset, ensuring its robustness and reliability. The use of Convolutional Neural Networks (CNN) and meticulous data labelling has allowed the model to accurately recognize fires under various conditions, including different lighting and environmental scenarios. The successful detection of fires in real-world tests underscores the model's efficacy, providing a reliable tool for early fire detection and prevention.

Furthermore, the comprehensive system design of the autonomous drone was crafted with precision to meet specific environmental requirements. This included the integration of thermal cameras, GPS navigation, and real-time communication capabilities, which together ensure that the drone can operate autonomously in challenging terrains and provide continuous monitoring without human intervention.

The robustness of the system architecture allows for effective and reliable performance, even in diverse and complex forest environments. In conclusion, the successful development and deployment of the autonomous drone system for early detection of forest fires represent a milestone in environmental technology. This research not only highlights the potential applications of such systems in real-world scenarios but also underscores the importance of integrating advanced AI and drone technologies in safeguarding our natural resources. The precise identification and rapid response capabilities of the system promise to enhance safety measures, offering a reliable and innovative tool for protecting forests and communities from the threat of wildfires.

REFERENCES

- [1]. Choudhary C., Shukla, P., *A Robust Machine Learning Model for Forest Fire Detection Using Drone Images*, *Advances in Aerial Sensing and Imaging*, pp. 129-144, 2024.
- [2]. Puttapirat P., Woradit K., Hesse H., Bhatia D., *FireFly Project: UAV Development for Distributed Sensing of Forest Fires*, *International Conference on Unmanned Aircraft Systems (ICUAS)*, pp. 594-601, IEEE, 2024.

- [3]. Filist S., Al-Kasasbeh R. T., Tomakova R. A., Al-Fugara A. K., Al-Hababbeh O. M., Shatolova O., Maksim I., *An unmanned aerial vehicle autonomous flight trajectory planning method and algorithm for the early detection of the ignition source during fire monitoring*, International Journal of Remote Sensing, Vol. 45, No. 12, pp. 4178-4197, 2024.
- [4]. De la Fuente R., Aguayo M. M., Contreras-Bolton C., *An optimization-based approach for an integrated forest fire monitoring system with multiple technologies and surveillance drones*, European Journal of Operational Research, Vol. 313, No. 2, pp. 435-451, 2024.
- [5]. Bauhus J., Forrester D. I., Gardiner B., Jactel H., Vallejo R., Pretzsch H., *Ecological Stability of Mixed-Species Forests*, Pretzsch, H., Forrester, D., Bauhus, J. (Eds), Mixed-Species Forests, Springer, Berlin, Heidelberg, 2017.
- [6]. Lundquist J. E., Camp A. E., Tyrrell M. L., Seybold S. J., Cannon P., Lodge D. J., *Earth, wind, and fire: Abiotic factors and the impacts of global environmental change on forest health*, Castello, J. D., Teale, S. A. (Eds), Forest Health: An Integrated Perspective, pp. 195–244, Cambridge: Cambridge University Press, 2011.
- [7]. Cours J., Bouget C., Barsoum N., et al., *Surviving in Changing Forests: Abiotic Disturbance Legacy Effects on Arthropod Communities of Temperate Forests*, Current Forestry Reports, Vol. 9, pp. 189–218, 2023.
- [8]. Negru N., Radu S. M., Soica A., *Air Quality Monitoring and Photovoltaic Impact Assessment in Valea Jiului*, 25th International Carpathian Control Conference (ICCC), pp. 1-6, IEEE, 2024.
- [9]. Samuil I., Stancioiu L., Ionica A. C., Leba M., *Possibilities of Adopting Electric Vehicles in the Agritourism Development Context*, 18th Iberian Conference on Information Systems and Technologies (CISTI), pp. 1-6, IEEE, 2023.
- [10]. Rus C., Lupulescu E., Leba M., Risteiu M., *Advanced Mathematical Modeling and Control Strategies for Autonomous Drone Systems*, 25th International Carpathian Control Conference (ICCC), pp. 1-6, IEEE, 2024.
- [11]. Narahari S. C., Polaboina U. R., Rishika K., Gudipalli A., *IoT-based fire and traffic density detection using AI-based drone*, AIP Conference Proceedings, Vol. 2966, No. 1, AIP Publishing, 2024.
- [12]. Gamulescu O., Leba M., Ionica A., *Exploring the Convolutional Neural Networks Architectures for Quadcopter Crop Monitoring*, World Conference on Information Systems and Technologies, pp. 225-234, Cham: Springer Nature Switzerland, 2024.

CHALLENGES IN INTEGRATING ARTIFICIAL INTELLIGENCE FOR ENHANCED ROBOTIC AUTONOMY AND INTERACTION

ALEXANDRU COSTINAȘ¹, MARIUS LEONARD OLAR², SEBASTIAN DANIEL ROȘCA³

Abstract: In recent years, the integration of artificial intelligence (AI) into robotic systems has opened new horizons across various fields such as industrial production, healthcare, transportation, and space exploration. This article presents how AI enhances robots' capabilities in perception, planning, and executing complex tasks. Deep learning and reinforcement learning algorithms enable robots to analyze sensory data in real-time, make predictions, and make autonomous decisions in dynamic and unpredictable environments. We also address the challenges related to safety, ethics, and human-robot interaction, emphasizing the need for clear regulations and stringent ethical standards. The case study presented illustrates the successful implementation of AI in robotic applications, showcasing the potential of this technology to revolutionize how robots operate and interact with the surrounding world. The conclusions highlight the importance of interdisciplinary collaboration to advance the effective development and deployment of AI in robotics.

Key words: Artificial intelligence, Robotic systems, Deep learning, Safety, Interdisciplinary collaboration

1. INTRODUCTION

The integration of artificial intelligence (AI) into robotic systems has made significant progress in various areas, such as healthcare, transportation, industrial manufacturing, and space exploration. The robots' improved capabilities, attributed to artificial intelligence, have allowed for more sophisticated perception, detailed planning, and the execution of complex tasks. In this literature review, we aim to synthesize current research on the impact of AI on robotics, focusing on technological advances, applications, challenges, and the need for ethical standardization and regulation [1].

¹ Ph.D., Eng., teseract@gmail.com

² Ph.D., Eng.

³ Ph.D., Eng.

Technological advancements in AI-enhanced robotics have revolutionized sensory perception, planning, and execution of complex tasks. Deep learning and consolidation algorithms now allow robots to analyze sensory data in real time and interact effectively with their environment, and based on convolutional neural networks (CNNs) computer vision is added for accurate object recognition and classification [8]. In planning and decision-making, AI allows robots to understand what the optimal actions are and navigate complex environments, such as autonomous cars that can dynamically plan routes and avoid obstacles [9], [12]. In the execution of complex tasks, AI-equipped robotic arms improve efficiency and precision in production, and in the medical field, surgical robots use AI to assist in delicate procedures [7], [11].

AI-powered robots have revolutionized various fields by increasing automation and efficiency. In industrial production, they perform repetitive tasks with increased precision and speed, reducing human errors and labor costs [6]. In healthcare, AI-enhanced robots facilitate minimally invasive surgery, rehabilitation, and patient care, providing more precise options and shorter recovery times [2], [4]. In transportation [13], [15], AI has led to the development of autonomous vehicles, which promise safer and more efficient travel, interpreting sensory data to navigate and make decisions in real time, avoiding collisions [3], [10]. In space exploration, autonomous robots, such as the Mars rovers, use AI to navigate and conduct scientific experiments on other planets, expanding human capabilities beyond Earth.

The implementation of AI in robotics poses significant safety challenges and requires rigorous testing and validation to ensure safe operation in various environments, along with robust mechanisms to prevent accidents due to the unpredictability of AI decisions [14]. Ethical considerations are key, addressing issues such as job abolition, privacy, and the moral implications of autonomous decision-making, with the need for clear regulations and strict ethical standards to guide the responsible development of AI in robotics [5]. Additionally, effective human-robot interaction (HRI) is important for successful AI integration, requiring the development of intuitive and secure interaction protocols to ensure risk-free collaboration between robots and humans.

2. ADVANTAGES OF IMPLEMENTING AI IN ROBOT MANAGEMENT

Implementing artificial intelligence (AI) in driving robots brings significant benefits, improving safety, efficiency, and accessibility. AI reduces human error by quickly processing sensory data and adapting in real time to road, traffic, and weather conditions. Thus, AI-equipped vehicles can anticipate and react more effectively to potential hazards, preventing accidents. These vehicles also optimise routes and contribute to a smoother flow of traffic, saving time and fuel.

Autonomous vehicles offer mobility solutions for people who cannot drive, such as the elderly and those with disabilities, and can operate continuously, making them ideal for transport and delivery services. AI also supports the transition to electric vehicles, reducing emissions and promoting cleaner energy sources. In addition, improved efficiency and safety lead to significant cost savings for users and businesses, and the development of AI vehicles creates new jobs and drives economic innovation.

The user experience is enhanced by the convenience and personalization offered by AI vehicles, which allow passengers to relax or work during their journey. AI systems learn users' preferences, providing an adapted driving experience. Autonomous vehicles also generate and analyze data to improve performance and safety, and AI-based predictive maintenance prevents breakdowns and extends the life of vehicles, ensuring reliable performance. These advantages demonstrate the transformative potential of AI in robot driving, promising a safer, more efficient and sustainable future of mobility.

3. THE OBJECTIVE OF THE PROJECT

The aim of this paper is to investigate the challenges associated with integrating artificial intelligence (AI) into mobile robots, with a particular emphasis on enhancing the efficiency and coordination of AI algorithms. The research focuses on identifying obstacles that hinder optimal algorithmic performance and exploring solutions to improve the synchronization and interaction of AI components within mobile robotic systems. By addressing these challenges, the paper seeks to advance the development of mobile robots that operate with greater autonomy, precision, and adaptability in dynamic environments.

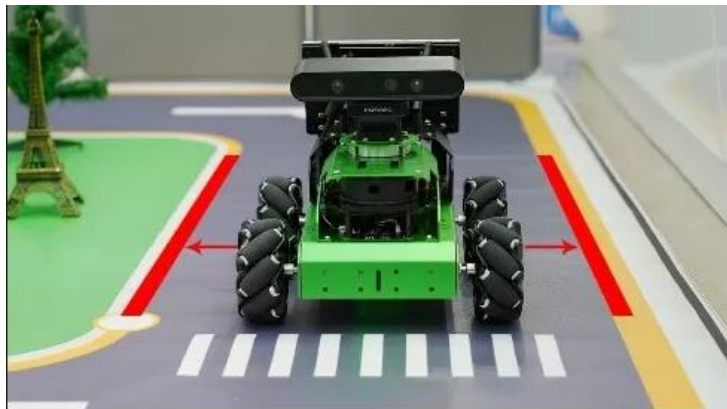


Fig.1. AI controlled mobile robot

4. HYPOTHESES OF THE WORK

Hypothesis 1: The integration of deep learning algorithms into robotic systems significantly enhances their autonomy and interaction in challenging environments where they encounter obstacles.

Justification 1: Deep learning algorithms are capable of extracting and integrating information from complex data, which can improve robots' ability to make real-time decisions and interact more effectively in difficult situations or where they face obstacles

Hypothesis 2: Data security and privacy issues represent a major challenge in integrating AI into mobile robotic systems, as well as other types of robotic systems, affecting both performance and the acceptability of advanced robotic technologies.

Justification 2: The use of AI in robotics involves collecting and processing a large volume of data, which raises significant concerns about the protection of sensitive information and the security of the data systems accessed.

5. DISADVANTAGES OF IMPLEMENTING AI IN ROBOT DRIVING

The implementation of AI in robot management faces significant technical and operational challenges. The complexity and reliability of AI systems are major concerns, as they must operate flawlessly in unpredictable scenarios to ensure safety. In addition, the development and maintenance of AI-based vehicles are costly, requiring substantial financial investments in advanced sensors, computing power, and continuous updates.

Ethical and social concerns also have drawbacks for AI-based vehicles. The possible migration of jobs, such as those of truck and taxi drivers, could lead to economic and social problems, including unemployment and the need for retraining. In addition, the programming of ethical decision-making in AI systems is complex, raising questions about how to prioritize lives in unavoidable accidents and the responsibility of these decisions.

Security and privacy issues are critical challenges for AI-powered vehicles. These vehicles are vulnerable to cybersecurity threats, such as hacking, which can lead to accidents and data breaches. In addition, the extensive collection of data by autonomous vehicles raises privacy concerns, requiring robust data protection measures.

Addressing these drawbacks requires a comprehensive approach, including technological innovation, regulatory frameworks and social adaptation to ensure safe and ethical implementation.

Integrating AI into robot management offers numerous benefits, including safety, efficiency, and economic benefits. However, there are technical, moral, and privacy challenges that need to be addressed to ensure the widespread adoption and responsible deployment of autonomous vehicles.

6. LIMITS OF IMPLEMENTING AI IN ROBOT MANAGEMENT

The implementation of AI in driving robots is limited by several technological constraints. Sensor limitations, especially in adverse weather conditions, affect the vehicle's ability to accurately perceive the environment. In addition, the substantial computing power required to process real-time data from multiple sensors poses challenges related to hardware requirements, power consumption, and heat management, making it difficult to operate efficiently and reliably.

Regulatory and infrastructure challenges also hinder the widespread adoption of AI-enabled vehicles. The evolution of legal and regulatory frameworks, which vary by region, complicates the implementation process. In addition, the current road infrastructure is not fully equipped to support autonomous vehicles, requiring significant upgrades and investment in features such as dedicated lanes, advanced traffic management systems, and vehicle-to-infrastructure communication capabilities.

Human factors and social acceptance further limit the integration of AI into driving robots. Public confidence in the safety and reliability of autonomous vehicles is

essential, but it remains low due to major accidents and safety concerns. Effective interaction between human drivers and AI-powered vehicles is essential, especially during the transition period, when both types of vehicles share the road. Overcoming these challenges requires technological advancements, standardized regulations, infrastructure development, and efforts to build public trust through testing and extensive education.

7. FUTURE DIRECTIONS OF AI DEPLOYMENT IN ROBOT DRIVING

The future of AI deployment in robot driving will see significant technological advancements, including improved sensor fusion, improved machine learning algorithms, and the potential integration of quantum computing. These advances will create more accurate, reliable and efficient autonomous vehicles capable of handling complex driving scenarios and processing large amounts of data in real time.

The development of infrastructure and ecosystems will also play a crucial role. The deployment of a smart infrastructure with vehicle-to-infrastructure communication systems and the deployment of 5G networks will improve real-time data exchange and traffic management. Additionally, cities can develop dedicated lanes for autonomous vehicles, reducing interactions with human-driven vehicles and improving overall traffic flow.

Regulatory and ethical frameworks, together with improving human-AI interaction, are essential for the successful integration of AI-enabled vehicles. Standardized global regulations and robust ethical guidelines will ensure safe and transparent implementation, while user-friendly interfaces, driver assistance solutions, and public education programs will build trust and acceptance. Public-private collaboration will be key to creating policies, standards and infrastructure to support the safe and efficient adoption of autonomous vehicles.

Table 1 summarizes these advantages and disadvantages, current limitations and future development directions of the implementation of AI in robot management.

Table 1. Comparative table of the advantages and disadvantages, current limitations and future development directions of implementing AI in robot management

Aspect	Advantages	Disadvantages	Limitations	Future directions
Safety	<ul style="list-style-type: none"> Reducing human error 	<ul style="list-style-type: none"> Technical failures or software errors that can lead to dangerous situations 	<ul style="list-style-type: none"> Limitations of sensors in adverse weather conditions 	<ul style="list-style-type: none"> Improved sensor fusion
Efficiency	<ul style="list-style-type: none"> Optimized route planning Improved traffic flow 	<ul style="list-style-type: none"> High computational requirements that can raise problems of power consumption and heat dissipation 	<ul style="list-style-type: none"> High computational requirements 	<ul style="list-style-type: none"> Improved machine learning algorithms Quantum Computing

CHALLENGES IN INTEGRATING ARTIFICIAL INTELLIGENCE FOR ENHANCED
ROBOTIC AUTONOMY AND INTERACTION

Accessibility	<ul style="list-style-type: none"> • Mobility for non-drivers <ul style="list-style-type: none"> • 24/7 operation 	<ul style="list-style-type: none"> • High development and maintenance costs 		
Medium	<ul style="list-style-type: none"> • Emission reduce • Promoting the adoption of electric vehicles 			
Economic	<ul style="list-style-type: none"> • Reduction of operational costs <ul style="list-style-type: none"> • New economic opportunities 	<ul style="list-style-type: none"> • Job cuts • Professional retraining 		
User experience	<ul style="list-style-type: none"> • Comfort and convenience • Adaptive learning 			<ul style="list-style-type: none"> • User-friendly interfaces • Driver support and transition solutions <ul style="list-style-type: none"> • Education and training
Use of data	<ul style="list-style-type: none"> • Data-driven insights • Predictive maintenance 	<ul style="list-style-type: none"> • Privacy concerns 		
Regulation and infrastructure		<ul style="list-style-type: none"> • Regulatory uncertainty • Infrastructure requirements 	<ul style="list-style-type: none"> • Regulatory uncertainty • Infrastructure requirements 	<ul style="list-style-type: none"> • Standardized regulations • Smart infrastructure <ul style="list-style-type: none"> • 5G connectivity <ul style="list-style-type: none"> • Frequencies dedicated to autonomous vehicles
Ethics and social		<ul style="list-style-type: none"> • Ethical decision-making • Ethical Concerns in Unavoidable Accident Scenarios 		<ul style="list-style-type: none"> • Clear ethical guidelines • Collaboration between the public and private sectors
Cybersecurity		<ul style="list-style-type: none"> • Cybersecurity risks 		

8. CONCLUSIONS

The integration of artificial intelligence (AI) in autonomous driving systems presents a multitude of advantages, including enhanced road safety, improved traffic efficiency and optimization, increased accessibility for individuals unable to drive, and substantial economic gains. Nevertheless, this advancement also encounters significant challenges, such as the technological limitations of sensors, high computational demands, the absence of a standardized regulatory framework, and the need for specialized infrastructure. Additionally, societal skepticism and issues related to social acceptance pose further obstacles. Future efforts should prioritize technological innovation, the development of intelligent infrastructure, the establishment of comprehensive global and ethical regulations, and the encouragement of collaboration between public and private sectors. Although AI-driven robotics holds significant promise for industries such as transportation, healthcare, and space exploration, its success hinges on addressing these challenges in a cohesive and sustained manner, ensuring adherence to ethical and safety standards, and enhancing human-robot interactions to fully harness the potential of AI-enhanced robotics.

REFERENCES

- [1]. Smith, J., Brown, A., "Omnidirectional Mobile Robots: Design and Applications," *Robotics Journal*, 2020.
- [2]. Lee, K., Park, S., "Machine Learning Approaches for Autonomous Navigation," *Journal of Artificial Intelligence Research*, 2019.
- [3]. Miller, T., "Supervised and Unsupervised Learning for Robotics," *International Journal of Robotics Research*, 2018.
- [4]. Javed, A. R., Saadia, A., Mughal, H., Gadekallu, T. R., Rizwan, M., Maddikunta, P. K. R., Hussain, A., "Artificial intelligence for cognitive health assessment: state-of-the-art, open challenges and future directions," *Cognitive Computation*, Vol. 15, No. 6, pp. 1767-1812, 2023.
- [5]. Kunze, L., "Artificial Intelligence for Long-Term Robot Autonomy: A Survey," University of Oxford, Oxford, Oxfordshire, GB.
- [6]. KUKA AG, "KUKA AG Annual Report 2020," 2020.
- [7]. Krizhevsky, A., Sutskever, I., Hinton, G. E., "ImageNet classification with deep convolutional neural networks," *Communications of the ACM*, Vol. 60, No. 6, pp. 84-90, 2017.
- [8]. LeCun, Y., Bengio, Y., Hinton, G., "Deep learning," *Nature*, Vol. 521, No. 7553, pp. 436-444, 2015.
- [9]. Sutton, R. S., Barto, A. G., "Reinforcement learning: An introduction," MIT Press, 2018.
- [10]. Thrun, S., "Toward robotic cars," *Communications of the ACM*, Vol. 53, No. 4, pp. 99-106, 2010.
- [11]. Yang, G. Z., Cambias, J., Cleary, K., Daimler, E., Drake, J., Dupont, P. E., Taylor, R. H., "Medical robotics—Regulatory, ethical, and legal considerations for increasing levels of autonomy," *Science Robotics*, Vol. 2, No. 4, eaam8638, 2017.
- [12]. Samuil, I., Stancioiu, L., Ionica, A. C., Leba, M., "Possibilities of Adopting Electric Vehicles in the Agritourism Development Context," In *2023 18th Iberian Conference on Information Systems and Technologies (CISTI)*, pp. 1-6, IEEE, June 2023.

[13]. Rus, C., Leba, M., Risteiu, M. N., Marcus, R., "Modeling and Simulation of Electric Vehicle Driveline," In *2023 18th Iberian Conference on Information Systems and Technologies (CISTI)*, pp. 1-6, IEEE, June 2023.

[14]. Rus, C., Leba, M., Risteiu, M., Marcus, R., "Vehicle Control Modeling and Simulation for Small Electric Car Case," In *2023 24th International Carpathian Control Conference (ICCC)*, pp. 388-393, IEEE, June 2023.

[15]. Rus, C., Leba, M., Negru, N., Marcus, R., Risteiu, M., "Electric vehicles in smart grid and smart city for Petroșani case," In *MATEC Web of Conferences*, Vol. 342, p. 05002, EDP Sciences, 2021.

This article was reviewed and accepted for presentation and publication within the 11th edition of the International Multidisciplinary Symposium "UNIVERSITARIA SIMPRO 2024".

RESEARCH ON REDUCING PM10 PARTICLES IN THE JIU VALLEY AREA AS A RESULT OF USING PHOTOVOLTAIC PANELS IN ELECTRICITY PRODUCTION

ALEXANDRA SOICA¹, NICOLETA NEGRU², SORIN MIHAI RADU³,
ANGELA EGRI⁴

Abstract: Air quality in industrial areas is a pressing concern due to its significant impact on public health and the environment, especially regarding PM10 particle pollution. Effectively mitigating these risks requires practical solutions. The adoption of photovoltaic panels for energy production emerges as an attractive option to address environmental pollution and promote sustainable development. This study aims to comprehensively analyze the potential of photovoltaic panels in reducing PM10 particle levels in the Jiu Valley region, an area primarily dominated by the mining industry. The research includes an assessment of air quality and PM10 particle pollution levels in the Jiu Valley, along with a detailed analysis of the energy potential of photovoltaic panels in the region. Statistical analysis was conducted to compare PM10 particle levels in the air with and without the use of photovoltaic panels, particularly in relation to those emitted by the mining industry. The findings provide valuable insights into the effectiveness of photovoltaic panels in mitigating PM10 particle pollution in the Jiu Valley, thus advocating for a sustainable approach to managing air quality in industrial areas.

Key words: air quality, photovoltaic panels, pollution, environment, industrial areas.

1. INTRODUCTION

Air pollution is a pressing concern, particularly in regions characterized by intensive mining and coal-fired power generation. The mining industry and associated activities contribute significantly to atmospheric pollution, releasing particulate matter and other pollutants into the air. Of particular concern are particulate matter with a diameter of less than 10 micrometers (PM10), which pose serious health risks due to

¹ Ph.D., Assistant Prof. Eng., University of Petroșani,
alexandra_valynikalay@yahoo.com

² Ph.D., Student Eng., University of Petroșani, negru.ioananicoleta@yahoo.ro

³ Ph.D., Prof. Eng., University of Petroșani, SorinRadu@upet.ro

⁴ Ph.D., Associate Prof. Eng., University of Petroșani, AngelaEgri@upet.ro

their ability to penetrate deep into the respiratory system. In this context, the reduction of pollution from coal-fired power plants is paramount [1], [21], [23] [25], [28].

These facilities are major sources of air pollutants, emitting significant amounts of PM10 particles, Sulphur dioxide (SO₂), nitrogen oxides (NO_x), and other harmful substances into the atmosphere [2]. Efforts to mitigate pollution from coal-fired power generation are critical for safeguarding public health and mitigating environmental degradation [3], [4]. One potential solution being explored is the adoption of cleaner energy technologies, such as photovoltaic (PV) solar panels, as alternatives to coal-fired power plants [5]. By harnessing solar energy to generate electricity, PV panels offer a sustainable and environmentally friendly alternative to traditional coal-based power generation. This shift towards renewable energy sources has the potential to significantly reduce air pollution, improve air quality, and mitigate the adverse health effects associated with coal-fired power generation [6], [22], [24].

PM10 particles are a type of air pollutant consisting of solid and liquid particles suspended in the air, with a diameter of less than 10 micrometers. These particles are highly diverse in composition, including dust, smoke, smog, and other fine substances, and their sources can vary, including industrial, vehicular, agricultural, or natural processes such as soil erosion. Due to their small size, PM10 particles can be inhaled and penetrate deeply into the human respiratory system. The effects of PM10 particles on human health are considerable and varied. These particles can cause irritation of the respiratory tract, exacerbating symptoms of asthma and other lung conditions. Moreover, PM10 particles can enter the bloodstream, having harmful effects on the cardiovascular system and increasing the risk of conditions such as heart attacks and strokes. Additionally, exposure to PM10 is associated with increased premature mortality, hospital admissions, and other health problems [7], [26], [29].

The Jiu Valley, situated in southwestern Romania, stands as one of the country's significant mining centers, boasting a longstanding tradition in coal extraction. Over the years, mining has served as the primary economic driver in the region, providing employment opportunities and contributing to local development. However, with the decline in coal usage as a primary energy source, the Jiu Valley has faced a challenging transition towards more sustainable alternatives. Resizing mining activities and the closure of certain mines became inevitable with changes in the energy industry and growing concerns regarding the environment. Nonetheless, these transition actions have not been without challenges, and one of the most significant issues is the air pollution specific to the area. The mining industry and related activities have been the primary contributors to air pollution in the Jiu Valley. Processes involved in coal extraction and processing have generated significant emissions of particulate matter, noxious gases, and other atmospheric pollutants. This pollution has had a significant impact on the quality of life of residents in the area, directly affecting community health and well-being. Monitoring air quality in the Jiu Valley has become a priority for authorities in an attempt to understand and manage the pollution's impact on human health and the surrounding environment. Sampling campaigns and data analysis have revealed elevated levels of particulate matter, nitrogen oxides, and other toxic substances in the air breathed by residents in the area [8], [30], [33], [35], [36].

Addressing this issue requires an integrated approach and cooperation among various stakeholders, including local authorities, mining companies, local communities, and non-governmental organizations. Investments in cleaner and more sustainable technologies, as well as the promotion of renewable energy, can contribute to reducing pollution and improving air quality in the Jiu Valley [9]. Ultimately, managing pollution in the Jiu Valley represents not only a challenge but also an opportunity to transform the region into a healthier and more sustainable place where people can live and work in a safe and clean environment [29], [31], [32], [34].

In the Jiu Valley, where air pollution, especially PM10 particles, poses a significant challenge, the deployment of photovoltaic panels represents a promising solution for reducing the pollutant impact of industrial and mining activities. Photovoltaic panels are devices that convert sunlight into electrical energy without emitting pollutants into the atmosphere or generating waste. These panels can be installed on buildings, open land, or specially constructed structures, generating clean electrical energy that can be used to power local consumers or integrated into electrical grids. By harnessing solar energy, dependence on traditional energy sources such as coal, which are associated with significant emissions of PM10 particles and other atmospheric pollutants, can be reduced.

Moreover, installing photovoltaic panels can contribute to diversifying the region's energy mix and increasing renewable energy production capacity. This can have long-term benefits for the environment and the health of residents by reducing air pollution and improving air quality. In addition to the environmental benefits, implementing photovoltaic panels in the Jiu Valley can create economic and local development opportunities. The construction and installation of these systems require local labor and resources, which can stimulate economic growth and job creation in the community [9]. In the specialized literature, there are scientific papers that analyze the impact of pollution on the production of electricity from renewable sources, as well as the impact of the use of sustainable (non-polluting) electricity production installations on the reduction of pollution in certain areas of the world.

In the paper by Mardani, Hoseinzadeh and Garcia [10], the impact of aerosols on solar power generation in Tehran, Iran is explored. Tehran, despite its high solar energy potential due to significant levels of solar radiation, faces severe air pollution challenges. This study aims to develop predictive models for solar attenuation caused by particulate matter (PM2.5 and PM10) using both remote sensing data from the NASA CERES syn 1-deg product and local observations from 2014 to 2020. The researchers found that the models performed better in predicting aerosol attenuation in the colder months (November, December, January) with correlation coefficients of 0.1553, 0.2926 and 0.1341, respectively. On average, aerosols accounted for a loss of 8.30% of total solar radiation. This was validated with RMSE and MBD values of 14.09% and 10.89%. The study highlights the significant impact of aerosols on solar power generation and suggests that the developed models can improve the feasibility and siting of PV plants by considering the attenuation effects of aerosols [10], [27].

In the work of Zheng, Lu, and Zhao [11], the impact of high-velocity longitudinal airflow on dust removal and power output characteristics of photovoltaic (PV) panels is explored. The study investigates how dust accumulation on photovoltaic

panels decreases their photoelectric conversion efficiency and proposes a dust removal method using high-speed longitudinal airflow to improve output power. Using commercial CFD software, researchers simulate the dust removal process and establish a model to analyze the output characteristics of PV panels under the influence of high-velocity air flow. The study examines various factors such as tilt angles, dust particle sizes, airflow velocities and blowing times to determine their effects on dust removal efficiency. The results show that as the tilt angle, airflow velocity, and blowing time increase, the dust removal rate and output power of the PV panel also increase. The optimal conditions for dust removal are identified, demonstrating significant improvements in power output, which can guide the practical application of high-velocity airflow in maintaining PV panel efficiency [11].

In the paper by Khan and Bounade [12], the authors explore strategies to mitigate PM2.5 air pollution in OECD countries. The study investigates the effects of green investment, digitalization, renewable energy and economic growth on PM2.5 air pollution over the period 1990-2020. The authors use advanced econometric techniques, especially the quantile moment regression method (MMQREG), to analyze the data. Their findings indicate that green investments, digitization and renewable energy have a significant positive impact on reducing PM2.5 air pollution, while economic growth tends to exacerbate it. The study highlights the importance of adopting a holistic approach that combines green investment and digitization to effectively mitigate PM2.5 pollution, protect public health and promote sustainable economic growth. The paper also highlights the critical role of renewable energy and green investments in achieving long-term environmental sustainability. It calls on decision-makers to implement support measures for green technologies and digital solutions to improve air quality. In addition, the study provides insights into the different effects of these factors in different quantiles, providing a comprehensive understanding of their impact on PM2.5 air pollution. The authors conclude by recommending policies that encourage green investment and digitization as key strategies to reduce air pollution and promote sustainable development in OECD countries. The paper contributes to the existing literature by providing empirical evidence of the benefits of integrating green and digital technologies into environmental policy frameworks [12].

In the paper of Haramaini et al. [13], the authors investigate how socio-economic factors influence the adoption of solar panels in urban areas of developing countries. This study uses a quantitative, associative research method and uses correlation analysis to understand the relationship between variables such as education level, income, and public perception of alternative energy with the use of solar panels. The study identifies several key socio-economic factors that significantly affect solar panel adoption, including number of prosumers, total kWh exports, gross regional domestic product (GRDP), total investment, total electricity load, EV home load and air quality. The research demonstrates that there are distinct relationships between these socio-economic variables and solar panel adoption, highlighting the importance of factors such as government policies, economic resources and environmental awareness in promoting the use of renewable energy. The results suggest that higher levels of education and income are positively correlated with increased adoption of

solar panels, while factors such as proximity to the capital and better air quality also play significant roles. The findings provide valuable information for policy makers to formulate effective strategies to promote solar energy, ensure sustainable energy development and reduce environmental impact in urban areas of developing countries [13].

In the paper of Bošnjaković et al. [14], the authors analyze the environmental effects of photovoltaic (PV) plants. The study highlights the importance of renewable energy, especially photovoltaic and wind, in addressing climate change and increasing energy security. However, PV plants have environmental impacts such as greenhouse gas (GHG) emissions, land use, water consumption and waste generation. Although the operation of PV plants generates minimal emissions, significant emissions occur during the production, transport and installation of the components. These emissions will decrease with the increase in the share of renewable energy and the improvement of production technologies. Land use for PV installations is a critical issue, and the authors estimate that there is sufficient land available, but emphasize the need for careful planning to minimize impacts. Water consumption in PV systems is relatively low, but manufacturing and recycling processes can consume significant amounts of water, requiring full life cycle assessments. Biodiversity impacts include habitat loss due to deforestation for PV installations, although well-managed solar farms can increase biodiversity. Noise pollution from inverters, transformers and cooling fans is another issue addressed, with recommendations for noise reduction. End-of-life management of PV systems emphasizes the need for efficient recycling and reuse to minimize waste. A significant increase in PV waste is predicted until 2050, highlighting the importance of developing sustainable recycling technologies and policies [14].

2. MATERIALS AND METHODS

Solar energy represents a promising and sustainable solution for meeting the growing global demand for electricity. Among the key components of solar energy systems are solar panels, which capture sunlight and convert it into usable electrical energy. In this chapter, we explore three main types of solar panels: monocrystalline, polycrystalline, and thin-film. Each type has its own unique characteristics, advantages, and applications.

Monocrystalline solar panels are made from single-crystal silicon, giving them a uniform appearance and high efficiency. They are known for their sleek black appearance and superior performance in areas with limited space. Monocrystalline panels are often used in residential and commercial installations where space is a premium and maximum efficiency is desired.

Polycrystalline solar panels are manufactured from multiple silicon crystals, resulting in a speckled blue appearance. While slightly less efficient than monocrystalline panels, polycrystalline panels offer a cost-effective solution for larger installations where space is not a constraint. They are commonly used in utility-scale solar farms and large commercial projects.

Thin-film solar panels are constructed using thin layers of photovoltaic material deposited onto a substrate, such as glass or plastic. They are lightweight, flexible, and less expensive to produce compared to crystalline silicon panels. Thin-film panels are suitable for applications where weight, flexibility, or aesthetics are important factors, such as building-integrated photovoltaics (BIPV) and portable electronic devices.

To assess the performance of these solar panel types in the Petrosani region, we collected climate data, including average temperatures, sunlight duration, and cloud cover, from reliable sources. Using MATLAB, we conducted a comprehensive analysis to estimate the energy output of each panel type throughout the year. MATLAB, a high-level programming and numeric computing platform, enabled us to simulate and model the performance of solar panels accurately. By correlating the climatic variables with solar panel performance, we validated our results and gained insights into the suitability of different panel types for the local climate conditions. Through this analysis, we aim to provide valuable insights into the selection and deployment of solar energy systems in the Petrosani region, ultimately contributing to the transition towards a more sustainable and renewable energy future. The climate data provided in the tabular format below has been obtained from specialized sources (National Meteorological Administration of Romania) [15] and describes the climatic conditions of the Jiu Valley region, particularly Petrosani, Hunedoara. These data points encompass various meteorological parameters crucial for understanding the environmental context and assessing the feasibility of solar energy utilization in the region.

Table 1. Climatic data from Petrosani [15]

Month	Avg. Min Temp (°C)	Avg. Max Temp (°C)	Sunny Days	Partially Cloudy Days	Overcast Days	Rainy Days
January	-3	3	5	10.8	15.2	12.3
February	-3	3	4	9.5	14.8	12.9
March	1	7	3.7	11.8	15.5	15.4
April	6	14	3.6	14	12.4	17.4
May	11	19	2.5	17.6	11	19
June	14	22	3.8	18.4	7.8	18
July	17	25	6.8	19.1	5.1	15.8
August	17	25	7.2	17.8	5.9	12.8
September	13	20	6.1	13.5	10.5	11.6
October	8	16	7.8	11.5	11.7	11.2
November	3	9	6	10.4	13.5	12.3
December	-2	4	6.9	9	9	13.3

These data points (Table 1) encompass average minimum and maximum temperatures, the number of sunny days, partially cloudy days, overcast days, and rainy days for each month of the year. They serve as fundamental inputs for analyzing the solar potential and suitability of implementing solar panel systems in the region. By considering these climatic factors, one can assess the expected performance and efficiency of solar panels in harnessing solar energy throughout the year. Additionally,

these data aid in formulating strategies for optimizing solar energy utilization and mitigating potential environmental impacts.

3. RESULTS

The first step in our entire research was the interpretation and visualization of climate data for the region of Jiul Valley, Petrosani, Hunedoara, using the MATLAB programming language [16], [17]. We imported the climate data and stored this information in appropriate variables, including the average minimum and maximum temperatures for each month, as well as the number of sunny, partly cloudy, cloudy, and rainy days [18]. Then using this organized data, we made the performance graph of the electricity production estimated to be produced for monocrystalline, polycrystalline and thin film solar panels for each month of the year in Petrosani, (Fig 1).

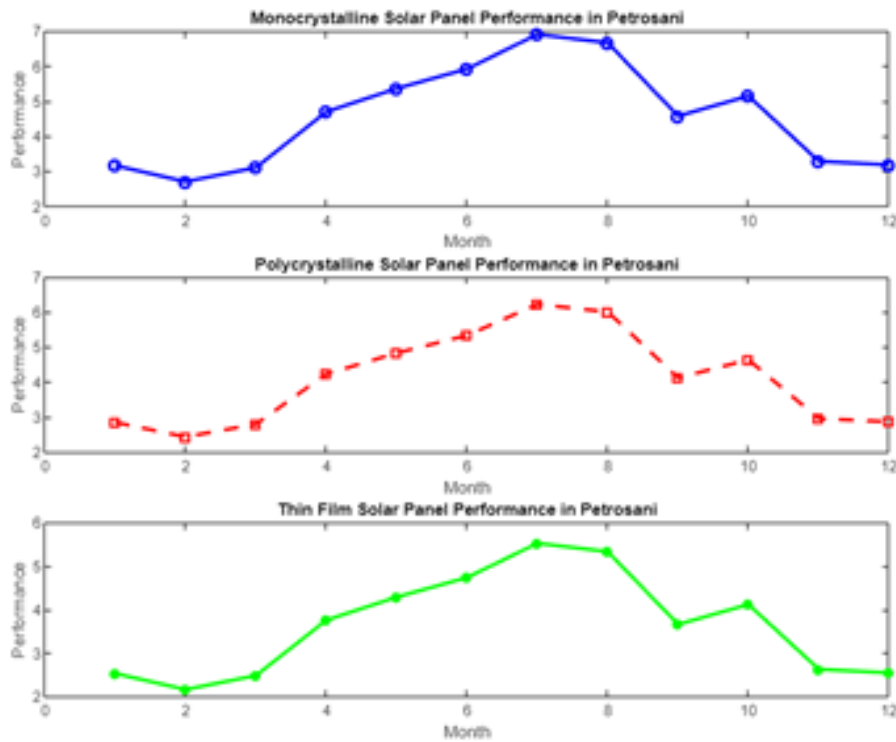


Fig. 1. Solar panel performance graph

In our analysis, we observed that monocrystalline panels consistently exhibited the highest energy output throughout the year. This is attributed to their higher efficiency and superior performance in varying light conditions. Monocrystalline panels are particularly effective during periods of low sunlight, such as winter months, making them well-suited for regions with fluctuating weather patterns like Petrosani.

Polycrystalline panels also demonstrated satisfactory performance, albeit slightly lower than monocrystalline panels. Their cost-effectiveness and moderate efficiency make them a viable option for larger installations where space is not a constraint. However, their energy output may fluctuate more significantly in response to changes in sunlight intensity.

Thin-film panels, while lightweight and flexible, exhibited the lowest energy output among the three types. Despite their lower efficiency, thin-film panels offer advantages in specific applications where weight and flexibility are critical factors. However, in Petrosani's climate, characterized by seasonal variations in sunlight and temperature, thin-film panels may not be the most efficient choice for maximizing energy production.

The temperature graph illustrates the monthly variation in average minimum and maximum temperatures in Petrosani (Fig 2). We observed that temperatures tend to be lowest during winter months (December to February) and highest during summer months (June to August). These temperature fluctuations can impact the performance of solar panels, with higher temperatures generally leading to decreased efficiency.

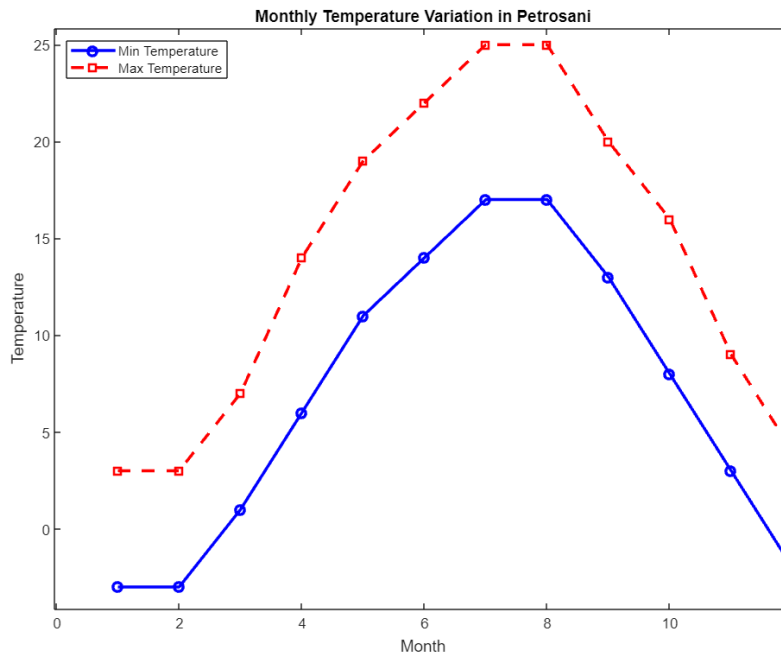


Fig. 2. Temperature Variation

The sunlight and cloud cover graph depicts the number of sunny, partially cloudy, overcast, and rainy days for each month (Fig 3). We found that Petrosani experiences a relatively high number of sunny days during summer months, which corresponds to increased solar energy production. However, the region also experiences frequent cloud cover and rainy days, particularly during spring and autumn, which can reduce solar panel efficiency.

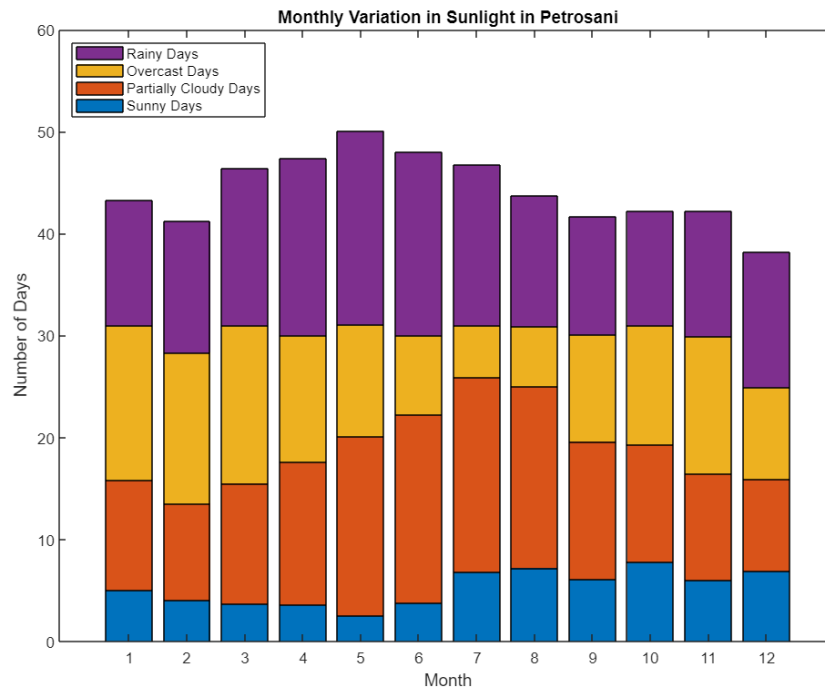


Fig. 3. Sunlight and cloud cover in Petrosani

By analyzing these results (Fig 4), we can gain valuable insights into the performance of different solar panel types in Petrosani's climate. Monocrystalline panels emerge as the most reliable option for consistent energy production throughout the year, followed by polycrystalline panels. Thin-film panels, while offering flexibility, may not be the optimal choice for maximizing energy output in Petrosani's climate. These findings can inform decision-making processes regarding the selection and deployment of solar energy systems in the region, contributing to the transition towards a sustainable energy future.

The research aimed to evaluate through a realistic simulation the potential reduction of PM10 particles in Petrosani through the implementation of photovoltaic (PV) panels for the production of electricity. Petrosani currently faces significant air pollution with an annual average concentration of PM10 at $35 \mu\text{g}/\text{m}^3$, mainly due to coal-fired power generation and other sources such as mining operations and industrial activities [19]. In order to make a realistic simulation, we took into account the total annual electricity consumption in Petrosani, which includes the residential, commercial and industrial sectors. The population of Petrosani is approximately 31,044 inhabitants, and the average consumption of electricity per capita is 2,800 kWh per year. This results in a total residential consumption of 86.9 GWh. In addition, taking into account the energy consumption of the commercial, industrial and institutional sectors, we estimate an additional 50% on top of residential consumption, bringing the total commercial, industrial and institutional consumption to 130.35 GWh. Therefore, the total annual combined electricity consumption is 217.25 GWh.

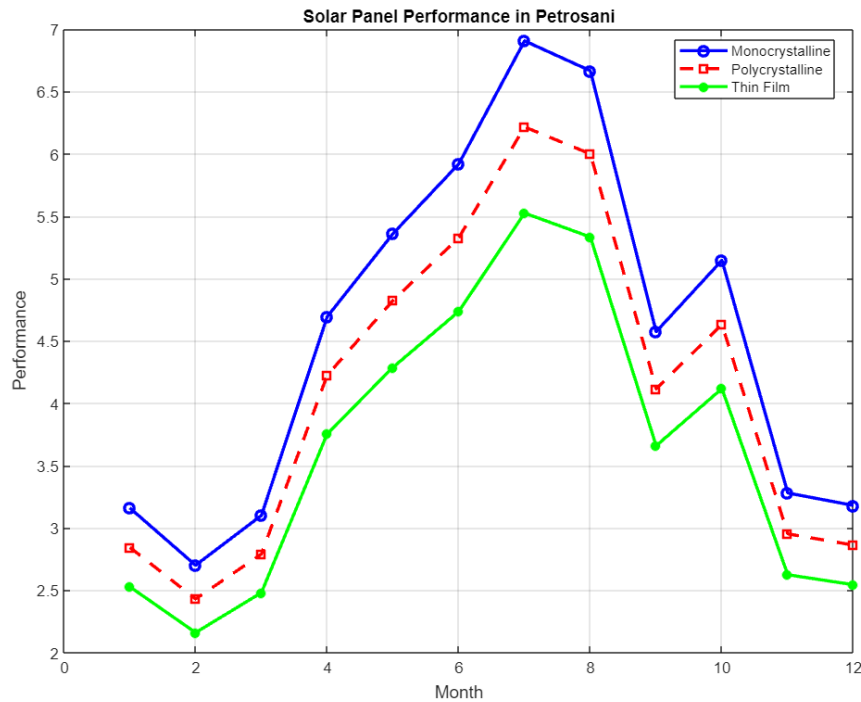


Fig. 4. Solar panel performance in Petrosani

Initially, 90% of Petroșani's energy comes from coal, contributing significantly to PM10 emissions, the remaining 10% from renewable sources. The simulation assumes a gradual increase in the proportion of solar energy by 10% annually, up to a realistic maximum limit of the PV installation, starting from an estimated current coverage of 0.5 km² and aiming to cover approximately 5 km² by the end of the simulation period. The photovoltaic panels have an efficiency of 18% and the average daily solar radiation is about 5 kWh/m² for sunny days.

PM10 emission factors include contributions from power generation (coal) at 0.1 μg/m³ per MWh and from other sources such as mine tailings and traffic, which account for 50% of the initial PM10 concentration.

The simulation integrates these data points and assumptions to model the potential reduction in PM10 concentrations over a 10-year period by gradually installing solar panels, replacing coal-fired power. The concentration of PM10 from other sources remains constant to ensure a realistic model.

The results showed a steady decrease in PM10 concentrations over a 10-year period (Fig 5). Initially, PM10 levels saw moderate reductions as the proportion of solar power in the electricity mix gradually increased. Each year, the area covered by photovoltaic panels increased by 10%, which corresponded to a greater amount of coal-based energy being replaced by solar energy. By the end of the ten-year period, PM10 levels had fallen significantly, reflecting the impact of increased use of solar panels. However, PM10 concentrations never fell below contributions from other sources, ensuring that the model remained realistic and not overly optimistic.

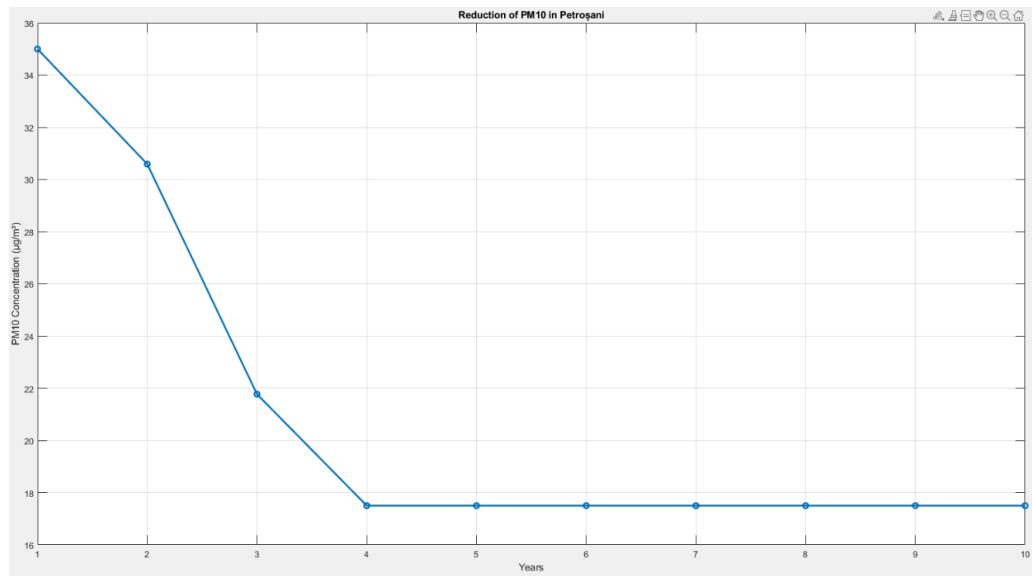


Fig. 5. Simulation of gradual reduction of PM10 concentration in Petrosani through the implementation of photovoltaic panels

The implementation of photovoltaic panels in Petrosani demonstrates the potential to significantly reduce PM10 levels, helping to improve air quality. However, persistent contributions from other sources of PM10, such as mining operations and industrial activities, highlight the need for a comprehensive approach to pollution reduction. Addressing all major contributors is crucial to ensuring a cleaner environment in Petrosani. This research highlights the importance of integrating renewable energy solutions while simultaneously managing other sources of pollution to achieve substantial air quality improvements. The data and results obtained are based on the assumption that approximately 5 km² of solar panels will be installed during the simulation period.

The conducted study demonstrates a significant decrease in the levels of PM10 particles in the air when photovoltaic panels are used compared to periods without their use.

The results comparing the reduction of PM10 particle levels achieved by the photovoltaic panels with the emissions from the mining industry, offer a perspective on the efficiency of this renewable energy solution. The analysis reveals the potential energy generation capacity of photovoltaic panels in the Jiu Valley region, highlighting their role in sustainable energy production [20].

4. CONCLUSIONS

The study clearly demonstrates that the implementation of photovoltaic (PV) panels in Petrosani has a significant potential to reduce PM10 levels. Through a realistic simulation, taking into account the total annual electricity consumption and the gradual increase in the installation of photovoltaic panels, the research highlights several key findings.

First, the switch from coal-based energy to solar energy can lead to a substantial decrease in PM10 concentrations. The simulation showed a consistent and gradual reduction in PM10 levels over the ten-year period, confirming that increasing the share of solar energy in the electricity mix effectively reduces emissions from coal-fired power plants. This reduction is crucial to improving air quality and mitigating the negative health effects associated with PM10 particles.

Second, the results highlight the importance of a gradual and planned approach to the adoption of renewable energy. Starting from a modest initial coverage of 0.5 km² and aiming to cover approximately 5 km² by the end of the simulation period, the study illustrates how systematic and incremental increases in solar power capacity can achieve significant environmental benefits. This approach ensures that the transition is both feasible and sustainable.

In addition, the findings highlight that while solar power can significantly reduce PM10 levels, other sources of PM10, such as mining operations and industrial activities, remain a challenge. The simulation accounted for constant contributions from these sources, ensuring that the model remained realistic. Therefore, a comprehensive pollution management strategy addressing all major contributors is essential to achieve substantial improvements in air quality.

The study also highlights the dual benefits of adopting photovoltaic panels. Beyond reducing PM10 levels, the transition to renewable energy contributes to broader environmental sustainability goals. It helps reduce dependence on fossil fuels, reduce greenhouse gas emissions and promote cleaner, healthier air for local people.

In conclusion, the implementation of photovoltaic panels in Petrosani is a promising solution for reducing PM10 levels and improving air quality. The research provides valuable insights into the potential environmental and health benefits of renewable energy adoption. It also highlights the need for an integrated approach to pollution management that addresses both energy production and other significant sources of PM10. By continuing to invest in and support the adoption of renewable energy technologies, Petrosani can pave the way to a cleaner and more sustainable future for its residents and the wider Jiu Valley region.

REFERENCES

- [1]. Zhou S., He, H., Zhang L., Zhao W., Wang, F., *A Data-Driven Method to Monitor Carbon Dioxide Emissions of Coal-Fired Power Plants*. *Energies*, 16(4), 1646, 2023.
- [2]. Nnaji C. C., Chibueze C., Afangideh C. B., *The menace and mitigation of air pollution in the built environment: A review*. *Nigerian Journal of Technology*, pp. 12-29, 2023.
- [3]. Deonarine A., Schwartz G. E., Ruhl L. S., *Environmental Impacts of Coal Combustion Residuals: Current Understanding and Future Perspectives*. *Environmental Science & Technology*, 57(5), pp. 1855-1869, 2023.
- [4]. Gopinathan P., Subramani T., Barbosa S., Yuvaraj D., *Environmental impact and health risk assessment due to coal mining and utilization*. *Environmental Geochemistry and Health*, 45(10), pp. 6915-6922, 2023.
- [5]. Hasan M. M., Hossain S., Mofijur M., Kabir Z., Badruddin I. A., Yunus Khan T. M., Jassim E., *Harnessing solar power: a review of photovoltaic innovations, solar thermal systems, and the dawn of energy storage solutions*. *Energies*, 16(18), 6456, 2023.

- [6]. **Yanto D. T. P., Akhmadeev R., Hamad H. S., Alawadi A. H. R., Abdullayev A. B., Romero-Parra R. M., Fooladi H.,** *Development and investigation of a pollutants emission reduction process from a coal-gasification power plant integrated with fuel cell and solar energy*. International Journal of Low-Carbon Technologies, 18, pp. 1120-1133, 2023.
- [7]. **Guascito M. R., Lionetto M. G., Mazzotta F., Conte M., Giordano M. E., Caricato R., Contini D.,** *Characterisation of the correlations between oxidative potential and in vitro biological effects of PM10 at three sites in the central Mediterranean*. Journal of Hazardous Materials, 448, 130872, 2023.
- [8]. **Gaman A. N., Simion A., Simion S.,** *Air quality monitoring in the eastern Jiul Valley*. In MATEC Web of Conferences (Vol. 389, p. 00044). EDP Sciences, 2024.
- [9]. **Itu R. B., Şoica A.,** *The Reintegration of The Surfaces Affected by the Phenomenon of Subsidence through the Cultivation of Trees with High Energy Value*, Revista De Gestão Social E Ambiental, 18(3), e06506, 2024.
- [10]. **Mardani M., Hoseinzadeh S., Garcia D. A.,** *Developing particle-based models to predict solar energy attenuation using long-term daily remote and local measurements*. Journal of Cleaner Production, 434, 139690, 2024.
- [11]. **Zheng C., Lu, H., Zhao W.,** *Research of dust removal performance and power output characteristics on photovoltaic panels by longitudinal high-speed airflow*, Energy, 304, 132202, 2024.
- [12]. **Khan Y., Bounade C. D.,** *Particulate matter 2.5 air pollution mitigation strategy: the role of green investment, digitalization, and renewable energy in the organization for economic co-operation and development (OECD) countries*. Clean Technologies and Environmental Policy, pp. 1-15, 2024.
- [13]. **Haramaini Q., Setiawan A., Sidiq M. H., Brilliawan A. S., Garniwa I.,** *Exploring the Relationship between Solar Panel Adoption and Socio-Economic Factors: A Case Study of Urban Households in Developing Countries*. Journal of Electrical Systems, 20(6s), pp. 2685-2705, 2024.
- [14]. **Bošnjaković M., Santa R., Crnac Z., Bošnjaković T.,** *Environmental Impact of PV power systems*. Sustainability, 15(15), 11888, 2023.
- [15]. National Meteorological Administration, Romania, 2024.
- [16]. **Rus C., Lupulescu E., Leba M., Risteiu M.,** *Advanced Mathematical Modeling and Control Strategies for Autonomous Drone Systems*. In 2024 25th International Carpathian Control Conference (ICCC) (pp. 1-6). IEEE, 2024.
- [17]. **Rus C., Leba M., Sibisanu R.,** *SOS-My Grandparents: Using the Concepts of IoT, AI and ML for the Detection of Falls in the Elderly*, In World Conference on Information Systems and Technologies (pp. 164-173). Cham: Springer Nature Switzerland, 2024.
- [18]. **Rus C., Leba M.,** *Autonomous Smart Electric Vehicle Integrated into a Smart Grid Type System*, In EURECA-PRO Conference on Responsible Consumption and Production (pp. 45-50). Cham: Springer International Publishing, 2022.
- [19]. **Rus C., Marcus R., Pellegrini L., Leba M., Rebrisoreanu M., Constandoiu A.,** *Electric cars as environmental monitoring IoT Network*. In IOP conference series: materials science and engineering (Vol. 572, No. 1, p. 012091). IOP Publishing, 2019.
- [20]. **Marcus R., Rus C., Leba M., Risteiu M.,** *Electric Vehicles Between Recycling and Sustainable Development-@. ro*. In International Conference on Computers Communications and Control (pp. 47-62). Cham: Springer International Publishing, 2022.
- [21]. **Handra A.D., Popescu F.G., Păsculescu D.,** *Utilizarea energiei electrice: lucrări de laborator*, Editura Universitas, 2020.
- [22]. **Fiță N.D., Radu S.M., Păsculescu D., Popescu F.G.,** *Using the primary energetic resources or electrical energy as a possible energetical tool or pressure tool*, In International conference KNOWLEDGE-BASED ORGANIZATION, vol. 27, no. 3, pp. 21-26. 2021.

- [23]. Popescu F.G., Păsculescu D., Păsculescu V.M., *Modern methods for analysis and reduction of current and voltage harmonics*, LAP LAMBERT Academic Publishing, ISBN 978-620-0-56941-7, pp. 233, 2020.
- [24]. Irimie S.I., Radu S.M., Petrilean D.C., Andras A., *Reducing the environmental impact of a gas operated cogeneration installation*, MATEC Web Conf. Volume 121, 8th International Conference on Manufacturing Science and Education – MSE “Trends in New Industrial Revolution” Environmental Engineering, 2017.
- [25]. Vasilescu G.D., Petrilean C.D., Kovacs A., Vasilescu G.V., Pasculescu D., Ilcea G.I., Burduhos-Nergis D.P., Bejinariu C., *Methodology for assessing the degree of occupational safety specific to hydrotechnical construction activities, in order to increase their sustainability*, Sustainability, Jan 21;13(3):1105, 2021.
- [26]. Petrilean D.C., Irimie S.I., *Carrying out and analysing the real and optimum energetic balance of thermal consumers issuing from the outline of the balance SC SEWS Romania SRL Alba Iulia*, Research Scientific Report, University of Petroșani, 2013.
- [27]. Andras A., Popescu F.D., Radu S.M., Pasculescu D., Brinas I., Radu M.A., Peagu D., *Numerical Simulation and modeling of mechano–electro–thermal behavior of electrical contact using comsol multiphysics*. Applied Sciences, 14(10):4026, 2024.
- [28]. Petrilean D.C., *Compresoare eliciodale*, Editura Tehnica-Info, 2006.
- [29]. Petrilean D.C., *Termodinamica tehnica si masini termice*, Editura A.G.I.R., 2010.
- [30]. Petrilean D.C., Stanilă S., Dosa I., *A mathematical model for determining the dimensionless heat flux with application in mine environment*, Environmental Engineering and Management Journal, Vol.16, No. 6, 1249-1414, 2017.
- [31]. Csaszar T., Pasculescu D., Darie M., Ionescu J., Burian S., *Method for assessing energy limited supply sources, designed for use in potentially explosive atmospheres*, Environmental Engineering and Management Journal 11, no. 7, 1281-1285, 2012.
- [32]. Arad S., Marcu M., Pasculescu D., Petrilean D.C., *Aspects of the electric arc furnace control*, Proceeding. of international symposium advanced engineering & applied management, Faculty of Engineering Hunedoara, 2010.
- [33]. Stepanescu, S., Rehtanz, C., Arad, S., Fotau, I., Marcu, M., Popescu, F. *Implementation of small water power plants regarding future virtual power plants* 10th International Conference on Environment and Electrical Engineering, pp. 1-4, IEEE, 2011.
- [34]. Fiță N. D., Lazăr T., Popescu F. G., Pasculescu D., Pupăză C., Grigorie E., *400 kV power substation fire and explosion hazard assessment to prevent a power black-out*, International Conference on Electrical, Computer Communications and Mechatronics Engineering-ICECCME, pp. 16-18, 2022.
- [35]. Fita N.D., Obretenova M.I., Pasculescu D., Tatar A., Popescu F.G., Lazar T., *Structure and analysis of the power subsector within the national energy sector on ensuring and stability of energy security*, Annals of „Constantin Brâncuși” University of Târgu Jiu, ENGINEERING SERIES, Issue 2/2022, pp.177-186, 2022.
- [36]. Petrilean D.C., *Elaborating and Analysing the Real Balance of Heat for the Steam Generator RGL 10/DD* Annals of the University of Petrosani, Mechanical Engineering, Volume 10, 155-160, 2008.

This article was reviewed and accepted for presentation and publication within the 11th edition of the International Multidisciplinary Symposium "UNIVERSITARIA SIMPRO 2024".

MODELLING AND IMPLEMENTATION OF THE DASHBOARD INTERFACE FOR ELECTRIC VEHICLES USING ADVANCED SIMULATION TECHNOLOGIES AND NAVIGATION APIS

VICTOR TRIOHIN¹, TUDOR MANOLE²

Abstract: This paper presents the design and implementation of a digital dashboard interface for electric vehicles using advanced simulation technologies and navigation APIs. The proposed dashboard system integrates real-time data processing and visualization to provide critical information to the driver, enhancing both the safety and efficiency of electric vehicle operation. Developed on a low-cost embedded platform, the system utilizes a combination of GMap.NET for mapping and navigation, the OpenWeatherMap API for real-time weather updates, and the Geoapify API for route planning and navigation functionalities. The graphical interface, created using Windows Forms and C#, includes features such as speed indicators, battery level indicators, navigation aids, and current weather information. A simulation program was developed to demonstrate the system's capabilities, including real-time updates of vehicle parameters such as speed, battery level, and remaining range. The simulation adjusts these parameters based on user inputs and driving conditions, providing an accurate representation of the vehicle's performance. The study highlights the system's adaptability to various vehicle models with minimal modifications and its potential for future enhancements, such as integrating additional sensors and incorporating AI algorithms for improved performance. The research underscores the importance of user-friendly interfaces and real-time data integration in modern electric vehicles, offering a scalable and cost-effective solution for enhancing electric vehicle usability.

Key words: real-time data processing, user interface, vehicle management, simulation program, embedded platform

1. INTRODUCTION AND LITERATURE REVIEW

The on-board computer system of an electric vehicle (EV) is a vital component that significantly enhances the driving experience by providing essential information for monitoring and controlling the vehicle. As the automotive industry moves towards more advanced and intelligent systems, the need for efficient, cost-effective, and customizable

¹ Ph.D., Student Eng., victortriohin@upet.ro

² Ph.D., Student Eng.

dashboard interfaces becomes increasingly important. These interfaces not only improve the usability and safety of EVs but also contribute to a more sustainable and enjoyable driving experience.

The existing commercial car computer systems are often prohibitively expensive and lack the flexibility required for customization and expansion. This limitation has created a demand for innovative solutions that can provide real-time vehicle data and navigation functionalities without the high costs associated with commercial products. Addressing this gap, our research focuses on developing a digital dashboard interface for electric vehicles using advanced simulation technologies and navigation APIs. The paper by Parth Bhatnagar et al. [1] addresses the issue of range anxiety among electric vehicle (EV) owners. It introduces "EV-Connect," a mobile application designed to optimize EV range by providing users with real-time battery status updates, route optimization suggestions, a charging station locator, and a community platform for EV enthusiasts. The authors begin with a comprehensive literature survey of existing mobile applications and their features related to EV management. They detail the development of EV-Connect using Django and Firebase for backend functionalities and Flutter for frontend development. The app integrates several APIs, including Google Maps for navigation, Open Weather Map for weather updates, and Open Charge Map for charging station locations, offering a robust tool for EV owners. Results demonstrate the app's effectiveness in enhancing the EV user experience, reducing charging costs, minimizing grid stress, and promoting efficient use of renewable energy sources. The authors emphasize addressing "range anxiety" to facilitate broader EV adoption, highlighting the need for ongoing collaboration, adaptive solutions, and continuous improvement based on user feedback. Future work includes integrating data from EV built-in systems for more accurate information and further enhancing the app to meet user needs. This research underscores the critical role of smart EV charging solutions in promoting sustainable transportation and improving the overall user experience for EV owners [1].

The paper by Shyba Zaheer et al. [2] delves into the real-time monitoring of lithium-ion battery health within the framework of Industry 4.0. The study highlights the development and deployment of a dashboard utilizing STM32 microcontrollers, advanced sensor technology, and data analytics to provide continuous insights into battery performance, including state of charge (SOC) and temperature. Integrating IoT principles, the system aims to enable predictive maintenance and optimize resource utilization, enhancing operational efficiency and reliability in industrial settings. The paper highlights the significance of lithium-ion batteries in electric vehicles (EVs), noting their high energy density and extended driving range. It addresses safety concerns such as thermal runaway, fires, and explosions, which can occur due to overcharging or physical damage. The authors detail the development of the dashboard using STM32 microcontrollers, advanced sensors, and data analytics to monitor SOC and temperature continuously. The methodology includes the design and implementation of charging and discharging processes, sensing of current, voltage, and temperature, data processing using MATLAB, and the display of real-time information through a user-friendly dashboard. The results indicate effective monitoring of battery health, with SOC variations and temperature stability being accurately tracked during charging and discharging conditions.

The paper by Agnieszka Dudziak et al. [3] explores the evolution and impact of modern vehicle communication systems, specifically focusing on intelligent car dashboards equipped with multimedia and internet connectivity. The study examines various types of dashboard interfaces, including analogue switch dashboards (ASD), gesture/speech controlled dashboards (GSD), and touch screen dashboards (TSD), assessing their convenience and safety from the driver's perspective. The authors conducted a comprehensive literature review, highlighting current trends in vehicle technology and the shift from mechanical controls to interactive touch panels, voice, and gesture control systems. This shift is driven by advancements in technology and the need for efficient handling of multiple functions within vehicle infotainment systems. The research methodology involved a survey of 863 drivers with varying levels of experience and driving environments. The survey aimed to gather opinions on the three types of dashboard interfaces, focusing on their usability and safety implications. The analysis employed correspondence and decision tree analyses to evaluate the data and identify significant differences in driver assessments based on demographics and driving conditions.

The study underscores the importance of aligning vehicle control systems with driver needs and safety, highlighting that the development of these systems should continue to evolve towards more intelligent and autonomous solutions. The findings emphasize the necessity for ongoing user feedback and adaptive solutions to enhance the driving experience and promote road safety [3].

The paper [4] addresses the challenge of creating an affordable, customizable car dashboard. It focuses on displaying real-time vehicle data such as speed, engine RPM, fuel levels, and battery status, using a Raspberry Pi 3 single-board computer. The dashboard receives data from the vehicle's CAN bus via an OBD-II cable. The study reviews existing commercial car computer systems, noting their high costs and limited customization options. It then details the design and implementation of a digital dashboard that is cost-effective and adaptable to various vehicles with minimal physical or software modifications. The authors highlight the potential for future enhancements, such as integrating GPS modules and inertial measurement units (IMUs). The system architecture includes a low-cost embedded platform optimized for graphical design. This platform processes and displays critical vehicle information interactively in real-time, ensuring that the final device is both affordable and highly functional. The paper concludes by demonstrating the feasibility and performance of the digital dashboard, emphasizing its adaptability and the ease of future upgrades. This research contributes to the development of accessible and customizable vehicle management systems, aligning with the broader goals of enhancing electric vehicle usability and driver experience.

2. IMPLEMENTATION

2.1. Graphical interface

The graphical interface of the dashboard system is developed using Windows Forms and the C# programming language, offering an interactive and intuitive

experience for the user. The graphical interface includes a series of elements that provide essential information and functionalities for the driver:

- Speed indicator: displays the current speed of the vehicle, allowing the driver to monitor and adjust the speed while driving;
- Maps and navigation: offers navigation functions, including route planning, turn-by-turn directions, and displaying points of interest along the route. These functionalities are integrated into the graphical interface to help the driver navigate efficiently to their destination;
- Current weather information: displays information about current weather conditions, such as temperature, humidity, wind speed, and visibility to help the driver make informed decisions during the trip;
- Energy consumption graph: includes a graphical representation of the energy consumed per hour. This graph provides detailed information about the vehicle's energy consumption over time, helping the driver to monitor and optimize energy usage;
- Gear indicator: Shows the current gear position of the vehicle. The positions include Park (P), Reverse (R), Neutral (N), Drive (D), and Sport (S). This helps the driver know the operational state of the vehicle;
- Tire pressure: indicates the current tire pressure, which is shown as 2.0 bar. Proper tire pressure is crucial for safe driving, optimal fuel efficiency, and tire longevity;
- Distance driven: shows the total distance the vehicle has travelled, which can be useful for maintenance schedules and overall vehicle usage tracking.
- Battery capacity, temperature, and drivable time: displays the total capacity of the vehicle's battery, allowing the driver to understand the maximum energy storage. Additionally, it shows the battery temperature, which helps in assessing the battery's performance and health. The indicator also provides the remaining drivable time, enabling the driver to manage energy consumption and plan charging stops efficiently;
- Other useful information: the graphical interface also includes other elements, such as a visual representation that adjusts the display according to the time of day (Day/Night Mode) for optimal visibility and reduced eye strain during night-time driving; the cellular signal strength, indicating the availability of a 5G connection for navigation, communication, and other connected services; a top-down view of the car showing its current state, such as whether the doors are closed and lights are off, to help the driver ensure that all parts of the car are in the correct state before and during driving; and the current time and date to help the driver manage their schedule with real-time information.

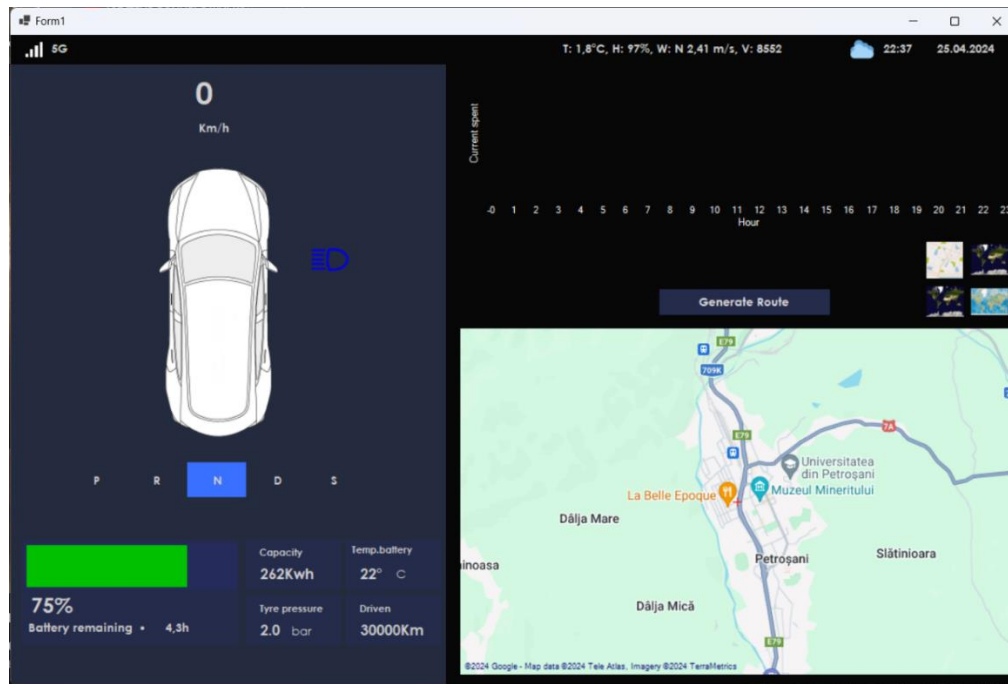


Fig.1. The graphical user interface

2.2. Design and ease of use

The graphical interface is carefully designed to be easy to use and understand, considering that the driver needs to primarily focus on driving the vehicle. The design is simple and intuitive, with accessible control elements strategically placed to allow quick and efficient access to information and functionalities. The graphical interface can integrate advanced technologies such as high-resolution displays, voice commands, and touch interfaces to offer an enhanced and more intuitive user experience. These technologies can help reduce distractions and improve safety while driving.

2.3 Navigation functions in the on-board computer system

The navigation functions are designed to help the driver plan and follow routes to destinations, providing precise directions and route information to facilitate the journey. The system allows the user to input the desired destination by directly selecting a point on the map, providing an intuitive and efficient way to set navigation goals without the need for typing addresses. Users can also select multiple points on the map, and the system will calculate the route based on all of them. By enabling multiple destination inputs and optimizing routes accordingly, the navigation system greatly enhances trip planning capabilities, making it a powerful tool for both everyday use and professional applications. This leads to time savings, reduced travel stress, and improved overall efficiency on the road. Once the destination is entered, the system calculates the fastest or shortest possible route. During the journey, the system provides visual

directions to follow to reach the destination. These directions include turns, traffic lights, pedestrian crossings, and other important landmarks along the route (Figure 2).



Fig.2 Temperature, time, date and other information

Additionally, the map can be visualized in three different modes: satellite view, terrain view, and standard map view (Figure 3). This functionality allows users to choose the most suitable view for their needs. For instance, the satellite view offers a detailed aerial perspective, which can be particularly useful for identifying landmarks and navigating in unfamiliar areas. The terrain view highlights geographical features, making it ideal for routes through mountainous or rural areas where understanding the topography is important. The standard map view provides a clear and straightforward representation of roads and infrastructure, which is useful for everyday driving in urban or suburban environments. These visualization options can significantly enhance the driver's ability to plan and navigate routes effectively. For example, when traveling through a densely populated city, the standard map view can help identify the best streets to avoid traffic congestion. In contrast, when driving in the countryside or mountainous regions, the terrain view can help anticipate changes in elevation and road conditions. The satellite view can assist in recognizing specific buildings or landmarks, making it easier to find exact destinations in complex settings like large campuses or industrial areas. By offering these versatile map visualization modes, the system ensures that drivers can adapt their navigation experience to different driving conditions and personal preferences, ultimately improving safety, convenience, and efficiency on the road.

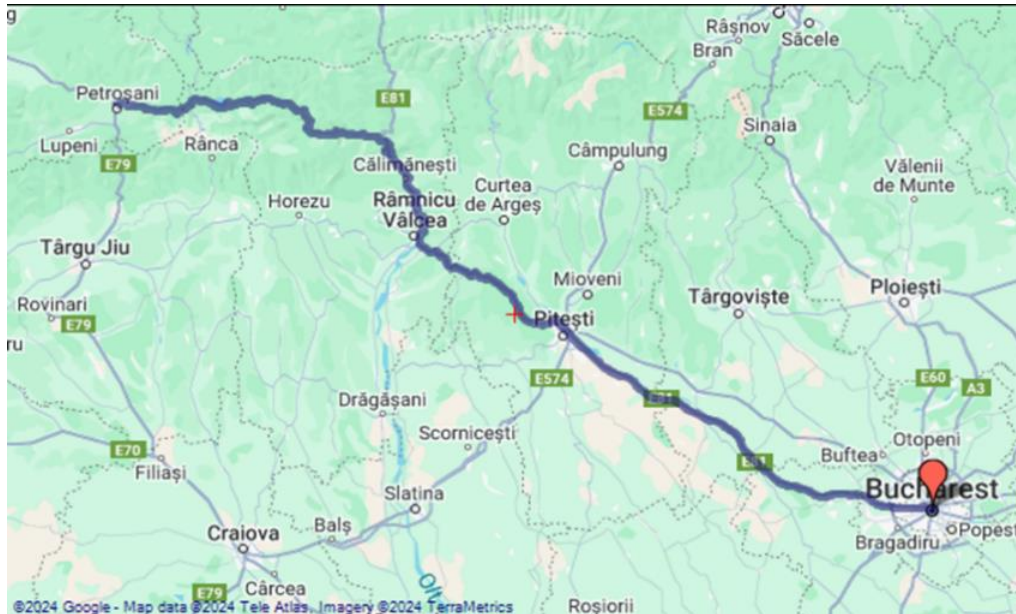


Fig.3 Navigation system

3. TECHNOLOGIES USED

3.1 GMap.NET

GMap.NET [5] is a mapping and map display technology that offers a robust and user-friendly interface for integrating interactive maps into .NET applications. In the on-board computer system of an electric car, GMap.NET is used to display maps, including street maps, terrain maps, satellite maps, and others. These maps are displayed within the graphical interface of the on-board computer system, providing the user with a visual view of the area they are in and the planned route. The user can interact with the displayed maps using a mouse or other interaction devices. For example, the user can zoom into a specific area of the map, scroll to explore adjacent areas, or click on points of interest to obtain additional information. In addition to displaying basic maps, GMap.NET also allows for the addition of extra elements to the maps, such as markers, route lines, polygons, and others. These elements can be used to highlight planned routes, electric vehicle charging stations, or other relevant points of interest.

3.2. OpenWeatherMap API

The OpenWeatherMap API [6] provides access to detailed weather data such as temperature, humidity, wind speed, and more for locations worldwide. In the on-board computer system of an electric car, the OpenWeatherMap API is used to provide up-to-date weather information and assist the driver in making route and driving decisions. Weather data obtained through the OpenWeatherMap API is displayed within the graphical interface of the on-board computer system, allowing the user to see current weather conditions and consider this information when planning the trip.

3.3. Geoapify API

The Geoapify API [7] offers various routing and navigation functionalities, which are used in the on-board computer system of an electric car to provide the driver with useful and precise information related to the planned route and travel conditions. Road maps are displayed within the system's graphical interface using data obtained through the Geoapify API. These maps include the planned routes, points of interest, and other relevant travel information.

4. DRIVING SIMULATION

To demonstrate the functionality and features of the interface, a simulation program was created for an electric car [8], [9]. The simulation begins with the initialization of the car's parameters and the initial driving conditions [10], [11]. This includes the car's weight, battery capacity, motor power, friction coefficients, and other relevant parameters. The objective is to calculate the car's speed based on acceleration, car mass, and other influencing factors using the derived formulas [8], [12].

Initialization parameters

The initial parameters for the electric car simulation are as follows:

- Weight of the car (W): The weight of the car.
- Battery capacity (C): The battery capacity.
- Motor power (P): The motor power.
- Rolling resistance coefficient (k_r): The rolling resistance coefficient.
- Aerodynamic drag coefficient (C_d): The aerodynamic drag coefficient.
- Frontal area (A): The frontal area.
- Air density (ρ): The air density.

Driving Forces

The forces acting on the car are calculated as follows:

1. Rolling resistance force (F_r)(1):

$$F_r = W \cdot k_r \quad (1)$$

where:

- W is the weight of the vehicle.
 - k_r is the rolling resistance coefficient.
2. Aerodynamic drag force (F_d)(2):

$$F_d = 12 \cdot \rho \cdot C_d \cdot A \cdot v^2 \quad (2)$$

where:

- ρ is the air density.
- C_d is the drag coefficient.
- A is the frontal area.
- v is the vehicle velocity in meters per second (m/s).

3. Motor force (F_m)(3):

$$F_m = P \cdot 1000 \cdot v \quad (3)$$

where:

- P is the motor power in kilowatts (kW). The factor 1000 converts kilowatts to watts for consistency in units.
- v is the vehicle velocity in meters per second (m/s).

Vehicle dynamics

The total driving force and the resulting acceleration are determined using the following equations:

1. Total driving force (F_t)(4):

$$F_t = F_m - F_r - F_d \quad (4)$$

where:

- F_m is the motor force.
 - F_r is the rolling resistance force.
 - F_d is the aerodynamic drag force.
2. Acceleration (a)(5):

$$A = F_t/m \quad (5)$$

where:

- F_t is the total driving force.
- m is the mass of the vehicle.

Simulation of speed

To determine the speed of the car over time, the following kinematic equations are used:

1. Velocity $v(t)$ (6):

$$v(t) = v_0 + a \cdot t \quad (6)$$

Where:

- $v(t)$ is the velocity at time t .
- v_0 is the initial velocity.
- a is the acceleration.
- t is the time.

2. Position $s(t)$ (7):

$$s(t) = s_0 + v_0 \cdot t + 1/2 \cdot a \cdot t^2 \quad (7)$$

Where:

- $s(t)$ is the position at time t .
- s_0 is the initial position.
- v_0 is the initial velocity.
- a is the acceleration.
- t is the time.

The car's motion is simulated using a set of predefined formulas [8]. This approach facilitates the assessment of the vehicle's range and performance throughout the route. The simulation continuously monitors and updates the battery level based on the car's energy consumption and additional factors such as energy regeneration during braking (Figure 4).

Parameters such as the coefficient of friction, aerodynamic drag coefficient, frontal area, and motor power are dynamically adjusted in real-time, taking into account driving conditions like speed, gear selection, and terrain.

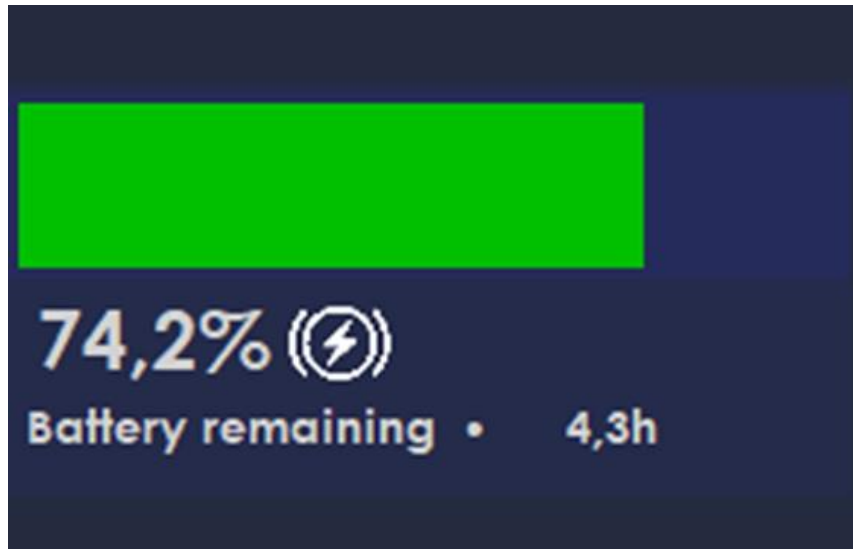


Fig.4. Regeneration of energy during braking

Users can change gears according to driving requirements, and the simulation adapts the car's performance accordingly. During the simulation, visual feedback is provided to the user, displaying essential information such as current speed, battery level, and remaining range.

By persistently updating the car's parameters and offering real-time feedback, this simulation serves as a comprehensive tool for evaluating the vehicle's range, performance, and energy efficiency.

This methodology not only enhances the understanding of the car's capabilities but also aids in optimizing driving strategies to improve performance and conserve energy. Future advancements may include more detailed terrain modelling and the integration of real-world driving data to further enhance the accuracy and applicability of the simulation. In addition to the benefits related to reducing energy consumption, such a system can help in the fight to reduce pollution, thus ensuring an effective sustainable framework [13].

5. CONCLUSIONS

This paper presents the design and implementation of a digital dashboard interface for electric vehicles, utilizing advanced simulation technologies and navigation APIs. The developed system demonstrates a significant improvement in providing real-time vehicle data and enhancing the overall driving experience through a user-friendly interface. The integration of GMap.NET, OpenWeatherMap API, and Geoapify API has enabled the creation of a robust and interactive dashboard that offers comprehensive navigation, weather updates, and vehicle performance metrics.

The use of Windows Forms and C# for the graphical interface ensures an intuitive and accessible user experience, allowing drivers to focus on the road while accessing essential information effortlessly.

The simulation program, which includes real-time adjustments of vehicle parameters based on user inputs and driving conditions, provides an accurate representation of vehicle performance and assists in route planning and energy management.

The findings highlight the potential for future enhancements, such as integrating additional sensors and improving AI algorithms to further refine the system's capabilities. This research underscores the importance of real-time data processing and user-friendly interfaces in modern electric vehicles, offering a scalable and cost-effective solution for enhancing vehicle usability and driver satisfaction.

The proposed digital dashboard interface represents a significant advancement in electric vehicle technology, contributing to safer, more efficient, and enjoyable driving experiences. The system's flexibility and potential for continuous improvement align with the evolving needs of EV drivers and support the broader adoption of electric vehicles.

Future work will focus on expanding the system's functionalities and ensuring seamless integration with emerging automotive technologies.

REFERENCES

- [1]. **Bhatnagar P., Gururaj H. L., Shreyas J., Aithal H.,** *ElectroPath: A Predictive Model for Electric Vehicle Range Optimization Through Mobile Application,* International Conference on Emerging Technologies in Computer Science for Interdisciplinary Applications (ICETCS), pp. 1-6, IEEE, April 2024.
- [2]. **Zaheer S., Krishna A., Surendran A., Sreedeeepam D.,** *Design and Implementation of a Dashboard for Battery Health Monitoring in Context to Industry 4.0,* 2024.
- [3]. **Dudziak A., Kuranc A., Zajac G., Szyszlak-Barglowicz J., Slowik T., Stopka O., Stopková M.,** *Smart solutions in car dashboard interfaces as a response to needs of drivers and their assessment, Case Studies on Transport Policy,* Vol. 16, p. 101194, 2024.
- [4]. **Benedetti D., Agnelli J., Gagliardi A., Dini P., Saponara S.,** *Design of a digital dashboard on low-cost embedded platform in a fully electric vehicle,* IEEE International Conference on Environment and Electrical Engineering and 2020 IEEE Industrial and Commercial Power Systems Europe (EEEIC/I&CPS Europe), pp. 1-5, IEEE, June 2020.
- [5]. GMap.NET, *GMap.NET Documentation,* Retrieved April 22, 2024, from <https://github.com/radioman/greatmaps>.
- [6]. OpenWeatherMap, *OpenWeatherMap API,* Retrieved April 22, 2024, from <https://openweathermap.org/api>.
- [7]. Geoapify, *Geoapify API,* Retrieved April 22, 2024, from <https://www.geoapify.com/api/>.
- [8]. **Lynn D. K., McCormick J. B., Bobbett R. E., Derouin C. R., Nachamkin J., Kerwin W.,** *Determination of vehicle rolling resistance and aerodynamic drag,* 29th IEEE Vehicular Technology Conference, Arlington Heights, IL, USA, pp. 292-295, 1979.
- [9]. **Samuil I., Stancioiu L., Ionica A. C., Leba M.,** *Possibilities of Adopting Electric Vehicles in the Agritourism Development Context,* 18th Iberian Conference on Information Systems and Technologies (CISTI), pp. 1-6, IEEE, June 2023.

[10]. **Rus C., Leba M., Risteiu M. N., Marcus R.,** *Modeling and Simulation of Electric Vehicle Driveline*, 18th Iberian Conference on Information Systems and Technologies (CISTI), pp. 1-6, IEEE, June 2023.

[11]. **Rus C., Leba M., Risteiu M., Marcus R.,** *Vehicle Control Modeling and Simulation for Small Electric Car Case*, 24th International Carpathian Control Conference (ICCC), pp. 388-393, IEEE, June 2023.

[12]. **Rus C., Leba M., Negru N., Marcus R., Risteiu M.,** *Electric vehicles in smart grid and smart city for Petroșani case*, MATEC Web of Conferences, Vol. 342, p. 05002, EDP Sciences, 2021.

[13]. **Negru N., Radu S. M., Soica A.,** *Air quality monitoring and photovoltaic impact assessment in Valea Jiului*, 25th International Carpathian Control Conference (ICCC), pp. 1-6, IEEE, 2024.

ENERGY TRANSITION AS THE NECESSITY FOR ACHIEVE A CLIMATE-NEUTRAL EUROPE

ILIE UTU¹, MARIA DANIELA STOCHITOIU²

Abstract. By 2030, the EU has to be on a clear trajectory towards an energy system decarbonate. In addition to cost benefits, climate and energy security, the energy transition is coming and with new challenges as the system adapts. Reducing carbon emissions represents a difficult task for Romania as well as EU that claims for a diversified mix and strategy.

Key words: climate-neutral, greenhouse gas emissions, energy transition.

1. INTRODUCTION

The energy transition represents a global change in the type that supply and consume energy. A key aspect of the energy transition is the replacement of fossil fuels (coal, oil, gas) with renewable resources.

The energy transition is could consider an element of sustainable energy policy that maximize the wellbeing of the humanity, assuring an equilibrium between competitiveness of the energy producers and environmental protection taking into account the energy systems challenges. [1], [2], [3], [17], [21].

The European Green Deal has the goal for a climate-neutral Europe by 2050 and the main objective is to reach net zero by that year, as the amount of carbon dioxide (CO₂) emitted into the atmosphere to be equal to the amount of CO₂ removed from the atmosphere. At the world level, it is estimated that natural absorbers (forests, soil, oceans) remove between 9.5 and 11 gigatons of CO₂ / year. Nowadays, global CO₂ emissions (37.8 gigatons in 2021) exceed natural CO₂ removal capacity. From this reason, measurements to reduce CO₂ emissions and increase capacity are needed simultaneously of CO₂ removal. The European climate law applied from July 2021, sets an intermediate target for the amount of greenhouse gas emissions to be achieved by 2030, 55% lower than in 1990 [2], [4], [18], [23].

The target could become a 57% reduction, if the increase in the absorptive capacity of the land is achieved and forests to 310 million tons of CO₂ by 2030 as stipulated by regulation 839/2023.

¹ Associate Prof. Eng., Ph.D. University of Petrosani, ilieutu@upet.ro

² Associate Prof. Eng., Ph.D. University of Petrosani, danielastochitoiu@upet.ro

The development of sustainable energy policy in Romania is considering as a rapidly and continuous process for ensuring optimal solutions of long term for customers [20].

All countries in the region have reduced greenhouse gas emissions (GHE) compared to 1990, the below figure shows the evolution of GHE in Romania for the last two decades (fig.1).

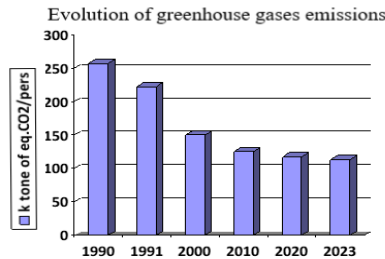


Fig.1. The evolution of GHE in Romania for the last two decades

Based on implementation of clean technologies or de-pollution technologies Romania achieved the largest reduction, from 257 thousand tons of CO₂ equivalent to 110 thousand tons of CO₂ equivalent in 2023.

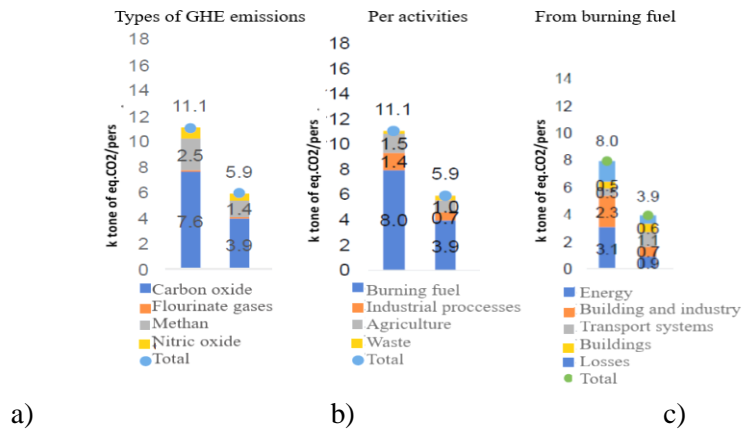


Fig.2. Detailed evolution of gas emissions in Romania

Relative to the population, greenhouse gas emissions decreased from 11.1 tons per capita to 5.9 tons/pers. Most of these emissions consisted of emissions of carbon oxides (66%) and methane (23%). [5], [6], [2].

Romania stands out among the countries in the region due to its double weight in greenhouse gas emissions methane, a gas that does not stay in the atmosphere as long as CO₂, but because it absorbs a lot more solar energy has a much higher greenhouse effect (fig.2a). The most polluting activities remained fuel-burning activities, which generated 3.9 tons/pers. of greenhouse gases in 2022 (fig.2b). The rest of the greenhouse gas emissions were due to industrial processes (0.7 tons/ pers.) and agriculture (1 tons/ pers.).

In Romania, agriculture is polluting more than industrial processes. Most of the pollution resulting from the burning of fuels as is generated by the transport sector and energy sector (fig.2c).

Compared to 1990, pollution in the energy sector has decreased (from 3.1 tones/pers. to 0.9 tons/pers.), but in the transport sector it increased (from 0.5 tones/pers to 1.1 tons/ pers). [7], [8], [9], [10].

The other two sources of pollution by burning fuel are representing by construction sector and buildings. Compared to 1990, pollution in the construction sector decreased (from 2.3 tons/pers. To 0.7 tons/pers.), and building pollution increased (from 0.5 tons/ pers. to 0.6 tons/ pers.).

Romania has reduced GHE emissions from 2022 by 56% compared to 1990, above the target of 55% set by the European Commission for 2030. However, efforts to reduce pollution have to be in line to achieve climate neutrality by 2050. Romania emits gases with GHE effect of 133 tons CO₂ equivalent further, which means the need to reduce emissions in parallel to the increase in the CO₂ absorption capacity of land and forests. This capacity will increase to 49.3 tons of CO₂ equivalent, above the target of 26.5 tons of CO₂ equivalent set for 2030 by the European Commission, Romania being the only country in the region with such a performance under the conditions in which the surface forested area increased slightly up to 30% of the country's surface in 2022.

2. DECREASING POLLUTION MEASURES

In the last 6 years, the structure of electrical energy production electrical was strongly influenced by the retreat of coal or hydrocarbon power plants or groups generators from operation.

During the period September 2017 – June 2023 were retreated from operation capacities totaling an installed capacity of 5508 MW in Romania. So, the capacity installed in the energetic power reached a historic low of 18.254 MW in 2023. In Romania, some capacities were installed as power plants put in operation about 624 MW, most of the power, installed photovoltaic farms – 496 MW, but they did not compensate the decommissioning of two coal-fired units from CE Oltenia, last year. [11], [12], [13], [3].

While wind and solar power were touching production records in Europe, flexibility system becomes vital for accelerating the transition energy, which it still based on fossil sources. Lignite is remaining an important source for electricity production, currently covering almost 18% of total electricity production at the national level.

There is a set of measures that is recommended for reducing pollution, all of them have the same importance and also reinforce each other:

- first, expanding the use of technologies based on renewable energy sources for the generation of electricity is approaching and started many years ago.

The mix of usable of renewable resources depends on existing technologies, availability resources, the climatic conditions determined by the geographical position

of Romania. In Romania, the renewable resources used in order of importance are the waters (35.6%), the wind (16.3%) and the sun (7.7%) [14], [19], [22].

- second, increasing energy efficiency can reduce the amount of energy required. Romania had the third highest energy efficiency in the region last year.
- third, public spending for environmental protection they can finance measures where ecological balances are precarious and natural capacity of CO₂ absorption can be improved.

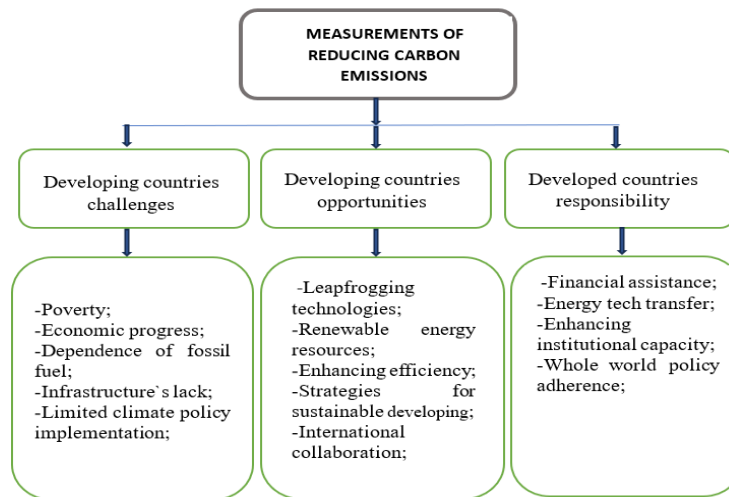


Fig.3. Climate change and build a low-carbon for a sustainable future

Of course, these expenses depend on the fiscal space in the budgets national. In Romania, in the period 2017-2022, the annual public expenses for environmental protection were the lowest.

Reducing carbon emissions represents a difficult task all over the world that claims for a diversified strategy. Each nation, regardless of its present quantity of emissions, has a specific role in this world effort. International collaboration, shared responsibilities, and coordinated efforts can help nations to tackle climate change and build a low-carbon for a sustainable future.

3. ENERGY TRANSITION AT THE MOMENT OF TRUTH

Without sufficient mineral resources, without processing units, without sufficient equipment factories, without mature technologies, Romania and all countries of European Union are engaged in a historic process of economic transformation, with the energy transition at the center. About 85% of a solar panel ,70% of an offshore wind turbine, 41% of the electrolyzes necessary for the development of the hydrogen industry or 71% of electric cars are produced in China, which is the largest global supplier of technology for the projects of green energy. These aspects are hard to be reach or overtake by EU [3], [4], [15]

The energy sector transition in Europe recorded crucial advances in 2023 as the system energetically emerged from a period characterized by high prices and government intervention. But although the EU has strengthened its energy ambitions from renewable sources in response to emerging crises in the last three years.

Improving efficiency in the energy sector is crucial in the clean energy transition process. In addition to reducing greenhouse gas emissions, investments in energy efficiency have the effect of increasing the share of renewable energy and combating energy poverty. Moreover, investments in this objective can create jobs, improve the quality of life and reduce social costs. At the same time, energy efficiency goals must be achieved without affecting productivity. In this transition process, Romania has the advantage of having gas reserves, which will help to have a phased energy transformation, and in addition, but the local market needs storage capacities. [5], [6], [16].

Beyond the moral aspect, of sustainability green transition involves major expenses. The European Commission estimates the costs for the European Union at 700 million euros annually until 2030, or around 5% of the EU's gross domestic product. Probably, each member state of the European Union requires comparable outgoings. The financial sources could be different. In addition to European funds, financing for green transition can be obtained on an internal basis through environmental taxes and green bond issuance. For Romania, between 2017 and 2023, green taxes accounted for 2.1% of GDP annually, representing almost all from energy taxes meanwhile, private sector obligations amounted to USD 0.5 million in 2022 and USD 0.2 million in 2023. For the first time, in February 2024 were issued two million euros of sovereign bonds. [3], [6], [16].

Volumes attained from both funding sources have the potential to be high in the next years. Romania is holding a comparative advantage in green transition relative to other countries, which must be maintained in order to achieve the goal of climate neutrality by the year 2050.

4. CONCLUSIONS

The growth of Romania's electric power sector is essential to the country's overall development since it must guarantee physical availability. continuously to provide power at a cost reachable by customers. The electricity sector's decarbonization reflects a quick and essential step to accomplish the goals that Romania has set for itself in the energy sector and climate change, necessitating an adjustment to sector by boosting electricity safety, promoting social and economic development as component of sustainable development.

REFERENCES

- [1]. **Golovanov N., s.a.** *Eficienta energetica. Mediul. Economia moderna*, Editura Agir, Bucuresti, 2017
- [2]. **Gheorghe St., Lazaroiu G., s.a** *Surse regenerabile de energie electrica in sistemul electroenergetic*, Editura Agir, Bucuresti 2015.

- [3]. **Stochitoiu M.D., Utu I.**, *Challenges of the European energy transition*, vol XXIV, Annals of the University of Petrosani, Universitas Publishing House, 2022.
- [4]. www.irena.org
- [5]. www.energy.ec.europa.eu
- [6]. www.mesagerulenergetic.ro
- [7]. **Momete, D.C.**, *The management of energy sources and resources of Romania: a challenge in the current geopolitical context*, U.P.B.Sci. Bull., Series B, Vol. 68, No. 1, 2006
- [8]. www.globalcarbonatlas.org
- [9]. www.repower.world
- [10]. www.worldenergy.org
- [11]. **Utu, I., Pasculescu, D.**, *Power Quality Study in Order to Comply with European Norms*. Supplement of "Quality - Access to Success" Journal, Vol.18, S1, January, pp. 366-371, 2017.
- [12]. **Stochitoiu M.D., Utu, I.**, *Some aspects about using the modern high efficiency motors for driving the conveyor belts in lignite open pits*. Proceedings of the 7th International Symposium Occupational Health and Safety, SESAM, Poiana Brasov, octombrie 2015.
- [13]. **Tăbăcaru T., Utu I.**, *Mașini electrice și acționări: culegere de probleme*. Universitas, Publishing House, Petroșani, 2012.
- [14]. **Tăbăcaru-Barbu T., Utu I., Tăbăcaru-Barbu I.C.**, *Simulation of a D.C. Drive Static Converter Fed*, Annals of University of Petrosani, 2003.
- [15]. **Utu I., Stochitoiu M. D.**, *Applications of power electronics in electromechanical drives from mining plants*. Annals of University of Petrosani, 2011.
- [16]. **Păsculescu D., Utu I.**, *Increasing the quality of protections for high-voltage power lines*. Publicat in Revista Calitatea, Supplement of "Quality - Access to Success" Journal, Vol.18, S1, January, pp. 234-239, 2017.
- [17]. **Samoilă L., Utu I.**, *Senzori și traductoare – Principii de funcționare*, Editura Univeristas, Petroșani 2010.
- [18]. **Popescu F.G., Slusariuc R., Utu I., Cucaila S., Stochitoiu M. D.**, *Study of the dependence of bending resistance in correlation to temperature of a conductive material*, International Multidisciplinary Scientific GeoConference Surveying Geology and Mining Ecology Management, SGEM 18(4.1), pp. 643-650, 2018.
- [19]. **Slusariuc R., Samoilă L., Utu I., Popescu F.G., Handra A. D.**, *SCADA systems analysis for industrial processes*, Annals of University of Petrosani, Electrical Engineering, Vol. 21, Petroșani, pp.17-22, 2019.
- [20]. **Stochitoiu M.D., Marcu M., Utu I., Niculescu T., Popescu F.G.**, *Modern concepts and its application for energetically security requirement at different connected sources*. International Multidisciplinary Scientific GeoConference Surveying Geology and Mining Ecology Management, SGEM Volume 18, Issue 2.1, pp. 591 – 596, 2018.
- [21]. **Utu I., Marcu M., Niculescu T., Popescu F.G., Slusariuc R.**, *The use of semiconductor materials in the construction of modern equipment for adjustable drive of power equipment from a lignite open pit*. International Multidisciplinary Scientific GeoConference Surveying Geology and Mining Ecology Management, SGEM Volume 18, Issue 2.1, pp.805 – 812, 2018.
- [22]. **Utu I., Marcu M., Popescu F.G., Stochitoiu M. D., Rada A.C.**, *Determination of the optimum operating regime for two power transformers 35 / 6,3 kV*, Annals of University of Petrosani, Electrical Engineering, Vol. 22, pp.71-76, Petroșani, 2020.
- [23]. **Lazăr T., Marcu M.D., Utu I., Popescu F.G., Păsculescu D.**, *Mașini electrice - culegere de probleme*, Editura UNIVERSITAS, Petroșani, pp.197, 2023.

ANALYZING THE IMPACT OF MOTOR IMAGERY IN A BCI VIDEO GAME

SEBASTIAN DANIEL ROSCA¹, MONICA LEBA², DRAGOS PASCULESCU³, LEON PANĂ⁴, FLORIN GABRIEL POPESCU⁵

Abstract: This study presents the current concerns of Brain-Computer Interfaces in the context of current advances in signal preprocessing and monitoring and identification of brain activity and behavior in the context of motor imaging. It also aims to identify the possible involvement of mechanisms specific to motor execution as a form of control based on the simulation of motor function. In this paper we developed an algorithm to quantify the effects produced by the kinesthetic imagery of an upper limb as a mental training method used as input for a video game. We also propose the advanced technique used to preprocess EEG raw data recorded from three healthy subjects, followed by a power spectral density analysis to produce a graphical representation of the beta power spectrum.

Key words: BCI, EEG, PSD, motor imagery, MATLAB.

1. INTRODUCTION

EEG is an important part of BCI and serves as a basic methodology for acquiring and analyzing the activity of the brain to allow for direct interaction between the human cortex and external devices. Due to the non-invasive nature of EEG and its applications in different areas, such as cognitive enhancement, assistive technology, and rehabilitation, there has been a significant stir of interest in EEG-based BCI recently.

With uses far beyond its original medical focus, Brain-Computer Interfaces (BCIs) have actually become a fast-expanding area of study in recent years. These innovative systems are revolutionizing the way humans connect with technology and opening up new possibilities across various domains.

Brain-Computer Interfaces (BCIs) hold significant potential in the research, treatment, and forecasting of neurological disorders. They can identify distinct signal

¹Ph.D Student Eng., University of Petrosani, sebastianrosca91@gmail.com

²Prof. Ph.D Eng., University of Petrosani, monicaleba@yahoo.com

³Ph.D Associate Prof. Eng., University of Petroșani, pdragos_74@yahoo.com

⁴Ph.D., Lecturer, Eng., Mircea cel Batran Naval Academy, leon_pana@yahoo.com

⁵Ph.D Associate .Prof. Eng., University of Petrosani, floringabriel82@yahoo.com

patterns associated with particular disorders, such as Parkinson's disease, to facilitate early identification and enhance diagnostic accuracy. In the treatment of Alzheimer's disease, BCIs have demonstrated potential in augmenting cognitive performance and enhancing memory through neural feedback mechanisms [1], [17], [21], [27]. For those who suffer from severe impairments, BCIs extend a tremendous deal of improvement in communication. These interventions are most valuable for patients suffering from diseases such as cerebral stroke, amyotrophic lateral sclerosis, spinal column injury or who are totally paralyzed. For those unable to speak the goal of Brain-Computer Interface (BCI) technology is to facilitate communication by directly translating brain intent into executable commands [2], [18], [22].

BCIs have altered assistive technology, enabling inventive methods to improve accessibility for people with physical and neurological limitations. By enabling direct interaction between the human cortex and external equipment, BCIs allow users to control assistive tools through neural activity. Innovative applications encompass neural-controlled prostheses, speech-generating technological devices, and systems for smart homes adapted for accessibility [3], [19], [25].

Signal preprocessing is the major step toward improving the performance of BCI systems through the reduction of these aforementioned artifacts and enhancement of the signal quality. As research in this area keeps on expanding, BCI technology offers the potential to alter human-computer interaction and create new paths for medical applications and assistive technologies [4], [23], [26].

In the last years, Brain-Computer Interface technology, especially employing electroencephalography (EEG) signals for motor imagery (MI) activities, has been one of the important fields of investigation.

In the recent years, there has been increasing interest in BCI technology, especially in those based on motor imagery (MI) and electroencephalography (EEG). The eventual goal of this technology aims at improving direct communication between the cortex and external devices; hence it provides a wide range of applications for the assistive technologies and rehabilitation field.

Current research concentrates on the development of deeper signal processing techniques, studying innovative feature extraction methods, and applying more advanced classification algorithms in order to substantially enhance the efficiency and dependability of MI-based BCI systems [5], [20].

The electroencephalogram (EEG) is a critical tool in the monitoring of cerebral activity and behavior; however, the recorded signals usually contain artifacts that may critically affect the analytical outcome. The sources of these artifacts may be ocular movements, muscular activity, and electrical interference from external sources [6].

Electroencephalogram (EEG) plays a crucial function in recognizing brain activity and behavior. But the recording electrical activity is always affected with artifacts and then affects the analysis of EEG signals. So, it is vital to develop algorithms to properly recognize and collect the clean EEG data while encephalogram recordings. Several approaches have been presented to remove artifacts; however, the study on artifact removal seems to remain an open problem [7], [24].

Despite significant progress, there is still an open issue with the artifact elimination of the EEG signals. Researchers in that respect keep on developing new

methods to improve both artifact detection and removal techniques' accuracy and effectiveness [8]. The major developments of the ongoing research in the field are creating automated, robust systems that should not only handle different artifact kinds but also preserve in essence the underlying brain-activity signals.

2. MOTOR IMAGERY AS A BCI SOLUTION

Motor-related brain activity plays a crucial role in association with motor imagery tasks as part of a significant paradigm in BCI research.

In this context, the paradigm of motor imagery is very important, considering that numerous studies have shown that both motor execution and motor imagery are closely related. A study shows that both motor imagining and the execution of walking actions engage overlapping motor-cognitive activations [9], particularly in beta and alpha strength variation patterns [9]. According to the Motor Simulation Theory, up to a certain point, the neural mechanisms behind motor imagery and motor execution are the same, at which point an inhibitory mechanism suppresses muscle activation and the resulting movement between overt action and plan encoding [10]. In theory, this presupposes that imagery practice has a form of control based on the simulation of motor function, which shows significant implications for motor learning and rehabilitation [11].

3. THE STUDY OF THE BETA WAVE

Electrical brain potentials can be captured by minimally invasive contact using headset-type EEG devices. Using this method, the waveforms and differentiated frequencies are measured while the brain activity of a region is associated with simultaneous electrical activity. Taking into account the localization of specific regions linked to motor imagery tasks, beta waves present a particular interest. Beta waves, which present oscillations in frequency between 13 - 30 Hz, are produced in the contralateral motor cortex but also in the somatosensory cortex [12], [13].

During concentration, beta wave activity is increased at the level of the frontal and occipital lobes and lower at the level of the temporal lobe [14].

The beta waves present a typical amplitude between 5 - 20 μ V and a waveform as presented in Fig. 1.



Fig.1. Theta rhythm waveform [15]

4. PUSH MENTAL TASK - CASE STUDY

To implement the case study, we selected three healthy subjects who participated in a mental command training scenario used as a control input for a BCI video game developed by us previously. For the real-time measurement of brain

waves, we used a neural headset equipped with 5 EEG channels with electrodes placed in the key points of the brain as shown in Fig. 2.

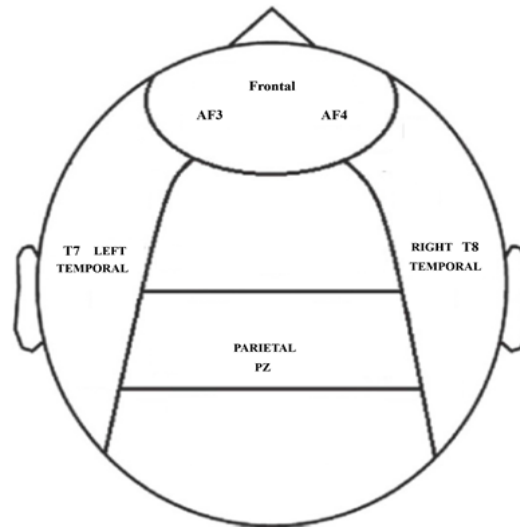


Fig. 2. Emotiv Insight headset - channel location

To train the mental task, each subject had to imagine a kinesthetic complex of arm movement that formed the push task in the time interval between the moment of pressing the training button of this command and the appearance of the pop-up window confirming the training. The mental training scenario is presented in Fig. 3.

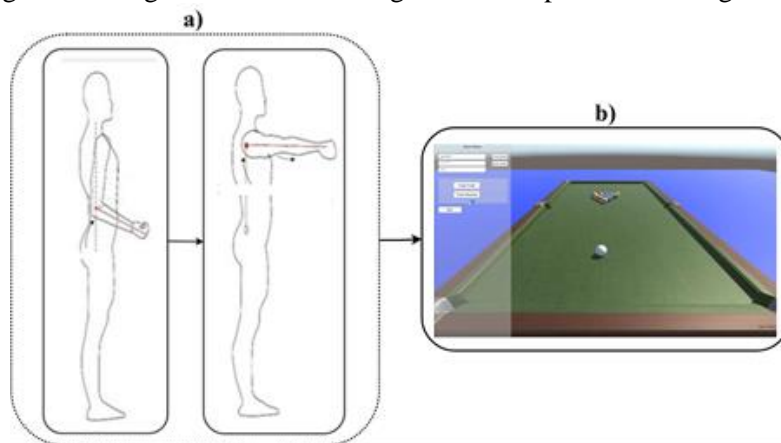


Fig.3. Train push mental task - Mental Pool Game [16]

As shown in Fig. 3. a), the kinesthetic movement complex is composed of a flexion movement of the elbow joint, followed by the same movement of the shoulder joint and an extension of the elbow joint. The interface of the chosen BCI game, made in Unity3D, on which each subject must focus for 9 seconds to memorize the trained mental command, is shown in Fig. 3 b).

5. EEG DATA ANALYSIS AND RESULTS

Each EEG dataset recorded through Emotiv Xavier TestBench software and saved in CSV format was analyzed in an algorithm developed by us, integrated in the MATLAB programming language, to determine the power spectral density distribution (PSD) of beta brainwave. The algorithm description is presented in Fig.4.

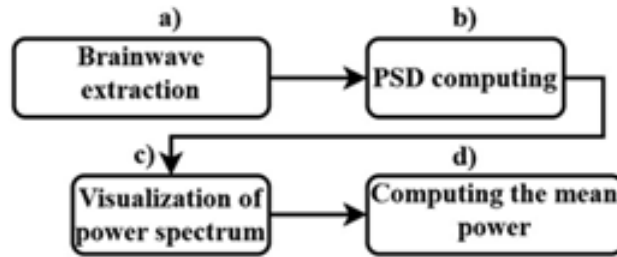


Fig.4. Determination of PSD in beta wave specter

The third step, presented in Fig. 4 c), aims to create a graphical representation of the beta power spectrum, representing the power in decibels (dB) reported to the beta rhythm frequency as a limiting point on the x-axis to the imposed frequency domain.

The fourth stage, illustrated in Fig. 4 d), calculates the average power in the beta frequency band (13 - 30 Hz) for each EEG channel by averaging the PSD values in this frequency range. The results obtained are stored in a table format included in a CSV file.

The results of beta power spectrum estimation (a) and mean power calculation (b) for subject S1 are shown in Fig. 5.

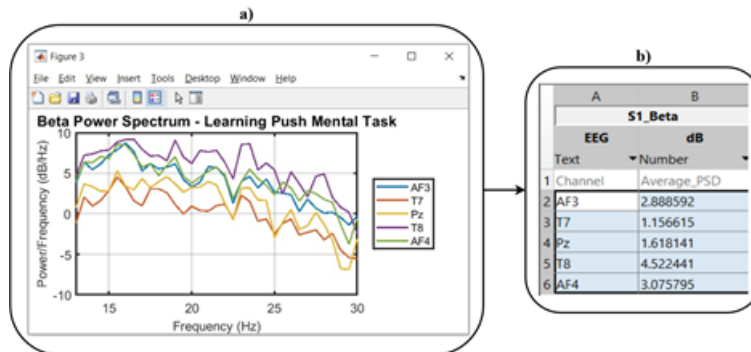


Fig.5. Result of PSD estimation for push mental task - S1 subject case

This result shows, in the case of subject S1, significant temporal asymmetry with stronger right temporal activation, while bilateral frontal activity and moderate parietal activity indicate the right-hemisphere dominance in complex upper limb movement imagery. The results obtained as a result of applying the same algorithm to the EEG dataset related to subject S2 are shown in Fig. 6.

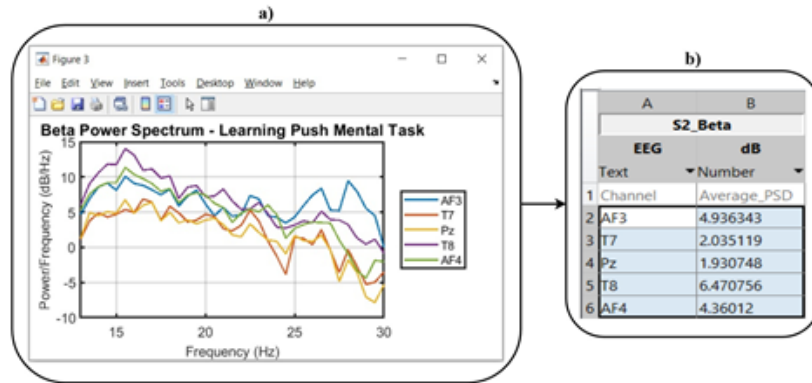


Fig.6. Result of PSD estimation for push mental task - S2 subject case

As the estimation results are presented in the case of subject S2, it can be said that this pattern shows overall higher activation levels compared to S1, particularly in the temporal and frontal regions, while maintaining a similar distribution pattern of right-hemisphere dominance.

The results of PSD estimation for the beta spectrum applied over the subject S3 dataset are presented in Fig. 7.

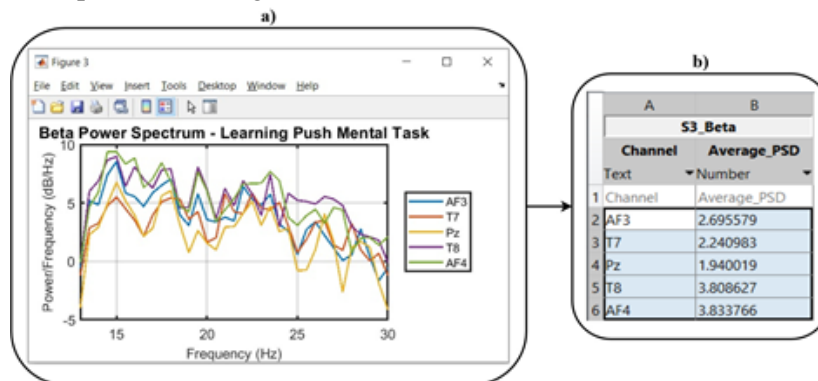


Fig.7. Result of PSD estimation for push mental task - S3 subject case

The beta power distribution during the mental push task for S3 shows moderate temporal asymmetry with slightly higher right temporal activation, while bilateral frontal activity and lower parietal activity demonstrate a more balanced activation pattern, suggesting less pronounced right-hemisphere dominance in complex upper limb movement imagery compared to S1 and S2.

6. CONCLUSIONS

The study of the activation of brain patterns on five EEG channels positioned in key regions of the brain through the prism of signal processing, filtering in the field of beta waves, power spectrum analysis, but also PSD calculation confirming the reliability of this approach in detecting the motor intention.

Also, the application of a training strategy based on kinesthetic motor imagery can prove effective, as evidenced by the consistent beta power distribution patterns across subjects. The neural mechanisms specific to complex motor planning and execution simulation were observed from the temporal asymmetry in conjunction with bilateral frontal activation and consistent parietal engagement.

Next, we propose to extend the study also to the intentional action of the learned mental command to discover if comparable mental models are involved.

REFERENCES

- [1]. **Yang R.**, *Research progress and application of Brain-Computer Interfaces in the diagnosis and treatment of neurological diseases*, 2024 5th International Conference on Electronic Communication and Artificial Intelligence (ICECAI), p. 626-630, 2024.
- [2]. **Salunkhe A.S., Salunkhe A.S.**, *From Science Fiction to Reality: Exploring Brain-Computer Interfaces and their Human Applications*, International Journal of Innovative Science and Research Technology (IJISRT), vol. 9, p. 208-213, 2024.
- [3]. **Ünlü S.C.**, *Enhancing Accessibility through Brain-Computer Interfaces (BCIs) in Assistive Technology*, Human Computer Interaction, Vol. 8, No. 1, 2024.
- [4]. **Xin C.**, *Research on Signal Preprocessing Methods based on Brain-computer Interface*, MedScien, vol.1, no.7, issue 7, 2024.
- [5]. **Ghumman M.K., Singh S., Kaur M., Ghumman**, *Investigation of EEG Signal Classification Techniques for Brain Computer Interface*, International Journal of Engineering and Advanced Technology (IJEAT), ISSN: 2249-8958 (Online), Vol. 9, Issue 3, February 2020.
- [6]. **Jiang X., Bian G.B., Tian Z.**, *Removal of Artifacts from EEG Signals: A Review*, Sensors (Basel, Switzerland), 19(5), 987, 2019.
- [7]. **Thottempudi P., Kumar V., Deevi N.**, *EEG Artifact Removal Strategies for BCI Applications: A Survey*, Majlesi J. Electr. Eng., Vol. 18, No. 1, pp. 187-197, 2024.
- [8]. **Mustile M., Kourtis D., Edwards M.G., Donaldson D.I., Ietswaart M.**, *Neural correlates of motor imagery and execution in real-world dynamic behavior: evidence for similarities and differences*, Frontiers in Human Neuroscience, 18, 1412307, 2024.
- [9]. **Hurst A.J., Boe S.G.**, *Imagining the way forward: A review of contemporary motor imagery theory*. Frontiers in human neuroscience, 16, 1033493, 2022.
- [10]. **Frank C., Krautner S.N., Rieger M., Boe, S.G.**, *Learning motor actions via imagery—perceptual or motor learning?* Psychological Research, 88(6), pp. 1820-1832, 2024.
- [11]. **Gwon D., Won K., Song M., Nam C.S., Jun S.C., Ahn M.**, *Review of public motor imagery and execution datasets in brain-computer interfaces*, Frontiers in human neuroscience, 17, 1134869, 2023.
- [12]. **Rosca S.D., Leba M., Sibisanu R.C., Panaite A.F.**, *Brain controlled lego NXT mindstorms 2.0 platform*, In 2021 International Seminar on Intelligent Technology and Its Applications (ISITIA), pp. 325-330, 2021.
- [13]. **Lim S., Yeo M., Yoon G.**, *Comparison between concentration and immersion based on EEG analysis*, Sensors, 19(7), 1669, 2019.
- [14]. **Houssein E.H., Hammad A., Ali, A.A.**, *Human emotion recognition from EEG-based brain-computer interface using machine learning: a comprehensive review*, Neural Computing and Applications, vol. 34, no. 15, pp. 12527-12557, 2022.
- [15]. **Rosca S., Leba M., Ionica A., Gamulescu, O.**, *Quadcopter control using a BCI*, In IOP Conference Series: Materials Science and Engineering, Vol. 294, No. 1, pp. 012048, IOP Publishing, 2018.

- [16]. **Handra A.D., Popescu F.G., Păsculescu D.,** *Utilizarea energiei electrice: lucrări de laborator*, Editura Universitas, 2020.
- [17]. **Fîță N.D., Radu S.M., Păsculescu D., Popescu F.G.,** *Using the primary energetic resources or electrical energy as a possible energetical tool or pressure tool*, In International conference KNOWLEDGE-BASED ORGANIZATION, vol. 27, no. 3, pp. 21-26. 2021.
- [18]. **Csaszar T., Pasculescu D., Darie M., Ionescu J., Burian S.,** *Method for assessing energy limited supply sources, designed for use in potentially explosive atmospheres*, Environmental Engineering and Management Journal 11, no. 7, 1281-1285, 2012.
- [19]. **Popescu F.G., Păsculescu D., Păsculescu V.M.,** *Modern methods for analysis and reduction of current and voltage harmonics*, LAP LAMBERT Academic Publishing, ISBN 978-620-0-56941-7, pp. 233, 2020.
- [20]. **Pana L., Janusz G., Pasculescu D., Pasculescu V. M., Moraru R. I.,** *Optimal quality management algorithm for assessing the usage capacity level of mining transformers*, Polish Journal of Management Studies 18, no. 2, 233-244, 2018.
- [21]. **Dobra R., Buica G., Pasculescu D., Leba M.,** *Safety management diagnostic method regarding work cost accidents from electrical power installations*. Proc. 1st Int. Conf. on Industrial and Manufacturing Technologies (INMAT), Vouliagmeni, Athens, Greece. 2013.
- [22]. **Stepanescu, S., Rehtanz, C., Arad, S., Fotau, I., Marcu, M., Popescu, F.** *Implementation of small water power plants regarding future virtual power plants* 10th International Conference on Environment and Electrical Engineering, pp. 1-4, IEEE, 2011.
- [23]. **Fîță N. D., Lazăr T., Popescu F. G., Pasculescu D., Pupăză C., Grigorie E.,** *400 kV power substation fire and explosion hazard assessment to prevent a power black-out*, International Conference on Electrical, Computer Communications and Mechatronics Engineering-ICECCME, pp. 16-18, 2022.
- [24]. **Marcu M., Niculescu T., Slusariuc R. I., Popescu, F. G.,** *Modeling and simulation of temperature effect in polycrystalline silicon PV cells*, IOP Conference Series: Materials Science and Engineering, Vol. 133, No. 1, pp. 012005, 2016.
- [25]. **Popescu F.G., Arad S., Marcu M.D., Pana L.,** *Reducing energy consumption by modernizing drives of high capacity equipment used to extract lignite*, Papers SGEM2013/Conference Proceedings, Vol. Energy and clean technologies, pp. 183 - 190, Albena., Bulgaria, 2013.
- [26]. **Popescu F.G., Marcu M.D.,** *Electronică de putere*, Editura Universitas, Petroșani, 2021.
- [27]. **Petrilean D. C.,** *Transmiterea căldurii*, Editura Universitas, 2016.

INCREASING THE TRANSMISSION CAPACITY OF 220kV LINE USING A STATIC SYNCHRONOUS SERIES COMPENSATOR

MARIA DANIELA STOCHITOIU¹, ILIE UTU²

Abstract As the Romania grid's electrical utility industry develops and grows, many changes, including more production stations, transmission lines, and loads are encountered. A Static Synchronous Series Compensator is a FACTS device. This paper is focusing on the theoretical study of series compensation method using Static Synchronous Series Compensator (SSSC) in Romanian Electricity Transmission network as national developing plane installation in the 220 kV axis Urechești – Târgu Jiu Nord – Paroșeni – Baru Mare – Hășdat.

Key words: congestions, energy transition, dynamic stability, compensation, power system

1. INTRODUCTION

The availability of the power transmission network is available to anyone. There are areas of the network where operating regimes that surpass the technical transit limits on elements are regularly observed and leading to the emergence of congestions that the Romanian Transmission System Operator (TSO) should handle, including by redispatch measures, given the operating regimes resulting from transactions on the wholesale electricity market. These redispatch strategies cause market distortions while also increasing TSO operating expenses. These operational issues can be resolved by Static Synchronous Series Compensator for transmission lines compensation well as power oscillations dumping [13], [16], [19], [21].

Static power-electronic devices known as FACTS devices are installed in AC transmission networks. Its use shunt or series compensation to increase the controllability, dynamic stability, and power transfer capabilities of the networks. Static synchronous series compensator (SSSC) is a FACTS device, that uses a voltage-source converter (VSC), and it is coupled in series with the transmission line via a coupling transformer [1], [3].

¹ Associate Prof. Eng., Ph.D. University of Petrosani, danielastochitoiu@upet.ro

² Associate Prof. Eng., Ph.D. University of Petrosani, ilieutu@upet.ro

INCREASING THE TRANSMISSION CAPACITY OF 220kV LINE USING A STATIC SYNCHRONOUS SERIES COMPENSATOR

The longitudinal static synchronous series compensator (SSSC) is a FACTS device, the SSSC uses a voltage-source converter (VSC), and it is coupled in series with the transmission line via a coupling transformer. In order to modify the flow of both active and reactive power in the transmission line, the converter produces a variable AC voltage source that is supplied to the series coupling transformer. Three fundamental components of Static Synchronous Series Compensator are: Power source; coupling transformer; voltage source converter (VSC). Two variants are possible:

- the conventional SSSC, connected to the transmission line through a transformer,
- SSSC device without the transformers, connected to the transmission line through multilevel inverters [2], [15], [18].

The SSSC can be considered functionally as an ideal generator that can be operated with a relatively small DC storage capacitor in a self-sufficient manner to exchange reactive power with the AC system or, with an external DC power supply or energy storage, to also exchange independently controllable active power, analogously to a STATCOM [3], [14], [17], [20].

Its output is a series-injected voltage that models a controlled inductive or capacitive reactance by leading or lagging the line current by 90° . The equivalent line impedance can be changed, and the SSSC can improve the line's capacity for active power transfer. Furthermore, the energy system can benefit from additional functions and services offered by the highly controllable SSSC device.

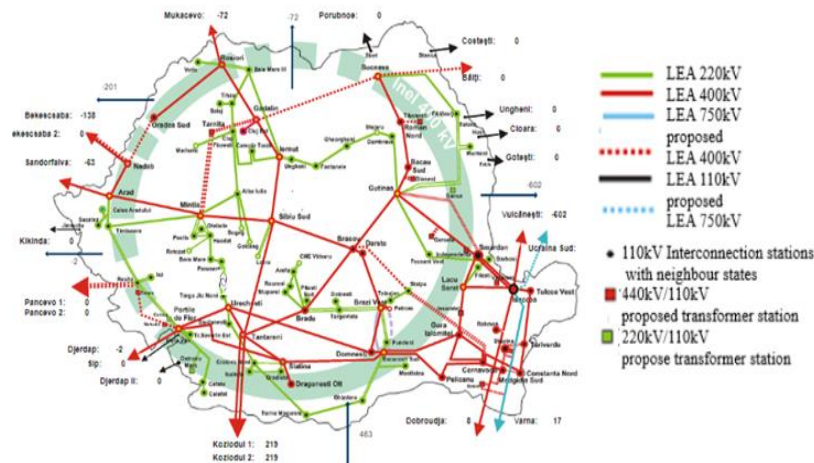


Fig.1. The national power system

The length of LEA between Tg.Jiu Nord power station and Paroseni power station is about $L = 38\text{km}$ and works at 220 kV , $f = 50\text{Hz}$. The specific parameters of electrical line are: Inductivity $l_0 = 1,3\text{ mH/km}$; Capacity $c_0 = 5\text{ nF/km}$ [4], [5].

This line is considered without losses, and in the middle, it could be installed an SSSC. It is supposed that for a dephasing between the ends of line $\theta = 30^\circ$. The maximum transmitted power on the uncompensated line can be calculated followed the next steps including the specify parameters [4], [6], [7]:

- the phase constant

$$\beta = 0,016 \text{ rad/km} \quad (1)$$

- the transmission angle

$$\varphi_L = \beta \times L = 0,016 \times 38 = 0,628 \text{ rad} = 36^\circ \quad (2)$$

- the characteristic impedance

$$Z_C = \sqrt{\frac{l_0}{C_0}} = \sqrt{\frac{1,3 \times 10^{-3}}{7 \times 10^{-9}}} = 425 \Omega \quad (3)$$

- the nominal power

$$P_N = \frac{U_N^2}{Z_C} = \frac{220^2}{510} = 113,89 \text{ MW} \quad (4)$$

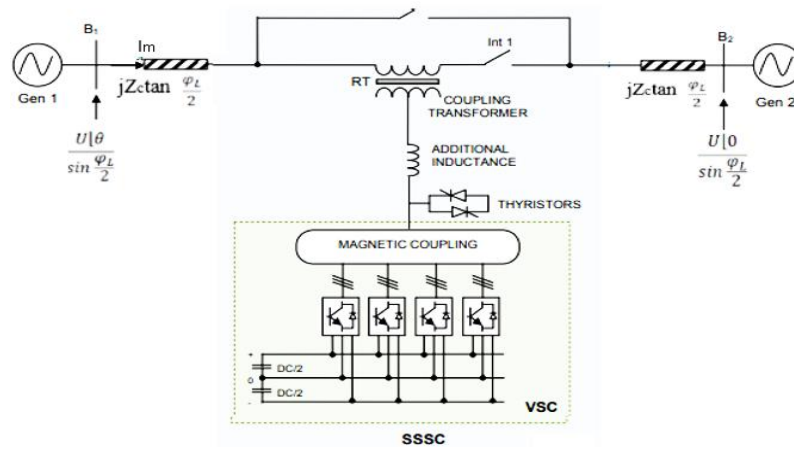


Fig.2. Static Synchronous Series Compensator structure

If U_1 represents the voltage in Tg Jiu Nord Power Station and U_2 represents the voltage in Paroseni Power Station and $U_1 = U_2 = U$, SSSC injected reactive voltage U_{SSSC} could be determine as:

$$\frac{U|\theta}{\sin \frac{\varphi_L}{2}} - jZ_C \tan \frac{\varphi_L}{2} \cdot \underline{I_m} = \underline{U_m} - \frac{U_{SSSC}}{2} \quad (5)$$

$$\frac{U|0}{\sin \frac{\varphi_L}{2}} + jZ_C \tan \frac{\varphi_L}{2} \cdot \underline{I_m} = \underline{U_m} + \frac{U_{SSSC}}{2} \quad (6)$$

$$\underline{U_{SSSC}} = j \cdot \frac{L_m}{I_m} U_{SSSC} \quad (7)$$

The current I_m is diphased behind of U_{SSSC} taking into account that the voltage is increasing into the current direction. From the above equations result:

$$\underline{U}_m = \left(\frac{U_s \cdot \cos \frac{\theta}{2}}{\cos \frac{\varphi_L}{2}} \right) \left| \frac{\theta}{2} \right. \quad (8)$$

$$\underline{I}_m = \left(\frac{U \cdot \sin \frac{\theta}{2}}{Z_C \sin \frac{\varphi_L}{2}} + \frac{U_{SSSC}}{2Z_C \tan \frac{\varphi_L}{2}} \right) \left| \frac{\theta}{2} \right. \quad (9)$$

So, the active power circulation is obtained:

$$P = U_m \cdot I_m = \frac{U^2 \sin \theta}{Z_C \sin \varphi_L} + \frac{U \cdot U_{SSSC} \cdot \cos \frac{\theta}{2}}{2 \cdot Z_C \cdot \sin \frac{\varphi_L}{2}} \quad (10)$$

The current in the middle of the line in the case of compensation using capacitors batteries is:

$$I_m = \frac{U \cdot \sin \frac{\theta}{2}}{(1 - k_m) \cdot Z_C \sin \frac{\varphi_L}{2}} \quad (11)$$

Where $k_m = 0,5$ represents the compensation factor, so $I_m = 1,61$ u.r.

On the other hand, using an SSSC, for an angle $\theta = 30^\circ$, the current (rel.9) expressed in u.r in the middle of the line is:

$$I_m = \frac{\sin \frac{\theta}{2}}{\sin \frac{\varphi_L}{2}} + \frac{\sin \frac{\theta}{2}}{\sin \frac{\varphi_L}{2}} = \frac{\sin \frac{30}{2}}{\sin \frac{36}{2}} + \frac{U_{SSSC}}{2 \tan \frac{36}{2}} = (0,837 + 0,837)$$

The numerical result is based that the two parts are equal and the injected voltage by SSSC is:

$$U_{SSSC} = 2 \times 0,837 \times \tan 18^\circ = 0,544 \text{ u.r.}$$

$$U_{SSSC} = 0,544 \times 220 = 108,86 \text{ kV}$$

$$V_{SSSC} = \frac{U_{SSSC}}{\sqrt{3}} = 62,92 \text{ kV}$$

The resulted active power for a injected constant voltage for a constant reactive power, expressed in u.r., is:

$$P = A \cdot \sin \theta + B \cdot \cos \frac{\theta}{2} \quad (12)$$

$$\text{Where } A = \frac{1}{\sin \varphi_L} = \frac{1}{\sin \frac{\pi}{5}} = 1,7 \text{ and}$$

$$B = \frac{U_{SSSC}}{2 \sin \frac{\phi_L}{2}} = \frac{0,544}{2 \sin \frac{\pi}{10}} = 0,88$$

12): The maximum value of active power expressed in u.r. is it obtained from (rel.

$$\frac{\partial P}{\partial \theta} = 0 \rightarrow A \cdot \cos \theta - B \cdot \sin \frac{\theta}{2} = 0 \quad (13)$$

As $\cos \theta = 1 - 2 \sin^2 \frac{\theta}{2}$, obtain the next equation:

$$A (1 - 2 \sin^2 \frac{\theta}{2}) - B \cdot \sin \frac{\theta}{2} = 0$$

Being $x = \sin \frac{\theta}{2}$, the above equation becomes:

$$2Ax^2 + Bx - A = 0 ; \rightarrow 2 \cdot 1,7 \cdot x^2 + 0,88 \cdot x - 1,7 = 0$$

For the angle $\epsilon (0-\pi)$ the variable x takes positive values, as for $x > 0$ it obtains:

$$x = 0,58 \rightarrow \theta = 72^\circ$$

The maxim active power (.13) for the above θ is:

$$P_{\max} = 1,7 \cdot 0,95 + 0,88 \cdot 0,8 = 2,33 \text{ u.r} \quad (14)$$

$$P_{\max} = 2,33 \cdot P_N = 2,33 \cdot 113,89 = 265,36 \text{ MW}$$

The active power with SSSC for $\theta = 0^\circ$, becomes $P = B = 0,88 \text{ u.r}$, respectively $P = 0,88 \cdot P_N = 100,20 \text{ MW}$. [8], [9]. In this situation the voltage in the middle of the line has the same value as without SSSC device:

$$U_m = \frac{\cos \frac{\theta}{2}}{\cos \frac{\phi_L}{2}} = \frac{\cos 0^\circ}{\cos \frac{36}{2}} = 1,05 \text{ u.r.} \quad (15)$$

The voltages two the SSSC device limits are:

$$\begin{aligned} \underline{U}_1 &= U_m [0 - j \frac{U_{SSSC}}{2}] = 1,05 [0 - j \frac{0,544}{2}] = 1,09 [-15^\circ] \\ \underline{U}_2 &= U_m [0 + j \frac{U_{SSSC}}{2}] = 1,05 [0 + j \frac{0,544}{2}] = 1,09 [15^\circ] \end{aligned} \quad (16)$$

2. CONCLUSIONS

SSSC is used to improve the steady state stability of 220kV transmission lines in this study, the effectiveness of SSSC is to enhance the voltage profile and reduction of active and reactive losses, moreover, SSSC is working effective in increasing the maximum power transfer limit of the system.

REFERENCES

- [1]. **N. Hingorani, L. Gyugyi**, *Understanding FACTS*, 1st ed. New York: John Wiley & Sons, Inc, 2000.
- [2]. **Eremia M., Sanduleac M., s.a.**, *Dispozitive FACTS. Concepte și aplicații în energetică*, Ed. Agir, Academia de Stiinte Tehnice din România, 2017
- [3]. www.entsoe.eu
- [4]. www.transelectrica.ro
- [5]. **N. Golovanov, s.a.** *Eficiența energetică. Mediul. Economia modernă*, Editura Agir, București, 2017.
- [6]. **Saurabh Pingale, Alviya Mahevas, s.a** *An overview of static synchronous series compensator*, Journal of Research in Engineering and Applied Sciences, vol.05, 2020.
- [7]. www.economica.net
- [8]. www.energynomics.ro
- [9]. **[Kumar A., s.a]**, *Power system stability Enhancement using FACTS controllers*, International Conference on Emerging Trends in Electrical Engineering and Energy Management (ICETEEEM), 2012.
- [10]. www.irena.org
- [11]. www.energy.ec.europa.eu
- [12]. www.mesagerulenergetic.ro
- [13]. **Utu, I., Pasculescu, D.**, *Power Quality Study in Order to Comply with European Norms*. Supplement of "Quality - Access to Success" Journal, Vol.18, S1, January, pp. 366-371, 2017.
- [14]. **Stochițoiu M.D., Uțu, I.**, *Some aspects about using the modern high efficiency motors for driving the conveyor belts in lignite open pits*. Proceedings of the 7th International Symposium Occupational Health and Safety, SESAM, Poiana Brasov, octombrie 2015.
- [15]. **Tăbăcaru T., Uțu I.**, *Mașini electrice și acționări: culegere de probleme*. Universitas, Publishing House, Petroșani, 2012.
- [16]. **Tăbăcaru-Barbu T., Uțu I., Tăbăcaru-Barbu I.C.**, *Simulation of a D.C. Drive Static Converter Fed*, Annals of University of Petrosani, 2003.
- [17]. **Uțu I., Stochițoiu M. D.**, *Applications of power electronics in electromechanical drives from mining plants*. Annals of University of Petrosani, 2011.
- [18]. **Samoilă L., Uțu I.**, *Senzori și traductoare – Principii de funcționare*, Editura Univeristas, Petroșani 2010.
- [19]. **Popescu F.G., Slusariuc R., Utu I., Cucaila S., Stochitoiu M. D.**, *Study of the dependence of bending resistance in correlation to temperature of a conductive material*, International Multidisciplinary Scientific GeoConference Surveying Geology and Mining Ecology Management, SGEM 18(4.1), pp. 643-650, 2018.
- [20]. **Stochitoiu M.D., Marcu M., Utu I., Niculescu T., Popescu F.G.**, *Modern concepts and its application for energetically security requirement at different connected sources*. International Multidisciplinary Scientific GeoConference Surveying Geology and Mining Ecology Management, SGEM Volume 18, Issue 2.1, pp. 591 – 596, 2018.
- [21]. **Utu I., Marcu M., Popescu F.G., Stochitoiu M. D., Rada A.C.**, *Determination of the optimum operating regime for two power transformers 35 / 6,3 kV*, Annals of University of Petrosani, Electrical Engineering, Vol. 22, pp.71-76, Petroșani, 2020.

CHARGING THROUGH ELECTRIC FIELD - THE LIMITING ELECTRIC CHARGE OF PARTICLES IN ELECTROSTATIC FILTERS

ANDREI CRISTIAN RADA¹

Abstract: The technological process of electrostatic precipitators involves several interconnected physical mechanisms. In practice, one of the main challenges is the removal of the layer of collected particles from the collection surface, as cleaning methods can reintroduce particles into the gas flow, thereby reducing collection efficiency. Other factors affecting the performance of electrostatic precipitators include the uneven distribution of gas velocity, the bypassing of electrified regions by particle-laden gas flows, and the re-entrainment of particles during periods when the collected material is not being removed.

Key words: electrostatic filters, electric charge, Corona effect, particle separation.

1. INTRODUCTION

Charging particles with an electric charge is the fundamental step in the electrostatic filtration process. Due to the significance of Coulomb's force, it is desirable for particle charging to occur at a high potential. Although electric precipitation is possible under conditions of bipolar charging, unipolar charging is far more efficient and, therefore, more commonly used. Fundamentally, there is no difference between positive and negative charging; both are equally effective for the same applied potential.

In practice, however, the choice of polarity is determined by other factors. For industrial filtration, negative polarity is preferred due to its greater stability and higher voltage and current values. For air purification, positive polarity is favored because it generates a smaller amount of ozone. In both cases, the primary criterion is to achieve the highest possible number of charged particles.

In principle, particles in gases can become charged through various mechanisms. In fact, uncharged particles are extremely rare and are considered exceptions. For instance, natural fog carries a significant electric charge due to the effects of cosmic radiation.

¹ Ph.D., Lecturer Eng., University of Petroșani, radaandreicristian@gmail.com

In many applications, the flue gas environment and the composition of fly ash are such that the layer of collected particles limits the maximum usable voltage and current.

Due to the inherent complexities of the electrostatic precipitator process and the difficulty in justifying limits in practical applications, developing a fundamental model that adequately describes the electrostatic deposition process remains a formidable challenge [2].

To separate particles from a biphasic medium using an electrostatic precipitator, the following operations are required:

- charging the particles in the biphasic medium with an electric charge;
- moving the dust particles toward the collection electrodes;
- depositing the particles onto the collection electrodes;
- removing the material from the collection electrodes for disposal outside the electrostatic precipitator.

Each electrostatic filter consists of two main parts: the collection chamber, through which the gas flow to be purified passes, and the electrical equipment that supplies the chamber with high-voltage direct current. Inside the chamber are the primary components of the system: the collection electrodes and the discharge electrodes (Corona).

2. CORONA DISCHARGE IN DIRECT CURRENT

Corona discharge is an autonomous and incomplete discharge that occurs at a certain potential difference applied to an electrode with a small curvature, forming a limited zone around it known as the corona discharge layer.

The optical characteristic of the corona discharge layer is a pale bluish luminescence, resulting from the recombination of ions accompanied by faint crackling sounds.

The phenomenology of unipolar corona discharge in direct current depends on the polarity of the applied voltage.

In the case of negative polarity, the corona discharge is characterized by the following stages:

- weak current generation: Ionization processes occur when the discharge is not autonomous, and no luminescent phenomena are observed;
- appearance of Trichel pulses: These are characteristic pulses that indicate the onset of a more defined discharge, with a higher rate of ionization;
- formation of a luminous corona around the emission electrode: A visible bluish glow appears around the discharge electrode, marking the active corona region;
- development of streamers: These are elongated, branching structures that form as a result of the corona discharge, which may eventually lead to a full breakdown if conditions allow [2], [3], [6].

In the initial stage, near the electrode with a small curvature radius, electrons appear either by detachment from a negative ion or through secondary emission.

As ionization processes intensify (see fig. 1), the electric field strengthens, and positive charge accumulations begin to form in the region.

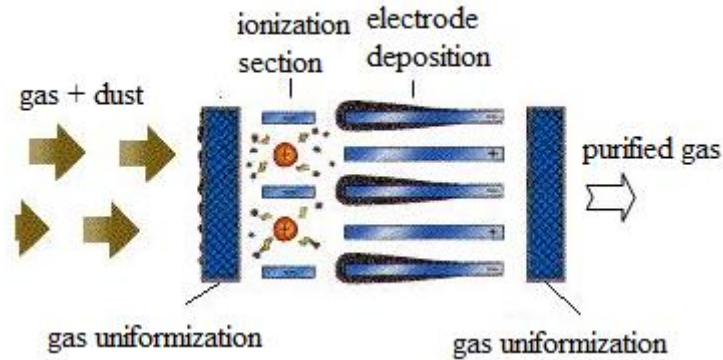


Fig.1. The ionization process

In the dark zone immediately adjacent to the emission electrode, the processes of ionization and excitation are slowed down.

As the electrons travel toward the anode, they lose some of their initial energy, and the intensity of the field gradually decreases. Electrons attach to molecules, leading to the formation of negative ions, characteristic of negative corona discharge.

After the dark zone, there follows a region of high concentration of positive ions, which leads to the uniformization of the field and thus a reduction in its intensity. The processes of ionization and excitation decrease to zero, and the Faraday dark zone appears [5].

The initial intensity of the discharge electric field is determined by the electrical conditions required for the onset of the corona discharge.

The threshold for the onset of corona discharge depends on several factors:

- the radius of the curvature of the electrode,
- the shape of the emission electrode,
- the shape of the collection electrode,
- the distance between the electrodes,
- the polarity of the emission electrode,
- the shape of the applied voltage wave on the emission electrode,
- the temperature of the medium,
- the pressure of the medium.

All of these factors cannot be captured by mathematical expressions to determine the exact threshold for the onset of corona discharge.

F.W. Peek, generalizing the results, provided a formula for the initial intensity required for the onset of corona discharge. The formula is typically expressed as:

$$E_i = A \cdot \delta \cdot \left(1 + \frac{B}{\sqrt{r}} \right) \text{ [kV/cm]} \quad (1)$$

For gases that have the same number of molecules per unit volume, the product of the coefficients A and B is a known quantity. For a curvature radius of the emission electrode ranging from $3,7 \times 10^{-4}$ m to $11,6 \times 10^{-4}$ m the coefficients have the following values: $A = 31,02$ and $B = 0,308$.

3. ELECTRIC CHARGING OF PARTICLES IN ELECTROSTATIC FILTERS

Numerous experimental investigations have concluded that most particles found in various natural suspensions or resulting from certain industrial processes carry electric charges, with uncharged particles being extremely rare. For example, measurements of the free electric charges on raindrops indicate that the average charge ranges from 10 to 100 elementary charges per drop, depending on altitude and storm intensity.

Laboratory studies have shown that in the case of fine particles in the air, nearly all particles are charged (equally positive and negative), and the average charge per particle increases with the particle's diameter. Similar investigations on other fine particles have revealed significant electric charges on aerosols. The natural electric charges occurring in industrial aerosols have also been extensively studied.

These measurements have shown that most industrial dispersions are charged, with the charge typically distributed equally between positive and negative, making the particle suspension electrically neutral as a whole. The average particle charge is small but not negligible [5].

Specific charges of particles generated from furniture grinding processes were found to be on the order of 10^4 elementary charges per gram, representing only 5%-10% of the charge obtained through the corona effect in precipitators.

Industrial steam generally exhibits an even lower charge, often zero or close to zero in most cases.

Despite the numerous possibilities for particle charging, only a few are effective in air purification. Most methods produce ambipolar charging with a low charge. As the number of charged particles increases, it becomes evident, for example, that doubling the charge doubles the separation force, thereby reducing the size of the precipitator required.

As a general principle, economic considerations dictate that particle charging should be as high as possible. Theories and extensive experience have concluded that high-potential unipolar corona discharge is by far the most effective method for producing highly charged particles for air purification purposes.

Consequently, researchers have focused their attention on charging methods that utilize the corona effect (or "cold plasma").

Particles present in a gas carry an electric charge accumulated due to frictional phenomena (triboelectrification), thermal effects, or natural terrestrial radiation. The magnitude of the electric charge accumulated by a particle depends on its intrinsic properties (such as electrical resistivity and permittivity), as well as the electric field existing in the given space.

However, these charges are typically too small for an externally applied electric field to significantly alter the trajectories of these particles. Effective action of an electric field requires the particles to carry as large an electric charge as possible.

As demonstrated in previous chapters, such an electric charge can only be accumulated when particles pass through a region with an electric field sufficiently intense to produce strong gas ionization.

To explain the process of charging particles with electric charge, the following considerations will focus exclusively on spherical particles [5].

An intense electric field causes all ions to move along the field lines, leading to collisions between the particles and the ions. These collisions ultimately result in the ionization of the particles: this is the mechanism of charging through an electric field. For particles with diameters larger than $1\text{ }\mu\text{m}$, this charging mechanism is predominant.

In practice the field charging mechanism is predominant for particles with diameters greater than $0,5\text{ }\mu\text{m}$. The diffusion charging mechanism predominates for particles with diameters smaller than $0,2\text{ }\mu\text{m}$. For particles with diameters between $0,2\text{ }\mu\text{m}$ and $0,5\text{ }\mu\text{m}$, both processes are significant.

4. ELECTRIC FIELD CHARGING - LOAD LIMIT CHARGE

The mechanism by which a particle can become electrically charged will be explained by illustrating how a certain number of ions accumulate on its surface, their motion being driven by the action of an electric field.

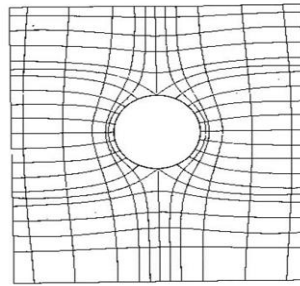


Fig.2. Electric field lines and equipotential lines for a conducting sphere in a uniform field

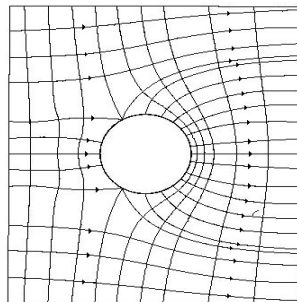


Fig.3. Electric field lines and equipotential lines for a partially charged conducting sphere in a uniform electric field

Let us first consider a conductive particle in the shape of a sphere with a radius a , carrying a negative electric charge of $-q$, and placed in an electric field (Fig. 4). The goal is to identify the forces acting on a negative ion with charge $-e$, located at a point A , such that $OA = a(1+v)$, where v is a multiplication coefficient. Only the radial component of each force will be considered, treating as positive those forces that tend to push the ion away from the particle.

The electric field E exerts a force F on the ion, given by the relation:

$$\vec{F}_1 = -e \cdot \vec{E} \quad [\text{mN}] \quad (2)$$

and its component according to the OA direction:

$$F_1 = -e \cdot E \cdot \cos \theta \quad [\text{mN}] \quad (3)$$

where θ is the angle between Ox and OA.

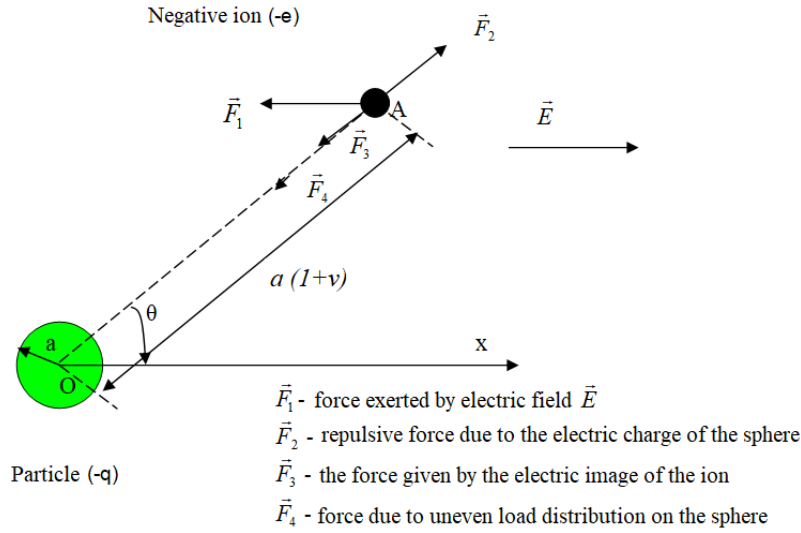


Fig.4. The forces exerted on a negative ion in the proximity of an electrically charged particle

The negative electric charge of the sphere repels the negative ion with a force given by Coulomb's law:

$$\vec{F}_2 = \frac{1}{4 \cdot \pi \cdot \epsilon_0} \cdot \frac{(-e) \cdot (-q)}{[a \cdot (1 + v)]^2} \cdot \vec{r} \quad [\text{mN}] \quad (4)$$

respectively:

$$F_2 = \frac{1}{4 \cdot \pi \cdot \epsilon_0} \cdot \frac{e \cdot q}{[a \cdot (1 + v)]^2} \quad [\text{mN}] \quad (5)$$

The electric image of the ion in relation to the sphere (particle) (Fig. 5) exerts an attractive force on it, given by the expression:

$$F_3 = \frac{1}{4 \cdot \pi \cdot \epsilon_0} \cdot \left[\frac{R_v \cdot a}{(R_v^2 - a^2)^2} - \frac{a}{R_v^3} \right] \cdot e \cdot (-e) \quad [\text{mN}] \quad (6)$$

where R_v is given in (Fig. 5.).

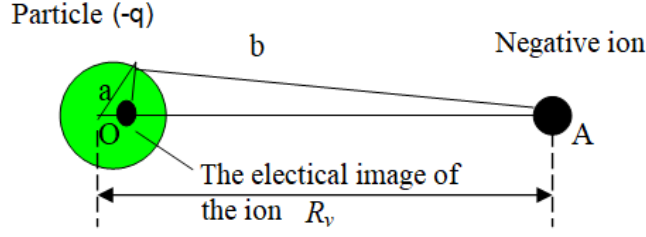


Fig.5. Define the geometric quantities needed to calculate the force created by the electric image of the ion

The non-uniformity of the electric charge distribution on the surface of the particle leads to the appearance of a force, whose radial component is given by the relation:

$$F_4 = -\frac{2 \cdot E \cdot e \cdot \cos \theta}{(1 + \nu)^3} \quad [\text{mN}] \quad (7)$$

The radial component of the total force acting on the particle, charged with the electric charge obtained by the algebraic summation of the radial components of the forces F_{1-4} , is given by the relation:

$$F_T = -E \cdot e \cdot \cos \theta \cdot \left[1 + \frac{2}{(1 + \nu)^3} \right] + \frac{e}{4 \cdot \pi \cdot \epsilon_0 \cdot a^2} \cdot \left[\frac{q}{(1 + \nu)^2} - \frac{e}{4 \cdot \nu^2} \cdot \frac{2 \cdot (1 + \nu)^2 - 1}{(1 + \nu)^3 \cdot \left(1 + \frac{\nu}{2} \right)^2} \right] \quad [\text{mN}] \quad (8)$$

If this component is negative, the ion moves closer to the considered spherical particle. However, the total force F_T determines the movement of the ion only when the distance between the ion and the particle is sufficiently small, thus only for low values of ν , which leads to the expression:

$$F_T = -E \cdot e \cdot \cos \theta \cdot \left[1 + \frac{2}{(1 + \nu)^3} \right] + \frac{e}{4 \cdot \pi \cdot \epsilon_0 \cdot a^2} \cdot \left[\frac{q}{(1 + \nu)^2} - \frac{e}{4 \cdot \nu^2} \right] \quad [\text{mN}] \quad (9)$$

As observed in the previous relation, the total force F_T depends on the angle θ between the direction of the electric field E and the direction of motion of the considered ion. Let the charge of the particle be q . Under these conditions, the force F_T becomes zero when the angle θ has the value θ_0 , given by the relation:

$$\cos \theta_0 = \frac{1}{4 \cdot \pi \cdot \epsilon_0 \cdot E \cdot a^2} \cdot \left[\frac{(1 + \nu)^3}{(1 + \nu)^2 + 2} \right] \cdot \left[\frac{q}{(1 + \nu)^2} - \frac{e}{4 \cdot \nu^2} \right] \quad (10)$$

For the intensity of the electric field $E = 1800 \text{ V/m}$, the radius of the particle $a = 10 \text{ }\mu\text{m}$, the elementary charge $e = 1,6 \times 10^{-19} \text{ C}$, and the particle's electric charge equal to 10.000, 30.000, and 38.000 elementary charges, Pauthenier and Moreau-Hanot plotted the points where the radial electric field cancels out and changes its sign (Fig. 6.).

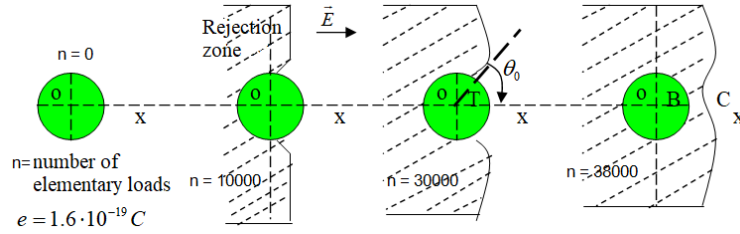


Fig.6. The evolution of the repulsion zone in the vicinity of the particle for various sizes of the electric charge load and $E = 1800 \text{ V/m}$.

If the electric charge of the particle is small, the interaction force between the ion and the particle is negative (causing the ion to move closer to the considered particle) regardless of the distance OA (value of v), which leads to an increase in the charge accumulated on the surface of the sphere (particle). If the charge of the particle q increases, $\cos\theta_0$ increases (i.e., θ_0 decreases), so the repulsion zone closes around the sphere (Fig. 6). Therefore, at a certain point, the particle will be completely surrounded by a repulsion zone that the ions can only overcome if thermal agitation gives them enough kinetic energy.

Thus, as long as the electric charge on the surface of a particle does not reach a limiting value, certain negative ions in the vicinity of the particle, accelerated by the electric field, can be attracted (accumulated) by it [1].

The equation $F_T = 0$ cannot be solved algebraically; however, in the region where $v \ll 1$ and $\frac{e^2}{a^2 \cdot v^2}$ are negligible, the expressions for the force F_T and $\cos\theta_0$ can be written as:

$$F_T = -3 \cdot E \cdot e \cdot \cos\theta + \frac{e \cdot q}{4 \cdot \pi \cdot \varepsilon_0 \cdot a^2} \quad [\text{mN}] \quad (11)$$

$$\cos\theta_0 = \frac{q}{4 \cdot \pi \cdot \varepsilon_0 \cdot 3 \cdot E \cdot a^2} \quad (12)$$

The electric charge accumulated on the particle will reach a limiting value q_p^s when $\theta_0 = 0$, that is, when the ions can no longer reach the surface of the sphere. In this case, the expression for the limiting electric charge can be written as:

$$q_p^s = 4 \cdot \pi \cdot \varepsilon_0 \cdot (3 \cdot E \cdot a^2) \quad [\text{C}] \quad (13)$$

Defining the ratio:

$$\lambda = \frac{q'}{q_p^s} = \frac{q}{4 \cdot \pi \cdot \varepsilon_0 \cdot (3 \cdot E \cdot a^2)} \quad (14)$$

we obtain the following expression for F_T :

$$F_T = E \cdot \cos \theta \cdot [y_1 + (\lambda - 1) \cdot y_2] + \frac{y_3}{a^2} \quad [\text{mN}] \quad (15)$$

$$y_1 = e \cdot \frac{3 \cdot (1 + v) + 2 \cdot \cos \theta}{\cos \theta \cdot (1 + v)^3} \quad (16)$$

$$y_2 = \frac{3 \cdot e}{\cos \theta \cdot (1 + v)^2} \quad (17)$$

$$y_3 = \frac{1}{4 \cdot \pi \cdot \varepsilon_0} \cdot \frac{-e}{4 \cdot v^2} \quad (18)$$

Pauthenier and Moreau-Hanot noted that the ion repulsion zone completely surrounds the sphere when the value of the ratio λ is 1.014, and it increases very rapidly if λ continues to grow. However, according to the definition, the ratio λ cannot exceed unity (the electric charge accumulated through this mechanism cannot exceed the limit charge q_p^s). The net value exceeding unity of the ratio λ can be explained by the fact that this particle charging mechanism neglects the phenomenon of charge by diffusion (the capture of ions that move due to the diffusion phenomenon).

Under these conditions, Pauthenier and Moreau-Hanot plotted the curve $F_T(v)$ for $\lambda = 1.014$. The negative ion under consideration is subjected to a repulsive force in a region with a width of 1 μm , which is equivalent to 12 times the average mean path of an ion in air. For this reason, the probability of an ion reaching the surface of the sphere due to thermal agitation is very low [3], [4]. This leads to the conclusion that the additional electric charge that can reach the particle's surface through this path is negligible compared to the amount of charge already accumulated. To generalize this result, Pauthenier and Moreau-Hanot calculated the values of the ratio λ , creating a repulsion zone of 1 μm for different particle sizes (see Table 1). In the table, it is observed that the ratio λ increases as the particle radius decreases. Pauthenier and Guillien compared the calculated limit value of the electric charge with the measured values, using large steel balls. The deviations between the experimental results and those calculated with the equations:

$$F_T = -3 \cdot E \cdot e \cdot \cos \theta + \frac{e \cdot q}{4 \cdot \pi \cdot \varepsilon_0 \cdot a^2} \quad [\text{mN}] \quad (19)$$

$$\cos \theta_0 = \frac{q}{4 \cdot \pi \cdot \varepsilon_0 \cdot 3 \cdot E \cdot a^2} \quad (20)$$

are 1-2%.

Table 1. The values of λ

$a = 3 \times 10^{-4} \text{ mm}$	$\lambda = 1,1$
$a = 5 \times 10^{-4} \text{ mm}$	$\lambda = 1,04$
$a = 10^{-3} \text{ mm}$	$\lambda = 1,014$
$a = 2 \times 10^{-3} \text{ mm}$	$\lambda = 1,0028$

In the case where the particles have significant electrical resistivity (located in the range of insulating materials), the expression for the limit of the accumulated electric charge can no longer be calculated using relations 19 and 20 [3], [4].

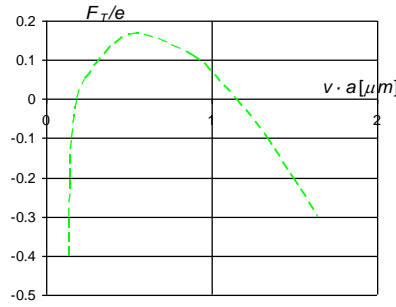


Fig.7. Curve of variation of the force F_e with v

Brigard finds the following calculation relation:

$$q_p^s \approx 4 \cdot \pi \cdot \varepsilon_0 \cdot (p \cdot E \cdot a^2) \quad [\text{C}] \quad (21)$$

where: $p = 1 + 2 \cdot \left(\frac{\varepsilon_r - 1}{\varepsilon_r + 2} \right) = \frac{3 \cdot \varepsilon_r}{\varepsilon_r + 2}$, with ε_r the particle's electrical permittivity.

In the case where the dimensions of the particles are comparable to the mean free path of ions in air $\lambda_{air} = 0,065 \mu\text{m}$, Cochet proposes a calculation expression for the limit of the electric charge, similar to the relation: $q_p^s \approx 4 \cdot \pi \cdot \varepsilon_0 \cdot (p \cdot E \cdot a^2)$ where only parameter p is changed:

$$q_p^s = \left\{ \left(1 + \frac{\lambda_{air}}{a} \right)^2 + \left(\frac{2}{1 + \frac{\lambda_{air}}{a}} \right) \cdot \left(\frac{\varepsilon_r - 1}{\varepsilon_r + 2} \right) \right\} \cdot \pi \cdot \varepsilon_0 \cdot (2 \cdot a)^2 \cdot E \quad [\text{C}] \quad (22)$$

where: λ_{air} is the mean free path of ions in the air, ε_r is the relative permittivity of the particle, and E is the electric field intensity.

Using the above relation, curves were created showing the variation of the accumulated electric charge for different values of the electric field intensity, depending on the particle diameters, at a temperature of 150°C (Fig. 8) (the permittivity is conventionally considered: $\varepsilon_r = 10$) [3], [4].

According to (Fig. 8), for an electric field intensity of $E = 3 \times 10^5$ V/m, a particle with a diameter of $d_p = 0,1 \mu\text{m}$ will accumulate 5 elementary electric charges, while for $d_p = 9 \mu\text{m}$, the number of accumulated elementary charges will be 10,000.

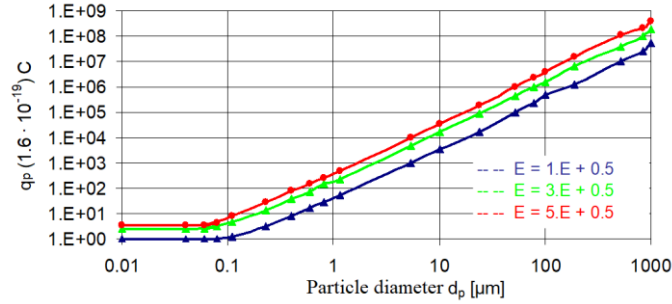


Fig.8. The charging of particles with electric charge as a function of their diameter for different values of electric field intensity.

From the previously presented information, it can be observed that thermal agitation can only have a negligible influence on the value of the limit electric charge accumulated by a particle with a radius around $1 \mu\text{m}$, placed in an electric field.

The expression for the electric charge as a function of time is:

$$q = q_p^s \cdot \frac{t}{t + \tau_q} \quad [\text{C}] \quad (23)$$

where: τ_q is a time constant, called the characteristic charging time, which depends on the density of negative ions and their mobility: $\tau_q = \frac{4 \cdot \varepsilon_0}{\mu \cdot n_i \cdot e}$ where μ and n_i represents the density of negative ions.

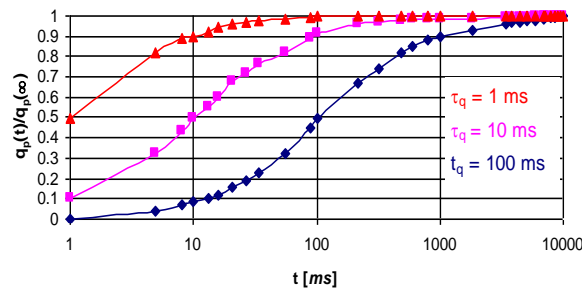


Fig.9. The evolution of the process of charging particles with electric charge over time for characteristic charging times of 1, 10, and 100 ms, using Cochet's relation

Using relation 22 for determining the limiting electric charge, in (Fig. 9) the charge of the particles is shown for different values of the charging time τ_q . It can be observed that for a particle characterized by a specific charging time of $\tau_q = 1$ ms, the

charge accumulated after a time interval of $t = 10$ ms is approximately 10% of the value q_p^s (the charge that would be accumulated over a very long time interval, identical to the limiting charge), while for a particle with $\tau_q = 100$ ms, the accumulated charge will be 90% of the value q_p^s .

4. CONCLUSIONS

The charging of particles by an electric field is a crucial process in the operation of electrofilters, achieved by generating an intense electric field between electrodes. The ions generated by corona discharge move toward the particles, transferring their electric charge.

Particles have a limiting electric charge that can be reached during the charging process. This limit is determined by the balance between electrostatic forces, the dielectric resistance of the medium, and the electrostatic repulsion effects between the already deposited ions and those in motion.

To maximize the efficiency of electrofilters, it is essential to adjust the operating parameters to ensure that the particles reach the optimal electric charge without exceeding the charging limit. This involves precise control of the electric field and environmental conditions, as well as the proper selection of insulating materials.

In practice, achieving and maintaining the limiting electric charge may be affected by the accumulation of deposits or degradation of insulating materials. Ongoing research in the development of more durable materials and electric field control technologies can help overcome these limitations, enhancing the durability and efficiency of electrofilters.

REFERENCES

- [1]. Anghelescu, L., Handra, A.D., Rada, A.C., *The electricity supply to the electric traction system*, Annals of the „Constantin Brancusi” University of Targu Jiu, Engineering Series, 2021.
- [2]. Handra, A.D., Păsculescu, D., Uțu, I., Marcu, M.D., Popescu, F.G., Rada, A.C., *Tehnici de optimizare în energetica*, Editura Universitas, Petrosani, 2022.
- [3]. Nibeleanu, Ș., Artino, A., Napu, S., *Instalații de separare a prafului cu electrofiltre*, Editura tehnică, București, 1984.
- [4]. Popa, G.N., *Contribuții privind îmbunătățirea performanțelor unor electrofiltre industriale pentru sisteme bifazice gaz-particule solide*, teză de doctorat, Facultatea de Electrotehnică și Electroenergetică, Universitatea „Politehnica” Timișoara, 2004.
- [5]. Rada A., C., *Fundamental mechanisms of electrostatic dedusting - diffusion charging of particles in electrofilters*, Annals of Constantin Brâncuși University of Târgu-Jiu - Engineering Series, Nr.3, pp. 48-53, 2024.
- [6]. Samoila B.L., Arad L.S., Marcu M.D., Popescu F.G., Utu I., *Contributions in Modern Electrical Engineering Higher Education Using Dedicated Applications*, International Symposium on Fundamentals of Electrical Engineering, Bucharest, 2018.

EVOLUTION OF ELECTRICITY PRODUCTION FROM THERMOELECTRIC POWER PLANTS IN ROMANIA: AN ECONOMETRIC APPROACH

NADIA ELENA STOICUTA¹

Abstract: This paper analyzes the evolution over time of electricity production from thermal power plants in Romania, by applying an ARMA (Auto Regressive Moving Average) model. The study uses statistical data over a period of 32 years (1992-2023). The results obtained show that time has a significant impact on electricity production from thermal power plants, its negative value indicating that, as time increases, the value of the dependent variable decreases. Also, the first-order moving average component has a significant impact on the dependent variable, the positive value indicating that previous errors have a positive influence on the current values of the time series.

Key words: electricity production, thermoelectric power plants, ARMA model.

1. INTRODUCTION

In the context of the global energy transition and efforts to reduce greenhouse gas emissions, the analysis of electricity production from thermal power plants in Romania becomes particularly relevant.

The European Union has implemented strict policies to reduce greenhouse gas emissions, including by promoting the transition to renewable energy sources and modernizing thermal power plants to make them more efficient and less polluting. In the European Union, it represented approximately 36% of total electricity production in 2022, a decrease of 3.1% compared to the previous year [3]. Germany and Poland are among the EU member states that rely most on thermal power plants, using mainly coal and natural gas for electricity production. In recent years, electricity production from renewable sources has increased significantly in the EU, exceeding production from all fossil sources combined for the first time in 2022 [4].

Romania has a diversified energy profile, with a mix of renewable and non-renewable energy sources. Thermal energy production in Romania is influenced by the available natural resources and national energy policies.

¹ Ph.D., Lecturer Eng. Mat., University of Petroșani,, stoicuta_nadia@yahoo.com

In Romania, thermal power plants play a crucial role in the national energy mix, providing a significant part of the country's electricity needs. These plants use fossil fuels, such as coal and natural gas, to generate heat, which is then converted into electricity.

The production of electricity from thermal power plants is essential for ensuring the stability and continuity of the electricity supply, especially during peak consumption periods. It contributes significantly to Romania's energy security, providing a reliable source of energy that can be quickly adjusted according to demand.

In recent years, Romania has seen a significant increase in electricity production from renewable sources, such as wind and solar energy, thus reducing dependence on fossil fuels. However, thermal power plants remain an important component of the energy mix, ensuring grid stability and the ability to respond quickly to demand fluctuations.

In the context of the global energy transition and efforts to reduce greenhouse gas emissions, the analysis of electricity production from thermal sources becomes particularly relevant. Even though national and European policies promote the transition to cleaner energy sources, thermal power plants continue to play an essential role in ensuring energy security in the medium term.

In the literature, there are a number of recent studies on the analysis of electricity production from power plants. A recent article that studies the theoretical aspects of the different types of heating installations that can be implemented in buildings, as well as information on the algorithms for calculating the heat demand for heating and hot water preparation, according to current regulations, was reported by Dinu and collaborators in the paper [1]. Also, Stoicuta analyzed the evolution of total electricity production by categories of power plants in Romania over a period of 26 years (1992–2017), in the article [2]. This paper aims to perform an econometric analysis of electricity production from thermal power plants in Romania, identifying the determining factors.

2. ECONOMETRIC ANALYSIS OF ELECTRICITY PRODUCTION FROM THERMAL POWER PLANTS IN ROMANIA

The production of electricity from thermal power plants in Romania plays a significant role in the country's energy mix. Thermal power plants use fossil fuels, such as coal, natural gas and fuel oil, to generate electricity.

These plants contribute to ensuring energy stability and security, having the ability to produce energy constantly, regardless of weather conditions. Currently, in Romania, there are seven thermoelectric power plants in operation, in Rovinari and Turceni - Gorj and in Ișalnița and Craiova - Dolj, in Bucharest (South and West), in Paroșeni - Hunedoara.

2.1. Trend Analyses

The following figure shows the evolution over time of electricity production from thermal power plants in Romania, between 1992 and 2023. The statistical data are analyzed over a period of 32 years and are provided by the National Institute of Statistics [5].

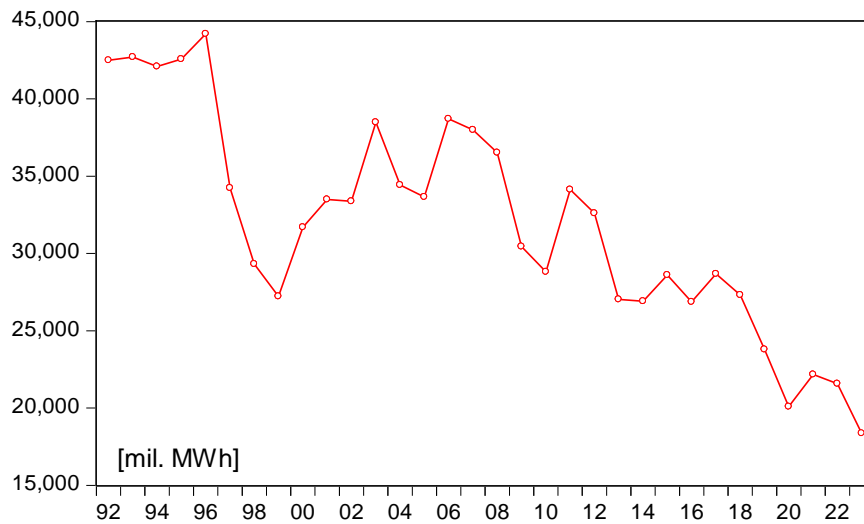


Fig.1. Electricity production from thermoelectric power plants in Romania

Analyzing the above representation, we notice that the graph shows a general downward trend in electricity production from thermal power plants over the analyzed period. This indicates a reduction in dependence on thermal power plants or a transition to other energy sources.

Around 1996, there is a sharp decline in production, followed by stabilization at a lower level. This decline can be associated with changes in energy policy, infrastructure modernization or the closure of old plants. După 1998, graficul arată fluctuații semnificative, cu vârfuri și minime. Aceste fluctuații pot fi cauzate de variații sezoniere, cererea de energie, prețurile combustibililor sau alte factori economici și politici.

By 2022, electricity production from thermal power plants had fallen to around 20,000 million MWh, suggesting a significant reduction compared to the beginning of the period under review.

The long-term downward trend may indicate a transition to cleaner and more sustainable energy sources, such as wind, solar or nuclear power. Changes in energy production may reflect national energy policies, infrastructure investments and environmental regulations.

Fluctuations and declines in production can have an impact on local and national economies, especially in regions dependent on the energy industry.

2.2. Descriptive data and assessments

In 2022, the total installed capacity of thermal power plants in Romania was approximately 32.4% of the total electricity generation capacity. In 2023, electricity production from thermal power plants was 18,367 million MWh, down 14.8% compared to the previous year. The benefits of thermal power plants are that they can operate continuously and ensure constant energy production. They can also be used to cover consumption peaks and stabilize the electricity grid. The major disadvantages of this form of electricity production are high operating and maintenance costs, especially in the context of rising fuel prices, and the burning of fossil fuels that generate greenhouse gas emissions and air pollutants.

The following table presents the values of the main descriptive indicators of electricity production.

Table 1. Descriptive indicators

	Y
Mean	31892.25
Median	32148.50
Maximum	44209.00
Minimum	18367.00
Std. Dev.	6998.514
Skewness	0.022270
Kurtosis	2.217773
Jarque-Bera	0.818485
Probability	0.664153
Observations	32

The electricity production from thermal power plants during the analyzed period is approximately 31892.25 million MWh, which suggests that, on average, the annual production was around this value. As for the median, it represents the middle value of the data, and it is observed that it is very close to the mean, which indicates a relatively symmetrical distribution. The maximum represents the highest value of electricity production during the analyzed period, which is 44209.00 million MWh, and the minimum represents the lowest value of electricity production from thermal power plants during the analyzed period, which is 18367.00 million MWh.

Standard deviation measures the dispersion of values from their mean. A higher value indicates greater variability in electricity production. Skewness measures the symmetry of the data distribution. A value of 0.022 indicates a nearly symmetrical distribution, meaning that the data is not significantly skewed. Kurtosis measures the "sharpness" of the data distribution. A value of 2.217 indicates a slightly flatter distribution compared to a normal distribution (which has a kurtosis of 3).

The Jarque-Bera test is used to check whether the data follows a normal distribution. A probability of 0.66, which is greater than 0.05, indicates that the data follows a normal distribution.

2.3. The econometric model

To perform the econometric analysis of electricity production from thermal power plants, we will use the following notations:

To analyze the evolution of electricity production from thermal power plants in Romania, we will use an ARMA (1,1) (Auto Regressive Moving Average) model defined by the following expression:

$$Y_t = c + \phi_1 Y_{t-1} + \theta_1 \varepsilon_{t-1} + \varepsilon_t, t = \overline{1, 32} \quad (1)$$

where $Y = (y_t), t = \overline{1, 32}$ represents the output variable and is given by the time series of electricity production from thermal power plants. The unit of measurement used is millions of MWh;

- c the model constant;
- ϕ_1 is the first-order autoregressive coefficient;
- θ_1 is the coefficient of the first-order moving average;
- ε_t is the error at time t of the model.

Table 2 introduces both the coefficient values from the ARMA model and the values of the statistics applied in the econometric modeling.

Table 2. Coefficients and values of statistical tests

Dependent Variable: Y				
Method: ARMA Maximum Likelihood (OPG - BHHH)				
Sample: 1992 2023				
Variable	Coefficient	Std. Error	t-Statistic	Prob.
C	1325077.	340428.3	3.892383	0.0006
T	-644.2080	169.5736	-3.798988	0.0008
AR(1)	0.216210	0.172102	1.256290	0.2198
MA(1)	0.634965	0.192523	3.298123	0.0027
SIGMASQ	8.010774	2652118.	3.020519	0.0055
R-squared	0.831169	Mean dependent var		31892.25
Adjusted R-squared	0.806157	S.D. dependent var		6998.514
S.E. of regression	3081.274	Akaike info criterion		19.07234
Sum squared resid	2.56E+08	Schwarz criterion		19.30136
Log likelihood	-300.1575	Hannan-Quinn criter.		19.14825
F-statistic	33.23090	Durbin-Watson stat		1.956609
Prob(F-statistic)	0.000000			
Inverted AR Roots	0.22			
Inverted MA Roots	-0.63			

In the context of the ARMA model, SIGMASQ represents the residual variance of the model. This is a measure of the variability of the residual errors of the model. In other words, SIGMASQ indicates how much the observed values of the dependent variable Y vary from the values estimated by the model. A lower value of SIGMASQ indicates that the model fits the data better because the residual errors are smaller. Conversely, a higher value suggests greater variability in the errors and therefore a poorer fit of the model.

The following figure represents the real values and those adjusted by the ARMA(1,1) model of electricity production from thermal power plants.

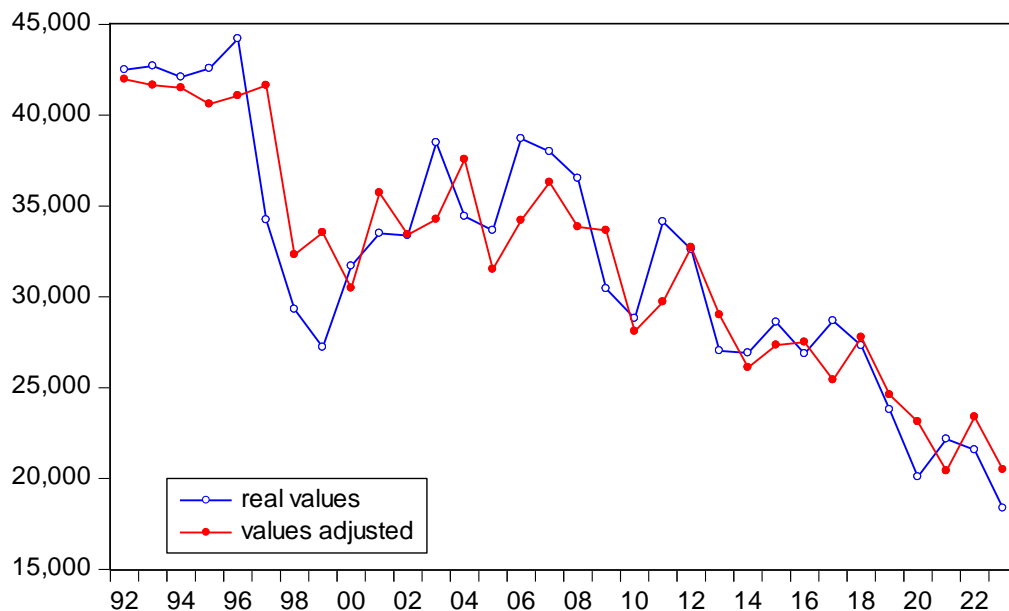


Fig.2. Actual values (blue) and adjusted values (red) through the ARMA model

As can be seen, the two plots are close enough to say that the ARMA(1,1) model performs well.

The stability of the ARMA model is essential to ensure that the long-term predictions of the model are reliable and that the model does not produce explosive or oscillating values. This is determined by the roots of the characteristic polynomials of the autoregressive (AR) and moving average (MA) components (Figure 3).

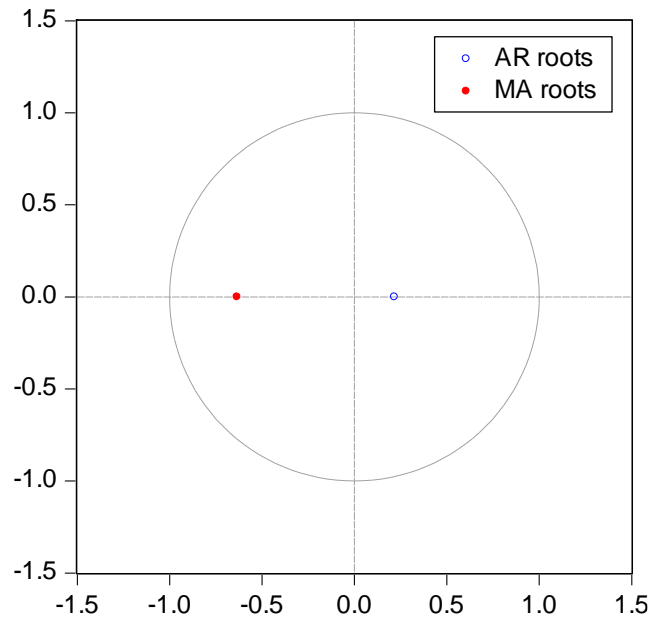


Fig.3. Inverse Roots of ARMA Polynomials

The impulse response shows how long the effect of a shock on the time series lasts. In a stable model, the impact of a shock should diminish over time.

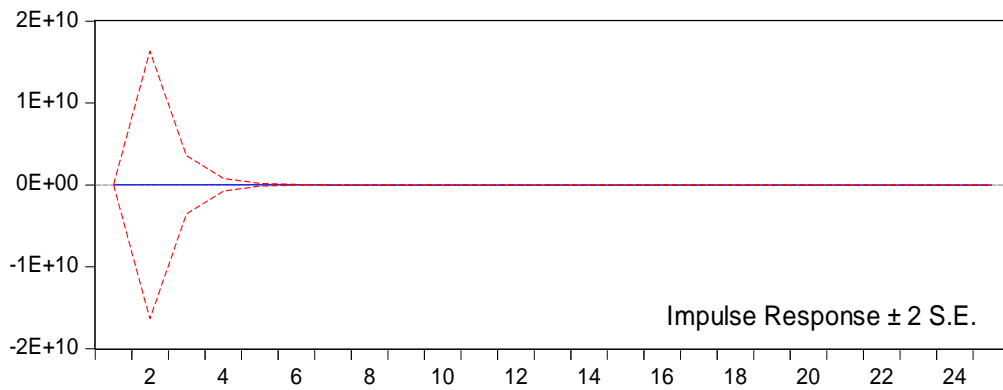


Fig.4. Impulse response

The impulse response is useful for understanding the dynamics of a time series and assessing the stability of the model. It can also be used to analyze the effects of policies, external shocks, or other factors on the variable under analysis.

The following table presents the results of the autocorrelation and partial autocorrelation analysis for a time series, along with the corresponding Q-statistics and p-values.

EVOLUTION OF ELECTRICITY PRODUCTION FROM THERMOELECTRIC POWER
PLANTS IN ROMANIA: AN ECONOMETRIC APPROACH

Table 3. Correlogram of residuals

Sample: 1992 2023						
Included observations: 31						
Autocorrelation	Partial Correlation		AC	PAC	Q-Stat	Prob
. .	. .	1	0.038	0.038	0.0480	0.827
*** .	*** .	2	-0.353	-0.355	4.4401	0.109
. * .	. .	3	-0.085	-0.062	4.7067	0.195
. .	. * .	4	-0.027	-0.169	4.7351	0.316
. * .	. .	5	0.081	0.039	4.9932	0.417
. .	. * .	6	-0.065	-0.170	5.1665	0.523
. .	. .	7	0.010	0.057	5.1704	0.639
. * .	. *** .	8	-0.123	-0.260	5.8406	0.665
. *** .	. *** .	9	-0.207	-0.213	7.8360	0.551
. * .	. .	10	0.138	-0.037	8.7684	0.554
. *** .	. * .	11	0.248	0.095	11.905	0.371
. .	. .	12	0.038	-0.001	11.984	0.447
. *** .	. * .	13	-0.214	-0.141	14.594	0.333
. * .	. * .	14	-0.093	-0.072	15.109	0.371
. * .	. * .	15	0.206	0.094	17.821	0.272
. * .	. .	16	0.095	0.028	18.434	0.299

The analysis of autocorrelation and partial autocorrelation suggests that there is no significant autocorrelation in the residuals of the time series at the analyzed lags, as the p-values are greater than 0.05 for all lags. This indicates that the model used to generate the time series is appropriate and there is no significant residual autocorrelation.

3. RESULTS AND DISCUSSION

Analyzing the results obtained using the Eviews 10.1 program, we can draw the following conclusions:

- The value of the constant is statistically significant ($p < 0.05$), which suggests that it has a significant impact on the dependent variable. This represents the base value of the time series when all other variables are zero.
- The coefficient for time is statistically significant ($p < 0.05$), which suggests that time has a significant impact on the dependent variable. The negative value indicates that as time increases, the value of the dependent variable decreases.
- The value of the AR(1) coefficient is not statistically significant ($p > 0.05$), suggesting that there is no significant first-order autocorrelation in the data. However, the positive value indicates a slight positive dependence between the current and previous values of the time series.

- The MA (1) coefficient is statistically significant ($p < 0.05$), which suggests that the 1st order moving average component has a significant impact on the dependent variable. The positive value indicates that past errors have a positive influence on the current values of the time series.
- The value of the R-squared coefficient of determination suggests that approximately 83.12% of the variation in the dependent variable is explained by the model.
- The F statistic, which has a value of 33.23090, shows that the model is statistically significant ($p < 0.05$), which suggests that at least one of the coefficients is different from zero.
- The Durbin-Watson statistic, with a value of 1.956609, suggests that there is no significant autocorrelation of the residuals.
- The values of the roots of the characteristic polynomials indicate the stability of the ARMA model, since the roots lie inside the unit circle (i.e., the absolute values of the roots are less than 1).
- In the graph in Figure 4, the impact of the shock diminishes over time, indicating the stability of the model. On the other hand, the amplitude of the impulse response indicates the magnitude of the shock's effect on future values of the time series. A large impulse response suggests that the shock has a significant impact on the time series. The initial response is significant, but it stabilizes quickly.
- The sign of the impulse response (positive or negative) indicates the direction in which the shock affects the time series. In the impulse response graph, initial fluctuations around zero suggest that the shock has a variable impact on the time series.

To reduce dependence on fossil fuels, some thermal power plants have started to use biomass and other alternative fuel sources. This can help reduce carbon emissions and promote energy sustainability.

Thermal power plants can be integrated with renewable energy sources, such as solar and wind power, to create a more balanced and sustainable energy mix. This can help stabilize the electricity grid and reduce dependence on fossil fuels.

Investment in research and development is essential to improve the efficiency and sustainability of thermal power plants. The development of new technologies and processes can help reduce costs and minimize environmental impact.

4. CONCLUSIONS

Romania aims to reduce its dependence on fossil fuels and increase the share of renewable sources in the energy mix. However, thermal power plants will continue to play an important role in ensuring energy security in the short and medium term.

To reduce the impact on the environment, it is necessary to modernize existing thermal power plants and implement more efficient and less polluting technologies. For example, the use of combined steam-gas cycles can increase efficiency and reduce emissions.

In the long term, the transition to renewable energy sources is essential to reduce dependence on fossil fuels and combat climate change. However, thermal power plants will continue to play an important role in the energy mix in the medium term.

Governments play a crucial role in promoting energy sustainability by implementing strict policies and regulations on emissions and energy efficiency. Financial incentives and subsidies can encourage the modernization of thermal power plants and the transition to cleaner energy sources.

In conclusion, thermal power plants remain an essential component of the energy mix both in Romania and globally, but the transition to cleaner and sustainable energy sources is imperative to ensure a sustainable and environmentally friendly energy future.

REFERENCES

- [1]. **Dinu R.C. Stan Ivan S. E., Digă M., Stănescu D.G.,** *Influence of Thermal Agent Production Method on Thermal Energy Costs*, International Conference on Electromechanical and Energy Systems (SIELMEN), Craiova, Romania, pp. 1-8, 2023.
- [2]. **Stoicuta N., Stoicuta O.,** *The Analyze of the Electrical Energy Production in Romania by Categories of Power Plants*, 2018 International Conference on Applied and Theoretical Electricity (ICATE), Craiova, Romania, 2018, pp. 1-6, 2018.
- [3]. **Eurostat. Electricity and heat statistic** https://ec.europa.eu/eurostat/statistics-explained/index.php?title=Electricity_and_heat_statistics [Accessed on 2.12.2024]
- [4]. **E-nergia** <https://e-nergia.ro/puterea-instalata-in-termocentrale-a-crescut-in-romania-in-anul-2022-date-transelectrca> [Accessed on 9.12.2024]
- [5]. **Institutul Național de Statistică** <http://statistici.INSSE.ro:8077/tempo-online/#/pages/tables/insse-table> [Accessed on 2.12.2024]

DEVELOPMENT OF A BCI VIDEO GAME FOR MENTAL STATE RECOGNITION

SEBASTIAN DANIEL ROSCA¹, SIMONA RIUREAN², GABRIELA POPESCU³, TEODORA LAZAR⁴, FLORIN GABRIEL POPESCU⁵

Abstract: This paper explores the applications of BCI technology in video games, ranging from medical to innovative gaming experiences. The research considers neurogaming platforms combining BCI and EEG for real-time insight into the cognitive state of players. Additionally, it investigates the use of EEG for emotion classification in gaming contexts. In this paper we develop a video game based on BCI that studies the influence of alpha and beta waves in installing the emotional state of happiness, together with normal state and relaxing state. As a solution to capture EEG signals, we propose to use a neural headset with a single detection electrode that was originally developed for an entertainment game, being augmented with a development board for signal extraction.

Key words: BCI, EEG, low alpha waves, low beta waves, happy.

1. INTRODUCTION

BCIs facilitate direct interaction between the human cortex and external devices, enabling individuals to control technology through thought. This technology is particularly beneficial for persons with severe motor impairments, such as those caused by diseases such as spinal cord injury or amyotrophic lateral sclerosis (ALS).

BCIs generally capture brain signals using methods like electroencephalography, which analyzes brain's electrical activity via electrodes placed on the surface of the scalp. Ensuring accurate signal acquisition and processing remains a significant hurdle due to noise and artifacts in the data.

Brain-Computer Interface (BCI) technology has made significant strides in its application to video games over the years, offering innovative ways for players to interact with virtual environments using their thoughts.

¹Ph.D Student Eng., University of Petrosani, sebastianrosca91@gmail.com

²Ph.D Associate Eng., University of Petrosani, sriurean@yahoo.com

³Student Eng., University of Petrosani, ghetaugabry@yahoo.com

⁴Ph.D. Lecturer Eng, University of Petroșani, teomititica@yahoo.com

⁵Ph.D Associate .Prof. Eng., University of Petrosani, floringabriel82@yahoo.com

We present a brief history of BCI's integration into gaming. In the early stages, BCI technology was primarily focused on medical applications and research. However, as the technology advanced, researchers and developers began to explore its potential in the gaming industry. The use of BCI in gaming started to gain traction in the early 2000s. Researchers began experimenting with EEG-based systems to control simple game elements, laying the groundwork for more complex applications [1].

The development of consumer-grade EEG headsets, such as the Emotiv EPOC+, played a crucial role in making BCI technology more accessible to game developers and players [2]. These devices allowed for easier integration of brain signals in gaming experiences.

As BCI technology improved, it found applications in serious games designed for training and rehabilitation purposes. For example, in 2019, the serious game PROEZA was developed to train users in controlling a hand prosthesis using BCI. This game integrated EEG signals captured by an Emotiv EPOC+ headband with the Unity game engine [3]. Researchers have also explored using BCI-enabled video games to enhance cognitive skills like attention and concentration. Studies have shown that mental training through BCI applications can improve these abilities over time [2].

In recent years, BCI technology in gaming has seen further advancements: the development of more sophisticated algorithms and machine learning techniques has improved the accuracy and responsiveness of BCI systems in gaming contexts; there's been an increased focus on creating immersive gaming experiences that incorporate BCI technology, enabling players to control game elements with their thoughts more seamlessly [4]. The combination of BCI with augmented reality and virtual reality technologies provide new opportunities for creative gaming experiences [5].

As BCI technology continues to evolve, its potential in gaming is expanding. Researchers are exploring ways to use BCI for enhancing player engagement and immersion in games, creating adaptive gameplay experiences based on a player's cognitive state, and developing new genres of games that are specifically designed around BCI interaction.

While BCI in gaming is still a developing field, it has enormous potential for altering how we interact with video games in the future [1].

2. Neurogaming platforms

Neurogaming platforms combine Brain-Computer Interfaces and EEG with video games, enabling the examination of the cognitive state of players in real time by linking brain activity with game actions. Brain-Computer Interface EEG data during gaming provide a continuous objective measurement of the player's cognitive state without interrupting gameplay and offer deeper insights into gaming experiences. While it is common to use this approach for assessing task engagement and arousal, a standard method has not been brought into being yet [6].

A study conducted by McMahan, Parsons, and Parberry demonstrated the effectiveness of EEG in assessing cognitive workload during video game play. The researchers used an off-the-shelf EEG device, the Emotiv EPOC headset, to analyze brain activity during different gaming [7].

Dehais et al. proposed a neuroergonomics framework that maps undesirable neurocognitive states within a two-dimensional space of task engagement and arousal, which can be applied to understanding gaming performance. The framework identifies specific mental states like mind wandering and effort withdrawal, which could be used to analyze how game elements influence players' cognitive states and performance [8].

A recent study evaluated cognitive attention levels of subjects using EEG data while they played three distinct genres of VR video games: Exergames, Challenging Puzzlers, and Casual Games [9]. The researchers studied the brain's activity in the alpha band, comparing IAF - individual alpha frequency and PSD - power spectral density values to detect changes indicating concentration states. Additionally, they examined FAA - frontal alpha asymmetry from the left and the right brain hemispheres [9].

EEG-based neurogaming platforms have shown potential in detecting cognitive decline. A study using a single-channel EEG system with an interactive assessment tool demonstrated the potential for extracting cognitive decline biomarkers in seniors at various clinical phases of cognitive impairment [10]. This approach could potentially aid in an early diagnosis of conditions like Alzheimer's disease.

3. EEG FOR ESTABLISHING HUMAN EMOTION

Combining features from the EEG dataset obtained from both time-domain, frequency-domain, and time-frequency analysis using the Discrete Wavelet Transform (DWT) through a hybrid domain can affect the decision-making process of emotion classification. The emotions in the EEG data set are often divided into four types based on model arousal-valences: those with positive valences with high arousal represented as happy and relaxed, and those with negative valences with low arousal represented by bored and stressed [11], [12], [13].

Most neurophysiological studies correlate emotional activity with the structure of the amygdala as part of the temporal lobe but also with the frontal lobe. Also, happy emotion phenomena can be correlated with brainwave power distribution estimation in the Alpha and Beta bands [14], [15].

An increased presence of low alpha waves (8-10 Hz) located in the frontal lobe may be closely aligned with the state of relaxation induced by mindfulness-based meditation, while increases in beta power together with increased lower alpha reflect networks involved in specific feelings and thoughts related to compassion and gratitude [16], [17].

4. APPROACHED METHOD TO MEASURING EEG SIGNAL

To measure the user's EEG signals, we chose a MindFlex neural headset equipped with a dry metallic detection electrode placed on the forehead at the location of the frontal pole of the brain (FP1) and two reference electrodes placed on the earlobes.

We choose this solution because it offers an inbox circuit-level processing in addition to amplification and digitization. This approach allows data processing based

on Fast Fourier Transform (FFT) to generate power values in the spectrum of different brain wave patterns. This headset transmits the ThinkGear Data Values encapsulated in ThinkGear packets, represented as a sequential stream of bytes. In addition to signal strength values, it can transmit values related to the level of attention and meditation but also to all major frequency bands of the brain [18].

To be able to extract the signals directly from the MindFlex headset circuit data flow via a USB port, we implemented a hardware connection based on the Arduino nano V3 development board, as presented in Fig. 1.

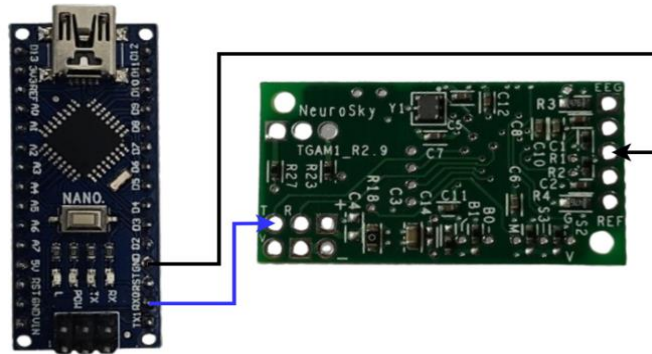


Fig.1. Hardware diagram Arduino Nano V3–Neurosky TGAM1 board

As shown in Fig. 1, we connected the Rx receiver pin of the Arduino to the T transmitter pin of the MindFlex board to enable the UART (Universal Asynchronous Receiver-Transmitter) hardware serial communication protocol between the boards.

The result of MindFlex neural headset integration with the development board is presented in Fig. 2.



Fig.2. MindFlex neural headsets after hardware upgrades

Next, we implemented a code in the Arduino Integrated Development Environment (IDE) that uses the `<Brain.h>` library (<https://github.com/kitschpatrol/Brain>), available by the General Public License (GNU), for parsing the data. We aimed to obtain processed data every second at the Neurosky TGAM1 chip baud rate, related to signal EEG quality, attention, low alpha waves that it associated with relaxation and meditation, and low beta waves that it associated with active thinking and focus. Each data point is then transmitted over the serial interface in CSV (Comma-Separated Values) format to be used as input to trigger a specific action in a BCI video game.

5. THE IMPLEMENTATION OF BCI VIDEO GAME

To be able to decode the user's emotional state, we developed a BCI-based video game based on a five-step algorithm, presented in Fig. 3, which we implemented in the Java-based Processing high-level programming language through the open-source sketchbook software, Processing 4.

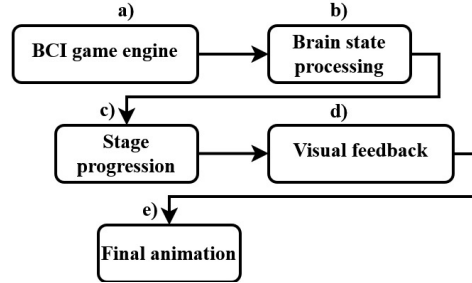


Fig.3. The implementation of emotional state decoding BCI video-game

The first step has the role of implementing the game variables that manage the number of stages set to three, to the current stage, but also the target brain state tracked from three target states that are chosen pseudorandomly. It also sets a series of timers, both to measure the user's performance and to trigger the closed or open state of a padlock animation generated as a reward based on the state reached by the user.

The second step aims to update the user's brain state in the category of normal state or emotion, such as relaxed or happy, by comparing the low alpha and low beta wave values obtained from the processed data as a result of reading the brain signals received from the Arduino board through the serial port. This classification is obtained by comparing the read values with a set of predefined minimum and maximum thresholds proposed by Hadi et al. in the domain of the tracked brain waves, presented in Table 1.

Table. 1. The threshold value for low alpha and low beta waves [19]

Mental condition	α (Min– Max)	β (Min – Max)
Normal	11000 – 150000	13000 – 150000
Happy	50000 – 150000	150000 – 300000
Relax	150000 – 260000	150000 – 250000

The third step verifies each step's completion by marking the current state as successful if it matches a target of 2 seconds in which the user focused and maintained the set emotion or normal state as appropriate. At the same time, it imposes a time limit of sixty seconds within which the imposed state must be reached; otherwise, the stage is counted as a failure. In case of success, a countdown is initialized, which will be displayed in the form of a numerical animation, marking a three-second countdown between stages. The implementation of the third step with open padlock state animation is presented in Fig. 4.

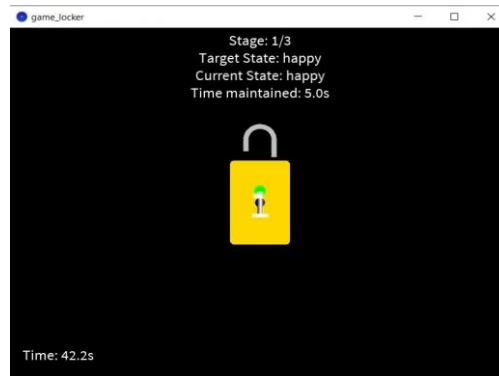


Fig.4 The first stage of BCI game with happy state recognition

The fourth step implements a series of animations to improve the user's perception of game dynamics offered as a reward to the action performed from rendering a closed padlock shown in Fig. 5. a), marked by a green pulsating indicator whose intensity is marked by the power developed by the user feeling experience. At the same time, a render of an open padlock, shown in Fig. 5. b), may or may not be marked by the pulsating indicator, depending on the presence or absence of maintaining the emotion, but it is certainly marked by the numerical animation of the three-second countdown.

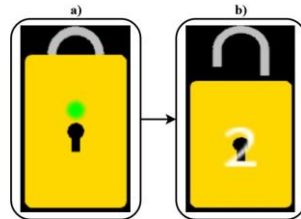


Fig.5 The interstage animation of paddlock

The last step represents the completion of all stages and aims to display an animation of total stars accumulated by the user as a result of accomplishing the imposed state. Along with the number of accumulated stars, represented between two and five, each user is being rewarded with one star for fulfilling the condition of the stage, displaying the related message, the completion times, and the achieved states for each stage. The final scene result of the BCI video game is presented in Fig. 6.

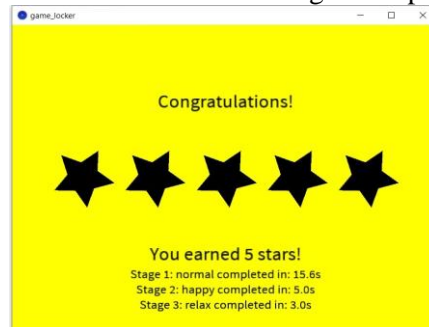


Fig.6 The final scene of BCI video game

6. CONCLUSIONS

BCI technology in gaming aims to change the way players engage, the mode of interaction based on immersive experiences, with the role of unlocking experiences between cognitive health and emotional well-being.

Through this study we found that the analysis of low alpha and low beta waves obtained as a result of preprocessing EEG signals at the circuit level by the MindFlex neural headset produces optimal results in the detection of the emotional state of happiness. This is influenced by the user's imagined experiences and produces better results in the case of imagining a scenario in which he associates the emotion with seeing a close person again, as shown in Fig. 4 reported to the time of maintaining the state. Also, we found that relaxation can be improved when the user was focused on his breath and maintained a defocused eye gaze.

Further, we want to extend the study to the gamma waves in the frontal lobe, as it is known this phenomenon can produce a decrease in the power spectrum related to responses to videos that evoke happiness.

REFERENCES

- [1]. **Hong S.**, *A review of Brain Computer Interface : Applications and potential* SunKee Hong, Computer Science, Medicine, 2013.
- [2]. **Garg D.**, *Cognitive Assessment and Enhancement through Video Gaming using Brain Computer Interface (BCI)*, IJRDO - Journal of Business Management, 3(12), pp.26-37, 2017.
- [3]. **Vega I., Adarve C., Villar-Vega H., Páramo C.**, *Serious game for real-time brain-computer interface training*, Journal of Physics: Conference Series, Vol. 1418, No. 1, pp. 012011, 2019.
- [4]. **Shafeeg A., Shazhaev I., Tularov A., Shazhaev I., Mihaylov D.**, *BCI Tech in Gaming Training and Education*, Indonesian Journal of Computer Science, Vol. 12, pp. 411 - 423, 2023.
- [5]. **Stephanidis C.**, *Intelligent and ubiquitous interaction environments*, 2009.
- [6]. **Parsons T.D., McMahan T., Parberry I.**, *Classification of video game player experience using consumer-grade electroencephalography*, IEEE Transactions on Affective Computing, 13(1), pp. 3-15, 2020.
- [7]. **McMahan T., Parsons T.D., Parberry, I.**, *Modality Specific Assessment of Video Game Player's Cognitive Workload Using Off-the-Shelf Electroencephalographic Technologies*, Dept. Comput. Sci. Eng., Univ. North Texas, Denton, TX, USA, 2014.
- [8]. **Dehais F., Lafont A., Roy R., Fairclough S.**, *A neuroergonomics approach to mental workload, engagement and human performance*, Frontiers in neuroscience, vol. 14, 268, 2020.
- [9]. **GomezRomero-Borquez J., Puerto-Flores J.A., del-Valle-Soto C.**, *Mapping EEG Alpha Activity: Assessing Concentration Levels during Player Experience in Virtual Reality Video Games*, Future Internet, 15 (8), 264, 2023.
- [10]. **Molcho L., Maimon N.B., Pressburger N., Regev-Plotnik N., Rabinowicz S., Intrator N., Sasson A.**, *Detection of cognitive decline using a single-channel EEG system with an interactive assessment tool*, medRxiv, 2020-08, 2020.
- [11]. **Lim M. X., Teo, J.**, *Predicting game-induced emotions using EEG, data mining and machine learning*, Bulletin of the National Research Centre, 48(1), 57, 2024.

- [12]. Galvão F., Alarcão S.M., Fonseca, M.J., *Predicting exact valence and arousal values from EEG*. Sensors, 21(10), 3414, 2021.
- [13]. Kumar G.S., Sampathila N., Martis, R.J., *Classification of human emotional states based on valence-arousal scale using electroencephalogram*. Journal of Medical Signals & Sensors, 13(2), pp. 173-182, 2023.
- [14]. Suhaimi N.S., Mountstephens J., Teo J., *EEG-based emotion recognition: a state-of-the-art review of current trends and opportunities*, Computational intelligence and neuroscience, 2020(1), 8875426, 2020.
- [15]. Halim N.F.A., Fuad N., Marwan M.E., Nasir, E.M.N.E.M., *Emotion state recognition using band power of eeg signals*. In Proceedings of the 6th International Conference on Electrical, Control and Computer Engineering: InECCE2021, Kuantan, Pahang, Malaysia, 23rd August, pp. 939-950, 2022.
- [16]. Pratiwi M., Wibawa A.D., Purnomo, M.H., *EEG-based happy and sad emotions classification using LSTM and bidirectional LSTM*. In 2021 3rd international conference on electronics representation and algorithm (ICERA), pp. 89-94, 2021.
- [17]. Viczko, J., Tarrant, J., & Jackson, R., *Effects on Mood and EEG States After Meditation in Augmented Reality With and Without Adjunctive Neurofeedback*, Frontiers in Virtual Reality, 2, 618381, 2021.
- [18]. He R., *Observing Brainwaves when Playing Games Using a Ruby-based Wireless Brainwave Measurement System*, International Journal of High School Research, 4(3), 2022.
- [19]. Hadi S., Sholahuddin A., Rahmawati L., *The design and preliminary implementation of low-cost brain-computer interface for enable moving of rolling robot*, In 2016 International Conference on Informatics and Computing (ICIC), pp. 283-287, 2016.

DIRECT ROTOR FLUX-ORIENTED CONTROL OF INDUCTION MOTORS USING HYSTERESIS CURRENT CONTROLLERS AND VSI INVERTER

OLIMPIU STOICUTA¹, VALI – CHIVUTA SIRB², NADIA ELENA STOICUTA³

Abstract: This article details the modeling and simulation of a direct rotor flux-oriented vector control system, incorporating hysteresis current controllers and a voltage source inverter (VSI). The simulations is conducted using Matlab-Simulink. The numerical analysis investigates the effects of sampling time on the discretization of speed, rotor flux, and electromagnetic torque controllers, as well as on the rotor flux observer.

Key words: rotor flux-oriented control, induction machines, simulation.

1. INTRODUCTION

Direct Rotor Flux-Oriented Control (DRFOC) is an advanced and effective technique for optimizing the performance of induction motors, widely used in industrial applications.

This method allows for the decoupling and independent control of the rotor flux and electromagnetic torque of the induction motor, similar to DC motors, thus facilitating precise and rapid control of these variables [1], [4], [5], [11].

The integration of hysteresis current controllers and a voltage source inverter (VSI) within the DRFOC system brings significant benefits in terms of stability and dynamic response of the induction motor [2].

Considering these aforementioned advantages, this article aims to elucidate, through numerical simulation in Matlab-Simulink, the impact of sampling time and discretization methods used in the controllers and the rotor flux observer on the dynamic performance of the DRFOC system, thus providing valuable insights for the improvement and optimization of industrial applications of induction motors.

¹ Ph.D., Assoc. Prof. Eng., University of Petroșani, stoicuta_olimpiu@yahoo.com

² Ph.D., Lecturer Eng., University of Petroșani,, sirb_vali@yahoo.com

³ Ph.D., Lecturer Eng. Mat., University of Petroșani,, stoicuta_nadia@yahoo.com

$$a_{11} = -\left(\frac{1}{T_s \cdot \sigma} + \frac{1 - \sigma}{T_r \cdot \sigma}\right); a_{13} = \frac{L_m}{L_s \cdot L_r \cdot T_r \cdot \sigma}; a_{14} = \frac{L_m}{L_s \cdot L_r \cdot \sigma}; a_{31} = \frac{L_m}{T_r}; a_{33} = -\frac{1}{T_r};$$

$$b_{11} = \frac{1}{L_s \cdot \sigma}; T_s = \frac{L_s}{R_s}; T_r = \frac{L_r}{R_r}; \sigma = 1 - \frac{L_m^2}{L_s \cdot L_r}; K_T = \frac{3}{2} \cdot z_p \cdot \frac{L_m}{L_r}.$$

In previous relationships, the following notations were used: R_s, R_r – stator and rotor resistances; L_s, L_r – stator and rotor self-inductances; L_m – mutual inductance; T_s, T_r – stator and rotor time-constants; σ – leakage coefficient; z_p – number of pole pairs; J – moment of inertia of the rotor; F – friction coefficient; K_T – torque constant; T_M – instantaneous electromagnetic torque of the motor; T_F – static friction torque; F – the coefficient of viscous friction; T_L – load torque; ω_r – mechanical angular speed of the rotor; $\underline{i}_s = i_{ds} + j \cdot i_{qs}$ – space vector of the stator current; $\underline{\psi}_r = \psi_{dr} + j \cdot \psi_{qr}$ – space vector of the rotor flux; $\underline{u}_s = u_{ds} + j \cdot u_{qs}$ – space vector of the stator voltage; $j = \sqrt{-1}$.

The mathematical model of the induction motor is written in a stationary reference frame fixed to the stator (d - q).

Relations (1) and (2), after discretization using the trapezoidal robust method, become [10]:

$$\begin{bmatrix} i_{ds}[(k+1) \cdot T_e] \\ i_{qs}[(k+1) \cdot T_e] \\ \psi_{dr}[(k+1) \cdot T_e] \\ \psi_{qr}[(k+1) \cdot T_e] \end{bmatrix} = A_d \cdot \begin{bmatrix} i_{ds}[k \cdot T_e] \\ i_{qs}[k \cdot T_e] \\ \psi_{dr}[k \cdot T_e] \\ \psi_{qr}[k \cdot T_e] \end{bmatrix} + B_d \cdot \begin{bmatrix} u_{ds}[k \cdot T_e] \\ u_{qs}[k \cdot T_e] \end{bmatrix} \quad (3)$$

$$J \cdot \{\omega_r[k \cdot T_e] - \omega_r[(k-1) \cdot T_e]\} = \frac{T_e}{2} \cdot \{N[k \cdot T_e] + N[(k-1) \cdot T_e]\} \quad (4)$$

where: $A_d = \left(I_4 - A_k \cdot \frac{T_e}{2}\right)^{-1} \cdot \left(I_4 + A_k \cdot \frac{T_e}{2}\right); B_d = \left(I_4 - A_k \cdot \frac{T_e}{2}\right)^{-1} \cdot T_e \cdot B;$

$$N(\tau) = T_M(\tau) - T_F(\tau) - F \cdot \omega_r(\tau) - T_L(\tau);$$

$$A_k = \begin{bmatrix} a_{11} & 0 & a_{13} & a_{14} \cdot z_p \cdot \omega_r[k \cdot T_e] \\ 0 & a_{11} & -a_{14} \cdot z_p \cdot \omega_r[k \cdot T_e] & a_{13} \\ a_{31} & 0 & a_{33} & -z_p \cdot \omega_r[k \cdot T_e] \\ 0 & a_{31} & z_p \cdot \omega_r[k \cdot T_e] & a_{33} \end{bmatrix}$$

In order to obtain relation (3), it was assumed that: $u_{ds}[k \cdot T_e] = u_{ds}[(k+1) \cdot T_e]$ and $u_{qs}[k \cdot T_e] = u_{qs}[(k+1) \cdot T_e]$; when the sampling time (T_e) has a very small value. The T_e denotes the sampling time used in the discretization of the mathematical model of the induction motor.

- **The flux analyzer (AF).** This block is defined by the following relations:

$$\begin{cases} |\psi_r[k \cdot T_n]| = \sqrt{\psi_{dr}^2[k \cdot T_n] + \psi_{qr}^2[k \cdot T_n]} \\ \sin(\lambda_r[k \cdot T_n]) = \frac{\psi_{qr}[k \cdot T_n]}{|\psi_r[k \cdot T_n]|}; \cos(\lambda_r[k \cdot T_n]) = \frac{\psi_{dr}[k \cdot T_n]}{|\psi_r[k \cdot T_n]|} \end{cases} \quad (5)$$

- **The torque calculation block (C_lM_e).** The C_lM_e block is defined by the following equations:

$$M_e[k \cdot T_n] = K_a \cdot |\psi_r[k \cdot T_n]| \cdot i_{qs\lambda_r}[k \cdot T_n]; \quad K_a = \frac{3}{2} \cdot z_p \cdot \frac{L_m}{L_r} \quad (6)$$

- **The direct and inverse Clarke transformation (TS).** These blocks are defined by the following equations:

- **The direct Clarke transformation (TS [A])**

$$\begin{cases} i_{ds}[k \cdot T_n] = i_a[k \cdot T_n] - i_{s0}[k \cdot T_n] \\ i_{qs}[k \cdot T_n] = \frac{1}{\sqrt{3}} \cdot (i_b[k \cdot T_n] - i_c[k \cdot T_n]) \end{cases} \quad (7)$$

where:

$$i_{s0}[k \cdot T_n] = \frac{1}{3} \cdot (i_a[k \cdot T_n] + i_b[k \cdot T_n] + i_c[k \cdot T_n]); \quad i_c[k \cdot T_n] = -(i_a[k \cdot T_n] + i_b[k \cdot T_n]).$$

- **The invers Clarke transformation (TS [A]⁻¹)**

$$\begin{cases} i_a^*[k \cdot T_n] = i_{ds}^*[k \cdot T_n] \\ i_b^*[k \cdot T_n] = -\frac{1}{2} \cdot i_{ds}^*[k \cdot T_n] + \frac{\sqrt{3}}{2} \cdot i_{qs}^*[k \cdot T_n] \\ i_c^*[k \cdot T_n] = -\frac{1}{2} \cdot i_{ds}^*[k \cdot T_n] - \frac{\sqrt{3}}{2} \cdot i_{qs}^*[k \cdot T_n] \end{cases} \quad (8)$$

In the previous relations, i_a , i_b and i_c are the three-phase components of the stator current (stator line currents); i_{s0} is the homopolar component of the spatial phasor of the stator current; i_a^* , i_b^* and i_c^* are the three-phase components of the command stator current.

On the other hand, i_{ds} and i_{qs} are the d - q components of the space vector of the stator current, and i_{ds}^* , i_{qs}^* are the d - q command components of the space vector of the stator current.

- **The direct and inverse Park transformation (TA).** These blocks are defined by the following equations:

- **The direct Park transformation (TA D[λ_r])**

$$\begin{bmatrix} i_{ds\lambda_r}[k \cdot T_n] \\ i_{qs\lambda_r}[k \cdot T_n] \end{bmatrix} = D[\lambda_r[k \cdot T_n]] \cdot \begin{bmatrix} i_{ds}[k \cdot T_n] \\ i_{qs}[k \cdot T_n] \end{bmatrix} \quad (9)$$

- *The inverse Park transformation ($TA D[-\lambda_r]$)*

$$\begin{bmatrix} i_{ds}^*[k \cdot T_n] \\ i_{qs}^*[k \cdot T_n] \end{bmatrix} = D[-\lambda_r[k \cdot T_n]] \cdot \begin{bmatrix} i_{ds\lambda_r}^*[k \cdot T_n] \\ i_{qs\lambda_r}^*[k \cdot T_n] \end{bmatrix} \quad (10)$$

where:

$$D(\lambda_r[k \cdot T_n]) = \begin{bmatrix} \cos(\lambda_r[k \cdot T_n]) & \sin(\lambda_r[k \cdot T_n]) \\ -\sin(\lambda_r[k \cdot T_n]) & \cos(\lambda_r[k \cdot T_n]) \end{bmatrix}$$

- **The rotor flux controller (PI_P)**. The transfer function, in the Z-domain, of this controller is [6], [7]:

$$G_p(z) = \frac{i_{ds\lambda_r}^*(z)}{\varepsilon_1(z)} = K_p \cdot \left(1 + \frac{1}{T_p} \cdot \frac{T_n}{2} \cdot \frac{z+1}{z-1} \right) \quad (11)$$

where

$$\begin{aligned} \varepsilon_1[k \cdot T_n] &= |\psi_r^*[k \cdot T_n]| - |\psi_r[k \cdot T_n]| \\ K_p &= \frac{T_r}{2 \cdot L_m \cdot T_{d1}^*}; \quad T_p = T_r; \quad T_r = \frac{L_r}{R_r} \end{aligned} \quad (12)$$

and T_{d1}^* is a imposed constant time.

- **The torque controller (PI_M)**. In this case, the transfer function, in the Z-domain, of this controller is [6], [7]:

$$G_M(z) = \frac{i_{qs\lambda_r}^*(z)}{\varepsilon_2(z)} = K_M \cdot \left(1 + \frac{1}{T_M} \cdot \frac{T_n}{2} \cdot \frac{z+1}{z-1} \right) \quad (13)$$

where

$$\begin{aligned} \varepsilon_2[k \cdot T_n] &= M_e^*[k \cdot T_n] - M_e[k \cdot T_n] \\ K_M &= \frac{T_{d1}^*}{K_a \cdot |\psi_r^*| \cdot T_{d2}^*}; \quad T_M = T_{d1}^* \end{aligned} \quad (14)$$

and T_{d2}^* is a imposed time constant ($T_{d2}^* > T_{d1}^*$).

- **The speed 2DOF controller ($PI_W + C_{FF}$)**. In order to better control the speed response of the vector control system, a 2DOF speed controller is used (2DOF ~ Two-Degrees-of-Freedom Controller) [3]. The reference electromagnetic torque of the induction motor, in the case of using the Z-transform, is:

$$M_e^*(z) = C_{FF}(z) \cdot \omega_r^*(z) + M_1^*(z) \quad (15)$$

where $M_1^*(z) = G_\omega(z) \cdot \varepsilon_3(z)$

In relation (15), C_{FF} is the feed forward component of the 2DOF controller, and G_ω is a PI speed controller (PI - proportional-integral controller).

The feed forward component of the 2DOF controller is defined by the following relationship

$$G_{FF}(z) = \frac{-J \cdot \left(\frac{\omega_n}{2}\right)^2}{\frac{2}{T_n} \cdot \frac{z-1}{z+1} + \omega_n} \quad (16)$$

where: ω_n is the bandwidth of the vector control system ($\omega_n = \frac{1}{T}$, T - is the imposed time constant of the vector control system).

On the other hand, the transfer function of the PI speed controller (PI_W) is:

$$G_\omega(z) = \frac{M_1^*(z)}{\varepsilon_3(z)} = K_\omega \cdot \left(1 + \frac{1}{T_\omega} \cdot \frac{T_n}{2} \cdot \frac{z+1}{z-1}\right) \quad (17)$$

where

$$\varepsilon_3[k \cdot T_n] = \omega_r^*[k \cdot T_n] - \omega_r[k \cdot T_n]$$

$$K_\omega = \frac{T_4 \cdot (1 + \rho^2)}{2 \cdot K_4 \cdot T_{d2}^*}; \quad T_\omega = 4 \cdot \frac{T_{d2}^* \cdot (1 + \rho^2)}{(1 + \rho)^3}; \quad \rho = \frac{T_{d2}^*}{T_4}; \quad K_4 = \frac{1}{F}; \quad T_4 = \frac{J}{F} \quad (18)$$

All the previously presented controllers have been discretized using the trapezoidal method.

- **The hysteresis current controllers (C_H).** In this case, the PWM (Pulse-width modulation) pulses for the VSI inverter are generated using the following relationships:

$$S_1[k \cdot T_n] = \begin{cases} 0 & \text{if } \varepsilon_4[k \cdot T_n] \leq -\Delta_h \\ 1 & \text{if } \varepsilon_4[k \cdot T_n] \geq \Delta_h \\ S_1[(k-1) \cdot T_n] & \text{if } |\varepsilon_4[k \cdot T_n]| < \Delta_h \end{cases}; \quad \varepsilon_4[k \cdot T_n] = i_a^*[k \cdot T_n] - i_a[k \cdot T_n] \quad (19)$$

$$S_2[k \cdot T_n] = \begin{cases} 0 & \text{if } \varepsilon_5[k \cdot T_n] \leq -\Delta_h \\ 1 & \text{if } \varepsilon_5[k \cdot T_n] \geq \Delta_h \\ S_2[(k-1) \cdot T_n] & \text{if } |\varepsilon_5[k \cdot T_n]| < \Delta_h \end{cases}; \quad \varepsilon_5[k \cdot T_n] = i_b^*[k \cdot T_n] - i_b[k \cdot T_n] \quad (20)$$

$$S_3[k \cdot T_n] = \begin{cases} 0 & \text{if } \varepsilon_6[k \cdot T_n] \leq -\Delta_h \\ 1 & \text{if } \varepsilon_6[k \cdot T_n] \geq \Delta_h \\ S_3[(k-1) \cdot T_n] & \text{if } |\varepsilon_6[k \cdot T_n]| < \Delta_h \end{cases}; \quad \varepsilon_6[k \cdot T_n] = i_c^*[k \cdot T_n] - i_c[k \cdot T_n] \quad (21)$$

where Δ_h is the hysteresis band of the current controllers.

- **The rotor flux observer.** This observer uses as inputs the rotor speed as well as the d - q components of the stator currents of the induction motor. This observer is defined by the following mathematical relations:

$$\frac{d}{dt} \begin{bmatrix} \hat{\psi}_{dr} \\ \hat{\psi}_{qr} \end{bmatrix} = F \cdot \begin{bmatrix} \hat{\psi}_{dr} \\ \hat{\psi}_{qr} \end{bmatrix} + H \cdot \begin{bmatrix} i_{ds} \\ i_{qs} \end{bmatrix} \quad (22)$$

where

$$F = \begin{bmatrix} -\frac{1}{T_r} & -z_p \cdot \omega_r \\ z_p \cdot \omega_r & -\frac{1}{T_r} \end{bmatrix}; H = \begin{bmatrix} \frac{L_m}{T_r} & 0 \\ 0 & \frac{L_m}{T_r} \end{bmatrix} \quad (23)$$

The discrete model of the rotor flux observer (22) is given by the following relation

$$\begin{bmatrix} \hat{\psi}_{dr}[(k+1) \cdot T_n] \\ \hat{\psi}_{qr}[(k+1) \cdot T_n] \end{bmatrix} = F_d \cdot \begin{bmatrix} \hat{\psi}_{dr}[k \cdot T_n] \\ \hat{\psi}_{qr}[k \cdot T_n] \end{bmatrix} + H_d \cdot \begin{bmatrix} i_{ds}[k \cdot T_n] \\ i_{qs}[k \cdot T_n] \end{bmatrix} \quad (24)$$

where:

$$F_d = \sum_{i=0}^3 \frac{F_k^i \cdot T_n^i}{i!}; H_d = \sum_{i=0}^2 \frac{F_k^i \cdot T_n^{i+1}}{(i+1)!} \cdot H \quad (25)$$

$$F_k = \begin{bmatrix} -\frac{1}{T_r} & -z_p \cdot \omega_r[k \cdot T_n] \\ z_p \cdot \omega_r[k \cdot T_n] & -\frac{1}{T_r} \end{bmatrix} \quad (26)$$

The previous relationships are obtained based on the ZOH (Zero Order Hold) discretization method. For the purpose of discretization, the matrices F_d and H_d are truncated (terms for which the sampling time (T_n) has an order greater than three are neglected).

In the previous relationships, T_n is the sampling time used in the discretization of the relationships that define the control algorithm for the vector control system of the induction motor.

3. THE SIMULATIONS RESULTS

In order to highlight the effects of sampling time on the dynamic performance of the vector control system, we will use a 3kW induction motor with the electrical and dynamic parameters presented in Table 1.

In numerical simulation tests, the sampling times used are:

- Case 1: $T_n = 20[\mu s]$; $T_e = 1[\mu s]$;
- Case 2: $T_n = 100[\mu s]$; $T_e = 1[\mu s]$.

Table 1. The electrical and mechanical parameters of the induction motor [2]

	Name	Value		Name	Value
R_s	<i>Stator resistance</i>	2.0975 [Ω]	J	<i>Motor inertia</i>	0.1[kg·m ²]
R_r	<i>Rotor resistance</i>	2.0625 [Ω]	F	<i>Friction coefficient</i>	0.04[N·m·s/rad]
L_s	<i>Stator inductance</i>	0.1202 [H]	n_N	<i>Rated speed</i>	705 [rpm]

L_r	Rotor inductance	0.1263 [H]	z_p	Number of pole pairs	4
L_m	Mutual inductance	0.1158 [H]	f_N	Rated frequency	50 [Hz]
U_N	Rated voltage	380 [V]	M_N	Rated torque	40 [N·m]

In the case of both tests conducted through simulation, it is assumed that the induction motor operates in load, with a load torque equal to its rated torque. On the other hand, in the simulations the hysteresis band of the current controllers is $\Delta_h = 1/12 [A]$ and bandwidth of the vector control system is $\omega_n = 100 [rad / s]$. In order to tune the controllers, the following time constants were used: $T_{d1}^* = 1 [ms]$; $T_{d1}^* = 7.5 [ms]$.

The simulation results are presented in the following figures.

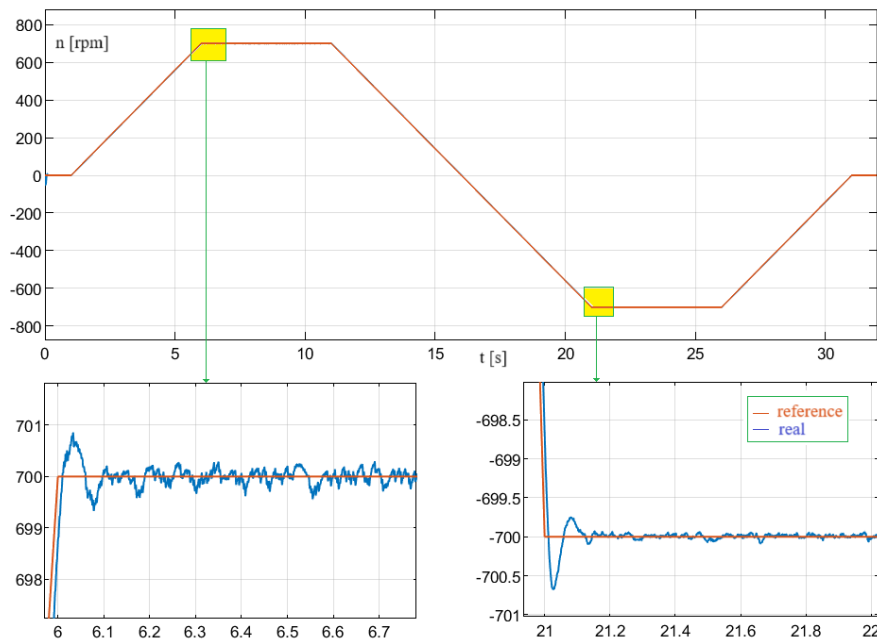


Fig.2. The time variation of the induction motor speed ~ Case 1

From Fig. 2, it can be observed that the speed of the induction motor stabilizes rapidly, indicating good dynamic performance of the vector control system when using a sampling time of 20 $[\mu s]$.

DIRECT ROTOR FLUX-ORIENTED CONTROL OF INDUCTION MOTORS USING HYSTERESIS CURRENT CONTROLLERS AND VSI INVERTER

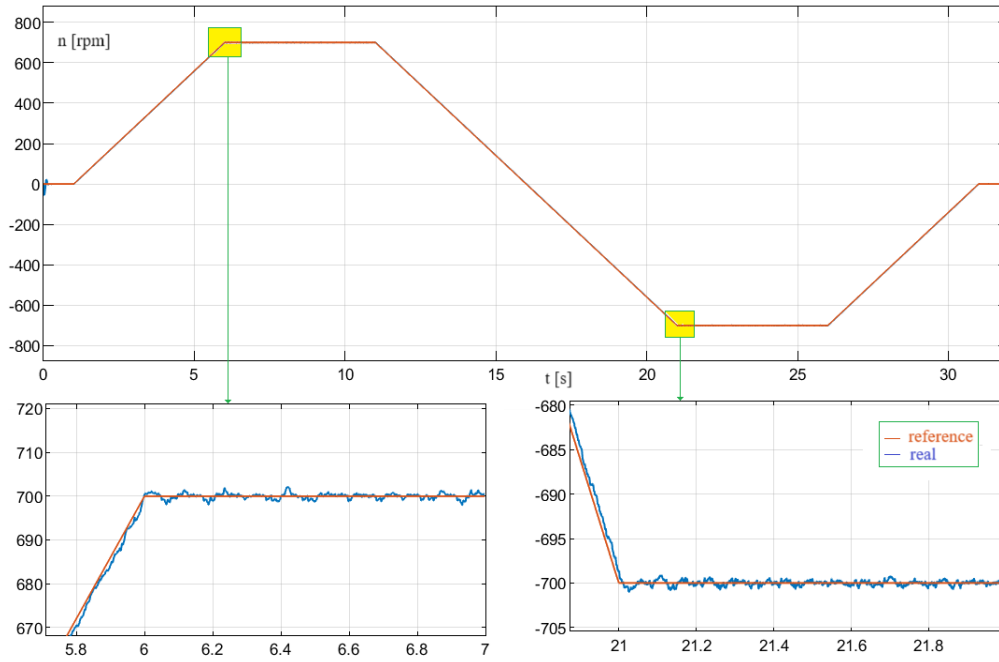


Fig.3. The time variation of the induction motor speed ~ Case 2

On the other hand, from Fig. 3, it can be observed that the speed of the induction motor exhibits larger oscillations and slower stabilization compared to Case 1, suggesting poorer dynamic performance due to the larger sampling time.

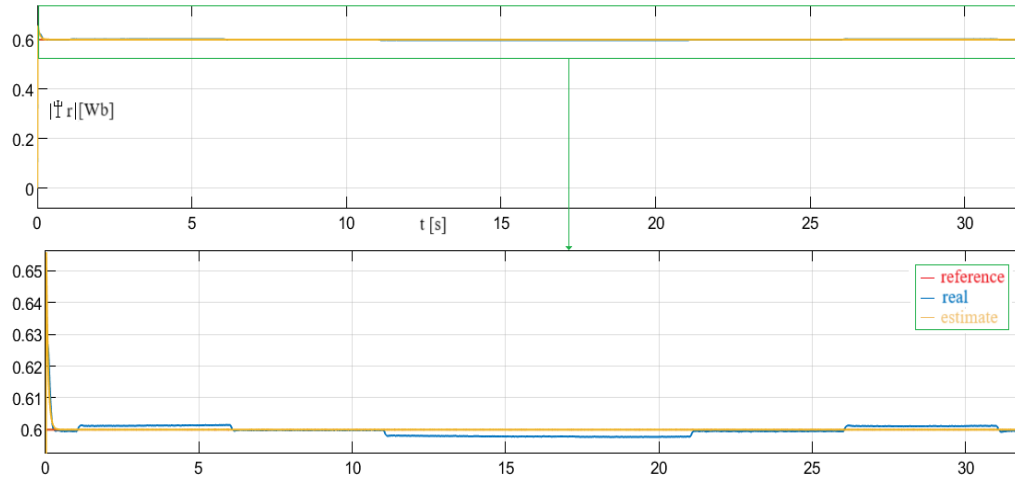


Fig.4. The rotor flux space vector - absolute value ~ Case 1

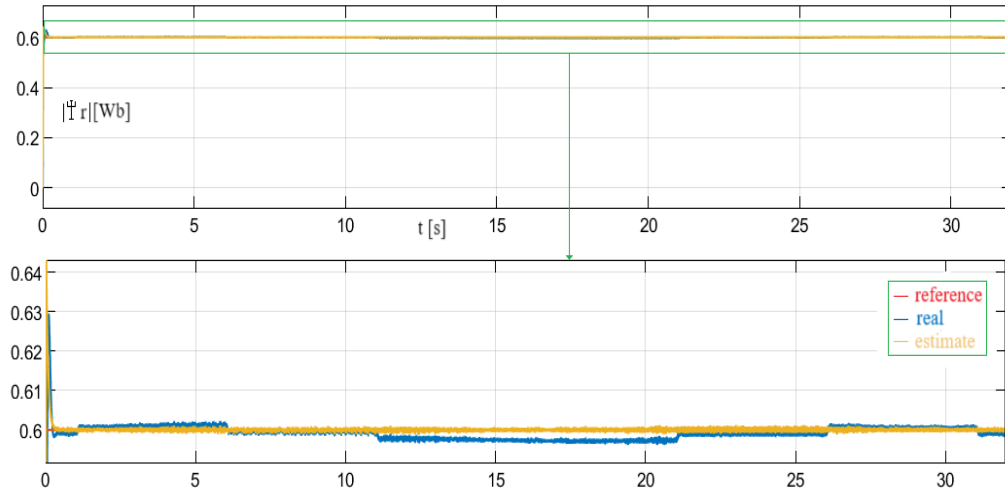


Fig.5. The rotor flux space vector - absolute value ~ Case 2

From Fig. 4 and Fig. 5, it can be observed that the absolute value of the spatial vector of the rotor flux of the induction motor is considerably more stable and constant in Case 1, compared to Case 2, where more pronounced variations and reduced stability are manifested. These observations suggest a significant negative influence of a larger sampling time on the performance of the vector control system.

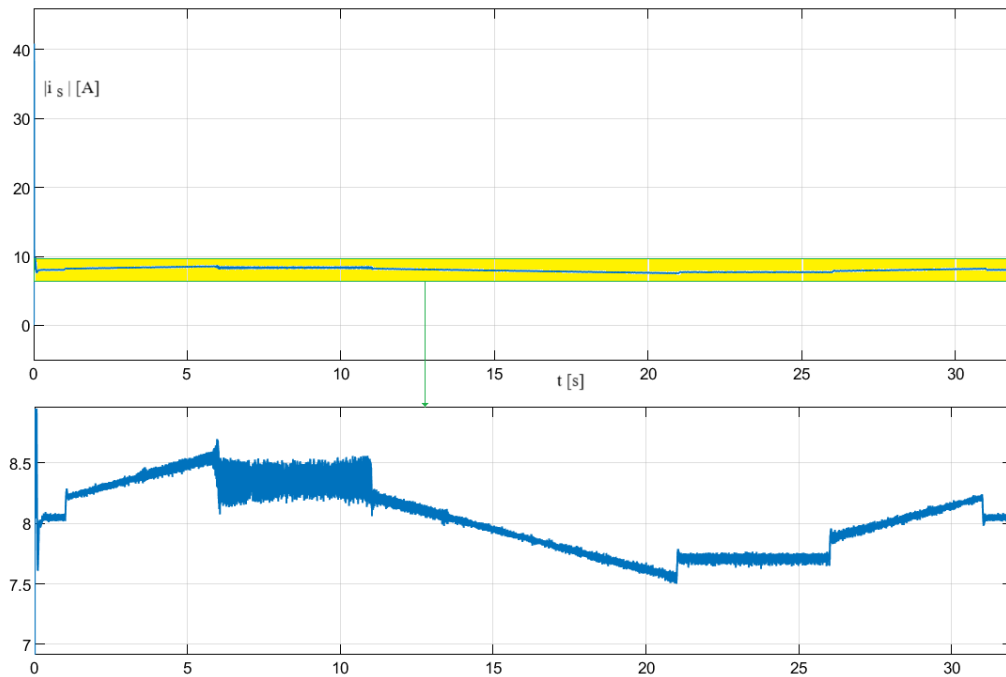


Fig.6. The stator current space vector - absolute value ~ Case 1

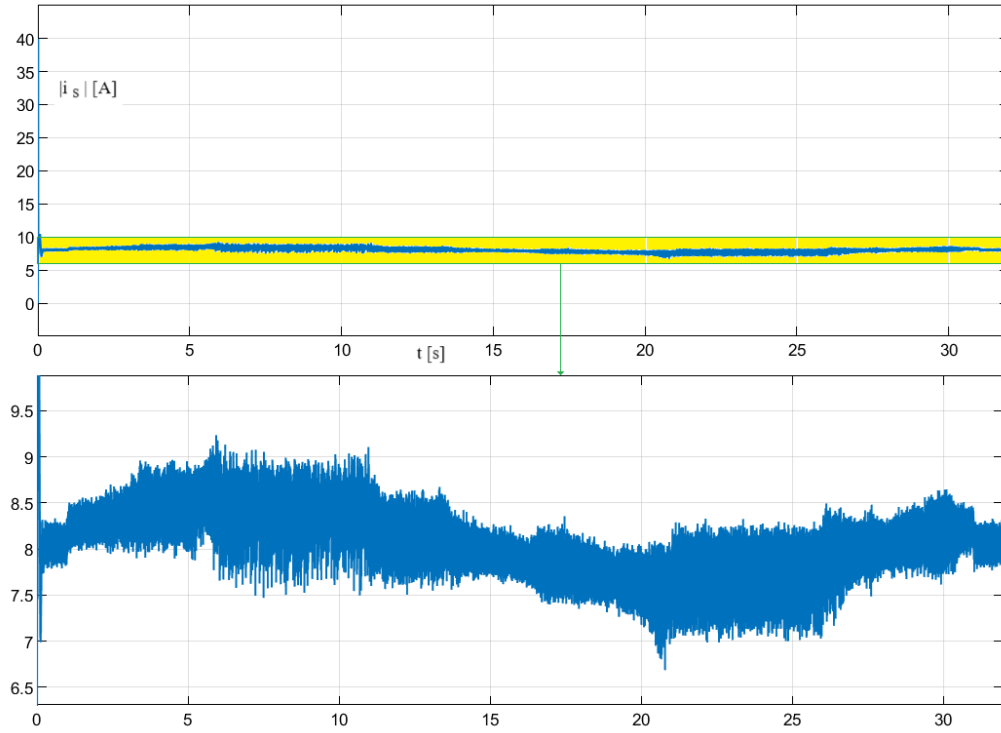


Fig.7. The stator current space vector - absolute value ~ Case 2

Analyzing Fig. 6 and Fig. 7, it is found that in Case 1, the absolute value of the spatial vector of the stator current has much smaller fluctuations and much better stability compared to Case 2.

4. CONCLUSIONS

Direct Rotor Flux Oriented Control (DRFOC) significantly improves the dynamic performance of induction motors, ensuring precise control of flux and electromagnetic torque. Simulations have shown that a smaller sampling time (20 [μ s]) provides superior stability and performance compared to a larger sampling time (100 [μ s]).

The detailed mathematical models presented in this article, along with the results obtained from Matlab-Simulink simulations, provide valuable support for experts in the field of induction motor control.

The research presented in this article can be extended in the future to optimize the selection of sampling time and control strategy, so that the efficiency and reliability of the induction motor control system are significantly improved. Additionally, the integration of emerging technologies, such as machine learning and artificial intelligence, can facilitate the development of advanced control and predictive maintenance methods for these motors.

REFERENCES

- [1]. **Boldea I., Nasar S.A.**, *Vector Control of AC Drives*, CRC Press, 1992.
- [2]. **Bitoleanu A., Popescu M., Suru V.**, *Experimental Evaluation of Rotor Field orientation Control and Hysteresis Controller for Induction Traction Motor*, 12th International Symposium on Advanced Topics in Electrical Engineering (ATEE), Bucharest, Romania, pp. 1-6, 2021.
- [3]. **Gogea A., Stoicuta O., Pana T.**, *Comparative Analysis Between the PI Speed Controller and Two-Degrees-of-Freedom Speed Controller for Induction Motor Drive*, 2019 8th International Conference on Modern Power Systems (MPS), Cluj-Napoca, Cluj, Romania, pp. 1-6, 2019.
- [4]. **Kelemen A., Imecs M.**, *Field-oriented AC Electrical Drives*, Romania Academy Publishing House, Bucharest, 1989.
- [5]. **Pana T., Stoicuta O.**, *Stability of the Vector Drive Systems with Induction Motors*, Mediamira Publishers, 2016.
- [6]. **Pana T., Stoicuta O.**, *Controllers tuning for the speed vector control of induction motor drive systems*, IEEE International Conference on Automation, Quality and Testing, Robotics (AQTR), Cluj-Napoca, Romania, pp. 1-6, 2010.
- [7]. **Stoicuta O., Pana T.**, *Asymptotic stability study of induction motor sensorless vector control systems with MRAS observer*, IEEE International Conference on Automation, Quality and Testing, Robotics (AQTR), Cluj-Napoca, Romania, pp. 1-6, 2016.
- [8]. **Stoicuta O.**, *The utilization of the S-Function block in simulation of the Luenberger rotor flux observer for induction motors*, Annals of the University of Petrosani, Electrical Engineering, Vol.18, pp. 31- 46, 2016.
- [9]. **Stoicuta O.**, *The utilization of the S-Function block in simulation of the mathematical model of induction motor with iron loss*, Annals of the University of Petrosani, Electrical Engineering, Vol.18, pp. 5-20, 2016.
- [10]. **Stoicuta O., Campian H., Pana T.**, *The Comparative Study of the Stability of the Vector Control Systems That Contain In the Loop Luenberger and Kalman Type Estimators*, IEEE International Conference on Automation, Quality and Testing, Robotics, Cluj-Napoca, Romania, , pp. 113-117, 2006.
- [11]. **Vas P.**, *Vector Control of AC Machines*, CRC Oxford, 1990.

INDEX OF AUTHORS

A

ANTIPOVA T., 155
ANTONOV A.E., 25, 79
APOSTU S., 169

B

BEIU C., 25, 79
BORODAY V., 89
BUICĂ G., 25, 79

C

COSTINAȘ A., 307

D

DOBRA R., 79
DINEA D.I., 69

E

EGRI A., 315

F

FOTAU D., 35, 273

G

GABOR D., 263
GHICAJANU (CAȘOTĂ) M.I., 237

I

IACOBESCU DINEA D.C., 69
ITU R.B., 169

K

KNYSH V., 115

L

LAZAR T., 177, 383
LEBA M., 69, 123, 141, 347
LOBONȚ L., 247

M

MAGYARI M., 133, 273
MANOLE T., 295, 329
MARCU M., 69, 177
MOLDOVAN C., 133
MOLDOVAN L., 133
MORARU R.I., 7, 51, 121
MUNTEAN E., 123
MUNTEAN L., 207
MURESAN-GRECU F., 51, 177

N

NAIDA V., 89
NEGRU N., 169, 315
NESTEROVA O., 89

O

OLAR M.L., 307

P

PANAITE F.A., 97
PANĂ L., 107, 347
PANCIU A., 247
PARAIAN M., 263
PASCULESCU D., 25, 79, 177, 347
PATRASCOIU N., 197
PĂUN A.P., 185
PETRILEAN D.C., 237
PLAHUNOV O., 115
POPA C.M., 185
POPESCU F.G., 107, 177, 347, 383
POPESCU G., 383

R
RAD M., 35
RADU M.A., 285
RADU S.M., 315
RÂȘNOVEANU S., 133
RISTEIU M., 25, 79, 177
RIUREAN S., 155, 383
ROSCA S.D., 69, 107, 307, 347, 383
RUS C., 141, 295

S
SALASAN D., 35
SHYKHOV S., 115
SIBIȘANU R., 295
SÎRB V., 391
SÎRBU V., 35
SOICA A., 169, 315
STEPANEK A., 97
STOCHITOIU M.D., 43, 341, 355
STOICUTA N.E., 373, 391
STOICUTA O., 391

Ș
ȘIMON-MARINICĂ B., 207
ȘUVAR M., 207

T
TĂZLĂUANU A., 263
TRIOHIN V., 329

U
UTU I., 43, 341, 355

V
VASS Z., 207

Z
ZERBES M.V., 247
ZSIDO S., 273

REVIEWERS:

Marius Daniel Marcu Ph.D.,
 Dragos Pasculescu Ph.D.,
 Nicolae Patrascoiu Ph.D.,
 Florin Gabriel Popescu Ph.D.,
 Razvan Slusariuc Ph.D.,
 Maria Daniela Stochitoiu Ph.D.,
 Olimpiu Stoicuta Ph.D.,
 Ilie Utu Ph.D.